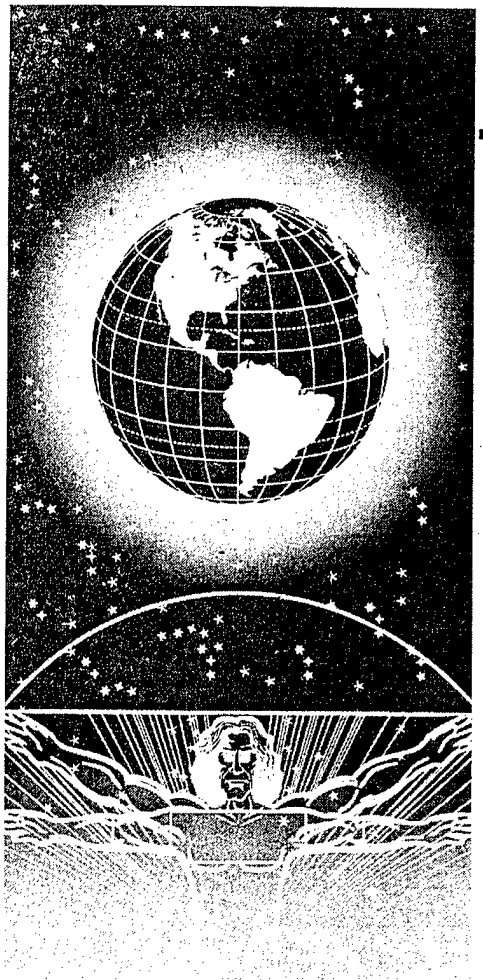
AFRL-HE-WP-TR-2003-0064



UNITED STATES AIR FORCE RESEARCH LABORATORY

AUTOMATIC LEGIBILITY CONTROL (ALC) OF ELECTRONIC DISPLAYS

Keith T. Burnette

BURNETTE ENGINEERING
4881 ARABIAN DRIVE
FAIRBORN OH 45324-9732

FEBRUARY 2003

FINAL REPORT FOR THE PERIOD 19 AUGUST 1994 TO 11 FEBRUARY 2003

20030715 020

Approved for public release; distribution is unlimited

Human Effectiveness Directorate
Crew System Interface Division
2255 H Street
Wright-Patterson AFB OH 45433-7022

NOTICES

When US Government drawings, specifications, or other data are used for any purpose other than a definitely related Government procurement operation, the Government thereby incurs no responsibility nor any obligation whatsoever, and the fact that the Government may have formulated, furnished, or in any way supplied the said drawings, specifications, or other data, is not to be regarded by implication or otherwise, as in any manner licensing the holder or any other person or corporation, or conveying any rights or permission to manufacture, use, or sell any patented invention that may in any way be related thereto.

Please do not request copies of this report from the Air Force Research Laboratory. Additional copies may be purchased from:

National Technical Information Service
5285 Port Royal Road
Springfield, Virginia 22161

Federal Government agencies and their contractors registered with the Defense Technical Information Center should direct requests for copies of this report to:

Defense Technical Information Center
8725 John J. Kingman Road, Suite 0944
Ft. Belvoir, Virginia 22060-6218

DISCLAIMER

This Technical Report is published as received and has not been edited by the Air Force Research Laboratory, Human Effectiveness Directorate.

TECHNICAL REVIEW AND APPROVAL

AFRL-HE-WP-TR-2003-0064

This report has been reviewed by the Office of Public Affairs (PA) and is releasable to the National Technical Information Service (NTIS). At NTIS, it will be available to the general public.

This technical report has been reviewed and is approved for publication.

FOR THE COMMANDER

MARIS M. VIKMANIS
Chief, Crew System Interface Division
Air Force Research Laboratory

REPORT DOCUMENTATION PAGE

Form Approved
OMB No. 0704-0188

Public reporting burden for this collection of information is estimated to average 1 hour per response, including the time for reviewing instructions, searching existing data sources, gathering and maintaining the data needed, and completing and reviewing the collection of information. Send comments regarding this burden estimate or any other aspect of this collection of information, including suggestions for reducing this burden, to Washington Headquarters Services, Directorate for Information Operations and Reports, 1215 Jefferson Davis Highway, Suite 1204, Arlington, VA 22202-4302, and to the Office of Management and Budget, Paperwork Reduction Project (0704-0188), Washington, DC 20503.

1. AGENCY USE ONLY (Leave blank)	2. REPORT DATE	3. REPORT TYPE AND DATES COVERED
	February 2003	Final: 19 August 1994 to 11 February 2003

4. TITLE AND SUBTITLE
Automatic Legibility Control (ALC) of Electronic Displays

5. FUNDING NUMBERS
C F33615-94-C-3801
PE 62201F
PR 2403
TA 04
WU 70

6. AUTHOR(S)
Keith T. Burnette, Ph.D.

7. PERFORMING ORGANIZATION NAME(S) AND ADDRESS(ES)
Burnette Engineering
4881 Arabian Drive
Fairborn, Ohio 45324-9732

8. PERFORMING ORGANIZATION REPORT NUMBER

9. SPONSORING/MONITORING AGENCY NAME(S) AND ADDRESS(ES)
Human Effectiveness Directorate
Crew System Interface Division
Air Force Research Laboratory
Air Force Materiel Command
Wright-Patterson AFB, Ohio 45433-7022

10. SPONSORING/MONITORING AGENCY REPORT NUMBER
AFRL-HE-WP-TR-2003-0064

11. SUPPLEMENTARY NOTES

12a. DISTRIBUTION/AVAILABILITY STATEMENT
Approved for Public Release; Distribution is Unlimited

12b. DISTRIBUTION CODE

13. ABSTRACT (*Maximum 200 words*)

Pilot legibility requirements are investigated to establish a basis for implementing automatic control over electronic and conventional displays, in day through night aircraft cockpit viewing environments. Applicable legibility test results, published by different experimenters over much of the past century, are examined and analyzed, and comparisons are used to assess their validity as display control criteria. The mathematical model of the human visual system developed provides a basis for the design of display automatic legibility controls, suitable for use in aircraft cockpits, by predicting the pilot's image difference luminance requirements, in the presence of luminance specularly and diffusely reflected from the display viewing surfaces, and with discrete and distributed glare sources incident on the pilot's eyes. Although this general automatic legibility control (ALC) model and the automatic brightness control (ABC) model, used in the newer Boeing airliners, appear quite different, comparisons show that, when properly implemented, the two models give equivalent results. The advantage of the ALC model is its greater design flexibility, owing to its better defined physical relationship to vision. Various practical design choices that should be taken into consideration to achieve a successful application of automatic legibility controls are explored in the balance of the report. This includes, for example: methods of achieving compatibility with light reflective, transflective, emissive and transmissive operating mode displays; the relative merits of viable alternatives to the recommended constant legibility control characteristic strategy; interactions between controls for legibility and sensor-video signal conditioning; the type and need for pilot legibility trim controls; and possible response time conpensations for the light and dark adaptation of the pilot's eyes during the following glare source exposures.

14. SUBJECT TERMS
Electronic Displays, Aircraft Cockpit Lighting, Pilot or Aircrew Legibility Requirements, Design Criteria, Night Vision, Human Visual System Model, Grey or Gray Shade Control, Color Picture Rendition, Glare Source Exposure, Veiling Luminance, Contrast, Video Signal Conditioning

15. NUMBER OF PAGES
425

16. PRICE CODE

17. SECURITY CLASSIFICATION OF REPORT	18. SECURITY CLASSIFICATION OF THIS PAGE	19. SECURITY CLASSIFICATION OF ABSTRACT	20. LIMITATION OF ABSTRACT
Unclassified	Unclassified	Unclassified	UL

THIS PAGE INTENTIONALLY LEFT BLANK

FORWARD

The legibility requirements and automatic legibility control techniques described in this technical report represent the culmination of thirty years of sporadic research into this specialized area of aircraft cockpit control-display systems and the design criteria they should meet to satisfy the control and information display needs of pilots and other aircrew members. The current technical report was prepared as a part of Contract Number F33615-94-C-3801, entitled "Criteria Development for High Technology Cockpit Devices," which was originally scheduled to be carried out during period from 19 September 1994 until 19 January 1999.

Although a preliminary report containing select portions of the information presented in the current report was prepared during the first two years of the contract, as an ancillary part of providing design criteria, in technical support of closely related research then being conducted by the USAF, an unforseen event resulted in the analyses of pilot legibility requirements and their application to the automatic legibility control of aircraft cockpit displays becoming the major emphasis during the completion phase of the contract. The unforseen event was a limitation of available Department of Defense funds, which caused the contract to be suspended on 12 March 1997, through the issuance of a Partial Stop Work Order by the USAF. Since the research efforts underway at the time were incomplete, but a report to conclude the effort was still sought by the USAF, the emphasis of the report was shifted to a compilation and presentation of research and analyses previously conducted, the substance and implications of which were apparently not yet recognized, since they have neither been applied to military aircraft cockpits nor adequately documented in the literature. In retrospect, the scope of the documentation effort needed to complete a report that adequately describes the legibility requirements of aircrews, as a function of day and night ambient illumination and glare source viewing conditions experienced in aircraft cockpits, and the implementation of display automatic legibility controls, with aircrew-adjustable trim controls, capable of satisfying these requirements in aircraft cockpits, was vastly underestimated, in that the preparation of the report required from 11 September 2001 and 11 February 2003, to complete.

This contracted investigation was sponsored and technically monitored by the United States Air Force Wright Laboratory, Flight Dynamics Directorate, Air Force Materiel Command, Wright-Patterson Air Force Base, Ohio. Mr. Walter Melnick was the Air Force Project Engineer for the first two years and a half of the contract. For the balance of the contract, Mr. Richard Moss served as the Air Force Project Engineer. Due to the reorganization of USAF research laboratories, from throughout the country in October 1997, the organization that Mr. Moss directs became a Branch within the Human Effectiveness Directorate, Air Force Research Laboratory (AFRL), Air Force Materiel Command, at the time of the reorganization. Dr. Keith T. Burnette served as the principal investigator for Burnette Engineering during the duration of the contract.

THIS PAGE INTENTIONALLY LEFT BLANK

TABLE OF CONTENTS

CHAPTER 1 Introduction 1

CHAPTER 2 Aircraft Cockpit Electronic Display Information Legibility Control Considerations 8
2.1. Rationale for Using the Objective Legibility Requirements of Pilots as a Basis for the Implementation of Automatic Legibility Control 9
2.2. Electronic Display Operating Mode and Technology Compatibility with Automatic Legibility Control 9
2.3. Light Reflective Mode Aircraft Cockpit Displays 11
2.3.1. Legibility Considerations for Conventional Aircraft Instruments 12
2.3.2. Legibility Considerations for Light Reflective Mode Electronic Displays 14
2.4. Light Transflective Mode Aircraft Cockpit Displays 15
2.4.1. Legibility Considerations for Conventional Aircraft Panels and Controls 15
2.4.2. Legibility Considerations for Light Transflective Mode Electronic Displays 16
2.5. Light Emissive Mode Aircraft Cockpit Displays 16
2.5.1. Legibility Considerations for Cathode Ray Tube Displays 19
2.5.1.1. Monochrome CRT Displays 19
2.5.1.2. Color CRT Displays 21
2.5.2. Legibility Considerations for Light Emitting Diode Displays 22
2.5.2.1. Monochrome LED Displays 26
2.5.2.2. Color LED Displays 27
2.6. Light Transmissive Mode Aircraft Cockpit Displays 28
2.6.1. Legibility Considerations for Conventional Light Transmissive Mode Displays 30
2.6.2. Legibility Considerations for Electronic Light Transmissive Mode Displays 31

CHAPTER 3 Pilot Legibility Requirements 33
3.1. Image Legibility Variable Dependences 34
3.1.1. Luminance Functional Description and Variables 39
3.1.2. Practical Legibility Variables 40
3.1.3. Common Misconceptions 40
3.1.4. Analysis Approach for Interpreting Published Data 41
3.1.5. Definition of Practical Legibility Test Variables 41
3.2. Image Critical Detail Dimension 44
3.2.1. Form Identification Dependence on the Image Critical Detail Dimension 44
3.2.2. Image Difference Luminance Relationship to Minimum Separable Visual Acuity 48
3.3. Image Difference Luminance Requirements 50
3.3.1. Qualitative Comparisons of Historic Image Difference Luminance Characteristics 50
3.3.2. Quantitative Comparisons of Historic Image Difference Luminance Characteristics 53
3.3.2.1. Comparisons of the Image Identification Task Data of Different Experimenters 54
3.3.2.2. Comparisons Between Image Identification and Image Detection Task Data 56
3.3.2.3. Quantitative Image Difference Luminance Characteristic Comparison Conclusions 60
3.3.3. Comparisons with Jainski Data 61
3.3.4. Influence of Pilot Legibility Performance Criteria 63
3.3.4.1. Day Versus Night Adjustments Between Legibility Performance Levels for Ideal Imagery Using Image Difference Luminance Multipliers 64
3.3.4.2. Prediction of Image Difference Luminance Multipliers to Change the Legibility Performance Levels of Ideal Imagery 65
3.3.4.3. Prediction of Image Difference Luminance Multipliers Needed to Legibility Present Information in Aircraft Cockpits 68

3.3.5. Dependence of Jainski Data on Cockpit Luminance Environment 71
3.3.6. Discussion of Key Legibility Dependence Features of Jainski's Data 73
3.3.6.1. Ideal Panel and Surround Luminance Conditions 74
3.3.6.2. Observations on Effects of Panel and Surround Luminances 74
3.3.6.3. Effect of Display Location: Head-Up or Head-Down 74
3.4. Empirical Representation of Ideal Legibility Requirements 75
3.4.1. Mathematical Modeling of Ideal Image Legibility Characteristics 76
3.4.2. Perceived Image Difference Luminance Requirements Equation 79
3.5. Discrete and Distributed Glare Source Induced Veiling Luminance 83
3.5.1. The Historic Origins and Generalization of Veiling Luminance 84
3.5.1.1. Discrete Glare Source Veiling Luminance Dependences 86
3.5.1.2. Discrete and Distributed Glare Source Veiling Luminance Dependences 87
3.5.1.3. Effect of Veiling Luminance on the Perceived Image Contrast 87
3.5.2. Veiling Luminance Dependence on the Illuminance of a Discrete Glare Source 88
3.5.2.1. Glare Source Experimental Data 88
3.5.2.2. Derivation of Equation for Veiling Luminance from Experimental Data 91
3.5.2.3. Assessment of the Accuracy of Jainski's Experimental Data 95
3.5.2.4. HDD and HUD Veiling Luminance Dependence on Glare Source Illuminance 99
3.5.3. Veiling Luminance Dependence on the Glare Source Angular Position with Respect to the Pilot's Line of Sight 104
3.5.3.1. Description of Jainski's Glare Source Angular Dependence Test Data 104
3.5.3.2. Analysis and Interpretation of Jainski's Glare Source Angular Dependence Test Data 106
3.5.3.3. Derivation of Veiling Luminance Angular Dependence from Experimental Data 111
3.6. Veiling Luminance Representations for Spatially Discrete Glare Sources 113
3.6.1. Empirical Equations for Discrete Glare Sources Based on the Data of Jainski 115
3.6.1.1. Combined Illuminance and Angular Dependences 115
3.6.1.2. Image Difference Luminance Requirement for a Discrete Glare Source 116
3.6.2. Comparison of Veiling Luminance Test Results of Different Experimenters for Discrete Glare Sources 117
3.6.2.1. Empirical Representations of Veiling Luminance Test Results 117
3.6.2.2. General Discussion of Veiling Luminance Test Results 122
3.6.2.3. Comparisons with Holladay Veiling Luminance Test Results 126
3.6.2.4. Comparisons with Nowakowski Veiling Luminance Test Results 132
3.6.3. Eye Pupil Diameter and Area Variable Dependences 136
3.6.3.1. Pupil Areas Predicted by Riggs' Rule of Thumb 137
3.6.3.2. Holladay's Pupil Area Experimental Findings 137
3.6.3.3. Other Pupil Area Experimental Findings 139
3.6.3.4. Comparison of Pupil Area Predictions 141
3.6.3.5. Comparison of Pupil Areas with the Predictions of Riggs' Rule of Thumb ... 143
3.6.3.6. Conclusions for Eye Pupil Area Variable Dependences 145
3.7. Elements of a Theory for the Origin and Functionality of the Veiling Luminance Induced by a Discrete Glare Source 145
3.7.1. Theoretical Origin of Veiling Luminance 146
3.7.2. Psychological Response to Scattered Glare Source Light 150
3.7.2.1. Veiling Luminance Angular Response Relationship to the Visual Task Performed 150
3.7.2.2. Comparison of Image Difference Luminance Requirements for Image Detection and Identification Tasks 151
3.7.2.3. Blackwell Image Detection Task Data and Commentary 153
3.7.2.4. Visual Task Related Confirmations and Comparisons of Blackwell's Results 158
3.7.3. Physiological Response to Scattered Glare Source Light 160

3.7.3.1. Interpretation of Stiles and Holladay Image Detection Task Experimental Data 161
3.7.3.2. Interpretation of Nowakowski and Jainski Identification Task Experimental Data 162
3.7.3.3. Interpretation of Blackwell's Image Detection Task Experimental Results ... 163
3.7.3.4. Implications of the Spectral Receptivity of Retinal Receptors under Photopic, Mesopic and Scotopic Light Adaptation Viewing Conditions 164
3.7.3.5. Influence of Photopic, Mesopic and Scotopic Adapted Viewing Conditions on the Performance of Image Detection and Identification Tasks 168
3.7.3.6. Interpretations Based on the Physical Geometry of the Retina and of its Light Receptors 170
3.7.3.7. Interpretation of Image Size or Critical Detail Dimension Dependence of Image Difference Luminance using Spatial Frequency Dependent Contrast Sensitivity Functions 173
3.7.3.8. Implications on Human Visual Capabilities of the Constraints Imposed by Retinal Cone and Rod Light Receptors 176
3.7.3.9. Implications of Image Size and Blackwell's Common Image Difference Luminance Inflection Point on the Transition Between the Use of Cone And Rod Light Receptors 176
3.7.3.10. Implications of Image Size on the Blackwell Image Difference Luminance Plateau Effect and on the Transition Between the Use of Cone and Rod Light Receptors 180
3.7.3.11. Dependence of Rod and Cone Receptor Usage Based on Experimental Design 182
3.7.3.12. Veiling Luminance Angular Response Conclusions 183
3.7.4. Influence of the Pupil Area of the Eyes on Veiling Luminance 184
3.7.5. Conclusions to the Theory of Veiling Luminance Induced by Discrete Glare Sources . 189
3.8. Veiling Luminance Representations for Spatially Distributed Glare Sources 190
3.8.1. General Case of the Discrete Glare Source Formulation of Veiling Luminance 191
3.8.2. Distributed Glare Source Formulation of Veiling Luminance 193
3.8.3. Comparison of Discrete and Distributed Glare Source Formulations of Veiling Luminance 195
3.8.4. Empirical Model for Distributed Glare Source Veiling Luminance 200
3.8.5. Validation of Empirical Model for Distributed Glare Source Veiling Luminance 202
3.8.6. Quasi-Theoretical Model for Distributed Glare Source Veiling Luminance 208
3.8.7. Validation of the Quasi-Theoretical Model for Distributed Glare Source Veiling Luminance 211
3.8.8. Conclusions for Veiling Luminance Induced by Spatially Distributed Glare Sources .. 213
3.9. Practical Aircraft Cockpit Display Legibility Requirements 215
3.9.1. General Legibility Equation as Formulated for Aircraft Cockpit Applications 216
3.9.2. Adaptation of General Legibility Equation to the Visual Requirements of Pilots 216
3.9.2.1. Minimum Contrast Requirement for Video Information in High Light Ambients 218
3.9.2.2. Minimum Image Difference Luminance Requirements for Video Information in High Light Ambients 218
3.9.2.3. Image Difference Luminance Requirements for Video and Multicolor Information in Night Light Ambients 220
3.9.3. Minimum Image Legibility Requirements Equation for Aircraft Cockpit Displays 222
3.9.4. Generalized Image Legibility Equation for Aircraft Cockpit Displays 223
3.9.5. Interpretation of the Image Difference Luminance Requirements Equation 225
3.9.6. Origin of Aircraft Electronic Display Minimum Image Difference Luminance Requirements 226
3.9.7. Predicting the Veiling Luminances Experienced in Operational Aircraft Cockpits 227

3.9.7.1. Comparison of Operational Aircraft and Veiling Luminance Model Predictions 228
3.9.7.2. Assessment of Using a Rough Approximation to Represent Veiling Luminance 229
3.10. Conclusions 231

CHAPTER 4 Historical Perspective of Automatic Brightness Controls (ABCs) and Automatic Legibility Controls (ALCs) 233
4.1. Initial Versions of Automatic Brightness Controls 233
4.2. Boeing Automatic Brightness Control 234
4.2.1. Boeing ABC System Control Law Algorithm 235
4.2.2. Interpretation of Boeing ABC System Control Law Algorithm 236
4.2.2.1. Display Brightness Control Equation 236
4.2.2.2. Compensation of Display Image Difference Luminance Requirements for Glare 237
4.2.2.3. Image Difference Luminance Forward Field of View Glare Gain Compensation Multiplier 237
4.3. General Automatic Legibility/Brightness Control 240
4.3.1. Composite Display Grey Shade and Image Difference Luminance Control 240
4.3.2. Grey Scale Relative Luminance Function 241
4.3.3. White Image Difference Luminance Level Control Function 241
4.4. Summary of Features Shared by Boeing ABC and General ALC 242

CHAPTER 5 General Automatic Legibility Control (ALC) Law 244
5.1. Emulation of Conventional Electromechanical Aircraft Instrument Legibility using Electronic Displays 245
5.2. Comparison of the General and the Boeing Automatic Brightness Control Laws 247
5.2.1. Commonality Between General and Boeing Control Laws 247
5.2.2. Evaluation of Equivalence of Gain Compensation Equations 249
5.3. Human Visual System Control over the Legibility of Perceived Visual Scenes 253
5.3.1. Historic Context for Considering the Adequacy of Aircraft Display Legibility 254
5.3.2. Quantifying Electronic Display Picture Legibility in Terms of Relative Luminance 256
5.3.3. Munsell System Characterization of Color and Grey Shade Perception 259
5.3.4. Comparison of Human Visual Perception and Display Image Rendition Capabilities 262
5.3.5. Perception of Grey Shades on Electronic Displays 264
5.3.6. Image Rendition Requirements for Video Portrayals on Electronic Displays 266
5.3.6.1. Relationships to Replicate Real-World Scenes in Electronic Display Pictures 267
5.3.6.2. Equating Munsell Value Scale and Electronic Display Relative Luminance Levels 272
5.3.6.3. Electronic Display Image Rendition Requirement Conclusions 273
5.3.7. Constant Legibility Control Capability of the Human Visual System 273
5.3.8. Extension of Perceptible Grey Scale Range Through Spatially Selective Adaptation 275
5.4. General Automatic Legibility Control Law Application Considerations 276
5.4.1. Context for Assessing the Legibility of Electronic Displays on Aircrew Performance 278
5.4.2. Fixed Maximum Display Luminance Control Law 280
5.4.2.1. Legibility Expectations for Displays Operated at Maximum Luminance in Daylight 280
5.4.2.2. Conclusions for Displays Operated at Maximum Luminance in Daylight 281
5.4.3. Merrifield and Silverstein Brightness Control Law 282
5.4.4. Rationale for Using the Constant Legibility Control Law 284
5.4.5. Control Law Slope and Night Image Difference Luminance Level Interactions 284
5.5. Automatic Legibility Control Implementation and Adjustment Considerations 285

5.5.1. Circumstances Requiring Aircrew Trim Control Adjustments to Display Legibility 286
5.5.2. Implementation of Single Aircrew Adjustable Legibility Trim Controls 287
5.5.3. Implementation of Dual Aircrew Adjustable Legibility Trim Controls 289
5.5.4. Choice of Settings for the Constant Legibility Control Law Equation Parameters 290

CHAPTER 6 Sensor-Video Signal Conditioning 291
6.1. Control of the Sensor-Video Information Content Depicted on Electronic Displays 293
6.1.1. Conditioning Sensor-Video Signals During Display 293
6.1.1.1. Gamma Compensation of CRT Video Displays 293
6.1.1.2. Conventional Aircraft CRT Display Conditioning of Sensor-Video Signals ... 295
6.1.1.3. An overview of Conventional Aircraft CRT Display Signal Conditioning 297
6.1.2. Conditioning Sensor-Video Signals Prior to Display 298
6.2. Signal Conditioning for Digitally Encoded Sensor-Video Signals 300
6.2.1. Human Perception and Extraction of Information from Pictures on Digital Displays ... 301
6.2.2. Digital Processing and Conditioning of Sensed Video Signals Prior to Display 303
6.2.3. Special Considerations for Color Digital Displays 307
6.3. Comparison of Legibility Control and Signal Conditioning Techniques for Different Types of Electronic Displays 309
6.3.1. Applying Signal Conditioning to Active Matrix Liquid Crystal Displays 309
6.3.2. Perceived Legibility Effects Associated with the Application of Signal Conditioning ... 310
6.3.3. Display Technology Limitations on the Signal Conditioning and Legibility Control of Electronic Display Pictures 312

CHAPTER 7 Practical Aircraft Manual and Automatic Legibility Control Implementation Considerations 314
7.1. Specular Reflection Component of the Background Luminance of Electronic Displays 315
7.1.1. Conditions under Which the Legibility of Electronic Displays is Influenced by Specularly Reflected Luminance 315
7.1.2. Techniques for Measuring the Luminance Specularly Reflected from Electronic Display Surfaces 316
7.2. Legibility Requirement Dependence on the Types and the Locations of Cockpit Displays 318
7.3. Aircrew Control Over Electronic Display Legibility 320
7.3.1. Electronic Display Image Difference Luminance Manual Control Characteristics 322
7.3.1.1. Image Difference Luminance Versus Control Knob Rotation Angle Characteristic 323
7.3.1.2. Separation of Aircrew Manual Control and Display Controller Characteristics 323
7.3.2. Interfacing Aircrew Legibility Controls with Image Difference Luminance Controllers for Electronic Displays 325
7.3.2.1. Interchangeability Criteria for Aircrew Manual Controls 328
7.3.2.2. Absolute Control Interface Protocol 328
7.3.2.3. Relative Control Interface Protocol 329
7.3.2.4. Comparison of Absolute and Relative Control Interface Protocols 330
7.3.3. Electronic Display Manual Legibility Control Options 330
7.3.3.1. Individual Electronic Displays Operated Using Dedicated Manual Controls .. 331
7.3.3.2. Multiple Electronic Displays Operated in Unison Using a Common Manual Control 331
7.3.4. Electronic Display Automatic Legibility Control Options 333
7.3.4.1. Multiple Individual Electronic Displays Operated Using Dedicated ALCs 333
7.3.4.2. Multiple Electronic Displays Operated in Unison Using a Single ALC 334
7.3.4.3. Multiple Individual Electronic Displays Operated Using Dedicated ALCs and Both Individual and Common Legibility Trim Controls 335
7.3.5. Integration of Manual with Automatic Control Techniques 336

7.4. Coordination of Multiple Light Sensors, Automatic Legibility Controls and Displays 337
7.4.1. The Effect of Static Illuminated and Shadowed Areas on ALC Controlled Displays ... 338
7.4.2. The Effect of Dynamic Flight Maneuvers on ALC Controlled Displays 339
7.4.2.1. The Implications of Control Technology Limitations 340
7.4.2.2. The Implications of Aircrew Visual Response Time Limitations 340
7.4.2.3. Compensation for Aircrew Visual Response Time Limitations 341
7.5. Digital Control Signal Compatibility Considerations 341
7.5.1. Display Image Difference Luminance Controller Step Size Criteria 343
7.5.2. Sampling Criteria for Automatic Legibility Control Light Sensor Signals 344
7.5.2.1. Light Sensor Range and Step Size for Minimum Legibility Video Displays ... 345
7.5.2.2. Light Sensor Range and Step Size for Optimum Legibility Video Displays ... 348
7.5.3. Interface Compatibility for Digital Control Signals 349

CHAPTER 8 General Conclusions Regarding the Applicability of Automatic Legibility Controls to Aircraft Cockpit Displays 351
8.1. Principal Conclusion Reached Regarding the Applicability of Automatic Legibility Control to Aircraft Cockpit Displays 351
8.2. Constraints on the Automatic Control of Display Legibility, Imposed by Changes in Aircrew Information Requirements, for Different Mission Segments 352
8.3. Constraints on the Automatic Control of Display Legibility, Imposed by the Time Dependence of Changes in Aircrew Light and Dark Adaptation 354
8.3.1. General Background Information on the Two Phase Process of Dark Adaptation 355
8.3.2. Legibility Considerations Attributable to the Light and Dark Adaptation Responses of Pilots under Daylight Viewing Conditions 357
8.3.3. Legibility Considerations During Aircrew Exposures to Glare Sources at Night 359
8.3.3.1. Legibility of External Night Scenes While Being Exposed to a Glare Source . 359
8.3.3.2. Legibility of Cockpit Display Information While Being Exposed to a Glare Source 362
8.3.4. Legibility Considerations Following Aircrew Exposures to Glare Sources at Night 362
8.3.4.1. Legibility of External Night Scenes after an Exposure to a Glare Source 363
8.3.4.2. Legibility of Cockpit Display Information after an Exposure to a Glare Source 372
8.3.5. Effects of Different Choices of Automatic Legibility Control Options at Night 376
8.3.6. Conclusions Regarding the Constraints Imposed by Aircrew Light and Dark Adaptation on the Legibility of Automatically Controlled Displays 377
8.4. Automatic Legibility Control Adjustment Strategy for Use with Existing Electronic Displays ... 382
8.5. Importance of Using Automatic Legibility Controls from the Perspective of the Aircrew 383
8.6. Strategy to Implement a Common Automatic Legibility Trim Control That Permits Aircrew Members to Adjust the Legibilities of Multiple Displays Concurrently 383
8.7. Overall Conclusions Regarding the Application of Automatic Legibility Control to All of the Displays in an Aircraft Cockpit 384

LIST OF REFERENCES 386

APPENDIX A Quantitative Data for Image Difference Luminance Versus Background Luminance Comparisons 397
A.1. Comparisons of Different Experimenters Image Identification Test Data 397
A.1.1. Chapanis Data 397
A.1.2. Aulhorn and Harms Data 397
A.1.3. Comparisons of Chapanis and Aulhorn and Harms Data 400
A.2. Comparisons of Image Detection and Image Identification Test Data 402
A.3. Luminance Ratio Baseline for Assessing Quantitative Comparisons Results 406
A.4. Comments on the Validity and Accuracy of the Quantitative Comparison Results 408

CHAPTER 1

Introduction

Conventional electromechanical aircraft instruments and integrally illuminated panel and switch legends are highly legible, and require no intervention by the pilot or other aircrew members to remain at or above minimum required legibility levels, as ambient light levels change naturally during the course of full daylight aircraft operations. In comparison, for the aircrew to achieve and maintain the levels of information legibility needed to perform different aircraft missions at night, it is necessary for the aircrew to intervene, through the adjustment of the luminance levels of the instrument and panel lighting. Past investigations show that the image difference luminance level settings of pilots at night, that is, the differences between the luminances of the images being read and the luminances of the background area with no imagery displayed, differ depending on the external visual tasks associated with the type of mission segment being flown. Once dark adaptation consistent with a particular visual task is achieved, further intervention does not occur unless the crew members' adaptation state is disturbed. Mission segments with visual tasks that require good dark adaptation, such as night dive bombing, result in the pilots selecting image difference luminance level settings for displays that are lower than is the case for mission segments that do not require good dark adaptation, such as flying high-level navigation legs under instrument flight rules. These settings are, moreover, made in advance, in anticipation of the mission segment(s) in which good dark adaptation will be needed.

The introduction of electronic displays into aircraft cockpits has changed the information legibility experience of aircrew members, in varying degrees, under both day and night viewing conditions. Under daylight viewing conditions, conventional instruments automatically maintain the image difference luminance levels of their imagery above the minimum required levels for good legibility, as the ambient illuminance incident on the display changes. Although these conventional displays do not automatically compensate for exposure of the eyes to glare sources in the pilot's field of view, the high reflectances of the images depicted on the displays usually provide reflected luminance levels that are sufficient to exceed the pilot's minimum legibility requirements. In comparison, electronic displays require either active control by the aircrew or an automatic control subsystem to maintain legibility at or above the minimum required levels under daylight viewing conditions. At night, the control requirements for achieving and maintaining satisfactory legibility for electronic displays are very similar to those for conventional electromechanical instruments, however, until recently, the electronic displays have used individual luminance controls whereas the conventional instrument lighting is grouped by information type and operated using common controls. The primary direct impact of the need for aircrew members to control the legibility of electronic displays manually under both daylight and night viewing conditions is an increase in their task loading, which can result in a degradation in mission performance during high workload mission segments.

The principal purpose of this report is to describe an automatic legibility control technique that retains the existing ability of pilots to adjust the legibility of the electronic display portrayals to suit their personal preferences and needs for legibility, but, thereafter, is capable of automatically maintaining the legibility of the displays, at the constant level set by the pilot, throughout the full range of ambient illumination and glare source viewing conditions experienced in aircraft cockpits. Although this automatic legibility control technique is capable of being used to assure that the legibility needs and setting preferences of pilots are fully satisfied, the ability to achieve fully effective operation of automatic legibility controls is conditioned upon several external application constraints that can potentially restrict the effectiveness of the technique. Foremost among these external constraints are the capabilities, and any associated technological limitations, imposed by the design of the total cockpit control-display system. Additional constraints are imposed by the need to configure the automatic legibility control law parameters for use with different types of aircraft cockpit electronic displays, and by the practical considerations associated with the implementation techniques selected both to apply the automatic legibility control and to provide the pilot with satisfactory legibility trim and manual backup control capabilities.

A thorough understanding of the pilots legibility requirements, and of the physical significance of the terminology used in the control laws is also needed to achieve correctly configured and effectively implemented automatic legibility controls. Some of the topic areas dealt with in this latter context include the following: the critical role played by the perceived image difference luminance and the reflected background luminance levels of display pictures and real-world visual scenes in establishing the legibility of the information being viewed; the legibility control dependence of different types of aircraft cockpit electronic displays; the light variables and relationships that are responsible for the legibility of the information depicted on electronic displays; the legibility requirements of pilots and other aircrew members as a function of ambient illumination and glare source exposures; and the formulation of mathematical models to represent the legibility requirements of pilots.

Properly applied automatic legibility controls do not directly control the legibility of the grey shades and chromaticities depicted on electronic displays but can influence their legibility indirectly. The information legibility interrelationship between the image difference luminance control function performed by automatic legibility controls on the displayed pictures, and the image grey shade and chromaticity modulation function performed by the display image generation computer, also needs to be understood to achieve effective sensor-video and color display picture presentations. Consequently, techniques that allow the legibility of these presentations to be controlled on electronic displays are described and relationships that allow the grey shades and chromaticities present in real-world visual scenes to be faithfully rendered in electronic display picture presentations are presented.

The automatic brightness and legibility control laws, described in this report were originally formulated independently by Merrifield and Silverstein of Boeing and the author, respectively, at about the same time in the late 1970s. Since these control laws have both been previously introduced, the purpose of describing them again in this report is to elaborate upon and hopefully clarify aspects of their formulation, development, application, integration and use with aircraft cockpit displays that have not been previously published. As will be shown later in the report, both control laws can be configured to produce nominally the same results. Consequently, either control law can be used to overcome the legibility problems that caused operational fighter aircraft cockpits equipped with earlier versions of automatic brightness control designs to be judged as unsatisfactory by the military pilots who experienced them. Although information has been added in this report to improve the interpretation of these control laws, and refinements have been introduced to aid in their configuration and to enhance their implementation, in other respects the original control laws remain effectively unchanged.

Unlike the Boeing Commercial Airplane Company, which has successfully used its automatic brightness control in commercial airliners for more than twenty years, no existing operational military aircraft are similarly equipped, even though the likelihood of aircrews experiencing periods of high task loading in military aircraft is much more probable. Owing to this situation, another purpose of this report is to attempt to establish the merits and build confidence in the practical feasibility of applying automatic legibility control to the electronic displays installed in military aircraft cockpits. Although a variety of approaches have been employed in this report in seeking to attain this goal, the greatest effort has been expended in trying to provide, to the extent that available experimental data permits, a factual and theoretically consistent scientific foundation to serve as an explanation of and a validation for the empirically derived equations that represent the legibility requirements of pilots and from which the automatic legibility control law used to control electronic displays was derived.

The balance of this chapter is devoted to providing summary descriptions of the contents of the remaining chapters of the report. In addition to the descriptions of the contents of each chapter, commentaries on the information contained in the chapter or, alternatively, explanations of the reasons the information is being presented have also been included. In some of the more technically involved chapters, the preceding treatment has been extended to related groups of sections and to the individual sections within chapters.

The purpose of Chapter 2 is to describe the need to exercise control over the image difference luminance levels of the information presented on aircraft cockpit electronic displays to achieve and maintain adequate legibility and to describe how the control requirements are influenced by the use of different types of electronic

displays. At the beginning of the chapter, the practical effects on pilot performance of the failure to provide adequate displayed information legibility and legibility control are described together with the advantages offered by applying automatic legibility control. This is followed by a description of the rationale for using the objective legibility requirements of pilots, as a basis for the implementation of automatic legibility controls. Specific methods used to implement either manual or automatic control over the legibility of electronic displays depend on whether the operating mode of the display is emissive, transmissive, reflective or transflective. None of these modes, as implemented by current state-of-the-art electronic display technologies, can take full advantage of the pilot's visual capabilities, and all require some form of legibility control as ambient light levels and glare source exposure conditions change. Design criteria relevant to the application of either manual or automatic legibility control to these electronic display operating modes, and a sampling of the display technologies that can be used to implement them, are described in the last four sections of Chapter 2.

The purpose of Chapter 3 is to develop a mathematical model for an image difference luminance control law that is capable of being used to control any electronic display so that the legibility requirements of pilots and other aircrew members can be satisfied and, furthermore, so that their visual performance can, if an election is made to do so, be maintained at a constant level in changing aircraft cockpit ambient illumination and glare source viewing conditions. This objective is based on the fundamental conclusion of Chapter 2 that it should be possible to formulate a single set of pilot legibility requirements, which can be applied to the design and implementation of any electronic display, independent of the operating mode and technology selected to present the information to be displayed. The mathematical model developed in Chapter 3 is derived from published experimental legibility requirement test results gathered by a variety of experimenters over a period of nearly a century. The derivation approach involves a process of integrating the results obtained from a detailed comparative examination of the published experimental test data to form a self-consistent empirically-based theory and predictive model for the legibility of any type of display. While the experimental data analyzed in this chapter is relatively well established, the relationships derived and the conclusions reached are subject to interpretations by the author. For this reason, an attempt has been made to include a more thorough presentation of the data analyzed than would normally be the case, the intent being to permit the reader to assess the validity of the final legibility control law developed.

The development of legibility requirements for pilots and other aircrew members described in Chapter 3 can be logically divided into three major topic areas. The first topic area is concerned with the formulation of an empirical model to represent a pilot's information legibility requirements in the absence of glare, and is described starting at the beginning and proceeding up to Section 3.5 of Chapter 3. A second topic area is concerned with the formulation of empirical models to represent the effects on display legibility caused by the exposure of the pilot's eyes to discrete and to distributed sources of glare that are within the pilots field of view while attempting to read information from a display, and is described starting at Section 3.5 and continuing up through Section 3.8 of Chapter 3. The third and final topic area is concerned with an adaptation of the two preceding models that makes them suitable for use for use as a practical automatic legibility control law in operational aircraft cockpits and is described in Section 3.9.

In the initial sections of Chapter 3, the variables and published experimental data that are pertinent to achieving legible information presentations on electronic displays installed in aircraft cockpit viewing environments are examined and compared. The purpose of the section is to identify those variables and points of commonality between the data of different experimenters that are critical for the determination of a pilot's legibility requirements. Section 3.1 is primarily concerned with the identification and discussion of image legibility variables. Section 3.2 provides a discussion of the influence that the critical detail dimensions of imagery have on the image difference luminance and contrast requirements of pilots. Section 3.3 presents the best available experimentally derived image difference luminance and contrast requirements data, together with a discussion of the influence that the pilot's visual performance level and the surround and panel luminances have on luminance and contrast requirements. As a culmination to the analysis of the basic legibility requirements of pilots and other aircrew members, presented in the earlier sections, Section 3.4 introduces and describes an empirical model to represent a pilot's legibility requirements. The model presented was formulated subject to the constraints that the design of the information to be displayed must

conform to ideal legibility characteristics and can only be utilized in the absence of glare. Luminance compensations to permit adjusting for less than ideal image designs or display image renditions are available in the literature, but the inclusion of these techniques exceeds the scope of the present report. Methods of adjusting ideal display information legibility requirements, for the presence of glare in the pilot's field of view, are described starting with Section 3.5 of Chapter 3.

In Sections 3.5 through 3.8 of Chapter 3, experimental data, concerning the effect on the pilot's ideal legibility requirements caused by exposures to discrete and distributed sources of the glare, within the pilot's field of view, are introduced, examined and compared. The description of the effects of glare sources begins in Section 3.5 with the introduction of veiling luminance, as the quantity perceived by an aircrew member as a direct result of exposure to either a discrete or distributed source of glare, and of published experimental data concerning the illuminance and glare source angular orientation dependences of veiling luminance. Next, in Section 3.6, the veiling luminance results of the various experimenters are analyzed and an empirical representation of veiling luminance is formulated in terms of its dependence on the illuminance and angular orientation of discrete glare sources, with respect to the pilot's line of sight. In Section 3.7, elements of a theory for the origin and functionality of the veiling luminance induced by a discrete glare source are introduced; the psychological and physiological responses to the glare source light scattered within the eyes are described; the influence of the pupil area of the eyes on veiling luminance induced is analyzed; and some conclusions regarding the theory of the veiling luminance induced by a discrete glare source are presented. Section 3.8 derives an empirical model for the veiling luminance induced by distributed glare sources, but because it also encompasses the effects of discrete glare sources, it represents the culmination of the development of the veiling luminance model.

Finally, the empirical display legibility requirement findings developed earlier in Chapter 3 are adapted in Section 3.9 to a practical automatic legibility control law that is suitable for use with the combination of stress, task loading and environmental conditions experienced by aircrew members in aircraft cockpits during daylight and night flight operations. After introducing a general legibility control equation, formulated to apply to aircraft cockpit applications, pilot visual requirements that are accepted as being applicable to aircraft cockpit settings are described, and an equation capable of satisfying a pilot's minimum legibility requirements is presented. Methods of generalizing this equation for use with virtually any type of information to be presented in on aircraft cockpit displays are described in the balance of the section.

In Chapter 4, automatic brightness controls are first considered from a historical perspective and the distinction between automatic brightness controls and automatic legibility controls are described. Although the performance of the initial automatic controls was judged to be unsatisfactory by military aircraft pilots, automatic brightness controls subsequently introduced by Boeing have been judged to provide satisfactory performance by commercial airline pilots. The Boeing automatic brightness control law algorithm is introduced in the second section of Chapter 4 and is then interpreted in the balance of the section. An image difference luminance requirements equation, for information presented on instrument panel mounted displays exposed to incident ambient light, is considered first. Following this, the gain compensation multiplier technique used by Boeing to correct this equation for the presence of a glare source, such as the sun, that is located within the pilot's forward field of view is considered. The significant automatic brightness control advancement by Boeing is ascribed to the incorporation of this gain compensation multiplier into the automatic control law algorithm to account for the effects of glare sources on the pilot's display image difference luminance requirements. Next, the application of an automatic legibility control intended for use with color active matrix liquid crystal displays in the Lockheed Advanced Tactical Fighter, the predecessor of the F - 22, is described in generic terms. The section concludes with a summary of the features shared by the Boeing automatic brightness control law and the general automatic legibility control law.

The general automatic legibility control law developed in Chapter 3 is described in greater detail in Chapter 5. The purpose of Chapter 5 is to compare the general automatic legibility control law with other control techniques and, in particular, with those techniques that have been found satisfactory, in some sense, by pilots and other aircrew members. This more in-depth treatment, of the general automatic legibility control

law, starts with a description of the emulation of the natural legibility control characteristics of conventional electromechanical instruments in changing ambient illumination environments using automatically controlled electronic displays. Since these conventional displays are considered legible by aircrew members, they provide a comparison baseline for assessing the legibility control characteristics of electronic displays operated using different automatic control characteristics.

In the second section of Chapter 5, the general automatic legibility control law is mathematically compared with the Boeing automatic brightness control law. The reason this comparison is being made is because the Boeing automatic brightness controls have undergone extensive operational usage in commercial aircraft cockpits, where it has been favorably received by airline pilots. This comparison shows that although the mathematical formulations of the two control laws cause them to appear quite different, their generic control characteristics are, from a functional standpoint, essentially equivalent.

Human visual system control over the legibility of perceived visual scenes is considered in the third section of Chapter 5, to provide a basis for comparing the general automatic legibility control law with other existing manual and automatic control techniques. The purpose of this section is to describe both qualitatively and quantitatively the factors that influence the legibility of both real-world visual scenes and electronic display grey shade and chromaticity encoded renditions of real-world visual scenes. To achieve this purpose, the section provides relationships between the real-world and display information presentation viewing conditions needed to provide satisfactory legibility. The legibility requirements for these two viewing conditions can be either very similar or very different from one another, depending on the spatially selective adaptation of the light receptors in the viewer's eyes, which, in turn, depend on the relationship between the light reflection properties of the real-world scenes and those of the electronic display viewing surfaces. An important practical consequence of this spatially selective light adaptation capability, which is also described, is an apparently related capability by the human visual system to impose its own version of constant legibility control on the information portrayed by electronic displays, when the imagery is depicted at sufficiently high levels of image difference luminance and contrast.

Based on the information presented in the earlier sections of Chapter 5, the fourth section describes application considerations for the general automatic legibility control law by drawing comparisons to the results to be expected from using other existing manual and automatic control techniques. As a prelude to this comparison, a brief context for assessing the legibility of electronic displays on aircrew performance is introduced. After the introduction of this background information, implementations of the general automatic legibility control law, which are intended to emulate the following: conventional displays; the use of fixed maximum display image difference luminances, under daylight viewing conditions; the Merrifield and Silverstein brightness control law; and a constant legibility control law, are described. The final topic considered in the section involves the interactions that exist between the selection of the slope of the general automatic legibility control law, for operating displays under daylight viewing conditions, and the image difference luminance level settings of electronic displays at night.

The fifth and final section of Chapter 5 is concerned with the adjustment capabilities of aircrew legibility trim controls and other implementation considerations associated with using automatic legibility controls. As a starting point for assessing these implementation considerations, circumstances in which aircrew trim control adjustments are needed to control the legibility of electronic displays are described. Next, implementations involving the use of single and dual aircrew-adjustable trim controls are described and compared. The section concludes with a description of the effects of the parameter values chosen for use with the constant legibility control law equation.

Sensor-video signal conditioning of monochrome video and color information presentations to enhance their interpretability by aircrew members is described in Chapter 6. The conditioning of signals, to enhance an aircrew member's ability to extract information from a display presentation, is actually a separate topic from the image difference luminance level at which the information has to be portrayed on the viewing surface of an electronic display to make it legible. In particular, signal conditioning relates to the ability of the aircrew to

exercise control over the information content of the picture that is being displayed, whereas legibility relates to their ability to control how readily the picture information content can be perceived by the aircrew.

Sensor-video signal conditioning is considered as a topic in this report for two reasons. The first reason is that the brightness and contrast controls used historically in aircraft cockpits to control the depictions of sensor-video information on cathode ray tube displays not only cause the legibility of the display presentations to be controlled, as the names of the controls imply, but also serve to integrate the conditioning of sensor-video signals, although not as distinct separable control functions. The second reason is that the effectiveness achievable in the transfer of information to the aircrew, through the conditioning of monochrome and color sensor-video signals, is influenced by the legibility levels of the electronic display pictures used to portray this information to the aircrew members. Differences in the effectiveness that can be achieved in conveying information to the aircrew from display information presentations of sensed real-world scenes depicted using integrated versus separate signal conditioning and legibility control are considered in the first section of the chapter. This is followed by a discussion of the design criteria for digitally encoded sensor-video signals. In the final section of the chapter, the practical legibility control and signal conditioning that is feasible using cathode ray tube, active matrix liquid crystal and other types of electronic displays are compared.

Chapter 7, examines an assortment of practical considerations involved in the implementation of both manual and automatic legibility controls in aircraft cockpits. The five major implementation considerations treated in this chapter include the following: the specular reflection component of the reflected background luminance of electronic displays; the dependence of aircrew legibility requirements on the types and locations of electronic displays in the cockpit; aircrew control over the legibility of electronic displays; the coordination of multiple light sensors, automatic legibility controls and displays; and compatibility considerations for digital control signals.

If accurate automatic legibility control is to be achieved, under any combination of ambient illumination and glare source viewing conditions, the effect of the specular as well as the diffuse reflected luminances from electronic display viewing surfaces must also be considered. Because specular reflections only become important under a few practical viewing conditions, and to simplify the descriptions in the earlier chapters of the report, the effects of specular reflections, while mentioned, are not specifically treated during the formulation of the empirical image difference luminance requirements equation in Chapter 3 or in the succeeding chapters. In the first section of Chapter 7, the effects of luminances specularly reflected from the viewing surfaces of electronic displays are considered, together with a discussion of methods available to implement the measurement of this variable and its incorporation into automatic legibility control laws.

In the second section of Chapter 7, the dependence of the legibility requirements of aircrew members on the types and locations of electronic displays used in aircraft cockpits is explained. An important and not generally recognized practical implication of these display and cockpit location dependent differences in aircrew legibility requirements is also introduced and described. Namely, each electronic display must be individually controlled if equal legibility, across all the displays in a cockpit, is to be achieved concurrently. A practical consequence of the need to apply an individualized control signal to each display is that it is not possible to use a common control that is directly connected, or one that is connected using isolation amplifiers, to operate multiple electronic displays in unison, and still be capable of achieving and maintaining equal legibilities at different display locations in the cockpit. Furthermore, this is true irrespective of whether the displays are manually or automatically controlled, unless the common control signal is applied as a trim control input to multiple individual display automatic legibility controls, as is described the third section of Chapter 7, rather than directly to the control inputs of the displays.

The third section of Chapter 7 considers different methods that can be used to provide aircrews with the ability to exercise control over the legibility of electronic displays. A variety of different aspects of this issue are dealt with in the section. The overall objective of the section is to present information that can be used to assure that aircrews have at their disposal the means to be able to intervene to satisfy their personal preferences and needs for display legibility, whether they are operating electronic displays in a manual control

mode, an automatic control mode or in the preferred configuration, where the choice of the control mode is selectable by the aircrew member. Topics discussed in the section include the following: the overall manual control input versus image difference luminance output characteristic that electronic displays should exhibit, and the separation of this overall input to output transfer characteristic into distinct aircrew manual control and display image difference luminance controller characteristics; the considerations involved in establishing a defined interface between display image difference luminance controllers and either manual or automatic legibility controls; the options and implications related to the implementation of individual and common manual electronic display legibility controls; the options and implications related to the implementation of different electronic display automatic legibility control configurations; and the considerations influencing the integration of manual with automatic control techniques, to implement an aircrew selectable mode switching control capability.

The fourth section of Chapter 7 describes the considerations involved in the coordination of multiple light sensors, automatic legibility controls and electronic displays. Placements of light sensors in the cockpit and methods of applying their measurement results to maintain adequate legibility on electronic displays operated using automatic legibility controls, in the context of static illuminated and shadowed areas in the cockpit, are discussed first. This is followed by a description of the effects, of dynamic flight maneuvers, on the legibility of information portrayed on electronic displays operated using automatic legibility controls. The description includes a discussion of the implications of likely control technology limitations, of visual response time limitations of the aircrew and suggests control techniques suitable for dealing with these potential limitations.

The final section of Chapter 7 describes compatibility considerations for digital control signals. In particular, criteria for making the sizes of the discretely incremented luminance steps, produced when digital image difference luminance controllers are used to operate electronic displays, small enough to avoid causing the aircrew to perceive distracting visual effects are described. Based on the resultant discrete step sizes and the aircrew's image difference luminance requirements, examples of the derivation of sampling criteria for digitized light sensor signals for sensor-video displays operated at two different legibility levels are provided. This section is concluded with a description of some considerations involved if a standardized digital image difference luminance controller interface, compatible with both manual and automatic legibility controls, is to be employed.

The final chapter, Chapter 8, describes some of the more important conclusions reached during the course of this investigation regarding the development and application of automatic legibility controls, for use in operating aircraft cockpit displays, under the gamut of day through night viewing conditions. This chapter also considers the effects of the time dependent light and dark adaptation of aircrew members when operating cockpit displays using automatic legibility controls under day and night viewing conditions.

CHAPTER 2

Aircraft Cockpit Electronic Display Information Legibility Control Considerations

The evolution of military aircraft flight capabilities has been paralleled in the cockpit by a gradual transition from conventional electromechanical instruments to electronic controls and displays. This transition has led to improved flexibility in the control and display of information and, in some instances, to smaller and more reliable cockpit equipment, but, it has also sometimes led to a degradation in the legibility of the information presentations and to added pilot task loading.

Display legibility reductions, which are sufficient to add to the time it takes to read a display's information accurately, increase the pilot's workload. In the recent past, highly legible conventional displays, characterized by low to moderate reliability and high maintenance, have been retrofitted with higher reliability, and potentially lower maintenance, electronic display counterparts, which provide adequate but lower legibility information portrayals. In a few instances, these retrofits resulted in replacing legible conventional displays with reflective operating mode electronic displays that were only marginally legible in low ambient daylight viewing environments. Since instrument retrofits typically occur one display at a time, the increase in the workload is incremental and, consequently, is unlikely to draw an immediate response from aircrews. The inclusion of automatic legibility control cannot be used to compensate for inadequate innate display legibility, but for displays that can be made legible it can lead to a reduction in a pilot's workload.

Displays that need to be manually controlled by the pilot, to maintain their legibility in changing ambient illumination daylight environments, add an ancillary task to the mission-related tasks already being performed and, thereby, increase the pilot's workload. The reductions in pilot task loading, made possible by using automatic legibility controls, are most pronounced in cockpits that employ multiple electronic displays. Cockpit designs that allow the legibility controls for electronic displays to be ganged together and operated using a single common manual control, in concept, improve the workload situation in comparison to using individual manual controls, but still require the pilot to divert time and attention from mission-related tasks to control the legibility of the displays, and, as is described in Chapter 7, common manual controls cannot maintain optimum display legibility in time changing viewing environments. Awareness by pilots of the demands placed on their time, by the need to control the legibility of cockpit displays, unfortunately, encourages the adoption of a strategy involving the operation of electronic displays at their maximum luminance levels during daylight missions, to avoid having to make manual legibility control adjustments. This, in turn, leads to an increase in maintenance and a reduction in the operating life of most electronic displays.

The primary benefit expected from the use of automatic legibility control is the ability to maintain the information displayed in aircraft cockpits at a constant legibility level and in so doing retain a perceptually invariant electronic display picture appearance in changing ambient illumination environments. A display with imagery perceived to be the same, each time it is viewed, allows the information portrayed to be read more consistently and with a smaller dwell time on each display in the instrument crosscheck. Although this benefit is quite small for displays portraying simple information, such as numerics, it becomes progressively more important in the transition from numeric, to alphanumeric, to graphic, and finally to video image portrayals. Invariance in the perception of electronic pictures, achieved through automatic legibility control, allows the visual identification characteristics of display imagery such as graphic symbols, video target signatures and so forth to be more readily learned and recognized, even in time variant presentation formats.

The addition of color coding to information presentations allows additional information to be conveyed to the pilot with no increase, and in some cases with a decrease, in the workload experienced. By maintaining constant legibility, the perception of the colors, selected to encode the information presented by displays, also remains constant. This constant legibility control strategy for automatic legibility control reduces the possibility that information will be misidentified, owing to perceived changes in either encoded display grey shades or colors that would otherwise occur, when the ambient illumination conditions incident on a display changes, and

the legibility of the display is not manually compensated by an aircrew member.

The first section in this chapter starts with a description of the rationale for using pilot legibility requirements as the basis for the implementation of automatic legibility control. In the second section, considerations associated with making automatic legibility control compatible with different display operating modes and technologies are introduced. The remaining four sections discuss the design criteria necessary to achieve adequate legibility using four different display operating modes and how this influences achieving compatible automatic legibility control implementations. It should be noted that the substantiation and reference citations for the legibility capabilities of the human visual system, asserted in this chapter, are provided later in the report. In this sense, this chapter, at least in part, represents a technical introduction to the balance of the report.

2.1. Rationale for Using the Objective Legibility Requirements of Pilots as a Basis for the Implementation of Automatic Legibility Control

It is taken as a fundamental theoretical fact that it is only by virtue of the light entering the eyes, where it is sensed and then perceived by a pilot, that the information contained in a visual scene can be conveyed to a pilot, whether that light emanates from cockpit display information presentations or from other areas within the total field of view from which light is incident simultaneously on the eyes. Although this statement of fact can be dismissed for being unnecessary, since it is a statement of the obvious, it follows directly from it that the light received by the eyes must meet the same minimum legibility requirements irrespective of the origin of that light. It can, therefore, be concluded that the legibility requirements for visual information, when specified in terms of the light entering the pilot's eyes, are the same, independent of the operating mode of the display techniques employed, that is, whether the light emanating from the display is based on reflected, transflected, emitted or transmitted light, and despite the technologies used to implement the specific display operating modes. Consequently, for the information presented to the pilot to be legible under all cockpit illumination conditions, the light reflected, transflected, emitted, or transmitted from conventional aircraft cockpit instruments and their electronic display counterparts must meet the same legibility requirements and light entering the eyes becomes a universal medium with which to specify these legibility requirements.

As just stated, when the pilot's visual requirements are expressed relative to the light entering the eyes, then these requirements become equally applicable to all types of displays; however, the design strategies necessary to adapt these requirements to different display operating modes, and, more specifically, to their individual display technology variations, differ depending on the interactions between the incident ambient illumination and the specific light modulation technique employed. Translating the pilot's visual requirements into a baseline of common display legibility requirements provides a universally applicable specification, in terms of which the performance of any type of display can be assessed or, alternatively, designed to satisfy the pilot's legibility requirements.

Based on the preceding considerations, it can be concluded that to be able to implement an automatic legibility control successfully, a mathematical model must exist that can predict the pilot's legibility requirement's for any given set of ambient illumination conditions that might be encountered in an aircraft cockpit. The pilot's legibility requirements and an automatic legibility control model to predict them are described in Chapter 3. The remainder of this chapter is devoted to an exploration of the differing relationships between the pilot's legibility requirements, which are to be considered inviolable, and the four different display operating modes and a selection of their supporting technologies.

2.2. Electronic Display Operating Mode and Technology Compatibility with Automatic Legibility Control

Although the pilot's legibility requirements are independent of the display operating mode and technologies employed to satisfy the pilot's legibility requirements, the display implementation techniques

needed to satisfy these requirements are unique to the display operating mode and technologies employed. The variations in the display implementation techniques result from the different ways that display operating modes and technologies use external and internally generated light to make information legible. As an example of this assertion, the reflection of ambient light from the viewing surface of a display can result in either an enhancement or a degradation in the legibility of the display information depending on whether the operating mode of the display is either reflective or transflective as opposed to being either emissive or transmissive, respectively.

Independent of the operating modes and technologies used to implement a display, each display technique must be capable of satisfying three primary interrelated viewing condition requirements to achieve and maintain the legibility of displayed information in aircraft cockpits. The first of these requirements is that the information presented on a display of any type must continue to be legible in the presence of high ambient light that is incident upon and, consequently, is reflected as a background luminance from the viewing surfaces of the display. A second requirement is that the displayed information must continue to be legible when the sun or another high ambient discrete or distributed source of light is incident on the pilot's eyes, while the pilot is attempting to read the information on an aircraft cockpit display. The third requirement is that displayed information must continue to be legible at low level daylight, dusk and night ambient illumination levels.

Besides the preceding display viewing condition requirements, an environmental illumination exposure interrelationship that typically exists between the first two viewing condition requirements, described in the preceding paragraph, results in a design constraint on the application of automatic legibility control to cockpit displays. This constraint stems from the fact that in an aircraft cockpit environment, when sunlight illumination is incident on the pilot's eyes, it is unlikely that high ambient illuminance will be simultaneously incident on the information depicted on displays installed in the cockpit's instrument panels (e.g., illuminance levels incident on the instrument panels of C-130 aircraft under this condition have been measured at levels less than 100 fc). Conversely, when sunlight illumination is incident directly on the cockpit displays, it is unlikely that substantial glare effects will be simultaneously be incident on the pilot's eyes. The constraint imposed by this environmental illumination exposure interrelationship is that both the illumination incident on a display and the glare source exposure of the pilot's eyes must be accounted for separately, if an effective implementation of automatic legibility control to cockpit displays is to be achieved.

The display operating mode descriptions provided in the balance of this chapter are intended to permit elaborating on the common legibility considerations associated with each of the four display operating modes; to provide examples of different technological implementations of a particular display operating mode; and to describe, in general terms, how each display operating mode can be interfaced with an automatic legibility control to cause the information it displays to satisfy the pilot's legibility requirements. Because the number of possible technological implementations for each display operating mode is very large, detailed technological implementation examples provided later in this chapter have been restricted to descriptions of the design considerations associated with making two historically significant implementations of light emissive mode displays, namely cathode ray tube (CRT) and light emitting diode (LED) displays, compatible with the pilot's legibility requirements in military aircraft cockpits.

It should be noted, that the descriptions of display operating modes and technologies used in this chapter to introduce their associated legibility considerations, should not be construed as a review of, nor a commentary on, the ultimate viability of the operating modes or technologies for use in aircraft cockpits. The latter topic is considered beyond the scope of this report. For this reason, display technology descriptions are dealt with only to the depth needed to illustrate the legibility considerations being described for a particular display operating mode. As an exception, detailed descriptions are provided for the CRT and LED display examples, cited above, to illustrate the large implementation differences that exist for the same operating mode using different display technologies. The CRT and LED display examples were selected for use in this comparison because properly designed electronic displays using these two technologies have more than a twenty-year historical record of being compatible with the legibility requirements of pilots flying operational military aircraft missions.

2.3. Light Reflective Mode Aircraft Cockpit Displays

Among the available display operating modes, light reflective mode displays come the closest to mimicking the light reflection properties of the natural world to which human vision has for so many years been exposed. In fact, from a visual perception standpoint, this display medium is almost ideally suited for the presentation of information in aircraft cockpits. The principal reason for this is the way that human vision naturally adapts to changing ambient illumination conditions. In particular, changes in the incident ambient illuminance in the range from 10,000 fc down to 23 fc, using a nominally constant spectral distribution illumination source, have been shown to produce no visually perceptible change, in either the perceived grey shade or color relationships, for the reflective media so illuminated. Stated in another way, the relative luminance levels, hues and saturations of the displayed color information does not change, and, consequently, the visual appearance of reflective mode displays should remain essentially invariant in changing ambient illumination conditions.

A physical property shared by all light reflective mode displays is the need for an external, or an internal (i.e., integral), source of illumination, incident from in front of the display's viewing surface, to make the information portrayed by the display legible. Control over the legibility that is attainable using this display technique is, therefore, dependent on the illuminance provided by the cockpit ambient illumination environment that the pilot happens to be experiencing when the display has to be read and on an auxiliary source of illumination, when the cockpit ambient illumination is insufficient to provide the legibility necessary to read the display information. In the latter context, all light reflective mode displays need a source of illumination to make the information they display legible under dusk through night viewing conditions, when the ambient illumination in the cockpit is inadequate to make the displayed information legible.

The image difference luminance levels that are perceived by the pilot to be associated with the imagery portrayed by all light reflective mode displays are controlled by the reflectances used to render the imagery and the illuminance incident at each location across the display's viewing surface. An important insight into the legibility requirements for light reflective operating mode displays can be illustrated by considering the effect of a shadow cast on part of a display's surface. A shadow causes the display surface reflected luminances to be reduced, which in turn causes an observer to perceive the legibility of the shadowed part of the display's viewing surface to be reduced, in comparison to the fully illuminated part of display. Since the image contrasts, of the information presented on these displays, are determined completely by the reflectances of the individual picture elements on reflective operating mode electronic displays, and through the selection of the diffuse reflective materials used to fabricate the light reflective viewing surfaces of conventional reflective operating mode displays, this fact allows the following general conclusion to be reached, regarding the legibility of reflective operating mode displays. Because the reflectances and, consequently, the contrasts of the pictures portrayed on these displays remain fixed, when a shadow is cast on a part of the display's viewing surface, it can be concluded that the change in the display legibility, between the fully illuminated and shadowed parts of display pictures, is due to the difference in the absolute image difference luminances reflected by the two parts of the display picture, rather than by the contrasts of the information content of the pictures. The point of this example was to show that the legibility of reflective operating mode displays is attributable, not only to the contrasts of the information depicted on the displays but is also determined by the absolute image difference luminance levels of the imagery depicted, an aspect of legibility that is applicable to all display operating modes and, more generally, to all visually perceived information.

Electronic versions of light reflective mode displays operate by modulating the light reflected from individual picture elements in the display viewing surface. Like other electronic display operating modes, light reflective mode displays can be used to depict numeric, alphanumeric, graphic, video and color image presentations. This is accomplished by electronically controlling the reflectances of the individual picture elements that form the display's viewing surface, between maximum and minimum reflectance states, and thereby modulate the reflected external or internal illumination to achieve the desired on, off, or intermediate levels of grey shades. Color presentations can be achieved through the use of reflective primary color picture elements or a matrix of primary color filters that are in registration with a display surface having controllable

reflectance color, or neutral-color, picture elements. As the result of technological problems with the implementation of this display technique, no displays that use the reflective mode for graphics, video or color presentations are currently suitable for use in operational aircraft cockpit applications.

In the balance of this section, the legibility properties of light reflective mode displays will be discussed. In the first subsection, the legibility of conventional electromechanical aircraft instruments will be considered in terms of their historic applications. Following this, a less in-depth discussion of the legibility properties of electronic versions of the reflective operating mode display technique will be considered.

2.3.1. Legibility Considerations for Conventional Aircraft Instruments

Conventional electromechanical instruments are examples of reflective operating mode displays. The legibility of the information portrayed by any aircraft cockpit instrument is determined by the display image and background luminance levels present when they are viewed, coupled with the effects of the luminance levels, present in the balance of the crew member's field of view. For reflective mode displays, the image and background luminance levels are determined by the reflectances of the painted or otherwise treated display image and background surface areas of conventional instrument faceplates, and by the illuminance level available to illuminate these reflective image and background areas. At night, the illuminance required to raise the display image and background reflected luminance levels to the point that they become legible is typically provided by internal bezel mounted incandescent filament light bulbs, known as wheat lamps, that, via integral edge or wedge lighting techniques, couple and attempt to distribute the lighting over the instrument faceplate evenly. In earlier times, lighting applied external to the instruments was used to make the display information legible at night. The use of cockpit flood lighting was supplanted by post lighting, which eventually was replaced by the internal integral lighting. During the day, the illumination of the cockpit by the ambient illumination that happens to be incident upon it at any given point in time is relied upon to provide the source of incident illuminance required to stimulate the display image and background reflected luminances of conventional aircraft cockpit instruments.

Conventional electromechanical instruments typically present information using white diffuse reflecting characters or symbology painted on a black diffuse reflecting background. The white and black employed are specified to meet FED-STD-595, Color Number 37875 and 37038, respectively. As such, the matte white is supposed to have a nominal diffuse reflectance, R_1, of 0.875 fL/fc and the matte black, a reflectance, R_2, of 0.038 fL/fc (i.e., the last three digits in the colors numerical designation). Excluding the effects of reflections from the instrument antireflection coated glass cover plates, the electromechanical instrument information presentations may be seen to have a contrast, C, given by the following equation:

$$C = \frac{\Delta L}{L_2} = \frac{L_1 - L_2}{L_2} = \frac{R_1 E_A - R_2 E_A}{R_2 E_A} = \frac{R_1 - R_2}{R_2} \qquad (2.1)$$

$$\therefore C = (0.875 - 0.038)/0.038 = 22.0 .$$

The quantities L_1 and L_2 in these equations are the luminances diffusely reflected by the white and black painted instrument surfaces, respectively, where a uniform, diffuse illuminance, E_A, is incident on the instrument's faceplate.

The preceding contrast is much higher than the required minimums, for the numeric, alphanumeric or symbolic (graphic) imagery presented on electronic displays. MIL-L-85762, which contains the first legibility specification for electronic displays, requires minimum contrasts of 1.5, 2.0 and 3.0, respectively, for images meeting minimum recommended size requirements for aircraft instruments (i.e., 0.2 inches or 5.08 mm), when they are viewed by the pilot at a nominal viewing distance of 28 inches and under the specified sunlight readability combined specular and diffuse reflectance test condition.

The military specifications for integrally illuminated conventional instruments, such as MIL-L-27160

(USAF) and MIL-L-25467, besides specifying the paint characteristics also set a minimum contrast of 12 for white on black presentations. A 44% reflective gray color, FED. STD. 595, Color Number 36440, is also specified for use with conventional instruments in applications where an information presentation can be enhanced through the use of a background luminance level beyond that of the black background. The test to verify whether or not the contrast requirements have been satisfied is specified to occur under uniform diffuse illumination, with the luminance measurements taken normal to the instrument surface and with the cover plate removed. Subject to these test conditions and the reflectances of the white, gray and black paints, it is not clear why the contrasts specified by these specifications are set to such low values; however, these specification contrasts are still well in excess of the minimum contrast requirements needed to make the information legible to pilots.

As reflective operating mode displays, conventional aircraft instruments exhibit constant contrast under any ambient illumination condition from full direct sunlight to full darkness. Because the pilot's minimum requirements for contrast progressively increases as the ambient illuminance available to illuminate the instrument decreases, reflective mode displays become progressively less legible as the illuminance incident on the instrument decreases. It is under reduced daylight ambient illuminance conditions that the high contrasts of conventional cockpit displays are actually needed to maintain instrument information at legible luminance levels. At ambient illuminance levels starting at from about 3 down to 1 foot-candle (fc), it becomes necessary to illuminate the instrument faceplate to maintain adequate legibility at progressively lower dusk and night ambient illumination levels.

It is at times when conventional instruments are night lighted, to make their information presentations legible, that it becomes evident the luminance of the imagery depicted on the display is the control variable of concern for achieving adequate display legibility, rather than the contrast of the imagery, which, as shown by Equation 2.1, is constant. Although it is a commonly held belief that the contrast of reflective mode display imagery is primarily responsible for controlling their legibility, as a practical matter, it is the image and background luminances reflected from the display surfaces that control the legibility of the images depicted on these, or any other displays. While, as the previous discussion indicated, this is quite evident at night, it is also true during the day. This latter point is clearly illustrated by the earlier common-experience example of a shadow passing over a reflective mode display and, in doing so, causing a reduction its legibility. Since a shadow has no influence on the fixed contrast of the display presentations, it is the reduction in luminance that leads to the reduction in the display legibility observed.

In daylight, the fixed contrast of the reflective operating mode conventional displays guarantees that, as the ambient illuminance incident on a display changes, both the image and background luminance levels will slavishly track the change. At a particular level of incident illuminance, the quantities actually sensed by the pilot are the image difference luminance levels, $\Delta L = L_1 - L_2$, associated with the image presentation on the display, and the background luminance, L_2, upon which the image difference luminance is superimposed. Increasing the image difference luminance or decreasing the background luminance, within a relative dynamic sensitivity range of about one hundred to one, causes images to be perceived as having increased legibility. Likewise, legibility is reduced by reversing this process. The contrasts of images, as defined by Equation 2.1, and knowledge of the background luminance, within a particular display presentation, are also valid measures of the perceived image legibility conveyed by the superposition of the image difference luminance onto the background luminance, and as the equation shows a knowledge of two of these three variables causes the third to be known precisely as well.

At night, the contrasts between the instrument reflected image and background luminance levels remains fixed at its daylight level. However, in this case, internally generated illumination, which is controlled by the pilot, is necessary to augment the dwindling night ambient illumination and, thereby, limit the decrease in the image difference luminance and background luminance levels at high enough values so that the fixed contrast of the presentation remains adequate to maintain the legibility of the information. Increasing the illumination incident on the display, using either its internal lighting or external lighting, increases both the image difference luminance and the background luminance in direct proportion, and as indicated by Equation 2.1 the contrast

remains constant. The aspect of this result, which is of interest, is that in spite of the constant contrast the increase in the image difference luminance causes the perceived legibility of the display information to increase.

To apply automatic legibility control to conventional reflective mode displays would require sensing the illuminance incident on the display and, when the ambient illuminance drops to a sufficiently low level, to control the internal integral source of illumination so as to progressively compensate for any further reductions in the ambient illumination incident on the display. Although this compensation would have to be activated at very high illuminance levels to maintain the legibility of the displays at an absolutely constant level, this is both impractical and unnecessary on displays having the high reflectances required by conventional aircraft electromechanical instrument display specifications. It is impractical because the existing integral illumination techniques for these displays cannot produce highlight white luminance levels much above 1 fL. It is unnecessary because of the perceptual invariance of reflective mode display presentations for ambient illumination conditions down to about 23 fc, as was previously described. In spite of the aforementioned invariance in the appearance of colors and grey shades, as the illuminance incident on a reflective mode display is reduced from 10,000 to 23 fc, the legibility of the information does decrease starting in the vicinity of 1,000 fc, in conjunction with a gradual degradation in the pilot's visual acuity. The high contrasts present in conventional reflective mode displays are sufficient to maintain adequate, though not constant, legibility between ambient illumination levels of 23 fc and nominally 1 fc. Based on the previous reasons, it is concluded that the application of automatic legibility control to integrally illuminated conventional reflective operating mode instruments would serve no useful purpose, except under dusk and lower night ambient illumination viewing conditions.

2.3.2. Legibility Considerations for Light Reflective Mode Electronic Displays

A variety of reflective operating mode display technologies have been investigated for possible applications in aircraft cockpits but for one reason or another most of them have been found inadequate to satisfy the performance or environmental operating requirements of military aircraft. The Electrophoretic display technology provides high reflectance white on black display presentations, but has an on-to-off cycling life limitation that makes the technology unsuitable for use in aircraft displays. Electrochromic displays, which have been extensively researched over many years, change color under electronic control but suffer both response time and cycle life limitations. Electronic displays based on some of the many available liquid crystal display technologies have come the closest to being realized in aircraft cockpit compatible reflective mode implementations. This approach is considered further below because it is used in aircraft cockpits and because it emphasizes some limitations associated with achieving adequate legibility using reflective mode electronic displays.

Some reflective operating mode liquid crystal displays, designed to portray numeric or limited alphanumeric information, have been installed in retrofit applications in commercial and some military aircraft cockpits and also in electromechanical instruments during aircraft upgrades. Because most of the liquid crystal display technologies that are compatible with an aircraft cockpit operating environment use polarizers as an integral part of their design, the maximum reflectance of the characters presented on these displays is typically less than 0.15 fL/fc as opposed to the 0.875 fL/fc previously cited for white paint on conventional aircraft instrument characters. The visual result of this reflectance relationship is that the characters portrayed on these liquid crystal displays are perceived as presenting dark gray characters on a black background in all but the highest daylight ambient illumination conditions experienced in the cockpit. Because the black background of these displays is typically of much lower reflectance than that of the 0.038 fL/fc diffuse reflectance of black paint specified for conventional instruments, the characters on these displays typically provide relatively good legibility when the displays are exposed to direct sunlight illumination. Unfortunately, when the sun is in the pilot's forward field of view rather than illuminating the display, the ambient illuminance incident on the display is reduced and the reflected luminance of the characters becomes insufficient to make them legible, unless the glare effects produced by the sun exposure of the eyes are small, due, for example, to the discrete or

spatially distributed glare source being oriented at a very large angle, with respect to the pilot's line of sight to the display.

A potential solution to the preceding legibility problem for small reflective mode liquid crystal displays would be to supplement the ambient illuminance incident on the display surface, using a light source integral to the display to increase the luminance reflected by the display information presentation to a level that is consistent with satisfying the pilot's minimum required legibility requirements. The practical problem in implementing this approach is that the integral night lighting of current reflective operating mode displays is usually only just adequate to provide the supplemental illumination needed to make these instruments legible under dusk and night viewing conditions. The efficiency of the existing wedge and edge lighting techniques used on conventional reflective mode electromechanical displays, would have to be significantly enhanced to make it feasible to apply these techniques to reflective mode displays under even low level daylight viewing conditions. Alternative lighting techniques and technologies for use with reflective mode display surfaces remain to be investigated.

The legibility limitations described in the previous two paragraphs for small area reflective mode liquid crystal electronic displays only become more severe for large area fully addressable reflective mode liquid crystal displays. Presumably, it is for these reasons that no large area reflective operating mode electronic displays suitable for use in aircraft cockpits have, as yet, been developed.

2.4. Light Transflective Mode Aircraft Cockpit Displays

Integrally illuminated control panels and controls with illuminated markers are an example of conventional displays that employ the light transflective mode of operation. Under dusk and night ambient illumination conditions, the integrally illuminated panels operate by displaying their information using the light transmissive mode, with integral internal lighting used to backlight translucent materials and thereby make the information depicted using masked openings in otherwise opaque panel surfaces legible. In daylight, the information displayed on the panel operates in the reflective operating mode. In this case, the masked openings in the opaque panel and control surfaces expose the same translucent materials to the ambient illuminance incident upon them within the cockpit and in so doing stimulate a diffuse reflected luminance from the translucent materials.

2.4.1. Legibility Considerations for Conventional Aircraft Panels and Controls

As the name implies, the term transflective represents the result of combining optical properties from the transmissive and reflective operating modes into a single display operating mode that utilizes both properties to display information. From a legibility perspective, the daylight operation of light transflective mode displays, using the reflected ambient illumination to make the display information legible, means these displays possess the same legibility advantages and are constrained by the same limitations as reflective mode displays, which have already been described.

Under dusk and night ambient illumination conditions, when the illuminance incident on the reflective display information becomes too low to reflect a sufficient luminance level to make the displayed information legible, the integral backlighting is turned on initially to augment and eventually substitute for the lack of adequate reflected luminance. Other than the difference between illuminating the display information from the rear rather than from the front there is no difference between legibility considerations for conventional reflective and transflective mode display operations at night.

The value of using automatic legibility control and the measures needed to implement it for use with conventional light transflective mode displays are essentially the same as those described earlier for conventional light reflective mode displays. In other words, automatic legibility control can be used to control

the backlighting of conventional light transflective mode displays at night, but offers no meaningful legibility benefit under daylight viewing conditions.

2.4.2. Legibility Considerations for Light Transflective Mode Electronic Displays

The electrooptical designs of light transflective mode electronic displays are typically very complex in comparison to their conventional display counterparts. In this case, the display panel picture elements must not only be alterable using electronic control but must also convey the same grey shade and color information when operated in either the reflective mode in daylight or the transmissive mode at night. Like reflective mode electronic displays, no large area light transflective mode electronic displays have been developed yet, which meet the legibility requirements of pilots in aircraft cockpits. Small area light transflective mode electronic displays for use in the portrayal of numeric and limited alphanumeric presentations have been developed and applied in limited numbers to aircraft, based on the use of different implementations of the liquid crystal display technologies. A description of the various techniques used to implement electronic displays, using the transflective operating mode, are considered beyond the scope of this report.

The daylight legibility problems, ascribed earlier to light reflective operating mode liquid crystal displays are, in general, also shared by their light transflective operating mode display counterparts. The considerations that influence the application of automatic legibility control to these displays are also essentially the same and, therefore, will not be repeated. An advantage of this operating mode is that the design of a backlight to augment the reflected image difference luminance levels of light transflective operating mode displays, under daylight ambient illumination viewing conditions, is technologically less difficult to achieve than is the front integral illumination of reflective operating mode electronic displays. This advantage is typically countered, at least for large area displays intended for use in applications requiring multipurpose information presentations, by the significant increase in the electooptical design problems associated with the technological implementation of effective transflective operating mode electronic displays.

2.5. Light Emissive Mode Aircraft Cockpit Displays

The light emissive operating mode of electronic display is characterized by the ability to control the spatial and temporal modulation of the luminance and chromaticity, of the light radiated by the display media toward the pilot, by exercising control over the electrooptical process used to generate the light. The effectiveness of the light emissive display mode is conditioned by the ability of the display designer to effect control over the emitted luminance levels and chromaticities of the light that the display media generates, and over the reflections of ambient light, from the materials used to fabricate the display, including the optical filters used to control the magnitude of the display's reflected background luminance levels.

An ideal aircraft cockpit light emissive display would allow the image difference luminance emitted by the display to be controlled from the off state up to the maximum image difference luminance level needed to make the display's monochrome or color imagery legible, at a glance, in worst case daylight ambient illumination conditions. It would, moreover, permit all colors (i.e., any luminance and chromaticity combinations) that are perceptible by a human, and needed for a particular display application, to be made legible under any ambient illumination condition. Finally the ideal light emissive display would, when exposed to incident ambient light, reflect so little of the ambient light back toward the pilot that its effect, when the lowest emitted luminance level used to convey information to the pilot is superimposed upon it, would not be perceptible, either as an increase in that image difference luminance level or as a shift in its color.

Light emissive display technologies that have been previously evaluated for use in military aircraft cockpits include the following: cathode ray tubes (CRTs); flat panel CRTs, including field effect displays (FEDs); light emitting diodes (LEDs); alternating current (AC) and direct current (DC) planar gas discharge; thin film electroluminescence (TFEL); vacuum fluorescence; direct view incandescent filaments; fiber optic light

piped displays, operated using light bulbs or LEDs; and a variety of lesser known techniques. None of these display technologies would fully qualify as ideal light emissive operating mode displays. From the perspective of meeting the pilot's visual requirements, only the CRT, LED, direct view incandescent filament and fiber optic light piped display technologies have been successfully applied in aircraft cockpits, and only then in applications that limit the image rendition capabilities required of the display.

All of the light emitting electronic display technologies considered for use in military aircraft have one or more legibility control performance characteristic shortcomings. One problem shared by all of the technologies is the difficulty of achieving adequate legibility under full sunlight viewing conditions. Another problem, associated with only some technologies, relates to the difficulty associated with achieving adequate dimming control over the full on-to-off emitted luminance range of the displays. The specifics of the individual display technologies determine the precise form of the design measures that have to be taken to compensate for these problems. As a practical matter, no existing electronic display technique, despite its operating mode, can take full advantage of a pilot's visual capabilities even under ideal ambient illumination viewing conditions. The reason for this is that, despite the operating mode used, no existing electronic display can create all of the grey shade and chromaticity combinations, that is, the colors, that a human is capable of perceiving.

The applications of direct view incandescent filament displays have historically been restricted to the presentation of numeric, and a segmented form of alphanumeric, information, by presenting the incandescent filaments against a black background. While these displays can be made legible in direct sunlight, they have operating lifetime problems and shift in color from white toward red as they are dimmed. The capabilities and limitations of the other three light emissive operating mode techniques are described later in this section.

From the standpoint of being able to render the full gamut of colors a human is capable of perceiving, existing color CRT displays operated in a darkened environment come the closest to fulfilling the capabilities of the ideal display at the present time, although other electronic display technologies may offer greater potential for the future. Having said this, the CRT still has some significant limitations in this respect. In particular, while color CRTs can provide the luminance dynamic range needed to display colors that are perceptible as bright whites through dark blacks (i.e., a range of about 30 to 1), in a single picture, the human visual system is capable of simultaneously perceiving a much larger range (i.e., a range greater than 800 to 1). Likewise, the limited color saturations of the red, green and blue primary colors used to generate pictures on existing CRTs also restrict the palette of mixed colors that can be rendered by typical CRT displays to less than half the size of the color palette that a human is capable of perceiving.

As a practical matter, the effectiveness that must be achieved by the optical design techniques used to effect control over the background luminance levels reflected by a display, in the presence of incident ambient illumination, is much less than the previously stated requirement for ideal light emissive operating mode displays. Although, to be ideal in the strictest sense, a light emissive display would have to reflect no luminance, this objective is not physically feasible for any display technology, since all materials reflect some light. An alternative optical design goal for ideal display legibility is to reduce the reflected display luminance to a level that is too low for a human to be able to perceive it, while much higher image difference luminance levels are being used to portray information to the pilot. Although this approach has the potential to provide ideal display legibility, for most display applications it still represents an excessive legibility requirement. A still more practical alternative is to take advantage of the limitations on luminance dynamic ranges that are actually needed to convey information to the pilot reliably, rather than to strive to display the complete range of colors, the pilot is capable of perceiving. Because a picture portrayed on a display at absolute image difference luminance levels slightly above the minimum levels needed to render the grey shade and chromaticity content of the picture naturally, for a particular display reflected background luminance viewing condition, cause the eyes' light receptors to adapt photochemically to the higher picture image difference luminance levels, this produces both a rendition of grey shades and chromaticities that would be perceived as fully satisfactory by a pilot and a reflected display background luminance level that would be perceived as black. This topic is discussed further in Chapter 5, where it is shown that other aspects of vision allow objectively satisfactory grey shade or color encoded presentations to be attained, without resorting to attempts to make the display

background reflected luminance imperceptible.

In spite of the fact that color rendition, image difference luminance control and the reflected background luminance of displays have been treated separately in the preceding discussion, because the methods of optimizing each of these aspects of an electronic display's performance differ, depending on the specific display technology implementation techniques being used, these three legibility design factors are interactive and must be considered together when attempting to satisfy a pilot's visual requirements. The reason for this is that the light adaptability of the human visual system, for any given set of ambient illumination conditions, does not predict a single set of display image legibility requirement characteristics but, rather, a family of such characteristics, any one of which would be equally suitable for meeting a pilot's visual requirements. Display image legibility requirement characteristics are considered in greater detail in Chapter 3.

The display physical parameter that distinguishes which of the family of human image legibility requirement characteristics applies to a particular display over the range of ambient illumination conditions experienced in an aircraft cockpit is its reflected background luminance. Displays having higher reflected background luminance levels, under a specific ambient illumination viewing condition, must have a correspondingly increased image difference luminance emission capability if the same legibility, as that of a lower reflected background luminance display, is to be achieved.

The ultimate restriction on how much the maximum image difference luminance of a light emissive electronic display can be decreased while still achieving a fixed level of legibility, under daylight ambient illumination conditions, occurs for two different display viewing conditions. One condition corresponds to the sun being positioned in the pilot's forward field of view. Under this display viewing condition, the sun acts as a source of glare, that is, light from the sun is scattered into the pilot's line of sight to the display being viewed, thereby causing a veil of luminance perceived as coming from the space between the pilot's eyes and the display. The effect of the superimposed veiling luminance is to create a lower limit on the perceived reflected background luminance of the display that is being viewed. Consequently, this also imposes a lower limit on the display emitted luminance requirements that must be met to compensate for the combined reflected background luminance and the perceived veiling luminance against which the imagery is contrasted. Electronic displays that can produce legible imagery at reflected background luminance levels that are greatly reduced in comparison to the luminances reflected from bezels, panels and other adjacent cockpit surface areas are the ones most strongly influenced by this effect.

The practical effect of the veiling luminance induced in the pilot's eyes is, therefore, to impose a requirement that the luminance dynamic range, spanned by the grey scale excursions of the affected displays, be operated at elevated absolute image difference luminance and contrast levels, with respect to the measurable reflected background luminance of the displays, to compensate for the legibility degradation caused by the veiling luminance induced in the pilot's eyes, by their exposure to a glare source. Stated in another way, to maintain the same level of picture legibility when veiling luminance is present as when it is absent, the absolute image difference luminance (i.e., and contrast) of the displayed picture must be increased to match the lower limits on these variables imposed by the level of veiling luminance induced in the pilot's eyes, by their exposure to a glare source. Moreover, this requirement applies to all display operating modes and technologies, not just to light emissive electronic displays.

The other display viewing condition that places a limit on how low the image difference luminance of display imagery can be made with no reduction in legibility is imposed by the photopic vision limit of the cone receptors in the pilot's eyes. Reductions in the image difference luminance of display imagery must be accompanied by corresponding reductions in the reflected background luminance of the display, through the use of optical design techniques such as filtering, for example, to maintain the display legibility at a constant level. Constant legibility imagery implies that the spatial luminance variations that render the grey shade encoded shape of an image, and that must be seen to permit it to be visually identified, will remain equally perceptible under changing viewing conditions.

Based on the critical detail dimensions of each image, a lower emitted luminance level exists, below which further reductions cannot be made without degrading the legibility of the image, irrespective of how low the reflected background luminance can be made. This legibility limit is generally recognized to exist for any type of display under night viewing conditions, but the effect can also occur under lower level daylight viewing conditions. In the latter case, displays with very low background reflected luminance levels and that, consequently, can be made legible at comparably reduced absolute image difference luminance and contrast levels, in high ambient incident illuminance environments, can with the same contrast become only marginally legible or even illegible when their reflected background luminance and image difference luminance levels are reduced into the range of values that would more typically be associated with the image difference luminance level limits of night vision.

2.5.1. Legibility Considerations for Cathode Ray Tube Displays

Cathode ray tube (CRT) displays are probably the best known and most widely used examples of a light emissive electronic display technology that is suitable for the portrayal of color or monochrome flexible information format picture presentations. This technology is characterized by an ability to design displays that can produce high image emitted luminance outputs of the order of up to several thousand foot-Lamberts (fL) of luminance in either monochrome or color, for display active area dimensions of up to 6 x 6 inches and for much larger screen dimensions at lower maximum image emitted luminance levels. This makes these displays suitable for use in a wide range of applications and for use in ambient illumination environments that include night, low level daylight and, with adequate design precautions, full daylight viewing conditions.

The optical design difficulties for aircraft CRT displays, in high ambient illumination environments, result from the fact that the CRT's light emissive phosphors are deposited inside the CRT's clear glass envelope and are therefore directly exposed to the high ambient illumination, which is incident on the display surface. Because the phosphors closely approximate perfectly diffuse reflecting (i.e., Lambertian) surfaces of about 0.85 fL/fc of diffuse reflectance, an unfiltered display, in a 10,000 foot-candles (fc) incident illuminance viewing condition, would reflect as much as 8,500 fL of luminance equally in all directions from each illuminated point on the display surface. Thus, in spite of the CRT's ability to generate image highlight luminances of several thousand foot-Lamberts, when this emitted luminance is superimposed onto the even higher luminance reflected from the display's glass encased phosphor surface, the CRT has very limited utility for use in high ambient illumination environments, such as those experienced by the pilots of military aircraft. Through the use of optical filters and the judicious choice of image information presentation techniques, both monochrome and color CRTs have been designed to be able to produce legible display presentations in both military and commercial aircraft cockpits.

2.5.1.1. Monochrome CRT Displays

Through the insertion of light attenuative optical filters in front of a CRT display, the background luminance reflected by the filtered display can be reduced by a larger fractional amount than the display image difference luminance emitted through the filter. By maximizing the difference between the reflective and transmissive fractions by using a green bandpass optical filter, in conjunction with a narrow bandwidth green emitting P-43 phosphor CRT display, the F-15 was the first military aircraft to employ a sunlight legible multipurpose electronic display. This display had an active area that was 3.84 inches square and it emitted 200 fL of luminance, as measured through its filter on raster line peaks, while diffusely reflecting only 0.0025 fL/fc of incident ambient illumination.[1]

In a 10,000 fc incident illuminance test environment, the F-15 CRT display could produce its 200 fL luminance output through an approximately 13% transmissive filter with a 25 fL reflected background luminance. The result was a raster line with a contrast of eight. This translates to an ability to display somewhat in excess seven grey shades with a $\sqrt{2}$ luminance ratio separation in a 10,000 fc illuminance test

environment (i.e., the display background luminance level is counted as the first grey shade level). If specular reflections from the CRT's antireflection coated faceplate and other optical filter and glass envelope surfaces are taken into account, then the contrast is reduced to 4.67. The number of grey shades is reduced from seven to six when the specular (mirror) reflectance component is combined with the filtered diffuse reflectance of the CRT phosphor.

The addition of graphics imagery to the raster video presentations on the F-15 monochrome vertical situation display (VSD) was accomplished using stroke writing during the raster retrace time periods. This results in a superposition of the luminance of the graphics symbology onto the grey shade encoded luminance of the raster scanned video pictures. From a visual perspective, the result of the superposition of the images is a presentation with fixed image difference luminance graphics symbology floating on top of the spatially variant peak image difference luminance levels of the video picture.

Following the F-15 CRT, a variety of military aircraft have been equipped with monochrome P-43 phosphor CRT displays and green bandpass absorption filters. Although the image difference luminance levels generated by a raster written CRT drops in direct proportion to the increase in the display active surface area being raster scanned, improvements in the efficiency of P-43 phosphor CRTs permitted the F-16, for example, to use 4 inch square active area CRTs and the F-18 to use 5 inch square active area CRTs. Subsequent phosphor improvements have allowed monochrome green CRTs of up to 6 inches square to be used in more recent military aircraft. For the 6 inch square CRTs, no study could be found to verify that the same legibility level attained with the early versions of the F-15, F-16 and F-18 displays has been achieved on these later, larger area displays.

The key to the legibility of the preceding displays was the use of narrow emission spectral bandwidth CRT phosphors with the green bandpass absorption filters. While these filters transmit 13% of the green narrow band P-43 phosphor light emission, they pass a much lower percentage of the nominally white ambient illumination incident on the display. The ambient light transmitted to the phosphor following attenuation by the filter is green, but because it is of greater spectral bandwidth than the display's green light emissions, it is attenuated by more than the 13% transmittance of the filter for P-43 phosphor light, when it is retransmitted back out of the display following its reflection by the CRT phosphor. The overall effect of the filter placed over the aircraft CRT was to reduce incident ambient illumination to 0.0025 fL/fc on the F-15 display and to less than 0.0020 fL/fc on later displays.

By way of comparison, the use of a 13% transmissive neutral density filter (i.e., to give the same emitted luminance as the bandpass filtered CRTs), because it attenuates all light wavelengths equally, transmits both 13% of the incident ambient light and 13% of the filtered light reflected by the surfaces of the CRT. Assuming a CRT having a 0.85 fL/fc reflectance, the overall diffuse reflectance, R_D, of the neutral density filtered display would be as follows:

$$R_D = (0.13)(0.85\,\mathrm{fL}/\mathrm{fc})(0.13) = 0.0144\,\mathrm{fL}/\mathrm{fc}\,, \tag{2.2}$$

that is, a factor of seven higher than the diffuse reflectance of the green bandpass filtered monochrome CRTs. Since the legibility achieved on the previously described military displays only just exceeded the minimum requirements for military aircraft applications, this makes it clear that the introduction of the narrow bandwidth light emission phosphors and absorption bandpass filters, played a pivotal development role in making the first sunlight readable raster-written CRT displays to be used in military aircraft cockpits feasible.

The need for any type of display to meet or exceed a peak image difference luminance requirement of 200 fL for CRT raster lines or an area-averaged image difference luminance requirement of 160 fL, to make grey shade-encoded video imagery legible, is a minimum pilot vision requirement, which must be met under the veiling luminance viewing conditions, induced by the sun acting as a glare source.[2,3] Displays with higher image difference luminance emissions would satisfy this requirement and would also permit higher reflected luminance levels to be used, with no loss of legibility. The origins of the preceding minimum display image

difference luminance requirements are discussed in greater detail in Section 3.9.

The maximum emitted luminance achievable by raster scanned CRT displays is determined by the active area of the display, which can be activated by the scanned CRT electron beam spot, and by the instantaneous image difference luminance saturation limit of the phosphor, as the electron beam drive excitation is increased in intensity. Up to the phosphor saturation limit, intensifying the electron beam (i.e., adding more electrons per unit area) increases the emitted luminance of the CRT spot, but, thereafter, the emitted luminance does not appreciably increase, and the percentage of the beam energy converted to heat, rather than light output, continues to increase.

The time available to raster scan a picture onto a CRT is fixed by the need to refresh the picture periodically, to avoid the picture being perceived to flicker. By making the CRT's luminous spot larger (or smaller), and concurrently drawing proportionately fewer (or more) scan lines by moving the beam slower (or faster), while staying within the allotted fixed time to scan an entire picture of fixed area, does not change the average maximum image difference luminance that the display can achieve. In comparison, making the luminous spot size larger (or smaller), while scanning the same area and number of lines, does increase (or decrease) the area-averaged display emitted luminance, by changing the extent to which the gaussian spot spread functions of adjacent lines overlap. However, changing the spot size also introduces issues of how accurately spatially distributed images can be rendered on the viewing surfaces of CRT displays, as the spot sizes become larger, and the increasing ease of visually discriminating individual scan lines within images, as the spot sizes become smaller. The point of the preceding information is that to enable increases to be made in the emitted luminance of a particular CRT display, without degrading its picture image quality, fundamental technological improvements must be achieved either in its phosphor luminous efficiency or in its phosphor saturation limit.

On stroke-written CRT displays, the image difference luminance of the displays can be increased by decreasing the beam speed used to draw the images, while holding the beam spot size fixed. Even with the instantaneous emitted luminance level of the CRT spot saturated, increasing the time that it takes the spot to translate over a fixed distance on the display surface causes the time averaged luminance to increase. The disadvantage of moving the electron beam at a lower speed over the surface of the display is that the display area, which can be written upon, is reduced. This translates into being able to write fewer lines, characters and graphic symbols. In comparison to raster-writing, the time available for stroke-writing is reduced, due to additional time spent moving the beam from one writing location to another. In spite of the latter shortcomings, the stroke writing technique has been used extensively for the presentation of graphics information on electronic displays in aircraft cockpits, and, in particular, for the portrayal of color encoded information on aircraft cockpit CRT displays.

2.5.1.2. Color CRT Displays

In concept, the light emission capabilities of color CRT displays are no different from their monochrome display counterparts, except that the use of a shadow mask, with red, green and blue phosphor dots, stripes, and so forth, limit the area of the display surface that has phosphor coverage. Lacking full screen phosphor coverage causes a perceived reduction in the image difference luminance of the white emissions from the display, due to the area averaging by the human visual system of the light emitted by the excited red (R), green (G) and blue (B) phosphors with the areas surrounding the phosphors that do not emit light. The white emitted luminance output may also be limited by the luminance saturation levels of the individual RGB phosphors and by the primary color mixing proportions needed to achieve a particular white chromaticity specification, for the pictures to be portrayed. If a single primary color is to be displayed, then the area-averaged emitted luminance levels, of any one of the three juxtaposed primary color phosphor light emitting areas operating alone, would be less than one third of the luminance of monochrome displays using the same primary color phosphors.

An even more important problem with color CRTs is the lack of an effective means of optically filtering the

displays. Multi bandpass optical absorption color filters, which are commonly called color notch filters, have spectral attenuation characteristics that are little better than neutral density filters in reducing the ambient light diffusely reflected from the viewing surface of color CRT displays. To achieve an effective color notch filter, for use with a black matrix CRT, the RGB primary color phosphor spots would have to be deposited upon, and in registration with, the corresponding primary colors of a matrix absorption bandpass filter affixed inside the CRTs glass envelope. This form of optical filtering would provide emitted luminances, from the primary color spots, comparable to those of monochrome CRTs, that is, area-averaged emitted luminances of less than a third of those of their monochrome CRT counterparts, and would also provide the needed effective color notch optical filtering of incident ambient illumination. Lacking effective color filtering, color CRT displays must produce much higher emitted luminance levels than their monochrome counterparts to achieve the same level of sunlight legibility. Since achieving the requisite image difference luminance levels in the raster scan mode is not currently possible, aircraft applications of color CRTs in military aircraft have been restricted to the use of stroke-writing to present the higher emitted luminance levels of the color graphics symbology, with raster-writing reserved for use in providing the lower image difference luminance levels needed to fill large areas of background colors.

The use of stroke-writing to implement well conceived color information format designs can be an effective approach for many different aircraft applications, however, it does impose severe restrictions on the flexibility of the information presentation techniques that can be employed. Stroke-writing in monochrome or color limits the total area of the symbology that can be displayed to a fixed maximum amount, which cannot be increased, no matter how large the display active area available for the presentation of information becomes. This is true because a higher writing speed would be required to permit stroke writing over a larger area of the display surface, which, in turn, would result in a reduction in the emitted luminance of the display imagery. Since full color image presentations, and most color images on background color presentations, require raster writing to achieve adequate area coverage on a display, it is not feasible to accurately replicate color aeronautical charts, color maps or other similar types of imagery using stroke writing.

2.5.2. Legibility Considerations for Light Emitting Diode Displays

Light emitting diode (LED) displays can produce overall legibility performance very similar to that of CRT displays in head-down military display applications involving monochrome image presentations. Lacking an efficient blue LED, in a geometric form suitable for use in flat panel dot-matrix displays, this display technology has been restricted to using mixtures red and green primary colors in multicolor LED displays. The legibility problems for LED displays, like those of CRT displays, are most severe under high ambient illumination viewing conditions. Although the fundamental physical properties of these two technologies bear few similarities and their design considerations therefore differ in significant ways, some aspects of the electrooptical designs needed to make CRT and LED displays legible in sunlight are similar.

As is true for all dot-matrix displays, the matrix array of LEDs that form the display's surface can be addressed with information one line at a time, in time sequence, rather than one spot at a time, as for the CRT. While some dot-matrix displays have an active element driver associated with each picture element, which allows the picture elements to be driven almost continuously, dot-matrix displays, which lack this feature, are driven sequentially one row or column at a time. For displays of equal overall efficiency, the effect of this dot-matrix display picture element (pixel) drive technique is to extend the period of time each LED pixel is driven, as compared with the time a CRT spot (i.e., CRT pixel) is driven. Consequently, for LED and CRT displays, to have the same time-averaged emitted luminance outputs, the instantaneous magnitude of the emitted luminance from the pulsed LED would have to be reduced, in comparison to the corresponding maximum instantaneous emitted luminance of the CRT spot, in direct proportion to the ratio between the CRT spot dwell times and LED drive times.

As the physical dimensions of the active surface areas of either CRT or LED displays used to portray information increase, higher instantaneous luminances and drive power levels per CRT spot area and LED

pixel must be achieved to hold the time and area averaged image difference luminances of these two display technologies constant as the CRT spot dwell times and the LED line drive times decrease. Eventually, as the display size continues to be increased, and the instantaneous CRT beam or LED drive currents are increased, to maintain a constant time-averaged emitted luminance, a limit is reached beyond which the emitted luminance of the light pulses from the phosphors and the LEDs become saturated. The physical cause of luminance saturation is related to the finite density of photon emission sites within the phosphor and LED materials and to the effects of current induced heating. Further display size increases after luminance saturation is reached cannot be achieved without causing a reduction in the display's average emitted luminance output. The onset of this emitted luminance saturation limit would be significantly extended for dot-matrix displays having integral pixel drivers that can be operated continuously. However, technology problems, associated with the integration of display pixels with their drivers have prevented producing displays, using any of the light emissive mode display technologies, that can meet a pilot's legibility requirements in an aircraft cockpit, under worst-case daylight ambient illumination viewing conditions.

The display size limitation just described was overcome for LED dot-matrix displays by using independently driven display modules designed to be abutted on all four sides, without the loss of pixel resolution across the boundaries of adjacent modules. Each module acts as a constant legibility display. Thus, through the addition of modules, the overall display can be made as large as is required to satisfy a display application, without having any degrading impact of the display legibility. Design considerations for modular LED displays were described in an earlier article by the author.[4] These considerations were also described, but in less detail, in a more recent overview of LED display technology advancements and applications in a section of the book Display Engineering entitled Addressing Techniques.[5] The two preceding references include different illustrations of some sunlight legible LED displays that have been developed. LED displays of up to five by five inches in active area, assembled using nominally one inch square 64 pixel/inch modules, were successfully developed[6] and judged to be satisfactory by pilots in flight simulator and flight test environments while depicting electronic attitude director indicator,[7] electronic horizontal situation indicator and electronic map formats,[8] portrayed using monochrome green graphic information presentations.

The shortcomings of the modular LED display technique, just described, are related primarily to its cost, which is high owing to the following design considerations: (1) the small tolerances on module dimensions and positioning that must be met; (2) the need for custom high current silicon integrated circuit drivers, which must be mounted on the modules to reduce the number of electrical interconnections between the module and the display back-frame mother board; and (3) the need for efficient heat sinking to transport heat out the rear of the display, to achieve and maintain adequate electrical to light conversion efficiencies by the LEDs. Unfiltered luminance emissions from LED displays built to meet the preceding requirements were roughly several hundred foot-Lamberts.

The light emission from planar LED surfaces occurs with approximately equal luminance emitted in all directions into the hemisphere in front of its surface. This angular emission feature is shared with the CRT display, but the physical geometry and phenomenon responsible for causing light emissions differ. The result in both instances is that the image emitted luminance is constant as a function of the pilot's viewing angle with respect to the display. Furthermore the background luminances reflected from the surfaces of these displays are also essentially constant as a function of the display viewing angle. For this reason, both display techniques produce imagery that is equally legible, despite the pilot's viewing angle with respect to the display, up to the point that the perceived foreshortening of dimensions of the images displayed can limit their legibility at large angles. Reasons underlying the fact that the legibility of information presented on LED displays is constant as a function of the angle from which they are viewed are considered as a part of the more in-depth discussion of the LEDs that follows.

The materials from which LEDs are made are usually nearly transparent to the color of the light they emit and to longer wavelengths in the visible spectrum; shorter wavelengths are absorbed. Approximately 70% of the ambient spectral luminance incident on a plarar surface LED enters the material, for each wavelength of the light present in the incident light spectrum. The balance of the incident ambient light is specularly reflected

from the LEDs front surface, and in doing so retains the same color spectral distribution as the ambient light that was initially incident on the LED surface. For the ambient light transmitted into the LED material, the LED acts like a low pass color absorption filter. Thus, for example, the ambient light that passes through yellow-green emitting Gallium Phosphide (GaP) LEDs looks amber in color when held up to sunlight but appears a darker reddish brown when ambient light passing through the LED is reflected back out its front surface. The additional coloration of the reflected light is due to the blue through dark green components of the incident ambient light spectrum being further selectively attenuated on the reflective pass through the GaP LED. The result of this filtering action by the LED on incident ambient light is that the color of the broad bandwidth light spectrum reflected by the display differs significantly from its narrow bandwidth (i.e., approximately 25 nm at the half intensity points) yellow-green emission color, thereby producing an inherent "color contrast." This color contrast feature is shared with CRT displays, whose unfiltered reflected light typically appears gray independent of the display's light emission color capabilities.

The high specular reflectance of LEDs is due to their high refractive indices, which are typically about n = 3.4 or higher. The Fresnel reflectance for normally incident light is given by the equation

$$R = \left(\frac{n_I - n_T}{n_I + n_T} \right)^2 = 0.298 , \tag{2.3}$$

where $n_I \approx 1$ for air and $n_T \approx 3.4$ for the GaP LED. Another interesting result of the high LED refractive index is that the angle at which total internal reflection occurs for light generated by the LED is quite small. This angle is determined using Snell's Law, which can be expressed in equation form as

$$n_I \sin \theta_I = n_T \sin \theta_T . \tag{2.4}$$

For light emitted parallel to the LED's surface, that is, for $\theta_I = 90°$, the corresponding angle at which light is incident from inside the LED on its surface, θ_T, can be calculated as follows:

$$\sin \theta_T = \frac{n_I}{n_T} = \frac{1}{3.4} \tag{2.5}$$

$$\theta_T = 17.1° .$$

The result calculated using Equation 2.5 shows that, when light internal to the LED is incident on its surface at angles greater than 17.1°, all of the light incident on the LED surface is totally internally reflected. Since the light emitted at the LED junction emanates from each point, with equal probability, in all directions into a spherical solid angle, only the fraction of the light directed into a cone subtending 34.2° will be directly emitted into the hemisphere in front of the display. Consequently, for the GaP LEDs being used in this example, only 2.2% of the light generated is directly emitted through the front surface. This result may be calculated using the following equation:

$$\Omega = \frac{A}{\rho^2} = \frac{1}{\rho^2} \int_0^{2\pi} \int_0^{\theta} \rho^2 \sin \theta \, d\theta \, d\phi$$

$$= 2\pi \int_0^{\theta} \sin \theta \, d\theta = 2\pi \left[1 - \cos \theta \right] . \tag{2.6}$$

where Ω is the subtended light emission solid angle, A is the circular light emission area at the surface of the LED, ρ is the distance from the LED junction to the emission area on its surface and the area integral is expressed in terms of the standard spherical coordinate system angles θ and ϕ. Substituting the limiting angle for light emitted from the LED into Equation 2.6, the following value is obtained for the LED emission solid angle, expressed in sterradians:

$$\Omega(\theta = 17.1°) = (0.044)\, 2\pi = 0.278 . \tag{2.7}$$

If this emission solid angle is expressed as a ratio, in relation the total 4 π radian spherical solid angle into which the LED junction emits light, then the fraction of the light emitted by the LED junction, which is transmitted through the LED's front surface, can be expressed, as follows:

$$\frac{\Omega(\theta = 17.1^\circ)}{4\pi} = 0.022 . \qquad (2.8)$$

Since LEDs emit equal amounts of light toward their front and rear surfaces, the light mirror reflected from the LEDs rear surface electrode, nearly doubles the front surface output luminance. A small amount of emitted light is also radiated out the edges of the LED. However, due to the small aspect ratio of the solid angle subtended by the edges of a LED, with respect to the full 4 π sterradians of a sphere (i.e., LEDs are typically very thin in comparison to their surface area), only a very small percentage of the device output occurs through these surfaces. Although this light leakage does not affect the useable output of the LED, it can lead to a low level of optical coupling if measures are not taken to cause it to be absorbed.

The point of the preceding discussion of LED light emission design is that more than 95% of the light generated by an LED remains internal to the device, where through multiple reflections it is eventually absorbed, giving off heat. Stated in another way, if the light generated within a LED could be translated into a visible output, the efficiency of the LED would be increased twenty-fold, as would its emitted luminance. In theory, if a LED is coated with a material that gradually transitions, from the refractive index of the LED to that of air, it would permit all of the light striking the front surface of the LED to be emitted. Materials with this property have been made for small refractive index changes, but research on materials suitable for use with LEDs has been quite limited. Attempts have also been made to increase the luminance output of LEDs using multilayer interference films, which in concept can perform the same function. Again, the research performed has been very limited. Finally, shaping the rear surface of a LED so that the light reflected from that surface strikes the front surface within its 34.2° emission angle cone is another method that can be used to increase efficiency of LEDs.

Practical LEDs, using a conformal coating of the LEDs to protect them from surface contaminants, do provide a modest increase in the emitted luminance achieved. The overall result, for the practical monochrome green dot-matrix LED displays, developed to provide sunlight readable imagery in aircraft cockpits, are power consumptions essentially the same as those for monochrome green sunlight readable CRT displays intended to portray the same information and having the same active area dimensions.

Like CRT displays, optical filtering is crucial for making LED displays readable in sunlight. Unlike CRT displays, the diffuse reflectance from the LED materials themselves is very low; often much less than 0.01 fL/fc, as compared with the 0.85 fL/fc of a CRT phosphor. The diffuse reflectance associated with LED displays is due primarily to the ceramic substrates on which they are mounted and the metalization runs used to provide electrical power to the LEDs. With the use of antireflection coatings, the diffuse reflectance of the entire LED module assembly can be reduced to the order of about 0.01 fL/fc. In fact, dot-matrix LED displays, with their faceplates and filters removed, are legible with sunlight incident directly on the display's viewing surface, if the luminance levels incident on the display viewing surface at specular reflection angles are at sufficiently low levels.

The inherently low diffuse reflectance of well designed LED displays causes the optical filtering applied to be aimed primarily at reducing specular reflections from both the LED and optical filter internal and external surfaces to an appropriately low level. The principal components of these optical filters are typically as follows: a bandpass absorption filter, which limits the ambient light entering the LEDs to nominally the same chromaticity of the light emitted; a neutral density circular polarizing filter, to quench specular reflections; multilayer antireflection coatings, to reduce front and rear surface reflections of the composite filter; optical cements, to refractive index match and join the layers of the filter; and a transparent metal layer, to control electromagnetic interference.

Since the absorption bandpass filter's function is, in part, to limit the ambient light wavelengths reaching the circular polarizer to those for which its performance is optimal and, in part, to cause a small further attenuation of the display diffuse reflectance, the transmittance of this filter to the design color is typically very high approaching that of clear glass for the emission color of interest. The polarizer/bandpass filter combinations have transmittances that can approach 40%, for the color spectrum of the display emitted luminance, with the attenuation being attributable almost exclusively to the one pass linear polarizing effect of the neutral density circular polarizing filter. The overall effect of the composite optical filter on the previously described LED displays is to cause them to emit and reflect luminance levels very similar to those of aircraft monochrome CRT displays, even though the physical phenomenon involved are almost entirely different.

2.5.2.1. Monochrome LED Displays

Green light emitting diode (LED) displays were the first dot-matrix electronic displays to be used in operational aircraft. The application occurred in the F-16 aircraft and consisted of a 1 x 3 inch active area display, with a 64 pixel/inch viewing surface and formed using 1 x 1 inch square, four-edge abuttable LED display modules. In the F-16, the display is called the Data Entry Display (DED). The display is mounted on the underside of the glare shield, with its viewing surface flush with the front of the glare shield, where it receives full exposure to incident ambient illumination and is reported by F-16 pilots to be readable in direct sunlight.

Although the basic design of the DED would permit the portrayal of real-time dynamic graphics imagery, the use of the DED in the F-16 is restricted to the presentation of time-changing alphanumeric information. MIL-L-85762 requires that graphic displays possess a contrast of three or greater and an image difference luminance of 100 fL. For alphanumeric characters 0.2 inches high, with a character stroke width of 12 to 20% of the character height, MIL-L-85762 requires a reduced contrast of two, rather than the three for graphics, but still maintains the minimum luminance requirement of 100 fL.

The reduction in the MIL-L-85762 contrast requirement from three, for graphics, to two, for alphanumerics, to one and a half, for numerics, is due to the reduction in the number of characters that make up the respective sets of characters, from which the identification of a specific character must be discriminated. Since the numeric character set of 10 characters is a subset of a 36 alphanumeric character pool, and the alphanumeric pool is usually a subset of a still larger graphic character pool, the critical detail dimensions of the characters that must be discriminated become progressively smaller as the size of each pool of characters becomes larger. Because higher contrasts are needed to permit achieving equal legibility, when smaller critical detail dimensions are to be discriminated, the larger the size of the character pool, for a set of characters of a particular height classification, the higher the contrast must be to make the entire character set legible.

The preceding relationship, for character sets of different sizes, also applies to the minimum emitted luminance requirements needed to overcome the legibility degradation effects of the veiling luminance induced by exposure to glare, due to the sun. Since the veiling luminance is perceived as the result of glare source light scattered within the eyes into the line of sight to the display that is being viewed by the pilot, this luminance adds to the measurable luminance reflected by the display. The result is that the luminance emitted by the display imagery is contrasted against this composite background luminance. With the glare fixed, and the ambient illuminance incident on the display fixed, the contrast requirements also apply to the display emitted luminance requirements. Consequently, since graphics requires 100 fL to overcome the effect of glare source induced veiling luminance, alphanumeric character sets only require 100 fL x 2/3 = 66.7 ft, and numerics require only 100 fL x (1.5)/3 = 50 fL, rather than the 100 fL specified in MIL-L-85762.

For the case of the F-16 DED, described earlier, the alphanumeric character height was 0.15 inches rather than 0.20 inches. Using the linear compensation approximation of MIL-L-85762, the contrast must be increased by a factor of 4/3 (i.e., 0.2"/0.15"). This factor also applies to the alphanumeric image difference luminance requirements. The contrast and emitted luminance requirements for the DED based on MIL-L-

85762 are 4/3 (2) = 2.67 and 4/3 (66.7 fL) = 88.9 fL, respectively. The satisfaction of F-16 pilots with the Data Entry Display is therefore predicted by the legibility requirements of MIL-L-85762. Although the preceding image difference luminance legibility requirements were introduced in the context of LED display legibility requirements, they have general applicability to any type of display and are considered further in Section 3.9.

2.5.2.2. Color LED Displays

One of the more attractive features of color LED displays is the narrow spectral distribution of their color emissions. Due to this feature, the chromaticities of red and yellow-green LED light outputs fall essentially on the spectral locus of the 1931 CIE Chromaticity Diagram, and are, therefore, fully saturated colors. Moreover, because the red to yellow-green segment of the spectral locus approaches a straight line, colors mixed with red and yellow-green LED light such as orange and yellow are also very nearly fully saturated colors. This gives multicolor LED displays the potential of being very useful for the presentation of aircraft signal colors in applications such as collision avoidance, radar homing and warning, and warning and caution signal annunciations.

As the emission colors from LEDs progress from infrared, to red, to yellow, to green, to blue and eventually to violet, the semiconductor material energy bandgap required to permit the shorter wavelength color emissions becomes progressively larger. To produce blue or violet emissions from a LED, the single crystal material employed requires such a large electron transition energy bandgap that the single crystal material appear clear (i.e., it passes all visible wavelengths with almost no attenuation). Two materials that are clear in their single crystalline form and have been shown to permit blue emissions are zinc sulfide (ZnS) and silicon carbide (SiC). In theory, and as confirmed by experiment, materials having large energy band gaps are capable of having dopant materials added during their fabrication that would permit colors with lessor bandgaps to be excited. In concept then, ZnS and SiC are not only capable of producing blue light but also the other two additive color primary colors, green and red. Despite these positive theoretical considerations, both of these materials have been found to possess severe technological limitations, that make it difficult to use them to fabricate efficient color LEDs.

For ZnS, the principal problem has been the inability to form the requisite p-type region of the p-n diode junction. Light emission occurs when minority carriers are injected into the depletion region between the p-type and n-type doped sides of the junction. The injection stimulates the recombination of holes and electrons, and the desired light emission. In the mid-1970's, the USAF Aerospace Research Laboratory developed an efficient blue ZnS metal insulator semiconductor junction that avoided the need for forming a p-n junction within the single crystal ZnS. This research was terminated during the early stages of the program, for reasons unrelated to the technology, and in spite of the rapid development progress being achieved by USAF personnel.

Light emission from SiC, when subjected to an electric field, was first observed in the early part of the 20th century, however, the phenomenon responsible for the light emission was not understood until after the invention of the diode and the transistor in the late 1940s at Bell Laboratories. Although many investigations of SiC as a host material for light emitting diodes have been conducted, progress with this material has been restricted by several severe material processing problems related to its high melting temperature, its hardness, and, possibly foremost, to the fact that it forms more than one single crystalline phase having different crystalline atomic structures that during early processing attempts underwent a conversion from a structure suitable for the formation of LEDs to one that was incompatible with this objective.

Although blue SiC LEDs have been reported in the literature and occasionally have also been produced for sale, the technology has historically been hampered by the inability to grow single crystals, in large enough sizes, to permit the development wafer processing techniques similar to those that are routinely applied to silicon-based diodes, transistors, and integrated circuits. Reports of 1 ½ inch diameter colorless, transparent

SiC wafers by Wright Laboratories* in 1994 and subsequent progress with epitaxial growth of single crystal SiC have resulted in the production and sale of single lensed LEDs, which produce light that is a blue-white in color, and has been used, for example, to make commercially available high intensity flashlights. The status of ongoing research, if any, on the application of this technology to the development of full-color dot matrix displays is unknown.

The fact that the preceding candidate materials, for use in making full color LED displays are clear and colorless, with smooth planar surfaces, means they would have very low diffuse and high specular reflectances. These materials, like the other LEDs already described, would require care in treating the surfaces on which the LEDs are mounted, to reduce diffuse reflections, and would also need circularly polarizing filters and antireflection coatings, to reduce specular reflections. Furthermore, because the design of LED displays do not rely solely on the use of narrow bandpass absorption filters, with the attendant high stopband attenuations needed to make CRT displays legible, the low inherent diffuse reflectances of LED displays allow them to be made legible even though they have much lower emitted luminance outputs than CRT displays, before applying optical filtering. Like color CRTs and color active matrix liquid crystal displays this technology would also benefit from the application of a mosaic array of primary color bandpass absorption filters that are in spatial registration with the corresponding emissive primary color LEDs.

2.5.3. Legibility Considerations for Fiber-Optic Light Piped Displays

Fiber-optic light piped electronic displays provide yet another example of the vast differences in techniques employed to implement light emissive operating mode display technologies. Although sunlight readable versions of this display have been demonstrated, using fixed information format color coded bargraph and circular dial instruments, the application of this technology to aircraft cockpits seems to have been restricted to numeric readout displays. The electronically controlled light sources used with these displays are most typically incandescent filament light bulbs, although any source of high intensity light could be used.

Either diffuse reflecting or specular reflecting fiber-optic surface designs can be used to implement the viewing surfaces of fiber-optic light piped numeric readout displays. Reducing the reflections for these two approaches are analogous to the respective techniques used for CRT and LED displays having similar reflective properties. Because the image difference luminance outputs, associated with the fiber-optic display technique, are typically much higher than they are for either CRT or dot-matrix LED displays, these displays should be compatible with the pilot's legibility requirements in the presence of sun induced veiling luminance. Since the implementation of automatic legibility control with this display technology should be essentially the same as for the other light emissive operating mode display technologies, it is not considered necessary to treat this subject for the fiber-optic display technology.

2.6. Light Transmissive Mode Aircraft Cockpit Displays

Electronic displays, using the light transmissive operating mode of electronic display, are characterized by the ability to control the spatial and temporal modulation of the luminance and chromaticity of the light radiated by the display media toward the pilot, by exercising control over the electrooptical process used to modulate the luminance emanated by the display's backlight. The effectiveness of the light transmissive display mode is conditioned by the ability of the display designer to affect control over the modulation of the emitted luminance levels and chromaticities of the light emanated by the display media, and over the reflections of ambient light from the materials used to fabricate the display, including the optical filters used to control the magnitude of the display's reflected background luminance levels.

---

* Gaffney, Timothy R. "Building Better Microchips" subtitled "Wright Lab Forms Research Group on Silicon Carbide," Dayton Daily News, Tuesday, November 29, 1994, Section B, Page 5.

The legibility dependence of light transmissive mode displays, on the ambient illumination and glare source conditions experienced in aircraft cockpits, is essentially the same as the legibility dependence of light emissive mode displays. Likewise, both of these display operating modes are dependent on light generated within the display, and emanated from their viewing surfaces, to make the information they portray legible. The physical distinction between the light transmissive and light emissive operating modes is commonly held to be associated with the way these displays modulate the light emitted from their viewing surfaces. For light emissive operating mode displays, the information to be conveyed to the pilot is modulated onto the light emitted from the display, as an integral part of the process of generating the light. The concurrent generation and information modulation, of the light produced by light emissive displays, most commonly occurs within the viewed surfaces of the display. However, the light can also be generated remotely and either viewed through transparent optical elements or conveyed to the display surface via fiber optics. Light transmissive operating mode displays modulate information onto the light emitted from the display by using either passive or electronically controlled light transmissive media and a separate source of backlighting generated either directly behind the viewing surface or at a remote location and light piped to the back of the viewing surface.

Backlights that produce an approximately uniform distribution of luminance over the entire rear surface of the image modulation media are a common feature of all of the light transmissive mode displays that are suitable for use in aircraft cockpits. Because the backlights are physically separate from the display's light modulation media, the image difference luminance levels of the spatially distributed patterns of information, portrayed across the surfaces of these displays at any instant of time, can be controlled simultaneously through the control of the emitted luminance of the backlight. The instantaneous spatially distributed patterns of information, portrayed across the surfaces of these display is established by using the display media to control the selective transmission, absorption and reflection of the light incident on the display media, from the backlight. The full practical significance of this ability to separate the control of the information portrayed, from the control of the image difference luminance of the resulting display presentation, and the implications, on the legibility and interpretability of displayed information, caused by enabling an independent capability to control the modulation of information and the luminance of the resulting presentation, for other display operating modes, are considered in Chapters 5 and 6.

Conventional transmissive mode displays typically use a multilayer viewing surface to modulate the light they transmit with a static spatial pattern of grey shade and chromaticity encoded information, which is conveyed to the aircrew via the modulated light when the display backlight is activated. Different layers of this light transmissive viewing surface are typically used independently to control the spatial pattern of the information to be conveyed, to absorb or reflect all but the desired transmitted color and to control the overall light reflective properties of the display, with respect to incident ambient light.

For electronic versions of light transmissive mode displays, the luminance emitted by the backlight is modulated by controlling the transmittance of individual monochrome or primary color picture elements, between their "on" and their "off" states, to produce the grey shade levels and chromaticities to be conveyed to the aircrew via the display's luminance emissions. Like conventional transmissive mode displays, the electronically controllable versions of these displays also employ multiple layers. One of these layers contains the active electronic control elements for setting the transmittances of the individual picture elements. Another layer serves to insert a mosaic of primary color filters that are in geometric registration with the active control elements for color displays, or to insert uniform color absorption bandpass filters for use with monochrome displays. Other layers can contain polarizing, phase shift, antireflection, electromagnetic interference, absorption filters and so forth.

It should be noted that displays using images generated remotely and rear projected onto translucent viewing screens are generally considered to be transmissive operating mode displays, independent of the operating mode of the image generation source. Due to the high diffuse reflectances, associated with unfiltered rear projection screens, and the image difference luminance limitations typically associated with using electronic displays as image generation sources, sunlight readability is difficult to attain, for formulations of this display technique capable of presenting electronically alterable pictures. This display technique shares the

legibility problems of other transmissive and emissive operating mode displays, and, consequently, further specific details on this display technique are not considered in this report.

As previously described in the section on light emissive operating mode displays, no existing electronic display technique can create all of the grey shade and chromaticity combinations that a human is capable of perceiving, even under ideal ambient illumination viewing conditions. The difficulty encountered in achieving the full gamut of colors a human is capable of perceiving, using light transmissive operating mode electronic displays, is that as the spectral bandwidth of the red, green and blue optical filters used to form the primary color picture elements become narrower to produce more saturated primary colors, the light emission efficiency, and, consequently, the image difference luminance levels of the pictures rendered by the displays, are progressively reduced. A method adopted to compensate for this effect uses a backlight having high efficiency red, green and blue narrow bandwidth light emissions, rather than the wide spectral bandwidth white light of conventional transmissive mode display backlights. Because the mosaic primary color filter matrix also serves as an efficient optical filter to reduce reflections of incident ambient light, this approach has the potential of producing very legible displays with large color palettes. Technological limitations associated with this approach have to date resulted in displays with color light emission properties that are only comparable to color CRTs, but with the advantage of not having the display size and spatial image rendition restrictions associated with sunlight readable CRT displays.

Like their light emissive operating mode display counterparts, the light reflection properties of the viewing surfaces of light transmissive mode displays are dependent upon the specific display technology, the optical design, the materials used and fabrication techniques selected to minimize the light reflections associated with that specific technology. As previously stated, these issues are considered beyond the scope of the present report. A light reflective property that is common to all light transmissive mode display implementation techniques, and is worthy to note, is the reflective response of the display viewing surfaces to incident ambient illumination of any illuminance magnitude when the display's backlight is turned off. Under this condition, the information intended for portrayal on these displays should be either imperceptible or essentially imperceptible. This property is an integral part of the definition of light transmissive mode displays, since displays that do produce perceptible images under this condition with their backlight turned off, are, by definition, light transflective mode displays.

2.6.1. Legibility Considerations for Conventional Light Transmissive Mode Displays

Sunlight readable signal indicators and illuminated push-button switches are examples of conventional aircraft displays that operate in the light transmissive mode. Sunlight readability is typically achieved through the incorporation of optical filters that combine the properties of bandpass color absorption filters, to achieve the intended emitted luminance color, with viewing surfaces possessing Lambertian diffuse reflection characteristics. The combination of these two design features provides a sunlight readable information depiction when the display is activated, and a spatially uniform reflective viewing surface perceived to be blank when the display backlight is not activated. Furthermore, these displays remain legible, even when the display is exposed to a direct reflection of the sun at a specular viewing angle.

The backlight for these indicators and switches has historically been implemented using incandescent filament bulbs that emit a broad spectral distribution of white light when activated. Due to the unpredictable operating lifetimes of incandescent filament bulbs, an alternative more reliable light source is desirable, however, as yet no suitable substitute capable of generating a comparable white light spectrum has been developed, which is also capable of being readily dimmed for night operations. The increases in the luminous efficiencies of light emitting diodes, in combination with operating lifetimes of more than one hundred times that of incandescent filament bulbs, make them prime candidates for this application, in those instances where the necessary identification and signal colors can be obtained. MIL-L-22885, the General Specification for illuminated Push Button Switches details the requirements and test procedures for these devices. MIL-S-38039, the General Specification for Illuminated Warning, Caution and Advisory Systems and MIL-STD-411,

the Military Standard for Aircrew Station Signals, details the requirements and test procedures for signal indicators.

The emitted luminance of signal indicators is required to exceed 150 fL under daylight viewing conditions and is required to be a minimum of 15 fL when the cockpit lighting is turned on, for use under night viewing conditions. In practice, both the sunlight readable signal indicators and the illuminated push button switches, in operational use in aircraft cockpits, produce emitted luminance levels significantly above the minimum 150 fL luminance requirement for these displays (i.e., typically more than 800 fL). Because these displays are operated at such high luminance levels and, moreover, are maintained at different fixed settings, under daylight and night viewing conditions, the veiling luminance induced by glare sources, for either of these viewing conditions, should not create a legibility problem when reading these displays. An exception occurs for displays mounted on or flush with the top of the glare shield, when the sun happens to be located directly adjacent to the display. The latter viewing condition is sometimes called blinding glare, and is equivalent to the head-up display viewing condition where a display image overlays or is directly adjacent to the sun. Blocking the luminance from sun, is the only feasible method available that can compensate for this extreme viewing condition.

It should be noted that an advantage would accrue, particularly at night and when a night vision imaging system (NVIS) is being used, from automatically controlling the image difference luminance of all cockpit displays that emit light, but this is especially true for warning and master caution signal indicators, signal indicator panels and illuminated push-button switches. By operating signal indicator panels, and warning and caution indicators, at a small fixed multiple, of from three to fifteen, above the image difference luminance levels of the other displays in the cockpit, where multiples of three and fifteen, respectively, would suffice for the signal indicator panels and the warning and master caution signal indicators, their ability to attract a crew member's attention would be retained and their ability to interfere with the pilot's external night vision or with the NVIS would be minimized. Similar, although smaller, benefits would be derived from the application of automatic legibility control to set the legibility levels of illuminated push button switch display information.

Each of the preceding types of transmissive operating mode displays have been chosen for emphasis because of their large emitting areas and the high image difference luminance levels at which they are typically operated. For example, a single warning or master caution signal indicator, operated at 15 fL at night, emits many times the luminous intensity emitted by an electronic attitude director indicator (EADI) format depicted on a five inch square multipurpose display, even when EADI format is set to its maximum night luminance level. Stated in more practical terms, when cockpit displays of all types are set to the luminance levels they are typically operated at for good external night vision, a single warning or master caution signal indicator, operated at its minimum specified night level of 15 fL, would emit more light than all of the other continuously illuminated light sources in the cockpit combined. The use of automatic legibility control with the previously mentioned displays, would not only allow greatly reducing the potential for these displays to interfere, either with the pilot's external night vision or with the operation of the NVIS when it is in being used, it would also allow the operating hours between maintenance for these displays to be extended under both daylight and night operations.[9]

2.6.2. Legibility Considerations for Electronic Light Transmissive Mode Displays

Several different electronic display techniques based upon the light transmissive operating mode are currently in use in operational aircraft. Most of the applications involve retrofits of other less reliable display techniques in older aircraft, and are for the most part restricted to the display of numeric and alphanumeric information. A small but growing number of applications involve the use of color active matrix liquid crystal displays (AMLCDs), which are currently used as alternatives to color CRT displays, for the presentation of multicolor graphic and green sensor-video information.

The preceding light transmissive mode electronic displays share, as a common feature, the use of liquid crystal materials as the technology utilized to permit the exercise of electronic control over the modulation of

the light from their backlights. In spite of this apparently common feature, the optical design techniques, used to implement effective liquid crystal displays, differ greatly from one another. Although the expected variations, caused by the design approaches used by different manufacturers, are present, the more substantive differences are based on the types of liquid crystal material technologies used and on differences that this imposes on the implementation techniques needed to achieve legibility, for different types of information presentations in an aircraft cockpit viewing environment.

Despite the differences between the liquid crystal technologies, and the techniques used by different manufacturers to implement these light transmissive mode electronic displays, if the different display implementations are used to present the same monochrome or color information portrayal, and the chromaticities of the rendered imagery, the modulated image difference luminances emitted, and the background luminances reflected, from the display viewing surfaces are the same, then for practical purposes a pilot viewing light transmissive mode displays would be expected to judge the pictures portrayed to be indistinguishable. Moreover, this assessment should also be valid if the same chromaticities, image difference luminances, and background luminances, were to be emanated from light emissive operating mode displays portraying the same information. In other words, a pilot viewing light transmissive and light emissive operating mode displays would have no way of knowing how the light was generated and modulated within the displays. As such, the legibility requirements that light transmissive operating mode electronic displays must meet are the same as those previously described for light emissive operating mode displays. Furthermore, this means that the requirements that must be met to apply automatic legibility control to light transmissive and light emissive operating mode displays are also the same.

The fact that the information modulation and image difference luminance generation functions of light transmissive mode electronic displays are physically separated from one another, allows their respective impacts on the legibility of the displayed information to be more clearly discerned, than is the case for light emissive mode electronic displays, where these functions are integrated. Since color AMLCDs, currently in use or proposed for use in operational aircraft, have been successfully designed to satisfy the three primary ambient illumination viewing condition requirements, described in Section 2.2 near the beginning of this chapter, this technology will be used as an example throughout the balance of this report. For this reason, a more in-depth description of the details of the legibility capabilities and operation of the color AMLCD technology is deferred to the later chapters of this report.

CHAPTER 3

Pilot Legibility Requirements

In this chapter, specific human luminance requirements data will be presented together with some data supporting its validity. The purpose of the chapter is to discuss, develop and, to the extent possible validate, a mathematical model to represent a pilot's legibility requirements. To avoid unnecessary complexity in the formulation of the model, the analysis of relevant test data is initially restricted to ideal imagery, ideal physical viewing environments and static display conditions. Having formulated the ideal model, the effects of degraded environmental illumination conditions are then added. Analysis results that permit compensating the ideal luminance and contrast requirements for dynamic imagery, and other factors that can potentially degrade image legibility, are considered only in the context of applying adjustments to the model to accommodate the difference between laboratory and operational aircraft-based requirements near the end of this chapter. The latter approach differs from the historic approach of applying successive compensations for individual factors known to influence legibility.

Due to the complexity of the luminance variable interrelationships, a considerable portion of this chapter is concerned with interpreting and, where possible, providing information that validates the luminance and contrast requirements data being presented. The remainder of the chapter is concerned with a discussion of the available experimental and in-flight test information, and with an analysis of that information to show how it can be interpreted for application to integrated aircraft cockpit control-display system designs.

One of the primary purposes of this report is to describe some of the results of an approximately thirty year intermittent effort started in 1969 aimed at analyzing and correlating pilot legibility requirements data. The data analyzed was acquired largely through searches of the display and visual research literature. The analysis was restricted to studies treating color normal subjects with 20/20 or better static visual acuity. The goal of the analysis was to first establish a basic set of pilot legibility requirements valid for known: high image quality, low image complexity display imagery when-viewed under ideal environmental illumination conditions. With this accomplished, an empirical equation that describes ideal human legibility requirements for luminance and contrast was developed. The second part of the analysis goal was to develop techniques for describing the changes in the luminance and contrast requirements made necessary when either the information depicted by displays or the viewing conditions are no longer ideal. The present report is restricted to a description of display image legibility and how it is influenced by the combination of light reflected from aircraft cockpit instruments and panels and glare inducing illumination levels incident on a pilot or other aircrew member's eyes from within his or her instantaneous field of view. An empirically based model for describing a pilot's display image legibility requirements and for predicting the increase in these display image legibility requirements when discrete and/or distributed glare sources are introduced is presented in this chapter.

The major topics discussed in this chapter include the following: (1) the identification and discussion of pertinent image legibility variables; (2) a discussion of the influence that the critical detail dimensions of imagery have on a pilot's luminance and contrast requirements; (3) a presentation of the best available experimentally derived image difference luminance and contrast requirements data, with a discussion of the influence that the pilot's visual performance level and the surround and panel luminances have on luminance and contrast requirements; (4) the development of an empirical mathematical model representation of the ideal image legibility requirements of pilots; (5) an introduction and discussion of experimental data concerning the veiling luminance induced by both discrete and distributed glare sources; (6) the development, explanation and validation of an empirical mathematical model to represent the veiling luminance induced by discrete glare sources, in a form that is compatible with being incorporated into the ideal image legibility empirical model and, therefore, permit characterizing the effect that discrete glare sources have on a pilot's ability to read cockpit display information; (7) the elements of a theory for the origin and functionality of the veiling luminance induced by a discrete glare source; (8) the development, explanation and validation of a mathematical model to represent the veiling luminance induced by distributed glare sources, in a form that is compatible with being

incorporated into the ideal image legibility empirical model and, therefore, permit characterizing the effect that both discrete and distributed glare sources have on a pilot's ability to read display information; (9) a discussion of the practical considerations associated with applying the pilot image difference luminance requirements model to the automatic legibility control of aircraft cockpit displays, controls and instrument panels; and finally (10) limited conclusions concerning the applicability of the automatic legibility control model to operational aircraft.

3.1. Image Legibility Variable Dependences

To set the context in which the analysis contained in this chapter was conducted and upon which its results are based, a framework will first be introduced to aid in its interpretation. The intent of this section is to deal with this framework only in very general terms.

Figure 3.1 illustrates human control-display information processing in a simplified block diagram format. The information processing stages shown in the path between the Displays and Controls blocks have been used to characterize visually/mentally processed information for a very long time, however, except for the distinction between Image Identification and Image Significance, they were only revealed to be actual distinguishable mental processing stages for the first time in reaction time experiments by Sternberg.[10]

The mental processing stages shown in Figure 3.1 will be described using an aircraft mission involving the location of a target as an example. Initially, at a large range from the target, it cannot be seen. As the range to the target decreases it will first be "detected," that is, a dot or spot will become visually discernable with respect to the background visual scene but its shape will be sufficiently undefined that the nature of the object being viewed cannot be recognized. Further closure on the unknown object will cause it to continue to become larger until features of the target's shape become sufficiently discernable to permit the object being viewed to be recognized as a building, bridge, aircraft, tank, truck and so forth. With still further reductions in range, even smaller features of the now recognized object start to become discernable, eventually allowing "identification" of the object as a friend or foe, and if a foe its mental designation as the assigned target, as a target of opportunity and so forth. Image significance refers to issues such as visually discriminating the threat posed by the identified target and requires further closure on the target to ascertain. As shown in Figure 3.1, pilot decision making can start as early as the image recognition stage of information processing and, depending on the situation, could result in an immediate jump to response selection. In the case that the target is a bridge, for example, onboard navigation and intelligence information might be sufficient to allow the pilot to designate the recognized object as the assigned target, without the need to close in on it further to permit an unambiguous visual identification. In this case, image significance might, for instance, be the visual discrimination of weapons deployed by an adversary to defend the bridge.

In the preceding discussion of Figure 3.1, no mention was made of the image perception block that separates the displays and image pattern recognition blocks. Image perception or perceptibility relates to the ability of an observer to see an object or image. Image perception can be analogized to a three-dimensional adaptive filter, operating on the spatial, spectral and temporal components that make up the external scene and aircraft cockpit instruments viewed by the pilot, which is coupled to a sensor array, in this case the visual cortex of the brain, that is capable of extracting the information passed to it by the adaptive filter. While the human visual system is adaptive to a variety of changing conditions in the external scene and cockpit environments that influence image perception, there are physiological constraints on this adaptive capability that cannot be exceeded. In addition to the fact that this natural adaptive filtering by the human visual system acts to impose inherent constraints on the perceptibility of the information passed to the brain, the pilot's ability to recognize, identify and determine the significance of perceived imagery can be no better than the information available to be sensed at the input to this adaptive filter.

Atmospheric illumination, haze, fog and a variety of other inclement weather can impose conditions exceed the visual system's capability to perceive external scenes. In worst-case scenarios, these conditions

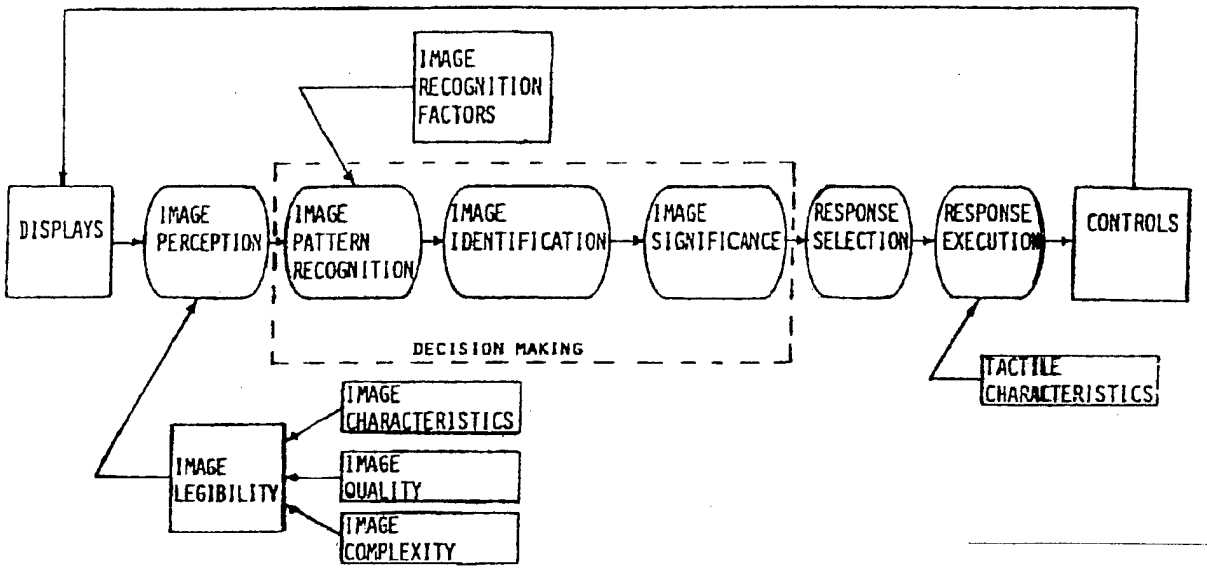


Figure 3.1. Human Control-Display Information Processing.

can completely prevent targets from being seen or, under slightly higher visibility conditions, they can restrict the ranges at which the pilot can be expected to recognize, identify and determine the significance of the imagery perceived. Alternative sensor-display systems must be relied on to circumvent these human visual system limitations. In analogy to the factors influencing the legibility of scenes external to the cockpit, the perceptibility of information displayed in the cockpit is in large part controlled by the inherent capabilities of the display technologies being used to meet the pilot's information needs and, consequently, on the information-display interface design specification implemented.

In the past, the perceptibility of information has been most comprehensively characterized through the specification of independent variables that are accessible external to the human's visual system and that are almost universally grouped under the general heading known as image legibility (i.e., the specifiable features of an image that make it discernable). The basic image legibility variables are most conveniently discussed and specified when they are divided into the three subcategory groupings shown in Figure 3.1. These three groupings of independent variables are categorized in Table 3.1 using the titles Image Characteristics, Image Quality and Image Complexity. Table 3.1 lists the more important variables under each of these legibility groupings and in addition separately lists legibility variables, which at progressively higher levels of legibility enables image recognition, identification and image significance to be perceived and interpreted by the pilot under the heading Recognition Factors. Other factors that can influence a pilot's overall performance, including visual performance, are grouped under the heading of Indirect Performance Factors. The primary purpose of the table is to give the reader an appreciation for the number of factors that can influence image legibility. Numerical values that have been found to provide optimum (ideal) visual performance are included in the table for some variables. The table includes most of the more important variables that influence information legibility, however, it is not intended to provide a complete listing of such variables. Variable entries in the table are considered, for the most part, self-explanatory and will be further explained only as the need to do so arises later in the report.

It should be noted that, in its simplicity, the diagram in Figure 3.1 fails to explicitly indicate the fact that information from throughout the human's instantaneous field of view is perceived not just information from the displays, as is indicated in the diagram. The figure also lumps image sensing and perception. These visual system functions are typically discussed separately, but for the purposes of this report it is not necessary to

Table 3.1. Factors that Influence Pilot Performance.

INDIRECT PERFORMANCE FACTORS

1. EXTERNAL ENVIRONMENT

HEAT	ACCELERATION	ILLUMINATION
NOISE	NUCLEAR RADIATION	VISIBILITY
VIBRATION	AIR COMPOSITION	PRESSURE

2. TASK LOADING

SPEED/ACCURACY REQUIREMENT — MULTIPLICITY OF TASKS (WORKLOAD)

3. INTERNAL ENVIRONMENT

MENTAL CONDITION
- MOTIVATION
- ATTENTIVENESS
- CONCENTRATION LEVEL
- PRIOR EXPERIENCE
- PERSEVERANCE
- MENTAL DEXTERITY
- STRESS-ANXIETY

PHYSICAL CONDITION
- COORDINATION
- STRENGTH
- ENDURANCE
- PHYSICAL DEXTERITY

LEGIBILITY FACTORS

IMAGE CHARACTERISTICS

LUMINANCE FACTORS

- L_S Display Symbol Luminance
- ΔL Image Difference Luminance
- ΔL_P Perceived Image Difference Luminance
- L_D Display Background Luminance
- L_P Panel Surround Luminance
- L_I Internal-Field Surround Luminance
- L_U External-Field Surround Luminance
- L_B Luminance of Sun or Bright Objects
- θ_H Horizontal Angle of Object
- θ_V Vertical Angle of Object
- α_C Critical Detail Dimension
- Stroke Width (% of Height): 12 - 20
- Aspect Ratio (Width to Height %): 50 - 100
- Slant; Vertical Best: < 10°

- Viewing Angle: < 30°

COLOR FACTORS (Hue, Purity)

- Color of Image
- Color of Background
- Color or Panel
- Color of Internal Surround Field
- Color of External Surround Field
- Color of Illuminance or Glare Source
- Color Signal to Noise Ratio

TIME FACTORS

- Image/Display Vibration
- Human Vibration
- Image/Display Acceleration
- Human Acceleration
- Image Velocity
- Information Update Rate
- Flicker Rate on Flash Rate Coded Information

IMAGE QUALITY

LUMINANCE FACTORS

- Relative Image Edge Gradient
- Picture Element Size-Dimensions X by Y
- Picture Element Density
- Luminance Uniformity
- Luminance Averaging Diameter/Task
- Image Registration
- Number of Comparatively Distinguishable
- Luminance Levels (Shades of Gray)
- Electrical/Optical Crosstalk

COLOR FACTORS

- Hue Uniformity
- Purity Uniformity
- Number of Comparatively Distinguishable Colors

TIME FACTORS

- Refresh Rate
- Persistence
- Image/Observer Relative Motion Induced Flicker
- Image Jitter

IMAGE COMPLEXITY

LUMINANCE FACTORS

- Number of Distinguishable Images Employed
- Luminance Image Clutter (Signal to Noise Ratio or the Image Rivalry Ratio)
- Image Spacing (% of Height): 26 - 63
- Word Spacing (% of Height): 60 Minimum
- Line Spacing (% of Height): 50 Minimum
- Image Location in Observer Visual Field

COLOR FACTORS

- Number of Distinguishable Color Coded Images for the Background Colors to be Used
- Color Image Clutter (Signal to Noise Ratio)

TIME

- Number of Changes in Display Background Luminance or Color Per Unit Time
- Rate of Change of Image Clutter in Display Background
- Number of Independently Moving Images
- Luminance Change Induced Flicker
- Luminance Constancy
- Color Constancy
- Image-Motion-Induced Image Periphery Flicker
- Image Motion in Spatially Discrete Steps

RECOGNITION FACTORS

IMAGE SHAPE

SCENIC/VIDEO

SYMBOLIC

- Symbol Shapes
- Alphanumeric Font
- Scale Font
- Graphics

IMAGE COLOR (Single, Multi, True and False Color Rendition)

INFORMATION FORMAT (Multiple Imagery)

IMAGE PLACEMENT

IMAGE DYNAMICS

IMAGE INFORMATION CONTENT (Expressed in Picture Elements Per Image)

TARGET DETECTION

TARGET IDENTIFICATION

DISPLAY SIZE

IMAGE SIGNIFICANCE

ALPHABETS USED - Number of CHARACTERS

VOCABULARY - COMPOUND SYMBOLS/WORDS

PRIOR EXPERIENCE (i.e., Realism, Familiarity)

INFORMATION CODING

- Shape - Number of Absolutely Distinguishable Shapes
- Image Texture - Hatching, Shading
- Colors (Symbol/Background) - Number of Absolutely Distinguishable Colors: 5 - 8
- Flash Rate - Number of Absolutely Distinguishable Flash Frequencies; Range: 0.25 - 12 Hz; 1/3, 1, 4 Hz optimum
- Luminance - Number of Absolutely Distinguishable Luminance Levels: 2
- Size - Number of Absolutely Distinguishable Sizes of Imagery

IMAGE/REAL WORLD DYNAMIC RELATIONSHIPS

- Motion Scaling
- Observer Perspective/Scaling of Imagery

IMAGE ORIENTATION WITH RESPECT TO OBSERVER

TIME - Display Information Update Rate

make this distinction.

The emphasis of this report is on pilot image perception (i.e., perceptibility) requirements or equivalently, if expressed in terms of external scene or display design variables, pilot image legibility requirements. It is the latter viewpoint that will be adopted throughout the balance of this report.

The data analysis approach adopted for use in this and subsequent sections of this report attempts to establish, through comparisons, that the data selected for examination from the experimental literature are valid and then attempts to identify any commonality or differences in the data and to resolve the sources of apparently conflicting results between the different studies. To do this involved: (1) initially becoming familiar with the available visual research data base,[11,12] (2) identifying significant variables and their interrelationships,[13,14] (3) converting the identified variables into basis sets of mutually exclusive variables,[15] and (4) establishing the quantitative relationships that exist between these variables.

3.1.1. Luminance Functional Description and Variables

Light, entering the eyes, contains all of the information the human is capable of sensing visually and therefore serves as the common point at which to interface the external independent variables upon which both human visual perception capabilities and display image legibility requirements can be characterized. The luminance functional,

$$L(r, \theta, \phi, \lambda, \psi, t) , \tag{3.1}$$

serves as a theoretical construct that completely describes the sensed visual scene and uniquely determines human visual performance when the full range of each of the independent variables it depends upon is specified. The luminance functional independent variables are defined as follows: the location within the observer's field of view, (r, θ, ϕ), the wavelength, λ, the phase, ψ, and the time, t. The spherical angle variables, θ and ϕ, define the direction of the line-of-sight followed by light entering the eyes from a point of origin for the spectral luminance magnitude, $L(\lambda)$, at a distance, r, from the eyes. At that point of origin, the spectral distribution of the luminance as a function of wavelength, λ, determines the color of light the human will sense, provided there are neither intervening nor more distant sources of luminance that can add to and

thereby alter the sensed spectral distribution. The phase, ψ, of light radiation emanating from most light sources found in nature is randomized and, in any event, the human is not able to observe the phase of light radiation directly. Observable visual effects, caused by the phased interactions of coherent laser light sources and the phased interactions of light radiation due to interference or diffraction effects, can create patterns with spatial, color and temporal dependences that are perceptible. Changes in the luminance functional as a function of the final variable, time, are primarily responsible for the information conveyed to an observer via the light perceived by the human visual system. To make this luminance functional description of the light to which the human visual system is exposed complete, it must be recognized that, as a further complication of this interface, binocular vision is based on each eye being exposed to a slightly different luminance functional.

3.1.2. Practical Legibility Variables

In general, the visual information perceived by a pilot does not relate directly, on a one-on-one basis, to the luminance functional variables. Instead, the information perceived depends on the integrated response of the brain to the multitude of signals sampled and sent to it by the discrete array of visual receptors in the eyes when they are exposed to the luminance functional spatial, spectral and temporal variables within the observer's field of view. By exploring and analyzing the relationships between these legibility variables, to achieve and maintain acceptable constant levels of visual performance, experimentally derived legibility requirements can be expressed entirely in terms of these external luminance functional variables.

As a theoretical construct, the luminance functional provides a valid means of visualizing an interface suitable for both display design engineers to derive design requirements for the specific display technology being applied and human factors engineers to specify the pilot's mission-oriented information legibility requirements. In practical terms, however, a set of variables that remain valid at the luminance functional interface but are easier to deal with need to be employed. Table 3.1 provides such a set of variables.

3.1.3. Common Misconceptions

The luminance functional was introduced in this report for the primary purpose of reminding readers that light, from the visual scene the observer is exposed to, conveys all of the visual information that a human is capable of extracting from his or her visual environment, and that includes the light emitted, transmitted, transflected or reflected from the electronic displays, which are the principal focus for the development of the legibility relationships described in this report. A common misconception among display manufacturers, display design engineers and some people who have written books on the subject of electronic displays, is that it is not possible to create a common set of legibility requirements applicable to any electronic display, independent of the display technology or display operating mode employed in its construction. According to this point of view and for reasons that are never explicitly identified, an implementation of one specific display technology, is claimed to be inherently more legible than all the others. These claims of superior legibility are usually based on subjective assessments of the legibility of displays, most typically using sources of simulated sunlight, but sometimes using direct sunlight. Less frequently the claims are based on laboratory measurements. However, in all instances where a demonstration or test seems to be valid, the tests have proven to be founded on incomplete simulations of the ambient illumination and glare source exposure conditions experienced by aircrew members in aircraft cockpits under operational flight conditions. Display technologies and operating modes afforded this special treatment have not surprisingly changed several times over the past thirty years, as the claims have been shown to be unjustifiable under closer examination or more thorough testing.

The most recent claims for special legibility properties involved backlighted color active matrix liquid crystal displays implemented using the transmissive operating mode. The development of more comprehensive tests to evaluate the sunlight readability of electronic displays, under the combined influence of diffuse and specular reflections and with compensation for sun glare induced veiling luminance, have shown the claims are unfounded but they nonetheless continue to persist. The fact that most display technologies

react very differently to exposures to natural ambient illumination, coupled with the large differences in the design and optical filtering approaches needed to achieve satisfactory legibility, aids in preserving this misconception. The other major factor contributing to this misconception is a failure to understand the full extent of the adaptive capabilities of the human visual system, which under less than complete illumination test conditions can leave the impression a display is more legible than it would be if exposed to more comprehensive ambient illumination tests.

3.1.4. Analysis Approach for Interpreting Published Data

The analysis approach, selected to establish the legibility requirements of pilots and other aircrew members involved analyzing published experimental test data, collected using essentially ideal imagery under nearly ideal task loading, viewing and environmental conditions, from as many experimenters as possible. The intent of selecting this approach was to create a situation where having once established a known baseline for ideal legibility image data, under ideal viewing conditions, it would then become easier to model the data and, afterwards, integrate the effect of legibility variables that degrade visual performance or, where possible, to simply to avoid such degrading influences.

The key to implementing this analysis approach involves the selection of published experiments that collected test data using test symbology of high image quality, low image complexity and using the simplest of visual tasks (i.e., so as to cause the test subjects to invoke the higher level mental information processes needed for image recognition, image identification and image significance determinations only to the minimum extent necessary to perform the experiment). By selecting published experiments in this fashion, all of the legibility variables in Table 3.1 except those being investigated could either be set to an ideal constant value or be eliminated. Since experiments involving humans are typically designed to reduce their complexity and use a small number of controlled test variables, with the balance held constant, the most difficult problem encountered implementing this approach involved finding published experiments that investigated a sufficient number of the legibility test variables of interest.

3.1.5. Definition of Practical Legibility Test Variables

The significant independent variables for determining fundamental legibility requirements in a simulated aircraft cockpit illumination test environment are listed from Table 3.1 as follows:

L_S = Display Symbol or Image Luminance
L_D = Display Background Luminance
L_P = Panel Luminance
L_U = Surround-field Luminance
L_I = Infield Luminance
L_B = Luminance of Sun or Other Glare Source
θ_H = Horizontal Angle of Glare Source
θ_V = Vertical Angle of Glare Source
F_T = Test Symbol Color
α_C = Symbol or Image Critical Detail Dimension

The light variables in the preceding variable test set are considered self-explanatory when their names are interpreted using the crewstation luminous variable geometry illustration shown in Figure 3.2. The illuminance of the glare source, E_B, incident on the cockpit and the illuminance incident on the displays and panels, E_P, are not shown in the above list, though they are shown in cockpit drawing of Figure 3.2, because they are not perceived light variables, but, rather, can stimulate the color and luminance variables in the above list through reflections.

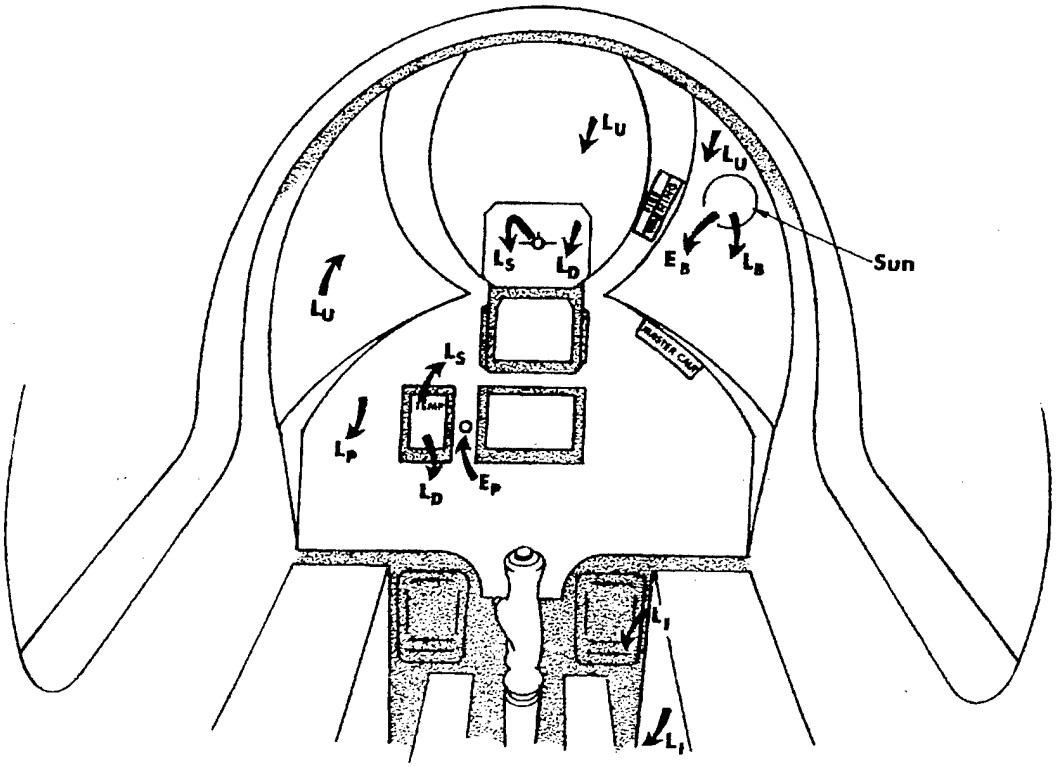
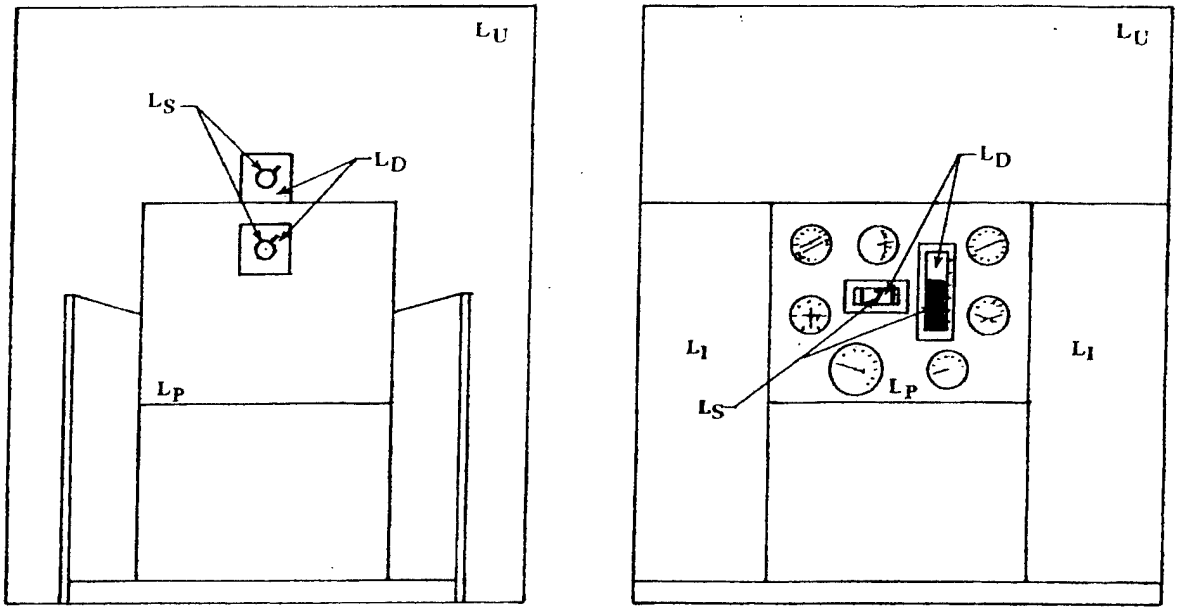


Figure 3.2. Crewstation Luminous Variable Geometry.



$\triangle L = L_S - L_D$ = Threshold Symbol Luminance
L_S = Symbol Luminance
L_D = Display Luminance

L_P = Panel Luminance
L_U = Surround - Field Luminance
F_T = Test Symbol Color
L_I = In-Field Luminance

Figure 3.3. Luminance Measurement Geometries and Variable Definitions.

Experiments identified, which satisfied the previously described analysis approach criteria, consisted of baseline visual acuity experimental tasks, with human visual performance assessed at a fixed 50%, 90%, 95% or 100% correct response legibility level and with the collection of luminance requirements limited to static display imagery. The test dependent variables used varied with the experimenters, but were limited to only two of the variables in the preceding list. One of these dependent variables was visual acuity or, equivalently, the inverse of visual acuity, the image critical detail dimension, α_c. The other dependent variable used in these experiments was the image (symbol) difference luminance, ΔL, that is, the luminance increment of the measurable image or symbol luminance level, either above or below, the measurable background luminance value, L_D. The defining expression for the image difference luminance, ΔL, can be expressed as follows:

$$\Delta L = L_S - L_D. \tag{3.2}$$

This quantity can be thought of as representing the absolute visual contrast between a symbol and its background. Furthermore, based on the evidence in the literature, this is the quantity most closely associated with the "luminance" magnitude visually perceived by a human when viewing an image.

In the earliest investigations of legibility that were found to treat the appropriate variables, only three variables were used rather than the complete set of variables included in the preceding list. The variables tested were the size of the test image critical detail dimension, α_c, the image difference luminance increment, ΔL, and the background luminance, L_D. Except for one experimenter, the legibility accuracy level selected to evaluate the experiment results was held constant. These experiments used dependent variables that are equivalent to either the image critical detail dimension or the image difference luminance, with the other two variables treated either as the independent variable or as a controlled parameter.

Although the earliest investigations analyzed use the image difference luminance, ΔL, to report experimentally derived legibility test results, it has become a common practice in the literature to express such results using a mathematically related variable, the relative contrast, C. The relative contrast, or simply the "Contrast," is defined by the following relationship:

$$C = \Delta L / L_D. \tag{3.3}$$

This variable is commonly expressed both as a ratio, which is sometimes called the "Contrast Ratio," and, when multiplied by 100, as a percent, "Percent Contrast." To interpret correctly which quantity is being referred to, care must be exercised when using contrast values, since the term contrast is used to describe each of these luminance ratios, as well as others that us different defining equations. The very large variations that occur in both the image difference luminance and in the contrast, as a function of changes in the independent variables, makes it virtually impossible to decide whether a stated value of contrast, C, refers to a ratio or a percent, based solely on the observation of the magnitude of the quantity. Because the relative contrast, C, is less meaningful, from a perceptual standpoint, than the image difference luminance, ΔL, the latter variable is used most often to present the experimental data contained in this report.

Figure 3.3 provides a symbolic representation, in a two dimensional format, of the simulated cockpit luminance environments used in two of the more thorough display image difference luminance requirements studies conducted to date. Both of the investigations simulated the illumination environments encountered in military aircraft cockpits. The cockpit mockup illustrated on the left shows the visual environment variables used in a study by P. Jainski,[16] and the one on the right shows the visual environment variables used in a study sponsored by the Air Force Flight Dynamics Laboratory, under contract to Westinghouse in 1969.[17] Both studies went to considerable effort and expense to represent the ambient light exposures pilots experience in flight accurately, and in physical geometries consistent with those of fighter aircraft cockpits. The Jainski investigation provided an accurate but austere representation of the cockpit physical geometry of the F-104G aircraft. Beyond its simulated head-up and head-down displays, the Jainski simulator was devoid of any of the instruments, controls or other accouterments normally expected in an aircraft cockpit, but the lighting simulator made up for this by providing an extensive capability for the exercise of experimental control over the internal and external luminance environment pilots would experience in an aircraft cockpit, from complete darkness to full daylight conditions. Conversely, the Westinghouse study, which was intended only to simulate high level

daylight ambient illumination conditions, provided a more accurate representation of the cockpit physical geometry, which included the use of an actual aircraft canopy, and a complement of aircraft instruments and controls, beyond the displays used for the tests. Light sources specifically designed by Westinghouse to simulate the spectral content and also the intensities of the sun and sky accurately were employed, however, the resulting illumination environment was limited by the inability to make small changes in the illuminance levels incident upon the cockpit, and, consequently, the tests resulted in a small number of experimental data points.

In the list of independent variables specified above, only changes in the test symbol color had a very small influence on the image difference luminance requirements reported by Jainski. The Flight Dynamics Laboratory investigation did not test for changes in the test image colors.

3.2. Image Critical Detail Dimension

The image critical detail dimension is a legibility variable that characterizes the smallest feature of an object that an observer must be able to discern to make it possible to recognize, identify or determine the significance of the object. Since each of these visual tasks would require discriminating successively smaller features of a complex military target that is to be recognized, identified and have its significance interpreted, each target actually has multiple critical detail dimensions. Furthermore, as the number of visually very similar friend and foe aircraft in an operational theatre increases, the critical detail dimensions of the target physical features that must be discerned to enable performing, for example, an image identification task, becomes progressively smaller, even for targets at a fixed visual range.

In practice, as a target moves closer to an observer, the angle subtended by target features that must be discerned to permit image recognition, identification and a determination of image significance to occur become progressively larger. As the target range decreases, each of the target critical detail dimensions that must be successively discerned to perform the different visual tasks eventually subtend an angle that matches the minimum subtended angle the observer is capable of perceiving, for the viewing conditions present at the time.

The minimum perceptible visual angle that a human is capable of visually discriminating, a perceptual variable, can, therefore, be equated to the analogous legibility variable, the minimum critical detail dimension that must be discerned, when the latter is expressed in angular measure. Taking the inverse of the minimum perceptible visual angle yields an alternative perceptual variable termed the minimum separable visual acuity.

In the first part of this section, the experimental basis for associating, the critical detail dimension of an image, a legibility variable, as a direct correlate to its perceptibility equivalent, the minimum separable visual acuity, will be presented. Having established this experimental basis for the fundamental role played by the critical detail dimension of an image, the second part of the section describes experimental data that shows the relationship between image difference luminance, the display background luminance and the critical detail dimension of an image.

3.2.1. Form Identification Dependence on the Image Critical Detail Dimension

The experimental data of Bitterman and Krauskopf [18] in Figure 3.4 shows image difference luminance thresholds for image detection and image form identification tasks. The results obtained for image form identification tasks show that symbol identification, for different simple geometric forms, is strongly correlated to the length of the critical detail dimension of the symbol. A further analysis of the experimental data collected by these investigators showed that symbol identification depends very little, if at all, on other geometric parameters, such as: length, width, height, symbol area, symbol perimeter, or on the ratio of a symbol perimeter to its area. The experimental data collected for the image difference luminance thresholds of triangles by

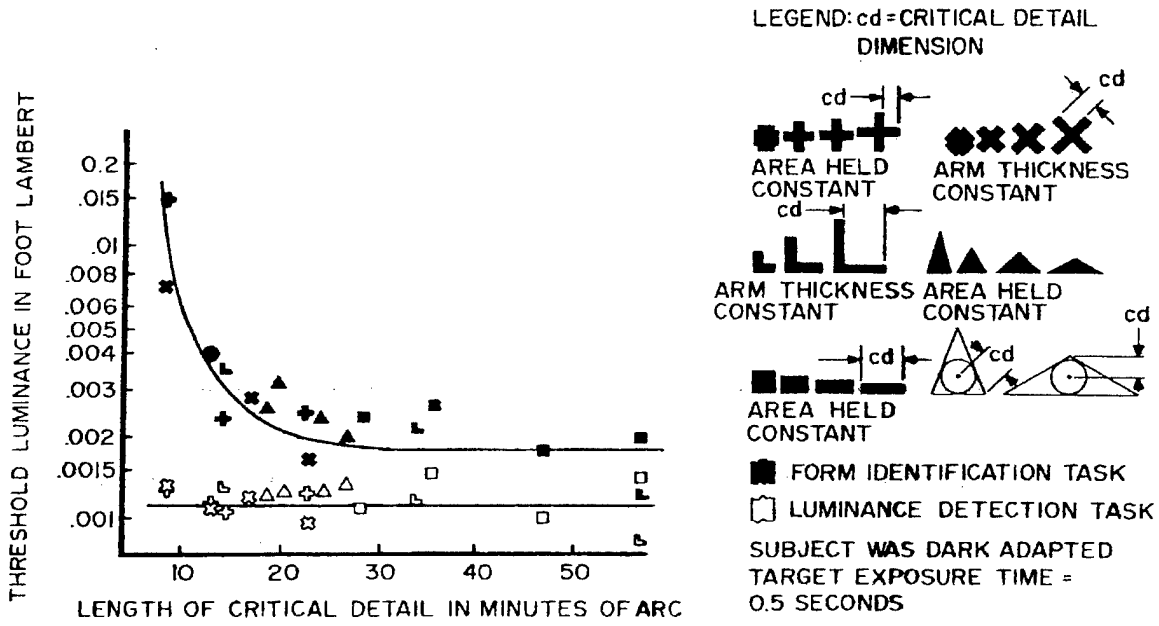


Figure 3.4. Image Detection and Form Identification Luminance Thresholds (Bitterman & Krauskopf, 1953).

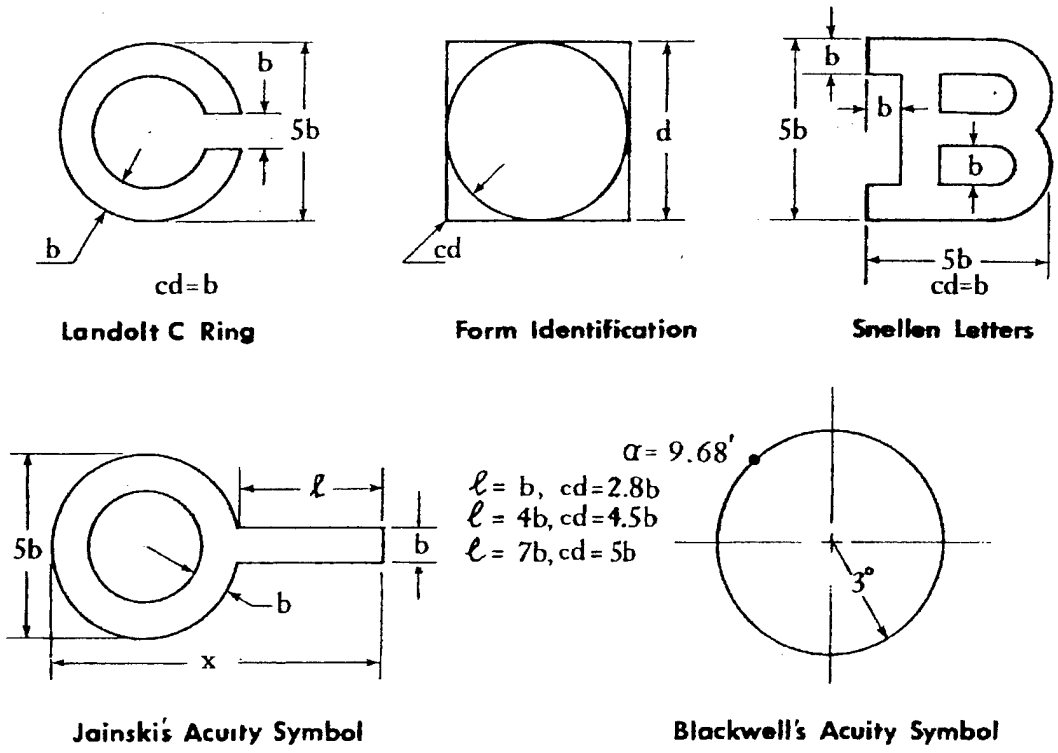


Figure 3.5. Visual Acuity Symbol Geometries and Critical Detail "cd".

Bitterman and Krauskopf, which was originally presented in a separate figure against the length of the triangles base, were incorporated into Figure 3.4 by replotting their results using the triangle critical detail dimensions shown in the triangle outlines in the legend of the figure.

Figure 3.5 illustrates a number of the symbol geometries used in minimum separable visual acuity testing in the past. It also shows the critical detail dimensions assigned to these visual acuity test images. Tests involving the Landolt C Ring require the test subject to identify in which of eight equal angular orientations the gap in the C is oriented. The form identification symbol shown in Figure 3.5 illustrates the critical detail dimension that must be discriminated to distinguish between a circle and a square, but the tests could also involve the use of other geometric symbols, such as those shown in Figure 3.4. Acuity tests using Snellen letters require the test subject to identify letters, presented randomly, from a Snellen letter alphabet set, that is designed using the criteria shown in Figure 3.5 for the Letter B. The critical detail dimension for the three digit numeric readout used in the Flight Dynamics Laboratory study most nearly corresponds to the Snellen letter measure illustrated.

The visual acuity symbol chosen by Jainski is not a particularly good symbol for visual acuity studies. Unlike the other visual acuity symbols shown in Figure 3.5, the one used by Jainski has several different critical detail dimensions, depending on the values assigned to its dimensions. This symbol is not in common use, and presented difficulties when attempting to assign critical detail dimensions to Jainski's experimental data. The following rationale, coupled with the need for the critical detail dimension magnitudes to adhere to the progressive ordering of their corresponding graphed characteristic curves, on the image difference luminance versus display background luminance plots, was used in making these assignments. Depending on whether the protrusion on the Jainski symbol is long ℓ = 7b, short ℓ = 1b or intermediate ℓ = 4b the symbol, as it is made either larger or more luminous, is recognized, respectively, first as a line for ℓ = 7b, first as a circle for ℓ = 1b and more indecisively as a rectangle for ℓ = 4b. The critical detail dimension, for the ℓ = 7b case, occurs when the circular bulge on the end of the line can first be discerned, that is for α_c = 5b with b expressed in angular measure. In a similar manner, the critical detail dimension, for the ℓ = 1b case, occurs when the direction of the protrusion can first be distinguished relative to the center of the ring. This occurs for α_c = 2.8b, which is small enough for the inner diameter of the ring, 3b, to first be resolved and then to act as a reference for comparing the outer radius of the ring, 2.5b, which cannot be resolved, with the radial distance to the end of the protrusion, 3.5b, which can be resolved. In the ℓ = 4b case, the diameter of the circle and the direction of the protrusion are resolved almost simultaneously at α_c = 4.5b.

The Blackwell acuity symbol is shown in Figure 3.5 because Blackwell's data[19] is used later in a comparison to Aulhorn and Harms[20] minimum separable visual acuity data and with the daylight difference luminance requirements determined in the formerly cited Flight Dynamics Laboratory cockpit illumination simulator investigation. Blackwell's visual acuity test symbol actually corresponds to an image detection rather than an image identification task. This is because the discrimination test involves correctly detecting the position of the circular spot (or alternatively at even lower image difference luminance levels simply detecting the presence or absence of a fixed spot) rather than correctly discriminating the shape of an image, as is required for form identification. The test subjects in Blackwell's tests had to discriminate the location of the spot in one of eight symmetrical positions correctly, relative to an illuminated red reference mark at the center of the circular locus that is not shown. Blackwell's image detection task produced image difference luminance requirement results that became progressively smaller as the background luminance was reduced under scotopic illumination levels. This result is very different from the image difference luminance requirement characteristics associated with discriminating an image's shape, at low background luminance levels.

Alphanumeric identification like symbol identification is based on the observer's ability to discern the critical detail dimension of an image. As a result, the conditions that must be met to permit symbol identification are the same as those required to permit alphanumeric identification. The truth of this assertion is demonstrated by the fact that, for equivalent symbol and background luminance conditions, the size requirements for alphanumerics, as determined by Shurtleff, et al,[21] and Howell and Kraft,[22] and the size requirements for symbols, as determined by Bowen, Andreassi, Traux, and Orlansky[23] and Steedman and

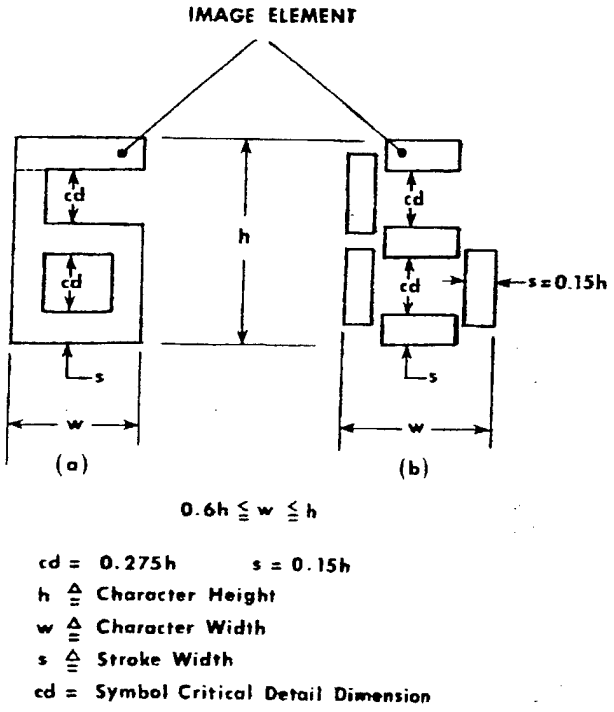


Figure 3.6. Reference Numeric Characters.
a) Continuous Stroke Image Elements
b) Continuous Bar Segment Image Elements

Baker,[24] are essentially the same (i.e., 15-20 minutes of arc for 99% identification legibility).

Character sets that meet the design criteria for Snellen letters produce essentially ideal image identification performance, however, a variety of alternative fonts with stroke widths of between 12 and 20% of the character height have been shown to produce equally good performance, provided they have the same critical detail dimension.[25] Figure 3.6 shows the critical detail dimensions for a numeric character having stroke width dimensions more typical of those found in actual display applications. The critical detail dimensions shown would be correct for a numeric character set made up of ten digits. In expanding from numeric to alphanumeric and then to graphic character sets, the critical detail dimension that must be seen typically becomes smaller as the number of characters in the set increases. Adding characters to a set, eventually increases the number of easily confused members within the set. This places additional emphasis on the observer being able to see the smallest dimensional features of characters, to be able to discriminate between them correctly.

The value in recognizing that ideal grey shade encoded images, graphic symbols, alphanumerics and numerics, having the same critical detail dimensions, also have the same legibility requirements, irrespective of large differences in their sizes, shapes and appearance, is that the same set of image difference luminance versus background luminance requirement characteristics can be used to represent all types of visual images. While alphanumeric characters and geometric symbols are among the simplest of ideal images, the critical detail dimension plays the same role in determining the legibility for more complex imagery, including imagery that is grey shade and/or color encoded. It should also be noted that, provided the degradation in the rendition of images caused by blur, distortion and so fort is not too severe, increases in image difference luminance of flawed imagery can often be used to compensate and thereby achieve visual performance equal to that for undegraded imagery having the same critical detail dimensions.

These preliminary investigations of legibility variable interrelationships resulted in the image difference luminance, ΔL, the background luminance, L_D, and the critical detail dimension, α_c, of imagery, being identified as the variables most crucial to a basic characterization of human image luminance requirements. The goal of the present analysis was to determine how the difference luminance, ΔL, must be changed to maintain a fixed level of performance as internal and external cockpit surround luminance variables, L_P and L_U respectively, are changed. As a reference baseline for this analysis all other image characteristic variables were considered to have fixed optimum performance values (e.g., static or slow-moving imagery, no vibration, no acceleration, and so forth).

3.2.2. Image Difference Luminance Relationship to Minimum Separable Visual Acuity

Minimum separable visual acuity data of Aulhorn and Harms,[26] corresponding to a 50% accuracy visual identification performance level, is shown for objects brighter than their backgrounds in Figure 3.7.A and for objects darker than their backgrounds in Figure 3.7.B. This data was collected with minimum separable acuity (i.e., image critical detail dimension) serving as the dependent visual test variable, image difference luminance as the controlled independent variable and display background luminance as a controlled independent parameter. Consequently, the original data of Aulhorn and Harms was plotted as shown in Figure 3.7.

Figure 3.7 also shows the average data complied by Moon and Spencer from six experimental studies using an error measure of about 50%.[27] These studies were conducted using illuminated dark printed images on light backgrounds. Unlike the threshold image difference luminances and corresponding low contrasts for the test images of the other experiments' data reported here, the contrast ratios of the test images, for the experimental results compiled by Moon and Spencer, were high and had fixed values as the illumination level was changed. These results are presented because, as may be seen in Figure 3.7B, they serve both as a bound on the visual acuity data of Aulhorn and Harms for negative contrast images and as a partial confirmation of the validity of their data.

In spite of the choice of dependent and independent variables used to collect the data shown in Figure 3.7, it is possible to replot the data in the format shown in Figure 3.8 with the image difference luminance on the ordinate, the display background luminance on the abscissa and the image critical detail dimension as a parameter. A display design advantage is also achieved by plotting the Aulhorn and Harms data in this way. Because the angular subtense requirements of an image's critical detail dimension are determined by minimum separable visual acuity angles, which the eyes can only just resolve, the curves of Figure 3.7 also represent image difference luminance characteristics for images with constant critical detail dimensions and at a constant level of human visual performance, that is, at constant legibility. This makes tracking the image difference luminance requirements, for any image having a known critical detail dimension and for a constant legibility level, directly readable from the graph in Figure 3.8.

After completing of the conversion of the Aulhorn and Harms data in the early 1970s, it was realized that the image difference luminance is a more sensitive measure of what the human is perceiving, than the image contrast measure used by Blackwell. Blackwell is reputed to have chosen to plot contrast as the dependent variable because, for moderate to high daylight viewing conditions the contrast becomes nearly constant, when plotted as a function of the background luminance, although it still exhibits a small but pronounced slope. When graphed as a full logarithmic plot of image difference luminance versus background luminance, with the angle subtended by the test image as a parameter, as shown in Figure 3.8, Blackwell's image detection task data only changes between two approximately constant positive slope values, for the range of image difference luminance values shown in the figure. The full extent of the changes in these characteristics are presented in figures and described in Section 3.7.

In comparison to Blackwell's image detection task data, two of the three critical detail dimension plots of the Aulhorn and Harm's data in Figure 3.8 exhibit zero slope for night display background luminance levels

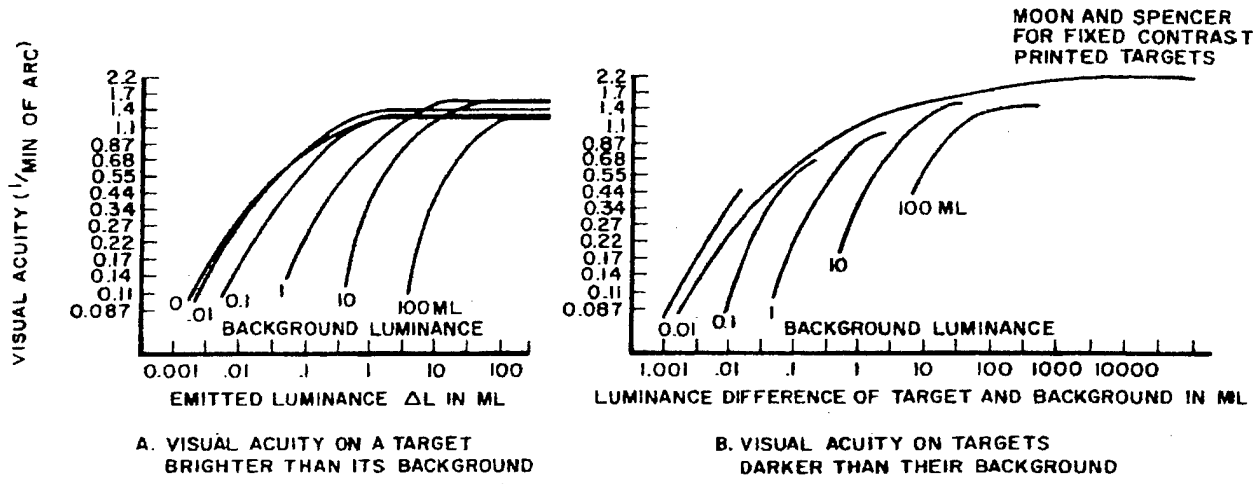


Figure 3.7. Minimum Separable Visual Acuity (Aulhorn and Harms).

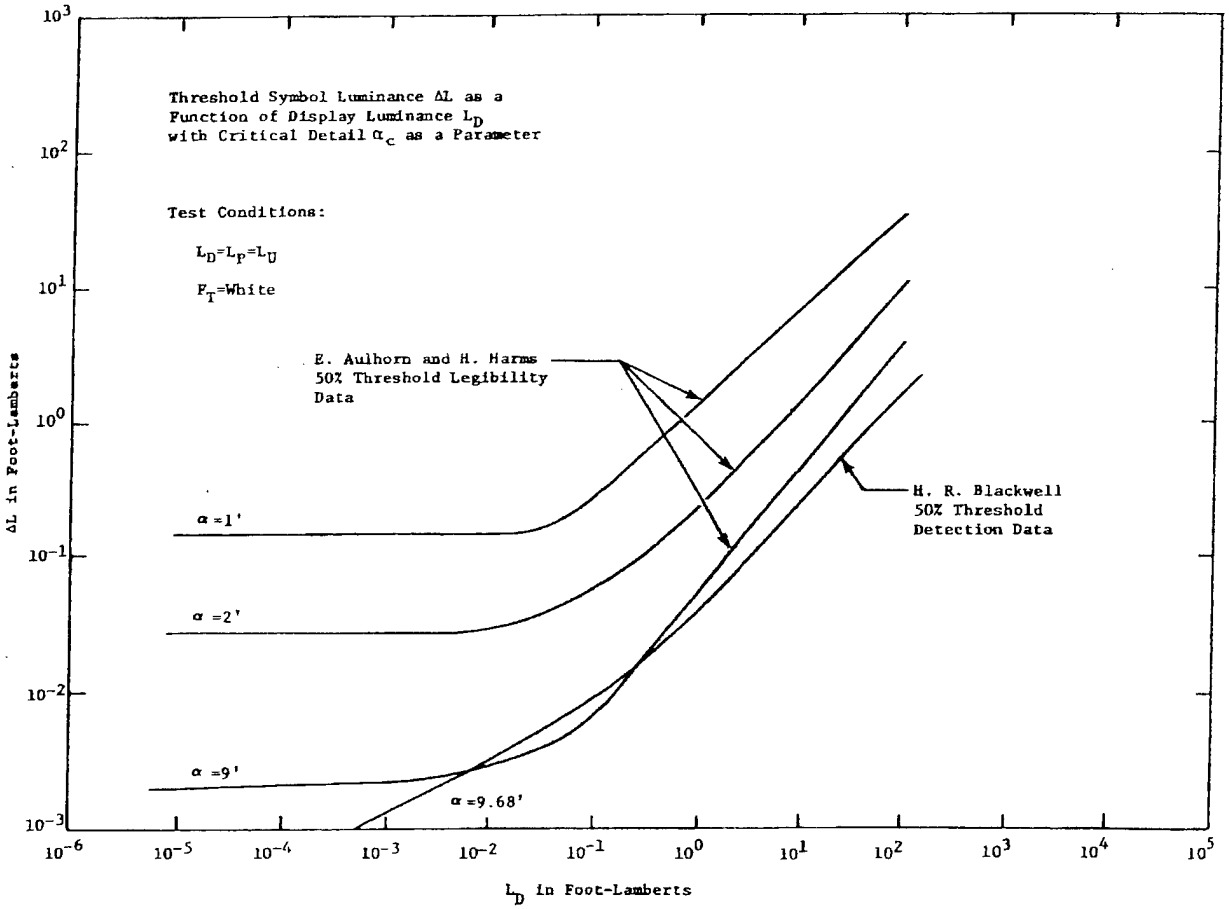


Figure 3.8. Aulhorn & Harms Minimum Separable Visual Acuity Data Replotted as Image Difference Luminance Versus Background Luminance with the Test Symbol Critical Detail Dimension as a Parameter.

in the scotopic range of vision, and transition in the mesopic vision region to an almost constant slope under daylight luminance levels, in the photopic range of vision. The correlation of these curves with the known ranges of the physiological sensitivity responses of the eyes' light receptors supports the view that image difference luminance closely tracks the information perception processes of the human visual system. The constant image difference luminance response at night also validates the logical expectation that to keep the eyes' high resolution cone light receptors active, which is a necessity to make image identification on cockpit displays possible at night, a minimum difference luminance level would have to be reached and, thereafter, be maintained as the background luminance is reduced. Consequently, this data presentation technique of Figure 3.8 does convey an immediate insight into the fact that underlying differences exist in the visual perception processes involved in image detection and image identification tasks, as evidenced by the different behaviors of the image difference luminance requirement characteristics for these two visual tasks under night background luminance levels.

3.3. Image Difference Luminance Requirements

Preliminary efforts to analyze image difference luminance data concentrated on making comparisons between the results of different experimenters to determine the commonality that might exist between their data. To perform this comparison, the image difference luminance versus display background luminance characteristic format of Figure 3.8 was employed, with the image critical detail dimension and the performance level of the subject serving as constant parameters. Although many legibility studies were found reported in the literature, few of these included the needed variables, and many of those that did either involved very limited ranges of the variables or key information was missing.

In this section, the validity of image difference luminance as a principal variable in establishing image legibility requirements is explored first from historical data comparison perspective and then through comparisons with the experimental test results of Jainski. Next, the effects of pilot visual performance criteria on the image difference luminance requirements are interpreted as a means of showing the consistency between the different experimenter's results. With the fundamental validity of Jainski's results confirmed through these comparisons, the significance of the Jainski findings are further expanded upon by introducing the effects of making changes in cockpit panel and external surround luminance levels, variables that were systematically explored only by the Jainski investigation. Finally, key legibility dependence features of the Jainski cockpit panel and external surround luminance test results are identified and described.

3.3.1. Qualitative Comparisons of Historic Image Difference Luminance Characteristics

Until 1971, when a summary paper entitled "The Status of Human Perceptual Characteristic Data for Electronic Flight Display Design" was presented at a North Atlantic Treaty Organization (NATO) Advisory Group for Aerospace Research and Development (AGARD) Symposium,[28] the only investigations found that came close to fully meeting the analysis criteria were the previously cited studies of Blackwell, Aulhorn and Harms, and King, Wolletin, Semple and Gottelmann and an investigation by Chapanis.[29] To more easily see the relationships that might exist, the data from each of these investigations were plotted on square full logarithmic graph paper, 22.5 inches on a side. The resulting graph was very cluttered, even at its full size, so the presentation of that information has been broken into separate smaller graphs this report.

Figure 3.8, introduced previously, shows the Aulhorn and Harms minimum separable acuity data for a 50% accuracy of image identification in a comparison with Blackwell's image difference luminance characteristic for the 50% accuracy of detection of a circular target subtending an angle of nominally ten minutes of arc. Figure 3.9 shows the 99% accuracy image identification data of King, Wolletin, Semple and Gottelmann, which includes a numeric readout display having an image critical detail dimension of 15.3 minutes of arc, in a comparison with the 50% accuracy image detection data of Blackwell, for a circular image subtending 9.68 minutes of arc, and obtained using two different experimental procedures. The higher of the

two Blackwell image difference luminance characteristics shown in Figure 3.9 is a plot of the same data as the Blackwell characteristic shown in Figure 3.8.

Figure 3.9 was originally published in the previously mentioned AGARD Symposium summary paper to demonstrate that parallel lines provide a reasonably good fit of both sets of data under daylight viewing conditions. Referring to Figure 3.8, it may be seen that two of the three characteristics of Aulhorn and Harms can also be reasonably well fit using straight lines parallel to the Blackwell 50% threshold legibility detection data. Each of the characteristics in Figure 3.8 were drawn by extracting the emitted luminances from Figure 3.7A corresponding to the intersections of straight horizontal lines, having visual acuities corresponding to the image critical detail dimensions shown in Figure 3.8, with the background luminance characteristics of Figure 3.7A. Because this figure contains only six background luminance characteristics, at multiples of ten between 100 and 0.01 mL (i.e., 92.9 and 0.00929 fL) and one at 0 mL, only six image difference luminance levels were available to draw the constant image critical detail dimensions characteristics shown in Figure 3.8. The zero background luminance characteristic was interpreted as being nominally 10^{-6} fL, typical of a dark room environment, and the coalescence of the characteristic with the 0.01 mL characteristic was interpreted as no change in the emitted luminance (i.e., image difference luminance) and, consequently, a zero slope below 0.01 mL. In the case of the nine minute of arc characteristic, the small slope shown below 0.002 fL of background luminance is due to the small image difference luminance between the 0 and 0.01 fL characteristics for the 0.111 visual acuity intercepts.

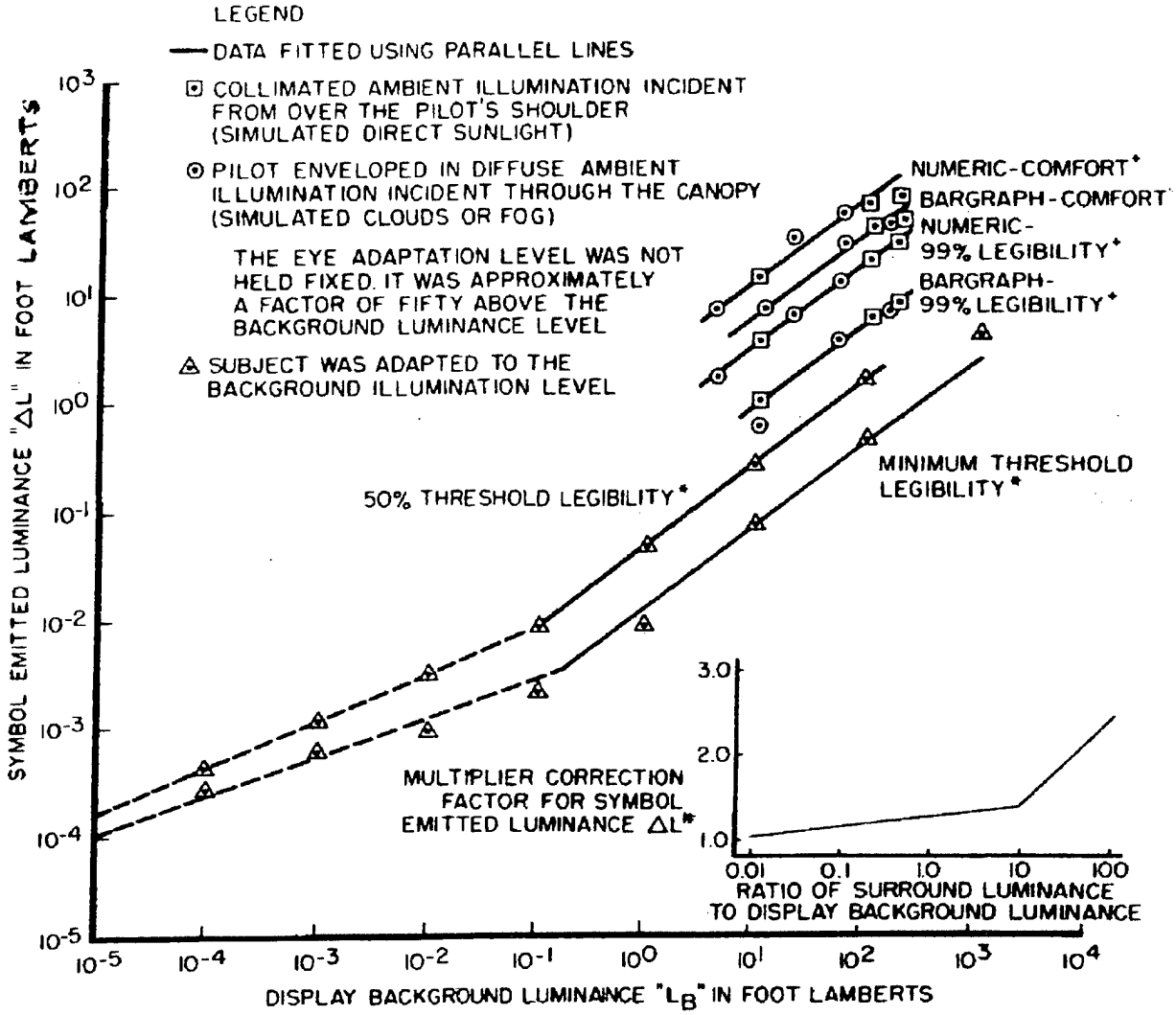
The point being made here is that due to their method of construction, the accuracy of the final characteristics shown in Figure 3.8 are limited. For example, whether due to the data itself, the accuracy of the original graph, or the accuracy of data extraction, the upper part of two minute of arc characteristic had to be fit with a curve rather than a straight line to cause the characteristic to pass through each of the points obtained from Figure 3.7A. This potential accuracy problem is accentuated for the nine minute of arc characteristic, having the deviant slope, since the 0.111 visual acuity intercepts with the background luminance characteristics correspond to the lower limit of the data collected by Aulhorn and Harms. In attempting to obtain a characteristic from the Aulhorn and Harms data that could be directly compared with the 9.68 minute of arc data of Blackwell, it became necessary to compromise the accuracy of this particular characteristic further by extrapolating the one millilambert background luminance characteristic to obtain one of the three data points responsible for the deviant slope of the characteristic. Despite these limitations, the resulting graph of Figure 3.8 shows that the Aulhorn and Harms data are in relatively good agreement with the results of Blackwell.

The preceding correspondence between parallel straight line curve fits of the Blackwell, Aulhorn and Harms, and King, et al, data, suggests that the image difference luminance requirements of an observer for different levels of performance accuracy, for different levels of reading task difficulty and for both the image detection and identification tasks are simply related to one another by a constant multiplication factor for the range of daylight display background luminance levels studied. This result is also consistent with the fact that, at the time, this adjustment technique had been used for years to extend the usefulness of Blackwell's 50% accuracy threshold detection legibility data, for the design of display imagery for use in image identification tasks having more stringent reading accuracy requirements.

In the original AGARD summary article, it was pointed out that if it were desired to make a more unbiased comparison between the Blackwell and King data, it would be necessary to correct for the difference in the surround luminance and display background luminance levels between the two studies. The full logarithmic graph in the insert to Figure 3.9 is a direct adaptation of a semilogarithmic graph presented in Figure 42 of a report by Carel, which Carel, in turn, attributed to a personal communication with Purdy.* The insert gives the image difference luminance (i.e., originally contrast) correction factor that was available, at the time, to adjust

---

* Purdy, W., "Outdoor TV," Carel attributed the data to a personal communication with Purdy regarding a study conducted by the General Electric Company, Ithaca, NY, in 1959.



DEFINITION OF TERMS:

COMFORT: The minimum difference luminance the pilot considered necessary to provide comfortable reading of the display.
99% LEGIBILITY: The reading accuracy criteria was 99% correct responses.
50% THRESHOLD LEGIBILITY: Correct detection occurred 50% of the time (6 second exposures).
MINIMUM THRESHOLD LEGIBILITY: The image was statistically detectable given sufficient time.

GEOMETRICAL FACTORS AFFECTING LEGIBILITY:

NUMERIC +: A three digit green electroluminescent phosphor readout was used. Viewed at 28 inches, the characters were 0.4 inches (50 minutes of arc) high, 0.28 inches (35 minutes of arc) wide and had a stroke width of 0.05 inches (6 minutes of arc).
BARGRAPH +: Overall, the green electroluminescent bargraph used was 5 inches high and 0.25 inches wide. The segments were 0.035 inches high and separated by 0.005 inch gaps. The bargraph reading scale was graduated in 0.25 unit steps from 0 to 6.25 units, each unit consisting of five electroluminescent segments.
THRESHOLD LEGIBILITY *: 50% threshold legibility was determined by scoring the number of correct responses to identifying the position of a lighted circular area, subtending 9.68 minutes of arc, in one of eight possible positions on a three degree radius circle. Minimum threshold legibility only required that the circle be identified as present or absent.

REFERENCES:

+ R.C. King, et. al., Aug. 1970 * H. Richard Blackwell, Tables 2 & 3, Nov. 1946 # W.L. Carel, Dec. 1966

Figure 3.9. Symbol Luminance as a Function of Display Background Luminance.

for an eye adaptation mismatch.[30] Using this graph, it can be seen that for a surround-field to display background luminance ratio of one hundred, the King image difference luminance requirements are a factor of nominally 2.3 times more stringent than would be required if there were no mismatch, as is the case for the Blackwell data.

In practical aircraft display applications the effect of an eye adaptation mismatch is expected to be important. This is true because proper filtering will generally reduce the background luminance level of a cockpit electronic display to one percent or less of the incident ambient illumination. Thus, whereas, the King experiments covered simulated sun ambient illuminance levels in the range of 500 to 10,000 foot-candles (fc), as measured on the instrument panel, and surround luminance levels in the range from 500 to 10,000 foot-Lamberts (fL), as measured on the diffusely transmitting constant luminance surfaces surrounding the cockpit, the display background luminances observed only ranged from 4 fL up to about 100 fL. The advantage of such a filtered display is that even under worst case ambient illumination and diffuse surround luminance conditions, 100 fL was the maximum difference luminance required from the numeric and bargraph display imagery to produce comfort level reading accuracies. A principal purpose of the present report is to provide information that will allow this type of luminance mismatch correction to be made more accurately, with a clearer understanding of the design factors involved and to incorporate it seamlessly into the automatic legibility control of cockpit displays. The Boeing automatic brightness control technique, described in Chapters 4 and 5 of this report, used Carel's "adaptation mismatch" correction factor.

Not shown in Figure 3.9 is the head-up display image data of Kelly, Ketchel and Strudwick.[31] Kelly, Ketchel and Strudwick collected 90% reading accuracy legibility data for a small number of individual data points using a head-up display combiner lens with background luminances between 6,000 to 8,200 fL, when back-illuminated with up to 10,000 fL of luminance. The resulting distribution of data points extended from just slightly above the extended 99% numeric data of King, Wolletin, Semple and Gottelmann on Figure 3.9 down to about two thirds of the luminance difference between the extensions of the 99% numeric and bargraph data. This data suggests that a straight line extension of the characteristics in Figure 3.9, for display background luminances up to nearly 10,000 fL, is approximately valid. Since the head-up display data of Kelly, Ketchel and Strudwick consisted of only a few discrete data points for the image size of interest, it has not been included in Figure 3.9.

3.3.2. Quantitative Comparisons of Historic Image Difference Luminance Characteristics

The ability to identify an image infers that the critical detail dimension of the image can be visually discerned, whereas the ability to detect an image infers only that the presence or absence of the image can be visually discriminated. Despite this fundamental difference in these visual tasks, the visual requirements for performing both of these tasks can be characterized using different luminance value combinations represented by the image difference luminance versus background luminance characteristics, which are associated with a particular critical detail dimension for an image identification task and with a particular image subtended angle for an image detection task. In this subsection the quantitative relationships between the constant critical detail dimension and constant image subtended angle characteristics of different experimenters are explored.

The quantitative comparisons of the historic image difference luminance versus background luminance data will be considered in the two subsections that follow. In the first subsection, quantitative comparisons between the image difference luminance versus background luminance characteristics of different experimenters, for visual tasks involving the identification of images, are considered. In the second subsection, the image difference luminance versus background luminance characteristics for image identification and image detection tasks are quantitatively compared.

3.3.2.1. Comparisons of the Image Identification Task Data of Different Experimenters

Chapanis,[32] like Aulhorn and Harms, collected minimum separable visual acuity data using a criterion of 50% accuracy of correct identification. A graph reported to be a synthesis of the Chapanis data was shown in Figure 43 of the report by Carel[33] and in Figure 99 of the report by Semple.[34] An enlarged copy of this graph of the Chapanis data is included as Figure A.1 in Appendix A. It shows constant contrast characteristics having parameter values of 100, 50, 30, 20, 10, 5 and 2 percent plotted with the critical detail dimension of an image, expressed in minutes of arc, on the ordinate, versus background luminance, expressed in foot-Lamberts, on the abscissa. The image identification task used in this investigation consisted of visually discriminating a space between two short straight lines, where the space was equal to the width of the lines. The ranges of the Chapanis experimental data extended from about 0.7 to 10 minutes of arc on the ordinate and from about 0.0015 to 100 fL of background luminance on the abscissa.

In comparison to the Chapanis image identification task, the Aulhorn and Harms investigation required test subjects to be able to discriminate between equal area circles and squares, the form identification task illustrated in Figure 3.5. To show the agreement that exists between the data of these experimenters, quantitative data was extracted from the Chapanis and Aulhorn and Harms visual acuity data for their respective images at critical detail dimensions of 2, 3.6 and 9 minutes of arc. The resultant tables of Chapanis and Aulhorn and Harms image difference luminance data are contained in Tables A.1 and A.2 of Appendix A, respectively. The procedure used to extract the data, the technique chosen to make the image difference luminance comparisons and the results obtained are described below.

Although the five-decade background luminance range cited previously for the Chapanis data is quite large, the horizontal line used to extract the two minute of arc data only intersected five constant contrast characteristics, with a background luminance range from 0.066 to 17.2 fL (i.e., less than three decades); the horizontal line for the 3.6 minute of arc data only intersected six constant contrast characteristics, with a background luminance range from 0.00109 to 6.1 fL (i.e., less than four decades); and the line for the nine minute of arc data, while intersecting all seven of the Chapanis constant contrast characteristics, still only had a background luminance range between 0.0019 and 11.1 fL (i.e., just less than four decades). Moreover, if the one photopic background luminance data point for the nine minute of arc characteristic of Chapanis is excluded, the number of background luminance data points available for comparison is reduced from seven to six and the range of the data is reduced to between 0.0018 and 0.105 fL (i.e., less than two decades). Characteristics representing the data of Chapanis are not shown in the figures, in part, because the restricted background luminance range does not offer an effective visual comparison and because of a two-decade gap between the last two data points on the nine minute of arc characteristic.

While the Aulhorn and Harms minimum separable acuity characteristics offered only six data points for each critical detail dimension value, five of those data points were evenly spaced at one decade background luminance intervals, and the last data point, corresponding to zero background luminance, extended the range of values covered by an additional four decades. For this reason, the Aulhorn and Harms minimum separable acuity characteristics were plotted on the previously mentioned large area graph for comparison with the Chapanis data. A version of these characteristics originally drawn in 1972 and previously published[35] is shown in Figure 3.8. The current extraction of data from the Aulhorn and Harms minimum separable acuity characteristics, which is contained in Table A.2 of Appendix A, resulted in a reduction in the slope of the nine minute of arc characteristic in the photopic background luminance range, but caused only minor changes to the other two characteristics. The quantitative data comparisons in Appendix A are based on the current data extraction.

Because of the full logarithmic relationship exhibited by the image difference luminance versus background luminance characteristics in the figures, the degree to which the two experimenters' data correspond has been evaluated by calculating the ratios between the larger and the smaller of the Chapanis and Aulhorn and Harms image difference luminance values, at common levels of background luminance. As may be seen by referring to Tables A.3, A.4 and A.5 in Appendix A, these ratios are compared in the tables

for each background luminance value, one pair of image difference luminance values at a time. The overall mean value of these ratios is also entered in the tables to serve as a measure of the mean separation between the constant image critical detail dimension characteristics of each experimenter.

In the comparison of the image difference luminance values for the two minute of arc critical detail dimension data, shown in Table A.3 of Appendix A, the mean value of the image difference luminance ratios was 1.26, with a maximum ratio for any individual background luminance of 1.51. To improve the accuracy of this comparison, the image difference luminance ratios corresponding to the Chapanis background luminance data points in Table A.1 of Appendix A were used. As previously stated, the larger range and the even spacing of the background luminance data of Aulhorn and Harms from Table A.2 permitted more accurate graphs of these characteristics to be drawn, particularly for the nine minute of arc data set. For this reason, it was expected that more accurate image difference luminance values could be extracted from graphs of the Aulhorn and Harms characteristics than would have been possible by graphing the Chapanis characteristics. This is the reason the background luminance data of Chapanis from Table A.1 was chosen to serve as the principal baseline for making the image difference luminance comparisons between the data of these two experimenters in Appendix A. This choice required drawing the Aulhorn and Harms characteristics to enable the extraction of image difference luminance values corresponding to the Chapanis background luminance values. The two minute of arc data in Table A.3, the 3.6 minute of arc data shown on the left-hand side of Table A.4 and the nine minute of arc data shown in Table A.5 had to be obtained in this manner from the graphed characteristics of Aulhorn and Harms.

The mean value of the image difference luminance ratios for the 3.6 minute of arc critical detail dimension data of Chapanis, at the background luminance data points shown on the left-hand side of Table A.4, was 1.18, with a maximum ratio for any individual background luminance of 1.37. To serve as a comparison with this result, the image difference luminance data of the two experimenters were also compared by drawing a graph of the 3.6 minute of arc data of Chapanis, which were better behaved and had minimum spacings between background luminance values of a decade or less, and then using the background luminance data points of Aulhorn and Harms, plus some intermediate values from their graphed characteristic, as a comparison baseline. The result of this comparison is shown on the right-hand side of Table A.4, and the overall mean value of the image difference luminance ratios for the background luminance data points of Aulhorn and Harms, was also 1.18, with the same maximum ratio for any individual background luminance of 1.37, since this data point was used in both sides of the table.

Finally, for the comparison of the image difference luminance values, for the nine minute of arc critical detail dimension shown in Table A.5 in Appendix A, an overall mean value of the ratios for the background luminance data points tested was 1.27, with a maximum ratio for any individual background luminance of 1.87. Excluding the image difference luminance ratio of 1.87, for the single background luminance data point of Chapanis, capable of being compared with the graphed Aulhorn and Harm's nine minute of arc characteristic, in the photopic background luminance range, reduced the mean ratio for this comparison to 1.17 and the maximum ratio for any comparison, at an individual background luminance value, to 1.41. In each case, a ratio of unity between the respective Chapanis and Aulhorn and Harms minimum separable acuity characteristics would correspond to an exact data match.

In spite of the restricted range of the Chapanis background luminance values over which the Chapanis and Aulhorn and Harms constant critical detail dimension characteristics can be compared, the comparison is nonetheless meaningful, since the two experiments should, in concept, yield very similar results in any range of background luminance values. To provide a numerical measure of the image difference luminance variable space, in which to assess the comparison results for the Chapanis and Aulhorn and Harms characteristics in Tables A.3, A.4 and A.5, the relative spacings among the 1, 2, 3.6 and 9 minute of arc image difference luminance characteristics of Aulhorn and Harms were calculated at the common background luminance values shown in Table A.2 of Appendix A. The resulting ratio separations between the characteristics are shown at five background luminance levels in Table A.10 of Appendix A.

Referring to Table A.10, it may be seen that the ratios between the two and nine and the one and nine minute of arc characteristics show that the size of the potential variable space, available to depict relative differences between the Chapanis and Aulhorn and Harms results, is quite large. The comparisons of the Chapanis and Aulhorn and Harms data in Tables A.3, A.4 and A.5 yielded mean image difference luminance ratios of 1.26, between the five data points of two minute of arc comparison, 1.18, between the six data points of the 3.6 minute of arc characteristic comparison, and 1.27, between the six data points of the nine minute of arc characteristic comparison. Because these image difference luminance ratios are quite small, when compared with the ratios that are possible, it is concluded that the Chapanis and Aulhorn and Harms data are in good agreement.

Although the close agreement between the experimental results of Chapanis and Aulhorn and Harms, should, at least in concept, be expected for testing the same visual perception effect, differences in test subject instructions, experimental procedures, test equipment, test images, controlled variables and so forth, typically make it possible to obtain different results for such comparisons, with no errors having been made by the experimenters, simply because unforseen variable dependences skew the expected results. In addition, because large variations are normally associated with human perception data, it is considered fair to conclude that the previously cited results of Chapanis and those of Aulhorn and Harms are in very good quantitative agreement.

3.3.2.2. Comparisons Between Image Identification and Image Detection Task Data

A more interesting quantitative comparison occurs between the image detection task results of Blackwell and the image identification task results of Aulhorn and Harms and of Chapanis, just described. The reason it is considered useful to make this quantitative comparison is the similarity exhibited in Figures 3.8 and 3.9, between the shape of the image difference luminance characteristics of Blackwell, for an image detection task, and the image identification task characteristics of Aulhorn and Harms and of Chapanis, for background luminance levels in the photopic vision range. This qualitative comparison result is not entirely unexpected because, as is described in Section 3.7, cone light receptors in the eyes are considered responsible for both image detection and identification under daylight viewing conditions. Conversely, the image identification and detection tasks are expected to produce results that differ both qualitatively and quantitatively in parts of the mesopic vision range and in all of the scotopic vision range. The reasons for the latter differences are further explored in Section 3.7.

Although no established theoretical basis exists for making quantitative comparisons between the image difference luminance characteristics for image detection and identification tasks, even in the photopic vision range, Figure 3.8 shows that the image detection data of Blackwell for a circular image subtending a total angle at the observer's eyes of 9.68 minute of arc is in fairly good quantitative agreement with the nine minute of arc critical detail dimension characteristic of Aulhorn and Harms, at least at the low end of the photopic luminance range. Based on the qualitative comparisons already made between the slope of the Blackwell characteristics, with the characteristics of Aulhorn and Harm's shown in Figure 3.8; with those of King, shown in Figure 3.9; and, in particular, with those of Jainski, to be considered later in this section and throughout the balance of the report, the deviant slope portion of the Aulhorn and Harm's nine minute of arc characteristic, shown in Figure 3.8 for the photopic background luminance range, may be an aberration. For this and other reasons described in Appendix A, another attempt was made to extract image difference luminance data from Figure 3.7A. As previously described, this update of the nine minute of arc critical detail dimension characteristic of Aulhorn and Harms resulted in a reduction in the slope of the photopic portion of the characteristic, which may be seen by referring to Figure A.2 of Appendix A, but did not materially affect the mean separation between the photopic portions of the two characteristics.

As a starting point for the quantitative comparison of the image difference luminance characteristics for image detection and identification tasks, the ratios of the larger to the smaller of the image difference luminance values, extracted from a graph of the 9 minute of arc Aulhorn and Harms and the 9.68 minute of arc Blackwell,

at each of nine background luminance levels in the range from 0.00167 to 9.2.9 fL, are shown in Table A.6 of Appendix A. This comparison was carried out because, as previously mentioned, nine minutes of arc was the practical upper limit on extracting data from the Aulhorn and Harms characteristics and Blackwell only had two image sizes in the range of critical detail dimensions investigated by Chapanis and Aulhorn and Harms, at 3.6 and 9.68 minutes of arc. To provide a measure of the effect of the difference between the image critical detail dimensions, a comparison was also made between the nine minute of arc data of Aulhorn and Harms and the ten minute of arc data of Chapanis, the maximum size tested by Chapanis.

The comparison of the Blackwell and Aulhorn and Harms data in Table A.6, yielded a mean image difference luminance ratio of 1.41. The mean of the two image difference luminance ratios between the Blackwell and Aulhorn and Harms characteristics in the photopic background luminance range was 1.77. This separation between the Blackwell and Aulhorn and Harms characteristics is greater than the mean ratio of 1.72 between the Aulhorn and Harm's 3.6 and 9 minute of arc characteristics (i.e., see Table A.10 of Appendix A). Thus, the nine minute of arc Aulhorn and Harms characteristic is slightly more than half way between the 9.68 minute of arc Blackwell characteristic and the 3.6 minute of arc Aulhorn and Harms characteristic, which are separated by a mean difference luminance ratio of 3.03. Although excluding the photopic data points from the comparison reduces the mean ratio from 1.41 to 1.31, as Figures 3.8 and A.2 show, the reduction is not meaningful. The likely reason for the reduction in mean separation between the characteristics is that the nine minute of arc Aulhorn and Harms characteristic crosses the Blackwell characteristic twice in the mesopic background luminance range. Since the shapes of the image identification and detection characteristics typically differ in the mesopic and scotopic background luminance ranges, the ratios simply indicate the inherent differences between the shapes of the two types of characteristics.

The comparison of the Chapanis ten minute of arc data in Table A.6, with the Aulhorn and Harms nine minute of arc data yielded a mean image difference luminance ratio of 1.34, or 1.25 if the photopic background luminance portion of the Aulhorn and Harm's nine minute of arc characteristic is excluded. A comparison of these mean image difference luminance ratios with the corresponding earlier ratios of 1.27, for the comparison of the Chapanis and Aulhorn and Harms nine minutes of arc critical detail dimension characteristics from Table A.5, and 1.17, if the photopic background luminance portion of the Aulhorn and Harm's nine minute of arc characteristic is excluded, gives an indication of the effect of the change in the critical detail dimensions used in the two comparisons. The preceding comparison shows that the effect of increasing the critical detail dimension of the Chapanis data, used in the comparison, from nine to ten minute of arc only increases the image difference luminance ratio by a factor of 1.072. It is considered valid to make the preceding comparison, in spite of the irregular spacing of the background luminance values at which comparisons were made, because both sets of characteristics had very similar background luminance levels.

The minimum separable visual acuity data of Chapanis, for a 50% accuracy of correct identification and a test image of ten minute of arc in critical detail dimension, nearly matches the 9.68 minute of arc Blackwell image detection data in Figure 3.8 for the characteristic in the figure labeled "50% Threshold Legibility," over the range from 10^{1} down to 10^{-3} fL of display background luminance. A distinction between the two characteristics occurs when the Chapanis characteristic reaches a zero slope, at a minimum image difference luminance level of about 0.00116 fL. This minimum image difference luminance level, which is a signature distinguishing feature of image identification task data, occurs at and below a background luminance of 0.0025 fL, down to the lowest data point for the Chapanis data at slightly more than 10^{-3} fL. In comparison, the image difference luminance of the Blackwell image detection task data continues to decrease as the background luminance becomes smaller.

The background luminances used in both the Blackwell and Aulhorn and Harms and the Chapanis and Aulhorn and Harms data comparisons, above, were those found when the data was extracted from the Chapanis 10 minute of arc characteristic, except that a data point was added at 0.9fL and 92.9 fL for the Blackwell and Aulhorn and Harms comparison owing to the existence of valid nearby data points for these two characteristics. A lack of Chapanis data above 9.37 fL of background luminance and a two-decade gap between the background luminance values on the Chapanis characteristic prevented making a valid estimate

of the missing point at 0.9 fL for use with this characteristic.

The interesting aspect of the preceding comparison is the degree of quantitative agreement that exists between the image difference luminance requirements for an image identification task requiring the discrimination of a nine minute of arc critical detail dimension and an image detection task requiring the discrimination of a circular image having a total subtended angle of 9.68 minutes of arc. If this relationship were to prove to be valid, it would suggest that when an image detection target has a total angle subtended equal to the the dimension marked "cd" in the portion of Figure 3.5 labeled "form identification," then the target and the image to be identified would have nominally the same image difference luminance requirements, in the photopic and a portion of the mesopic vision ranges. As Figure 3.5 illustrates, the size of the image to be identified is likely to be much larger than the size of the image to be detected. This target size relationship is consistent with the known need for a target to be at smaller range to permit identification to occur than is necessary to allow the same target to be detected, under the same viewing conditions. The cone light receptors in the eyes are used to perform both image identification and detection tasks under photopic viewing conditions, where the image difference luminance requirements are similar for both tasks, but under night viewing conditions rod light receptors are used to perform image detection tasks and cone receptors continue to be used to perform image identification tasks, at least for the small image sizes present in aircraft cockpits. This distinction between the day and night uses of the eyes' retinal light receptors is, therefore, also consistent with the preceding observed experimental similarities and differences in the respective image difference luminance characteristics as a function of the background luminance viewing conditions. These relationships are further considered in Section 3.7.

To more fully assess whether or not the quantitative correspondence noted above, between the Aulhorn and Harms and Blackwell characteristics for images that have critical detail dimensions approximately equal in size to total angle subtended by a target to be detected, was just a coincidence, the image difference luminance data of Chapanis for critical detail dimensions of nine and ten minutes of arc were linearly interpolated to provide a set of Chapanis image difference luminance levels corresponding to 9.68 minute of arc critical detail dimension images, which can be directly compared with the Blackwell characteristic for a 9.68 minute of arc circular target. This comparison is contained in Table A.7 in Appendix A. A similar comparison was also made between the image difference luminance values from the Blackwell image detection task characteristic for the 3.6 minute of arc circular target, and the values extracted from the Carel graph of the Chapanis data for the 3.6 minute of arc critical detail dimension images. The data for this comparison is contained in Table A.8 in Appendix A. For the 3.6 minute of arc image size and image critical detail dimension characteristics, comparisons were also made between both the Blackwell and Aulhorn and Harms data and the Blackwell and Chapanis data. To make these image difference luminance comparisons, the Aulhorn and Harms data was chosen to serve the comparison baseline. This choice was made because the even spacing between their background luminance values on a logarithmic scale permitted the Blackwell characteristic to be compared with the Aulhorn and Harms and Chapanis characteristics on an equal footing. The data for the latter comparison is contained in Table A.9 of Appendix A.

Comparisons between the 9.68 minute of arc Blackwell and the interpolated Chapanis characteristics, described at the beginning of the preceding paragraph and shown in Table A.7 of Appendix A, resulted in an overall mean image difference luminance ratio for the seven data points that could be compared of 1.42. The background luminance values at which the image difference luminance ratios were calculated corresponded to the values extracted from the Chapanis characteristics and covered a range from 0.00191 to 11.09 fL, just less than four decades. In this case, the Chapanis image difference luminance values were less than the Blackwell characteristic values throughout the background luminance range, except in the vicinity of the beginning of the zero slope portion of the Chapanis characteristic. At the photopic end of the background luminance range for the Chapanis data, the single image difference luminance data point approached to within a ratio of 1.11 below the Blackwell 9.68 minute of arc characteristic, at a background luminance value of 11.09 fL. This agreement between the Blackwell and Chapanis image difference luminance values in the photopic range, where the characteristics would be expected to agree, is considered very good, however, because only one point from the Chapanis characteristic is available for comparison, this result, by itself, cannot be

considered significant.

A maximum image difference luminance ratio of 1.77, of the 9.68 minute of arc Chapanis characteristic below the Blackwell characteristic, occurred at 0.0892 fL. This result is very similar to the image different luminance deviations, shown in Table A.6, where the maximum ratios of 1.66 for two points on the 9 minute of arc Aulhorn and Harms characteristic below the 9.68 minute of arc Blackwell characteristic, nearly agree both in their magnitudes and locations in the background luminance range. This deviation of the nine minute of arc Aulhorn and Harms characteristic below the Blackwell characteristic would have been expected to result in a slight reduction in the image difference luminance levels, at each background luminance level, causing it to agree better with the Chapanis comparison to Blackwell's characteristic, had data been available to plot an Aulhorn and Harms characteristic for a 9.68 minute of arc critical detail dimension image. This close agreement between the Blackwell and Chapanis data in the photopic background luminance range and the close agreement between the Aulhorn and Harms and Chapanis data in the mesopic background luminance range leaves unresolved the question of why the Aulhorn and Harms characteristic exhibits image difference luminance requirements that increase to a factor of nominally 1.75 higher than the Chapanis and Blackwell data in the photopic background luminance range.

In the second comparison introduced above between the 3.6 minute of arc characteristics of Chapanis and Blackwell, Table A.8 of Appendix A shows that the mean image difference luminance ratio of the six Chapanis data points available for comparison was 1.67 and the background luminance values at which the image difference luminance ratios were calculated covered a range from 0.011 to 6.08 fL, just less than three decades. In this case, the data points for the Chapanis characteristic were below the Blackwell characteristic throughout the entire background luminance range. Referring to Table A.8 in Appendix A, it may be seen that image difference luminance ratios, as high or higher than the 9.68 minute of arc Chapanis and Blackwell characteristic comparison in Table A.7, prevail throughout the range of background luminance values available to make this comparison. Unfortunately, like the 9.68 minute of arc characteristic comparison, there is only one photopic background luminance data point available for comparing the 3.6 minute of arc Chapanis characteristic, and it exhibits an image difference luminance ratio of 1.78 below the Blackwell characteristic at 6.08 fL of background luminance, a multiple of 1.6 greater than the deviation of the 9.68 minute of arc characteristic of Chapanis below the Blackwell characteristic. Thus, while the results are consistent, the level of quantitative agreement present in the photopic background luminance range between the Chapanis and Blackwell data does not provide convincing support for the existence of a relationship between the two characteristics.

The left-hand side of Table A.4 compares the Chapanis and Aulhorn and Harms image difference luminance data, for 3.6 minute of arc critical detail dimension images, using the same background luminance values employed in Table A.8 to compare the Blackwell and Chapanis data. As a result, the image difference luminance ratios in these two tables can be directly compared at each background luminance value. Likewise, the mean values of the image difference luminance ratios from both tables are also directly comparable. The mean image difference luminance ratio of 1.18 from the Chapanis and Aulhorn and Harms comparison show these experimenters' results are in very good agreement for the 3.6 minute of arc critical detail dimension images, whereas, the same ratio for the Chapanis and Blackwell data was, as reported in the previous paragraph, 1.67. However, and as previously described, only the photopic background luminance comparisons with Blackwell's image detection task data should be meaningful. As compared to the 1.78 image difference luminance ratio, between the single photopic Chapanis and Blackwell data points in Table A.8 at 6.08 fL of background luminance, the left-hand side of Table A.4 gives an image difference luminance ratio of 1.37, for the Chapanis and Aulhorn and Harms comparison. Referring to Figure A.2 of Appendix A, the Aulhorn and Harms characteristic is seen to be intermediate between the lower image difference luminance of the Chapanis photopic data point and the corresponding point on the Blackwell characteristic.

The final comparison introduced above is between data of Blackwell for an image subtending a total angle the 3.6 minute of arc and the image critical detail dimension data of both Aulhorn and Harms and Chapanis. Although Table A.8 already compares the characteristics of Blackwell with the image difference luminance

values extracted from the critical detail dimension characteristics of Chapanis, the comparison in Table A.9 of Appendix A uses the background luminance values of Aulhorn and Harms, from the right-hand side of Table A.4 as a comparison baseline, rather than the background luminance values of Chapanis. The limitations the latter comparison places on the accuracy of the Chapanis portion of the comparison with the Blackwell characteristic were described previously in relation to the comparison of the Chapanis and Aulhorn and Harms data in Table A.4. Except for adding image difference luminance data to Table A.9 at 0.0034 fL in the mesopic range and at 9.29 and 11.09 fL in the photopic range, in an attempt to improve the comparison of the Blackwell and Aulhorn and Harms characteristics, the background luminance values in the right-hand side of Tables A.4 and in Table A.9 are the same, and, consequently, allow direct comparisons to be made between the image difference luminance ratios on the right-hand side of Table A.4 with those in Table A.9.

The earlier comparison of the Chapanis and Aulhorn and Harms data for 3.6 minute of arc critical detail dimension images, on the right-hand side of Table A.4, yielded a mean difference luminance ratio of 1.18, showing the two experimenters' data is in good agreement. As was true for the comparison of the mean image difference luminance ratios in Table A.8, the comparisons in Table A.9 do not exhibit close agreement, however, this can in large part be attributed to the expected differences with Blackwell's data in the mesopic background luminance range. In the comparison of the Blackwell and Chapanis image difference luminance ratios in Table A.9 for the photopic background luminance range, the results obtained are essentially the same as those found previously for this comparison in Table A.8. The comparison between the Blackwell and Aulhorn and Harms image difference luminance ratios, corresponding to photopic background luminance levels, shows much better agreement between the two characteristics with a mean value of the ratio for this background luminance range being only 1.26.

3.3.2.3. Quantitative Image Difference Luminance Characteristic Comparison Conclusions

The result of comparing the Chapanis image difference luminance data with the Aulhorn and Harms image difference luminance characteristics for images having 2, 3.6 and 9 minute of arc critical detail dimensions was that on average the results are in close agreement, with a maximum mean image difference luminance ratio between any of the individual characteristics being 1.27 for the nine minute of arc characteristic comparison. Furthermore, for each critical detail dimension comparison the maximum separation between the image difference luminance values of the two experimenters occurred in the photopic background luminance range with the Chapanis data having the lower values in each instance. It is concluded from these comparisons that the image identification task data of Chapanis and the Aulhorn and Harms are in good agreement, considering the differences in the forms of test images being compared, the typical variability of human performance data and the ranges of the luminance variables being investigated.

In Section A.3 of Appendix A, image difference luminance values extracted from the Aulhorn and Harms minimum separable visual acuity characteristics of Figure 3.7A, for constant critical detail dimension values of 1, 2, 3.6 and 9 minutes of arc, were compared quantitatively by calculating the ratios between the image difference luminance values corresponding to each of the four constant critical detail dimension data sets at each of five common background luminance levels spaced one decade apart. The calculated values of these image difference luminance ratios are contained in Table A.10.

The evaluation of the image difference luminance ratios in Appendix A support several important conclusions reached later in this report, using other experimenters' data, concerning the mathematical modeling of human image difference luminance versus background luminance requirements. To be more specific, the principal conclusion supported by the Aulhorn and Harms data is that the constant critical detail dimension characteristics are parallel to each other, in the photopic background luminance range. The next most important conclusion supported by the data is that the slope of the characteristics is close to but less than unity when depicted on a full logarithmic graph of image difference luminance versus background luminance. A third conclusion supported by the Aulhorn and Harms quantitative data comparison was that the separations between the characteristics, as measured using the image difference luminance ratios, are much larger in the

lower half of the mesopic background luminance range than they are in the photopic part of the range. In relation to the last conclusion, a trend in the ratios in Table A.10 suggests that most of the change in the spacings, between the image difference luminance characteristics during the transition from photopic to scotopic background luminance levels, occur in the upper part of the mesopic background luminance range, below 3 fL and above 0.1 fL. As described in Appendix A, the limited data available from the single experimental graph of the Aulhorn and Harms results in Figure 3.7A was considered insufficient to treat this observed trend as a firm conclusion. It should be noted that while this relationship is satisfied by several of the Jainski image difference luminance characteristics, presented later in this chapter, it does not apply to the vast majority of Jainski's characteristics.

The overall conclusion with respect to the comparison of the Blackwell with the Chapanis and the Aulhorn and Harms image difference luminance data, for both the 3.6 and 9 minute of arc critical detail dimension characteristics, is that they are in reasonably good quantitative agreement, given the previously described variability expected in the image difference luminance data being compared. In spite of this relatively good quantitative agreement, a comparison of the graphed characteristics in Figure A.2 of Appendix A shows the Blackwell image difference luminance characteristic is above the Aulhorn and Harms characteristic for the 3.6 minute of arc comparison, and is below it for the 9 minute of arc comparison. This observable fact prevents reaching a firm conclusion on whether or not a real relationship exists between the image difference luminance requirements for image detection and identification tasks, based on the total subtended angle of an image to be detected being equal to the critical dimension of an image to be identified, without having image difference luminance characteristics at one or more additional critical detail dimensions to compare. Despite the fact that a firm conclusion on this point of comparison cannot be reached, based on the available comparison data, it is considered unlikely that the agreement that does exist between the characteristics is just a coincidence.

3.3.3. Comparisons with Jainski Data

The previously cited report by Jainski was acquired by a colleague from the German Air Force, with a summary translation from the Royal Air Force,[36] in the early 1970's. A cursory review of the report revealed numerous graphed characteristics similar to those in Figure 3.8. A closer examination of the report revealed that it provided the most thorough and best documented investigation of legibility data applicable to pilots performing image identification tasks conducted to date. Acquiring this report permitted an extensive effort, which had been conducted to glean additional information from the limited experimental data available in the literature, up to that time, to be concluded.

To gain confidence in the validity of the Jainski test results, that data was compared with the data of earlier experimenters. The results of these comparisons are described briefly below. First, Figure 3.10 compares the image identification data of the Flight Dynamics Laboratory investigation, for images subtending critical detail dimensions of 15.3 minute of arc data, with the comparable data of the Jainski investigation, for images with critical detail dimensions of 5.5, 8.8, 9.8, 11.0, 17.7, and 19.6 minute of arc. The results of the two studies may be seen to be consistent with one another, to the extent that the image difference luminance requirements for the King investigation are about a factor of six higher than those for the Jainski investigation, when data for images subtending critical detail dimensions of 15.3 minutes of arc are compared. The assessment that the results are consistent is based on the fact that the King investigation used a 99% rather than a 95% accuracy legibility performance level and, as was described in the preceding subsection, because the image difference luminance levels of their numeric readout display would have been higher by a multiple of about 2.3 to compensate for the effect of the factor of nearly one hundred mismatch between the surround-field and display background luminances. As is described starting in Section 3.5 of this chapter, the increase in the image difference luminance requirements for the display used in the King investigation is attributable to veiling luminance induced by the scattering of light in the pilot's eyes, due to a peripheral vision exposure to the external surround-field, while simultaneously attempting to read information from displays having low reflected background luminance levels.

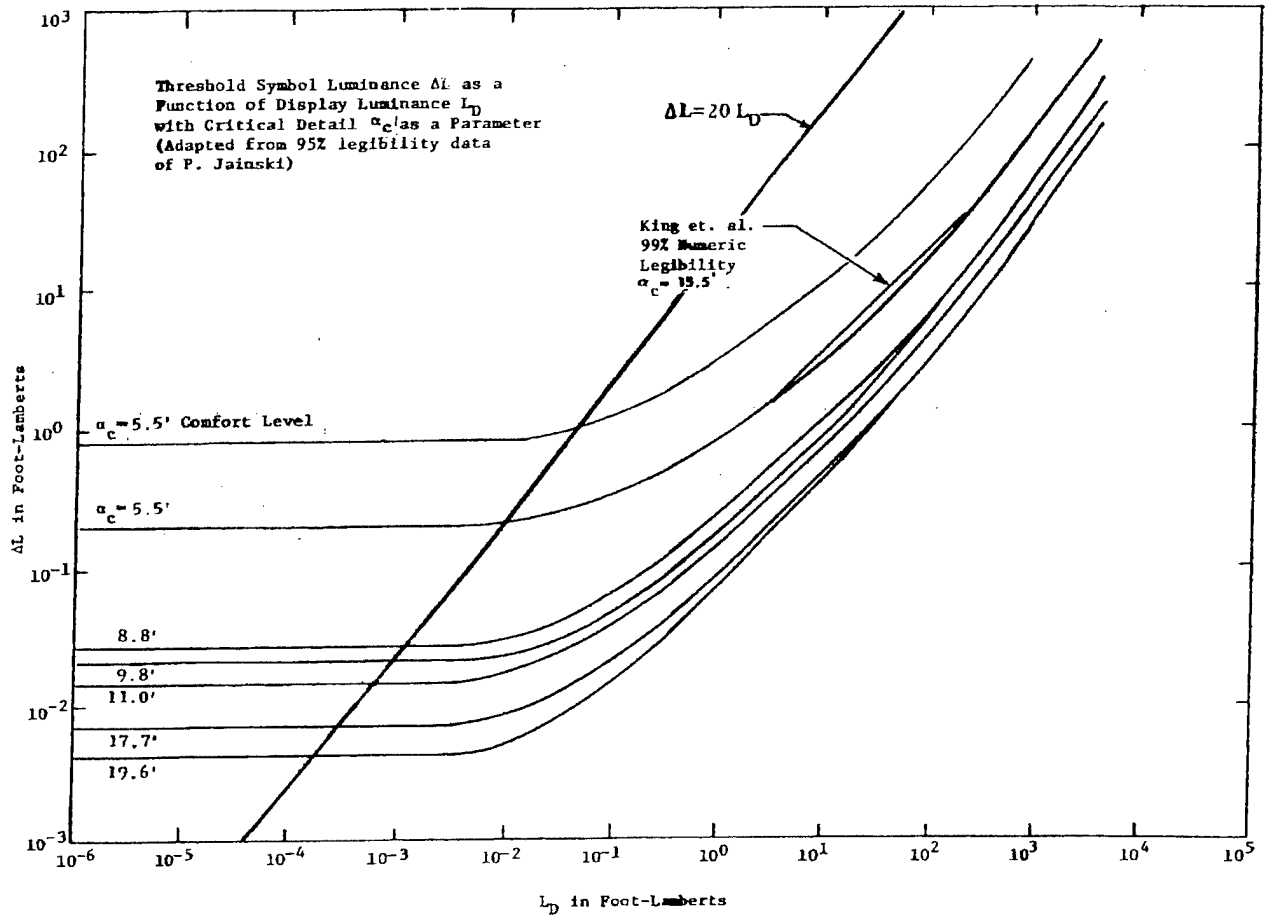


Figure 3.10. Image Difference Luminance Versus Background Luminance Data of Jainski, with Image Critical Detail Dimension as a Parameter, for Head-Up Display Presentations.

Under very high background luminance conditions, in the range of 6,000 to 8,200 fL, the previously introduced image difference luminance data of Kelly, Ketchel and Strudwick also agrees well with the results of Jainski, when the latter are extrapolated to the same display background luminance levels.

The data of the Jainski study can also be shown to be in good qualitative agreement with the 1956 minimum separable acuity data of Aulhorn and Harms[37] shown in Figure 3.8. Since the Aulhorn and Harms results correspond to a 50% probability of correct identification whereas the Jainski results correspond to a 95% probability of correct identification, a direct quantitative comparison of the two sets of data characteristics is not possible. Qualitatively, however, the former data is consistent with the latter data in that the nine minute of arc characteristic of Aulhorn and Harms is about a multiple of ten less in its image difference luminance requirements than the corresponding Jainski characteristics and the dependence of both sets of characteristics on the display background luminance are, even in quantitative terms, very similar to one another.

As a means of validating the test procedures and illumination test configurations used by Jainski, image difference luminance requirement experiments were also conducted employing the techniques of the now classical Blackwell contrast threshold image detection task experiments.[38] The image detection task data obtained by Jainski, in this manner, agreed closely enough with the results of Blackwell to convince Jainski that the experimental design and test setups were indeed valid. These result also show that the 95% accuracy results of Jainski can be directly compared, on a quantitative basis, with the 50% accuracy image detection

task results of Blackwell. Moreover, to make a more direct comparison of the image detection task data of Blackwell with the image identification task data of Jainski, the Blackwell data can first be adjusted to the 95% accuracy level, to match the Jainski tests, using a multiplier of nominally 1.8 taken from a probability of correct detection versus relative contrast conversion graph included as Figure 7 in the Blackwell article.

The preceding examples of the correspondence between the experimental data of Jainski and that of other experimenters was judged, for the purposes of this report, to be sufficient to substantiate the validity of Jainski's data for both night and daylight display background luminance levels. The desirability of establishing credence in the Jainski data stems from the following facts: Jainski's investigation is by far the best designed and most thorough study of image difference luminance requirements conducted to date, both in terms of the number of parameters controlled and the range of variables covered; Jainski's data corresponds to meaningful levels of task performance accuracy, namely 95%; and Jainski's data covers the range of display background, surround and panel luminance values encountered in aircraft cockpits.

3.3.4. Influence of Pilot Legibility Performance Criteria

Displays designed for aircraft cockpit use must provide imagery at image difference luminance levels sufficient to meet or exceed the pilot's minimum visual performance requirements. Since pilot's and other aircrew members are provided with controls that allow them to set the legibilities of their displays to suit their personal preferences, establishing the pilot's minimum visual performance requirements is necessary only as a means of specifying control-display systems that are can meet or exceed these requirements, and for determining the constant legibility image difference luminance characteristics that correspond to the minimum visual performance accuracy level that a pilot can tolerate and still perform his or her assigned mission. The latter constant legibility characteristics are needed to serve as a design baseline for cockpit instrument automatic legibility controls. The discussion that follows is intended to provide a rationale for using the image difference luminance characteristics of Jainski as that baseline, with appropriate adjustments to transition them from the nearly ideal conditions, under which the experimental data was collected, to the real world of operational aircraft cockpits.

The legibility performance to be expected when an image detection or identification task is being performed is one of the more important legibility parameters that influence the values of the image difference luminance requirements, ΔL, determined for a particular display image, task loading condition and viewing environment. Legibility performance is typically characterized in terms of the accuracy or, alternatively, the probability of a correct response, to be expected when a test subject in an experiment, or a pilot in a cockpit, attempts to perform an image detection or identification task. Like the experimental results described earlier in this chapter, legibility performance is quantified in the discussion that follows using the ratio of the number of correct responses to the total number of responses, expressed as a percentage.

The balance of this subsection is devoted to a discussion of the influence that the image difference luminance levels of display presentations can have on the legibility performance achievable by a person viewing the presentations. While increasing the image difference luminance and, hence, the contrast of a display presentation, with all other experimental parameters held fixed, is known to cause the probability of correctly detecting or identifying imagery in the display presentation to increase, the magnitude of the increase required to achieve any specific level of legibility performance is not currently predictable. As a part of this discussion, the practical difficulties associated with formulating a theory that is capable, even for ideal imagery and viewing conditions, of predicting test subject or pilot performance based on a knowledge of the display presentation legibility variables, are also explored in general terms.

In the three subsections that follow, factors are elaborated upon, which either affect the interpretation of legibility performance or serve to complicate the prediction of the corresponding required image difference luminance levels, or do both. The first factor is concerned with the difference between the magnitudes of the adjustment multipliers that must be applied to the pilot's image difference luminance requirements, under day

versus night viewing conditions, to achieve a particular change in the legibility performance of a test subject or pilot. A second factor concerns the fact that the information available in the literature is inadequate to permit predicting the changes in the performance levels to be expected as image difference luminance levels of displayed information are adjusted under fixed viewing conditions. The third, and final, factor to be considered concerns the need to apply an additional image difference luminance compensation multiplier to image difference luminance requirements established in a laboratory test environment, using ideal images under ideal viewing and task loading conditions, to attain levels of legibility performance that are acceptable to pilots under operational aircraft cockpit task loading and environmental viewing conditions.

3.3.4.1. Day Versus Night Adjustments Between Legibility Performance Levels for Ideal Imagery Using Image Difference Luminance Multipliers

As previously described, when comparing the 99% probability of correct image identification data of King et al, and the 50% probability of correct image detection data of Blackwell, a nominally constant performance compensation multiplier is valid as the display reflected background luminance changes for daylight viewing conditions. Similar comparisons between the image difference luminance characteristics of Jainski, corresponding to image identification performance at a 95% level of accuracy, and those of Aulhorn and Harms, corresponding to performance at a 50% level of accuracy, validates the daylight constant multiplier effect and also shows that a constant multiplier can also be applied to compensate for performance level differences at night.

A comparison of the critical detail dimension characteristic of Jainski, for 8.8 minute of arc in Figure 3.10, with the most nearly matched characteristic of Aulhorn and Harms, having a critical detail dimension of 9 minutes of arc and shown in Figure A.2 of Appendix A, gave a night multiplier of about 14, at a display background luminance of 10^{-5} fL, and a day multiplier of 2.88, at a display background luminance of 10 fL. It was considered valid to make this comparison with the head-up display data of Jainski because the visual conditions of the two tests were very nearly matched. For the Aulhorn and Harms tests, the observer's entire field of view was set to the display background luminance level, except the test symbol, which was higher by the image difference luminance value being experimentally determined. For Jainski's test, the luminance of the observer's field of view was at twice the level of the display background luminance (i.e., a 50% transmittance image combiner), except the in-field/panel luminance, which was at a much lower setting of 0.3% of the display background luminance. As shown by the results of Jainski, which are described in Section 3.3.5, these are equivalent viewing conditions and the results obtained should therefore be directly comparable.

As described previously, when the probability of correct image identification is fixed, as is true for all of the 50% accuracy image difference luminance characteristics of Aulhorn and Harms in Figure 3.8 or for the 95% accuracy characteristics of Jainski in Figure 3.10, it may be seen that an analogous effect to the one described in the preceding paragraph occurs, where the image critical detail dimension is the experimental test parameter under investigation. As is the case for the legibility performance compensation multipliers needed under night versus day reflected background luminance levels, the compensation multiplier required to make images having different image critical detail dimensions equally legible is also higher at night than under daylight display reflected luminance levels. It is likely that both results have a common origin in that the cone light receptors in the eyes are less sensitive at low luminance levels than they are at high levels.

The preceding comparisons show that the image difference luminance compensation multipliers needed to compensate for changes in legibility performance or image critical detail dimension changes, at night, are much larger than the corresponding daylight multipliers and, consequently, a single constant performance compensation multiplier cannot be used across the complete range of display reflected background luminances. It should also be noted that the transition from the night to daylight constant performance compensation multipliers appears to correspond to display background luminance levels in the mesopic range of vision, that is, it is associated with the adaptation transition between the scotopic and photopic ranges of luminance levels. These results also show that the absolute magnitude of the multiplier needed to compensate

the image difference luminance for a change in the legibility performance level, from 50 to 95% probability of correct identification, can be quite large.

3.3.4.2. Prediction of Image Difference Luminance Multipliers to Change the Legibility Performance Levels of Ideal Imagery

In the previously cited image detection experiments of Blackwell, a graph, designated in the article as Figure 7, was published that relates the probability of correct image detection to the relative contrast of the image. This legibility performance compensation relationship was established experimentally by Blackwell using 450,000 image detection task observations by taking the average of 1,500 individual probability curves and was found by Blackwell to conform to a Gaussian probability function.[39] Carel, citing the Blackwell article, published as Figure 41 of his report a plot of Blackwell's data as a straight line on a graph that used a probability scale on its vertical axis and a linear relative contrast scale on its horizontal axis.[40]

Because the Blackwell data conforms to a Gaussian probability density distribution it is sufficient to know two points on the corresponding Gaussian probability function to define the entire characteristic using standard tables of probability functions. To verify that the Blackwell graph does correspond to a properly scaled standard probability function, a graph was drawn for comparison using two known points on the Blackwell graph, namely, a relative contrast of unity at the 50% probability level and a relative contrast of 1.62 at 90% probability, where the latter value was used by Blackwell in an example. When these points were used to draw a straight line on a graph with a linear relative contrast scale as the ordinate and probability scaling on the abcissa, the resultant values were found to be consistent with six other points tested on the previously described Blackwell and Carel graphs. Furthermore, since the independent variable, x, in the standard probability function and Blackwell relative contrast, C, are related by the equation, $x = (C - \overline{C}) / \sigma$, where the mean value of the distribution is $\overline{C} = 1$, the standard deviation, σ, of the Blackwell data distribution can be calculated. From the standard probability function table, the value of x corresponding to a probability of 90% was found to be 1.2817, yielding an average value of the standard deviation of 0.48373 for the Blackwell data distribution.

As pointed out in the previous subsection, the graphs of image difference luminance versus background luminance, for the image detection task of Blackwell shown in Section 3.7, exhibit a dependence on the size of images similar to those for the day versus night image difference luminance characteristic dependences of Jainski's data on the critical detail dimensions of images for image identification tasks. Based on this comparison, it would be considered likely that the Blackwell performance compensation multipliers should also differ for scotopic and photopic background luminance viewing conditions. However, Figure 5 of Blackwell's article reports the values of a parameter that is inversely proportional to the slope of the probability versus relative contrast characteristics graphed as a function of the background luminance levels tested by Blackwell. The graph shows that the values of this parameter are constant, as a function of the background luminance, throughout the scotopic and photopic ranges. This result shows, therefore, that the relative contrast compensations to achieve specific changes in the probability of correct detection for the Blackwell data are unchanged throughout the scotopic and photopic background luminance ranges. The result also shows that the image identification characteristics of Jainski, Aulhorn and Harms and Chapanis are, in this respect, inconsistent with the image detection results of Blackwell.

Although Figure 5 of Blackwell's article showed that the values of the previously introduced Blackwell parameter, which is inversely proportional to the slope of the probability function versus relative contrast characteristic, is constant as a function of the background luminance level, Figure 6 of Blackwell's article shows that the same parameter is influenced by the angle subtended by the circular image to be detected. In particular, since the smallest image size shown in Figure 6 exhibits the largest value of this parameter, the slope of this probability characteristic would be the lowest for the image sizes tested by Blackwell. This result translates into the smallest image size tested, 3.6 minutes of arc, exhibiting the largest range of relative contrasts to span the zero to a 100% probability of correct detection range and the largest image size tested,

121 minutes of arc, exhibiting the smallest relative contrast range. Furthermore, the Blackwell results support a linear contraction of the relative contrast range in going from the smallest to the largest image sizes tested. The practical effect of this Blackwell finding is that adjustments to the image difference luminance versus background luminance characteristics, for images with smaller subtended angles, to a higher probability of correct detection, require a larger legibility performance compensation multiplier than would be required for images subtending larger angles.

The Blackwell relationship between the probability of correct image detection and the relative contrast of the image was subsequently recommended by Carel for use in adjusting relative image contrasts obtained from the image identification characteristics of Chapanis, to increase the legibility performance level for correct image identification from 50 to 99%. Carel stated that a factor of three was needed to achieve this adjustment, and an additional factor of five is then needed "to raise the picture from a ghost to a more substantial picture," which Carel referred to as "Muller's constant."[41]

Carel's image difference luminance ratio of three, to convert from 50 to 99% probability of correct identification, appears to have been obtained from the probability function graph by extracting the relative contrast of 2.12 corresponding to 99% and then converting the relative contrast to an image difference luminance ratio. This conversion is necessary because the relative contrast is defined by Blackwell as the difference between the image difference luminance at the new probability of correct identification, in this case the 99% level, and the 50% image difference luminance level, divided by the 50% image difference luminance level. The image difference luminance multiplier needed to convert from the 50 to the 99% level of correct identification can therefore be obtained by adding one to the relative contrast. The value of 3.12 obtained by Carel was then presumably rounded to 3.0.

The Muller constant adjustment is considered comparable to the increase by a multiple of about four in the image difference luminance, and three in the relative contrast, to adjust the 99% accuracy numeric characteristic of King, et al, to the "comfort level" shown in Figure 3.9. Increases in the image difference luminance, and the contrast, of a picture after the legibility performance reaches nominally 100% are dealt with in the next subsection.

The comparison in the previous subsection between the experimental image difference luminance characteristics of Jainski and those of Aulhorn and Harms serve a dual purpose, since the comparison not only shows the similarity between the shapes and slopes of the image difference luminance characteristics but also demonstrates that the magnitudes of the performance compensation multipliers required to adjust image difference luminance requirements at one level of performance to those required at a different level can be quite large. In the previous subsection, it was reported that the image difference luminance ratio between the Jainski 8.8 minute of arc 95% accuracy characteristic and the Aulhorn and Harms 9 minute of arc 50% accuracy characteristic at a photopic luminance of 10 fL was 2.88. To compare this result with the image difference luminance ratio prediction of the Blackwell probability function, the relative contrast of 1.80 corresponding to a 95% probability of correct identification, is added to unity to give 2.80 as the image difference luminance ratio compensation multiplier for the Blackwell image detection data. In this particular instance, the comparison result shows that the application of Blackwell's contrast correction factor for use with image identification task data, as recommended by Carel, does result in a satisfactory estimate of the image difference luminance compensation multiplier in the photopic background luminance range.

Although the preceding comparison shows the two compensation multipliers are in good agreement at the photopic background luminance level of the comparison, there are no other Jainski, Aulhorn and Harms and Blackwell characteristics having critical detail dimensions and image subtended angles in close enough agreement to allow the validity of this result to be confirmed. Since Carel provided no evidence or references to validate the application of contrast compensation relationship for Blackwell's image detection task data to image identification task data, the comparison of the Aulhorn and Harms data with the Jainski data, described above, is the only confirmation that the two types of visual tasks require the same probability of correct identification compensation multipliers. Beyond the comparison just made, no experimental evidence was

found in any of the published image identification task literature surveyed, to allow the values of the image difference luminance compensation multipliers needed to make changes in legibility performance levels predictable. While the comparison results, described above, increase the likelihood that the day compensation multipliers for both visual tasks are the same, and would therefore support Carel's recommendation, the only evidence available shows that the Blackwell probability of correct detection compensation multipliers cannot be applied to adjust the image difference luminance requirements for image identification tasks under night background luminance viewing conditions.

Since levels of human legibility performance much below a nominal 100% probability of correct image identification would not be acceptable during practical aircraft missions, the value of the preceding comparison lies in the fact that the data support the application of constant, albeit separate, legibility performance compensation multipliers under daylight and night viewing conditions. No comprehensive image difference luminance requirements data could be found in the literature, for the 95 to 100% visual performance range, except for the Jainski and King investigations already cited.

The data of King, Wolletin, Semple and Gottelmann show that a mean increase, by a performance compensation multiplication factor of nominally four, in the image difference luminance, ΔL, above the 99% legibility level is necessary for a pilot to respond that a comfort level has been achieved. Once the image difference luminance levels required to produce 100% legibility performance is exceeded, the experimental methods used to establish image difference luminance requirements become dependent on the subjective impressions, rather than the objective responds of the pilots viewing the test images, and the results, in turn, reflect human preference rather than need. This assertion is supported by the data of King, Wolletin, Semple and Gottelmann. More specifically, their results showed evidence of large increases in the variance of the image difference luminance data, when the 100% legibility performance level was exceeded during their comfort level tests.

It should be noted that the image critical detail dimension for the numeric readout character set used in the Flight Dynamics Laboratory experimental investigation was somewhat more than a factor of three larger than the smallest critical detail dimensions used for symbology in conventional electromechanical cockpit instrument displays, controls and panels. The smallest image critical detail dimension used in the Jainski experimental investigation, 5.5 minutes of arc, is, however, about the same size as the smallest critical detail dimensions used for time changing symbology in cockpit displays. Although, as subsequent data will show, the size of the minimum image critical detail dimensions used does have a significant effect on the minimum image difference luminance requirements of display symbology, Jainski's image difference luminance requirements data shows this is not sufficient to account for the much larger contrasts associated with conventional cockpit displays. As will be discussed later in this report, two factors account for this large difference in the image difference luminance requirements. One is that the legibility requirements of conventionally equipped cockpits were determined by experience-based demands, established in operational aircraft rather than in a simulated laboratory tasking environment. The balance of the difference in the legibility requirements is attributed to the need to make conventional reflective mode displays compatible with viewing information they present when a glare source, such as the sun, is located in the pilot's forward field of view.

The comparison data already presented show that the use of the legibility performance compensation multiplier technique is valid, provided that multipliers appropriate to the photopic and scotopic background luminance ranges are used. The principal disadvantage of this legibility compensation technique is that it still requires the estimation of the performance compensation multiplier to be used for the minimum critical detail dimension imagery that has to be resolved on a display and cannot be directly applied to aircraft cockpit legibility requirements.

3.3.4.3. Prediction of Image Difference Luminance Multipliers Needed to Legibility Present Information in Aircraft Cockpits

A major problem is encountered when an attempt is made to transition the image difference luminance requirements data, acquired using ideal images viewed under ideal conditions to an actual aircraft cockpit. The problem relates to the difficulty of predicting the ability of pilots to perceive information from multiple cockpit display information presentations, while the pilot is concurrently subject to the demands imposed by flying the aircraft in an environment with time-changing task loadings, which change depending on mission scenarios and segments assigned; by mental and physical stress; and by many other factors, listed in Table 3.1, that can influence a pilot's legibility performance. These demands are not encountered in the previously described experiments, and the theoretical modeling necessary to predict their effect on aircrew legibility requirements in aircraft cockpit environment, while continuing to advance, have not yet evolved to the point of making a theoretical predictive approach feasible.

The effect of these differences between the conditions experienced by pilots reading the information presented on cockpit displays and pilots participating in laboratory tests is the need for a large increase in the magnitudes of the absolute image contrasts (i.e., and of the corresponding image difference luminances), which are associated with the probability of correct identification versus relative contrast function. Another way of describing the change that occurs when transitioning displayed information to an operational aircraft cockpit is that the pilot's performance can be expected to decrease for the increased workload and less than ideal conditions present, and, consequently, increased magnitudes of absolute image contrast, and image difference luminance, would be needed to maintain the same legibility performance levels attainable for ideal imagery and workload conditions, at the reduced image contrasts established in laboratory tests. If Blackwell's results apply, and the image critical detail dimensions are the same in both environments, the relationship between relative contrast and the probability of correct identification should remain unchanged.

For purposes of a visual comparison, a line is drawn in Figure 3.10 and Figure 3.11 showing the image difference luminance relationship for display symbology having a fixed contrast of twenty. This line represents the relationship between ΔL and L_D for the white symbology on the black backgrounds of most aircraft electromechanical instruments, controls and panels. These figures show that under daylight viewing conditions the image difference luminance levels produced by the reflection of ambient light from the symbology of electromechanical instruments is much more than the level required even for comfort level viewing by the Jainski and Flight Dynamics Laboratory investigations.

Image difference luminance requirements for aircraft cockpit electronic displays, under daylight viewing conditions, are also substantially more than those shown in Figure 3.10 for the 5.5 minute of arc critical detail dimension. Assuming Blackwell's probability of correct detection versus relative contrast relationships can be applied to Jainski's image identification task data, and using these results to calibrate relative contrast, as was done earlier, standard probability function tables can be used to predict that a minimum relative contrast of 2.89, or an image difference luminance ratio of 3.89, is needed to adjust performance from the Blackwell 50 to 100% accuracy level. Since, as previously stated, a 2.80 multiple is needed to adjust the image difference luminance levels from the 50 to the 95% probability of correct identification results of Jainski, the 3.89 ratio represents an increase in the multiplier beyond the Jainski image difference luminance characteristics of 1.39. The application of this multiplier, in combination with the factor of five Muller constant recommended by Carel, that is, a total multiplier of about seven, is still insufficient to compensate for the difference between the image difference luminance requirements determined to be needed in a laboratory and those needed in operational aircraft cockpits.

An image difference luminance characteristic labeled "comfort level" was originally added in Figure 3.10 to permit a visual comparison of the effect of applying the multiple of four shift in the King, et al, image difference luminance characteristics, which was needed to increase the probability of correct identification from a 99% accuracy to the comfort level for their numeric readout data, to the Jainski 95% accuracy, 5.5 minute of arc critical detail dimension image difference luminance characteristic. In practice, the characteristic shown

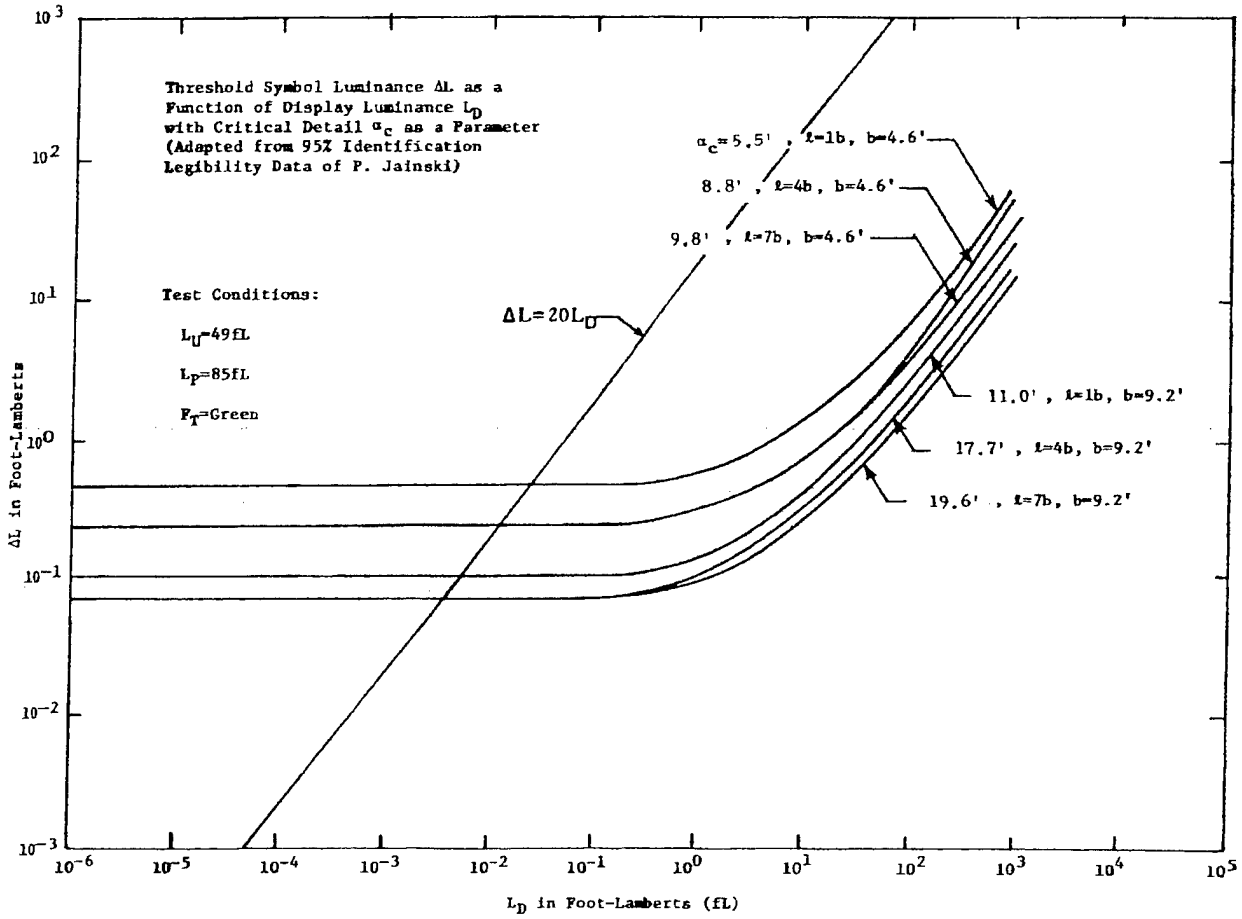


Figure 3.11. Image Difference Luminance Versus Background Luminance Data of Jainski, with Image Critical Detail Dimension as a Parameter, for Head-Down Display Presentations.

in Figure 3.10 is closer to a multiple of 3.5 higher than the Jainski 95% accuracy level characteristic in the photopic background luminance range and is 3.75 higher in the scotopic background luminance range. As such, the comfort level characteristic in Figure 3.10 is shown at about half of the multiple of seven increase, determined in the preceding paragraph using the Carel recommendation for legibility performance compensation. When this comfort level characteristic was originally added to Figure 3.10, nominally the same performance compensation multiplier was used for all display background luminance levels since no test data was available to permit adjusting it for the higher multipliers that may be needed under night viewing conditions.

Under aircraft cockpit night lighting conditions, the settings of the image difference luminance levels, ΔL, are commonly understood to be a matter of pilot preference. An investigation of aircraft cockpit night instrument lighting requirements was conducted from 1969 to 1971 by the Air Force Flight Dynamics Laboratory, employing a specially equipped T-39 aircraft and three night mission scenarios. This study showed that whether or not the missions required the pilots to be dark adapted to the external night scenes, pilots would on average adjust the image difference luminance levels of the instruments down to luminance levels approaching the 95% legibility level curves shown in Figure 3.10.[42] Furthermore, the image difference luminance level settings appear to have been made by the pilots in anticipation of the mission to be flown, either at the start or very early in the flight, and, afterwards, on average were left essentially unchanged for the remainder of the mission. These results differ from those attributed to commercial aircraft pilots, whose external night vision tasks are typically restricted to takeoff and landing at well-lighted airport runways, and

where instrument and panel lighting is typically controlled at luminance levels approaching the comfort level.

Despite the apparent conformity, cited above, between the cockpit display night lighting control strategies employed by pilots, when preparing to perform mission dependent visual tasks at night, significant differences between the image difference luminance level setting preferences of the instruments by individual pilots were also in evidence. In addition, the choices of luminance level settings for the individual instruments support two premises. The first premise is that, all other factors being equal, the night lighting levels of cockpit instruments are set by pilots to achieve approximately equal legibility across the instruments, rather than equal luminance. These settings, for example, resulted in instruments that had smaller critical detail dimension imagery, including those with time changing numeric information, being set to image difference luminance levels higher than those for instruments portraying information with larger critical detail dimension imagery.

A second premise is that the luminance level settings of the pilots, for some of the individual instruments, controllable portions of instruments and panels, were task dependent. On average, pilots dimmed displays, or portions of displays, portraying information not needed for the mission scenario being performed to image difference luminance levels too low to allow accurately reading the information being depicted. This, for example, included fixed format engine legends that were separately controllable from the time changing engine information being displayed. Similarly, the image difference luminance levels of select information, regarded as particularly important to the satisfactory performance of a mission, were increased to levels well above those used during the other missions flown. The principal example of this occurred for an electronic clock readout, used during a simulated low altitude night penetration and weapons delivery mission, which depended on dead reckoning for navigation, and, therefore, on time, speed and heading to make turns where ground checkpoints could not be located visually.

The preceding observations are included here to show that the night image difference luminance settings of pilots do at least conform to the constant night image difference luminance requirements shown in Figures 3.8 and 3.10 and, moreover, nominally agree with the levels of these requirements, shown in Figure 3.10. An additional purpose of describing night cockpit image difference luminance setting of military pilots is to point out that these levels are much lower than the levels normally considered suitable for good legibility, and, in fact approach the levels normally associated with a laboratory test rather than an aircraft cockpit environment.

Although the Jainski and Flight Dynamic Laboratory investigations represent an admittedly limited database of information to be drawn upon, the Jainski investigation alone increased the information available in the literature on this subject by an order of magnitude or more. Furthermore, the data that was found does appear to be self-consistent, and more importantly no data was found which was inconsistent. The only failing of the Jainski data is that it is directly applicable only for ideal imagery, collected under essentially ideal conditions, and therefore does not provide any inherent means, beyond the constant multipliers already described, to adjust the image difference luminance level characteristics to correct for the transition from the ideal to the realistic imagery and viewing conditions experienced by a pilots and other aircrew members in operational aircraft.

In the past, as today, when definitive design data is not available, the best information that is available has to be used. Using this premise, and based on the previously described validation of the historic practice of applying various multipliers to Blackwell's daylight contrast requirements data for 50% accuracy of correct detection, to make it suitable for use at higher performance levels, the present report will continue to use this now traditional approach. The difference, in the present instance, is that the approach will be applied to the experimental legibility characteristics of Jainski for image identification data rather than to the image detection data of Blackwell.

Other than the Muller constant, recommended by Carel, no information was found in the literature that attempted to deal with the question of how much to increase the image difference luminance requirements to compensate for the expected decrease in performance, which is attendant to the transition from ideal imagery and viewing conditions to an operational aircraft environment. Consequently, it can be concluded that no

validated theoretical method currently exists for predicting the absolute image difference luminance requirements needed at one legibility performance level from luminance requirements already available at another performance level. This limitation will simply be circumvented by using another approach to establish the absolute values of the pilot's legibility requirements under operational aircraft cockpit conditions. The alternative approach involves acquiring the necessary legibility requirements from military operational aircraft cockpit experience with actual electronic displays, subject to the proviso that pilots do consider the image difference luminances of the display information to be satisfactory to meet their information presentation needs.[43] This subject is dealt with in greater detail near the end of this chapter, in Section 3.9, in conjunction with adapting the legibility control model developed later in this chapter to meet the pilot's legibility needs in operational aircraft environments.

3.3.5. Dependence of Jainski Data on Cockpit Luminance Environment

Whereas the earlier experiments of both Blackwell, and Aulhorn and Harms had covered a wide range of display background luminance values, L_D, the other luminance fields including the surround-field luminance external to the aircraft, L_U, the cockpit panel luminance, L_P, and the infield luminance areas internal to the cockpit, L_I, were always maintained at the same luminance value as L_D. Jainski's 17.7 minute of arc critical detail dimension characteristic, corresponding to $L_P = L_U = L_D$ in Figure 3.12, shows that this is a nearly ideal luminance environment. This conclusion was reached by virtue of the fact that when this characteristic is compared with the characteristics in any of Jainski's other charts, it has the smallest image difference luminance level requirements for this critical detail dimension, irrespective of the values of the other surround-field and combined infield and panel luminance values tested. It should be noted that the distinction between the panel and infield luminances, present in the King, Wolletin, Semple and Gottelmann experiment was not present in the Jainski experiment, where the term infield luminance referred to both of these areas within the cockpit.

Figure 3.10 and 3.11, which were introduced previously for other purposes, are primarily intended to show the influence of changes in the critical detail dimensions of the test symbology on the image difference luminance requirements. The test conditions for the simulated head-down display (HDD) are indicated in Figure 3.11. The test conditions for the head-up display (HUD) data of Figure 3.10 are $L_U = 2\,L_D$ and $L_P = L_I = 0.003\,L_D$. Except for a change in the units of luminance in these figures, and the previously described changes to the labeling of the characteristics, these figures appear as size-scaled traced reproductions of the figures in the original Jainski report. The closeness in size of the 8.8 and 9.8 minute of arc critical dimensions of the data in these two figures, apparently resulted in a coalescence of the experimental data curves at high display background luminance levels, for the head-up display data on Figure 3.10 and for the low display background luminance levels for the head-down display data on Figure 3.11. Referring to the same figures, it may be seen that these relationships also hold true for the 17.7 and 19.6 minute of arc critical detail dimension data, which is also attributed to the small difference between their critical detail dimensions.

Although the head-up and head-down image difference luminance characteristics in Figures 3.10 and 3.11 appear to be quite different from one another, this difference is not because one test display simulates a head-up display and the other simulates a head-down display. The difference stems instead from the fact the differences in the panel and surround-field luminances, and how they relate to the display background luminance levels. This may be more readily seen by referring to Figures 3.12 and 3.13, but most readily when referring to Figure 3.13. These figures contain data extracted from Jainski figures that compiled HUD and HDD data separately and then were combined to create the presentation formats shown in Figures 3.12 and 3.13.

Figure 3.13 illustrates the dramatic influence surround and panel luminance levels have on the image difference luminance requirements at low display background luminance levels and the relatively small effect at high display background luminance levels. Figure 3.13 also shows the convergence of the image difference luminance requirement curves at high display background luminance levels. The coalescence of these

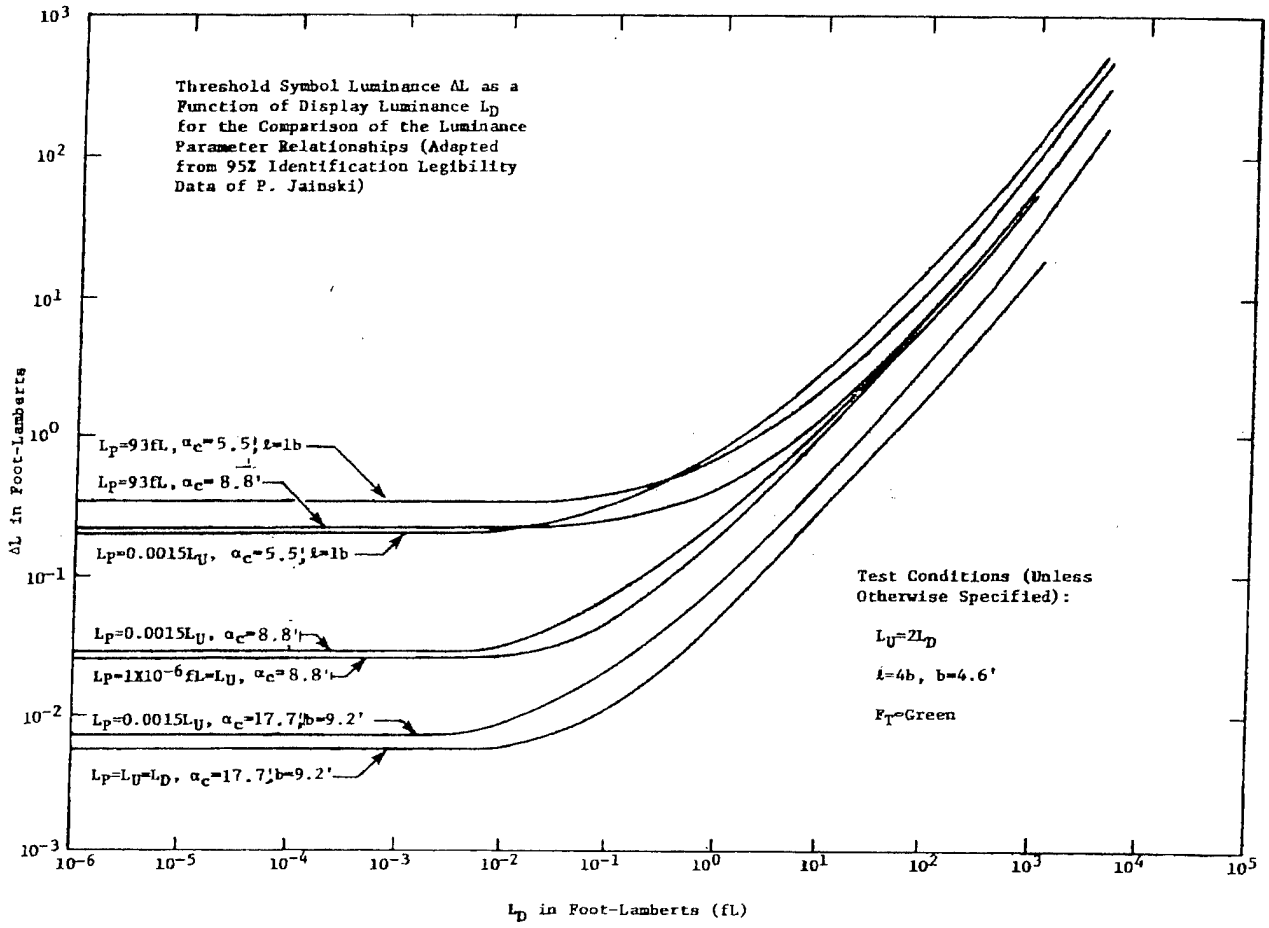


Figure 3.12. Comparison of Image Difference Luminance Versus Background Luminance Data of Jainski, with Panel Luminance as a Parameter, for Head-Up and Head-Down Display Image Presentations.

characteristics is consistent with the fact that all of the data in this figure is for a single test symbol and, therefore, all of the characteristics are for the same critical detail dimension. A similar combination of results occurs in Figure 3.12. This graph plots data for symbols having three different critical detail dimensions and shows that at high background luminance levels each of the three image sizes show a tendency to coalesce.

The dominant effect of changing the color of the test symbol, as determined by comparing image difference luminance requirements characteristics of Jainski that otherwise share the same independent variable parameter values, was that the results are inconclusive. Among the colors tested by Jainski: red, green, blue, white and yellow, blue and red were the only colors having characteristics with any apparent trend to their data. Test images rendered in blue tended to produce the highest image difference luminance requirements and red tended to produce the lowest difference luminance requirements, however, neither color was entirely consistent in doing this over the full range of the display background luminances, and for all of the parameter variations Jainski tested. Jainski's tests included two different critical detail dimension symbols rendered in each of the test colors and presented in both the HUD and HDD configurations. The variations tested were therefore quite limited.

As one of only two consistent trends, under higher display background luminance levels (L_D > 10 fL), red symbols on the average required slightly smaller image difference luminance values to make them identifiable than did the other colors. The only other consistent trend in Jainski's color data was that the ratio of the image

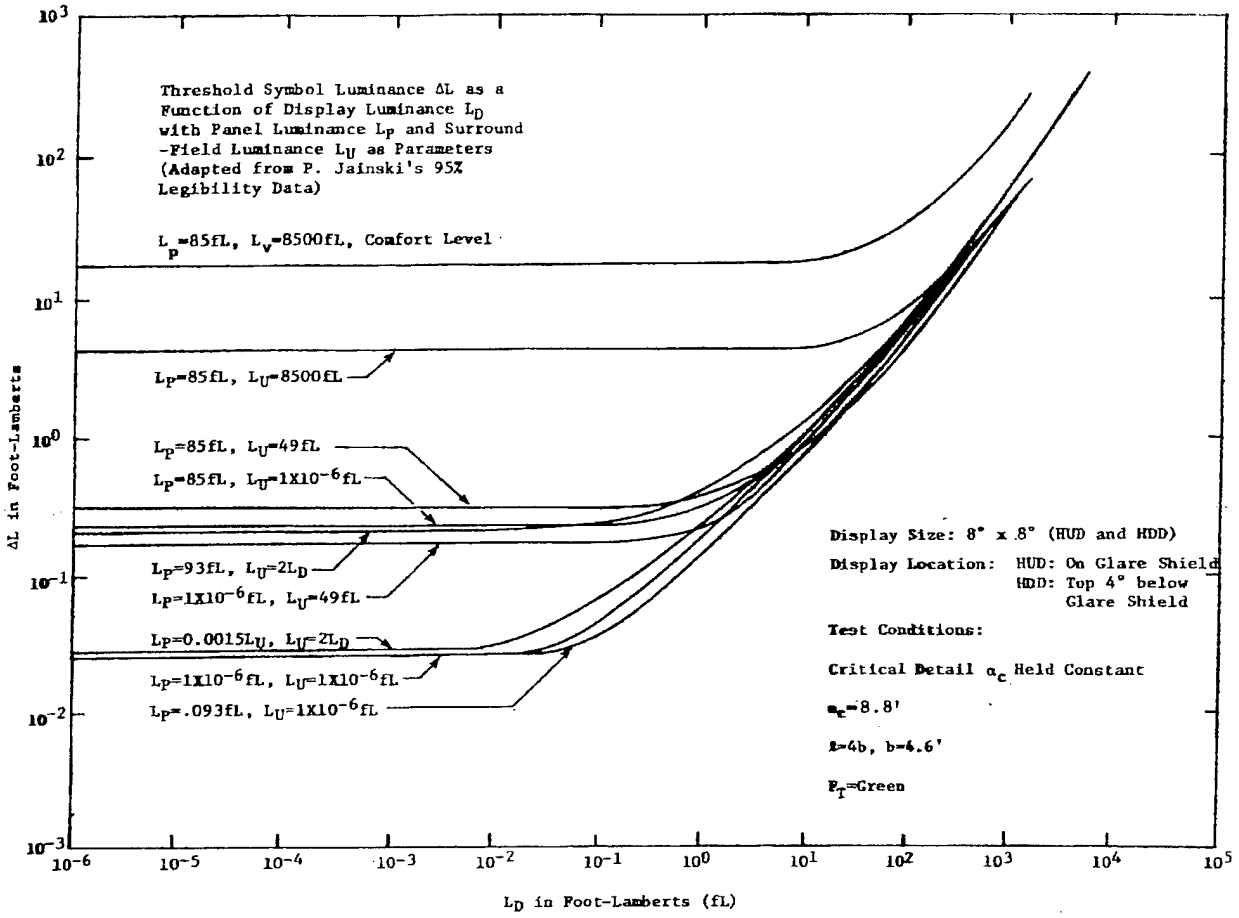


Figure 3.13. Image Difference Luminance Versus Background Luminance Data of Jainski, with the Panel and Surround-Field Luminances as Parameters.

difference luminance, between the most and least legible symbol colors, decreases from about three to one down to two to one, or less, in going from night to daylight display background luminance levels.

The small differences in the image difference luminance requirements resulting from changing the test symbol color are not considered large enough nor consistent enough to justify trying to draw conclusions, on the basis of color, for Jainski's threshold legibility data. Because the variability between test subject responses exceeded the differences introduced by changing the test symbol color, it is considered adequate to use the legibility data for green symbology to also describe the image difference luminance requirements for white, red, yellow and blue symbology. For the preceding reasons, only Jainski's data for green test symbols is shown in this report.

3.3.6. Discussion of Key Legibility Dependence Features of Jainski's Data

The development of a mathematical model to describe the legibility requirements of pilots, later in this chapter, is predicated on first modeling ideal legibility requirements and only later adding the effects of the non-ideal illumination environment conditions experienced in aircraft cockpits. In this section, the test data associated with illumination environment conditions that produce ideal, that is, optimum legibility performance, are identified and described. Next, the test data and effects produced by non-ideal panel and surround luminance levels are introduced and described. Finally, test data concerning the effects of the location of a

display in the cockpit, that is, whether it is used for head-up or head-down viewing, are identified and described.

3.3.6.1. Ideal Panel and Surround Luminance Conditions

The better visual acuity experiments conducted in the past, which are typified by the threshold of image detection experiments of Blackwell and the minimum separable acuity experiments of Aulhorn and Harms, had uniform luminance backgrounds on which the display symbology was superimposed; hence, in terms of the present variables, the condition $L_D = L_U = L_P$ was satisfied. In Figure 3.12, Jainski's data corresponding to this environmental luminance viewing condition for head-down displays is shown compared with the environmental luminance viewing condition of $L_U = 2L_D$ and $L_P = 0.0015L_U$ for head-up displays, at a critical detail dimension of 17.7 minutes of arc. Figure 3.13, in turn, shows that this latter luminance environment viewing condition is nearly ideal, in that it produces a minimum image difference luminance requirement.

The data of Figures 3.12 and 3.13, when considered together, therefore show that the following three luminance conditions: $L_P = L_U = 1 \times 10^{-6}$ fL and $L_P = 0.093$ fL; $L_U = 1 \times 10^{-6}$ fL and $L_P = L_U = L_D$; and, to a somewhat lesser extent, $L_P = 0.0015\ L_U$ and $L_U = 2\ L_D$ represent ideal luminance relationships for the identification of display imagery, having a particular critical detail dimension, and that this is true irrespective of the value assigned to the display luminance, L_D. An important practical consequence of this finding is that the image luminance requirements data of Figure 3.10 represent ideal difference luminance requirements (i.e., minimum requirements) and are approximately valid, not only for the head-up display panel and surround luminance condition used to acquire the data, but also specify the ideal head-down display image difference luminance requirements.

3.3.6.2. Observations on Effects of Panel and Surround Luminances

Referring again to Figure 3.13, several other data relationships are worth noting. First, the panel and surround luminance levels have a large influence on image difference luminance requirements only at low display luminance levels. At high display background luminance levels, the image difference luminance requirements are about the same for all of the panel and surround luminance conditions tested. Second, at low display background luminance levels, the image difference luminance requirements remain nearly optimum until photopic panel or surround luminance levels (i.e., levels in excess of the approximately 1 to 3 fL mesopic to photopic transition) are reached. This result may be seen by comparing the negligible change that takes place in ΔL when L_P is increased from 10^{-6} fL to 0.093 fL, with the factor of eight increase in the ΔL requirement that occurs when L_P is changed from 0.093 fL to 85 fL, where for both situations L_U is maintained fixed at 10^{-6} fL. Third, and finally, the characteristics of Figure 3.13 demonstrate that the image difference luminance requirement advantage that can be achieved, under daylight viewing conditions, from decreasing L_D to reduce ΔL (i.e., for example, through the application of optical filters to displays) is limited at low L_D values by the degrading effect that large constant values of L_P and L_U have on the image difference luminance requirement, ΔL.

3.3.6.3. Effect of Display Location: Head-Up or Head-Down

Jainski collected image difference luminance requirements data using a head-down display located on a simulated cockpit instrument panel as shown in Figure 3.3 and a visually identical head-up display located at the top of the display panel but with its test symbology collimated at infinity. Theoretically, the image difference luminance requirements for head-up and head-down display imagery subtending the same visual angle at the observer's eyes and under equivalent background luminance conditions should be identical. When the image difference luminance requirements for both of Jainski's display configurations are plotted together, as they are in Figures 3.12 and 3.13, the data corresponding to ideal viewing conditions, as specified previously in this section, are indeed very nearly identical for both the head-up and head-down displays. This

is true in spite of the fact that the head-up display condition $L_U = 2\ L_D$ at L_D = 1,000 fL makes L_U = 2,000 fL and $L_P = 0.0015 L_U$ = 3 fL, while the corresponding conditions for the head-down display are L_D = 1,000 fL, L_U = 1 x 10^{-6} fL and L_P = 1 x 10^{-6} fL or 0.093 fL. The high levels of display background luminance used in this example were chosen to emphasize the large differences between the surround, panel and display background luminance levels, and to show that similar or lower levels of panel and surround luminance have only a small effect on the image difference luminance requirements. It should be noted that this result is consistent with the predictions of the inset in Figure 3.9, for applying a correction factor to the image difference luminance, based on the value of the ratio between the surround and display background luminances.

An extremely important image difference luminance relationship can be recognized by observing the low level display background luminance dependence of ΔL on L_P and L_U in Figure 3.13. Raising either the panel luminance from L_P = 1 x 10^{-6} fL or 0.093 fL to L_P = 85 fL with L_U held at 10^{-6} fL or, alternatively, raising the surround luminance from L_U = 1 x 10^{-6} fL to L_U = 49 fL with L_P held at 10^{-6} fL produces equivalent image difference luminance requirements for the head-down display symbol identification task. This is true in spite of the fact that in the first case the panel enclosing the head-down display is bright, L_P = 85 fL, and the surround is dim $L_U = 10^{-6}$ fL, while in the second case, the panel enclosing the display is very dim, $L_P = 10^{-6}$ fL, and the surround is bright L_U = 49 fL. It appears from this dependence that the location of the display, be it in the bright or dim area, is not important. Instead, what is important is that raising either the panel or the surround luminance level into the photopic luminance range causes an increase in the display image difference luminance requirement. In addition, for Jainski's test geometry at least, the magnitude of the increased requirement on ΔL due to the panel luminance is equivalent to the ΔL increase required due to the change in the surround luminance.

Referring again to Figure 3.13 it may be seen that the non-ideal image difference luminance requirement characteristic corresponding to L_P = 93 fL and $L_U = 2\ L_D$ for the head-up display corresponds very closely with the equivalent L_P = 85 fL, L_U = 1 x 10^{-6} fL data for the head-down display. This data lends further credence to the finding that no changes in the image difference luminance requirements occur, for the Jainski tests, when the position of the head-up display is interchanged with that of the head-down display. Likewise, an interchange of the surround with the panel luminance levels is not expected to cause a change in the display image difference luminance requirements, when the display's position is held fixed. These results are very useful in generalizing Jainski's results and in fact are the reason no distinction has been made between the curves of head-up and head-down image difference luminance requirements data in any of the figures showing Jainski's data.

While the fact that Jainski's surround and panel luminance levels can be interchanged without changing the display image difference luminance requirements is useful, this should not be regarded as a general result that can be carried over to situations where Jainski's geometric relationships are not duplicated. Changing the display size or vertical position with respect to the panel, the size of the surround or panel, or any one of several other test factors, which were constant in Jainski's experiment, could change the relative magnitudes of the image difference luminance requirements when either the display positions or the panel and surround luminances are interchanged.

The underlying ideal legibility relationships identified in this section are nonetheless fundamental and should be valid even under modified geometric conditions. The complete legibility model that is developed later in this chapter allows the effects of different display locations, whether head-down, head-up or helmet-mounted and variations in the geometry of a cockpit to be taken into account in controlling the legibility of the respective displays.

3.4. Empirical Representation of Ideal Legibility Requirements

In the preceding section, a point was made to distinguish between ideal image legibility performance characteristics and viewing conditions from the balance of Jainski's experimental data. The intent of doing this

was to be able to identify and then select from Jainski's data those characteristics that can be considered ideal and therefore suitable for mathematical modeling, in accordance with the previously described analysis approach adopted for use in this report.

3.4.1. Mathematical Modeling of Ideal Image Legibility Characteristics

Based on the experimental data of Jainski,[44] ideal image legibility characteristics correspond to ambient/cockpit illumination conditions that satisfy the following criteria:

$$L_U \leq 2L_D\ ,\ L_P \leq 2L_D \text{ and } E_B = 0\ . \tag{3.4}$$

The experimental characteristics of Jainski, selected to meet these criteria, can then serve as a reference baseline from which to derive an empirically based mathematical model to represent the ideal image legibility characteristics. Once established, the model can then be modified to include the degrading influence of non-optimum panel luminance, surround luminance and glare source conditions.

Figure 3.10 provides a representative set of image difference luminance versus display background luminance characteristics that are valid for both head-up and head-down display presentations and also satisfy the ideal viewing condition criteria. These ideal characteristics are used as the reference baseline for the formulation of the mathematical model needed. It should again be noted that the purpose of this mathematical model representation is not to depict the various variable dependence facets of Jainski's experimental data accurately, but, rather, is to provide a general equation that can serve as a basis for representing constant perceived image difference luminance versus display background luminance legibility characteristics, a feature that is inherent in the threshold legibility data collected by Jainski.

The graph in Figure 3.10 shows Jainski's ideal legibility data plotted on logarithmically scaled x and y axes. It may be seen from this figure that the characteristics appear to approach straight line asymptotes at the low and high background luminance ends of the characteristics. For small values of the display background luminance, L_D, of nominally 0.003 fL and smaller, the image difference luminance characteristics of Jainski can be represented by the equation of a straight line parallel to the x axis as follows:

$$\Delta L = \Delta L_K\ . \tag{3.5}$$

The constant term, ΔL_K, represents the difference luminance values corresponding to the straight line asymptote intercepts of Jainski's characteristics with the y axis.

For large values of the display background luminance, L_D, of nominally 3 fL and larger, the experimental image difference luminance versus background luminance characteristics of Jainski can be approximately represented by the equation of a straight line tangent to the characteristics in the photopic background luminance range. A tangent rather than an asymptotic line is used because the pupils of the eyes reach their minimum diameters at background luminance levels between about three hundred and one thousand foot-lamberts, depending on differences in pupil diameter responses of the eyes between different individuals. This small pupil aperture, like the low f-stop settings on camera lenses, promotes the ability of the human visual system to achieve maximum visual acuity, and, beyond this luminance, the slope of the image difference luminance versus background luminance characteristics is shown by Jainski's results to increase to approximately unity. Since virtually all aircraft cockpit electronic displays, excepting head-up displays, operate at maximum background luminance levels of one hundred foot-lamberts or less, the slope for this lower portion of the background luminance range is used in the mathematical model, rather than the maximum slope reached by the constant image critical detail dimension characteristics of Jainski at the maximum background luminance levels tested.

The development of an equation for use in mathematically modeling the photopic background luminance region of the image difference luminance characteristics of Jainski, applicable to ideal images and viewing conditions, simply involves writing the equation of a straight line for logarithmically scaled image difference

luminance and background luminance axes. The general equation of a straight line having any orientation or position within a planar two dimensional orthogonal Cartesian coordinate system (i.e., a rectangular coordinate system) can be expressed by the following equation:

$$y - y_1 = m(x - x_1) . \tag{3.6}$$

This equation describes the locus of points anywhere on a straight line using the coordinate pair (x, y), where x is the distance, measured parallel to the x axis, from the y axis (i.e., the x = 0 locus) to any point on the line (i.e., the abscissa of the point) and y is the distance, measured parallel to the y axis, from the x axis (i.e., the y = 0 locus) to the same point on the line (i.e., the ordinate of the point). A line is defined when its slope, m, and any arbitrary point on the line (i.e., designated in the equation by the coordinate pair (x_1, y_1)) are specified.

The general equation of a straight line on a full logarithmic graph can be obtained by substituting the logarithms of the relevant luminance variables and constants into the preceding general equation for a straight line, thereby yielding the following expression:

$$\log_{10} \Delta L - \log_{10} \Delta L_1 = m(\log_{10} L_D - \log_{10} L_{D1}) . \tag{3.7}$$

The perceived image difference luminance and the display background luminance in this equation were previously defined. The constant luminance coordinate pair $(L_{D1}, \Delta L_1)$ and slope of the logarithmic line, m, are analogous to the coordinate pair (x_1, y_1) and the slope of the line, m, respectively, described previously for uniquely defining a straight line on a rectangular coordinate plot with linear axis scaling.

The preceding expression for a straight line on a full logarithmic graph can be further reduced by using the laws of logarithms to simplify it. Combining terms within the logarithms

$$\log_{10}\left(\frac{\Delta L}{\Delta L_1}\right) = m \log_{10}\left(\frac{L_D}{L_{D1}}\right) , \tag{3.8}$$

then taking the antilogarithm

$$\frac{\Delta L}{\Delta L_1} = \left(\frac{L_D}{L_{D1}}\right)^m , \tag{3.9}$$

and finally solving for the image difference luminance

$$\Delta L = \Delta L_1 \left(\frac{L_D}{L_{D1}}\right)^m . \tag{3.10}$$

This completely general equation always yields a straight line when plotted on a graph with full logarithmic scaling of its axes.

In the special case where the slope, m, is equal to zero, the power term evaluates to unity and Equation 3.10, the general equation for a straight line for full logarithmic axis scaling, then becomes the equation of a straight line parallel to the x axis,

$$\Delta L = \Delta L_1 . \tag{3.11}$$

By substituting the previously introduced y axis intercept of the low background luminance zero slope region of the Jainski characteristic, ΔL_K, into this equation for ΔL_1, it yields the formerly introduced equation for the low background luminance region of the Jainski characteristics, as is required.

To the first level of approximation, the Jainski experimental data shown in Figure 3.10 can be mathematically modeled as the summation of the previously introduced low and high display background luminance straight line (i.e., the lines are straight when plotted on a graph having logarithmic rather than linear axis scaling) representations of the image difference luminance versus background luminance characteristics of Jainski. The resultant expression formed by the summation of Equations 3.5 and 3.10, can be represented in equation form as follows:

$$\Delta L = \Delta L_K + \Delta L_1 \left(\frac{L_D}{L_{D1}} \right)^m . \tag{3.12}$$

Since the coordinate pair, (L_{D1}, ΔL_1), that defines the straight line asymptote of slope, m, to the Jainski characteristics can be any point on the line, the equations are simplified by choosing the coordinate point as ($L_{D1} = L_{DK}$, $\Delta L_1 = \Delta L_K$). This coordinate pair corresponds to the point where the line parallel to the x axis through the y axis intercept intersects the high background luminance asymptote of slope m. Making this substitution in the above equation and introducing an additional subscript, described below, the following final equation is obtained as the sought after approximate mathematical model to represent the ideal experimental data of Jainski:

$$\Delta L_P = \Delta L_{PK} + \Delta L_{PK} \left(\frac{L_D}{L_{DK}} \right)^m . \tag{3.13}$$

In this equation, the "P" subscript has been added to the image difference luminance variable and corresponding image difference luminance intercept constant to indicate that the Jainski data this equation mathematically models corresponds to the image difference luminance values "perceived" by the subject when viewing the test symbology (i.e., at the threshold level for 95% accuracy of identification). It should be noted that there is no relationship between the "P" subscript terminology used in the preceding equation and panel luminance term, L_P, introduced in the previously described experiments by the King, Wollentin, Semple, and Gottelmann, and used elsewhere in this report.

The values of constants ΔL_{PK} and L_{DK}, in the perceived image difference luminance equation above, are in practice parameters, which are dependent on the critical detail dimension of the image being identified and the applicable level of pilot visual performance. The value of the slope, m, of the daylight portion of the image difference luminance requirements characteristic is being treated as a true constant.

Equation 3.8 for the straight line tangent to the high display background luminance portion of Jainski's ideal characteristics in Figure 3.10 can be solved for the slope, m, by substituting the coordinate values for a second higher display background luminance point on the tangent, say ΔL_2 and L_{D2}. Making this substitution, the equation for the slope of the line, m, in terms of any two arbitrarily chosen points on the line, is as follows:

$$m = \log_{10} \left(\frac{\Delta L_2}{\Delta L_1} \right) \Big/ \log_{10} \left(\frac{L_{D2}}{L_{D1}} \right) . \tag{3.14}$$

Through a process of trial and error using this equation, the best curve fit obtained for the experimental data corresponded to a slope of

$$m = 0.9260 . \tag{3.15}$$

To model Jainski's data in Figure 3.10, using Equation 3.13, it is necessary to determine values for ΔL_{PK} and L_{DK}. The values of ΔL_{PK} can be extracted directly from Jainski's original ideal image difference luminance characteristics as the y axis intercepts for each of the test symbol critical detail dimensions. To demonstrate the correspondence between Jainski's experimental data and the mathematical model of it, as represented by Equation 3.13, the perceived image difference luminance, ΔL_P, and display background luminance, L_D, were set equal to the corresponding coordinates for maximum data points for Jainski's 5.5 and 19.6 minute of arc critical detail dimension characteristics shown in Figure 3.10, and Equation 3.13 was then solved for the only remaining unknown value in the equation, L_{DK}. The resulting equation may be expressed as

$$L_{DK} = 10^{\frac{1}{m} \log_{10} \left(\frac{\Delta L_{PK} L_{DM}^m}{\Delta L_{PM} - \Delta L_{PK}} \right)} , \tag{3.16}$$

where L_{DM} and ΔL_{PM} are the coordinates of the maximum point on each characteristic. The values extracted from Jainski's 5.5 minute of arc critical detail dimension characteristic were as follows: ΔL_{PK} = 0.200 fL, L_{DM} = 3,900 fL, and ΔL_{PM} = 573.3 fL. Using these constants in Equation 3.16, the value obtained for the x axis coordinate for the intersection of the two straight lines given by Equations 3.5 and 3.10 is L_{DK} = 0.7204 fL. In

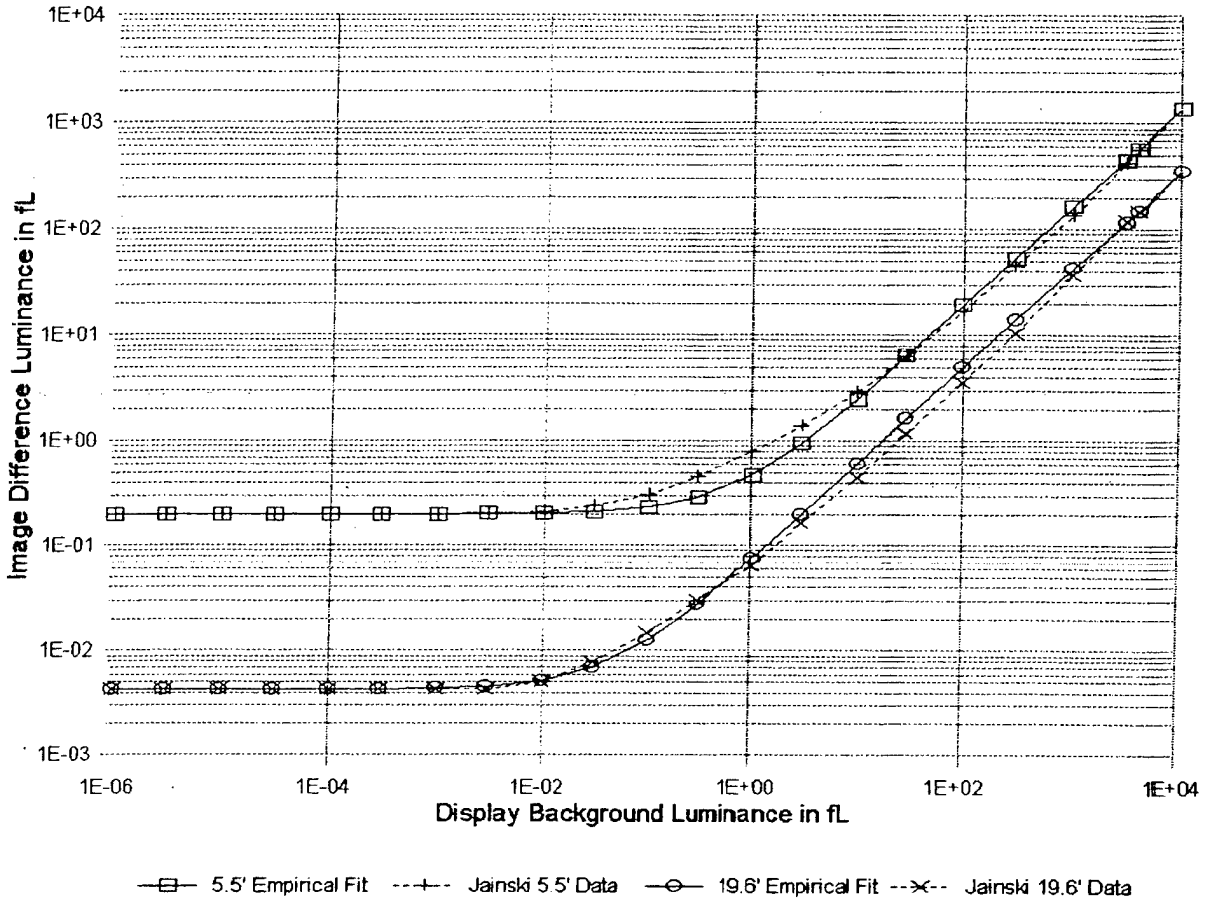


Figure 3.14. Comparison of Empirical Fit and Jainski Legibility Data, for the Two Extreme Critical Detail Dimensions and Ideal Viewing Conditions.

a similar fashion, the values extracted from Jainski's 19.6 minute of arc critical detail dimension characteristic were as follows: ΔL_{PK} = 0.0042 fL, L_{DM} = 3,900 fL, and ΔL_{PM} = 148.4 fL. Substituting these values into Equation 3.16, the value obtained for x axis coordinate for the intersection of the two straight lines given by Equations 3.5 and 3.10 is L_{DK} = 0.0478 fL.

Using values for m, L_{DK}, and ΔL_{PK}, presented above, for the 5.5 and 19.6 minute of arc critical detail dimension characteristics, Figure 3.14 shows the empirical model of Equation 3.13 overlayed on Jainski's experimentally determined characteristics, which were previously illustrated in Figure 3.10 (i.e., a tracing of Jainski's original characteristics converted to units of foot-Lamberts from apostilbs and then scaled down in size for inclusion in this report). The experimental characteristics in Figure 3.14 were generated using data points from Table 3.2, which, in turn, were extracted from the original report drawings published by Jainski. A comparison of these two sets of characteristics in Figure 3.14 shows that they are in reasonably good agreement, with the largest errors occurring for the 5.5 minute of arc characteristics, in the upper portion of the mesopic background luminance range.

3.4.2. Perceived Image Difference Luminance Requirements Equation

The preceding derivation of the perceived image difference luminance equation led to a result that is roughly equivalent to the mathematical model presented by Jainski to represent the experimental data, with

Table 3.2. Ideal Image Difference Luminance Data of Jainski.

L_D in fL	$\Delta L(\alpha_c = 5.5')$ in fL	$\Delta L(\alpha_c = 19.6')$ in fL
3.90×10^{3}	573.3	148.4
3.00×10^{3}	422.8	117.9
1.00×10^{3}	135.7	36.42
3.00×10^{2}	44.86	10.27
1.00×10^{2}	16.71	3.628
3.00×10^{1}	6.378	1.170
1.00×10^{1}	2.904	0.4481
3.00×10^{0}	1.379	0.1627
1.00×10^{0}	0.7847	0.06403
3.00×10^{-1}	0.4656	0.02938
1.00×10^{-1}	0.3100	0.01472
3.00×10^{-2}	0.2379	0.007727
1.00×10^{-2}	0.2112	0.004951
3.00×10^{-3}	0.2002	0.004198
1.00×10^{-3}	0.2002	0.004198
3.00×10^{-4}	0.2002	0.004198
1.00×10^{-4}	0.2002	0.004198
3.00×10^{-5}	0.2002	0.004198
1.00×10^{-5}	0.2002	0.004198
3.00×10^{-6}	0.2002	0.004198
1.00×10^{-6}	0.2002	0.004198

Notes: 1. Data extracted from Jainski's Figures (Bild) 53 and 54.
2. All data are valid to no more than three significant figures.
3. Units conversion equation: L(fL) = 0.09290304 L(asb)

the distinction that the slope, m, in Equation 3.13 must be equated to unity to yield expression developed by Jainski. To cast Equation 3.13 in the same form as the Jainski equation, an alternative formulation of the perceived image difference luminance equation can be obtained by factoring the perceived image difference luminance intercept constant, ΔL_{PK}, from Equation 3.13. The image difference luminance requirements characteristics that were experimentally determined by Jainski, for ideal images and viewing conditions, can therefore be equally well represented by the following alternate formulation of the previously introduced

empirical equation:

$$\Delta L_P = \Delta L_{PK}(\alpha_C)\left[1 + \left(\frac{L_D}{L_{DK}(\alpha_C)}\right)^m\right]. \tag{3.17}$$

This formulation of the equation for ΔL_P is the same as the one originally developed by Jainski, with the exception that the display background luminance ratio term shown in parentheses has been changed from the power of one to the power of "m" to permit a more accurate modeling of the previously presented experimental data. In addition, the dependence of the constant parameters on the critical detail dimension, α_C, of the image to which a specific instance of the equation applies has been included.

The method previously used to derive the values for the constant parameters L_{DK}, and ΔL_{PK} relied on the use of the maximum background luminance data points on the 5.5 and 19.6 minute of arc critical detail dimension experimental characteristics. Since there are two instances where separate experimental characteristics coalesce into a single characteristic a different method is used to model the intermediate characteristics in Figure 3.10.

Based on the observation that there is a discernable shift visible in the L_{DK} breakpoints to the right for increasing values of ΔL_{PK} in Figure 3.10 and lacking sufficiently precise data to permit a more accurate prediction, the shift in these breakpoints can be approximately represented by a straight line to connect the (L_{DK}, ΔL_{PK}) breakpoints to permit plotting the intermediate characteristics on the chart. Using a straight line approximation, the slope of the line can be determined using Equation 3.14, by substituting the appropriate constant parameters already determined for the 5.5 and 19.6 minute of arc critical detail dimension experimental characteristics, as follows:

$$m_K = \log_{10}\left(\frac{\Delta L_{PK}(\alpha_C = 5.5')}{\Delta L_{PK}(\alpha_C = 19.6')}\right) \Big/ \log_{10}\left(\frac{L_{DK}(\alpha_C = 5.5')}{L_{DK}(\alpha_C = 19.6')}\right). \tag{3.18}$$

Substitution of the values of the breakpoint coordinates, for the 5.5 and 19.6 minute of arc critical detail dimension experimental characteristics, into this equation allows the slope, m_K, of the locus of the intermediate characteristic breakpoints to be calculated as follows:

$$m_K = \log_{10}\frac{0.200}{0.0042} \Big/ \log_{10}\frac{0.7204}{0.0478} = 1.424086 \approx 1.424\,. \tag{3.19}$$

The equation of the straight line locus connecting the breakpoints on a full logarithmic graph can be written using Equation 3.9, with the appropriate changes of variables and constants as follows:

$$\Delta L_{PK} = \Delta L_{PK1}\left(\frac{L_{DK}}{L_{DK1}}\right)^{m_K} = \frac{\Delta L_{PK1}}{L_{DK1}^{m_K}} L_{DK}^{m_K}. \tag{3.20}$$

In this equation, L_{DK1} and ΔL_{PK1} are the coordinates of any known breakpoint on the locus of breakpoints. Arbitrarily choosing the coordinates of the 5.5 minute of arc breakpoint and substituting its values into Equation 3.20, the equation of the breakpoint locus can be expressed as follows:

$$\Delta L_{PK} = \frac{0.200}{0.7204^{1.424}} L_{DK}^{1.424} = 0.319040\, L_{DK}^{1.424} \approx 0.3190\, L_{DK}^{1.424}. \tag{3.21}$$

Since the values of ΔL_{PK} are known for each of the Jainski characteristics, intermediate between the 5.5 and 19.6 minute of arc characteristics, it remains to solve for the unknown in this equation, L_{DK}. The desired equation to permit the calculation of the x axis breakpoint coordinate, L_{DK}, can be written as follows:

$$\Delta L_{PK} = \frac{0.200}{0.7204^{1.424}} L_{DK}^{1.424} = 0.319040\, L_{DK}^{1.424} \approx 0.3190\, L_{DK}^{1.424}. \tag{3.22}$$

Table 3.3 lists the values obtained from the evaluation of Equation 3.22, for the experimental characteristics of Jainski shown in Figure 3.10. Figure 3.15 shows the characteristics generated by the mathematical model of Jainski's experimental data, that is, either Equation 3.13 or, equivalently, Equation 3.17, after substituting the values of the constant parameters given in Table 3.3. The 5.5 and 19.6 minute of arc characteristics are the same as those shown in Figure 3.14 since their constant parameters were the basis for the derivation of Equation 3.22, which enabled the calculation of the intermediate breakpoint values.

Table 3.3. Characteristic Breakpoints for Use in the Mathematical Model of Jainski's Ideal Image Difference Luminance Characteristics, in Figure 3.10.

Image Critical Detail Dimension expressed in Minutes of Arc		Approximate Ideal Image Difference Luminance Characteristic Breakpoints	
Actual	Approximate	$\Delta L_{PK}(\alpha_c)$	$L_{DK}(\alpha_c)$
5.50	5.5	0.2000	0.7204
8.84	8.8	0.0276	0.1793
9.82	9.8	0.0211	0.1458
11.00	11.0	0.0150	0.1168
17.68	17.7	0.0069	0.0677
19.64	19.6	0.0042	0.0478

As previously stated, the final mathematical model arrived at to approximate Jainski's ideal image difference luminance characteristics is given by either Equation 3.13 or, equivalently, in the format of the Jainski equation by Equation 3.17. The introduction of the slope, m, into these two equations was intended to permit achieving two goals. One goal, already described, was to more accurately represent the perceived image difference luminance requirements characteristics of Jainski in the photopic and mesopic ranges of background luminance values, in which electronic displays are expected to operate when installed in aircraft cockpits. A second goal was to produce a generalized mathematical model and, in particular, a model capable of being used to satisfy objectives that fundamentally differ from those of Jainski. This application of the equation is considered in detail in Chapters 4 and 5.

The apparent objective of Jainski in employing the slope value of m = 1, for the photopic background luminance range, was to achieve accuracy in characterizing the slope of the experimental characteristics for the maximum background luminance levels at which the data had been collected. Using a slope of unity rather than 0.926, to model the Jainski image difference luminance characteristics, results in larger differences between the experimental characteristics and the predictions of the model, in the mesopic and lower luminance portion of the photopic background luminance ranges. The slope value of m = 0.926, employed in this report to represent Jainski's experimental data, was selected to achieve approximately constant legibility characteristics, having their accuracy optimized for use in controlling electronic displays installed in aircraft cockpits. Later in this report, objectives other than constant legibility control are introduced, which use different values for the slope parameter, m, in Equations 3.13 or 3.17.

Two other points should be made before concluding the discussion of the portion of this report dealing with ideal legibility characteristics. First, it should be noted that the use of a unity slope in Jainski's theoretical model could produce a more accurate overall representation of the experimental data. No attempt was made to determine whether the slope of unity or 0.926 produces a more accurate representation of Jainski's data. The only objective in determining a specific value for the slope, m, and the other constant parameters, in

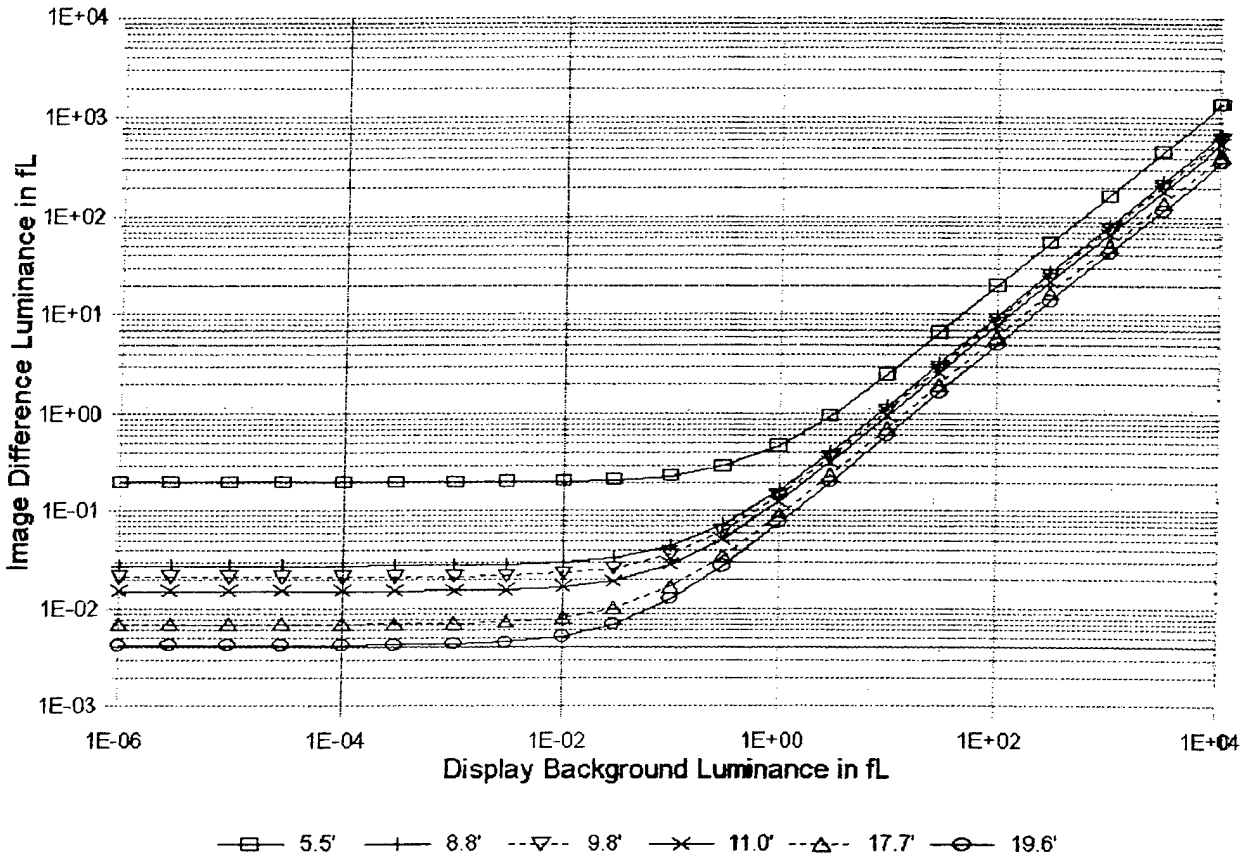


Figure 3.15. Empirical Fit of Jainski Legibility Data for Ideal Viewing Conditions, with the Critical Detail Dimension as a Parameter.

modeling the data of Jainski, was to show that the model can produce a reasonably accurate constant legibility control characteristic representation of the image difference luminance versus background luminance characteristics of Jainski, for ideal images and viewing conditions, and that the 0.926 slope produces a representation better suited for an aircraft cockpit implementation of cockpit display automatic legibility control. In the context of constant legibility control characteristics, it should be noted that a model having a slope somewhat less than unity is more accurate than a model using a slope equal to unity, for display background luminance levels of 3 to 300 fL, in the daylight viewing range. This choice of the slope also conforms more closely to the experimental results of the historic legibility experiments, previously described in this report, however, most of these investigations did not explore the higher background luminance levels included in the Jainski investigation.

3.5. Discrete and Distributed Glare Source Induced Veiling Luminance

The previously introduced empirical equation for the perceived image difference luminance for ideal imagery under ideal viewing conditions lacks any provision to account for other than ideal viewing conditions. As shown in the preceding sections of this chapter, panel, in-field and surround-field luminance levels that are nominally equal to or less than the display background luminance produce ideal display viewing conditions, that is, conditions under which the previously introduced empirical equation for the perceived image difference as a function of the display background luminance is directly applicable.

To accommodate aircraft cockpit panel, in-field and surround-field luminance levels that are of appreciably higher luminance than the background luminance level of the cockpit displays (i.e., and hence correspond to non-ideal viewing conditions) and/or if glare sources are present in the pilot's instantaneous field of view, the previously introduced empirical equation must be modified to incorporate a compensation variable referred to in this report by the name Veiling Luminance. As will be shown, this single variable can be used to account for the effects stemming from non-ideal viewing conditions present in the cockpit's internal and external illumination environment.

The balance of this subsection will be devoted to a description of veiling luminance, its visual significance, the manner used to introduce this compensation factor into the empirical equation, and the introduction and analysis of the experimental data needed for development of the empirical equations used to determine the veiling luminance for both discrete and distributed sources of glare illumination.

3.5.1. The Historic Origins and Generalization of Veiling Luminance

Veiling luminance, as used in this report, is a term representing the increase in the perceived background luminance in the foveal visual field when the eyes are exposed to either discrete or distributed sources of glare in the peripheral and/or parafoveal fields of view. The use of the term "Veiling Luminance" to describe the veil of light perceived to exist between the eyes and a display, when glare sources are present in the observer's field of view, appears to have first been coined by Holladay.[45] Veiling luminance, although described above as a compensation factor, is a real visual phenomenon, not simply an empirical adjustment factor. In the development of the veiling luminance relationships in this section an attempt is made to retain physical realism in the treatment of this variable.

The block diagram in Figure 3.16 represents an attempt to place veiling luminance in the context in which a pilot would encounter it in an aircraft cockpit illumination environment. The figure was prepared in the late 1970s to serve as an aid in describing the factors that influence the interaction between light and the pilot's vision. It is not intended to be an accurate representation of the actual physical interactions that occur in the human visual system, just a schematic representation of the overall interaction of the factors that influence human luminance perception in an aircraft cockpit illumination environment.

The block diagram begins, near its left-hand side, with the two sources of light responsible for all of the light stimulation the aircrew receives, namely, the atmospheric spectral luminance distribution, $L_A(\theta,\phi,\lambda,t)$, external to the cockpit, and the display emitted spectral luminance, $\Delta L(\theta,\phi,\lambda,t)$, generated within the cockpit. The block diagram ends, on the right-hand side of Figure 3.16, with the pilot's overall perception of the aforementioned light sources, as received through the intermediary optical transmission paths and media. It should be noted that emitted luminance, as used in the figure, should be interpreted in the generic sense to represent the light generated, transmitted or reflected by displays, panels, signal lamps, controls and so forth to convey information to the pilot via the human visual system.

Figure 3.16 shows three potential light transmission paths, for the light that enters an aircrew member's eyes, to follow. One of these paths, shown at the bottom of the figure, is the luminance generated or modulated by displays, panels and other light sources, internal to the cockpit, which are viewed either directly or indirectly. In this context, displays viewed indirectly refers to the unintended reflections of the interior of the cockpit from the windscreen or canopy. The figure does not explicitly show the indirect coupling of this source of light to the other paths in the figure, which are primarily concerned with the origins of display background and external ambient luminances.

The second light path in Figure 3.16 starts with light passed through and modified by the aircraft transparencies, such as the windscreen, windows or canopy. This spectrally attenuated and spatially modified version of the luminance incident upon the aircraft transparencies acts as an illumination source for luminance diffusely and specularly reflected from the interior cockpit surfaces, including panels, displays, clothing and so

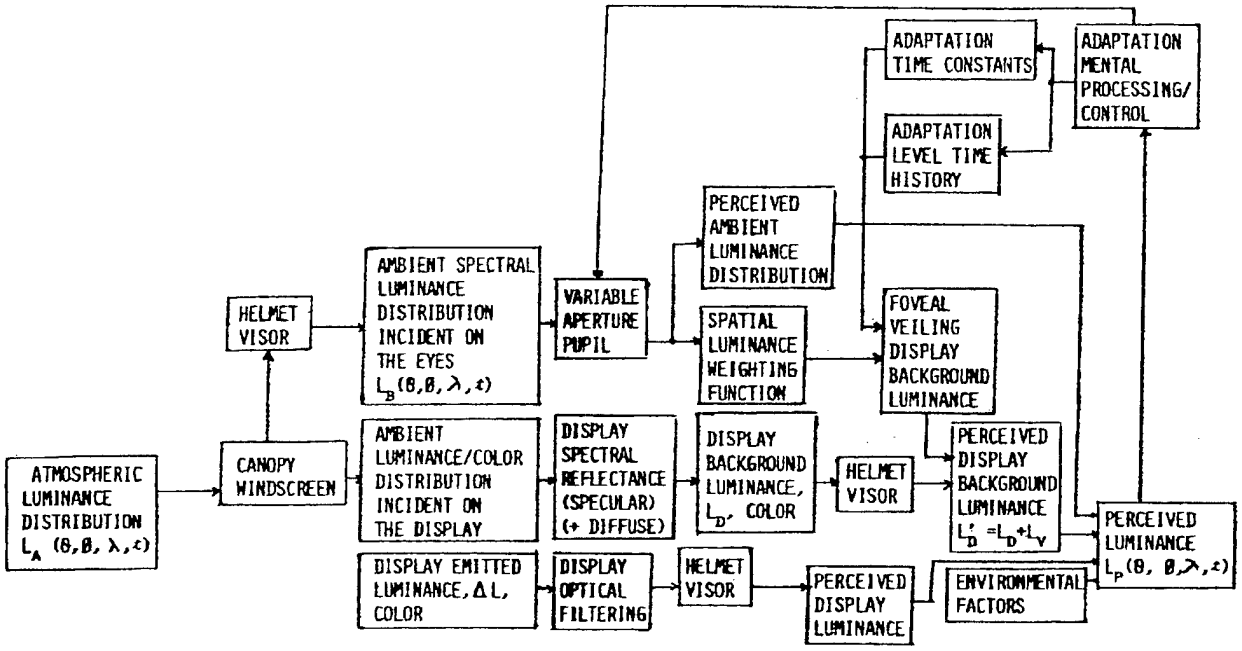


Figure 3.16. Luminance Perception Relationships.

forth. The luminance reflected from these surfaces is then further modified by passage through the helmet visor or sunglasses, if used, before becoming available for perception, as either display background luminance, L_D, or the panel or in-field luminances, L_P and L_I, respectively. It is into this primary path that the effect of veiling luminance is introduced as an additive modification to the display background luminance.

The third light path in Figure 3.16 involves luminance viewed directly, as seen through the aircraft windscreen or canopy and the helmet visor. This forward path is split after the atmospheric luminance distribution is modified by passage through the helmet visor and the variable aperture pupil of the eyes. Following the split shown in the figure, the primary luminance path corresponds to luminance directly imaged on the retina. This is the luminance perceived by the pilot to discern the scene external to the cockpit. Simultaneously a small fraction of the luminance, present at the split, is scattered during passage through the eyes. This event creates the perception that veiling luminance is superimposed on the display background luminance, as shown in the second transmission path, as described above. The additional box entitled "foveal veiling display background luminance" is inserted into this path to accept the additional inputs from the boxes labeled "adaptation time constants" and "adaptation level time history," and to adjust the veiling luminance accordingly. These factors are intended to indicate that the veiling luminance perceptual response to the glare source luminance scattered in the eyes is time dependent. This time dependence is influenced by electrochemical processes in the retinal sensors and elsewhere in the visual system (i.e., which includes signal transmission to and from and within the visual cortex of the brain), which are associated with the unconscious mental processing of the perceived luminance distribution, $L_P(\theta,\phi,\lambda, t)$. The dependence is also influenced by an unconscious mental control over the sensed magnitudes of the imaged scene luminances, via adjustments to the eyes' pupil areas that control the light admitted into the eyes. The impact of the time dependence of veiling luminance becomes important primarily under time variant night illumination conditions.

Dealing with the human visual system's responses to time dependent environmental lighting conditions was intentionally excluded from the consideration of ideal legibility requirements at the beginning of this chapter. Other than to include comments as to where time dependent visual effects would influence the current results, and a discussion of the likely effects of light and dark adaptation in Chapter 8, this subject is considered to be beyond the scope of the present report. Again, the block diagram of Figure 3.16 is only intended to

introduce the factors that influence pilot vision and not as an accurate representation of the interrelationships that are actually present in the human visual system.

Although the use of glare shields, helmet visors and similar devices allow the aircrew's exposures to external light to be attenuated or blocked, and night vision devices allow the amplification of incident light on a spectrally selective basis, military aircrews do not usually have access to a direct means for controlling their exposure to external light. It is therefore desirable to be able to predict the effect of external illumination changes on both aided and unaided eyes. The method proposed here for doing this involves compensating the optimum luminance perception curves of the ideal difference luminance requirements equation, Equation 3.13 or 3.17, for real-world cockpit viewing conditions.

3.5.1.1. Discrete Glare Source Veiling Luminance Dependences

A number of investigations have been conducted to assess the effect of glare sources on a person's ability to perceive display or real-world scene information. Most of the early studies appear to have been intended to determine the effect glare produced by vehicle headlights at night or under dusk viewing conditions. Investigations conducted include those by Sweet (1910)[46], Holladay (1926)[47], Nowakowski (1926)[48], Stiles (1929)[49], Crawford (1936, 1937)[50], Fry and Alpern (1954)[51], Moon and Spencer (1944)[52], Ireland, et al (1967),[53] and Hartmann (1963)[54].

Although each of these papers contributed to an understanding of the effects of glare, from a theoretical standpoint, the paper by Holladay was probably the most important. In it, Holladay introduced the concept of veiling luminance, that is, a transparent veil of light, which is induced in the viewer's eyes because of their exposure to a glare source somewhere in the viewer's instantaneous field of view. The effect of the veiling luminance is to mask (i.e., reduce the apparent or perceived contrast) of fixed luminance/contrast scene objects or display imagery that must be viewed through the veil of luminance. The physical phenomenon to which glare source induced veiling luminance has been ascribed is the scattering of light into the viewer's line of sight by imperfections in the ocular media within the eyes. The visual effect of veiling luminance is therefore analogous to the luminance of the light scattered into an observer's line of sight, when atmospheric haze or fog is present in the intervening space between the observer and the visual scene being viewed. As a practical matter, since the light from a glare source is only scattered into the viewer's line of sight after entering the eyes, veiling luminance, unlike the luminance scattered by haze or fog, is not a directly measurable quantity.

The method formulated by Holladay, to overcome this physical limitation on the measurement of veiling luminance, was to treat the effect of veiling luminance, on the legibility of a display image (or a real-world visual scene), as being directly analogous to the effect of an increase in background luminance, on the legibility of display imagery (or a real-world visual scene), while holding the image (or the scene) difference luminance constant. In practice, this is precisely the physical effect that the addition of veiling luminance has on the display (or on the real-world visual scene) background luminance, because, it increases the display (or the scene) background luminance perceived by the observer but in doing so does not change the image difference luminance.

The value of veiling luminance, L_V, can be determined using the following experimental procedure. First, in the presence of a glare source of illuminance, E_B, as measured at the observer's eyes, it is necessary to experimentally determine the image difference luminance, ΔL, required to cause an image being viewed on a display (or a visual scene) background luminance, of measured value, L_D, to be legible at the desired level of image identification accuracy. Second, when the same image (or the scene) is viewed in the absence of the glare, that is, when it is viewed under the conditions previously described as ideal, and with its image difference luminance set equal to the value determined in the first step, the increase in the value of the display (or the scene) background luminance, ΔL_D, required to reduce the image identification accuracy to the same level of performance as when glare is present is a direct measure of the veiling luminance, L_V. The value of the increase in the display (or the scene) background luminance, ΔL_D, can be determined either

experimentally, in a cockpit lighting simulator; through the use of previously tabulated legibility data, collected in either simulated or real-world atmospheric illumination environments; or by introducing a real veiling luminance between the display and the test subjects eyes, the technique employed in the first two of the three experiments published Holladay. In each case, the image identification accuracy, with and without a glare source present, must be the same.

The veiling luminance, L_V, for a particular display or real-world visual scene image can therefore be interpreted mathematically as the difference between two measurable quantities: the value of the background luminance with no glare present and the value of the background luminance with glare present, where in both cases the image difference luminance needed to make the display (or scene) image legible is the same. Because of this relationship, it is possible to account for the effects of a glare source, in the previously derived equations for the perceived image difference luminance requirements, Equations 3-13 and 3-17, by simply substituting the sum $L_D + L_V$ for L_D. The result of this substitution may be expressed in equation form as follows:

$$\Delta L_P = \Delta L_{PK}\left[1 + \left(\frac{L_D + L_V}{L_{DK}}\right)^m\right]. \qquad (3.23)$$

The explicit dependence of the break point coordinate constants, of this image difference luminance equation, on the image critical detail dimension has been dropped from this equation to simplify its appearance.

3.5.1.2. Discrete and Distributed Glare Source Veiling Luminance Dependences

In the investigation conducted by Holladay, it was found that the veiling luminance was dependent on the illuminance attributable to the glare source, as measured at the viewer's eyes, E_B, and on the angle, θ_B, between the glare source and the viewer's line of sight to the display images or real-world objects being viewed. It was further shown by Holladay that the veiling luminance response to a glare source located anywhere on a circular locus, which is at a fixed distance from the viewer and centered on the viewer's line of sight, is constant. Moreover, the veiling luminances induced by multiple discrete glare sources, located on the same circular locus, are directly additive. Based on Holladay's experimental results, it can be concluded that the individual contributions to veiling luminance from any number of discrete glare sources are additive, provided that appropriate angular weighting function adjustments are used to account for the effect of glare sources, at different subtended angles from the viewer's line-of-sight (i.e., on circular loci subtending different angles at the eyes). Holladay went on to formulate this result as an integral equation, using an angular weighting function to represent the relative effect of the glare source as a function of the angle it subtends to the viewer's line of sight, thereby allowing the effect of distributed glare sources to also be treated. This result has been verified by several of the experimenters cited above, and appears to have been accepted by those who did not attempt to confirm its validity, however, all of these experimental studies yielded different angular weighting functions. The results of these early experimenters will be compared with those derived from Jainski's test results later in this chapter.

3.5.1.3. Effect of Veiling Luminance on the Perceived Image Contrast

In the late 1960s, Jainski[55] conducted a very thorough investigation, which for the first time included full daylight glare source viewing conditions. In this investigation, Jainski also demonstrated that the effect of glare could be represented by a veiling luminance. In a viewing environment in which a significant background luminance level is already present, as the combined result of the direct exposure to the ambient illumination conditions present and of the ambient light reflected from real-world scenes or display viewing surfaces, these sources of background luminance are further increased by the amount of the glare induced veiling luminance. The resultant legibility of the real-world scene or display imagery, in the presence of a glare source, is consequently determined by the measurable image difference luminance (i.e., the emitted, reflected or

transmitted luminance) of the scene or display imagery as contrasted against the perceived background luminance; where, for a cockpit electronic display, the background luminance is made up of the combined effect of the background luminance diffusely and specularly reflected by the display (i.e., this includes reflections from the display faceplate, any optical or electromagnetic interference (EMI) filters used, interior filter and display surfaces and the filter and display media) and the veiling luminance induced in the pilot's eyes because of exposure to the sun or an alternative glare source.

Representing the veiling luminance as L_V, a new expression for contrast, C_P, in this case the perceived contrast during those periods when the pilot is exposed to glare, can be expressed as follows:

$$C_P = \frac{(L_S + L_V) - (L_D + L_V)}{L_D + L_V} = \frac{\Delta L_P}{L_D + L_V} = \frac{C}{[1 + L_V / L_D]}, \tag{3.24}$$

where the other variables are as previously defined. Although veiling luminance cannot be directly measured, it is none the less real and as the equation shows its effect is to raise the perceived level of background luminance and, consequently, cause the perceived contrast, C_P, to be reduced below the value that would be obtained if the display image contrast, C, were to be measured. It is for this reason that the minimum image difference luminance requirement in MIL-L-85762 is stipulated independently from the requirement for the measurable display image contrast. The image difference luminance requirement in MIL-L-85762 relates to the need to achieve an acceptable level of perceived image contrast, when glare is presence in the pilot's forward field of view, whereas the contrast requirement in MIL-L-85762 relates to the need to achieve an acceptable level of measurable display image contrast when high ambient illumination levels are directly incident on and reflected from the display.

It should be noted, in the equation for perceived contrast, that when the veiling luminance, L_V, is very small in comparison to the display reflected background luminance, L_D, then the perceived contrast, C_P, is approximately equal to the measurable display image contrast, C, that is

$$C_P \approx C, \quad \text{for} \quad L_V \ll L_D. \tag{3.25}$$

Conversely when the veiling luminance is very large in comparison to the display reflected background luminance, then

$$C_P \approx \frac{L_D}{L_V} C, \quad \text{for} \quad L_V \gg L_D, \tag{3.26}$$

and the perceived contrast is reduced in direct proportion to the increase in the veiling luminance.

3.5.2. Veiling Luminance Dependence on the Illuminance of a Discrete Glare Source

This subsection is devoted to developing the dependence of veiling luminance on the illuminance of discrete glare sources. It starts with an example of the experimental data collected by Jainski, for use in deriving the relationship between veiling luminance and the illuminance of a discrete glare source. Next the method used to determine veiling luminance values from Jainski's head-down display experimental data is described. Following this, comparisons are made between experimental data of Jainski, which include the illuminance of the glare source as either a variable or parameter, to assess the accuracy of the data. Finally, the differences between the dependences of veiling luminance on the illuminance of the glare source for head-down display (HDD) and head-up display (HUD) test configurations are considered.

3.5.2.1. Glare Source Experimental Data

As discussed previously in this section, veiling luminance is not a directly measurable quantity and it therefore has to be derived through the interpretation of other measured quantities. To characterize the effect of the illuminance of a discrete glare source on veiling luminance, Jainski made two sets of measurements for

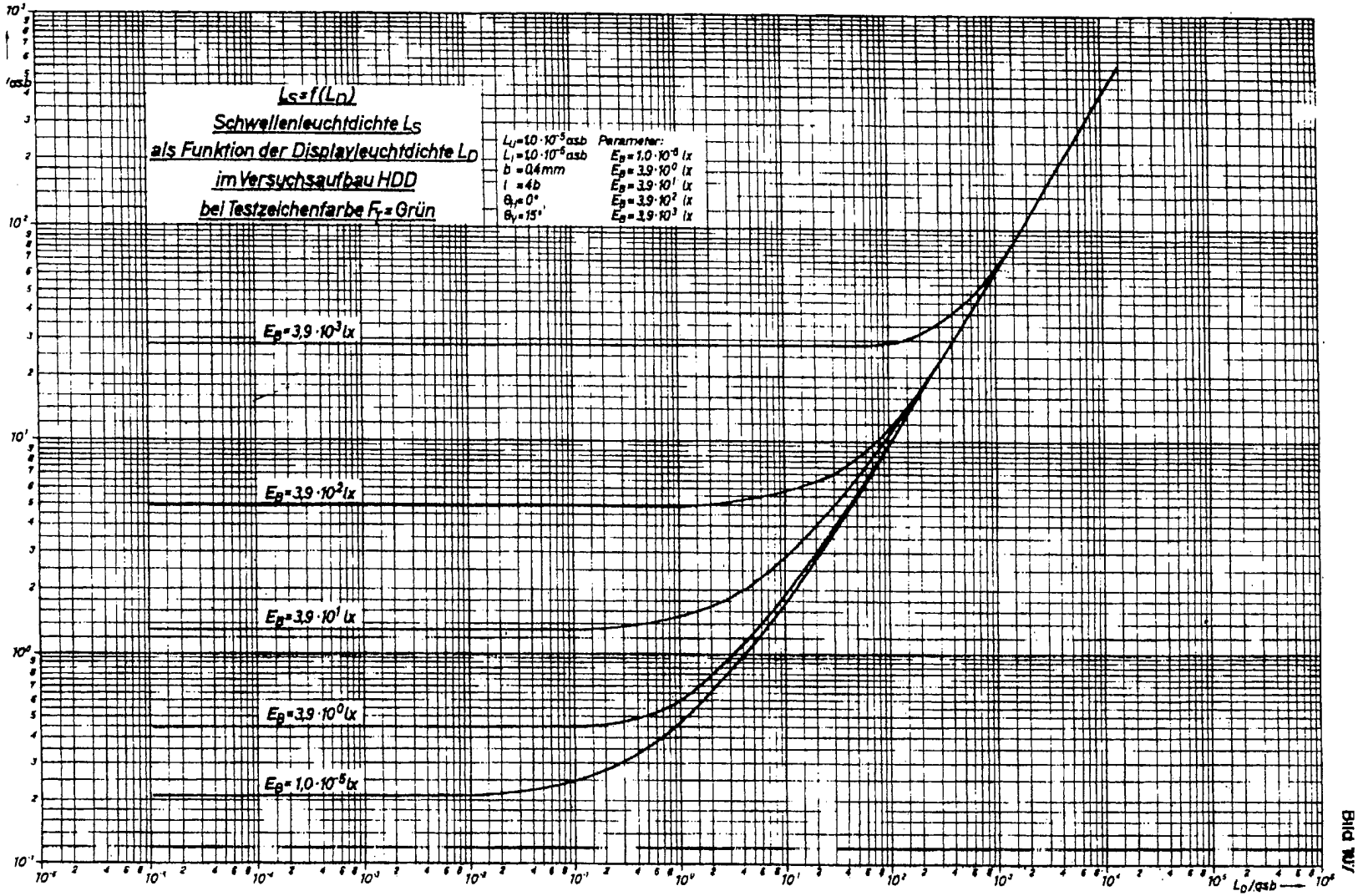


Figure 3.17. Scanned Copy of Jainski Figure 107 Showing Image Difference Luminance Dependence on Glare Source Illuminance as a Function of Display Background Luminance for the Head-Down Display Test Configuration.

both the head-down and head-up display test configurations.

In the first set of measurements, the image difference luminance requirements of the test subjects, as a function of the display background luminance, were characterized with a measure of the glare source illuminance controlled as a parameter and with the other independent variables held constant. Figure 3.17 shows the experimental results of Jainski's measurements for the HDD. The independent variables held constant for the HDD included the following: in-field and surround-field luminances, both set at 0.929×10^{-6} fL (i.e., 1×10^{-5} asb); the critical detail dimension of a green test symbol, set to 8.8 minutes of arc; and the angular position of the glare source, which was set at a horizontal angle of 0 degrees and a vertical angle of 15 degrees with respect to the subject's line of sight to the center of the display. The HUD was characterized in the same manner, using the same parameter and variable values, except that the in-field luminance was $L_I = 0.003\,L_D$ and surround-field luminance was $L_U = 2\,L_D$.

To interpret Figure 3.17 correctly, it is necessary to understand the illuminance variable nomenclature adopted by Jainski to characterize the effect of a glare source on the legibility of display imagery. The illuminance term, $E_{B\perp}$, was selected by Jainski to represent the directly measurable illuminance incident on a subject's eyes from the direction of the glare source. The quantity $E_{B\perp}$ is measured at the location of the subjects eyes, using a cosine receptor (i.e, an illuminance sensor having a Lambertian angular light receptivity characteristic) or Lambertian surface that is oriented perpendicular to an optical axis originating at the center of the glare source and terminating at the subjects eyes. Provided the glare source angular displacements are made at a fixed distance from the eyes this illuminance term remains constant. The illuminance, designated by Jainski as $E_{B\perp}$, is the quantity that would normally be called the illuminance of the glare source and is referred to elsewhere in this report as E_B.

The illuminance variable, used in equations and graphs by Jainski to characterize the effect of the glare source on the legibility of the test symbology, corresponds to the illuminance that would be measured using a cosine receptor having its surface oriented perpendicular to the test subject's line of sight to the center of the display. Jainski designated this measure of the glare source illuminance as E_B, however, except in those instances where it appears in scanned copies of Jainski's figures, this measure of the glare source illuminance will be referred to as E_{BJ}, and E_B will continue to be used to refer to the actual direct illuminance of the glare source. The relationship between E_{BJ} and $E_{B\perp}$, is as follows:

$$E_{BJ} = E_{B\perp}\cos\theta, \tag{3.27}$$

where θ is the angle between the line of sight to the center of the display and the glare source optical axis. In practice, E_{BJ} corresponds to the component of the illuminance of the glare source, which is incident on the eyes, along a direction from the point on the surface of the display being viewed, but since the light from the glare source enters the eyes from the glare source direction, rather than the display direction, it is not clear why this extra step was added by Jainski.

In terms of the terminology adopted for use in this report, Equation 3.27 can also be expressed as follows:

$$E_{BJ} = E_B\cos\theta, \tag{3.28}$$

where $E_B = E_{B\perp}$ was substituted into Equation 3.27 to obtain Equation 3.28. This equation is being introduced because Jainski's measure of the illuminance from the glare source, E_{BJ}, is angle dependent, whereas the direct illuminance from the glare source, E_B, is independent of the angle between the glare source and the pilot's line of sight to the display symbology. Because of its angle independence, it is the direct illuminance of the glare source, E_B, that is incorporated into the final veiling luminance empirical equations.

The glare source illuminance values, $E_{B\perp}$, that resulted in the constant illuminance characteristics shown in Figure 3.17 were 1.04×10^{-5} lux and from 4×10^{0} to 4×10^{3} lux in decade increments (i.e., about 1×10^{-6} fc and from 3.716×10^{-1} to 3.716×10^{2} fc in decade increments). The parameter values shown by Jainski in the figure were obtained by applying the $\cos 15^\circ = 0.966$ multiplier to the $E_{B\perp}$ glare source illuminance values, using Equation 3.27. Applying this multiplier to the number 4 yields 3.864 and after rounding to two places of

accuracy leads to the E_{BJ} illuminance parameter values (i.e., the term Jainski refers to as E_B) shown in Figure 3.17 of 1 x 10^{-5} and from 3.9 x 10^0 to 3.9 x 10^3 lux in decade increments. This change in the way the data is characterized does not alter the results in any way, just the way the data is reported.

In the second set of measurements conducted by Jainski, the image difference luminance requirements of the subjects were characterized as a function of Jainski's measure of the illuminance of the glare source, E_{BJ}, from nominally 1 x 10^{-6} fc to about 1,650 fc. The result of this test for the HDD is shown in Figure 3.18. In this test, the same set of independent variables, held constant in Figure 3.17, was also held constant in Figure 3.18, and in addition the display background luminance, L_D, was held constant at 1 x 10^{-5} asb (i.e., 9.29 x 10^{-6} fL).

For the Jainski test using the HUD configuration, the display background luminance, L_D, was also held constant at 1 x 10^{-5} asb (i.e., about 1 x 10^{-6} fL). The only difference for the HUD test is that the in-field luminance is given by the relationship, $L_I = 0.003 L_D$, a luminance magnitude too small to be measured, and the surround-field luminance is given by the relationship, $L_U = 2 L_D$. The independent variables were the same as for the HDD.

3.5.2.2. Derivation of Equation for Veiling Luminance from Experimental Data

To derive the relationship between the veiling luminance, L_V, and the component of illuminance, E_{BJ}, in the direction of the viewing axis to the display, it is necessary to first recognize that the image difference luminance versus display background luminance characteristic of Figure 3.17, that has an E_{BJ} value of 1 x 10^{-5} lx, corresponds to the glare source being turned off. With the glare source turned off and the other variable values held constant at the values listed in the legend of Figure 3.17, the E_{BJ} characteristic for 1 x 10^{-5} lx satisfies all the requirements for ideal image legibility. Consequently, this characteristic may be used in conjunction with Figure 3.18 to determine the values of veiling luminance for different glare source illuminance values using the previously described procedure of Holladay. In particular, for any value of E_{BJ} on the x axis of Figure 3.18, a corresponding value of L_S (i.e., Jainski's symbol for ΔL) can be read from the y axis. A line parallel to the x axis of Figure 3.17 through this value of L_S on the y axis intersects the 1 x 10^{-5} lx characteristic at a point having an x axis coordinate value of L_D.

The difference between this value of the background luminance, and the constant value of L_D of 1 x 10^{-5} asb in Figure 3.18, is equal to the equivalent veiling luminance, L_V. Since the 1 x 10^{-5} asb value of L_D is negligible compared to the L_D values that can be read from Figure 3.17, as the values of L_S (i.e., ΔL) increase above the minimum value in Figure 3.18, the veiling luminance can be read directly from the L_D axis of Figure 3.17. Figure 3.19 shows the relationship between the veiling luminance and glare source illuminance derived by Jainski using Figures 3.17 and 3.18.

Due to the straight line fit, of the dependence of veiling luminance on the illuminance of the glare source, illustrated in Figure 3.19, an empirical equation to represent this data can be expressed by the equation of a straight line, of slope, q, which was introduced previously, as follows:

$$y - y_1 = q(x - x_1). \tag{3.29}$$

In this case, $y = \log_{10} L_V$ and $x = \log_{10} E_{BJ}$, so the equation of a straight line depicted on full logarithmic coordinate axes can be expressed as:

$$\log_{10}\left(\frac{L_V}{L_{V1}}\right) = q \log_{10}\left(\frac{E_{BJ}}{E_{BJ1}}\right), \tag{3.30}$$

where the veiling luminance slope, q, can be determined using any two points on the straight line using the following equation:

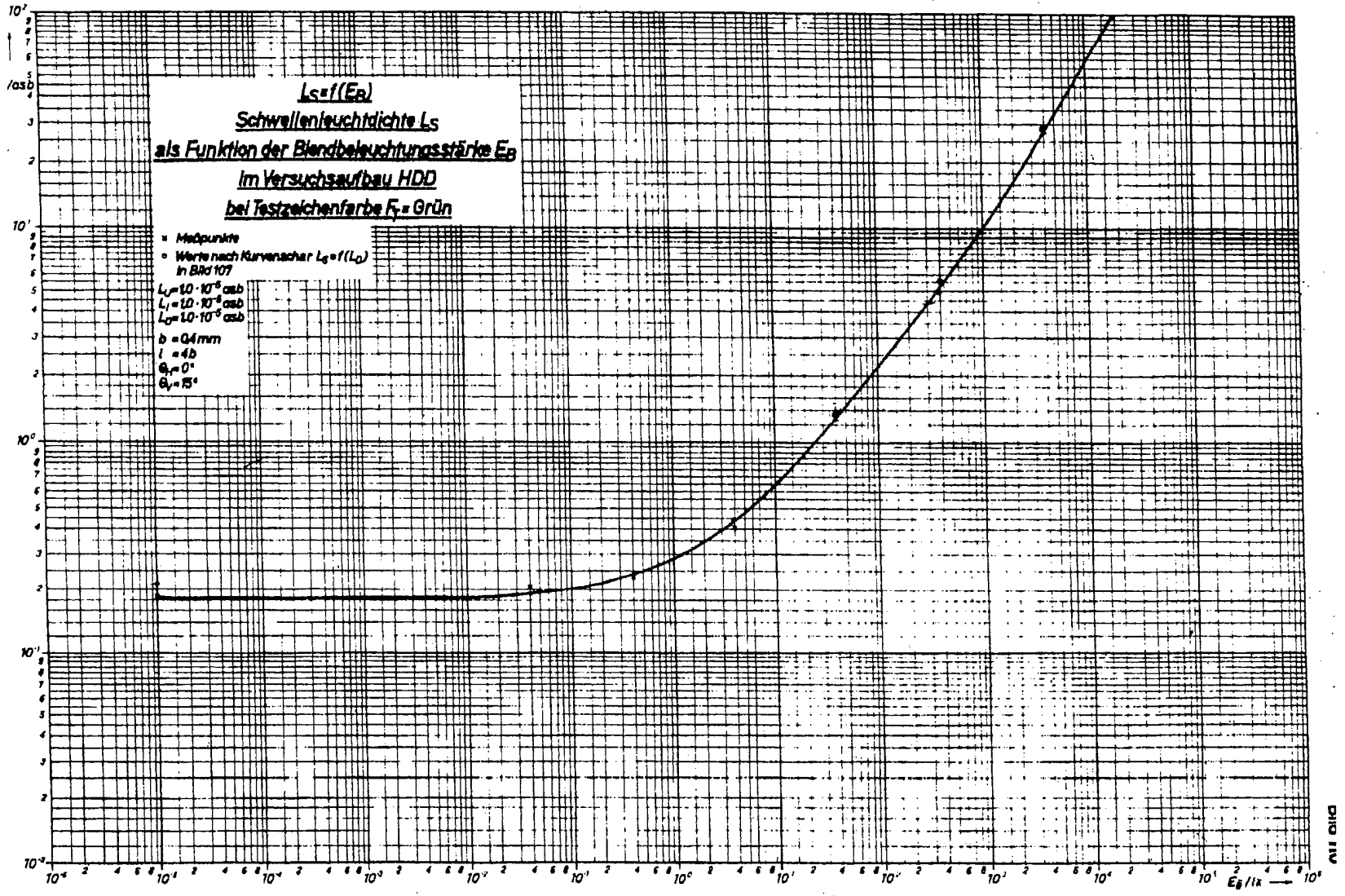


Figure 3.18. Scanned Copy of Jainski Figure 110 Showing Image Difference Luminance as a Function of Glare Source Illuminance for the Head-Down Display Test Configuration.

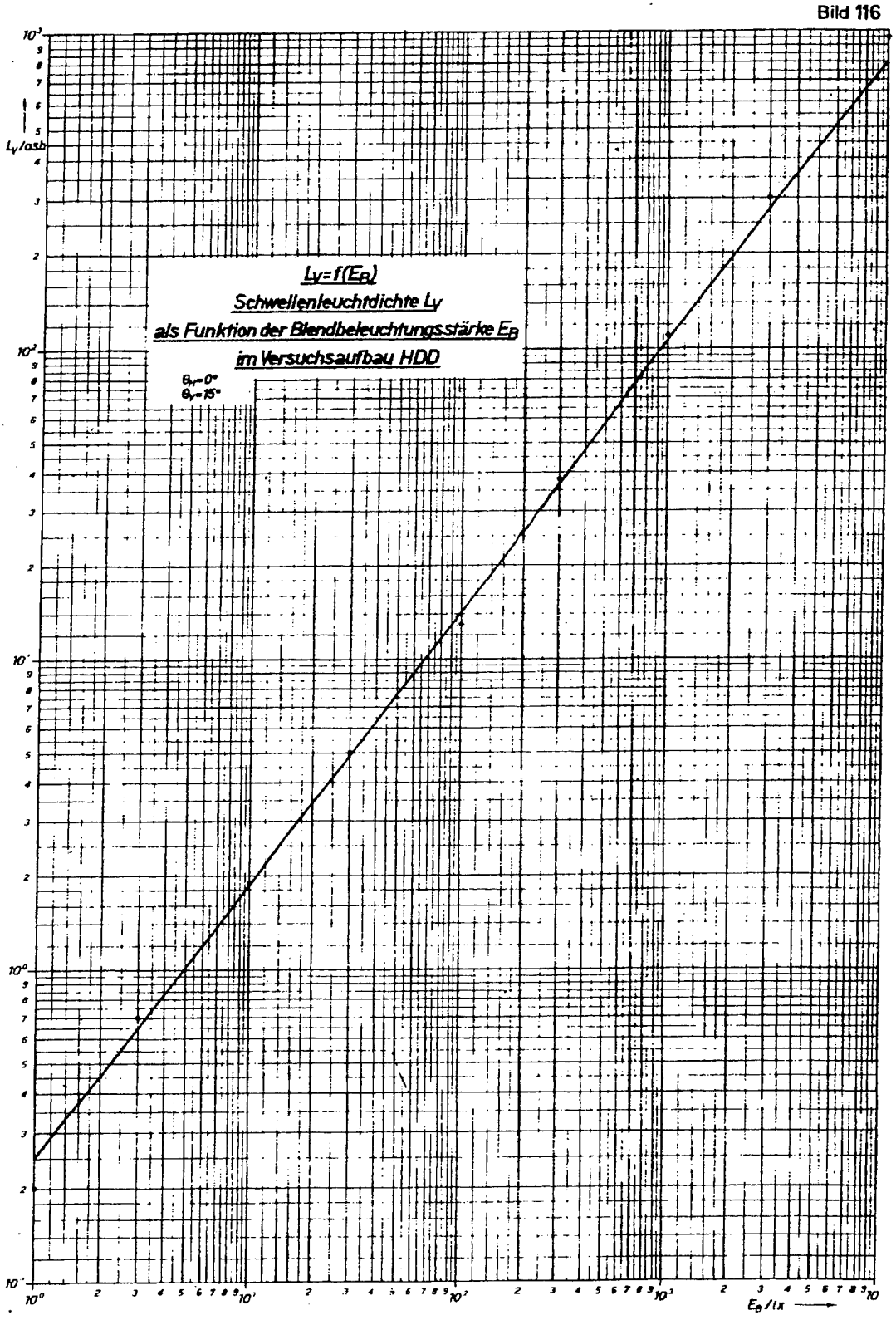


Figure 3.19. Scanned Copy of Jainski Figure 116 Showing Veiling Luminance Dependence on Glare Source Illuminance for a Head-Down Display.

$$q = \log_{10}\left(\frac{L_{V2}}{L_{V1}}\right) \Big/ \log_{10}\left(\frac{E_{BJ2}}{E_{BJ1}}\right). \tag{3.31}$$

Table 3.4 is a compilation of data points extracted from the originals of Jainski's figures, reproduced at a reduced size in Figures 3.17 and 3.18 (Jainski's Bild 110 and Bild 107, respectively) to fit the current report's page size. The table is intended to serve the dual purpose of verifying Figure 3.19 (Jainski's Bild 116) and to provide the experimental data needed to formulate the empirical equation for veiling luminance. The data, as extracted from Jainski's figures, is in units of lux (abbreviated lx) for illuminance and apostilbs (abbreviated asb) for luminance, since these are the units used in the Jainski's figures. These units are then converted to foot-candles (fc) for illuminance and foot-Lamberts (fL) for luminance.

Table 3.4. Veiling Luminance Experimental Data for Head-Down Display.

E_{BJ} in Lx to Bild 110&116	E_{BJ} in fc	L_S (*i.e.*, ΔL) in asb from Bild 110	L_V in asb from Bild 116	L_V in asb from Bild 107	L_V in fL
4×10^{0}	3.72×10^{-1}	4.42×10^{-1}	8.30×10^{-1}	8.83×10^{-1}	8.20×10^{-2}
4×10^{1}	$3.72 \times 10^{+0}$	$1.32 \times 10^{+0}$	$6.30 \times 10^{+0}$	$6.40 \times 10^{+0}$	5.95×10^{-1}
4×10^{2}	$3.72 \times 10^{+1}$	$5.25 \times 10^{+0}$	$4.75 \times 10^{+1}$	$4.70 \times 10^{+1}$	$4.37 \times 10^{+0}$
4×10^{3}	$3.72 \times 10^{+2}$	$2.75 \times 10^{+1}$	$3.65 \times 10^{+2}$	$3.65 \times 10^{+2}$	$3.39 \times 10^{+1}$

As previously described, the L_S (*i.e.*, ΔL) values extracted from Bild 110 (Figure 3.18) for each of the cited E_{BJ} values in the first column are used in Bild 107 (Figure 3.17) to obtain the L_V values in the fifth column of the table. These results are in relatively good agreement with the values of L_V in the fourth column of the table, which were extracted, using the E_{BJ} values in the first column, from Jainski's straight line curve fit of the veiling luminance versus glare source illuminance data shown in Bild 116 (Figure 3.19). The small circles on the graph represent Jainski's derivation of the veiling luminance versus glare source illuminance data using the method just described. The deviations in that data from the straight line fit of the data is commensurate with the deviations evident between the fourth and fifth columns of Table 3.4. The sixth column of the table labeled "L_V in fL" represents the veiling luminance data in the fifth column, expressed in apostilbs (asb), converted to units of foot-Lamberts (fL).

By substituting into the slope equation using the values of glare source illuminance and veiling luminance from the first and fourth data rows of the second and sixth columns, respectively, of Table 3.4, the following value is obtained for the slope of the line:

$$q = \log_{10}\left(\frac{33.9}{0.0820}\right) \Big/ \log_{10}\left(\frac{372}{0.372}\right) = 0.872. \tag{3.32}$$

Alternatively, if Jainski's curve fit data from the first and fourth rows of the first and fourth columns are used, then the slope obtained is $q = 0.881$, in agreement with the value of 0.88 determined by Jainski for the HDD.

Finally, by taking the antilogarithm of Equation 3.30, and rearranging the terms in the expression, the following equation for the veiling luminance as a function of the glare source illuminance can be obtained:

$$L_V(\theta_H = 0°,\ \theta_V = 15°) = \left(\frac{L_{V1}}{E_{BJ1}^{q}}\right) E_{BJ}^{q}. \tag{3.33}$$

The explicit values of the angles that are applicable to the data being modeled from Figures 3.17 and 3.18 has been added to the veiling luminance nomenclature, since the magnitude of the constant multiplier to be evaluated next depends on the angle subtended between the glare source and the pilot's line of sight to the center of the display. Substituting into the preceding equation the coordinate values of L_{V1} = 33.9 fL and E_{BJ1} = 371.6 fc, for one point on the line from Table 3.4, the final empirical equation for veiling luminance, expressed using Jainski's measure of the glare source illuminance, E_{BJ}, can be written as follows:

$$L_V(\theta_H = 0°,\ \theta_V = 15°) = \left(\frac{33.9}{371.6^{0.872}}\right) E_{BJ}^{0.872} = 0.1946\, E_{BJ}^{0.872}. \tag{3.34}$$

The glare source illuminance of magnitude, E_B, enters the eyes directly from the direction of the glare source and is subsequently scattered by the ocular media within the eyes into all of the retina's light receptors. This produces both foveal veiling luminance, which is perceived as coming from a direction from the display symbology being tested, and peripheral and parafoveal veiling luminances that reduce the contrast of the scene imagery located beyond the foveal field of vision. Only the effect of veiling luminance induced in the foveal region of the retina is dealt with in the present report. In the context just described, Jainski's measure of glare source illuminance, E_{BJ}, although acceptable as an alternative to using the direct glare source illuminance, E_B, fails to conform to the physical reality of the test configuration and, therefore, from a practical standpoint simply complicates the veiling luminance equation by introduces a term, which is itself dependent on the angle subtended by the glare source with respect to the pilot's central visual axis.

The substitution of E_{BJ}, from Equation 3.28, into the preceding empirical equation, Equation 3.34, and the substitution of the angle subtended by the glare source with respect to the line of sight, yields the following final empirical equation for the veiling luminance dependence on the glare source illuminance, E_B:

$$L_V(E_{BJ},\ \theta_B = \sqrt{\theta_H^2 + \theta_V^2}\ ) = 0.1946\, E_{BJ}^{0.872} = 0.1946\, (E_B \cos\theta_B)^{0.872}$$

$$L_V(E_{BJ},\ \theta_H = 0°,\ \theta_V = 15°) = 0.1946\, (\cos 15°)^{0.872} E_B^{0.872} \tag{3.35}$$

$$\therefore\ L_V(E_B,\ \theta_H = 0°,\ \theta_V = 15°) = 0.1888\, E_B^{0.872}.$$

This equation gives the veiling luminance in foot-Lamberts when the glare source illuminance value is expressed in foot-candles. It should be noted that the substitution of E_{BJ} from Equation 3.28 does not change the exponent in Equation 3.35. This is because the coordinates of the two E_{BJ} points used to calculate the slope term in Equation 3.31, occur in the equation in the form of a ratio, thereby causing the $\cos\theta$ angular components to cancel. The explicit glare source angle, to which this equation applies, has been specified in the veiling luminance variable because in the strict sense it is the only angle at which the test data, upon which the equation is founded, is valid. The angular dependence of veiling luminance to be examined later in this section uses this glare source angle as a reference glare source orientation for expressing the angular dependence of veiling luminance for head-down displays.

3.5.2.3. Assessment of the Accuracy of Jainski's Experimental Data

A number of Jainski's figures contain data that allow comparisons to be made for common data points collected in different tests at different times but under the same test conditions. In making comparisons between the data presented in these figures, Jainski's variable names, units and figure designations are used. Although some figures have been scanned from Jainski's report for use as examples to aid in visualizing the description of the data they contain, the copies are not considered to be of sufficient quality to permit the reader to do more than follow the data extraction techniques being employed. Attempts to verify the information presented in the current report should rely on either the original Jainski report or high quality copies of it, rendered either at full scale or enlarged.

Comparisons of individual values extracted from Jainski's image difference luminance, L_S (*i.e.*, ΔL),

requirements data for different values of glare source illuminance, E_B, are made in Table 3.5 for data collected using both the head-down and head-up display test configurations. The table is divided into four major columns. The first column gives the glare source illuminance values at which the experimentally determined values of image difference luminance appearing elsewhere in the table were collected. The second and third major columns include the image difference luminance data extracted from Jainski's figures for the HDD and HUD test configurations, along with comparisons and measures of the relationships between the data. The final major column in the table compares the HDD image difference luminance levels taken from Jainski's Bild 107 and illustrated in Figure 3.17 with those taken Jainski's equivalent figure for the HUD (i.e., from Bild 101).

The various experimental results in the HDD area of Table 3.5 are discussed first because they were found to be more self-consistent than was the case for the HUD data. Image difference luminance data from Figure 3.17 (i.e., Bild 107) and from Figure 3.18 (i.e., Bild 110) are shown in the first two columns in the HDD area of the table, in the same rows as the corresponding glare source illuminance levels tested. Each of the L_S (*i.e.*, ΔL) versus L_D characteristics shown in Figure 3.17 can be thought of as representing a distinct test run for each of the corresponding discrete levels of E_B tested. Only the L_{S1} data point from each E_B characteristic, corresponding to $L_D = 1 \times 10^{-5}$ asb, is included in the first column in the HDD area of Table 3.5. The second column in the HDD area of the table contains L_{S1} data extracted from Bild 110, which plots image difference luminance as a continuous function of the glare source illuminance, E_B, with the display background luminance set to $L_D = 1 \times 10^{-5}$ asb. A scanned copy of this data is illustrated in Figure 3.18.

If the data collected by Jainski had contained no test subject or experimental variability and no sources of measurement deviations, then Bild 107 and 110 should have yielded identical values of L_{S1} for the same E_B settings in Table 3.5. The difference between these sets of experimental data therefore provides a measure of the total error present in these Jainski experimental results. An indication of the level of the error present is shown in the third column of the HDD area of the table. The magnitudes of errors shown in the table for the HDD is surprisingly small, with the exception of the $E_B = 1 \times 10^{-5}$ lx glare source illuminance level. The latter reading is the one that would be expected to be most strongly influenced by the Shot noise and noise bursts inherent in the photomultiplier detector tube-based photometers available to make light measurements at the time of the experiments in the later part of the 1960's.

Besides the nearly random variations introduced by noise, data shifts between individual test runs would normally also be expected to occur. As a result of the separate effects of temperature induced drift of the measurement instrumentation and the documented variations known to be introduced by photometric measurement calibration errors, geometric (i.e., ratio) shifts can influence measurements made at any image difference luminance level, irrespective of its magnitude. While scant evidence of such shifts can be observed in the percentage error data in the HDD area of Table 3.5, its presence is suggested in the HUD area of the table, and in the data discussed subsequently in this subsection and in others to follow. The low level image difference luminance data and its high level of error will be discussed further near the end of this subsection.

The image difference luminance data presented in the HUD area of Table 3.5 was acquired and plotted in the same way as the HDD data, just described. The HUD data in the table were taken from Jainski's Bild 101 and Bild 103. These figures are directly analogous to Bild 107 (i.e., Figure 3.17) and Bild 110 (i.e., Figure 3.18) for the HDD. The data extracted from these figures for the HUD appear in the first and second columns in the HUD area of Table 3.5. As the third column of the HUD area of the table shows, a much higher level of total error is present for the HUD data than is the case for the HDD data. In fact, the total error for the HUD data in the table is on average larger that the percentage differences shown in the last column of the table, which compares the data in the first column of the HDD (Bild 107) and HUD (Bild 101) areas of Table 3.5.

Another way of comparing the respective HDD and HUD data in Table 3.5 is to compare the ratios of the image difference luminance levels between adjacent rows in the table (i.e., the rows of data are separated by rows containing the ratios, which to distinguish them are right justified and marked with a trailing Letter R to show they are ratios) that are the result of the equal multiple of ten changes in the glare source illuminance level settings between the adjacent rows. These ratios may be seen to decrease in a monotonic progression

Table 3.5. Comparison of Jainski Image Difference Luminance Requirements Data, L_S (*i.e.*, ΔL), for Different Values of Glare Source Illuminance, E_B.

Glare Source Illuminance E_{BJ} in lux & Ratio of Adjacent Levels-R	HDD Image Difference Luminance Values for $L_V = L_I = 1 \times 10^{-5}$ asb Separated by Luminance Ratios between Adjacent Levels (1)			HUD Image Difference Luminance Values for $L_U = 2L_D$ & $L_I = 0.003L_D$ Separated by Luminance Ratios between Adjacent Levels (1)			Percentage Difference between HDD&HUD L_S (*i.e.*, ΔL) Values $\frac{L_{S1} - L_{S3}}{(L_{S1} + L_{S3})/2}$ x 100 in %
	Bild 107 L_{S1} in asb & Ratio of Adjacent Levels-R	Bild 110 L_{S2} in asb & Ratio of Adjacent Levels-R	% Error: $\frac{L_{S1} - L_{S2}}{(L_{S1} + L_{S2})/2}$ x 100 in %	Bild 101 L_{S3} in asb & Ratio of Adjacent Levels-R	Bild 103 L_{S4} in asb & Ratio of Adjacent Levels-R	% Error: $\frac{L_{S3} - L_{S4}}{(L_{S3} + L_{S4})/2}$ x 100 in %	
3.9×10^3	28.2 (2)	27.9	+1.1	21.0 (2)	19.0	+10.0	+29.3
10-R	5.76-R	5.42-R		5.16-R	5.67-R		
3.9×10^2	4.90	5.15	-5.0	4.07	3.35	+19.4	+18.5
10-R	3.71-R	3.96-R		2.89-R	3.90-R		
3.9×10^1	1.32	1.30	+1.5	1.41	0.860	+48.5	-6.6
10-R	2.97-R	2.98-R		3.24-R	2.53-R		
3.9×10^0	0.445	0.437	+1.8	0.435	0.340	+24.5	+2.2
3.9×10^5-R	2.07-R	2.38-R		1.69-R	1.21-R		
1×10^{-5}	0.215	0.184	+15.5	0.258	0.280	-8.2	-18.2
	Bild 78			Bild 46			
1×10^{-5}	0.278			0.295			-5.9

Notes: 1. The values of the other variables held constant for each image difference luminance data point in this table are as follows: the display background luminance was $L_D = 1 \times 10^5$ asb, the test symbol critical detail dimension was $\alpha_c = 8.8$ minutes of arc, the horizontal glare source angle was $\theta_H = 0°$, and the vertical glare source angle was $\theta_V = 15°$.

2. These values are referred to in Section 3.5.2.4 when comparing HDD and HUD test results.

from top to bottom, for the HDD data from Bild 107 and Bild 110 and for the HUD data from Bild 103, but this progression of the ratios fails for the HUD data from Bild 101. This result suggests that one or more of the image difference luminance levels in Bild 101 are erroneous, since encountering physiological data that oscillates from higher to lower then higher values, in this fashion, would be extremely unusual. Unfortunately, with the exception of single data points, to be considered presently, Jainski reports no other data that permits additional direct comparisons of image difference luminance levels as a function of glare source illuminance setting for the HUD test configuration.

In spite of the preceding limitation, two additional comparisons between Jainski's data are possible. The first comparison involves single image difference luminance data points extracted from ideal HDD

characteristics, like those shown in Figure 3.10 (and from Jainski's equivalent HUD characteristics), at a display background luminance of $L_D = 1 \times 10^{-5}$ asb. These ideal characteristic data points, which were obtained from Jainski's Bild 78 and Bild 46 for the HDD and HUD, respectively, are shown in the bottom row in Table 3.5. Since no glare source was present, this test condition was equivalent to Jainski's tests with the glare source turned off, that is, with an illuminance of $E_B = 1 \times 10^{-5}$ lx. These data meet all the conditions ascribed to the other data reported in Table 3.5 and therefore are directly comparable to the two image difference luminance values for $L_D = 1 \times 10^{-5}$ asb and $E_B = 1 \times 10^{-5}$ lx appearing in the row of data immediately above them in the respective HDD and HUD areas of the table.

The preceding comparison of the single data points in Table 3.5 shows that three different values of image difference luminance exist in both the HDD and HUD areas of the table. In concept, if no subject variability or measurement differences were present in Jainski's test data, then individual data points for the HDD and those for the HUD should be identical. Since a dispersion of the data exists for both the HDD and HUD, the imaged difference luminance data points reported at the bottom of Table 3.5 provide a limited measure of the magnitude of the errors present in Jainski's experimental data. Computing the ratio between the difference between the maximum value of 0.278 from Bild 78 and the minimum value 0.184 from Bild 110, for the HDD at $E_B = 1 \times 10^{-5}$ lx, and the mean of these two numbers, expressed as a percent, yields a measure of the error present for the HDD data of 40.7%. Repeating this calculation using 0.295 from Bild 46 and 0.258 from Bild 101 for the HUD, yields a measure of the error present for the HUD data of 13.4%.

Although the Jainski report provides no direct way to assess the measurement accuracy and repeatability of Jainski's luminance test data, the report does provide test subject variability information that can be used as a baseline, for assessing the significance of the magnitudes of the differences between the data points. In particular, the mean data point of 0.278, which was extracted from Jainski's Bild 78 for the HDD and is shown in the last row of Table 3.5, exhibited a range of test subject data variability of from 0.20 to 0.42. These extremes produce a percentage test subject variability range for the HDD mean data point of 71% (i.e., calculated as the difference between the test subject variability extremes divided by their mean value, and expressed as a percentage, as before). The test subject variability extremes, for the mean data point of 0.295, which was extracted from Jainski's Bild 46 for the HUD and is shown in the last row of Table 3.5, were from 0.24 to 0.42, nearly the same values as for the HDD. These extremes yield a percentage test subject variability range for the HUD mean data point 61%. In comparison to these values of test subject variability, even the previously calculated 40.7% error between Jainski's maximum and minimum HDD image difference luminance values, at $E_B = 1 \times 10^{-5}$ lx, is, in relative terms, not that large. The error is also not that large when viewed relative its data collection range of six to seven decades. Although nothing of value, from a quantitative statistical standpoint, can be drawn from so few data points, note that the test subject data point mean of 0.278, for the HDD in the last row of Table 3.5, coincides with the mean of the three corresponding HUD data points (i.e., 0.258, 0.280, 0.295) from the HUD area of Table 3.5.

Besides the individual data point comparison at $L_D = 1 \times 10^{-5}$ asb and $E_B = 1 \times 10^{-5}$ lx, a second comparison is also possible. The second comparison involves the use of the entire ideal image difference luminance versus display background luminance characteristics from Bild 78 and Bild 46 for the HDD and HUD, respectively. Since, as previously described, each of these characteristics corresponds to an E_B value of 1×10^{-5} lx, that is, with the glare source illuminance turned off, the ideal characteristic for the 8.8 minute of arc critical detail dimension HDD image in Jainski's Bild 78, and illustrated in Figure 3.10, should, in concept, be identical to the corresponding $E_B = 1 \times 10^{-5}$ lx characteristic in Figure 3.17 (i.e., taken from Bild 107). Each of the preceding figures presented for a HDD have HUD counterparts in Jainski's report. In particular, Jainski's Bild 78 that plots L_S (*i.e.*, ΔL) versus L_D for a HDD, is equivalent to Bild 46 for a HUD, and, as has been previously stated, Bild 107 that plots L_S (*i.e.*, ΔL) versus E_B for a HDD is equivalent to Bild 101 for a HUD. Consequently, the ideal characteristic for a 8.8 minute of arc critical detail dimension HUD image from Jainski's Bild 46 should similarly, in concept, be identical to the corresponding $E_B = 1 \times 10^{-5}$ lx characteristic for a HUD from Bild 101.

Image difference luminance versus display background luminance requirements data extracted from the

figures referenced in the preceding paragraph have been included in Table 3.6. Comparisons are made in this table between 8.8 minute of arc critical detail dimension characteristics from Bild 78 and 107, for the HDD, and from Bild 46 and 101, for the HUD. Since, in concept, these respective characteristics are supposed to be identical, the percent errors reported in this table should be zero. To the extent that they are not equal to zero, they represent a measure of the magnitude of the total error present in these particular Jainski tests.

The comparison results in Table 3.6, like those in Table 3.5, are normalized using the mean of each pair of image difference luminance values and are then expressed as a percent error in the fourth and seventh columns of Table 3.6, to the right of the two columns of data extracted from the figures. Mean percent error magnitudes have been computed and included at the bottom of the table. The absolute values of the individual errors were used for this computation, which yielded 11.22% for the HDD and 14.38% for the HUD test configuration data. Image difference luminance error data between the 1×10^{-5} and 1×10^{-1} asb levels of display background luminance were excluded from the calculation of the overall mean errors since these values all measure essentially the same test condition along the low background luminance straight line portion of the characteristics. The error polarities have been retained in the table to show where the decreases in errors result from the curves crossing one another. This only occurred for the HUD data, where the image difference luminance level values from Bild 46 start higher than their corresponding values in Bild 101, at low display background luminance levels, but at 3×10^{2} asb and higher values of display background luminance the relationship is reversed.

Figure 3.20 shows a plot of the data points in Table 3.6, to provide a visual indication of the significance of the errors in Jainski's data, for what should be identical HDD and HUD characteristics, and also shows a visual comparison of the differences between the HDD and HUD characteristics. It can be observed that the dispersion, of the groupings of characteristics, due to error, for the range of intermediate to high display background luminance levels in Figure 3.20, is very similar to the groupings of characteristics shown in Figure 3.13. Although two of the three characteristics, having the lowest image difference luminance intercept points in Figure 3.13, duplicate two of the characteristics in Figure 3.20, the characteristics at other in-field luminance values confirm the relative agreement between 8.8 minute of arc critical detail dimension HDD and HUD data shown in the figure. These figures illustrate the fact that the characteristics are all very similar and their dispersion is within the bounds that could be expected as the result of measurement error shifts in the characteristics.

3.5.2.4. HDD and HUD Veiling Luminance Dependence on Glare Source Illuminance

In the preceding subsection, the test data in Tables 3.5 and 3.6 were assessed with respect to the accuracy of Jainski's experimental data using characteristics, which, at least in concept, should be identical if no errors were present. As previously mentioned, the two tables also include measures of the differences between the HDD and HUD in the last one or two columns of each table. These difference measures allow comparisons to be made between the percentage errors, for the presumptively identical image difference luminance characteristics for the HDD and the HUD, with the differences between the HDD and HUD data. In this subsection the differences between the HDD and the HUD will be assessed.

The mean of the individual percent errors, between the HUD image difference luminance characteristics listed in the second to the last column of Table 3.5, evaluates to a value of 22.1%. In comparison, the mean of the percent differences between the HDD and the HUD image difference luminance characteristics, from the last column in Table 3.5 is 15.0%. Since the mean error between the HDD and HUD characteristics is less than the mean error between two HUD characteristics that should be identical, this relationship suggests the differences between the Jainski image difference luminance versus glare source illuminance characteristics for the HDD and HUD test configurations are artifacts attributable to test errors, rather than being real. The errors present in the test results of Jainski preclude reaching a firm conclusion on whether the HDD and HUD characteristics are the same or differ in some respects. Additional sources of Jainski experimental data that bear on providing an answer to this question are described below.

Table 3.6. Comparison of Jainski Image Difference Luminance Requirements Data, L_s (*i.e.*, ΔL), as a Function of Display Background Luminance, L_D.

Display Background Luminance L_D in asb	HDD Image Difference Luminance Values for $L_U = L_I = 1 \times 10^{-5}$ asb			HUD Image Difference Luminance Values for $L_U = 2L_D$ & $L_I = 0.003L_D$			Percentage Difference between HDD&HUD L_s (*i.e.*, ΔL) Values	
	Bild 78 L_{S1} in asb	Bild 107 L_{S2} in asb	% Error: $\frac{L_{S1} - L_{S2}}{(L_{S1} + L_{S2})/2}$ x 100 in %	Bild 46 L_{S3} in asb	Bild 101 L_{S4} in asb	% Error: $\frac{L_{S3} - L_{S4}}{(L_{S3} + L_{S4})/2}$ x 100 in %	Bild 78/46 $\frac{L_{S1} - L_{S3}}{(L_{S1} + L_{S3})/2}$ x 100 in %	Bild 107/101 $\frac{L_{S2} - L_{S4}}{(L_{S2} + L_{S4})/2}$ x 100 in %
1×10^{4} *	540	420	25.00	635	710	-11.51	-16.17	-51.33
3×10^{3} *	185	157	16.37	195	220	-12.05	-5.26	-33.42
1×10^{3} *	68.0	63.3	7.16	72.0	76.0	-5.41	-5.71	-18.23
3×10^{2} *	24.8	23.5	5.38	26.5	27.0	-1.87	-6.63	-13.86
1×10^{2} *	10.4	9.70	6.97	11.7	10.8	+8.00	-11.76	-10.73
3×10^{1} *	4.3	3.77	13.14	5.10	4.27	17.72	-17.02	-12.44
1×10^{1} *	1.94	1.77	9.16	2.42	2.02	18.02	-22.02	-13.19
3×10^{0} *	0.93	0.83	11.36	1.26	0.99	24.00	-30.14	-17.58
1×10^{0} *	0.480	0.470	2.11	0.705	0.56	22.92	-37.97	-17.48
3×10^{-1} *	0.313	0.310	0.96	0.422	0.342	20.94	-26.66	-9.82
1×10^{-1} *	0.278	0.248	11.41	0.317	0.268	16.75	-13.11	-7.75
3×10^{-2}	0.278	0.223	21.96	0.295	0.258	13.38	-5.93	-14.55
1×10^{-2}	0.278	0.218	24.19	0.295	0.258	13.38	-5.93	-16.81
1×10^{-5} *	0.278	0.215	25.56	0.295	0.258	13.38	-5.93	-18.18
* Total (2)			134.58			172.57	198.38	224.01
* Mean			11.22			14.38	16.53	18.67

Notes: 1. The values of the other variables held constant for each image difference luminance data point in this table are as follows: the test symbol critical detail dimension was $\alpha_c = 8.8$ minutes of arc, the glare source illuminance was $E_B = 1 \times 10^{-5}$ asb, the horizontal glare source angle was $\theta_H = 0°$, and the vertical glare source angle was $\theta_V = 15°$, in applicable figures, which is equivalent to the source being turned off.

2. Only the the absolute values of numbers in rows marked with an asterisk are summed. Refer to the text of the report for an explanation.

3. Conversion of luminance in apostilbs (asb) to foot-Lamberts (fL): L (fL) = 0.09290304 L (asb).

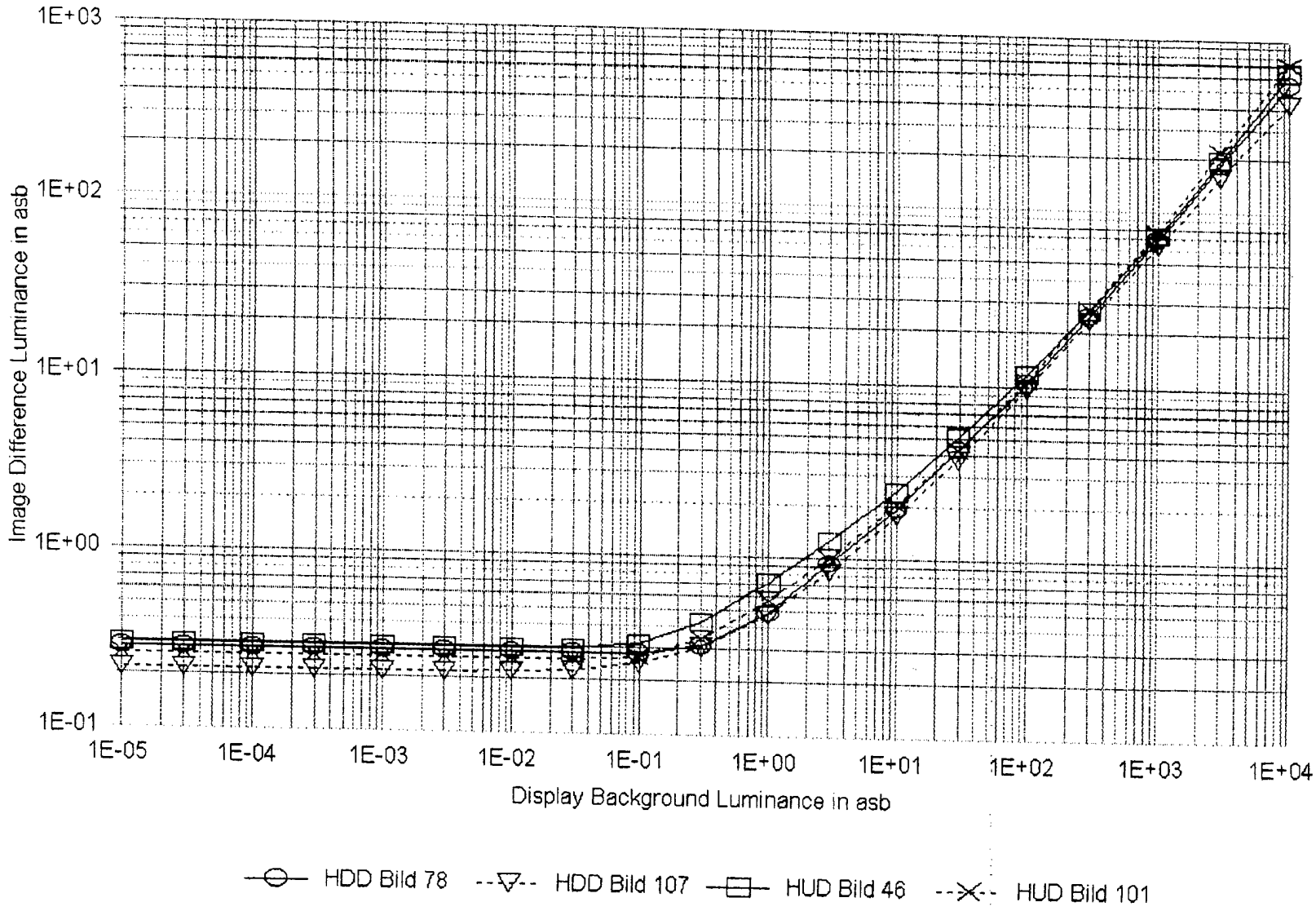


Figure 3.20. Comparison of Jainski 8.8 Minute of Arc Critical Detail Data Showing Errors for HDD and HUD Characteristics That Should Be Identical and the Differences Between HDD and HUD Characteristics.

In another series of experimental tests, distinct from the investigation of the dependence of image difference luminance requirements on the illuminance of a glare source and to be described in greater detail in the next subsection, Jainski also conducted investigations of the dependence of image difference luminance requirements on the angle subtended by the glare source, with respect to the test subject's line of sight to the center of the HDD display. Using the same values of the constant variables as in Table 3.5, and with a glare source illuminance setting of 4.0×10^3 lx, Jainski obtained the glare source angular dependence test results for the HDD test configuration shown in Figure 3.21. Moreover, the initial glare source orientation for this test was a horizontal angle of zero degrees and a vertical angle of 15 degrees. These are the same source angles applicable to the data in Table 3.5, and, consequently, the relevant data in Figure 3.21 is directly comparable to that in the table. The value of image difference luminance obtained from the angular dependence test was 21 asb, which differs from the 28.2 asb in Table 3.5 for the HDD, but matches the value listed in Table 3.5 for the HUD. This result is probably coincidental, however, it does show that the magnitudes of the errors present in Jainski's test data do not justify treating the image difference luminance dependence on glare source illuminance separately, for the HDD and HUD test data.

From a theoretical standpoint, the test conditions applicable to the data contained in Table 3.5, make it difficult to understand why a difference between the data obtained using the HDD and HUD test configurations should exist. The image difference luminance results of Table 3.5 were obtained for values of the luminance geometry variables cited in the table as $L_D = 1 \times 10^{-5}$ asb for both the HDD and the HUD, and with $L_U = L_I = 1 \times 10^{-5}$ asb for the HDD and with the combination of $L_U = 2L_D$ and $L_I = 0.003L_D$ for the HUD, that is, in total darkness. The consequence of this luminance geometry should have led to an unambiguous characterization of the glare source illuminance dependence of the test subject's eyes. To insure that this was the case during the tests, Jainski had to limit the glare source illuminance exposure to the eyes of the test subjects. Although exposure to the sun or another glare source, such as the moon, a flare or lightning at night, would result in a general illumination of an actual aircraft cockpit, to achieve the essential experimental separation of the glare source effects being tested from the effects of the luminance geometry variables, it was necessary for Jainski to restrict exposure solely to the test subject's eyes.

Differences between the HDD and HUD test results should be expected only when there are differences in the luminance geometries attributable to the HDD and HUD test configurations that are visible to the observers involved in the tests. In Figure 3.20, which illustrates the data in Table 3.6, the HDD and HUD luminance geometries do visibly differ from one another when the display background luminance levels increase, since the surround-field and in-field luminances are held at a level of $L_U = L_I = 1 \times 10^{-5}$ asb, for the HDD, whereas for the HUD these levels increase along with the display background luminance level following the equations $L_U = 2L_D$ and $L_I = 0.003L_D$. Although this report has lumped the HUD test conditions, just cited, in with the HDD ideal luminance conditions, and in so doing has called it an ideal viewing condition, in the transition region from night to day display background luminance levels, and at still higher display background luminance levels, the HUD characteristics tend toward slightly higher image difference luminance requirements than is the case for the HDD. The HUD Bild 46 data in Figure 3.20 illustrates this tendency, as do the HUD characteristics in Figures 3.12 and 3.13. Whether this tendency is real, or an error artifact, is difficult to determine accurately from Jainski's data. However, the previously described incorporation of the veiling luminance term into the mathematical model for the ideal image difference luminance characteristics, would produce the same tendency for the image difference luminance characteristics of a HUD to be higher than those of a HDD, when they are compared using the differences in the HUD and HDD viewing conditions described above.

Referring again to Figure 3.20, the lower solid curve for the HDD and the upper solid curve for the HUD are in relatively good agreement at both low and high display background luminance levels, but not in the previously discussed transition region from day to night. The similarly positioned dashed curves for the HDD and the HUD, acquired using the $E_g = 1 \times 10^{-5}$ lx characteristic, from the glare source illuminance characteristic figures for the HDD and the HUD, are in good agreement up to 1,000 asb of display background luminance. The last two columns in Table 3.6 endeavor to make the equivalence comparisons, illustrated in Figure 3.20 for the HDD and HUD characteristics, using image difference luminance data expressed in a

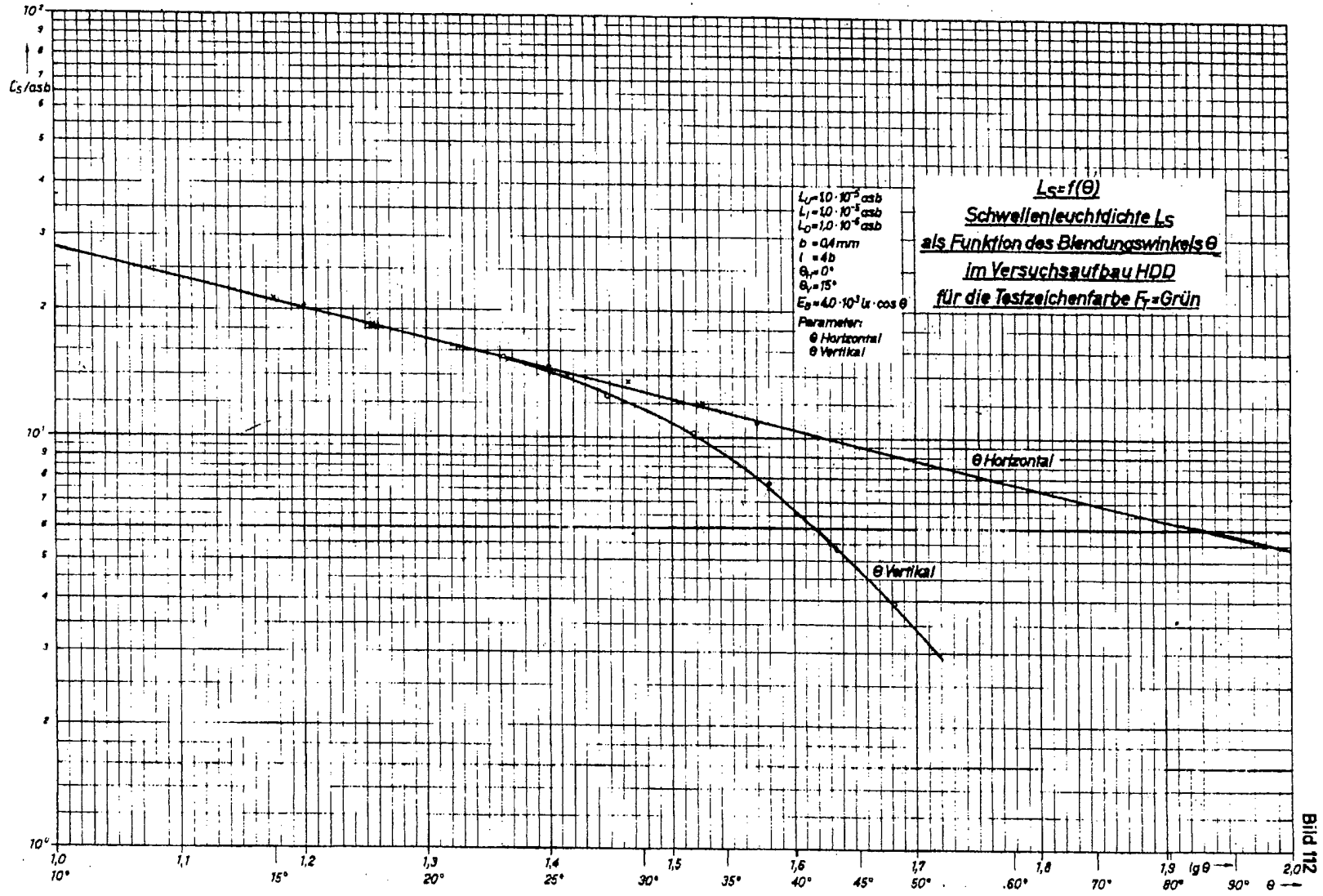


Figure 3.21. Scanned Copy of Jainski Figure 112 Showing Image Difference Luminance Requirements as a Function of the Angle Between the Glare Source and the Line of Sight to the Display for the Head-Down Display Test Configuration.

numerical format. Although the mean differences are slightly higher for these comparisons between the HDD and HUD data than are the mean errors within the respective HDD and HUD data, they are sufficiently similar to validate the earlier adoption of a single mathematical model to represent ideal HDD and HUD image difference luminance versus display background luminance characteristics.

The choice of the HDD data, to represent both the HDD and HUD glare source illuminance dependence of the image difference luminance requirements, is based on the exceptionally low error magnitudes present in Table 3.5 for the HDD test configuration data. In particular, the good correspondence between the data from Jainski's Bild 107 and Bild 110, as shown by the low error magnitudes in Table 3.5, caused these figures to be considered more suitable than the corresponding HUD figures to produce an accurate determination of veiling luminance as a function of the glare source illuminance.

3.5.3. Veiling Luminance Dependence on the Glare Source Angular Position with Respect to the Pilot's Line of Sight

The glare source illuminance dependence of veiling luminance, discussed in the preceding subsection, was determined with the glare source positioned fifteen degrees above and aligned horizontally at zero degrees, with respect to the test subject's line of sight to the center of the HDD or HUD configuration being tested. The test subject's response to the glare source is, however, determined by virtue of the veiling luminance scattered directly into the test subject's line of sight to the display, where the test symbol used to determine the image difference luminance required to achieve 95% image identification accuracy is located. Since veiling luminance is a real physical quantity and depends on the scattering of light from the glare source within the eyes, it can be expected to change in magnitude, as a function of the angle subtended by the glare source, with respect to the test subject's line of sight to the display image being tested. This angular dependence of veiling luminance will be explored in this subsection.

3.5.3.1. Description of Jainski's Glare Source Angular Dependence Test Data

Figures 3.21 (Bild 112) and 3.22 (Bild 106) show scanned copies of Jainski's image difference luminance requirements, L_S (*i.e.*, ΔL), expressed as a function of the total subtended angle, θ, between the glare source and the test subject's line of sight, to the center of the display under test for the HDD and HUD, respectively. The glare source illuminance used to collect the data in both figures was 4,000 lx (371.6 fc). The other test variables and parameters held constant are shown in Figures 3.21 and 3.22. It should be noted that, except for the $L_D = 1.55 \times 10^3$ asb (144 fL) characteristic shown in Figure 3.22 for the HUD, the variables and parameters have the same values as those in Figures 3.17, 3.18 and 3.19, for the HDD, and in Jainski's equivalent figures, for the HUD (i.e., Bild 101, Bild 103 and Bild 117, respectively).

The equation $E_B = 4.0x10^3\ lx \cdot \cos\theta$ that appears in both Figures 3.21 and 3.22 should be read as $E_{BJ} = 4.0x10^3\ lx \cdot \cos\theta$, using the terminology adopted for use in this report. This subject was previously described in relation to Equations 3.27 and 3.29. Since the actual glare source illuminance in both Figures 3.21 and 3.22 is $E_B = 4.0 \times 10^3$ lx, the $\cos\theta$ term in the figures should be ignored. The empirical equation for the veiling luminance dependence on the glare source illuminance, Equation 3.35, was previously adjusted to relate veiling luminance to the direct illuminance from the glare source, E_B, rather than to Jainski's measure of the glare source illuminance, E_{BJ}.

A reduced size scanned copy of Jainski's Bild 112, shown in Figure 3.21, portrays the decrease in image difference luminance requirements as the fixed illuminance glare source is moved away from the test subject's line of sight to the center of the head-down display. The actual test data starts at a vertical angle of 15 degrees and a horizontal angle of 0 degrees. For the characteristic marked "θ Vertical," the test data goes from 15 to about 48 degrees in the vertical direction. The balance of the characteristic shown in Figure 3.21 was extended by a straight line extrapolation by Jainski to higher and lower angles. In practice the eyebrows

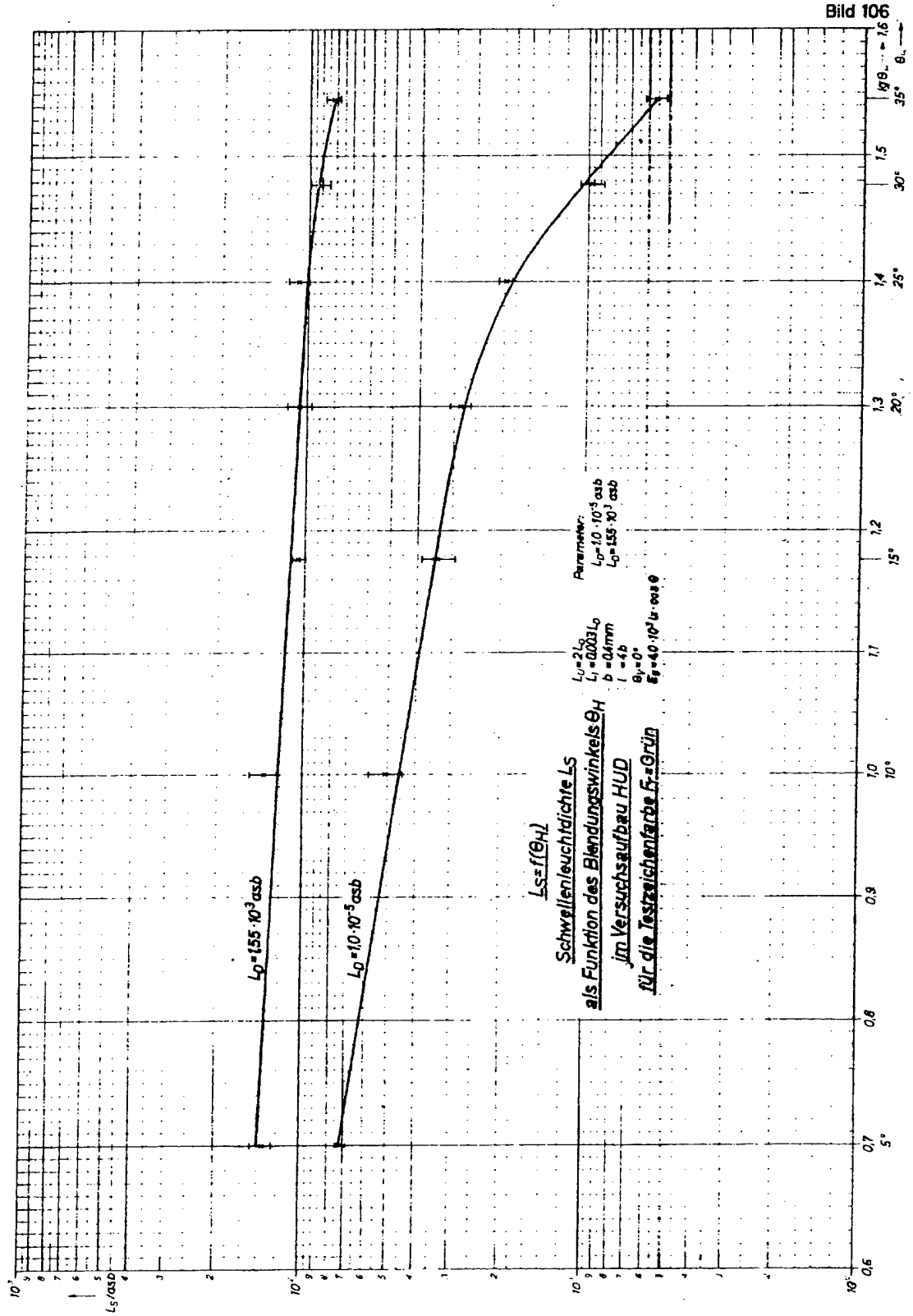


Figure 3.22. Scanned Copy of Jainski Figure 106 Showing Image Difference Luminance Requirements as a Function of the Horizontal Angle Between the Glare Source and the Line of Sight to the Display for the Head-Up Display Test Configuration.

limit the effect of a glare source on inducing veiling luminance, to a maximum vertical angle of about 48 degrees from the center visual axis. Either voluntary or involuntary movements of the eyebrows by a pilot or test subject can further reduce the vertical glare source exposure angle. The approximately 15-degree lower limit on Jainski's collection of data for vertical angles appears to have been imposed by practical dimensional constraints of the HDD test configuration. The angle required to clear the edge of the HDD panel was dimensioned, in a diagram (i.e., Bild 5) in the Jainski report, at 8 degrees above the center of the display. The angle subtended by the inner diameter of the glare source filter holder was not specified in Jainski's drawings of the test configuration but in the figure appeared to be only slightly less than 8 degrees. The combination of these two angles would have limited the subtended angle, between the center of vision and the center of the Jainski glare source, to a minimum of approximately 12 degrees in the vertical direction.

The characteristic in Figure 3.21 designated as "θ Horizontal" is more difficult to describe than was the case for the vertical angle. The data for this characteristic starts at the same angular coordinate as did the vertical characteristic, however, the glare source then is moved horizontally, on a fixed radius from the test subject's eyes, in a way that maintains the 15-degree initial vertical angle as it is moved to larger horizontal angles. For this characteristic the total subtended angle, θ, shown on the horizontal axis of the figure, is made up of both vertical and horizontal angle components. In the first 15 degrees of glare source motion (i.e., in the region extrapolated by Jainski to smaller angles in the figure) the source motion would be vertical for both the vertical and horizontal characteristics shown. Thereafter, the glare source is moved in the two separate directions already described, however, the horizontal motion is only out to about 37 degrees of total subtended angle, with the balance of the characteristic shown being a straight line extrapolation by Jainski out to beyond 90 degrees.

The angular dependence on the glare source, shown for the head-up display in Figure 3.22, is again straightforward to describe. To be consistent with the figures from which the illuminance dependence was previously obtained, only the $L_D = 1.0 \times 10^{-5}$ asb display background luminance characteristic is of current interest. In this case, because the vertical angle of the glare source, used to acquire the characteristic, was held fixed at 0 degrees, the horizontal angle, θ_H, shown in Figure 3.22, is equal to the total subtended angle, θ, employed on the horizontal axis of the HDD characteristics shown in Figure 3.21. The HUD characteristic data was collected with the glare source positioned at horizontal angles between 5 and 35 degrees and the characteristic was not extrapolated.

3.5.3.2. Analysis and Interpretation of Jainski's Glare Source Angular Dependence Test Data

The luminance geometry conditions held constant during the conduct of Jainski's angular dependence tests, including, in particular, the fact that the display background luminance was held constant at $L_D = 1.0 \times 10^{-5}$ asb, means, as has been described previously for the glare source illuminance dependence data, that no physical reason exists for making a distinction between the glare source angular dependence data, acquired using the HDD and HUD test configurations. In other words, except for the possible second order effects due to the HUD image being focused at infinity, and the fact that the HDD test configuration limits moving the glare source to much closer than 15 degrees from the test subject's line of sight, whereas the HUD combiner presents no such obstacle, the total darkness in the test environment should make the HDD and HUD tests identical, at least from the perspective of the glare source exposure of the test subject's eyes. The existence of these test condition similarities provides a reasonable basis for the expectation that were there to be no test subject variability or measurement errors present, then the HDD and HUD test configurations should yield identical image difference luminance versus glare source subtended angle dependences.

Based on the test results of the various early experimenters, introduced at the beginning of this section, a reasonable expectation should also exist that the veiling luminance response of the test subjects should be essentially the same, for a translation of the glare source along any radial direction from the center of the test subject's visual field of view. This is equivalent to assuming that the angular response of the eyes, due to movements in the location of a glare source, adhere to spherical angular symmetry. For this expectation to

be realized by Jainski's test results, the image difference luminance requirement should be the same for any particular total subtended angle, θ, along any radial originating at the test subject's center of vision. Due to Jainski's experimental design, the test subject's center of vision is forced to coincide with the center of the HDD or HUD, by virtue of the need to be able to bring the maximum image resolution capability of the eyes to bear, to enable the correct identification of Jainski's minimum separable acuity test symbol.

Referring to Figure 3.21, which depicts the image difference luminance response of the test subjects to the angular location of the glare source on full logarithmic axes, it may be seen that the image difference luminance characteristic initially starts to decrease, as a function of an increasing vertical angle, by following a straight line locus, and then, above about 25 degrees, gradually transitions to a much more rapid decrease with increasing angles, and, hence, to a characteristic with a much larger slope at 48 degrees. In contrast to this response for a vertical translation of the glare source, the horizontal translation of the glare source, at a fixed vertical angle of 15 degrees, produces a characteristic that is coincident with the vertical angle response, out to a total subtended angle of about 25 degrees, but then diverts from the vertical angle translation response characteristic, by continuing to follow the slope of the initial straight line decrease, out to about 37 degrees, Jainski's last data point. Observing the data points located beyond 25 degrees on the horizontal characteristic, rather than the straight line data fit applied by Jainski, shows that a slight trend exists toward a decrease in the response at angles greater than 30 degrees, however, the data is not definitive for either interpretation of Jainski's glare source angular response result.

In Figure 3.22, for the HUD, the horizontal translation response characteristic for the glare source, corresponding to $L_D = 1.0 \times 10^{-5}$ asb, starts following a straight line out to about 18 degrees and then, like the vertical translation characteristic for the HDD, transitions to a more rapid decrease with increasing angles out to its maximum translation angle of 35 degrees. Because this horizontal translation of the glare source occurs at a vertical angle of 0 degrees, and starts just 5 degrees from the test subject's line of sight, the initial magnitude of the image difference luminance is higher than it is for the HDD in Figure 3.21.

Comparisons between the two HDD and one HUD characteristics, reveal that both confirmations and contradictions exist, with respect to the expectations set forth in the first two paragraphs of this subsection, namely, that the angular response of the eyes to movements of the glare source should be spherically symmetric, and that the angular response characteristics for the HDD and HUD image difference luminance requirements should be the same, or, for Figures 3.21 and 3.22, at least self-consistent. Out to angles of 25 to 30 degrees in Figure 3.21, the spherical angle symmetry of the image difference luminance in response to the translation of the glare source seems to be confirmed. Beyond 25 degrees, Figure 3.21 appears to provide evidence that the spherical symmetry may no longer hold, however, the small number of data points, coupled with the measurement errors present and the fact that the data only goes to 37 degrees in the horizontal direction, casts doubt on whether this result is definitive. The HUD characteristic shown in Figure 3.22, also contradicts the horizontal angle response depicted for the HDD in Figure 3.21, and, in so doing, tends to confirm the gradual transition to a much more rapid decrease in the angular response, exhibited by the HDD vertical angle data in Figure 3.21 with increasing glare source angles.

Two further noticeable discrepancies between the characteristics exist, which do not quite rise to the level of being treated as contradictory results. One discrepancy is the fact that the transition to a higher rate of decrease for the HUD angular response characteristic starts at a subtended angle of 18 degrees whereas the one for the HDD vertical angle response characteristic does not start until reaching an angle of 25 degrees. The other discrepancy is that the image difference luminance magnitudes of 21 and 34 asb obtained, respectively, from the HDD and HUD characteristics, at a glare source total subtended angle of 15 degrees in both Figures 3.21 and 3.22, do not match, as they should if the angular response to the glare source location were spherically symmetric and if no errors were present. To put this difference in perspective, the first row in Table 3.5 shows data, from Figure 3.17 (i.e., Bild 107) and Figure 3.18 (i.e., Bild 110), collected by Jainski under an identical set of test conditions. In that table, with the glare source set to the same illuminance and positioned at the same angle, the image difference luminance determined for the HDD was 28.2 asb, for Figure 3.17, and 27.9, for Figure 3.18, rather than the 21 asb from Figure 3.21. From the earlier discussion of the

Table 3.7. Comparisons of Jainski's Image Difference Luminance, L_S (*i.e.* ΔL), and Veiling Luminance, L_V, Requirements as a Function of the Angular Location of the Glare Source for HDD and HUD Test Configurations.

Variable Descriptions	L_S (i.e., ΔL) or L_V Dependence on Total Subtended Angle, θ, in Degrees, between Glare Source and Test Subject's Line of Sight to the Display										
Vertical Displacement of Glare Source with respect to the Foveal Center of Vision for the HDD Test Configuration											
$\theta = \sqrt{0^2 + \theta_V^2} = \theta_V$	10*	15	20	25	30	35	37.2	40	45	48	50*
L_S in asb from Bild 112	28	21	17.1	14.2	11.7	9.1	8.0	6.7	4.8	3.9	3.4
L_V in asb from Bild 107	380	260	200	160	130	93	81	65	42	33	28
L_V in fL	35.3	24.2	18.6	14.9	12.1	8.64	7.53	6.04	3.9	3.1	2.6
Vertical then Horizontal Displacement of Glare Source with respect to the Foveal Center of Vision for the HDD Test Configuration											
θ_V	10	15	15	15	15	15	15				
θ_H	0	0	13.3	20	26	31.6	34				
$\theta = \sqrt{\theta_H^2 + 15^2}$	10*	15	20	25	30	35	37.2				
L_S in asb from Bild 112	28	21	17.1	14.4	12.7	11.4	10.8				
L_V in asb from Bild 107	380	260	200	165	140	122	114				
L_V in fL	35.3	24.2	18.6	15.3	13.0	11.3	10.6				
Horizontal Displacement of Glare Source with respect to the Foveal Center of Vision for the HUD Test Configuration											
$\theta = \sqrt{\theta_H^2 + 0^2} = \theta_H$	5	10	15	20	25	30	35				
L_S in asb from Bild 106	72	45.5	34	27	18.5	10.1	5.6				
L_V in asb from Bild 101	930	560	410	305	200	95	44				
L_V in fL	86.4	52.0	38.1	28.3	18.6	8.83	4.09				

* Jainski extrapolation of HDD data

accuracy of Jainski's data, it would be reasonable to conclude that the difference between 21 and 34 asb, obtained from Figures 3.21 and 3.22, respectively, is attributable to a combination of measurement error and test subject variability. The seven-degree discrepancy between the transitions to a higher rate of decrease for the HUD angular response characteristic could have a similar origin, but is more problematic, unless multiple test sessions were required to collect the data.

Numerical values of Jainski's image difference luminance requirements data, as extracted from Bild 112 and 106 (i.e., Figures 3.21 and 3.22) are included in Table 3.7. The table also shows the values of veiling luminance corresponding to Jainski's image difference luminance requirements data. The veiling luminance values were obtained from the figures cited in Table 3.7 using the technique previously described in this section

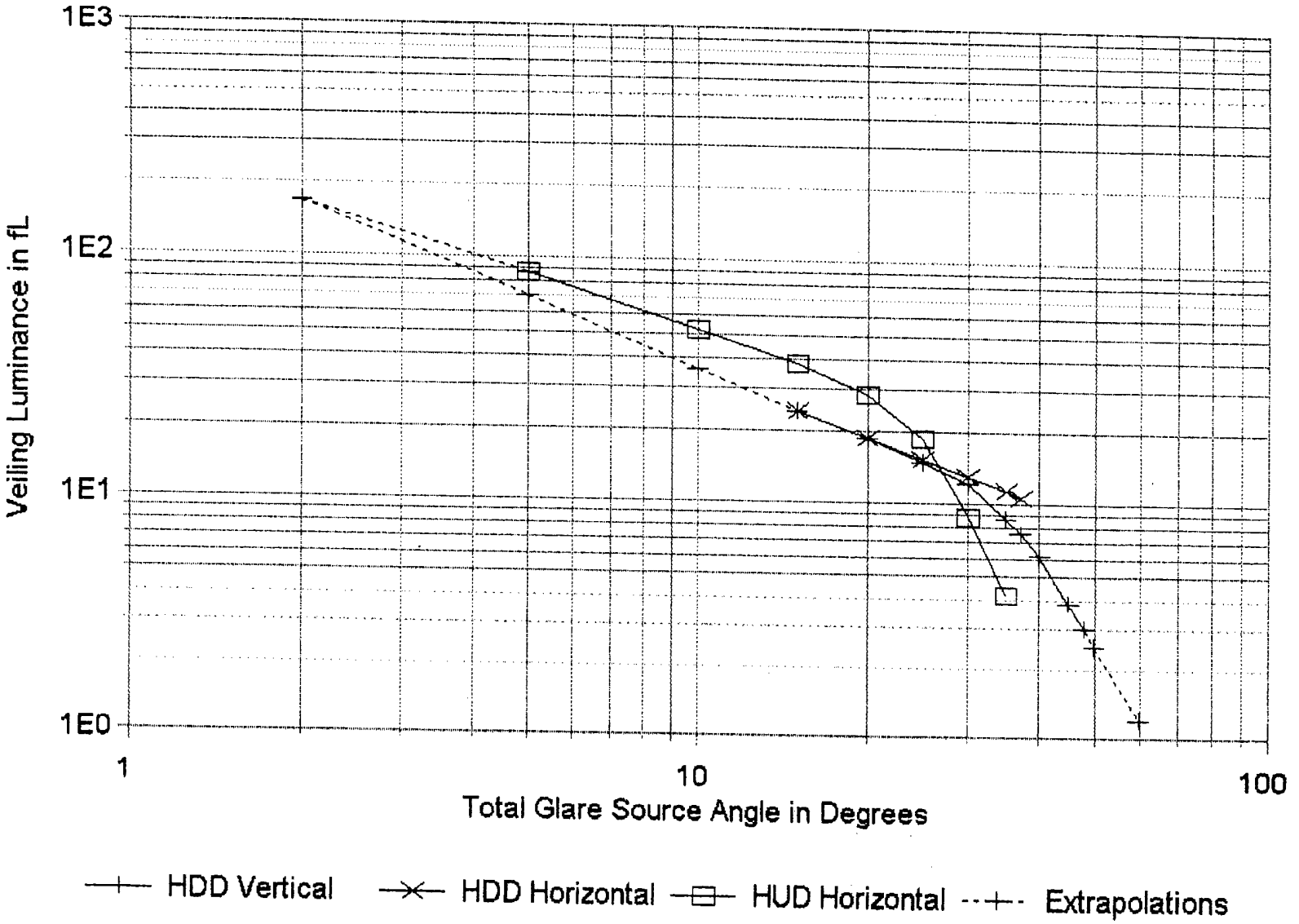


Figure 3.23. Comparison of Jainski Veiling Luminance Angular Dependence Characteristics for the Indicated Types of Glare Source Angular Displacements.

and then were converted from units of apostilbs to foot-Lamberts. The resulting three relationships between veiling luminance and the total angle subtended by the glare source with respect to the test subject's line of sight, from the fovea of the eyes to the center of the respective displays, are shown plotted in Figure 3.23.

Examining the angular response characteristics for the HDD and HUD test configurations in Figure 3.23 shows they do not overlap, as they should if the hypothesis that no difference should exist between the test subject's visual response to the angular displacement of the glare source, obtained using these two display test configurations, were correct, and if no errors were present in the Jainski test data. As previously described, one HDD data point, from Bild 107, collected under conditions identical to those in Figure 3.23 had an image difference luminance of 28.2 asb, for the glare source at a vertical subtended angle of 15 degrees, rather than the 21 asb, from Bild 112, used to obtain the veiling luminance of 24.2 fL shown in Figure 3.23. The veiling luminance, corresponding to the image difference luminance data point of 28.2 asb for the HDD, is about 375 asb, or 34.8 fL, whereas the veiling luminance at 15 degrees of glare source displacement for the HUD, from Table 3.7, is 38.1 fL, an error of 9%. As an addition source of comparisons, Figure 3.19 (Bild 116) gives veiling luminance as a function of glare source illuminance for the HDD at the same glare source angle. The equivalent Jainski figure for the HUD is Bild 117. These two figures yield veiling luminances of 34.4 fL for the HDD and 20.2 fL for the HUD, almost an exact reversal of the values obtained above from Figure 3.23.

If it were to be assumed that a measurement repeatability shift error, common to photometer measurements, resulted in the HDD vertical characteristic in Figure 3.23 being shifted to lower luminance values, then raising it, by the ratio of 28.2 divided by 21 asb along its entire length, and converting to veiling luminance would cause the HDD and HUD characteristics to be in much closer agreement for smaller glare source angles, but would still leave a discrepancy, at larger angles, in the breakpoint transition to the higher rate of decrease in the veiling luminance. As a practical matter, given the error levels that exist in the Jainski angular dependence characteristics, this data provides no experimental basis for treating the HDD and HUD characteristics in Figure 3.23 separately. Jainski, of course, had to treat each of the angular characteristics separately and, for this reason, also formulated individual equations for the HDD and HUD. These equations ignored the results beyond 25 degrees for the HDD and 15 degrees for the HUD. Contradictions and inconsistencies in the test data described here were not mentioned by Jainski, and, therefore, were not dealt with in the report.

The luminance geometry conditions present during Jainski's glare source tests, resulted, as has been previously described, in a test of the eyes' response to the angular displacement of the glare source. The physical differences between the HDD and HUD test configurations should not have been visible to the test subjects, due to the extremely low scene luminance levels maintained. This means that the only theoretical or physical difference between the HDD and HUD tests is the difference in the accommodation of the test subject's eyes, which results from the HDD image being in focus at the distance of the instrument panel display, and the HUD image being in focus at virtual infinity, due to its projection by the HUD image combiner optics. This difference in the focus of the eyes, when considered in the context of changes in the light scattering cross sections in the eyes that are responsible for inducing veiling luminance, should produce no more than second order effects, since scattering centers are predominant in the optical media behind the lens of the eye rather than in the lens and cornea. Due to level of error, present in Jainski's test results, there is no reason to expect that a second order effect would be discernable in the Figure 3.23 test data. In other words, although it is unlikely that the latter effect would justify a separate treatment of the HDD and HUD, even under the best conditions, the level of error, present in Jainski's test results, makes the need for this distinction questionable.

The combination of the known errors in Jainski's glare source angular dependence characteristics, and the preceding argument, justifies not creating separate mathematical models for the HDD and the HUD. Even if the characteristics shown in Figure 3.23 did represent accurate representations of different HDD and HUD characteristics, the tight grouping of the HDD vertical and HUD horizontal characteristics would allow the use of an average worst-case characteristic to approximate both dependences for the purposes of automatic legibility control modeling. Alternatively, if the characteristics shown in Figure 3.23 are different representations

of a single angular response characteristic, with the differences between the characteristics being attributable to errors, as has been shown above to be feasible, then, when looked upon as a grouping of characteristics they do exhibit an angular dependence trend, which, from the perspective of automatic legibility control, could also be approximately represented by a single angular response characteristic that produces a veiling luminance effect approaching a worst-case viewing condition.

3.5.3.3. Derivation of Veiling Luminance Angular Dependence from Experimental Data

Viewing Figure 3.23 from the perspective of modeling the data to approximate a worst-case veiling luminance scenario involves using the HUD horizontal characteristic at small glare source displacement angles and the HDD vertical characteristic for large glare source displacement angles. The HDD horizontal characteristic is being ignored, due to the lack of any data that extends beyond 37.2 degrees of glare source displacement and because the greatest difference between the horizontal and vertical characteristics occurs at this angle (i.e., the difference between 10.6 fL and 7.53 fL) and yields a mean error of only 8.5%, well within the demonstrated range of errors present in Jainski's test data.

Examination of Figure 3.23 shows that a straight line can be used, as an approximation, to represent the depicted dependence of veiling luminance, on the angle subtended by the glare source with respect to the test subjects line of sight to the display, at both small and large angles. Empirical equations to represent this angular dependence data can be expressed by the equation of a straight line, which was introduced previously,

$$y - y_1 = m(x - x_1). \tag{3.6}$$

In the present case, the requisite equations to represent the two straight line segments in Figure 3.23 that are to be modeled can be obtained by substituting $y = \log_{10} L_V$ and $x = \log_{10} \theta$ for y, y_1, x and x_1 in Equation 3.6, with the application of the appropriate subscripts. The resulting equation for straight line segments depicted on full logarithmic coordinate axes can be expressed as follows:

$$\log_{10}\left(\frac{L_V}{L_{V1}}\right) = m_{V\text{-}\theta} \log_{10}\left(\frac{\theta}{\theta_1}\right), \tag{3.36}$$

where the veiling luminance slope, $m_{V\text{-}\theta}$, can be determined using any two points on the straight line segments, using the equation:

$$m_{V\text{-}\theta} = \log_{10}\left(\frac{L_{V2}}{L_{V1}}\right) \Big/ \log_{10}\left(\frac{\theta_2}{\theta_1}\right). \tag{3.37}$$

The small and large angle extrapolations of the veiling luminance angular dependence characteristics shown in Figure 3.23 were obtained using straight line extensions of the test data in Table 3.7 plotted on full logarithmic graph paper ten inches square. At small angles, the two points used to calculate the slope of the HUD characteristic consisted of the point L_{V1} = 38.1 fL, at θ_1 = 15 degrees from Table 3.7, and the intersection point of the HUD and HDD characteristics, at L_{V2} = 169 fL and θ_2 = 2 degrees. The slope of the straight line segment can be calculated by substituting these values into Equation 3.37, yielding

$$m_{V\text{-}\theta}(\theta \le 15^\circ) = \log_{10}\left(\frac{169}{38.1}\right) \Big/ \log_{10}\left(\frac{2}{15}\right) = -0.7393 \approx -0.74. \tag{3.38}$$

At angles of 40 degrees and larger, the two points used to calculate the slope of the HDD vertical angle characteristic consisted of the intersection point of the straight line extrapolation of the HDD characteristic with the L_V = 1 fL locus, at L_{V1} = 1 fL and θ_1 = 64.7 degrees, and the point L_{V2} = 6.04 fL, at θ_2 = 40 degrees from Table 3.7. Substituting these values into Equation 3.37, the slope of the vertically displaced glare source HDD characteristic, shown extended as a straight line segment in Figure 3.23, can be calculated as follows:

$$m_{V\text{-}\theta}(\theta \geq 40^\circ) = \log_{10}\left(\frac{6.04}{1}\right) \Big/ \log_{10}\left(\frac{40}{64.7}\right) = -3.7398 \approx -3.74. \tag{3.39}$$

An alternative form of the general equation for the straight line segments of the veiling luminance angular dependence characteristics can be obtained by taking the antilogarithm of Equation 3.36. Solving for the veiling luminance and rearranging terms, this equation can be expressed in the following equivalent form:

$$L_V(\theta) = \frac{L_{V1}}{\theta_1^{m_{V\text{-}\theta}}}\theta^{m_{V\text{-}\theta}} = K\,\theta^{m_{V\text{-}\theta}}. \tag{3.40}$$

The value of the constant term, K, is therefore given by the equation

$$K = \frac{L_{V1}}{\theta_1^{m_{V\text{-}\theta}}}. \tag{3.41}$$

Evaluating the value of *K* for small angles,

$$K(\theta \leq 15^\circ) = \frac{L_{V1}}{\theta_1^{-0.74}} = \frac{169}{2^{-0.74}} = \frac{169}{0.599} = 282.3\ fL. \tag{3.42}$$

In a similar fashion, evaluating the value of *K* for large angles,

$$K(\theta \geq 40^\circ) = \frac{L_{V1}}{\theta_1^{-3.74}} = \frac{6.04}{40^{-3.74}} = \frac{6.04}{1.019 \times 10^{-6}} = 5.93 \times 10^6\ fL. \tag{3.43}$$

Based on the preceding results, the final equation for the veiling luminance angular dependence, on the glare source displacement for small angles, can be written as:

$$L_V(\theta \leq 15^\circ) = 282.3\,\theta^{-0.74}. \tag{3.44}$$

Likewise, the final equation for the veiling luminance angular dependence, on the glare source displacement for large angles, can be written as:

$$L_V(\theta \geq 40^\circ) = 5.93 \times 10^6\,\theta^{-3.74}\ fL. \tag{3.45}$$

Formerly, when mathematically modeling Jainski's ideal image difference luminance versus display background luminance characteristics, the final composite empirical relationship was formed by adding a constant low luminance term, which predominates at low display background luminance levels, to a second term that increased as the power of the display background luminance, and predominated at high display background luminance levels. To derive a combined angular dependence function, using the previously derived low and high angle components of the glare source induced veiling luminance, a different approach is necessary. The term that should predominate at low angles, which is given by Equation 3.44, evaluates to lower values at small angles than does the other term, given by Equation 3.45. Similarly, the term that should predominate at large angles, Equation 3.45, evaluates to lower values than Equation 3.44, for large angles. To accommodate this situation and still combine the equations through addition, as before, the individual terms must first be inverted so that they predominate in the desired low and high angular ranges. An equation that allows the two terms to be added, and also causes the correct term to predominate at the respective low and high glare source displacement angles, follows:

$$\frac{1}{L_V(\theta)} = \frac{1}{L_v(\theta \leq 15^\circ)} + \frac{1}{L_v(\theta \geq 40^\circ)}. \tag{3.46}$$

This relationship can also be expressed in the following equivalent form as follows:

$$L_V(\theta) = \frac{1}{\dfrac{1}{L_v(\theta \leq 15^\circ)} + \dfrac{1}{L_v(\theta \geq 40^\circ)}}. \tag{3.47}$$

Substitution the functional values of the veiling luminance terms from Equations 3.44 and 3.45 into this expression, the following equation is obtained for the empirical equation for the angular dependence of veiling luminance,

$$L_V(\theta) = \frac{1}{\frac{1}{282.3\,\theta^{-0.74}} + \frac{1}{5.93\times10^{5}\,\theta^{-3.74}}}. \tag{3.48}$$

By factoring out the first fractional term in the denominator of this equation and then multiplying the numerator and denominator of the factored equation by the denominator of the factored fractional term, Equation 3.48 can be reduced to the simpler form that follows:

$$L_V(\theta) = \frac{282.3\,\theta^{-0.74}}{1 + \frac{1}{2.099\times10^{4}\,\theta^{-3}}}. \tag{3.49}$$

The final veiling luminance angular dependence equation, which corresponds to the glare source illuminance of E_B = 371.6 fc (i.e., 4,000 lx), applicable to Figure 3.23, is then obtained by carrying out the division shown by the second term in the denominator of Equation 3.49. Performing this operation yields the following final empirical equation for the angular dependence of veiling luminance:

$$L_V(E_B = 371.6\,fc, \theta) = \frac{282.3\,\theta^{-0.74}}{1 + 4.764\times10^{-5}\,\theta^{3}}. \tag{3.50}$$

Figure 3.24 shows this empirical veiling luminance equation superimposed onto Figure 3.23, to permit a direct visual comparison with the two angular dependence characteristics from which it was derived. In this equation, the veiling luminance is expressed in units of foot-Lamberts and the angle is in units of degrees. The resulting empirical characteristic approximates the maximum veiling luminance values of the horizontal HUD characteristic, for small subtended angles between the glare source and the line of sight, and the maximum veiling luminance values of the HDD vertical characteristic, at large angles. In both the case of small and large angles, the empirical characteristic approaches the respective horizontal HUD and vertical HDD experimental characteristics of Jainski asymptotically. For angles, close to where the characteristics cross, the empirical characteristic takes on intermediate values, between the two experimental characteristics, approximately following the trend of the angular response of veiling luminance established by considering both experimental characteristics of Jainski as a valid grouping of dispersed data, representative of a single veiling luminance characteristic, as described previously.

3.6. Veiling Luminance Representations for Spatially Discrete Glare Sources

Up to this point, separate empirical equations for the dependence of veiling luminance on glare source illuminance and on the angle subtended by the glare source with respect to the pilot's line of sight have been introduced. The previously introduced equation for the glare source illuminance dependence of veiling luminance corresponds only to a glare source at a horizontal angle of zero degrees and a vertical angle of fifteen degrees. Likewise, the previously introduced equation for the angular dependence of veiling luminance corresponds only to a glare source illuminance of E_B = 371.6 fc (i.e., 4,000 lx). The purpose of this section is to develop empirical equations that apply approximately to all glare source illuminance values and displacement angles of interest for aircraft cockpit applications. The section starts by developing an empirical equation for the veiling luminance attributable to discrete glare sources. This result is then compared with the test results of earlier experimenters. The effects of changes in pupil area, in response to changing ambient illumination conditions, are then considered, in relation to the potential impact of this uncontrolled variable on the empirical veiling luminance model.

The applicability of the empirical equations, developed in this section, remains strictly valid only for ideal display images and/or real-world visual scenes, even though they permit accounting for the effects of non-ideal

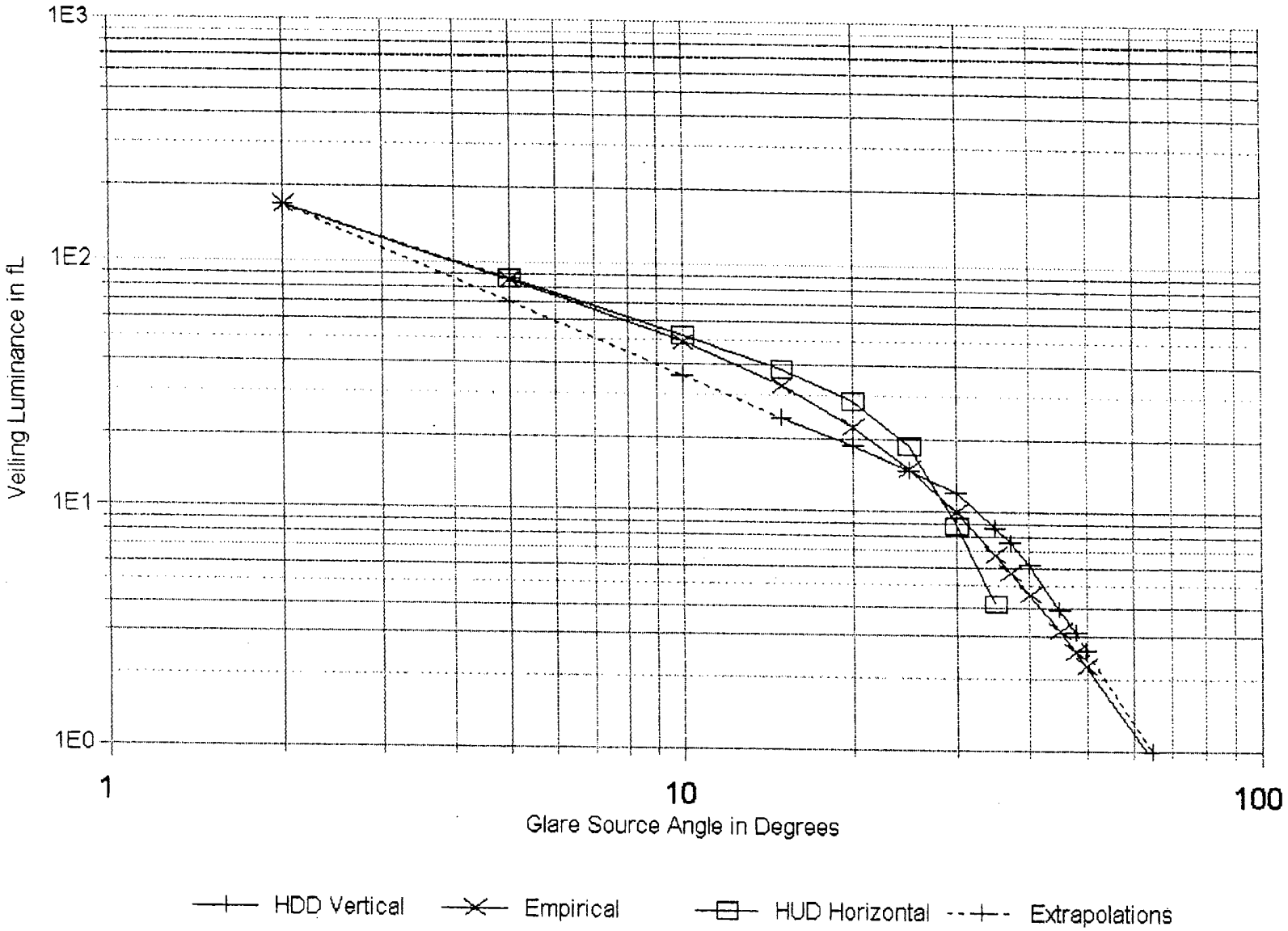


Figure 3.24. Comparison of Empirical Equation Predictions with Jainski's Veiling Luminance Angular Dependence Characteristics for the Indicated Types of Glare Source Angular Displacements.

viewing conditions. Although the equations developed are strictly valid only for ideal imagery (e.g., unblurred images viewed in the absence of vibration, acceleration and the other degrading effects listed in Table 3.1), the practical implementation of the veiling luminance model described in a later section, near the end of this chapter, circumvents this limitation.

3.6.1. Empirical Equations for Discrete Glare Sources Based on the Data of Jainski

In Section 3.5, the dependences of Jainski's veiling luminance test results on the illuminance of a discrete glare source and on the angular position of the discrete glare source with respect to the pilot's central vision axis were developed separately. In this subsection these dependences are combined to provide a single mathematical model for these veiling luminance dependences.

3.6.1.1. Combined Illuminance and Angular Dependences

In the most general case, when a dependent variable is functionally dependent on two or more independent variables, the functional dependence of the dependent variable must be stipulated for each possible combination of the independent variables. Stated in another way, the most general case infers that each change in value of one independent variable can result in a different functional relationship between the dependent variable and the remainder of the independent variables. For veiling luminance, the independent variables are the glare source illuminance and the angle between the glare source and the pilot's line of sight. In the most general case of the formulation of veiling luminance, the functional relationship between veiling luminance and its two independent variables, can therefore be expressed mathematically as follows:

$$L_V = K_D f(E_B, \theta) \tag{3.51}$$

where K_D is a proportionality constant that sets the correct magnitude of the veiling luminance induced by a discrete glare source.

The form of the functional dependence of veiling luminance expressed by Equation 3.51, allows the glare source illuminance and angular position independent variables to be functionally interdependent. If this functional interdependence between the veiling luminance independent variables were to be valid, then the dependence of veiling luminance on the glare source illuminance would have to be known at all angles rather than at only the single angle tested by Jainski in Figure 3.19. Alternatively, the veiling luminance angular dependence would have to be known at all glare source illuminances of interest, rather than at only a single value, as in Figures 3.21 and 3.22. Consequently, even if the spherically symmetric veiling luminance angular dependence, reported by Holladay and others, is valid, as was assumed to be true for the derivation of the empirical veiling luminance angular dependence equation in the last section, the veiling luminance angular dependence would still have to be known, at least along one radial from the center of vision, for each value of glare source illuminance of interest.

In practice, veiling luminance, and the image difference luminance used to measure its effects, are both always incident on the foveal light receptors of the eyes, from the direction of the center of the test subject's field of view (e.g., from the direction of the display being tested), irrespective of the actual angular position of the glare source, with respect to the pilot's line of sight. As described later in this section, this physical fact allows concluding that the effects of glare source illuminance and the angular position of the glare source on veiling luminance are not interdependent. Modifying Equation3.51 to express this functional independence, it can be written in the following alternative form:

$$L_V = K_D f(E_B) f(\theta) \tag{3.52}$$

The practical consequence of the functional independence, represented by this equation, is that the relationship between veiling luminance and the glare source illuminance, and the relationship between the veiling luminance and the angular position of the glare source, can be determined separately, as was done by

Jainski. Afterward, these functional dependences can be combined to form a single function, dependent on both the glare source illuminance and its angular position, using Equation 3.52.

In an earlier subsection, the relationship given by Equation 3.35 was developed to relate veiling luminance to the illuminance of the glare source. The constant multiplier in that equation was applicable only to the particular angular position of the glare source responsible for inducing the veiling luminance, which was specified at a horizontal position of zero degrees and a vertical position of fifteen degrees. Likewise, Equation 3.50 gives the relationship developed between veiling luminance and the angular position of the glare source that was responsible for inducing the veiling luminance. The constant multiplier in that equation was dependent of the magnitude of the glare source illuminance and the numerical value shown in the equation is applicable only for a glare source illuminance of 371.6 fc (i.e., 4,000 lx).

Either Equation 3.35 or 3.50 can be used as the basis for a composite empirical equation of the form of Equation 3.52. Arbitrarily choosing Equation 3.50 to serve as the basis, the following equality can be written:

$$L_V(E_B = 371.6\,fc, \theta) = \frac{282.3\,\theta^{-0.74}}{1 + 4.764x10^{-5}\,\theta^3} = 282.3\,f(\theta)\,. \tag{3.53}$$

However, from Equations 3.52 and 3.35 it is known that this equation can be expressed in still more general terms as follows:

$$L_V(E_B, \theta) = K_D\,E_B^{0.872}\,f(\theta)\,. \tag{3.54}$$

The illuminance dependent multiplier in Equation 3.53, that is, 282.3, must therefore satisfy the relationship

$$K_D\,E_B^{0.872} = 282.3\,. \tag{3.55}$$

Following the substitution of the value E_B = 371.6 fc, applicable to Equations 3.50 and 3.53, for the glare source illuminance, E_B, into Equation 3.55 the equation becomes:

$$K_D\,(371.6)^{0.872} = 282.3\,, \tag{3.56}$$

which can be solved for the constant K_D yielding a value of

$$K_D = 1.6203 \approx 1.62\,. \tag{3.57}$$

The final empirical veiling luminance equation, for the case where a discrete glare source is present in the observer's instantaneous field of view, that contains both the glare source illuminance and angular displacement dependences, can then be expressed as follows:

$$L_V(E_B, \theta_B) = \frac{1.62\,E_B^{0.872}\,\theta_B^{-0.74}}{1 + 4.764 \times 10^{-5}\,\theta_B^3}\,. \tag{3.58}$$

In this equation, the veiling luminance, L_V is in foot-Lamberts (fL), the glare source illuminance, E_B, is in foot-candles (fc) and the angle the glare source makes with the foveal line of sight, θ_B, is in degrees.

3.6.1.2. Image Difference Luminance Requirement for a Discrete Glare Source

As previously described near the beginning of Section 3.5, the veiling luminance, L_V, is added to the measured display or scene background luminance, L_D, to produce the perceived background luminance, $L_D + L_V$. In other words, the presence of veiling luminance, in the foveal field-of-view, or for that matter anywhere in the field of view, results in an increase in the measurable display background luminance to a perceived display background luminance value, L_D', where

$$L_D' = L_D + L_V\,. \tag{3.59}$$

In an analogous manner, substituting the modified background luminance into the equation for image difference luminance,

$$\Delta L = L_S - L_D, \tag{3.2}$$

in which both the symbol luminance, L_S, and the display background luminance, L_D, are measurable quantities, yields an equation for the modified difference luminance, in the presence of veiling luminance, as follows:

$$\Delta L' = L_S - L_D' = L_S - L_D - L_V = \Delta L - L_V. \tag{3.60}$$

The new image difference luminance, $\Delta L'$, is therefore equal to the measurable difference luminance, ΔL, reduced by the amount of the veiling luminance superimposed onto the display background luminance that is already present.

Finally, using L_D' in place of L_D in Equation 3.13 or 3.17 (or on the appropriate characteristic on Figure 3.10), a new value for the image difference luminance required to maintain legibility at the level it was at before introducing the veiling luminance can be obtained. Veiling luminance can therefore be accounted for in the perceived image difference luminance requirements equation, by writing it in the previously introduced modified form,

$$\Delta L_P = \Delta L_{PK}\left[1 + \left(\frac{L_D + L_V}{L_{DK}}\right)^m\right], \tag{3.23}$$

where m = .926 and, for a discrete glare source, L_V is given by Equation 3.58.

It should be noted that the value of the veiling luminance, L_V, induced, by light scattering and any potential retinal induction effects, associated with an exposure to a glare source, already takes into account changes in the pupil diameters of the eyes that accompany the increase in the background luminance perceived. This subject is discussed in more detail in succeeding sections of this chapter.

3.6.2. Comparison of Veiling Luminance Test Results of Different Experimenters for Discrete Glare Sources

In this section the empirical equations for veiling luminance, determined by five experimenters, will be compared, with each other and with the empirical equation derived to represent Jainski's discrete glare source test data, Equation 3.58. The results of these tests are, in several instances, very different from one another. To the extent that the information reported by the experimenters makes it possible to do so, the reasons for these differences are explored in this subsection.

3.6.2.1. Empirical Representations of Veiling Luminance Test Results

The veiling luminance equations presented below are first introduced in the same form in which they appeared in the articles from which they were taken. To simplify comparisons, the equations are then converted to a common set of units, namely, foot-Lamberts (fL) for luminance and foot-candles (fc) for illuminance. The conversion equations employed are as follows:

$$\begin{aligned} L_V(fL) &= \pi L_V(cd/ft^2) = 0.929\, L_V(mL) \\ L_V(fL) &= 0.2919\, L_V(cd/m^2) = 0.2919\, L_V(nt) \\ E_B(fc) &= E_B(lm/ft^2) = 0.0929\, E_B(lx) = 0.0929\, E_B(mc). \end{aligned} \tag{3.61}$$

In the last equation, the unit abbreviation, mc, stands for meter-candles or as it is more commonly known today, lux (lx).

The equation reported by Jainski, as representative of the test results obtained for angles between 5 and 38 degrees, is as follows:[56]

$$L_v(cd/m^2) = \frac{0.55\, E_B^{.88}(lx)}{\theta^{0.72}(deg)}. \tag{3.62}$$

The angular response indicated by this equation was determined for a single glare source illuminance of 4,000 lx (371.6 fc). The illuminance dependence was determined at a glare source angle of 15 degrees, with illuminance values varied between 1 lx (0.0929 fc) and 10,000 lx (929 fc). Applying the units conversions to the preceding equation, Jainski's equation can be expressed as follows:

$$\begin{aligned} L_v(fL) &= \frac{(0.2919)(0.55)(10.764)^{0.88}\, E_B^{.88}(fc)}{\theta^{0.72}(deg)} \\ &= \frac{1.3\, E_B^{.88}(fc)}{\theta^{0.72}(deg)}. \end{aligned} \tag{3.63}$$

Holladay's 1927 article reported a distinctly different test result for veiling luminance.[57] The empirical equation reported was as follows:

$$L_v(mL) = \frac{2.9\, E_B(lx)}{\theta^2(deg)}. \tag{3.64}$$

The angular dependence in this equation was determined for angles between 2.5 and 25 degrees, at a glare source illuminance level setting of 1 lx (0.0929 fc). Applying the units conversions to the preceding equation, Holladay's equation can be expressed as follows:

$$\begin{aligned} L_v(fL) &= \frac{(0.929)(2.9)(10.764)\, E_B(fc)}{\theta^2(deg)} \\ &= \frac{29\, E_B(fc)}{\theta^2(deg)}. \end{aligned} \tag{3.65}$$

The equation reported in Stiles' 1929 article[58] is very similar to that of Holladay's 1927 article, except the power of the angular dependence, which was 1.5 rather than 2. The empirical equation derived by Stiles to represent veiling luminance was expressed as follows in the article:

$$L_v(cd/ft^2) = \frac{4.16\, E_B(fc)}{\theta^{1.5}(deg)}. \tag{3.66}$$

This equation was determined from plots of effective background luminance, L_D', versus the glare source illuminance for values of illuminance between 0 and 1 fc, where the glare source test angles of 1, 2, 3, 5 and 10 degrees were parameters. Expressed in the terminology of this report, Stiles used the following equation to fit the experimental data:

$$L_D' = L_D + \frac{k\, E_B}{\theta^n}, \tag{3.67}$$

where the multiplier, k, is a proportionality constant.

In a plot of the exponent, n, versus the logarithm of the background luminance, L_D, Stiles data demonstrates support for an exponent of 1.5, for background luminances of zero up to 0.04 cd/ft^2 (0.126 fL), but, after that, the exponent was found to decrease reaching about 0.8 at 1 cd/ft^2 (3.14 fL). In the summary section of the article, Stiles concluded that the equation should not be used for display background luminances greater than 0.22 cd/ft^2 (0.69 fL). It should be noted that Stiles predicted value for the exponent of 0.8 at the highest background luminance level tested, 1 cd/ft^2, is not that different from the value of 0.72, shown in

Jainski's equation above, or the value of 0.74, used in this report's empirical representation of Jainski's data, Equation 3.58. Applying the units conversions to Stile's equation, it can be expressed as follows:

$$L_v(fL) = \frac{\pi(4.16)\,E_B(fc)}{\theta^{1.5}(deg)} = \frac{13.1\,E_B(fc)}{\theta^{1.5}(deg)}. \tag{3.68}$$

Jainski, in reporting empirical equations for Holladay, Stiles and Fry, listed only the angular range for which the equations are valid not the ranges over which the illuminance dependences are valid. The equation attributed by Jainski to Fry is as follows:

$$L_v(cd/m^2) = \frac{9.2\,E_B(lx)}{\theta(deg)(1.5+\theta(deg))}, \tag{3.69}$$

where Jainski states the equation is good for all angles. Applying the units conversions to the Fry equation, it can be expressed as follows:

$$L_v(fL) = \frac{(0.2919)(9.2)(10.764)\,E_B(fc)}{\theta(deg)(1.5+\theta(deg))} = \frac{9.2\pi\,E_B(fc)}{\theta(deg)(1.5+\theta(deg))} = \frac{28.9\,E_B(fc)}{\theta(deg)(1.5+\theta(deg))}. \tag{3.70}$$

In searching Jainski's five references to Fry, the above equation was found in an article, whose purpose was to explore the scattering theory of glare.[59] The equation was proposed, without further experimental testing, by Fry for the stated purpose of resolving the difference that can be noted above between the results obtained in the tests conducted by Holladay and those of Stiles. This equation is being compared with the others both to demonstrate Fry's assertion and because Fry and Alpern had conducted an earlier experimental investigation of the veiling luminance induced by glare sources, which they did not include in their comparison.[60] The results of the Fry and Alpern experimental investigation were similar to those of Holladay and Stiles except that the glare source angle exponent was 2.5. This investigation's results are not included in the present report for two reasons. First, the experimental test procedure used exposed both eyes to identical brightness comparison rectangles but only one eye to the glare source. No discussion or test results were presented to establish how the exposure of one rather than both eyes to the glare source might alter the test results. The second reason the results of Fry and Alpern are not included is that specific reference is made to confining the glare source light beam to an area smaller than the pupil diameter to eliminate effects caused by this variable.

The final empirical equation to be compared is one published by Nowakowski in 1926.[61] Nowakowski's technique for measuring the effect of glare was very similar to the techniques used by Holladay and Stiles, but differed from them in the way the results were characterized. Using fixed negative contrast letters on a white background, the illuminance incident on the letters needed to achieve threshold legibility was first determined with no glare present (i.e., an illuminance, E_{NG}, produces an image difference luminance, ΔL_{NG}, perceived against a white reflected background luminance, $L_{D\text{-}NG}$). Next, to achieve the same threshold legibility, with a glare source directed toward the test subjects eyes, the illuminance incident on the test letter had to be increased to compensate for the presence of the glare source (i.e., an illuminance, E_θ, produces an image difference luminance, ΔL_θ, perceived against a white reflected background luminance, $L_{D\text{-}\theta}$). Nowakowski defined his measure of the effect of glare as the ratio of the increase in illuminance incident on the letters needed to cause them to be legible, in the presence of the glare source, to the illuminance needed to cause the letters to be legible, in the absence of the glare source. Expressed as an equation, the glare metric, G, defined by Nowakowski can be written as follows:[62]

$$G = \frac{E_G - E_{NG}}{E_{NG}} = \frac{E_G}{E_{NG}} - 1 . \tag{3.71}$$

To make this measure, of the effect of glare, comparable with the other equations presented, it is necessary to express Nowakowski's measure in terms of veiling luminance. By multiplying the numerator and denominator of the preceding equation by the diffuse reflectance, R, of the white reflected background of the test letters, and then substituting the equivalent reflected luminance terms, for the glare and no-glare reflectance-illuminance products, this equation can be expressed, in terms of the luminances reflected by the white background that is common to the glare and no-glare tests, as follows:

$$G = \frac{R\,E_G - R\,E_{NG}}{R\,E_{NG}} = \frac{L_{D\text{-}G} - L_{D\text{-}NG}}{L_{D\text{-}NG}} . \tag{3.72}$$

The difference in the background luminance with and without glare is, however, just the previously introduced definition of veiling luminance, L_V, and the no-glare background luminance is the same as L_D, so, with a rearrangement of terms the equation becomes,

$$L_V = G\,L_D . \tag{3.73}$$

In other words, Nowakowski's definition of glare, which can take on values of zero and greater, is directly proportional to the veiling luminance measure of glare, originally defined by Luckiesch and Holladay.

Because Nowakowski's experimental techniques did not involve the direct measurement of any luminances and the reflectances of the test images and their backgrounds were not cited, the empirical glare equation of Nowakowski cannot be expressed directly in terms of veiling luminance, using absolute parameter values as has been the case for the other equations. Nowakowski also expressed his equation using the glare source candlepower (i.e., luminous intensity) and its distance from the eyes, instead of using the illuminance due to the glare source, as measured at the eyes. In spite of this difference in reporting methods used, Nowakowski did state that the glare source illuminance was measured and that the effect of glare was proportional this illuminance.

The following equation represents the proportionalities ascribed by Nowakowski to his results, which are relevant to the present investigation:

$$L_V \propto \frac{\cos\alpha}{\sin\theta} E_B . \tag{3.74}$$

The $\cos\alpha$ dependence was added by Nowakowski to account for a more rapid decrease in the effect of glare than the $1/\sin\theta$ dependence predicts for angles greater than 30 degrees. Values of the angle α contained in Nowakowski's Table 7 are reproduced in Table 3.8.

Table 3.8. Nowakowski's Values of the Angle α.

θ in degrees	30	40	50	60	70	80	90
α in degrees	0	14	30	44	58	73	88

In his article, Nowakowski attributed a physical significance to the angle, α, as the angle subtended by glare light, incident on the eye's retina, with respect to the normal to the retinal surface. Therefore, by inference, Nowakowski associated a cosine receptor response with the light reception properties of the retina's rod light receptors. In spite of this interpretation, Nowakowski stated in his article that the values of this angle, included in his table, were determined to match his empirical equation to his experimental data, rather than being based on an actual determination of the angle between the incident glare light and the normal to the

retina.

It should be noted that the use of illuminated negative contrast test images in the Nowakowski tests was one of the experimental design aspects common to the 1925 Luckiesch and Holladay article, an article that incidentally was cited by Nowakowski, and to the subsequent article published three months later in 1926 by Holladay. An important difference between these tests is that the letters, Nowakowski used, required the test subjects to perform a threshold form identification task, whereas the other two articles collected the relevant data using a variety of images in threshold detection tasks.

To more readily compare the angular dependences of the preceding equations, they have been normalized to have a value of unity at an angle of 2.6 degrees, the nominal radius of the fovea, as shown below:

Jainski: $\dfrac{L_V(\theta)}{L_V(2.6^\circ)} = \dfrac{(2.6)^{0.72}}{\theta^{0.72}}$ $\quad 5^\circ \le \theta \le 38^\circ$

Holladay: $\dfrac{L_V(\theta)}{L_V(2.6^\circ)} = \dfrac{(2.6)^2}{\theta^2}$ $\quad 2.5^\circ \le \theta \le 25^\circ$

Stiles: $\dfrac{L_V(\theta)}{L_V(2.6^\circ)} = \dfrac{(2.6)^{1.5}}{\theta^{1.5}}$ $\quad 1^\circ \le \theta \le 10^\circ$ $\quad 0 \le L_D \le 0.69\,\text{fL}$

Fry: $\dfrac{L_V(\theta)}{L_V(2.6^\circ)} = \dfrac{10.66}{\theta(1.5+\theta)}$ $\quad$ Any vertical angle

Nowakowski: $\dfrac{L_V(\theta)}{L_V(2.6^\circ)} = \dfrac{\sin(2.6)\cos\alpha}{\sin\theta}$ $\quad 10^\circ \le \theta \le 90^\circ$

Empirical Fit of Jainski Data: $\dfrac{L_V(\theta)}{L_V(2.6^\circ)} = \dfrac{(2.0298)\,\theta^{-0.74}}{1 + 4.764\times10^{-5}\,\theta^3}$ $\quad 5^\circ \le \theta \le 60^\circ$

The result of a comparison of these equations is shown in Figure 3.25. It is evident, from even a cursory examination of these veiling luminance characteristics, that the different experimenter's test results are not consistent. Furthermore, the large differences between the experimenters' results make it more likely that the test subjects are responding to real differences in the experimental tests conducted and not simply due to variability between test subject populations, light measurement techniques or in the experimental design techniques employed.

Figure 3.26 shows the computed values of veiling luminance, as a function of the glare source angle, for the previously introduced equations of the different experimenters. For this comparison, the glare source illuminance has been set to a value of 1 fc in each equation. An exception to this had to be made for Nowakowski's data. This characteristic was arbitrarily set to match the starting value of veiling luminance, at a one degree angle, of the empirical discrete glare source equation used to model the Jainski data. Excepting the characteristics for the Fry theory-based equation and for the empirical characteristic derived from Jainski results, and labeled Empirical, both of which have been extended to allow comparison at large angles, the other curves are stopped at the approximate upper limits of the experimental data. The small angle limits of validity for the experimental test data shown in Figure 3.26 are as follows: 1 degree for the Stiles data, 2.5 degrees for the Holladay data, 5 degrees for the Jainski data and 10 degrees for the Nowakowski data.

Figure 3.26 shows that all of the equations predict similar veiling luminances in the region of 10 degrees. It also shows that the equations of Holladay, Stiles and Fry and separately those of Jainski, Nowakowski and

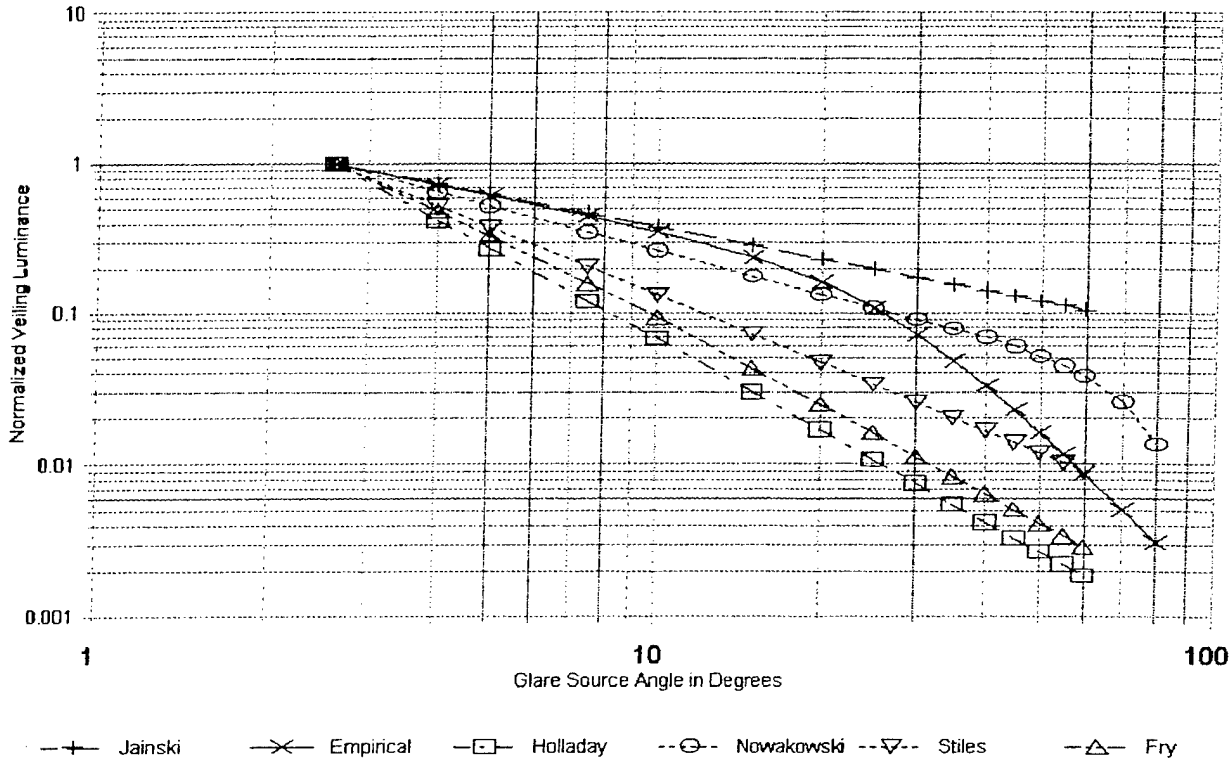


Figure 3.25. Comparison of Normalized Veiling Luminance as a Function of Glare Source Angle for Different Experimenter's.

the empirical model for Jainski's data, predict similar veiling luminances for angles less than ten degrees. Above 10 degrees, the equation labeled as Empirical has the same data trend as the Nowakowski equation, except that the reduction in veiling luminance occurs at smaller angles. Likewise, the Fry approximation of the Holladay and Stiles characteristics is seen to be in reasonably close agreement with the empirical model. It should be noted that the preceding comparisons were intended to highlight similarities between the veiling luminance angular characteristic predictions of the different experimenters' equations, and not to minimize the differences, which are clearly substantial.

3.6.2.2. General Discussion of Veiling Luminance Test Results

The veiling luminance illuminance and angular dependence data of Holladay[63], Stiles, [64] and of Fry and Alpern[65] predict a much sharper angular cutoff dependence with increasing glare source angles, θ_B, than does the data of Jainski and Nowakowski. The former studies were, however, conducted under quite different conditions, at least in comparison to the Jainski tests. In the first three investigations cited above, the test image background luminance areas, of up to a subtended angle of about 40 degrees, were illuminated; the glare source illuminances, as measured at the eyes, were low; and in each case a threshold of image detection task rather than a threshold of image identification task was employed. Nowakowski's tests also conformed to the first two test conditions, although the test range of glare source illuminances did go higher than those of the other experimenters (i.e., up to 6.1 fc), but, like Jainski, an image identification task was employed.

In a literature review of the effects of surround illumination on visual perception, Ireland identified 75 pertinent documents.[66] Among the documents evaluating the effect of glare source illuminance on veiling

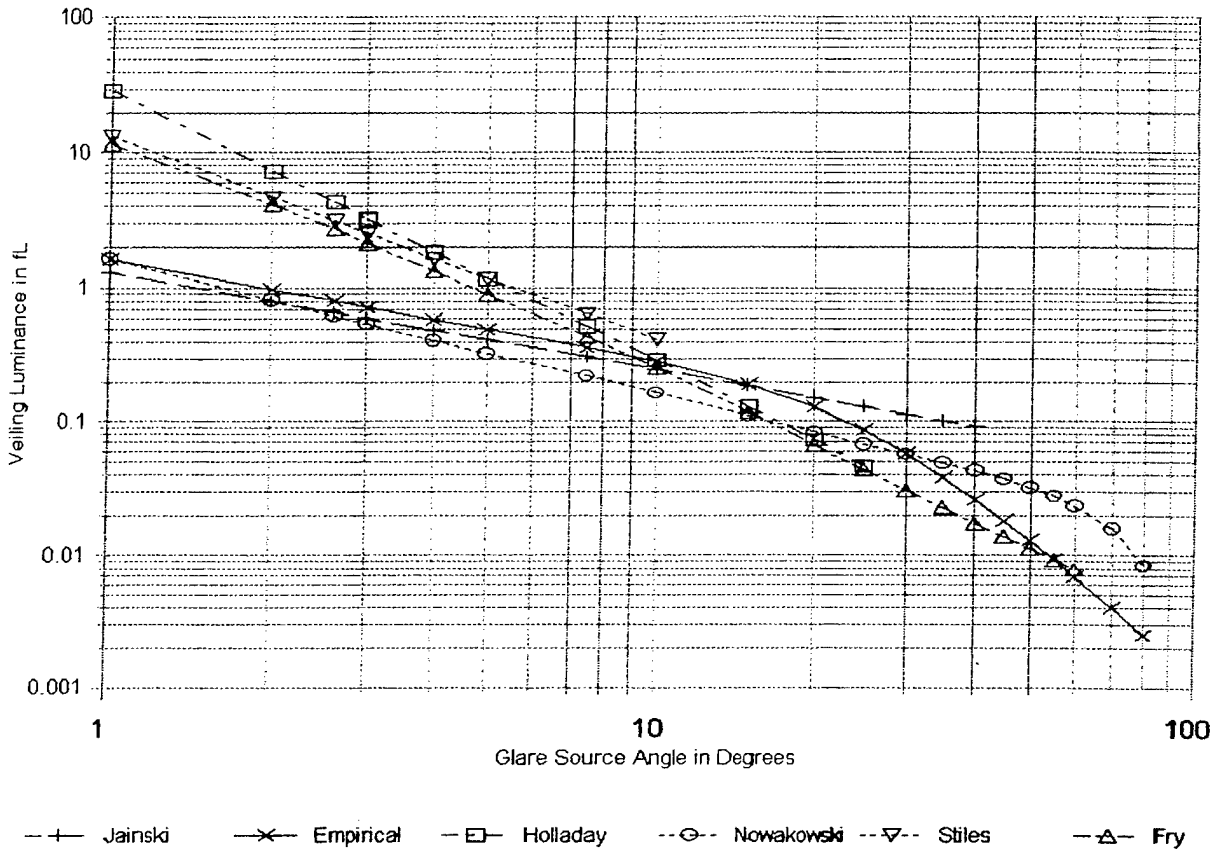


Figure 3.26. Comparison of Veiling Luminance Versus Glare Source Angle for Different Experimenters.

luminance, Ireland concluded that all found that the effect of glare, at a fixed glare source angle, θ_B, was directly proportional to the illuminance of the glare source, E_B, as measured at the eyes.[67,68,69] It should be noted that, in all of the investigations of veiling luminance reviewed, either the luminance or the area of an aperture placed in front of the glare source, or both, were varied to exercise control over the illuminance they produce at the eyes, not the glare source to observer separations. The exponent of 0.872, for the illuminance dependence of veiling luminance obtained by analyzing Jainski's data, is considered a refinement caused by the larger glare source illuminance range of the Jainski data, which is nominally four and a half decades rather than the approximately two-decade range of the earlier investigative results. In this context, and for the reasons previously described, the Jainski result is regarded to be in good agreement with the unity power of the earlier test results.

The 1937 article by Crawford references an earlier study by Crawford and Stiles,* which found that veiling luminance can be expressed by the equation,

$$L_V(cd/ft^2) = \frac{11.5\, E_B(fc)}{\theta^{2.1}}. \qquad (3.75)$$

Crawford compares this result with the previously presented results of Holladay and Stiles, and then goes on to say that a multiplier of ten and an exponent of two "are sufficiently near the truth for practical purposes."

* Crawford, B. H. and W. S. Stiles, J. Sci. Instrum., Vol. 12, 1935, p.177.

Crawford concluded this discussion by saying that these parameter values "are also supported by further work by Stiles and Crawford (1937)."

Two studies were cited by Ireland as raising questions, regarding the validity of using illuminance, measured at the eye, as a fundamental parameter in the glare source relationship. The first of these studies, and earliest study reviewed for the present report, on the visual effects of glare, was conducted by Sweet. This study, concluded that distance from a fixed glare source (i.e., zero to 100 feet from a 400 cd source) had no effect on test symbol perception.[70] Ireland in noting this conclusion went on to say that Miller and Mck Gray" had pointed out that the glare source in Sweet's study illuminated both the test objects and their backgrounds. Ireland concluded from this that the effect of glare alone was not studied, and the result obtained is therefore not relevant.

In the second study cited by Ireland, Nowakowski reported that the expected inverse square law distance relationship between glare and illuminance, as measured at the eyes, holds for exposures to a fixed magnitude candela source (i.e., a lamp specified in terms of luminous intensity), only if the glare source and test image being identified are both at the eye accommodation distance.[71] Ireland then went on to point out that Nowakowski had found that an inverse distance relationship, rather than the inverse square law distance relationship, holds when accommodation is maintained at a fixed near-field focal distance as the glare source is moved away.

The question of the influence that a glare source, not located in the plane of focus of the test symbol has on the veiling luminance induced, is important from a practical real-world aircraft environment standpoint. Glare sources such as the sun, the moon, flares, and so forth are at virtual infinity, while head-down displays require near-field focus. Eyes accommodated for focus at progressively nearer distances will certainly form progressively more blurred myopic images of distant glare sources. The defocused image of glare sources subtending small angles would result in a dispersion of the light incident on the retina and should therefore result in a reduction of the illuminance (i.e., luminous flux density) at the surface of the retina. This would not, however, change the total luminous flux entering the eyes from the glare source and would therefore be unlikely to alter the veiling luminance, induced by the scattering of light within the optical media of the eyes. In summary, blurring, of the glare source image on the retina of the eyes, would be expected to make it possible to directly illuminate part of the foveal area of the retina of the eyes, with of the defocused glare source image, only for small subtended angles between the glare source and the line of sight, but would not influence the induced veiling luminance.

Because of the potential importance of the preceding glare source distance finding, an examination Nowakowski's article was conducted to assess the conditions under which inverse distance illuminance relationship was found. This examination revealed two evident differences between this test by Nowakowski and the other tests reported. The first difference was that the inverse distance relationship reported by Nowakowski was obtained for a test letter viewing distance of 13 inches, much less than the distance used by the other experimenters and also much less than the typical 28 inches or greater viewing distance to cockpit instruments. This difference therefore provides a possible point of departure for explaining why only Nowakowski reported finding this glare source distance relationship. Because the inverse distance relationship would not be applicable in most instances in a cockpit, subsequent considerations of the Nowakowski test results in his report are restricted to results obtained for a test letter viewing distance of 26 inches.

The second evident difference is that Nowakowski conducted his tests with one of the test subject's eyes covered. Although Fry and Alpern's results were considered suspect because the test involved the use of both

---

* Stiles, W. S. and B. H. Crawford, Proc. Roy. Soc., B, Vol. 122, 1937, p. 255.

" Miller, P. S. and S. Mck Gray, "Glare - its Manifestations and the Status of Knowledge Thereof," Proceedings, Commission Internationale de l' Eclairage, 1928, pp. 239-291.

eyes to perform a brightness matching comparison, while only one eye was exposed to the glare source, covering one eye throughout the experiments does not create same likelihood for potential visual conflicts. For example, since only one eye was exposed to both the test image and glare source, the fact that the glare source will not illuminate precisely the same portions of the retina in both eyes, when the eyes are focused on an object at a distance of only 13 inches, can be discounted as the origin of the inverse distance relationship.

Nowakowski performed the evaluation of the effect of the distance of the glare source from the test subject, described above, using lamps with luminous intensities of 35, 90, 150 and 275 candela, although tabular and graphical results were presented only for the 35 and 90 candela luminous intensity lamps. In each case, the lamp was moved at integer multiples of 13 inches, between 13 and 169 inches, and the source angle was maintained at an angle of 40 degrees horizontal and zero degrees vertical from the test subjects line of sight. For this experiment, the test letters were viewed from a distance of 13 inches as the glare source was moved.

An examination of the glare metric versus inverse distance relationship data, from Table III of the Nowakowski article, entitled Glare and Distance, when graphed using full logarithmic rather than the linear axis scaling, used in Figure 4 of the Nowakowski article, revealed that the glare source distance dependence of the glare metric was neither inversely proportional to distance nor inversely proportional to the square of distance. Instead the data plotted as nominally straight line slopes, which were intermediate between the inverse distance, $1/d$, dependence, with a slope of -1, and the inverse square of distance, $1/d^2$, dependence, with a slope of -2, having slopes of -1.31, a $1/d^{1.31}$ dependence, for the 35 candlepower light source, and -1.42, a $1/d^{1.42}$ dependence, for the 90 candlepower light source. Thus while these glare source distance dependence relationships do not support Nowakowski's stated finding of an inverse distance dependence, they do confirm that the inverse square law distance relationship does not hold for this Nowakowski test condition.

Because Nowakowski had expected the visual effects of the glare to decrease in inverse proportion to the square of the distance of the glare source, rather in inverse proportion to its distance, the second experiment, mentioned above, was performed, with the test image and glare sources at equal distances of 13, 32.6 and 65 inches from the test subject, using 175 and 200 candlepower light sources. For this more limited test, Nowakowski reported the inverse square relationship did hold, and based on this finding, attributed the previously described inverse distance relationship result to the glare source being out-of-focus and producing a blurred image of the glare source on the eye's retina, due to the accommodation of the eye to the 13 inch test image viewing distance. Full logarithmic graphing of the results of this test, from Table IV of Nowakowski's article, resulted in a slope of -1.83 for the 175 candlepower source, with the data points for the three different image accommodation and glare source distances falling on the straight line. For the 200 candlepower source, a straight line could not be drawn through the data points at the three distances. A straight line of slope -1.93 drawn between the 13 and 65 inch data points caused the data point at 32.6 inches to be 28% below the line, however, a straight line with a slope of -2 could have been drawn and not exceed a maximum difference of 21% between any data point and the line. The results of this test are, considered to be in good agreement with a slope of -2 for an inverse square law relationship, as claimed by Nowakowski.

At an angle of 40 degrees, between the center of the glare source and the test subject's line of sight, it is considered unlikely that a blurred retinal image of a small glare source, 40 degrees from the fovea, could account for the failure of the square law glare-distance relationship, noted by Nowakowski at the 13 inch test letter viewing distance. The most convincing evidence that a glare source, which is not in focus, does not materially change the veiling luminance induced comes from Jainski's test results. In particular, Jainski's HUD data (i.e., with the test object focused at infinity and with the glare source at about 28 inches from the test subjects eyes) had image difference luminance requirements only slightly greater than for the HDD (i.e., where both the glare source and the test symbol were in focus at about 28 inches). Although this test condition is the reverse of Nowakowski's, with the image of the glare source on the eyes' retina being blurred because it is at a small distance, when eye accommodation is at a large distance, to permit perceiving the HUD test images, the image of the glare source on the retina is nonetheless blurred in both instances. Furthermore, since the comparison of the Jainski characteristics occurred for a glare source angle of fifteen rather than forty degrees,

if blurring, of the glare source image on the retina, was to affect the veiling luminance induced, the effect should be more pronounced under the Jainski test conditions.

Blurring of the glare source image on the retina of the eyes was not, however, the only uncontrolled independent variables that existed in the glare source distance tests conducted by Nowakowski, which could influence his test results. For example, neither the size nor the angle subtended by the glare source was stated by Nowakowski, and the description of the experimental procedures infers the angle subtended by the glare source was not held constant as its distance from the test subject was changed. The inverse square law distance dependence finding of Nowakowski, for test images and glare sources that are both at the same distance from the test subject, shows that the glare source was not so large as to invalidate the inverse square law distance relationship that holds for light sources that can be approximated as point sources of light, but, which no longer holds for light sources subtending sufficiently large subtended angles. Independent of whether this relationship is satisfied, and, as described later in this chapter, increasing the angle subtended by a fixed candlepower light source does influence the veiling luminance induced. Another potential origin, for at least part of the effect noted by Nowakowski, is that a progressive automatic contraction of the pupil area of the eyes occurs, when focusing on images at distances progressively smaller than 30 inches from the eyes, for a fixed illuminance incident on the eyes. Holladay's pupil area experiments, which are briefly discussed in Section 3.6.3.2, demonstrate the latter effect, and would predict progressively reduced veiling luminances, due to a reduction in the scattering of the glare source light, at Nowakowski's two smallest test image viewing distances.

While the two independent variables described in the preceding paragraph are considered to be the likely cause of the glare source distance effect revealed by the Nowakowski experiment, when using test characters at a 13 inch viewing distance, the information reviewed and evaluated for this report are considered inadequate to definitively explain or mathematically model this result. As previously stated, the veiling luminance model is based on experimental data collected for test image viewing distances, of nominally 28 inches or larger, applicable to the vast majority of cockpit display viewing conditions. The Nowakowski result, coupled with the automatic contractions of the eyes' pupil areas, documented by Holladay, raises a question of whether small viewing distances should not also be considered as a constraint, not only on the application of the veiling luminance model, but also on the information viewing distances, permitted in aircraft cockpits, with or without the presence of glare.

In concluding the general discussion of the veiling luminance test results contained in this subsection, it is again emphasized that while the veiling luminance dependence on the glare source angular positions, and the equations of the different experimenters that represent them, appear quite different, these differences are not as large as first impressions would suggest. To make further comparisons between the results of these experimenters, the differences that exist in their experimental design, geometric and lighting conditions must be considered. Some of these differences include the following: the size of the test image backgrounds; the focus of the glare source on the retina; the size and types of test images (e.g., a variable luminance detection spot,[72] printed characters with L_D variable,[73] a printed symbol with a veiling luminance overlay,[74] variable luminance symbols[75, 76]); the glare source angular ranges investigated; the background luminance ranges studied; and the range of the glare source illuminance levels tested. Comparisons under these differing conditions are made more difficult when experimental parameters are inadequately specified, and, unfortunately, except for the Jainski tests, this was a major limitation of all of the investigations reviewed. Nonetheless, some comparisons are possible and this is the primary emphasis of the two subsections that follow.

3.6.2.3. Comparisons with Holladay Veiling Luminance Test Results

The test technique used by Luckiesch and Holladay,[77] to measure veiling luminance, exposed the test subject to an actual veiling luminance. This was done by reflecting light from a 45-degree angled glass plate through which the test symbology is viewed. The test symbol was described as annular rings of gray paper, having a fixed inside diameter equal to 2 cm, and different annulus widths subtending angles, ω_s, between 0.75

and 12 minutes of visual arc when viewed at a distance of 344 cm. These test symbols were placed on a white illuminated background having a luminance, L_D, as measured, or viewed, through the angled glass. The test involved increasing the veiling luminance, L_V, and then measuring the image difference luminance, ΔL, and total apparent background luminance, $L_D + L_V$, which was varied from 0.1 to 400 mL (i.e., 0.0929 to 371.6 fL), when the additional veiling luminance caused the test symbol to become imperceptible. The relationship obtained using this test procedure was designated the "visibility-factor," V, by Luckiesch and Holladay, and was expressed as follows (i.e., when using the terminology of the present report):

$$V = \frac{L_D + L_V}{\Delta L} = 45(\omega_s - 0.5)^{0.4}. \qquad (3.76)$$

This equation was described as being valid for the range of annulus widths cited above and for total apparent background luminances between 1 and 400 mL. Below about 5 mL the visibility factor does not satisfy the equation, and decreases, at a progressively higher rate, down to the 0.1 mL, the lowest total apparent background luminance level tested.

The visibility factor, as defined above, may be recognized as the inverse of the universally accepted definition of contrast and, as such, should actually increase very slowly as the total apparent background luminance level increases above 5 mL, rather than remaining fixed as the right-hand side of Equation 3.76 would predict, if the equation were to be entirely consistent with the image detection results of Blackwell (i.e., with $L_V = 0$). This expectation is based on the 0.926 exponent on the $L_D + L_V$ term, in the image difference luminance requirements equation, Equation 3.23, for background luminance levels in the photopic vision range, where the equation is also applicable to the Blackwell image difference luminance versus background luminance characteristics. In practice, the latter dependence would have been unlikely to be noted for total background luminance levels of up to only 400 mL. In fact it has been common practice for more than fifty years in aircraft cockpit applications to ignore this small difference between the perceived and measured contrasts and simply assume that the perceived contrast is constant under daylight viewing conditions.

To characterize the veiling luminance induced by a glare source, the preceding experiment was repeated with a glare source introduced and the angled glass combiner and uniform veiling luminance source removed. The results of the revised test was that the preceding equation for the visibility factor continued to be valid, for a test range of background luminance values, L_D, from 0.1 to 100 mL, when the following relationship was substituted for the veiling luminance:

$$L_V(mL) = \frac{4\,E_B(lx)}{\theta_B^2(deg)}. \qquad (3.77)$$

This equation differs from the one presented above from Holladay's 1927 article, in that the constant multiplier is 4 rather than 2.9.

The stated range of test angles for the above equation was from 5 to 30 degrees in 5 degree increments, using 25, 100, 225, 400, 625 and 900 Watt lamps at the respective angles, as glare sources. The veiling luminances, when extracted from the graph in Figure 7 of the article, were found to range from about 0.5 mL (0.46 fL), at 30 degrees, to 30 mL (27.9 fL), at 3.75 degrees, for the single glare source illuminance characteristic shown in the figure. The characteristic was reported to be only one of many that space did not permit publishing, and was reported to be applicable to 100 lx of glare source illuminance, as measured at the eyes. The glare source distance was not reported, but as illustrated would be roughly 260 cm. With the target at 344 cm and this glare source distance the effects of accommodation and convergence of the eyes, which are discussed later, should not produce any complications with the validity of the results.

Although Holladay's 1926 article provided additional experimental detail, and reported many ancillary tests not described in the earlier article, the basic test procedure described above for measuring veiling luminance was essentially the same. The reported results for veiling luminance were also the same, except that the constant multiplier in the veiling luminance equation was revised from 4 to 4.3.

Holladay's 1927 article introduced a new approach for determining veiling luminance, and also introduced intentionally blurred test imagery, using an image projector to eliminate any visual effects that may have been caused by test image edges visible in the earlier tests. The angled glass formerly used to measure veiling luminance directly was eliminated in favor of extracting this information from zero glare characteristics, in the same fashion described previously for the Jainski experiments. As already indicated, the only difference in the results was a revision of the veiling luminance equation constant multiplier from 4.3 to 2.9. The new result is presented in the article with no mention of the change and, therefore, no explanation for why it occurred. Subsequent comparisons to Holladay's veiling luminance equation by other authors refer only to the 1927 test result.

In seeking to resolve the differences between the Holladay and Stiles veiling luminance angular response test results, the experimental data points reported in Table 2 of Holladay's 1927 article were plotted on full logarithmic graph paper. The data points in Table 2 of Holladay's article have been reproduced in Table 3.9, together with the results of an analysis performed by the author on the veiling luminance test data contained in that table. The plot revealed that despite the large data dispersion present at each angle tested, Holladay's equation to represent the data passed below the lowest point in range of the test data, at 20 degrees, by 17.6%. Based on this result, an attempt was made to fit the data with a straight line having a slope closer to that of the Stiles equation (i.e., 1.5 rather than 2). This data fit was successful for the data at 2.5, 5, 10 and 20 degrees, but a sharp drop in the test data, between 20 and 25 degrees, could not be reconciled with the smaller slope. The best fit of Holladay's data, for any single straight line characteristic, was as follows:

$$L_V = M(\theta) E_B = \frac{2.675}{\theta^{1.917}} E_B \,. \tag{3.78}$$

The $M(\theta)$ characteristic passes through the top point of the 2.5 and 25 degree data ranges and just within the top of the range for the data at 10 degrees. It also passes near the mean of the 5 degree data range and only 2.6% below the bottom point in the 20 degree data range (i.e., as compared with the 17.6% of Holladay's equation).

While examining the values of the angular dependence multiplier, $M(\theta)$, in Table 3.9, it was observed that for a particular background luminance value, L_D, these values trend toward a decrease in magnitude as the illuminance at the eye, E_B, is increased. Based on this observation, it was decided to test the use of an illuminance dependence like that found to hold for the Jainski veiling luminance data, with illuminance raised to the power of 0.872 rather than the value of unity employed by Holladay, to calculate the values of $M(\theta)$ from experimentally determined adaptive luminances, $L_D + L_V$. The results of this analysis are shown on the right side of Table 3.9. With the exception of the 5 degree data corresponding to a background luminance of 1 mL, the highest background luminance tested at 5 degrees, and the 2.5 degree data, the standard deviation of the data sets were reduced, in some cases substantially, for the balance of the data in the table. The maximum to minimum ranges of the data points were also reduced and the illuminance dependence trend was either eliminated or reduced. Furthermore, if the one data point at 2.5 degrees that corresponds to the 2 mL background luminance is excluded from consideration, the dispersion of the data at this angle also benefited substantially from the use of illuminance raised to the power of 0.872, rather than unity (i.e., a reduction in the standard deviation of the remaining three points from 0.0397 to 0.0102).

The new values of $M(\theta)$ obtained from the preceding analysis are shown on a full logarithmic plot in Figure 3.27. A best fit of the data using a straight line produced the following empirical equation:

$$L_V = M(\theta) E_B^{0.872} = \frac{2.907}{\theta^{1.912}} E_B^{0.872} \,. \tag{3.79}$$

This $M(\theta)$ result is essentially the same as the one described above for the best fit of Holladay's unmodified data, except that the characteristic passes 9.9% below the bottom point in the 20 degree data range. The sharp drop in the test data between 20 and 25 degrees was accentuated with this adjustment of Holladay's data.

Table 3.9. Veiling Luminance Data Adapted from Table 2 of the 1927 Holladay Article.

Experimental Test Data of Holladay using Terminology of this Report						Analysis of Holladay Test Data		
L_D in mL	E_B at the eye in lx	θ_B in degrees	ΔL in mL	Adaptive Luminance $= L_D + L_V$ corresponding to ΔL. $L_V = M E_B$ Holladay or $L_V = M E_B^{0.872}$ Empirical	$M(\theta)$M in mL/lx	Mean = $\bar{M}$ and Standard Deviation = σ	$M(\theta)$ in mL/lx	Mean = $\bar{M}$ and Standard Deviation = σ
1	1	5	.0225	1.122	.122		.122	
1	2	5	.0254	1.27	.135		.1475	
1	4	5	.0312	1.622	.155		.1857	
1	5	5	.0329	1.738	.148		.1814	
				Mean = $\bar{M}$	.14000		.15915	
				Standard Deviation = σ	.01458		.03009	
0.1	1	5	.0050	.209	.109		.109	
0.1	2	5	.0068	.299	.100		.1087	
0.1	4	5	.0090	.408	.077		.0920	
0.1	5	5	.0108	.525	.085		.1044	
				Mean = $\bar{M}$	.09275		.10353	
				Standard Deviation = σ	.01443		.00797	
0.01	.25	5	.00141	.043	.130		.1105	
0.01	.5	5	.00208	.071	.122		.1116	
0.01	1	5	.00338	.130	.12		.120	
0.01	2	5	.00452	.178	.084		.0918	
0.01	4	5	.00822	.372	.091		.1081	
0.01	5	5	.00879	.425	.083	$\bar{M}$ = 0.10635	.1020	$\bar{M}$ = 0.10991
				Mean = $\bar{M}$	.105		.10733	
				Standard Deviation = σ	.02126	σ = 0.02613	.00958	σ = 0.01538
0.001	.25	5	.00153	.0478	.187		.1568	
0.001	.5	5	.00174	.0562	.110		.1010	
0.001	1	5	.00254	.0912	.090		.0902	
0.001	2	5	.00550	.229	.114		.1246	
0.001	4	5	.00844	.385	.096		.1146	
0.001	6	5	.01160	.550	.092		.1151	
				Mean = $\bar{M}$	.11483		.11705	
				Standard Deviation = σ	.03667		.02291	
0.0002	.5	5	.00178	.059	.118		.1080	
Overall Mean, $\bar{M}$, for θ_B = 5 degrees.					.11276		.11929	
Overall Standard Deviation, σ, for θ_B = 5 degrees.					.02760		.02679	

Table 3.9. (Continued)

Experimental Test Data of Holladay using Terminology of this Report						Analysis of Holladay Test Data		
L_D in mL	E_B at the eye in lx	θ_B in degrees	ΔL in mL	Adaptive Luminance $= L_D + L_V$ corresponding to ΔL. $L_V = ME_B$ Holladay or $L_V = ME_B^{0.872}$ Empirical	$M(\theta)$ in mL/lx	Mean = $\bar{M}$ and Standard Deviation = σ	$M(\theta)$ in mL/lx	Mean = $\bar{M}$ and Standard Deviation = σ
0.01	.25	2.5	.00312	.118	.430	$\bar{M}$ = 0.3970 σ = 0.03966	.3618	$\bar{M}$ = 0.3627 σ = 0.0102
0.01	.5	2.5	.00521	.214	.408		.3734	
0.01	1	2.5	.0080	.363	.353		.353	
0.01	2	2.5	.0183	.933	.462		.5043	
Overall Mean, $\bar{M}$, for θ_B = 2.5 degrees.					.41325		.39813	
Overall Standard Deviation, σ, for θ_B = 2.5 degrees.					.04588		.07127	
0.01	1	10	.00143	.0437	.0337		.0337	
0.01	2	10	.00220	.076	.0330		.0361	
0.01	4	10	.00277	.100	.0225		.0269	
0.01	5	10	.00321	.120	.0220		.0270	
Overall Mean, $\bar{M}$, for θ_B = 10 degrees.					.02780		.03093	
Overall Standard Deviation, σ, for θ_B = 10 degrees.					.00642		.00469	
0.01	.25	20	.00059	.0141	.0164		.0137	
0.01	.5	20	.00070	.0182	.0164		.0150	
0.01	1	20	.00084	.023	.0130		.0130	
0.01	2	20	.00109	.0316	.0108		.0118	
0.01	4	20	.00145	.045	.0088		.0105	
Overall Mean, $\bar{M}$, for θ_B = 20 degrees.					.01308		.01280	
Overall Standard Deviation, σ, for θ_B = 20 degrees.					.00338		.00173	
0.01	2	25	.00082	.0213	.0056		.00617	
0.01	4	25	.00096	.0270	.0042		.00508	
0.01	5	25	.00096	.0275	.0035		.00430	
0.01	6	25	.00118	.0347	.0041		.00518	
Overall Mean, $\bar{M}$, for θ_B = 25 degrees.					.00435		.00518	
Overall Standard Deviation, σ, for θ_B = 25 degrees.					.00089		.00077	

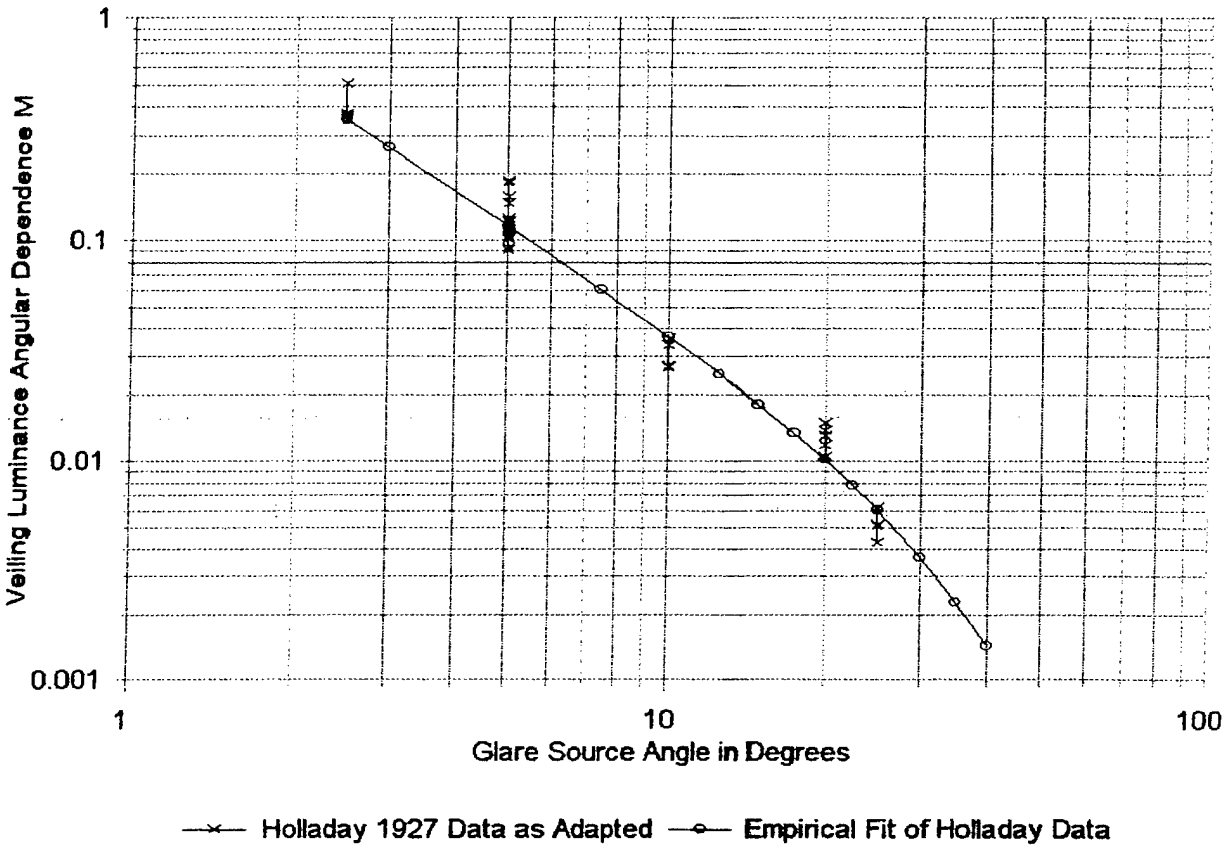


Figure 3.27. Veiling Luminance Angular Dependence Function, $M(\theta)$, Adapted from the 1927 Data of Holladay Using Illuminance Raised to the Power of 0.872.

Since the increased slope for Holladay's angular dependence characteristic occurs in the same range of angles as it does for the Jainski data, an equation like the one used previously to fit that data but adapted to the larger slopes of the Holladay and Stiles angular responses for small angles, was fitted to Holladay's data. The equation resulting from this attempt to curve fit Holladay's data is as follows:

$$L_V = M(\theta) E_B^{0.872} = \frac{1.544\,\theta^{-1.81}}{1 + 2.847 \times 10^{-5}\,\theta^3} E_B^{0.872} . \qquad (3.80)$$

The $M(\theta)$ function in this equation is plotted for comparison purposes in Figure 3.27. Although this equation fits Holladay's adjusted data better than a straight line, the improvement is marginal. In this case, the characteristic, predicted by the empirical equation, passes through the lowest point in the data range at 2.5 degrees, near the top of the 25 degree data range, and slightly below the mean for the 5 degree range, or, if the data corresponding to 1 mL of background luminance are excluded, slightly above the revised mean. At 10 and 20 degrees, the characteristic passes 1.9% above the top point in the range and 3.8% below the bottom point in the range, respectively. In other words, this fit of the data is only slightly better than the best straight line fit of the same data, given above by Equation 3.79. In spite of the preceding shortcoming, the empirical equation, with two slopes, has two advantages. The first advantage is that the angular dependence of this equation in good agreement with Stiles 1929 empirical equation for small angles. The second advantage is that the predicted characteristic passes through the portion of the 2.5 degree data range containing the consistent data points for that angle, rather than through the single inconsistent data point used by the preceding straight line fit equation and the empirical straight line fit equation published in the 1927 Holladay article.

Irrespective of how well the empirical equations fit Holladay's test data, if the individual experimental data points shown in Figure 3.27 are valid, then they do provide a clear visual indication of a change in the slope of the angular response characteristic, in the vicinity of 20 degrees, analogous to the one found for the Jainski data. Unfortunately no independent confirmation for this breakpoint was found in the literature, and, with none of Holladay's data extending beyond 25 degrees, no convincing experimental evidence exists to confirm the existence of the breakpoint.

In spite of the differences between the physical geometries of Holladay's experiment and that of Jainski's, namely, the fact that Holladay's glare source would be out-of-focus whereas Jainski's source would be in focus for the head-down display configuration and out-of-focus for the head-up display configuration, there is no evidence provided in any of the investigations reviewed that the physical differences between the experiments could account for the large observed differences in the measured angular weighting functions. It is, therefore, likely that the difference in the angular weighting functions is related either to the observer's level of light adaptation, which was high in the Jainski test (i.e., 371.6 fc) and low in the other tests (i.e., a maximum of 1 fc in the Holladay and Stiles tests), or to the difference in the visual task performed by the test subjects, image identification in the Jainski tests and image detection in the Holladay tests. The first of these possibilities was indirectly eliminated by the tests conducted by Nowakowski.

3.6.2.4. Comparisons with Nowakowski Veiling Luminance Test Results

The study by Nowakowski differed from that of Jainski, in that it used fixed contrast, 16 minute of arc, black printed letter characters attached to a white background, with a controlled source of incident illuminance, for its image identification tasks, rather than positive contrast test symbols with independently controllable background and image difference luminance levels. These studies also differed in many other ways. Some differences include the following: the attention paid to the experimental design; the selection of test subjects based on visual capabilities and age; the precision of control over the experimental equipment setups; the amount of data collected per experimental data point recorded; and the sophistication of the data collection and analysis techniques. Like most of the other veiling luminance angular dependence tests, reviewed for this investigation, Nowakowski's experiments can best be characterized as screening studies, intended to determine the responses of the general populace to glare, rather than a select group, such as pilots. Consequently, the results of Nowakowski can potentially encompass much greater variability than the results of Jainski. Despite the differences between the Nowakowski and Jainski studies, which relate primarily to the reliability of the test results, enough of the experimental design elements of the two studies were similar to conclude that it is valid to make comparisons. The comparison is also warranted, based on the need to understand why the glare source angular dependence of the Nowakowski empirical equation comes the nearest to matching that of the empirical equation developed in this report for the Jainski data.

Nowakowski's investigation of the dependence of the effects of glare on the angle subtended by the glare source, with respect to the test subject's line of sight, was conducted for a range of glare source illuminance levels, as measured at the eyes, of between 0.43 and 6.1 fc. This compares with a range of 0.023 to 0.56 fc, for Holladay, and 0 to 1 fc, for Stiles (i.e., the Stiles data was reported on a linear scale with the lowest data point other than 0 being 0.02 fc). Even though the Nowakowski tests included somewhat higher glare source illuminances, as measured at the eyes, than the other two experimenters, there is overlap between the test ranges. Nowakowski's metric for glare, the use of an image identification task rather than an image detection task, and the conduct of angular dependence tests at 13 and 26 inches rather than 135 inches for Holladay and 48 inches for Stiles, all differed from the procedures used in the Holladay and Stiles tests. In all other respects, however, the experiments were very similar. In spite of the many similarities, the veiling luminance angular response figures show that the results of the tests were very different.

Since the Nowakowski angular response characteristics much more nearly match those of Jainski's data, although the vast majority of the test conditions match those of Holladay and Stiles, it was concluded that a

more detailed analysis of Nowakowski's test results was warranted. Nowakowski's published data is contained in Table 3.10. The third and sixth columns in this table show the incident illuminance levels that were needed to make the test images legible, at a viewing distance of 26 inches, and in the presence of a 35 candela luminous intensity glare source, which was positioned at the different angles shown in the table, with respect to the test subject's line of sight. The illuminance data shown in the third column of the table corresponds to a vertical angle of zero degrees and to the horizontal angles shown in the table. The illuminance data in sixth column corresponds to a horizontal angle of 40 degrees and to the vertical angles shown in the table. Column One in Table 3.10 shows the compound angles subtended by the glare source with respect to the test subjects line of sight to the test symbols. These compound angles corresponds to the combination of the listed horizontal angles, θ_H, and vertical angles, θ_V, and are calculated using the equation,

$$\theta_B = \sqrt{\theta_H^2 + \theta_V^2}. \tag{3.81}$$

Nowakowski's test data in Table 3.10 was collected with the glare source maintained at the same radial distance from the test subject's eyes as the test image, thereby placing it in the same focal plane as the test image. This was also the case for the glare source data of Stiles and the head-down display data collected by Jainski. The calculated glare metric of Nowakowski, G, is shown in the remaining two columns of Table 3.10. The glare metric in the fourth column is for horizontal angle displacements of the glare source, and the one in seventh column is for vertical angle displacements, from an initial, fixed 40 degree horizontal angular displacement, orientation of the glare source.

Figure 3.28 shows veiling luminance plotted, as a function of the total glare source angular displacement, for both the Jainski and Nowakowski test results. Figure 3.24, introduced earlier to show Jainski's results, was modified to include the Nowakowski test results by applying a constant multiplier of 4.2885 to Nowakowski's glare metric values from Table 3.10. The multiplier was chosen to match the Jainski head-down display test configuration results to those of Nowakowski, numerically, at a horizontal glare source angle of 15 degrees, since this is the Jainski test configuration that Nowakowski's test setup and conditions most nearly match. At 15 degrees, Jainski's vertical and horizontal characteristics for the head-down display test configuration are coincident and the match is therefore made with the characteristic labeled J - HDD Vertical in the figure. The Jainski horizontal displacement characteristic is not shown because, on the scale of Figure 3.28, it is essentially coincident with the Nowakowski data points and, hence, to show it would interfere with their presentation. Jainski's horizontal characteristic is shown in Figure 3.23. Also, for purposes of comparison the empirical equation derived for Jainski's data is shown in Figure 3.28.

The plot of the scaled, and units converted, Nowakowski glare metric data points, from Table 3.9, versus the displacement angle of the glare source, in the full logarithmic format of Figure 3.28, reveals a characteristic that is decreasing at a rate similar to the veiling luminance data of Jainski, for small horizontal angular displacements of the glare source. As shown in Figure 3.23, Jainski's data for the head-down display test configuration, at horizontal angles greater than 30 degrees, shows only a possible onset of an increased rate of decrease from an otherwise essentially constant full logarithmic slope characteristic. Nowakowski's horizontal angle displacement data definitely starts to decrease at an increased rate, for large angles, but, due to the variability present in the data, the onset of this change could be interpreted to occur as early as somewhat less than 40 degrees or as late as 50 degrees. Jainski's horizontal data stops at about 37 degrees and, therefore, does not provide a clear breakpoint. Jainski's graphical plot of the veiling luminance response, to horizontal displacement angles, showed the small-angle, low-slope, portion of the characteristic extrapolated as a straight line out to 90 degrees, but stated in the text of the report that data was collected only out to 37 degrees. The preceding results of Nowakowski and of Jainski, using the head-down display test configuration, appear to confirm each other for both small and large horizontal displacement angles of the glare source (i.e., at least up to the upper angular limit of Jainski's data). Nowakowski's data, which shows a progressively greater rate of decrease of veiling luminance for angles up to 90 degrees, the largest angle for which data was collected, appears as if it were an extension of Jainski's results, for horizontal glare source displacement angles greater than 37 degrees.

Table 3.10. Dependence of Nowakowski Glare Metric on Glare Source Angle.

θ_B In Degrees	θ_H In Degrees	E_G [+] in fc	Glare Metric $G = \frac{E_G}{E_{NG}} - 1$	θ_V In Degrees	E_G [*] in fc	Glare Metric $G = \frac{E_G}{E_{NG}} - 1$
10	10	2.25	7.036			
15	15	1.86	5.643			
20	20	1.42	4.071			
30	30	1.11	2.964			
40	40	0.88	2.143			
44.72				20	0.71	1.367
50	50	0.76	1.714	30	0.55	0.833
56.57				40	0.42	0.40
60	60	0.66	1.357			
64.03				50	0.37	O.233
70	70	0.53	0.893			
72.11				60	0.33	0.1
80	80	0.44	0.571			
80.63				70	0.30	0
90	90	0.34	0.214			

Notes:

[+] Threshold illuminance incident on test image at image identification with light from a glare source incident on the eyes: 26 inch viewing distance with a 35 cd luminous intensity glare source at $\theta_B = \theta_H$ and $\theta_V = 0°$. With no glare, the illuminance threshold for image identification was $E_{NG} = 0.28$ fc. The data is reproduced from Table 5 of the Nowakowski article.

[*] Threshold Illuminance incident on test image at image identification with light from a glare source incident on the eyes: 26 inch viewing distance with a 35 cd luminous intensity glare source at $\theta_B = \sqrt{\theta_H^2 + \theta_V^2}$ and $\theta_V = 40°$. With no glare, the illuminance threshold for image identification was $E_{NG} =$ 0.3 fc. The data is reproduced from Table 6 of the Nowakowski article.

Other than to introduce his Table 6, which contained the data for the combined horizontal and vertical displacements of the glare source with respect to the visual axis direction, Nowakowski did not either plot or discuss this data. When this data is plotted, as is shown in Figure 3.28, it can be seen to produce a completely separate response characteristic. At the 40 degree horizontal and 0 degree vertical data point, this characteristic immediately starts decreasing, at a rate somewhat more rapid than the highest rate of Jainski's data, for vertical displacements of the glare source. Nonetheless, the Jainski and Nowakowski characteristics for a vertical displacement of the glare source, like their horizontal displacement counterparts, are in relatively

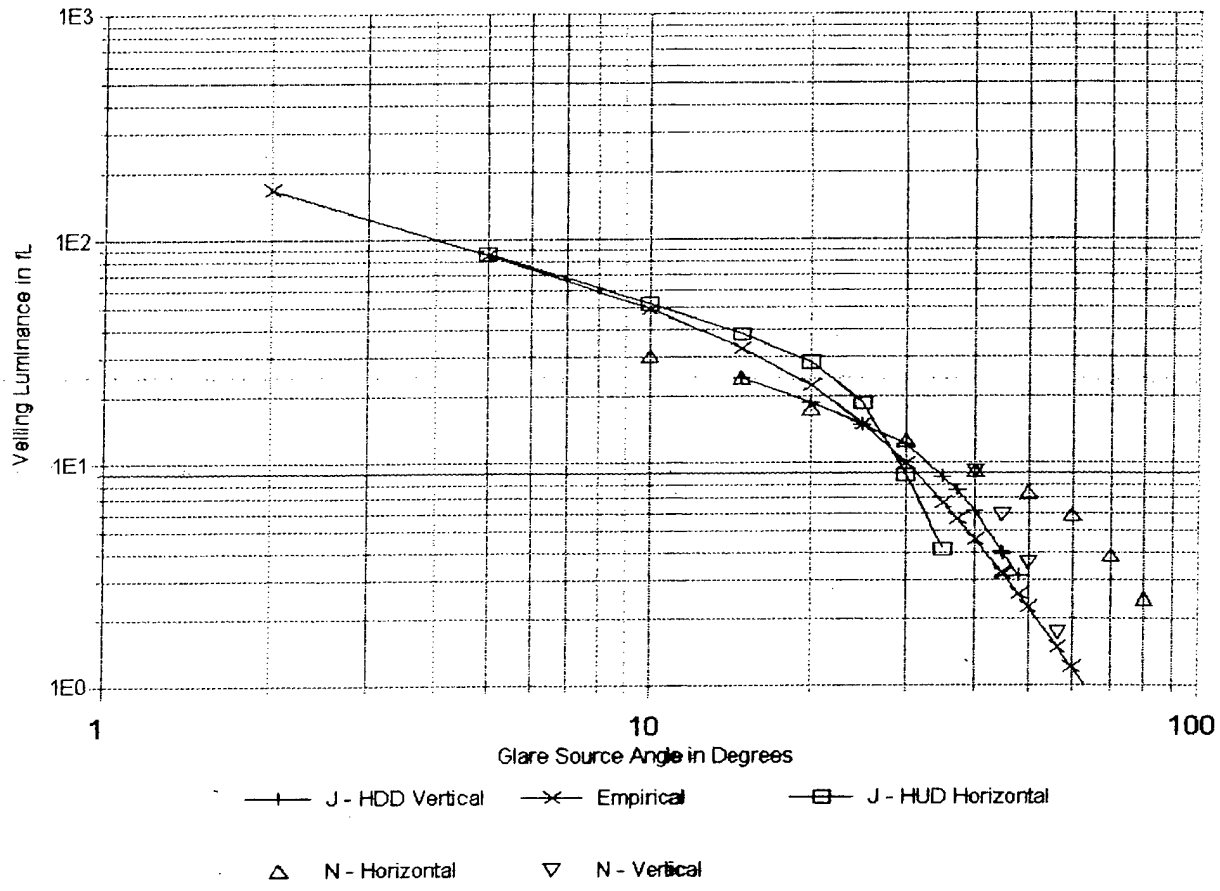


Figure 3.28. Comparison of Jainski (J) and Nowakowski (N) Veiling Luminance Angular Dependences.

good agreement. If the Nowakowski and Jainski sets of data are both valid, then their test results would appear to suggest that, at large angles, the angular response of the eyes stop being symmetric along all of the spherical angle radial directions, with the breakpoint occurring at smaller angles, for compound angles having a vertical component.

The problem with the preceding thesis, regarding the lack of angular symmetry in the human's veiling luminance glare source response, as previously discussed in relation to Jainski's angular response data, is that Jainski had conflicting results for horizontal angle displacements of the glare source. Jainski's angular response characteristic for horizontal displacements of the glare source, determined using the head-up display test configuration, is illustrated in Figure 3.28. This conflict occurs between Jainski's head-up and head-down display configurations, where the horizontal angle breakpoint for the HUD may be seen to occur at an even lower angle (i.e., between 20 and 25 degrees) than for the HDD vertical angle breakpoint (i.e., nominally between 30 and 35 degrees), and where the HDD horizontal angle glare source displacement data (see Figure 3.23) indicates no unequivocal evidence of a breakpoint out to 37 degrees, the last angle tested.

The relatively good agreement between the Jainski and Nowakowski results for both horizontal and vertical displacements of a glare source does point to a real difference in the results for these two displacement directions for large glare source subtended angles, despite the HUD evidence to the contrary. The investigations reviewed, while conducting the analyses of the present report, do not provide sufficient information to permit achieving a definitive resolution of these conflicting experimental results. The most likely

explanation for this conflict is expected to be related to the lack of control, exercised during the tests, over measures that can be initiated by test subjects to influence their exposure to glare. One measure a test subject can take to limit exposure to a glare source, which is at least partially effective, involves squinting of the eyes. This limits exposure for vertical angle displacements of the glare source, and can restrict exposures from other directions when used in combination with coordinated movements of the eyes and tilting of the head.

Among the investigations reviewed, only the one by Fry and Alpern mentioned using an overt technique to hold the test subjects head in a fixed location and orientation during the collection of data. The other tests relied on the primary test image visual detection or identification task to establish the test subject's line of sight, but this would not prevent squinting of the eyes, in conjunction with coordinated movements of the head and eyes to reduce glare exposure. The need for test subjects to be able to read the test imagery, when it is projected at virtual infinity for the Jainski HUD test configuration, would impose a more stringent constraint on the location of the test subject's head, but, again, should not prevent squinting of the eyes to reduce glare exposure. It should be noted that none of the veiling luminance tests used high enough glare source illuminance levels to force the test subjects to squint to limit, or avoid, visual discomfort. It should also be pointed out that it is unlikely that the experimenters would not have observed, and commented on, head movements during their tests.

It was previously concluded, in relation to the Jainski veiling luminance angular dependence response data, that experimental error or large subject variability was the most likely cause of the conflicting results. Furthermore, since no known physiological basis exists for expecting asymmetric angular response characteristics, due to light scattering by the optical media within the eyes, an average of the results was selected for use with the discrete glare source mathematical model of veiling luminance. Nowakowski's test results provide no compelling reason to change this approach for treating the veiling luminance angular response data, at least in the context of the automatic legibility control mathematical model. Provisions to accommodate the likelihood of squinting, in combination with head and eye movements, and any other measures a pilot might employ to reduce the effects of glare induced veiling luminance, probably do not need to be considered, when designing and deploying the light sensors needed to implement automatic legibility control in aircraft cockpits. The reason for this is that the failure to compensate for elective techniques used by pilots to reduce veiling luminance, in the design of the automatic legibility control, would simply cause the displays to be controlled at more legible levels than, would otherwise be the case, if the pilot were to take no measures to compensate for glare exposures.

3.6.3. Eye Pupil Diameter and Area Variable Dependences

In this section the factors that influence the pupil area of the eyes are introduced and described. The importance of the size of the pupil areas stems from the fact that the pupils act as optical apertures that directly control the total luminous flux that enters the optical media of the eyes at any instant in time and, consequently, the total quantity of light, per unit time, available to induce the perception of veiling luminance. An empirical equation, adequate to describe the veiling luminance induced by a discrete glare source, for the purposes automatic legibility control, has already been developed using the test results of Jainski. This equation already includes the effect of the changes in the pupil areas of Jainski's test subjects, as an implicit integral element of the empirical veiling luminance equation. It could therefore be argued that a determination of the explicit effect of pupil area on veiling luminance is an ancillary consideration, given the primary purpose of this report. However, since the changes in pupil areas of the eyes are limited by the finite upper and lower limits on their sizes, the constraints this variable imposes on the applicability of the empirical equation need to be explored.

Approximately one fourth of Holladay's 1926 article was devoted to descriptions of the results of investigations conducted to determine the dependence of the eye's pupil aperture diameter on a variety of different variables. The variable dependences that were investigated included the following: different background luminance levels, with the test subject's entire field of view uniformly illuminated at the same field luminance level; different illuminance levels of a glare source, as a function of its angular position; the two

preceding variables following momentary increases in the luminance and illuminance magnitudes, respectively; accommodation of the eyes to different distances; convergence of the eyes at different fixation point distances; and exposure of the eyes to different luminance levels of a uniform luminance circular source centered on the line of sight and subtending different angles between 2.5 and 10.7 degrees. None of the other articles reviewed added to this list of potential pupil area variable dependences.

3.6.3.1. Pupil Areas Predicted by Riggs' Rule of Thumb

As reported by Riggs,[78] in a section of Chapter 11 of the book "Vision and Visual Perception," entitled "Retinal Illuminance," the diameter of natural pupils range from nominally 8 to 2 mm, resulting in an area change of about sixteen to one, as the retinal illuminance increases from low to high values, or vice versa. Riggs went on to state the following rule of thumb, for predicting the area of the eye's pupil, in response to exposure to a field of light: "At high field intensities, the area of the pupil is reduced about 35% for each tenfold increase in field intensity," and then cited seven references implying they conform to this result. In the sentence following this quotation, Riggs made it clear that the reference to field intensity should be read as field luminance.

The previous quotation of Riggs' rule of thumb, for predicting changes in the pupil areas of the eyes, can also be stated in an alternative equivalent form that is better suited to being represented using an equation. In effect, Riggs states that at high, but unspecified, field luminances, and for a pupil area somewhere between 50.27 mm^2, for an 8 mm diameter pupil, and π mm^2, for a 2 mm diameter pupil, each factor of ten increase in field luminance causes a successive 0.65 multiple reduction in the pupil area. Since this algorithm represents a geometric progression, the pupil area, A_P, and field luminance, L_F, variables must satisfy a power-function relationship. Because of this relationship, the relationship between pupil area and field luminance, for Riggs' rule of thumb, plots as a straight line on a graph having logarithmically scaled axes, where the constant slope of the line is equal to the exponent of the power-function relationship. Based on the power-function relationship, Riggs' Rule of thumb can be expressed using either of the following two equivalent equations, one for the area of the pupil aperture and the other for its diameter:

$$A_P = A_{P1}\left(\frac{L_F}{L_{F1}}\right)^{-0.1871}$$
$$d_P = d_{P1}\left(\frac{L_F}{L_{F1}}\right)^{\frac{-0.1871}{2}}. \qquad (3.82)$$

The value of the exponent, - 0.1871, was chosen to cause the ratio of the two areas, A_P / A_{P1}, to equal 0.65, when the ratio of the field luminances, L_F / L_{F1}, is equal to a one decade change, that is, to a value of ten. In the second equation, for the pupil diameter, d_P, the exponent is divided by two, since it is the square of this variable that is proportional to pupil area. The preceding equations, relating pupil area and pupil diameter to the field luminance, allows Riggs' rule of thumb relationship to be used as a common comparison baseline, with the test results of other experimenters. Substituting a set of corresponding values of the pupil area, or pupil diameter, and field luminance for a single data point on an experimenter's pupil area, or pupil diameter, versus field luminance test characteristic into Equation 3.82, in place of the constants A_{P1}, or d_{P1}, and L_{F1}, allows a direct comparison to be made, in turn, between the predictions of Riggs' Rule of thumb, as expressed by Equation 3.82, and each of the other experimenters' test characteristics.

3.6.3.2. Holladay's Pupil Area Experimental Findings

Based on Holladay's 1926 findings, the pupil area is dependent on the luminance incident on the eyes from a uniform luminance field, L_F, or on the illuminance incident on the eyes from a glare source and on the angle the glare source subtends with respect to the line of sight. Using the nomenclature and terminology

adopted in this report to describe the variables, the empirical equation Holladay derived to express the variable dependence the pupil diameter of the eyes can be expressed is as follows:

$$d_P = d_{PMax}\, e^{-0.18\left(L_F + \frac{1.85}{(1.122)^{\theta_B}} E_B\right)^{0.4}}, \tag{3.83}$$

where d_{PMax} is the pupil diameter, with the iris aperture fully open and was expressed by Holladay in units of millimeters (mm). The field luminance, L_F, was reported to fill the field of view with a uniform luminance adapting field. In the equation, the glare source illuminance is expressed in units of lux, and the field luminance is expressed in units of millilamberts and covers a range of test values from 0.005 to 221 mL, where the latter value applies to the pupil reaching its minimum diameter. The angle subtended by the glare source, θ_B, is expressed in degrees and corresponds to tested angles from 5 to 30 degrees.

When describing the procedure used in the derivation of Equation 3.83, Holladay referred to the second term in the exponent of the above equation as the equivalent field luminance. The test procedure involved measuring the pupil diameters at 5 degree increments of the glare source angular position, for each subject, and then determining the equivalent field luminance from the previously measured pupil diameter versus field luminance characteristic, for that subject, with no glare source present. Other than to say that the glare source was placed two meters from the eyes and consisted of a ten inch diameter white diffusing tungsten filament globe, with an interposed disk having a circular opening, of unspecified diameter, very little information was provided concerning the glare source. The glare source illuminance, E_B, in the equation above, is expressed in lux, but its test values were not specified, except for the inference that they would give the same range of equivalent field luminance values as the range of field luminances tested.

Holladay's equation, when adapted to give the area of the pupil, A_P, can be written as follows:

$$A_P = \frac{\Pi}{4} d_P^2 = A_{P\text{-}Max}\, e^{-0.32\left(L_F + \frac{1.85}{(1.122)^{\theta_B}} E_B\right)^{0.4}}. \tag{3.84}$$

This equation accurately predicts the experimental results obtained by Holladay, for the decrease in pupil area, as either the field luminance or glare source illuminance is increased. It, however, is valid only down to areas approaching but not reaching the minimum pupil area of π of mm^2 and a corresponding pupil diameter of about 2 mm. The equation also predicts that increasing the angle subtended by the glare source with respect to the line of sight, from the center of the fovea to the fixation point, will increase the pupil aperture area, when the values of field luminance and glare source illuminance are held fixed. In other words, moving a discrete light source of uniform luminance and fixed illuminance, as measured at the eyes, to progressively larger angles with respect to the line of sight, would be expected to increase the pupil area, admit more of the light into the eyes and, consequently, increase the light scattered into the retina, as compared with the amount of light that would be scattered if the pupil aperture did not increase in area.

Another test Holladay performed that bears on the angular dependence of the pupil area contraction and expansion of the eyes, involved the use of a constant luminance circular light source of variable area placed 117 cm from the subject's eyes and centered on the line of sight and therefore on the fovea. The size of the area was changed by introducing disks, with circular openings of different diameters from 5 to 22 cm, in front of the light source, thereby causing the source to subtend angles, θ_S, in the range of 2.5 to 10.7 degrees at the test subject's eyes. Holladay reported a 32 to 5,700 mL light source luminance range and 1 to 420 lx illuminance range for the test. Empirical equations for the pupil diameter, d_P, derived by Holladay to approximate the test results obtained, are as follows:

$$\begin{aligned} d_P(mm) &= 6.1 + 0.5\log\Omega_S(sr) - \log E_B(lx) \\ d_P(mm) &= 5.6 - 0.5\log\Omega_S(sr) - \log L_B(mL), \end{aligned} \tag{3.85}$$

where the second equation can be derived from the first or vice versa using the following relationship between the glare source illuminance, E_B, and luminance, L_B:

$$E_B(lx) = \frac{10}{\pi} L_B(mL)\,\Omega_S(sr)\,. \tag{3.86}$$

The solid angle in sterradians subtended by the light source is given by the equation,

$$\Omega_S = \frac{A_S}{\rho^2} = \frac{\pi r_S^2}{\rho^2} = \frac{\pi(\rho\tan(\theta_S/2))^2}{\rho^2} = \pi(\tan(\theta_S/2))^2\,. \tag{3.87}$$

An analysis of these equations revealed, as expected, that increasing the area of the light source, without changing its luminance, results in a corresponding reduction in the pupil area. The analysis also showed that when the area of the light source is increased from the smallest area tested to the largest (i.e., an increase in the subtended light source solid angle from 14.3×10^{-4} sr to 278×10^{-4} sr), more than four times the light source illuminance is needed for the larger source to cause the same constriction of the pupil area. If all areas of the retina were to produce the same pupil area response to incident light, then it would be expected that, irrespective of the size of the area, the application of equal incident illuminances to different locations on the retina would produce the same pupil area constrictions. Instead, Holladay's results show that the constriction of the eyes' pupil areas, in response to illuminance directly incident on the fovea is much greater than it is for illuminance of the same magnitude incident on retinal areas outside the fovea. This result is consistent with the predictions of Equation 3.84, for the dependence of pupil area on the angular displacement of a discrete light source, with respect to the test subject's line of sight.

Due to the fact that the pupil diameter investigation leading to Holladay's Equation 3.83 did not include a test with the discrete light source at a subtended angle, θ_B, of zero degrees, the predictions of this equation cannot be directly compared with those for a discrete light source centered on the test subject's line of sight as given by Equation 3.85. Even though a direct quantitative comparison cannot be made, to the extent that the trends predicted by the two equations can be compared, they are found to give self-consistent rather than inconsistent pupil area predictions. To illustrate this point, for any given luminance level, common to the valid ranges of both equations, the pupil diameters are, as expected, smaller for the full field of view luminance exposure of Equation 3.83 than for the centered light source luminance exposure of Equation 3.85. The two equations are also self-consistent from the perspective that the predicted luminance level, required to reach the minimum 2 mm pupil diameter, becomes progressively larger as the area of the luminance source gets smaller.

The only other pupil area variable dependences studied by Holladay that are relevant to the present analysis are those due to accommodation and convergence. Based on test results of Holladay, the accommodation and convergence of the eyes only influence the pupil areas for eye fixation distances of less than approximately 28 inches. Under constant light source exposure conditions, which resulted in a maximum pupil diameter of about 5 mm (i.e., half way between the nominal 8 mm maximum and 2 mm minimum), changes in pupil diameter for fixation distances from 28 inches (0.75 meters) to four meters, the largest distance tested, were less than 10%. For fixation distances of less than 28 inches, the pupil area decreased rapidly and automatically down to 3 mm at very small viewing distances, even though the light source exposure conditions remained constant. Presumably for this reason, none of Holladay's other pupil diameter tests involved fixation distances of less than one meter.

3.6.3.3. Other Pupil Area Experimental Findings

To see how Holladay's 1926 test results compare with those of other experimenters, the pupil area analysis was expanded to include other easily accessed pupil diameter empirical equations. Three empirical equations cited by Wyszecki and Stiles[79] were evaluated. These equations are introduced in date order of publication.

The first equation was attributed to a 1936 article by Crawford[80] and is expressed as follows when using the terminology of this report:

$$d_P = 5 - 3\tanh(0.4\log L_F). \tag{3.88}$$

Although this equation appears quite different from Equation 3.83 of Holladay it can also be expressed in the following equivalent form:

$$d_P = 5 - 3\tanh(\log L_F^{0.4}), \tag{3.89}$$

where the field luminance, L_F, is raised to the power of 0.4, just as it is in Holladay's Equation 3.83. By definition, the function tanh x, where $x = \log L_F^{0.4}$, is given by the first equality in the following equation:

$$\tanh x = \frac{e^x - e^{-x}}{e^x + e^{-x}} = \frac{e^{2x} - 1}{e^{2x} + 1} = \frac{1 - e^{-2x}}{1 + e^{-2x}}. \tag{3.90}$$

Following the definition of $\tanh x$ in this equation, two equivalent alternative forms of the equation are shown. Factoring e^{-x} from the numerator and denominator of the defining equation yields the first of the two additional equations. The second is obtained by factoring e^x from the numerator and denominator of the defining equation.

The first of the alternative equations above shows, for positive values of L_F that approach zero, that x takes on large negative values, thereby causing the e^{2x} term in the numerator and denominator to approach zero, the value of $\tanh x$ to approach -1 and d_P to approach the upper pupil diameter limit $d_P = 8$ mm asymptotically. Likewise, the second of these alternative equations shows, for positive values of L_F, much larger than unity, that x takes on large positive values, thereby causing the e^{-2x} to approach zero, the value of $\tanh x$ to approach +1 and d_P to approach the lower pupil diameter limit $d_P = 2$ mm asymptotically. The selection by Crawford of the function $\tanh x$ for use in pupil diameter equation, Equation 3.88, both provides the previously described asymptotic behavior and causes the pupil diameter equation to be symmetric about the field luminance, $L_F = 1$ mL (i.e., 0.929 fL), where d_P takes a value $d_P = 5$ mm (i.e., for $L_F = 1$, x and $\tanh x$ both evaluate to zero).

The second listing, by Wyszecki and Stiles, of empirical pupil diameter equations was attributed to Moon and Spencer.* The Moon and Spencer empirical equation may be written, using the terminology of this report, as follows:

$$d_P = 4.9 - 3\tanh[0.4(\log L_F + 0.5)]. \tag{3.91}$$

This equation appears to be a refinement of Crawford's equation. It can also be written either as,

$$d_P = 4.9 - 3\tanh[\log(3.162\, L_F)^{0.4}], \tag{3.92}$$

or as,

$$d_P = 4.9 - 3\tanh[\log(1.585\, L_F^{0.4})], \tag{3.93}$$

where again the field luminance, L_F, is raised to the power of 0.4, just as in the Holladay's Equation 3.83.

The third equation cited by Wyszecki and Stiles is an empirical equation attributed to De Groot and Gebhard,**

$$\log d_P = 0.8558 - 4.01 \times 10^{-4}(\log L_F + 8.1)^3. \tag{3.94}$$

---

* Moon, P. and D. E. Spencer, "Visual Data Applied to Lighting Design," Journal of the Optical Society of America, Vol. 34, 1943, p.605.

** De Groot, S. G. and J. W. Gebhard, "Pupil Size as Determined by Adapting Luminance," Journal of the Optical Society of America, Vol. 42, 1952, p. 492.

By rearranging the terms in this equation it can also be expressed in an equivalent exponential form as follows:

$$\log\left(\frac{d_P}{7.17464}\right) = -4.01 \times 10^{-4}(\log L_F + 8.1)^3 \tag{3.95}$$

$$d_P = 7.17464\ 10^{-4.686 \times 10^{-4}(\log L_F + 8.1)^3)}.$$

Alternatively, by changing from the common logarithm, base ten to the natural logarithm, base e, as follows:

$$\log_{10}\left(\frac{d_P}{7.17464}\right) = \log_e\left(\frac{d_P}{7.17464}\right)\log_{10} e = 0.434294 \log_e\left(\frac{d_P}{7.17464}\right), \tag{3.96}$$

the pupil diameter can be expressed as,

$$d_P = 7.17464\ e^{-9.2334 \times 10^{-4}(\log_{10} L_F + 8.1)^3}, \tag{3.97}$$

or as,

$$d_P = 7.17464\ e^{-9.2334 \times 10^{-4}[\log_{10}(1.2589 \times 10^8 L_F)]^3}. \tag{3.98}$$

The last two forms of the De Groot and Gebhard equation are directly comparable to Equation 3.83 of Holladay, which is of the same form but has a different relationship for the field luminance in its exponent.

3.6.3.4. Comparison of Pupil Area Predictions

A comparison of the pupil area predictions of all of the aforementioned empirical equations was conducted. The results of this comparison are shown in Figures 3.29 and 3.30, which plot pupil area on linear and logarithmic ordinates, respectively, versus field luminance plotted on a logarithmic abscissa. It is evident from these two figures that the empirical pupil area predictions of the four experimenters differ markedly from one another. These differences are discussed below.

Although the differences between the pupil area predictions of the four empirical equations are large, particularly when the predictions of Holladay's equation are compared, graphical results from an investigation by Spring and Stiles*, which are shown in Figure 2.6 of the Wyszecki and Stiles book entitled Color Science,[81] place these differences in perspective. The Spring and Stiles graph is a plot of the pupil diameter of the eyes versus the product of field luminance and pupil area (i.e., this produce is referred to in the literature as retinal illuminance, although this is a misnomer) for twelve test subjects viewing a 52 degree uniform field, rather than the full field of view tested by Holladay. When these graphical results are compensated to allow plotting either pupil diameter or area versus field luminance, the data shows that the above four empirical equations fall within the range of pupil diameter or area versus field luminance variations that existed between different individuals in the Spring and Stiles tests. For the most rapidly changing data of Holladay, the pupil diameter rate of change as a function of the field luminance was, however, only slightly less than the highest rate recorded in the Spring and Stiles investigation.

Even though the minimum pupil diameters in the Spring and Stiles investigation only varied between 1.8 and 3 millimeters, for the twelve subjects included in their tests, the maximum pupil diameter range was from about 4.75 to 7.9 millimeters. Furthermore, the maximum slopes of the characteristics also varied significantly between individuals, from slopes greater than those of Holladay to slopes less than those of Crawford.

---

* Spring, K. H. and W. S. Stiles, "Variations of Pupil Size with Changes in the Angle at which the Light Stimulus Strikes the Retina," British Journal of Ophthalmology, Vol. 32, 1948, p. 340, or "Apparent Shape and Size of the Pupil Viewed Obliquely," British Journal of Ophthalmology, Vol. 32, 1948, p. 347.

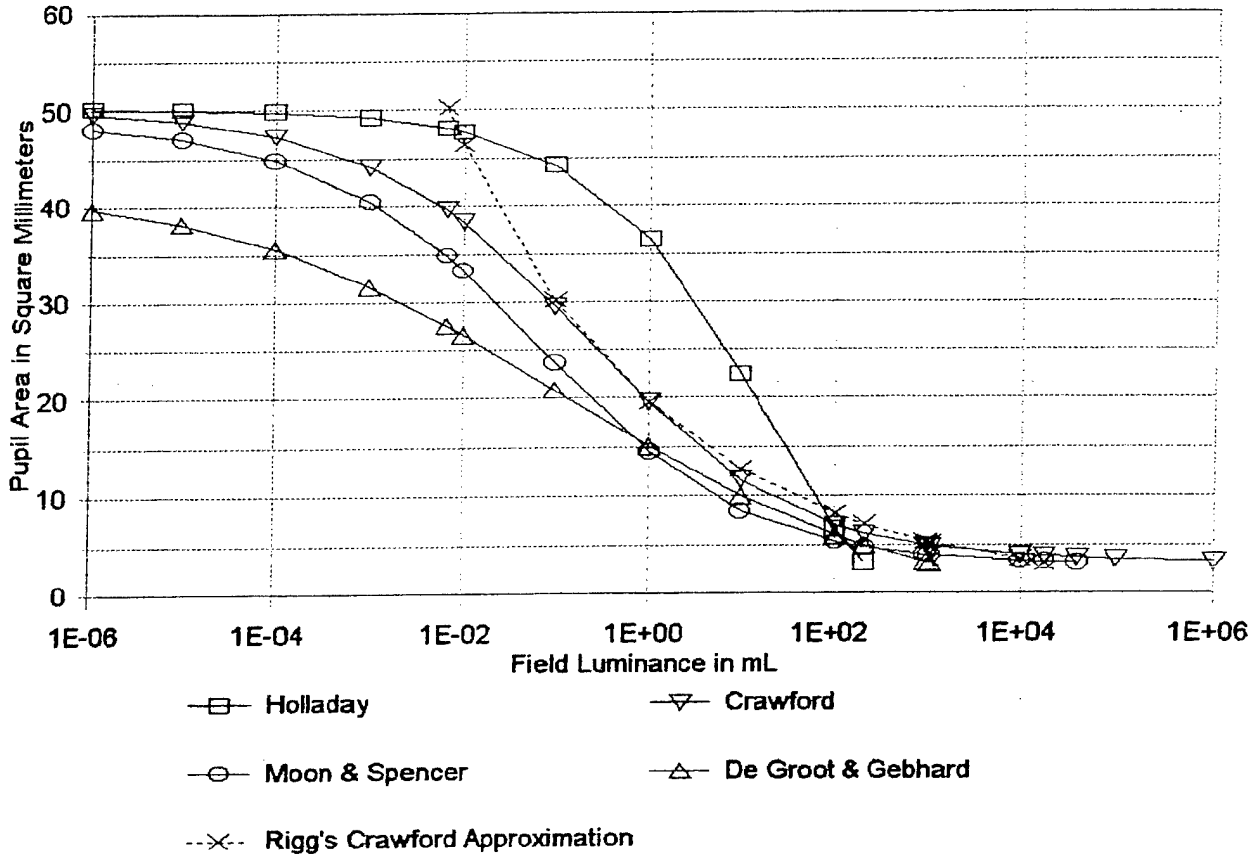


Figure 3.29. Semi-logarithmic Comparison Plots of Pupil Area Versus Field Luminance.

For three fourths of the individuals tested by Spring and Stiles, the minimum pupil diameter was either reached, or very nearly reached, for field luminances of between 1,300 and 3,000 mL (i.e., between 1,208 and 2,787 fL), although for five of the individuals tested the pupil area continued to decrease by as much as 0.3 mm out to the maximum field luminance - pupil area product tested, 100,000 Trolands (i.e., nominally to 6,400 mL, or 5,946 fL, of field luminance). To illustrate the variability in the Spring and Stiles experimental results further, one individual, Subject C, had a pupil diameter that increased rapidly from 3 mm, at 1,300 mL, to 5.7 mm, at 12.3 mL, and, after that, reached a maximum pupil diameter of 6.2 mm at 3.1 mL. By way of comparison Subject K had a pupil diameter that increased gradually from 2 mm, at 3,000 mL, to 7.3 mm, at 0.0024 mL, which was the maximum pupil diameter for this individual.

The preceding two examples give neither the most rapid nor the most gradual changes in pupil diameters for the subjects tested by Spring and Stiles, but they do show the large variability present in the test data. All of the subjects but one had either reached the maximum pupil diameter or were within 12% of reaching it at 0.0024 mL. Six of the test subject's pupil diameters continued to increase very gradually down to the lowest field luminance level tested. This luminance level was not stated but based on the graph had to be at least two decades below 0.0024 mL.

A part of the variability between individuals in the Spring and Stiles test results was attributed to the test subject's age by Wyszecki and Stiles. Holladay, and others made similar observation about their own results. Increasing age appears to most strongly limit the maximum pupil diameter. Potential explanations for the

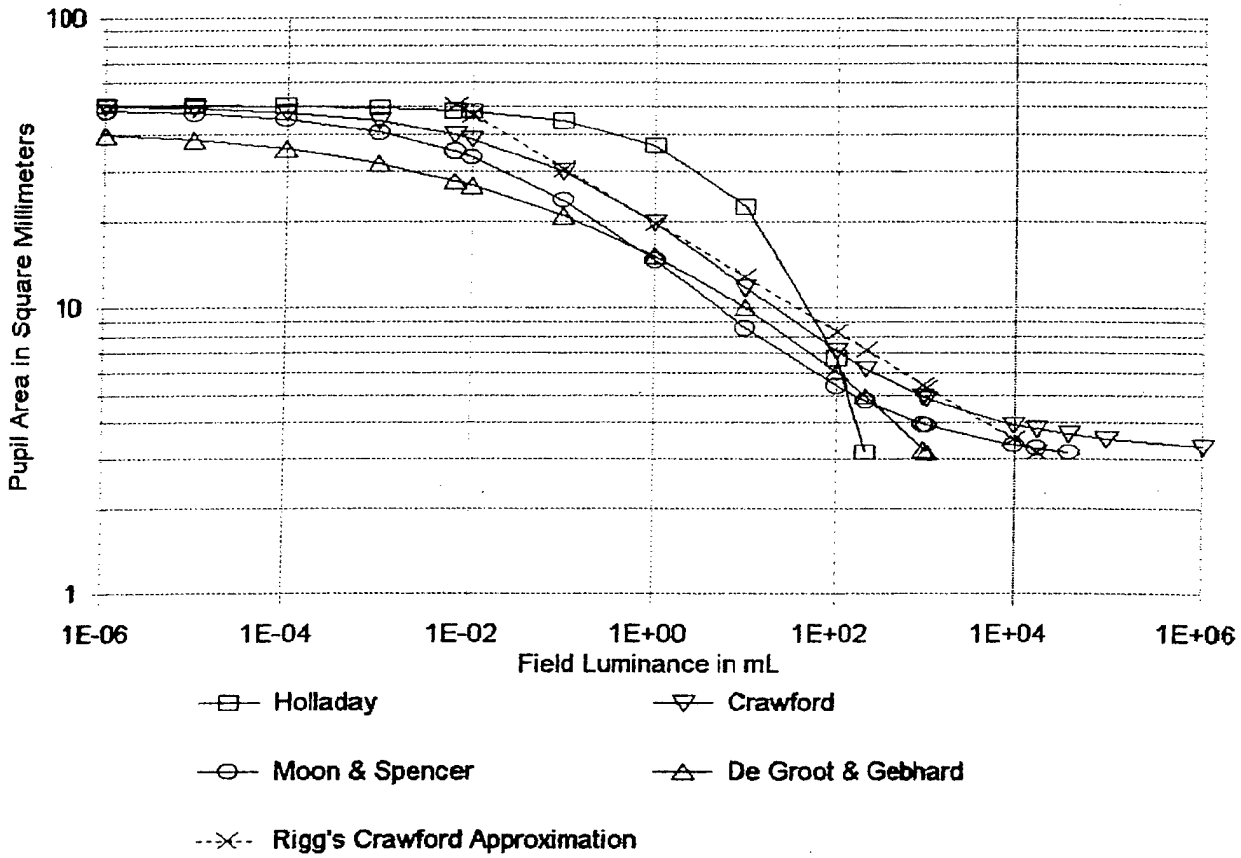


Figure 3.30. Full-logarithmic Comparison Plots of Pupil Area Versus Field Luminance.

balance of the variability present in the pupil size test results were not provided in the respective references studied.*

3.6.3.5. Comparison of Pupil Areas with the Predictions of Riggs' Rule of Thumb

Besides comparing the pupil area predictions of the four empirical equations, each equation was also compared with the pupil area dependence rule of thumb reported by Riggs, as represented by Equation 3.82. The experimentally determined pupil area empirical equations of Crawford, Moon and Spencer, De Groot and Gebhard and Holladay were matched to Riggs' rule of thumb, Equation 3.82, by using the pupil areas predicted by each of the respective experimenter's equations, at a field luminance of one milliLambert, as parameter value substitutions for the pupil area and field luminance in Equation 3.82.

For Crawford's pupil area and pupil diameter versus field luminance characteristics, the equations for Riggs' rule of thumb pupil area and diameter approximations were obtained by substituting a pupil area of A_{P1} = 19.635 mm,^{2} and d_{P1} = 5 mm, from the Crawford characteristic at L_F = 1 mL, into Equation 3.82, yielding the following equations:

* Restrictions on the scope of this investigation prevented acquiring for study the references which have been footnoted, with the exception of those in the appendix.

$$A_P = 19.635\, L_F^{-0.1871}$$
$$d_P = 5\, L_F^{-0.1871}. \qquad (3.99)$$

To make it easier to visualize the comparisons that follow, the pupil area approximation of Equation 3.99 for Crawford's empirical equation has been included in Figures 3.29 and 3.30. The Riggs' rule of thumb approximations, for each of the other experimenter's data, would plot as lines parallel to the line approximating Crawford's empirical equation in Figure 3.30, but shifted either to the left or right of that approximation. Only the approximation of Crawford's empirical equation is shown to avoid cluttering the figures.

The pupil area comparison of Riggs' rule of thumb approximation and Crawford's empirical equation, illustrated in Figures 3.29 and 3.30, produced a maximum error of 21% at 0.01 mL and peak errors of 17% elsewhere in the field luminance range from 0.01 to 17,900 mL, where Equation 3.99 predicts a pupil area of π mm^2 for a 2 mm diameter pupil. As Figure 3.30 illustrates, except for field luminances near 1 mL, where the two curves either briefly cross or are tangent to one another, and the pupil diameter is 5 mm, Crawford's equation predicts smaller pupil areas than does Equation 3.99, up to a field luminance of more than 1,100 mL (i.e., 1,022 fL), where Crawford's characteristic crosses Riggs' approximation of this characteristic, and then, asymptotically, approaches a pupil area of π mm^2.

The Riggs' rule of thumb equation, used to approximate the pupil area characteristic of Moon and Spencer, was obtained by substituting a pupil area of A_{P1} = 14.575 mm,^{2} from the Moon and Spencer characteristic at L_F = 1 mL, into Equation 3.82, yielding the following equation:

$$A_P = 14.575\, L_F^{-0.1871}. \qquad (3.100)$$

As expected, due to the similarity between the Moon and Spencer and Crawford equations, the comparison produced similar results. In this case, the comparison produced a maximum error 14.6% at 100 mL, and, at or near, double digit errors throughout most of a range from 0.01 to 3,648 mL, where the above equation predicts a pupil area of π mm^2 for a 2 mm diameter pupil. Like Crawford's equation, the Moon and Spencer modification predicts slightly smaller pupil areas than does Equation 3.100 over the preceding luminance range, with two exceptions. The exceptions occur between 0.01 and 1 mL, where the Moon and Spencer equation crosses the characteristic of Equation 3.100 twice, producing a 5.3% larger pupil area at 0.1 mL, and at a field luminance of somewhat more than 1,000 mL, where the Moon and Spencer empirical characteristic again crosses the Equation 3.100 characteristic and then asymptotically approaches π mm^2.

The De Groot and Gebhard empirical equation was approximated by substituting a pupil area of A_{P1} = 15.152 mm,^{2} from the De Groot and Gebhard characteristic at L_F = 1 mL, into Equation 3.82, yielding the following equation to represent Riggs' rule of thumb:

$$A_P = 15.152\, L_F^{-0.1871}. \qquad (3.101)$$

A comparison of these two equations showed that they agree to within 17.5% between field luminances of 0.1 and 400 mL, a more restricted range than for the two preceding comparisons. Pupil area predictions, of the De Groot and Gebhard empirical equation, are 35% and 28.6% smaller, at 0.01 mL and at 1000 mL, respectively, than those of Equation 3.101. The De Groot and Gebhard equation crosses the characteristic of Equation 3.101 twice, between 1 and 100 mL producing a 2% larger pupil area at 10 mL but otherwise predicts smaller pupil areas for the same field luminance values. Unlike the two preceding equations discussed, the De Groot and Gebhard empirical equation lacks a mathematical term to allow it to approach the minimum pupil area asymptotically. Because of this, the equation of De Groot and Gebhard evaluates to the nominal minimum pupil area of π mm,^{2} at a field luminance of 1,103 mL, whereas, Equation 3.101, for the Riggs' pupil area approximation, predicts a field luminance of 4,489 mL is required to reach this pupil area.

To represent Holladay's empirical equation adequately, using an equation of the form of Equation 3.82, would require using an exponent on the field luminance term that is a larger negative number than - 0.1871. Since this would no longer comply with the Riggs' rule of thumb, it would defeat the purpose of the comparison. Applying Equation 3.82, without modifications, to Holladay's empirical equation at a field luminance of 1 mL,

as was done for the other comparisons, resulted in the following equation:

$$A_P = 36.5\, L_F^{-0.1871}. \qquad (3.102)$$

This equation predicts a pupil area that is 26.9% larger than is predicted by the Holladay equation at 0.1 mL and 5.4 % larger at 10 mL. Beyond this range of field luminances, the errors become very large.

3.6.3.6. Conclusions for Eye Pupil Area Variable Dependences

Like the other tests conducted by Holladay, the pupil area investigation involved very few test subjects, typically no more than four. In addition, the investigations conducted could probably be best classified as screening studies, rather than complete experimental investigations. Furthermore, because all of the pupil area studies reported here were aimed at determining the responses of the general public, rather than for a select group having the above average visual capabilities of pilots, and who on average are also quite young, it is not clear how much reliance can be placed on any of the preceding numerical results. In a few cases the experimenters pointed out that a subject was young, and for those subjects the range of pupil area change was at or near the 2 to 8 mm pupil diameter limits.

In spite of the inconsistencies in the numerical results obtained, the preceding test results demonstrate two important general dependences of the pupil area response of humans. The first important pupil area dependence is the location on the retina illuminated by a light source. More specifically, when a light source of constant luminance and fixed area, which produces a constant illuminance as measured at the eyes, is focused on the retina, it causes a maximum contraction of the pupil area when the area of the retina containing the fovea is illuminated, and, as the image of the light source on the retina is moved progressively further away from the fovea, the pupil area becomes progressively larger. The second important dependence is that given by the Riggs' rule of thumb approximation, which has been shown to be a valid approximation, for three of the four experimenters' data, over a four to five order of magnitude change in the field luminance, but only over a two-decade range for Holladay's data. These pupil area dependences are considered further in Section 3.7.4, in relationship to the effect of pupil area changes on veiling luminances induced by discrete and distributed sources of glare.

3.7. Elements of a Theory for the Origin and Functionality of the Veiling Luminance Induced by a Discrete Glare Source

In this section various potential explanations of veiling luminance will be explored using the leads provided in the available experimental data. The intent of this analysis is to arrive at a theory-based explanation for veiling luminance and its relationship to the variables upon which it is dependent. This analysis will be divided into four interrelated parts for purposes of presentation. In the first part of the analysis, the primary emphasis is on the light stimulus element of the glare source induced veiling luminance theory. The second part of the analysis is primarily concerned with the element of the theory related to the human's psychological response to the glare source light, sensed by the eyes, and other factors that influence that response. The third part of the analysis discusses the theory, from the perspective of the human's physiological response to exposing the eyes to light from a glare source and other factors that influence that response. In the final part of the analysis, the effect of pupil area on the veiling luminance induced is considered.

In Section 3.7.1, information relevant to ascertaining the theoretical origin of veiling luminance will be considered. The two subsequent subsections, Sections 3.7.2 and 3.7.3, describe the probable psychological and physiological basis for explaining the apparent inconsistencies in the experimentally determined image difference luminance versus background luminance and veiling luminance angular response characteristics. In Section 3.7.4, the previously introduced experimental data on the variable dependences of pupil area are evaluated to see how they can be used to advance a theory of how pupil area influences veiling luminance. Conclusions, regarding the theory of the veiling luminance induced by discrete glare sources, are described

in the last subsection, Section 3.7.5.

3.7.1. Theoretical Origin of Veiling Luminance

The physical basis for employing the veiling luminance construct is that the eye's foveal sensors, while focused on a test symbol, will also receive part of the light incident from the parafoveal and peripheral visual fields, as the result of light dispersion from scattering centers suspended in the optical media of the eyes. By the standard of glass optics, the eyes are very poor lenses. Therefore, no doubt exists that this light scattering effect occurs and that it would, under glare source exposure conditions, produce at least a portion of the observed effect of glare source exposure, which in this report is characterized in terms of veiling luminance. This explanation for the origin of veiling luminance does not rule out the possibility that other phenomena contribute to the experimentally observed magnitudes of the veiling luminance induced by exposure to a glare source.

In discussing the results of the experimental studies that had been conducted, Holladay, under a section heading entitled "Theory of Dazzle-Glare, stated that "The seat of the phenomenon may be located in the: [82]

(a) Brain or central nervous system.
(b) Optic Nerve.
(c) Retina.
(d) Surface membranes of the eye.
(e) Media of the eye."

In the subsequent discussion of these possible origins of the phenomenon, Holladay allocated very little space to the first two. The first two choices described by Holladay, for the location of this phenomenon, namely, the brain or central nervous system and the optic nerve, offer little promise as possible locations for a phenomenon that could explain responses, perceived to be stimulated in the fovea, when a glare source exposes areas as remote as peripheral regions of the retina. Holladay mentioned a reflex action that stimulates both eyes, even when one is covered, attributed to a Frank Allen,* as a possibility for the brain or central nervous system location of the phenomenon, and a stimulation cross-coupling between optic nerve fibers, for the second possible location of the phenomenon. In both cases, Holladay pleaded ignorance as to magnitude and distribution of these potential phenomena.

The discussion in Holladay's article concentrated on the last three items in the preceding list, because these locations for coupling in the effects of glare light were considered the most probable to support explanations for the veiling luminance results observed through experiment. Holladay's comments on these potential explanations for the observed veiling luminance phenomenon are interspersed in the discussion of the merits of these explanations in the first subsection that follows.

In conducting the literature review for the present report, it was found that forty years after the publication of Holladay's investigations, the origin of the veiling luminance effect was apparently still not considered to be resolved. Following a literature search and analysis of earlier investigations,[83] Ireland again raised a question about whether veiling luminance is due to light scattering alone or is also in part caused by retinal induction. Retinal induction refers to the generation and transmission, over the optic nerves to the brain, of responses from foveal neurons that are, in turn, induced by the transmission through the retina cell structure of signals activated by peripheral or parafoveal light receptors directly exposed to light from the glare source. Although the available evidence does not permit completely ruling out the possibility that components of veiling

---

* Holiday's reference citation was as follows: Frank Allen, J.O.S.A. & R.S.I., p. 538; 1923 (The citation to the Journal of the Optical Society of America & Review of Scientific Instruments contained neither a volume number nor a month of publication.)

luminance are due to retinal induction, or light ducting and dispersion by the surface membranes of the eyes, it can be concluded that these contributions to veiling luminance are so small that they were not measurable, at least within the experimental accuracy of the experiments conducted.

Under the heading of "Influence of the Blindspot," Holladay[84] described a test in which a glare source producing 20 lx (1.86 fc) of illuminance, at the eye, was used to show that veiling luminance was induced even when the image of the glare source was restricted to the blind spot of one eye (i.e., the other eye being covered). Moreover, the level of veiling luminance induced in this test was commensurate with that induced when the glare source image was moved into adjacent areas of the retina populated by light receptors, just above and below the blind spot. This result is a clear indication that retinal induction, if operative, is not a major component in the veiling luminance effect.

Holladay did not perform a specific test to evaluate the influence on veiling luminance of glare source light exposures of the surface membranes of the eye. In discussing this possibility, Holladay referenced a study by P. W. Cobb,* as having shown that light shining upon the eye is transmitted through the sclera, cornea and iris and scattered over the retina. Holladay also commented that "a portion of the light entering the pupil, may by one or more reflections at the surfaces of the lens, cornea, and retina be scattered over the retina." In concluding this commentary, Holladay expressed the expectation that the light entering the eyes by these means would be "scattered more or less uniformly over the entire retina and therefore its distribution would be practically independent of the angle between the dazzle-source and the line of vision."[85]

Fry and Alpern [86] reported conducting an experiment similar to the test of the blind spot reported by Holladay. The results obtained confirm those of Holladay, although they did not specifically cite the Holladay article in the discussion of their result. Instead Fry and Alpern referenced an article by Schouten and Ornstein** in which an investigation of the veiling luminance induced by a glare source was conducted. According to Fry and Alpern, when describing the results reported by Schouten and Ornstein, the latter concluded that retinal induction is a more satisfactory explanation for the glare source induced veiling luminance phenomenon than is light scattering within the media of the eyes. Although the article also contained an experimental confirmation of Holladay's blind spot test result, Schouten and Ornstein had attributed the presence of the glare effect to stray light. As their justification for the stray light origin of the veiling luminance effect, when the glare source was imaged on the blind spot of one eye, Schouten and Ornstein cited an investigation they had conducted in which "spots of light were focused on the sclera in front of and behind the ora serrata and did find a difference (i.e., a veiling luminance effect) which they used as evidence for a physiological effect transmitted through the retina."[87]

A fundamental problem with the theory espoused by Schouten and Ornstein is that if "a physiological effect transmitted through the retina" (i.e., retinal induction) explains the magnitude of the veiling luminance induced when a glare source is imaged on the blind spot of one eye, then this source of veiling luminance should be present whenever the entire eye is exposed, irrespective of where the glare source is imaged on the retina. The existence of this effect would, therefore, predict a noticeable increase in the veiling luminance when a glare source image is moved from the blind spot to an area of the retina containing light receptors, since at that point the two veiling luminance effects, as happens for multiple glare sources, would become additive. Instead, the three experiments, just referred to, reported observing no change in the veiling luminance, during the translation of a light source image, on the retina, from the blind spot to adjacent areas of the retina populated with light receptors.

---

* Holiday's reference citation was as follows: P. W. Cobb, Lectures on Ill. Eng., 2, p. 525 (The cite lacked both a date and a publisher).

** Fry and Alpern's reference citation was as follows: J. F. Schouten and L. S. Ornstein, J. Opt. Soc. Am., 29, 168 (1939).

Fry and Alpern also annunciated another problem with the retinal induction explanation, by Schouten and Ornstein, of the veiling luminance the ...ad observed when the blind spot is illuminated by a glare source. In their article, Fry and Alpern concluded their discussion of this subject by stating that they had repeated the basic experiment conducted by Schouten and Ornstein, and in doing so had been unable to confirm their result. While it is possible that a real veiling luminance effect was observed by Schouten and Ornstein (leaving aside whether it was due to retinal induction or scattering), apparently the magnitude of the effect was too small to be measured by Fry and Alpern. The fact that the experimental techniques of Fry and Alpern were sufficiently sensitive to discern the veiling luminance associated with the blind spot shows the effect reported by Schouten and Ornstein is too small to explain the veiling luminance observed when the blind spot is illuminated. This test result by Fry and Alpern also appears to vindicate the previously described conclusion that Holladay had reached, through theoretical analysis using a thought experiment.

In Holladay's description of the scattering of light, by the optical media of the eyes, as a potential origin of the veiling luminance test results observed, a trial calculation to predict the total luminous flux density falling on the eye's fovea was carried out by incorporating the Rayleigh equation* for light scattering into the Holladay equation for total luminous flux density. The equation gives the angular distribution of the intensity of the light scattered within an optical media (i.e., within the eyes), which contains a density of optical imperfections capable of serving as scattering centers, in terms of the intensity of the incident light. Holladay, in commenting on the final integral equation, which was formulated to give the total luminous flux density incident on the fovea, expressed the view that the equation predictions are consistent with the results of the experiments conducted. This conclusion, however, must be interpreted in the context that the final equation of Holladay, with the adaptation of the Rayleigh scattering equation included, correctly predicted the observed trends in the experimental results, rather than their absolute values. Due to a lack of information, on several parameters in the final equation, such as refractive indices and the density of optical imperfections present in the optical media in the eyes, this equation could not be evaluated to the point where specific numerical value predictions were possible.

It was pointed out by Holladay that the scattering equation predicts that the total flux density should vary approximately as $\theta_B^{-1.1}$, for values of θ_B between 1 and 30 degrees.[88] This result compares with θ_B^{-2} for Holladay's experimental test results, with $\theta_B^{-1.5}$ for the experimental test results of Stiles and with $\theta_B^{-0.74}$ for the test results of Jainski, over the indicated range of glare source angles. Holladay did express concern that this angular dependence prediction did not more closely match the experimental dependence observed. However, clear reasons exist why the total flux density equation, as interpreted by Holladay, cannot make precise predictions of the veiling luminance angular dependence caused by a glare source. These reasons are considered in the following discussion.

From a current perspective, it would have to be concluded that the assumptions made by Holladay about the scattering geometry in the eye were greatly oversimplified. The most important example of this occurs in Holladay's formulation of the integral equation for the flux density sensed by the fovea. In this equation, a cosine receptor (i.e., Lambertian) angular receptivity characteristic was incorporated to represent the angular light reception properties of the foveal light receptors. However, as the result of experiments by Stiles and Crawford[89] in 1933, it is now known that the cone light receptors that populate the fovea of the eyes have angular light reception characteristics vastly more restrictive than those of the cosine receptor characteristics incorporated into Holladay's equation. For this reason, the significance of the retinal light receptor angular characteristics, and of the other assumptions implicit in the formulation Holladay's equation, are considered below. The primary purpose of the modifications and additions to be described below is to show how the accuracy of the predictions possible using Holladay's equation could be improved. The changes would, therefore, be expected to only lead to a refinement of Holladay's theory of light scattering, in the eyes, and not to a major modification of the theory.

---

* Holiday's reference citation was as follows: Lord Rayleigh, Phil. Mag., 41, pp. 107, 274, 447; 1917.

The largest difference in the predictions made using Holladay's theoretical light scattering equation would be expected to stem from introducing the rapid decrease in the angular receptivity characteristics of cone receptors (i.e., or more generally the retinal receptors) as the angle between scattered light and the center vision axis increases. This effect, which was referred to in the preceding paragraph, is known as the Stiles-Crawford effect. As a general indication of the magnitude of this effect, light entering the eye, from an angle near the outer edge of the pupil aperture, is sensed with a receptivity that is down to less than 20% of the peak receptivity of light, incident from the center of the pupil, even thought the luminance reaching the fovea is the same along both paths.[90]

The principal result of the Stiles-Crawford effect is to limit the volume of the eyes' media that can scatter light into the fovea's cone light receptors at an angle, which permits the scattered light to be sensed. This volume is defined by the common intersection of the glare source beam, within the eye's optical media, with a cone having a base slightly larger than the pupil area of the eye, and having its apex located at the foveal light receptor. This common volume would be at its maximum size, for small glare source angles, θ_B, when the beam is located very close to the central visual axis. As the glare source angle is increased, the scattering volume that is sensed, via the light scattered into the direction of the fovea, would continue to decrease in size until reaching its smallest volume at the glare source reaches the limiting angles of the human's field of view. Furthermore, based on the volume of the cone sensed and the intersection of the light beam with it, at small glare source angles, the decrease in the scattering volume as the angle subtended by the glare source, with respect to the observer's line of sight, increases in size, would be expected to at first occur slowly. For intermediate glare source angles, between nominally 25 and 45 degrees, the scattering volume would be expected to decrease in size more rapidly. Finally, at large glare source angles, of greater than about 45 degrees, the scattering volume, due to this effect alone, would again decrease in size more slowly. However, two additional effects described in the next paragraphs, would combine with the first scattering volume reduction effect to continue the rapid reduction in the scattering volume throughout the range of large angles.

The first of the two additional causes for reductions in the sensed luminous flux density of scattered light reaching the fovea, as the glare source angle, θ_B, is increased, is due to the foreshortening of the pupil aperture. Owing to the glare source beams passage through the pupil aperture at progressively more acute angles, with respect to the plane of the aperture, as the glare source angle increases, there is a change in beam shape from a circle to an ellipse, with its major axis being equal to the pupil diameter. This effective change in the shape of the pupil would result in a progressive foreshortening of the minor axis of the ellipse and to an attendant reduction in the beam area. Holladay did include this factor in the scattered luminous flux density equation, however, its effect would be relatively minor, for the glare source angle range restriction of 1 to 30 degrees, which Holladay placed on the validity of the luminous flux density equation. This is the case, because the reduction in the scattering volume, due to this effect, is proportional to the cosine of the glare source angle, following an adjustment for refraction of light, after it has passed through the lens of the eyes.

The second additional cause for reductions in the sensed luminous flux density of scattered light reaching the fovea, as the glare source angle, θ_B, is increased, is a progressive reduction in the beam luminous flux entering the eyes due to the increase in the fraction of glare source light that is not admitted into the eyes because it is specularly reflected from the multiple optical surfaces associated with the eye's cornea and lens. In restricting the validity of the luminous flux density equation to angles between 1 and 30 degrees, Holladay again incurred little error by ignoring this effect.

Based on the assumptions Holladay used to determine the luminous flux density incident on the retina cone receptors, the integrated result included light scattered toward the foveal cone receptors, from anywhere within the volume of the beam, admitted into the optical media of the eyes through their pupil apertures. In accordance with the reduced sizes of the scattering volumes described above, in comparison to those of Holladay, the larger scattering volume used by Holladay would be expected to result in an excessive estimate of the light sensed by the cone receptors for small glare source angles. This result is therefore consistent, at least in the direction of change, with the reduction in the angular weighting function response from the value of $\theta_B^{-1.1}$, predicted by Holladay's theoretical luminous flux density equation, to the slower response of the

angular weighting function derived from Jainski's test data, $\theta_\beta^{-0.74}$, for small angles. The changes in the scattering volume, described above, would be expected to produce a directly proportional change in the luminous flux density incident upon, and sensed by, the retina cone receptors. An analysis of Holladay's equation, modified to include the corrected scattering volumes, is beyond the scope of the present investigation. Nonetheless, the previously described trend in the reduction of the scattering volume, and, therefore, in the reduction of the luminous flux density incident upon and sensed by the retina cone light receptors, is consistent with the angular response characteristics predicted by the discrete glare source veiling luminance equation, derived from Jainski's test data for the full range of glare source angles tested, namely, Equation 3.58.

While the cumulative effect of the preceding results does not prove conclusively that no effects are present, due to retinal induction or the surface membranes of the eyes, they do prove that, if present, the effects are too small in magnitude to be measured with the equipment available at the time the various experimental tests were conducted, that is, so small that the effect is buried within the experimental error present during the tests. From this evidence and the preceding analysis, the author concludes that the predominant effect responsible for the veiling luminance, induced in the foveal region of the retina, is glare source light entering the eyes through their pupil areas, which is subsequently scattered into the direction of the foveal receptors, during the time of the lights' passage through the optical media of the eyes, contained within cones defined by apexes at the fovea and having the pupil apertures of the eyes as their base. Based on analysis results to be presented later, a similar explanation would apply for the experimental test results of Holladay and Stiles except that the angular responsivity function applicable to parafoveal rod receptors would have to be used in place of the angular responsivity function applicable to the cone receptors responsible for the Nowakowski and Jainski test results.

The investigation of veiling luminance in this report, is intended to establish the dependence of the legibility of information, presented on aircraft cockpit instruments and panels, as a function of the magnitudes and positions of glare sources, within the observer's field-of-view, and on the day through night viewing conditions encountered by the flight crew. By itself, the finding that veiling luminance is primarily due to the scattering of light within the eyes does not resolve the issue, raised by the published test data, that possibly more than one veiling luminance angular response function must be used to model the aircraft cockpit display legibility responses of pilots, who receive exposures to the veiling luminance induced by glare sources under ambient illumination conditions that extend from daylight to night. The balance of this section will be devoted to a further scrutiny of the origins of veiling luminance within the human visual system and to the development of experiment-based explanations for the observed veiling luminance angular response characteristics.

3.7.2. Psychological Response to Scattered Glare Source Light

The discussion of the human's psychological response to veiling luminance, which follows, proceeds with a brief review of previously introduced experimental findings, followed by an exploration of the role that the image detection or image identification visual task, assigned to a test subject, plays in determining the observed differences in veiling luminance angular response characteristics. Afterwards, the differences that exist between the image difference luminance versus background luminance characteristics, for image detection and image identification tasks, are presented and their implications are considered.

3.7.2.1. Veiling Luminance Angular Response Relationship to the Visual Task Performed

In experimental studies originally published by Luckiesch and Holladay in 1925[91] and by Holladay in 1926,[92] it was shown that the effect of one or more glare sources can be duplicated through the insertion of a uniform veiling luminance of the correct magnitude between the test symbol and the observer's eyes. In subsequent tests, published in 1927,[93] Holladay confirmed the 1925 and 1926 test results, using refined experimental test techniques and equipment. In this case, however, Holladay did not employ a physical source

of veiling luminance, as a direct comparative tool, for use in establishing the values of veiling luminance induced by a glare source. Instead, Holladay matched the image difference luminance values, determined with the glare source present, to image difference luminance requirements, determined with no glare source present, and, in this way, characterized the effect of the glare source in terms of an equivalent veiling luminance. Since the latter approach was also used by Stiles,[94] Crawford,[95] Fry and Alpern,[96] and Jainski, to produce their previously described experimental test results, the findings of all of these experimenters can be directly compared to one another. As shown previously, although Nowakowski used a different metric for characterizing the effect of a glare source, his data was also directly comparable with that of the other experimenters.

The veiling luminance angular dependence results, previously introduced in Section 3.6.2, show that while there are veiling luminance angular response differences among all of the experimenter's data, the large differences occur between the data sets of Holladay, Stiles, Fry and Alpern, and those of Nowakowski and of Jainski. In the discussion in Section 3.6.2, of the experimental design variables tested, a process of elimination resulted in a finding that the only meaningful difference between these two sets of experiments was the visual task performed by the test subjects. The primary experimental consideration used to reach this conclusion was the nominal confirmation of Jainski's angular test results by Nowakowski, for small angular displacements of the glare source, even though the test conditions used by Nowakowski conform much more closely to those of Holladay and Stiles than those of Jainski. It was reasoned that the overlap of Nowakowski's range of tested background luminances and of glare source illuminances, as measured at the eyes, with those used by Holladay and Stiles should have produced similar veiling luminance angular test results. The fact that a correspondence between these test parameters did not produce comparable results implies that the remaining differences between the experiments are responsible for the difference in the veiling luminance angular responses of the test subjects.

The principal difference remaining between the two sets of experiments is the behavioral psychology-based response of the test subject to the image detection tasks, used by Holladay, Stiles, Fry and Alpern, and to the image identification tasks, used by Nowakowski and of Jainski. This difference is founded in the need for the test subjects of Jainski and Nowakowski to use minimum separable acuity to identify a test image correctly, whereas the other experimenter's visual tasks only require detecting the presence or absence of an image.

Although the difference between image detection and identification tasks appears to be the most likely origin of the observed differences in the experimental veiling luminance angular responses, at least among the variables tested, one potentially important variable not included in any of the tests, except Jainski's, was the size of the test image. While the Nowakowski and Jainski test image sizes had image critical detail dimensions of twenty minutes of arc or less, test image sizes used by the other experimenters were in the range of one to two and one half degrees. To be able to explore further, both the effect of test image size, and the role that the difference between image detection and identification tasks play in causing the observed differences in the angular response characteristics, an alternative source of experimental data is needed. Since the image difference luminance versus background luminance characteristics, for image detection and identification tasks, are known to differ, these better established sets of experimental data are considered, compared and commented upon in the following three subsections.

3.7.2.2. Comparison of Image Difference Luminance Requirements for Image Detection and Identification Tasks

Earlier in this chapter, a sampling of image difference luminance requirements as a function of the display background luminance, for both image detection and image identification tasks, were presented in Figures 3.8, 3.9 and 3.10, and then qualitatively and quantitatively compared in Section 3.3. In this subsection, the earlier comparisons are summarized, as are the principal results of the comparisons, to provide a background for making comparisons with the experimental image detection data of Blackwell in the succeeding subsections.

Collectively, Figures 3.8, 3.9 and 3.10 provide a comparison of two of Blackwell's image detection task characteristics with the image identification task characteristics of several other experimenters. Image detection task data available for comparison in the figures includes the 50% probability of correct detection criterion data of Blackwell for a 9.68 minute of arc circular target, which can occupy one of eight possible positions on a 3 degree radius circle, and Blackwell's data, for the same size of circular target, but, in a centrally fixated static position, and collected using a minimum threshold of detection criterion. The image identification task data compared in the figures includes the following: a characteristic for the 9 minute of arc minimum separable acuity of Aulhorn and Harms; a characteristic for the 15.3 minute of arc critical detail dimension numeric character of King, Wollentin, Semple, and Gottelmann; and a characteristic for the 5.5 minute of arc critical detail dimension data of Jainski (i.e., the outside diameter of the ring on the Jainski symbol is 9.82 minutes of arc). As previously noted, to permit covering the full range of background luminance values, the Blackwell data shown in Figures 3.8 and 3.9 were extracted from contrast characteristics, curve fitted by Blackwell to the image detection data collected, rather than from the data tables published by Blackwell.

Because the image detection and identification characteristics, under moderate to high photopic background luminance levels, can be treated as approximately straight parallel lines, when graphed against logarithmically scaled image difference luminance versus background luminance axes, the ratios, between the image detection characteristics, for test images of constant size, and image identification characteristics, for test images of constant critical detail dimension, provide a means of comparing human visual performance for these otherwise dissimilar tasks and characteristics. The similarity between the test conditions of Blackwell and those of Aulhorn and Harms enhanced this comparison. Blackwell's image detection task used circular areas as test objects, and the image identification task of Aulhorn and Harms required their test subjects to discriminate correctly between circles and squares (i.e., see Figure 3.5). Moreover, both tests used a 50% accuracy of correct identification legibility criteria. These similarities in the tests, coupled with the similarities between the test results of these and other experimenters, in the photopic background luminance range, were interpreted to mean that the respective image difference luminance versus background luminance characteristics can be directly compared with one another, and, furthermore, the test results infer the existence of an underlying perceptual commonality between the image detection and image identification tasks, in the photopic background luminance range.

Figure 3.8 and Figure A.2, of Appendix A, show Blackwell's image detection characteristic, for a circular area image subtending an angle of 9.68 minutes of arc, intersecting the 9 minute of arc critical detail dimension characteristic of Aulhorn and Harms. The inference from this comparison, for photopic background luminance viewing conditions, is that the image difference luminance value needed to perceive a particular critical detail dimension would also allow an image subtending that same dimension to be detected. Although no other test data was found, to provide an independent confirmation of this specific result, the relationship makes good physical sense, in that the eyes' cone light receptors are generally accepted to be used to perform both image detection and image identification tasks in the photopic background luminance range. This result is also consistent with the practical requirement that a target must first be depicted, with a sufficient image difference luminance to allow it to be detected, before it becomes possible for it to be identified.

In this subsection the similarities between image difference luminance versus background luminance characteristics, for image detection and image identification tasks, have been reviewed to provide a basis for considering the differences between these characteristics, in the next two subsections. The purpose for exploring these differences between the image difference luminance versus background luminance characteristics, for image detection and image identification tasks, is to learn whether these differences are consistent with the previously described observed differences between the veiling luminance angular response characteristics, for image detection and image identification tasks. Before proceeding with the introduction of Blackwell's image difference luminance versus background luminance characteristics, in the next subsection, it should be noted that as a practical matter, it is the image identification task that is relevant to the pilot being able to read head-down, head-up and helmet-mounted display information, and, consequently, it is the image identification characteristics that are relevant to the topic of the automatic control of display legibility in aircraft cockpits, dealt with in this report. In addition, because the image difference luminance

needed to identify a target, at any background luminance level, is the same or larger than the corresponding image difference luminance required to detect the same target, a display whose image difference luminance is controlled to make a target identifiable will automatically provide sufficient image difference luminance to perform image detection on the display, should that be required.

3.7.2.3. Blackwell Image Detection Task Data and Commentary

Although the application of Blackwell's image detection requirements in aircraft cockpits is restricted primarily to the acquisition, by the pilot, of visual scene imagery external to the cockpit, an examination of the image detection data of Blackwell is still of value to permit a further exploration of the reasons for the differences between the human's response to image detection and image identification tasks. Figures 3.31 and 3.32 show the contrast versus background luminance data, contained in Tables 2 and 7 of Blackwell's November 1946 article, respectively, after it was converted to allow plotting image difference luminance versus background luminance.

Due to a limitation of the graphing capabilities of the spread sheet program used to plot Blackwell's data, straight lines connecting the data points could only be drawn by the program if the image difference luminance values, along the ordinate axis, were entered for each of the abscissa background luminance data points. Since the abscissa data points were all different, for the different target size characteristics from Blackwell's Tables 2 and 7, graphical interpolation was necessary to obtain the ordinate data points, shown connected by straight lines in Figures 3.31 and 3.32. This was accomplished by plotting Blackwell's data using straight lines to connect the adjacent data points on full logarithmic graph paper, 22.5 inches square, and then extracting the ordinate values, corresponding to the common abscissa data points. This procedure resulted in all of the characteristics in the figures having more data points than those contained in Blackwell's tables. Although the process of adding intermediate data points using straight line interpolations can be expected to have created errors in the computer generated characteristics in Figure 3.31 and 3.32, the characteristics do provide a reasonably good approximation of the Blackwell data plotted on the large area graph.

It should be noted that except for what appeared to be an accuracy check involving the repeat of one data point per characteristic, each at different background luminances, Blackwell typically only recorded data at decade sampling intervals. Two exceptions to this testing pattern occurred in Blackwell's first experiment. One exception was that between three and five data points were recorded in the decade interval centered on 0.001 fL for all of the characteristics. The other exception was that test results were recorded at or near both 1 and 3 fL for all but the 121.0' characteristic in the first experiment. The added emphasis on these areas of the characteristics by Blackwell is not considered accidental, since Blackwell had collected and analyzed extensive amounts of data while conducting preliminary experiments intended to refine the experimental procedures and to train test subjects.

Neither of the aforementioned sets of extra data points were collected in the second experiment, which was referred to by Blackwell as "the supplementary experimental program." In the second experiment, Blackwell, in comments based on the contrast results of the first experiment, noted that supplemental data was not needed below 10^{-5} fL. Blackwell also noted that, due to the large number of observations made in the first experiment, in the vicinity of 0.001 fL of background luminance, "less emphasis was necessary in the supplementary experimental program."

Figure 3.31 shows Blackwell's 50% probability of detection criteria data for circular test images (i.e., targets) subtending angles from 3.6 to 121.0 minutes of arc, and, for comparison purposes, image detection data for Holladay's intentionally blurred annular ring target is also shown. Figure 3.32 shows Blackwell's minimum threshold of detection criteria data for circular targets subtending angles from 0.595 to 360.0 minutes of arc. This latter series of tests was run by Blackwell, after the first experiment was completed, to evaluate the effect of very small and very large test images sizes. Because of the difficulties in achieving a 0.595' projected test image, of sufficient quality, and the fact that the 360.0' test image is the same size as the three

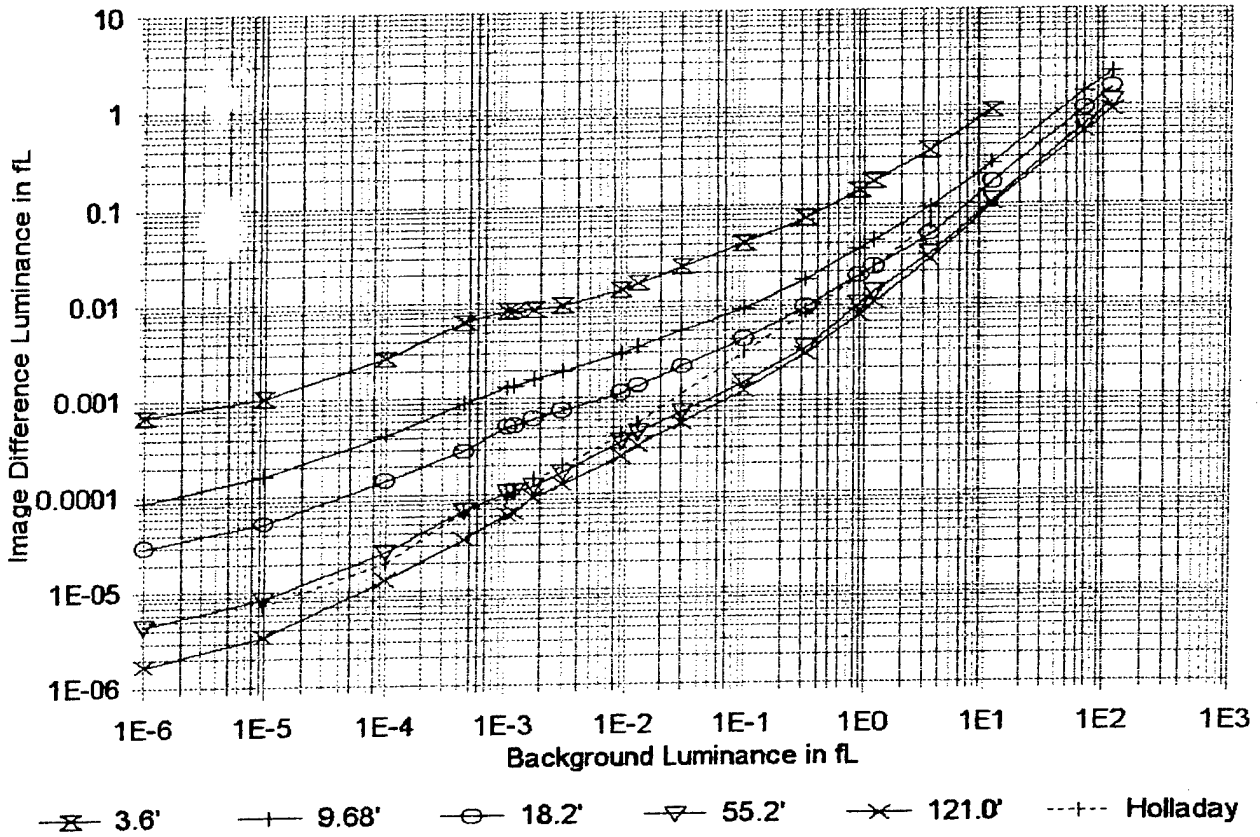


Figure 3.31. Blackwell Image Detection Data for 50% Threshold Legibility with the Angle Subtended by the Target, Expressed in Minutes of Arc, as a Parameter and with Holladay's 1927 Image Detection Data Superimposed.

degree radius circle on which the targets having eight possible target positions were placed in the first experiment, Blackwell decided to use centered fixed position targets for the second experiment. The 0.595' test image size was transilluminated using a specially designed rear projector, and a light pipe the size of the test image, embedded in and flush with the viewed surface of the screen. To make comparisons possible with the results of the first experiment, Blackwell included the five circular target sizes used in the first experiment in the second experiment. Blackwell indicated in the article that, owing to the first experiment, fewer background luminance sampling points were needed in the second experiment to document the results for these intermediate characteristics. Although the test subjects were thoroughly dark adapted in both experiments, additional testing, performed before the second experiment, had shown that the target exposure time had to be extended from six seconds, for the first experiment's visual task, to fifteen seconds to achieve reproducibility, for the modified visual task of the second experiment.

Based on Blackwell's experimental test results, the image detection characteristics in Figures 3.31 and 3.32 can be broken into three different background luminance segments. Above a transition region between about 1 and 3 fL of background luminance, all of the detection characteristics in Figure 3.31, including Holladay's, and all but the 0.595' characteristic in Figure 3.32, can be approximated by straight parallel lines of essentially the same slope as Jainski's image identification characteristics. As an additional common feature of this first segment, the image difference luminance requirements decrease as the target being detected increases in the size, with the changes in image difference luminance between adjacent characteristics becoming progressively smaller as the size of the target increases up to a sensitivity limit. This limiting

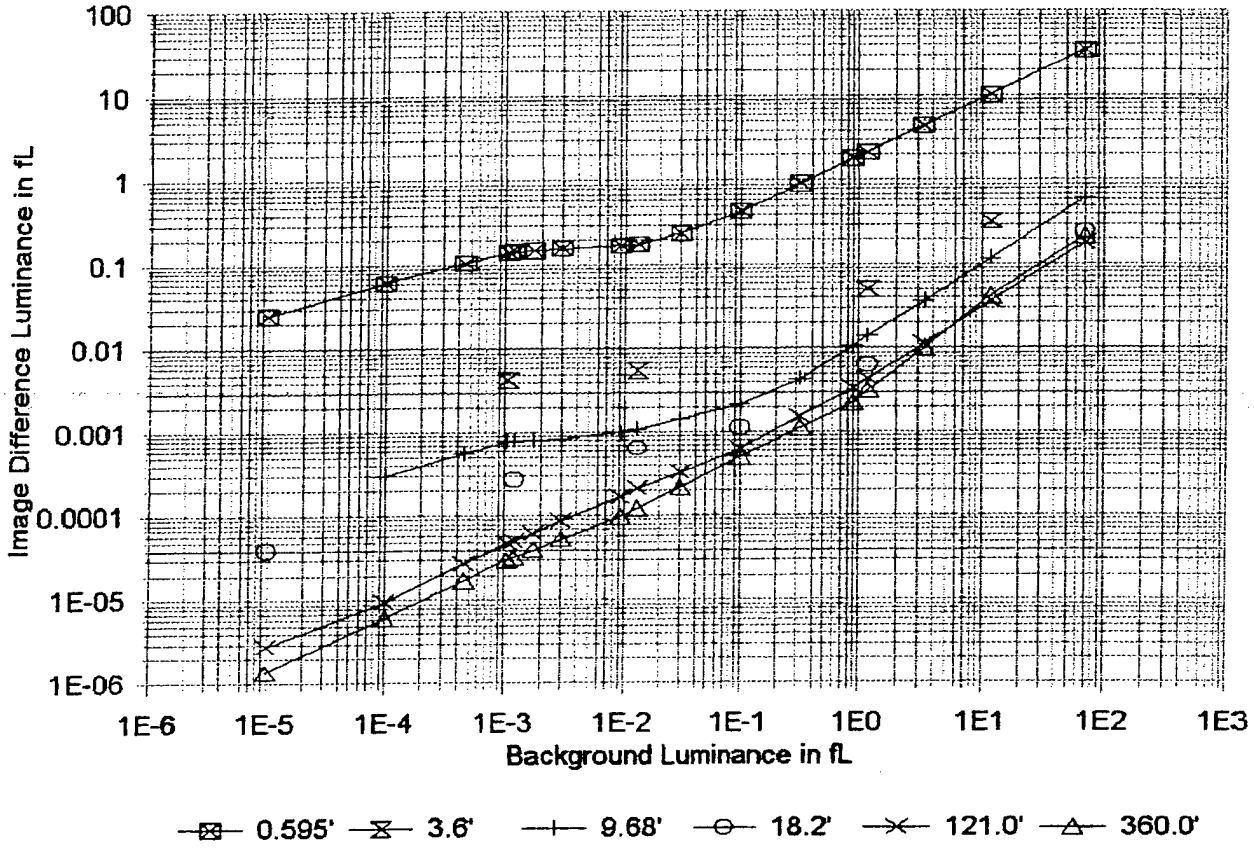


Figure 3.32. Blackwell (Nov. 1946) Image Detection Data for Minimum Threshold Legibility with the Target Subtended Angle, Expressed in Minutes of Arc, as a Parameter.

behavior, which was observed in the contrast versus background luminance characteristics of the first experiment, caused Blackwell to conduct the second experiment to permit exploration of the effect of both smaller and larger target sizes.

As indicated in Figure 3.32, the results of Blackwell's second investigation show that the 360' target size actually produced a higher image difference luminance requirement, above about 3 fL in background luminance, than did the 121' target size, whereas below 3 fL the larger target size produced lower image difference luminance requirements. Due to the high accuracy of Blackwell's data, the reversal in the positions of these characteristics in the vicinity of 3 fL cannot simply be discounted as an error. Moreover, this behavior is, at least in concept, consistent with the spacial frequency dependence of contrast sensitivity at low spatial frequencies (i.e., large image sizes) where contrast sensitivity decreases for larger or smaller spatial frequencies on either side of a maximum sensitivity value.

At the other extreme of the background luminance range, below nominally 0.001 fL, all of the image detection characteristics decrease at a somewhat larger slope than in the second, intermediate, background luminance segment. This behavior of the detection characteristics in the third background luminance segment is highlighted both because it is common to all of the detection characteristics and because it is also distinctly different from the behavior of image identification task characteristics, as exemplified by those of Jainski and of Aulhorn and Harms, for background luminances below 0.001 fL. Although the characteristics in the third background luminance segment, like those in the first, can be reasonably well approximated by straight lines, on the full logarithmic plot of Blackwell's data, for the background luminance range from 10^{-3} to 10^{-5} fL, the lines

so drawn are not approximately parallel as they are in the first background luminance segment.

The effect of changes in the test image size in the third background luminance segment may also be seen to produce much larger differences in the image difference luminance requirements in this segment than in the first, and although a target size related saturation limits on the sensitivity of the eyes still appears to be in evidence, it is not as pronounced as in the first segment. Figure 3.31 shows that all of the characteristics, extending below 10^{-5} fL down to 10^{-6} fL in background luminance, exhibit an apparent saturation limit on image difference luminance sensitivity as the background luminance is reduced. Since this limitation occurs for all of the characteristics, it can be concluded that this behavior is not a measurement error artifact of the very low luminance levels being measured for the larger target sizes.

Apart from serving the obvious function of a transition, between the image difference luminance requirements in the first and third background luminance segments, the intermediate background luminance segment exhibits some of the most interesting image difference luminance behaviors. First, in the transition from the first to the second segment, the slopes of the characteristics usually tend to decrease. Second, the slopes of the characteristics in the second and third segments both increase as the image size being detected increases. Third, the slopes of the characteristics for the two largest targets in Figure 3.31 (i.e., those corresponding to the 55.2 and 121.0 minute of arc target subtended angles) and Figure 3.32 (i.e., those corresponding to the 121.0 and 360.0 minute of arc target subtended angles), which, due to the scaling of these figures, appears to become very nearly the same for both the second and third segments, still exhibit a slope change anomaly (i.e., noted by Blackwell as a contrast discontinuity) in the vicinity of 0.001 fL. Fourth, the characteristics in the second segment of both figures almost, but do not quite, reach an image difference luminance plateau for the smallest target sizes as the background luminance decreases, before continuing to decrease with a greater slope in the third segment, and this trend continues, even though it becomes progressively less pronounced, as the target size is increased up to the largest target size tested.

To avoid creating a false impression of Blackwell's results, by adding straight lines between the individual data points for the 3.6' and 18.2' (i.e., minute of arc) target sizes in Figure 3.32, the intervening data points were not interpolated to fill in the additional common abscissa data point values needed to permit the graphing program to connect them with straight lines. In addition, due to a limitation of the program used to graph the data entered in the spread sheet, the figures were restricted to the simultaneous display of only six sets of data and, therefore, prevented showing the four supplementary data points, for the 55.2' target size collected by Blackwell. The four individual data points, corresponding to the 3.6' target size, were included in Figure 3.32 because they are necessary to provide a visual comparison with the new 0.595' target size data, included in Blackwell's second series of experiments, and to relate that data to Figure 3.31. The six individual data points corresponding to the 18.2' target size were included in Figure 3.32 because they illustrate the progression of the plateau effect for larger target sizes.

The image difference luminance values for the 55.2' target size (i.e., the data points that are not shown in Figure 3.32), were determined by Blackwell only over a three decade range, at background luminances of 0.885, 0.101, 0.0138 and 0.00119 fL. In the order of the background luminance abscissa points just cited, the ordinate values for the 55.2' target were 0.9, 8.7, 32.0, and 65.7% above the corresponding ordinate values for the 121.0' characteristic. The 55.2' ordinate data points therefore followed a path quite similar to the four central 18.2' minute ordinate points shown in Figure 3.32, except that they were closer to the 121.0' characteristic than to the 18.2' data points. The near coincidence of the 55.2' and 121.0' target data, at 0.885 fL of background luminance, close to the beginning of the first data segment, and the close approach of the 18.2' data points to the 121.0' target size characteristic in the photopic background luminance range, is further evidence of target size induced saturation limit on image difference luminance sensitivity.

Because of the contrast versus background luminance graph format, employed by Blackwell to depict his experimental results, many of the background luminance dependences that are evident in Figures 3.31 and 3.32, were not discernable to Blackwell. Paraphrasing Blackwell, the data from the second experiment (i.e., from his Table 7) was empirically fitted using the best-fitting curves consistent with the contrast versus

background luminance characteristics of the first experiment.[97] Blackwell also acknowledged, in commenting on the contrast versus background luminance figure, which resulted from the second experiment, that "it is evident that the precision of the results is significantly less than in the" first experiment. The point is that while Blackwell had implicitly assumed that the second experiment would produce results very similar to the first experiment, a reasonable expectation given the small change in the experimental design between the two experiments, a comparison in Figure 3.33 of the characteristics in Figures 3.31 and 3.32, representing the same target sizes in each figure, shows that significant differences exist between the test results obtained.

As expected, the shift from Blackwell's 50% probability of detection legibility criteria, for the first experiment, to a minimum threshold of detection legibility criteria, for the second experiment (i.e., a psychological change in the test subject's visual performance objectives), produced a reduction in the image difference luminance requirements, for all of the target size characteristics capable of being compared. However, contrary to expectation, the image difference luminance plateau effect, noted earlier in second background luminance segment, becomes much more pronounced, for the minimum threshold of detection legibility criteria characteristics, illustrated in Figure 3.32 for target sizes from 3.6' up to 55.2' (i.e., the data points for this image size are not shown), than it is for the 50% probability of detection legibility criteria characteristics, illustrated in Figure 3.31.

One consequence of the more pronounced plateau effect for the minimum threshold legibility criteria characteristics of Figure 3.32, which is not obvious unless the legibility criteria characteristics for each target size are plotted on the same graph to allow direct comparisons to be made, is that the plateau effect causes the minimum threshold legibility characteristics to more closely approach the 50% threshold legibility characteristics in the second background luminance segment. Figure 3.33 illustrates this behavior, and also graphically shows the distinctive difference between the image difference luminance requirement characteristics, for the two smaller target sizes being compared. The differences between these characteristics occur, even though Blackwell only changed psychological factors in going from the first to the second experiment. In particular, the image detection task was changed from circular targets, projected onto one of eight locations on a three degree radius circle for the 50% threshold legibility task, to being projected at a fixed central location for the minimum threshold legibility task. Moreover, for the image sizes shown in the figure, the same viewing conditions, targets and target projection techniques were used for both experiments.

As shown in Figure 3.33, after the minimum threshold legibility characteristics enter the third background luminance segment, they continue to approach the 50% probability of detection threshold legibility characteristics, from below, along reduced slope characteristics. Because Blackwell's second experiment only tested down to 10^{-5} fL, it is not known whether the two characteristics for each target size would eventually intersect slightly below 10^{-5} fL of background luminance at the minimum sensitivity limit. For each of the three target size characteristics compared, the luminance differences between the characteristics are clearly much smaller, at the lowest background luminance levels capable of being compared, than they are in the first background luminance segment.

Because of the thoroughness, attention to experimental detail, subject training, screening of test subjects, the data analysis techniques employed and the small error levels achieved, Blackwell's experiments have come to be regarded as a standard of comparison for other experimenters. To validate the experimental test setups being used, Jainski also performed specific experiments to permit comparisons to be made between Blackwell's results, for an image detection task, and analogous results obtained for the Jainski HUD and HDD test configurations. These comparisons for the HUD and HDD were presented in Figures 23 and 24, respectively, of Jainski's report. The close correspondence between the image difference luminance versus background luminance characteristics of Blackwell's image detection task and those of Jainski, were taken by Jainski as confirmation of the validity of the HDD and HUD test configurations.

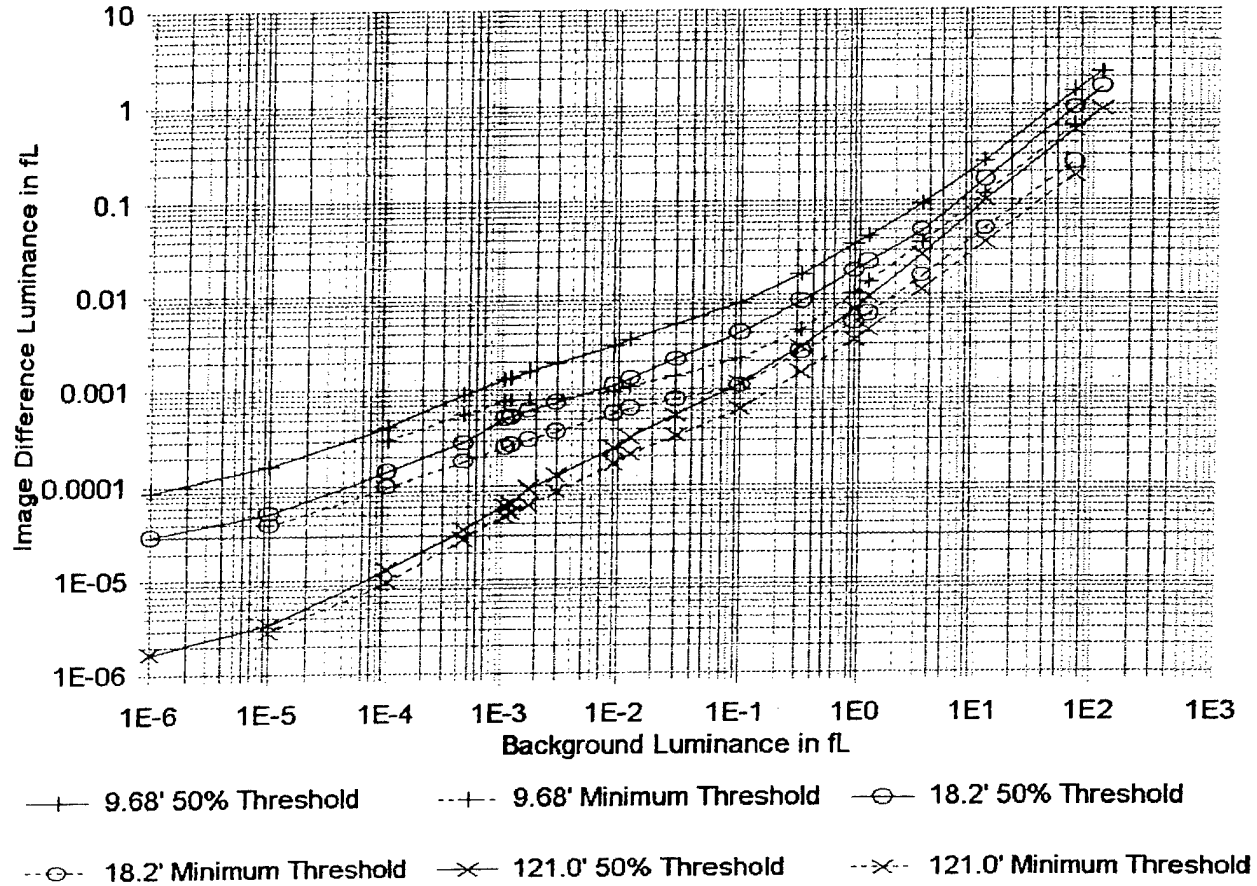


Figure 3.33. Comparison of Blackwell (Nov. 1946) Image Difference Luminance Requirements for Circular Targets Subtending the Same Angle using 50% Probability and Minimum Threshold Legibility Image Detection Criteria.

3.7.2.4. Visual Task Related Confirmations and Comparisons of Blackwell's Results

Figure 3.34 is included to illustrate the differences between the image identification task characteristics, collected by Jainski, and the image detection task characteristics, collected in the two experiments of Blackwell, by showing the upper and lower image difference luminance characteristic from each of the three sets of experiments. The minimum image difference luminance requirement limits that are applicable to image identification tasks, that is, the image difference luminance floor below which image identification cannot occur, at a particular image critical detail dimension, as the background luminance levels are reduced, may be seen to be distinctly different from the comparable image difference luminance requirements for image detection tasks. The principal difference is that rather than the image difference luminance requirements for image detection tasks reaching a lower limit, as they do for image identification tasks, the characteristics continue to decrease as the display background luminance is reduced. The point of these comparisons is that it is already an experimentally well established fact that a very fundamental difference exists between the perception and/or mental processing of information involved in the performance of image identification and image detection tasks.

The Holladay image detection target, as projected on the screen viewed by test subjects, was described by Holladay as a blurred annular ring of light having a maximum difference luminance on a 54.9' diameter circle (i.e., the diameter of this circle is dimensioned in Figure 1 of Holladay's 1927 article as 55 mm,

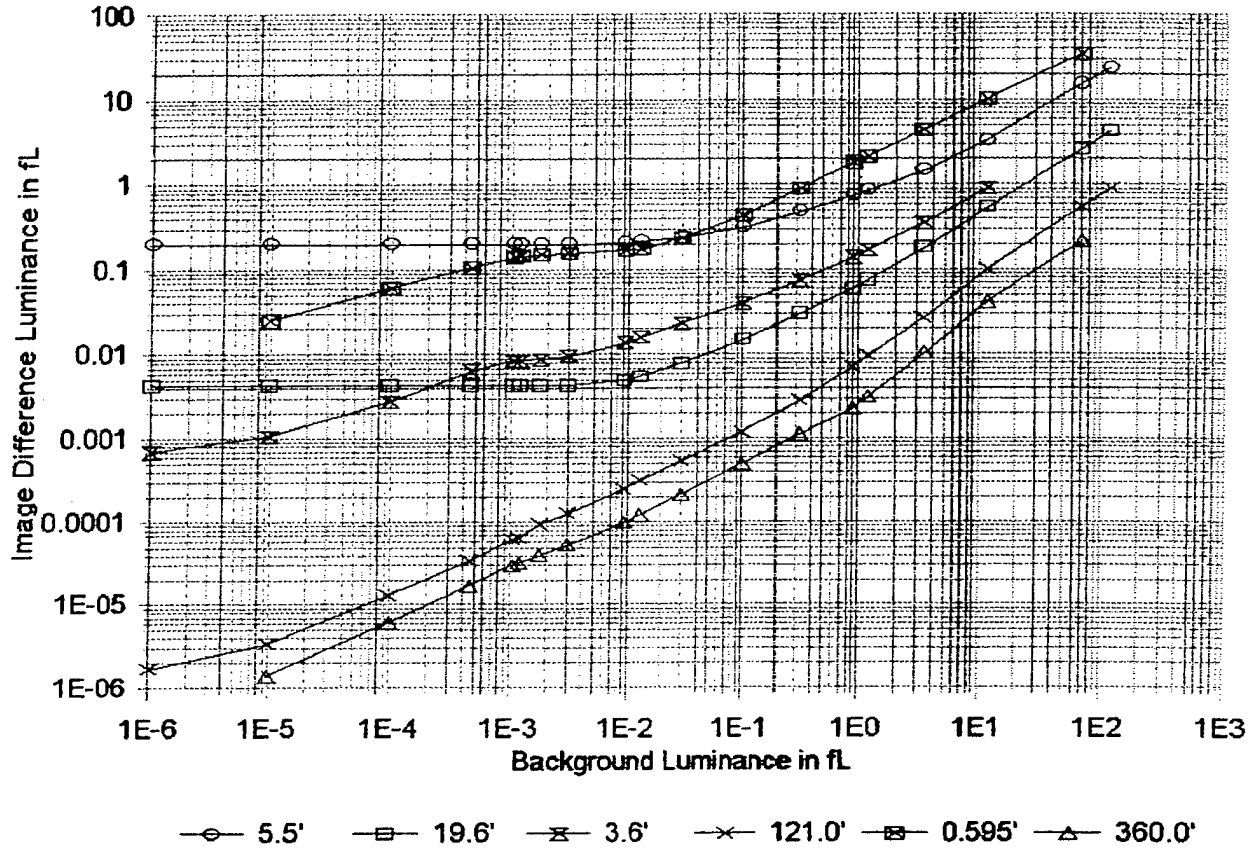


Figure 3.34. Comparison of Jainski Image Identification Data (5.5' & 19.6') with Blackwell Image Detection Data for 50% Threshold Legibility (3.6' & 121.0') and for Minimum Threshold Legibility (0.595' & 360.0').

which translates to 54.9 minutes of arc at the 344 cm viewing distance used by Holladay). The maximum difference luminance circle was shown centered in an annular ring having its radial width dimensioned as 37 mm in the figure, which converts to a subtended angle of 37'. As illustrated in Holladay's Figure 1, the maximum image difference luminance decayed radially both outward and inward toward a value of effectively zero at the ring's boundaries. No spatial distribution or additional dimensional information on the target was provided in Holladay's article.

Using the detection target just described, Holladay collected image difference luminance versus background luminance test results, which were presented in Figure 2, and the accompanying Table 1, of Holladay's 1927 article. A characteristic representing this data has been included in Figure 3.31, to permit it to be directly compared with Blackwell's data. This figure shows that the image detection test results of Holladay are, overall, consistent with those of Blackwell and Jainski, for a background luminance range from nominally 0.00019 fL to 2.8 fL, (i.e., the limits shown in Holladay's Table 1). This correspondence of results includes the following: a change of the image difference luminance characteristic, from a higher to a lower slope, in the 1 to 3 fL range, a plateau effect at the lower end of the second background luminance segment (i.e., in the decade above 0.001 fL) and a return to a higher slope at the beginning of the third background luminance segment.

Another notable feature of the image difference luminance requirement characteristic of Holladay, for an image detection task, is that it is just below Blackwell's characteristic for a target subtending an angle of 55.2

minutes of arc, in the third background luminance segment, but transitions to a location slightly above the 18.2 minute of arc characteristic, in the first background luminance segment. This shift could be indicative of a difference in the way that Holladay's visually more complex detection target is perceived, and/or mentally processed, when sensed in the third background luminance segment (i.e., which coincides with the scotopic vision range in humans), versus when it is perceived in the first background luminance segment (i.e., which coincides with the photopic vision range). It is interesting, and possibly also significant, that Holladay's target, previously described as blurred annular ring of light having a maximum difference luminance on a 54.9' diameter circle, has almost the same dimension as the outside diameter of Blackwell's 55.2' target circle, the image difference luminance characteristic to which Holladay's characteristic is nearly coincident in the scotopic vision range.

The task performed by Holladay's test subjects involved detecting the image difference luminance when an image appeared or disappeared. Even without this information, the unique signature of the image difference luminance requirements characteristic, obtained by Holladay, serves as an independent confirmation that the task, performed by Holladay's test subjects, was, indeed, an image detection rather than an image identification task. Based on this finding, it can be concluded that the differences in the angular response characteristics, obtained by experimenters using image identification and detection tasks, is yet another aspect of the fundamental psychological differences, which exist in the ways images, sensed by the eyes, are perceived and interpreted by the brain.

Assuming the differences in the veiling luminance angular response characteristics of the eyes observed by these experimenters are real, and there is no reason to believe otherwise, a question arises as to whether the explanation for the observed psychological differences between the results of image detection and image identification tasks also has a physiological component. The answer to this question will be explored in the next subsection.

3.7.3. Physiological Response to Scattered Glare Source Light*

The experimental evidence available to assist in the formulation a physiological explanation for the veiling luminance angular response discrepancies at small angles is quite limited. Nonetheless the information that is available is still quite important, since it provides experimental evidence to support the conclusion that the veiling luminance angular response model, derived from Jainski's data, is applicable for controlling the legibility of aircraft cockpit instruments, controls and panels not only under daylight but also under night viewing conditions, with equal validity. The importance of this finding is that it validates the applicability of the automatic legibility control model under the full range of illumination environments experienced by a pilot when flying an aircraft.

The balance of this section is devoted to the presentation of a variety of types of information, which, when considered as an integrated whole, show that the conclusion described in the preceding paragraph is correct. This presentation starts with a description of additional experimental results of Stiles, and an analysis of the data of Holladay, that are relevant to drawing a physiological distinction between the origins of their angular response characteristics with those of Jainski and Nowakowski. Following this, the image detection characteristics of Blackwell are interpreted in terms of the photopic, mesopic and scotopic regions of vision. To aid in this interpretive effort, the spectral sensitivity characteristic differences between rod receptors and cone receptors, both inside and outside the central fovea, are considered along with the changes in these characteristics as a function of the luminance level the observer is adapted to and the size of the test image. To permit these results to be interpreted in terms of the physiology of retinal receptors, the numbers,

---

* The factual information concerning the eyes that is presented in this section was taken primarily from the following books: Vision and Visual Perception and Color Science. See the list of references for complete reference citations.

geometries, densities and sizes of rod and cone receptors, within the eyes, are reviewed and their potential relationships to the image difference luminance versus background luminance characteristics and the angular dependence of veiling luminance are explored. An explanation of the image size and image critical dimension dependences, indicated by the threshold image difference luminance versus background luminance characteristics and the threshold spectral sensitivity versus wavelength data, is also described, couched in terms of the spatial frequency dependence of threshold contrast sensitivity, on the processing of visual information by the brain. Other factors that influence the type of retinal receptor selected by the brain for use in performing a visual task are also explored. This includes the following: the blind spot that appears in the center of the fovea at low enough light levels; the need to perceive the color of an image; the low luminance limit on cone receptivity; the high luminance rod saturation limit on receptivity; the size of an image or of its critical detail dimension; and the mesopic to scotopic transition. Published characteristics, showing the time dependence of dark adaptation and the factors that influence that time dependence, are also employed to aid in interpreting the retinal receptors used to carry out visual tasks. Next, the implications of a transition between cone and rod light receptors, is considered as a likely explanation for the plateau effect dependence on image size, in the image difference luminance characteristics of Blackwell. Following this, the differences between the two experimental designs used by Blackwell to present targets to test subjects, in combination with the sizes of the targets, are considered as a possible explanation for whether signals transmitted to the brain by cone or rod light receptors are used to perceive a particular target. The presentation of information is concluded with a description of the effect of differences in cone and rod angular receptivity, as the likely cause of the differences in the veiling luminance angular responses observed by the different experimenters.

3.7.3.1. Interpretation of Stiles and Holladay Image Detection Task Experimental Data

In the 1929 article of Stiles, the angular dependence of the veiling luminance equation is stated to be valid for glare source angles from 1 to 10 degrees, for display background luminances of from 0 to 0.69 fL (i.e., the reported test range went up to 6.79 fL), and for glare source illuminance levels from 0 to 1 fc. As previously described, the valid range for the power of 1.5 exponent on the veiling luminance angle dependence equation is shown in Figure 16 of the 1929 article by Stiles to extend only up to background luminances close to 0.04 cd/ft^2 (0.126 fL). Thereafter, the figure shows the power of the angular dependence of Stile's veiling luminance equation decreasing from 1.5 down to a value of 0.8 at a background luminance of 3.1 fL, the largest background luminance value shown in the figure. As noted previously, the nominal 0.8 final value of the power is only slightly greater than the powers found to fit the small angle veiling luminance data of Jainski and Nowakowski.

By comparison with Stiles test conditions, Holladay's 1927 test results were collected for angles from 2.5 to 25 degrees, for background luminances from 0.000186 fL up to 0.929 fL and for glare source illuminance levels, measured at the eyes, from 0.023 to 0.56 fc. As previously described, the angular dependence test results of Holladay can be interpreted as not that different from those of Stiles. In addition, at the 5 degrees angle chosen by Holladay to examine the effect of different background luminance levels on the values of the veiling luminance angular dependence function*, $M(\theta)$, the values of $M(\theta)$ corresponding to the highest background luminance level tested, 0.929 fL, were found to be inconsistent with the values of $M(\theta)$ collected at lower background luminance levels of 0.0929, 0.00929, 0.000929 and 0.000186 fL. This problem with Holladay's data, starting at background luminances somewhere between 0.0929 and 0.929 fL, agrees with Stile's admonition that the angular dependence of the empirical veiling luminance equation becomes invalid for background luminance levels above 0.69 fL (i.e., because the power on the angular dependence becomes smaller).

Stiles' findings, indirectly supported by the preceding analysis of the earlier findings of Holladay, indicate that the change in the angular dependence of veiling luminance occurs over a background luminance range

---

* Refer to Section 3.6.2.3, and Table 3.9.

which corresponds to the known transition from the high end of the mesopic vision range into the low end of the photopic vision range. Since photopic vision is associated with cone receptors, scotopic vision is associated with rod receptors and mesopic vision is associated with both types of receptors, the preceding results of Stiles and Holladay would suggest that, while detecting the test image, the subjects' eyes undergo a change from using rod receptors or a combination of cone and rod receptors to using cone receptors, alone, as the background luminance increases from the mesopic into the photopic luminance range.

It had initially been considered plausible that the differences between the experimenter's published veiling luminance angular response characteristics could be associated with the capture of instances, in a gradual transition, from the angular dependence of the eyes' rod receptors under scotopic night viewing conditions, through the mesopic range and up into the range of photopic daylight viewing conditions. The test results of Stiles and Holladay shows that this possible interpretation is incorrect. Instead, the veiling luminance angular dependences of Holladay and Stiles are constant in the scotopic and much of the mesopic vision ranges, and the transition in the angular characteristics occurs at the top of the mesopic vision range, over a background luminance range that is just somewhat less than a decade in extent.

Although the preceding physiological explanation for the differences in the angular weighting functions obtained from the experimental test results of Holladay and Stiles, and those of Jainski and Nowakowski, seems reasonable, by itself the explanation is incapable of resolving all of the compatibility issues, and in particular those raised by the test conditions associated with Nowakowski's experiment. In fact, the overall experimental evidence available from all sources points to the actual relationships being both multifaceted, and also quite complex, as will become progressively more evident, as the presentation and discussion of the available physiology related evidence progresses throughout the remainder of this section.

3.7.3.2. Interpretation of Nowakowski and Jainski Identification Task Experimental Data

In the Nowakowski 1926 article, the angular dependence of the veiling luminance is given by Equation 3.74 and is reported to apply for glare source angles from 10 to 90 degrees, for incident illuminance levels that equate to background luminances of from nominally 0.2 to 5 fL, and for glare source illuminance levels from 0.426 to 6.1 fc. The Nowakowski background luminance range of from 0.2 to 5 fL overlaps much of the 0.126 to 3.1 fL range of Stiles, where the transition in the angular dependence of the veiling luminance function occurs. The resolution of this apparent conflict between the result of Nowakowski and the results of Stiles and Holladay can be ascribed to the previously described psychological difference in the image identification and detection visual tasks being performed by the test subjects.

As previously stated, the fundamental differences in the image difference luminance versus background luminance requirement characteristics, for image detection and image identification tasks during dusk through night background luminance levels, provide unique signatures that distinguish between these psychological tasks as was illustrated in Figure 3.34. An examination of the image identification characteristics, as typified by those of Jainski plotted in Figure 3.10, shows evidence of a change in the image difference luminance characteristic occurring as background luminance levels decrease below about 3 fL down to somewhat above 0.003 fL. Thereafter, the image difference luminance characteristics, for the image identification task, remain constant down to the lowest levels a human can sense (i.e., slightly less than 10^{-6} fL), even though the last three decades of the decrease occur in the scotopic range of background luminance values.

To be able to identify images, rather than simply detect their presence or absence in a visual scene or on an aircraft cockpit display, a need exists to be able to resolve the critical detail dimensions of the display images. This need translates into a requirement for an observer to use the minimum separable visual acuity capabilities of eyes to resolve display images or real-world scene objects, which, in turn, establishes corresponding minimum image difference luminance requirement characteristics that are consistent with the required level of image identification performance. The need to be able identify displayed images, of the small sizes, and even smaller image critical detail dimensions, that are typically encountered on aircraft instruments

and panels, demands the use of foveal cone receptors, and the selective mental processing of information sensed by them to make the identification possible. Irrespective of how low the background luminance becomes, information sensed by foveal cone receptors must therefore be used by the brain to make image identification on cockpit displays possible. In comparison to this relatively straightforward and logically self-consistent composite psychological and physiological explanation for image identification on aircraft instruments and panels, the explanation for image detection can at best be described as complex and not readily amenable to being defined with any degree of precision.

3.7.3.3. Interpretation of Blackwell's Image Detection Task Experimental Results

An observer's ability to elect, at will, whether to perform an image detection, or an image identification, task, implies the existence of an underlying ability by the mind to segregate, select and then process distinct stimuli emanating from the eyes, and transmitted to the brain, which are associated with these two tasks. The need to be able to reconcile the veiling luminance angular response characteristic differences between the results of Stiles and Holladay, and those of Nowakowski, where both are attributable to the operation of the eyes under the same ambient lighting conditions, and where both could be operative simultaneously, within the observer's instantaneous field of vision, increases the likelihood that a part of the explanation for this difference is associated with the physiology of the eyes. To explore this possibility further, the image detection data of Blackwell will be considered in greater detail, in an attempt to determine the operative eye physiology, while performing image detection tasks.

In discussing the contrast sensitivity results, for image detection at the 50% threshold legibility accuracy level, Blackwell stated that "Two interesting aspects of the contrast sensitivity functions are apparent." One of these aspects was that "there is no appreciable change in the threshold contrast" at high background luminance levels. For image difference luminance thresholds, rather than contrast thresholds, this statement by Blackwell is equivalent to saying that the image difference luminance increases or decreases, approximately in direct proportion to a corresponding increase or decrease in the background luminance. The other aspect of interest, cited by Blackwell, was that "Each of the curves shows a discontinuity at approximately 7×10^{-4} footlambert." The discontinuity in question was actually an abrupt change in the slope (i.e., an inflection point) of the contrast versus background luminance characteristics used by Blackwell to fit the experimental data. After an "interrogation" of his test subjects, Blackwell concluded that this common anomaly in the characteristics was associated with a change in the test subject's scanning. "Since the test subjects were allowed to fixate where they chose, they used foveal vision at high brightnesses and parafoveal vision at low brightnesses." Blackwell's usage of the terminology high and low brightnesses, translates into high and low background luminances in the terminology used in this report.

In stating that "there is no appreciable change in the threshold contrast" at high background luminance levels, Blackwell cited his 121 minute of arc subtended angle test image data, as an example to illustrate his point. In a close examination of the 121' target size data, using the previously described 22.5 inch square full logarithmic graph of the Blackwell data, shown at reduced size in Figure 3.31, it was found that the Blackwell image difference luminance data points at 11.9 and 120.3 fL of background luminance, for the 50% threshold legibility characteristic upon which Blackwell based his statement, very nearly coincide with the 0.926 slope determined for Jainski's characteristics (i.e., the Blackwell slope was just slightly greater). A similar examination of the 121' target data points at 0.887, 11.1 and 70.8 fL of background luminance, for Blackwell's minimum threshold legibility characteristic in Figure 3.32 (i.e., which Blackwell did not comment on), confirmed the very close correspondence of the slope with that determined for Jainski's characteristics (i.e., the Blackwell slope was just slightly smaller). It should be noted that Blackwell's quoted assertion can be justified, if the data point at 11.9 fL for the 50% threshold legibility characteristic is not used and a straight line is drawn from a data point at 1.19 fL to the 120.3 fL point in Figure 3.31. In this case, the slope is still less than unity but is close enough to justify Blackwell's assertion.

Referring to Figure 3.34, it may be seen that the 121' 50% threshold and 360' minimum threshold

characteristics both show an increased slope in the image difference luminance characteristic between nominally 10 and 1 fL. This change in the slope is, however, likely to be only illusory, since the data points, at 3.4 fL on both characteristics, are the result of the previously described straight line interpolation needed to draw the characteristics using the graphing program, rather than being real data points. If the slope of the Jainski characteristics, which is applicable to the photopic vision range, is correct, then the downward shift that can be observed in Figure 3.34 for both of the characteristics, near 1 fL and below, would be associated with the photopic to mesopic vision transition, in the background luminance range of 1 to 3 fL, for these larger target sizes. All of the aforementioned variations are totally masked, when the data is plotted in the contrast versus background luminance format used by Blackwell.

At high background luminance levels, and down to and including the change in the characteristics at about 3 fL, Figure 3.34 shows that the image difference luminance requirement characteristics for image detection and image identification are very similar to one another. Below the 3 fL background luminance level, it may be seen that the image difference luminance requirement characteristics for image detection become much more complex than the image identification characteristics.

The other "interesting aspect" of the image detection characteristics, cited by Blackwell, appears different, when plotted as image difference luminance versus background luminance, than it does in Blackwell's contrast versus background luminance format. Namely, the common inflection point that appears at 0.0007 fL on Blackwell's contrast versus background luminance characteristics, instead appears at between 0.001 and 0.002 fL on the image difference luminance versus background luminance characteristics. This inflection point is quite evident even at the small sizes of the graphical presentations in Figures 3.31 and 3.32. As previously stated, Blackwell associated this anomaly in the contrast characteristics with a transition from using foveal cone receptors to parafoveal rod and cone receptors as the background luminance levels decrease through the inflection point. Based on the physiology of the eyes, this transition would have to represent a change from the test subject using either the cone receptors of the central fovea, or the cone and rod receptors that occupy the foveal annular ring surrounding the central fovea, within the mesopic vision range, to using rod receptors in the scotopic vision range below 0.001 fL, since only rod receptors are active in the scotopic range.

If the preceding assertion by Blackwell is valid, then it infers that the transition that occurs at the top of the mesopic vision range, from foveal cone receptors in the photopic vision range to foveal cone and rod receptors in the annular ring surrounding the central fovea in the mesopic vision range, was responsible for the change in the angular response characteristics of Stiles and Holladay. This result points to the possibility of the mesopic transition being more complex than simply a transition from cone to rod receptors. To explore the potential conflict between these two physiological transitions further, other sources of information concerning the operation of cone and rod receptors in the mesopic vision range are explored below.

3.7.3.4. Implications of the Spectral Receptivity of Retinal Receptors under Photopic, Mesopic and Scotopic Light Adaptation Viewing Conditions

Based on the light adaptive state of the eyes' light receptors, vision is divided in the literature into the categories of photopic, scotopic and mesopic. Photopic vision is associated cone light receptors, daylight vision and rapid adaptation between light levels. Scotopic vision is associated with rod light receptors, dark adapted night vision, and slow, or very slow, adaptation between light levels. Mesopic vision is an intermediate range of states between photopic and scotopic vision where both rod and cone receptors are credited with being operative.

The general consensus in the literature is that the eye's cone receptors are used to see both small and large images, which are perceived in color at photopic adaptation levels, whereas rod receptors are used to see large images, which are perceived to be achromatic (i.e., perceived in black and white), at scotopic adaptation light levels. Other than to identify the mesopic vision region as a three and a half to five decade range, over which the eyes transition from the scotopic visual receptivity characteristics, of rod receptors, to

the photopic visual receptivity characteristics, of cone receptors (i.e., the only visual region in which both types of receptors are credited with being functional), the literature provides very little unambiguous information concerning this visual range. It should be noted that even the preceding statement of the extent of the mesopic background luminance range is ambiguous, given the one and a half decade uncertainty in its specification. This uncertainty arises due to differences in the experimental variables and criteria, used in the literature to measure the extent of the mesopic vision range.

It should be noted that the ability to perceive the color of an image is a signature indication that the visual cortex of the brain is processing information sensed by the cone light receptors in the eyes. Likewise, the perception of an image as achromatic is a signature indication that the rod light receptors are being used. When the image difference luminance exceeds the minimum level needed to resolve the critical detail dimension of an image, and, thereby, make it identifiable, then its color will also be perceptible, however, this does not hold for the scotopic identification of images using rod receptors. Likewise, if the image difference luminance is only just sufficient to be able to detect the presence or absence of an image, it may still be perceived in color if the light adaptive state of the retinal receptors, the target size, and possibly other factors, are such as to cause the brain to select signals originated by cone receptors to be used to detect the image.

Among the attributes associated by a human, as the result of perceiving light sensed by the eyes, color is probably the most studied and least understood. The only aspect of color vision that will be addressed here is the spectral sensitivity response of the eyes to light at different wavelengths, and the changes that occur in that sensitivity as a function of the adaptive state of the eyes' light receptors. The visual tasks employed for these tests typically involve bipartite field brightness matches, and, therefore, are most nearly comparable to a detection task. The consensus concerning the results of this type of testing may be summarized by saying that the cone light receptors in the eyes are responsible for the spectral characteristics obtained under photopic viewing conditions, and rod light receptors are responsible for the different characteristics obtained under scotopic viewing conditions. The significant difference between the spectral characteristics attributable to sensing with cone and rod receptors causes a spectral sensitivity measurement to provide an unambiguous indication of whether cone receptors, rod receptors, or a combination of both, are operative. Unfortunately, difficulties in achieving repeatable test results, in the mesopic vision range, have resulted in very little published spectral sensitivity data, for this range of background luminance values. In the literature, this result is attributed to the inability to achieve test conditions that are sufficiently reproducible, to avoid inducing variations in the spectral characteristics because of changes in the adaptation level of the test subjects, within the mesopic transition range.

Both Judd,[98] of the National Bureau of Standards, and Bartlett[99] start their discussion of the human's spectral sensitivity characteristics by reporting on an investigation by Wald.* In Wald's investigation, a test image, subtending 1 degree of visual arc, was used to determine the spectral sensitivity characteristics for cone receptors, located in the central fovea, and for both cone and rod receptors, located 8 degrees above the fovea, in an area beyond the outer boundary of the 8.6 degree diameter parafovea, but within the 19 degree outside diameter of the perifovea. The resulting spectral characteristic for the photopic adapted foveal cones and the scotopic adapted perifoveal rods were individually in fair agreement with the results of other experimenters. It is considered significant that the spectral sensitivity characteristic of Wald, for photopically adapted perifoveal cones, was quite similar to the one for the foveal cones but with slightly lower overall sensitivity.

Constant luminance spectral sensitivity characteristics of cone light receptors in the central foveal (i.e., in the nominal 2 degree diameter area of the fovea that is free of rod light receptors) are reported by Judd[100] to be essentially invariant for photopic adapting luminances of from 1 to 10,000 fL. The maximum photopic spectral sensitivity for these cone receptors is found to occur at approximately 555 nm, and corresponds to spectral yellow-green light. For higher and lower wavelengths, the spectral sensitivity decreases, at first slowly,

* Wald, G., "Human Vision and the Spectrum," Science, Vol. 101, June 29, 1945, pp. 653-658.

and eventually by nearly five orders of magnitude, for blue and red spectral light at the practical spectral vision extremes of 380 and 780 nm, respectively (see $\bar{y}_\lambda$ color matching function, from Table 3.3 in Wyszecki and Stiles).[101]

The invariance in the spectral sensitivity characteristics claimed for cone receptors, at photopic levels, is also ascribed to rod receptors, at scotopic adapting field luminance levels.[102] The difference between these spectral sensitivity characteristics is that the sensitivity of rod receptors is greater, and the maximum sensitivity occurs at nominally 507 nm, for 0.00001 fL and lower constant luminance spectral sensitivity characteristics.

Judd also presented absolute spectral sensitivities for "the average normal eye," for constant luminance characteristics in the mesopic vision range that spanned the interval between the photopic and scotopic characteristics. The data was shown both in a table, Table 5, entitled "Absolute Luminosities (Lumens/ Watt)" and in an accompanying figure, Figure 2, which shows characteristics of the logarithm of spectral radiance versus the wavelength, with constant values of adapting luminance from 1 fL to 0.00001 fL, in decade increments, stipulated as parameter values. The table and figure were both attributed to a data analysis by Weaver,* using data originally reported by Jones.** The spectral characteristics, intermediate between 1 fL and 0.00001 fL, were described by Judd as having been determined by Weaver, through interpolation, and represent the spectral sensitivities of a combination of rods and cones in the mesopic vision range. In commenting on these results, Judd stated that "Although these intermediate data are subject to revision on the basis of further experimental study, they have served very satisfactorily and may be provisionally recommended."

In a discussion, preceding the introduction of the information in preceding paragraph, Judd stated that cone vision is usually assured by using 2 degree centrally fixated fields, for the measurement of the photopic characteristics of the central fovea cone receptors, and that 5 degree, or larger, centrally fixated fields are needed for measuring the spectral characteristics of rod receptors. The larger size of the photometric fields, needed to measure rods, was commented on by Judd to be necessary "because most observers have a central rod-free area of about 2 degrees." As represented by this data, the majority of the 48 nm shift in the peak spectral sensitivity, from 555 nm at 1 fL of adapting luminance, to 507 nm, at 10^{-5} fL of adapting luminance (i.e., a shift which is known as the Purkinje effect), occurs between about 0.2 and 0.001 fL. No explanation was given to aid in how to interpret or apply the interpolated mesopic spectral sensitivity transition characteristics, in relation to change from a 2 degree photopic to a 5 degree, or larger, scotopic centrally fixated test field.

The accepted photopic spectral sensitivity characteristic, for use in representing the response of cone receptors, was adopted as a standard by the International Commission on Illumination (i.e., Commission Internationale de l'Eclairage, abbreviated CIE) in 1924. The standard is considered applicable to images of 4 degrees and smaller in diameter and is described by Judd as differing, in the blue area of the spectrum, from the characteristic that would be adopted today. Still another photopic spectral characteristic was standardized by the CIE in 1964, for a large-field standard observer. This characteristic is reported to be applicable to visual fields subtending an angle greater than 4 degrees, and centered on the fovea.[103] The scotopic spectral sensitivity characteristic standardized by the CIE in 1951, to represent the response of rod receptors, was derived from the previously described experimental results of Wald, and those of Crawford.*** This

---

* Weaver, K. S., "A Provisional Standard Observer for Low Level Photometry," Journal of the Optical Society of America, Vol. 39, 1949, p. 278.

** Jones, L. A., "Summary of American Option BS/ARP 18, British Standard Specification for Fluorescent and Phosphorescent Paint," Transmitted to Dr. P. G. Agnew, Secretary, American Standards Association, June 2, 1942.

*** Crawford, B. H., "The Scotopic Visibility Function," Proceedings of the Physical Society, Vol. 62B, 1949, p. 321.

characteristic was further described by Wyszecki and Stiles as applicable to the mean spectral sensitivity, for "observers whose age does not exceed thirty, when observing at angles of not less than 5 degrees from the foveal center, under conditions of complete dark adaptation."[104]

In contrast to the gradual mesopic transition from photopic cone receptors to scotopic rod receptors described by Judd, Bartlett described experiments conducted by Kinney,* on rod receptors located 10 degrees from the center of the fovea and, therefore, in an area of the retina just inside the near periphery. Kinney's experiment was described as covering a range of five log units above the scotopic threshold, which consequently included the mesopic vision range. As reported by Bartlett, "Kinney found that peripheral luminosity curves remained basically scotopic with a maximum near 510 mμ for 3.5 to 4 log units above threshold, through the mesopic range (intermediate light adaptation)."[105] Bartlett went on to say that "At a 5 log unit level, the curve shifted its maximum toward 540 mμ and showed a small relative loss in sensitivity to the smaller wavelengths" and that "the effect of illumination of background was slight." Bartlett also noted that "Kinney's data are, among others, similar to those of Hsia and Graham (1952)."** In another chapter of the book Vision and Visual Perception, entitled "Discriminations that Depend on Wavelength," when referring to experiments conducted by Sloan,*** Graham makes the following general statement: "If the area of stimulation includes both cones and rods, the luminosity curve may be taken to represent cone function at high intensities and rod function at low intensities."[106]

In another reference to the 1928 experimental observations by Sloan, Bartlett made the following statements concerning the spectral sensitivity of cone receptors, in the foveal area of the retina: "For a size of stimulus that fell within the rod-free area, Sloan found that, under conditions of dark adaptation, the photopic luminosity curve changes shape with change in intensity level; in particular, the position of maximum luminosity changes from 555 to 540 mμ for intensities below 0.2 meter-candle"; (i.e., 0.2 lx or 0.0186 fc) "at intensities above this level and under conditions of light adaptation, the wavelength of maximum luminosity remains near 555 mμ."[107] This result is interesting because it shows that in an experiment, which attempted to restrict exposure of the fovea to its central 2-degree rod free area, no change in the observer's color sensitivity occurred down to 0.0186 fc. The shift in the spectral sensitivity maximum below this level, suggests a transition, from the use of cones, to the use of either parafoveal rods, or to a combination of parafoveal rods and cones, to make continued image detection possible, after reaching the sensitivity limit of central fovea cones. Because the previously cited results of Wald, for parifoveal cones, did not show any significant change in the shape of the spectral sensitivity characteristics in comparison foveal cones, only a slight overall reduction in sensitivity, the shift in the maximum of the spectral sensitivity characteristic below 0.0186 fc can be interpreted as a change from cones to rods. Wald's tests of parifoveal cone receptors did include low light levels, by virtue of using the cone phase of the two phase time dependence of the human's dark adaptation response, to separate the parafoveal cone and rod responses.

The preceding result of Kinney indicates that, for a location just inside the near peripheral area of the retina, the transition from rod to cone receptors occurs at the top rather than distributed across the entire mesopic vision range. Moreover, this result is consistent with the veiling luminance angular response transition of Stiles for nominally the same luminance range. The implication is that the Stiles and Holladay veiling luminance angular response transition is also between rod and cone light receptors.

---

* Kinney, J. A. S., "Comparison of Scotopic, Mesopic and Photopic Spectral Sensitivity Curves," Journal of Optical Society of America, Vol. 48, 1958, pp. 185-190.

** Hsia, Y. and C. H. Graham, "Spectral Sensitivity of Cones in the Dark Adapted Human Eye," Proceedings of National Academy of Sciences, Vol. 1, 1952, pp. 80-85.

*** Sloan, Louise L., "The effect of Intensity of Light, State of Adaptation of the Eye, and Size of Photometric Field on the Visibility Curve," Psychol. Monogr., Vol. 38, No. 173, 1928.

It should be noted that Kinney's results do not necessarily contradict the gradual mesopic transition between cone and rod receptors described by Judd, which involved a centrally fixated target, but it does point to a potential problem being able to predict which retinal receptor areas will be selected for use by an aircrew member, when the mind, rather than an experimental procedure setup and the instructions given to the test subjects, determines the retinal receptor signals to be used to detect a target, at any particular eye adaptation level. The literature reviewed does not provide information regarding the selection criteria used by the mind, to perform image detection or identification tasks, when the mind is free to direct the eyes to select the best signals present, from anywhere within the retina.

In discussing the breadth of human spectral sensitivity characteristic test results, Bartlett states that "The CIE luminosity curve for the Standard Observer is a representative scheme that by no means represents all the data of cone luminosity; in fact, the shape and position of the luminosity curve depends upon a considerable number of controlling variables."[108] One of Bartlett's examples is particularly relevant to the present analysis. In the example, Bartlett states that "an increase in the stimulus area results, even within an anatomically homogeneous area of the retina, in a decrease in threshold for a given wavelength (see, e.g., Graham and Bartlett, 1939)." This behavior is entirely consistent with the image difference luminance versus background luminance requirement characteristics, for both image identification and detection, in that these characteristics show progressively lower image difference luminance thresholds, as the image critical detail or target dimensions increase in size (i.e., at least up to limiting size values). An eye physiology-based explanation, for these behaviors, was not found in the literature reviewed. An alternative explanation for the test image size dependences of the spectral and image difference luminance sensitivities of the eyes is explored below.

3.7.3.5. Influence of Photopic, Mesopic and Scotopic Adapted Viewing Conditions on the Performance of Image Detection and Identification Tasks

Since image detection occurs over the full range of background luminance levels, to which the eyes can adapt, and since only cone receptors operate under viewing conditions, considered in the literature to be purely photopic, that is, for image difference luminance and background luminance level combinations that are greater than 3 fL, it can be concluded that both image detection and identification must be performed by retinal cone receptors under photopic viewing conditions. At the other extreme, practical night vision experience shows that image identification can occur under purely scotopic viewing conditions, where only rod receptors are operative, provided that the images have sufficiently large critical detail dimensions to permit them to be identified, using the groupings of rod light receptors in the eyes.

Direct experimental evidence of human image identification capabilities, at scotopic vision levels, has been reported by Bartlett, in the form of the time dependence of the dark adaptation recovery response of humans, following preadaptation exposure to a luminance of 1,500 mL (i.e., 1,394 fL). In particular, Figure 3.35 is a reproduction of Bartlett's Figure 8.7 of the book Vision and Visual Perception.[109] This figure shows threshold luminance versus time characteristics, with visual acuity as a parameter. The data depicted in this figure is attributed by Bartlett to Brown, Graham, Leibowitz and Ranken.** The test images, used to collect the threshold luminance versus time dependence characteristics of dark adaptation, were single dimensional line gratings, having lines and spacings of equal widths, in the range from 0.96 to 23.8 minutes of arc, as subtended

---

* Graham, C. H. and N. R. Bartlett, "The Relation of Size of Stimulus and Intensity in the Human Eye: II, Intensity Thresholds for Red and Violet Light," Journal of Experimental Psychology, Vol. 24, 1939, pp. 574-587.

** Brown J. L., C. H. Graham, H. Leibowitz, and H. B. Ranken, "Luminance Thresholds for the Resolution of Visual Detail During Dark Adaptation," Journal of the Optical Society of America., Vol. 43, No. 3, 1953, pp. 197-202.

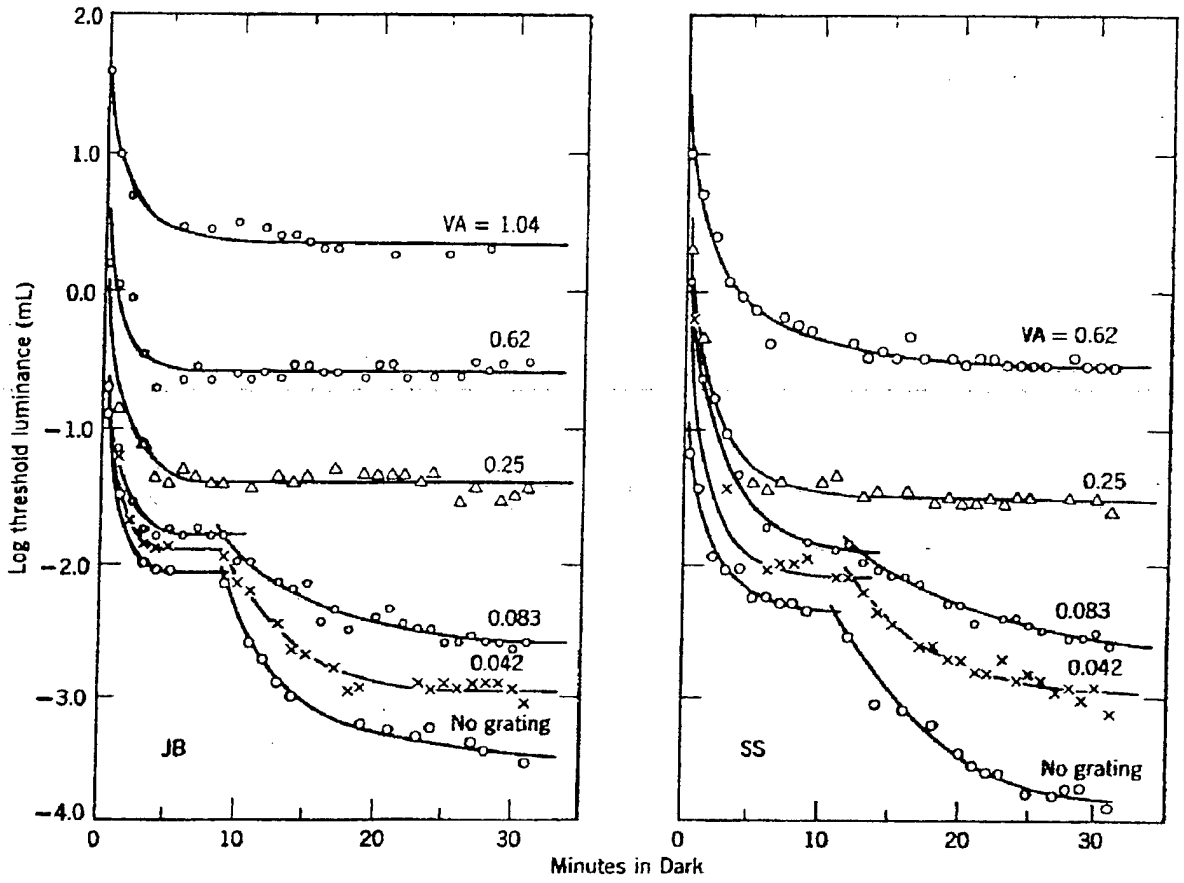


Figure 3.35. Dark Adaptation as Characterized by Determining the Threshold Luminance of a Line Grating Following a Preadaptation Luminance Exposure of 1,500 fL.*

at the eyes. The signature two phase response-time decay, to a fully dark adapted state, with the start of the second phase of dark adaptation being associated with the transition from mesopic to scotopic vision, is evident in these parametric characteristics. Based on these characteristics, the transition to scotopic adapted viewing of these gratings starts for line/spacing widths somewhere between 4 and 12 minutes of arc. For 4 minute of arc, and smaller line/spacing widths, the second slower dark adaptation phase does not occur. The shape and dimensions of the test field upon which the grating was superimposed was not specified. Although the commentaries in the literature are intentionally vague, with respect to identifying whether the mesopic adapted retinal light receptors are cones, rods or a combination of cone and rod receptors, following the transition to the second phase of dark adaptation, agreement exists that scotopic adapted rod light receptors are used, exclusively, to perform both image identification (i.e., minimum separable acuity) and detection tasks. For purposes of comparison, the experiment included a detection task in which the line grating was removed. This characteristic in effect served as a lower bound on the characteristics shown in the figure and consequently exhibited the lowest threshold luminance values and the largest sensitivities.

Unlike photopic image detection, no experimental tests were found which attempted to determine image difference luminance versus background luminance characteristics for image identification tasks under

* Figure 8.7 in Bartlett, N.R., Vision and Visual Perception, p. 195. Data from Brown, J. L., C. H.Graham, H. Leibowitz and H. B. Ranken, 1953, pp. 197-202.

conditions considered in the literature to be purely scotopic, that is, for image difference luminance and background luminance level combinations that are both less than nominally 0.001 fL. For that matter, with the exception of Blackwell's experimental results, surprisingly little direct experimental evidence, relevant to image detection tasks under photopic viewing conditions, was found in the literature. This may be true, because the common practice of extrapolating Blackwell's photopic image detection results, beyond the 120 fL background luminance limit of the data, has provided satisfactory predictions in the past.

3.7.3.6. Interpretations Based on the Physical Geometry of the Retina and of its Light Receptors

To permit a more in-depth exploration of the physiology of the eyes, and its potential relationship to the previously described experimental test results for the three adaptation regions, the physiology of the retinal receptors is considered in greater detail in this subsection. According to Brown's Figure 2.11, in the book Vision and Visual Perception[110], the spatial density of cones in the retina is highest in the central fovea, where cones are believed to be coupled one-on-one to the optic nerve pathways to the brain. Beyond the central fovea, the density of cones decreases, following what appears to be an exponential curve, to a nearly constant level in the middle peripheral regions of the retina beyond 20 degrees. The ordinate axis in Brown's Figure 2.11 is labeled "Number of rods and cones in an area 0.0069 sq mm" and shows the maximum number of rods and cones in the specified area to be about 1,975 and 1,843, respectively. This translates into maximum densities of retinal receptors being 286,100 rods/mm^2 and 267,100 cones/mm^2. Furthermore, if the light receptors in the retina are assumed to conform to a hexagonal packing structure, the preceding maximum rod and cone counts, in the specified 6,900 square micron area, would correspond to minimum center to center spacings of 2.009 microns for rods and 2.079 microns for cones. Using an external angle translation factor of 0.00345 degrees per micron (i.e., derived from similar conversions performed in Table 2.1 of Wsyzecki and Stiles[111]), the minimum separation of rods can be expressed as either 0.00693 degrees, or as 0.416 minutes of arc, and the minimum separation of cones can be expressed as either 0.00717 degrees, or as 0.430 minutes of arc. The central region of the fovea is also associated with the highest visual acuity (i.e., resolution) that the eyes are capable of achieving. From its maximum value in the center of the fovea, visual acuity thereafter decreases, again almost exponentially, as a function of increasing angles, from the edge of the central fovea.

The spatial density distribution of rods in the retina is more complex than for cones. It is reported that no rods exist in a central portion of the fovea, an area reported by Oesterberg* to be 1 degree in diameter and by Polyak** between 1.7 and 2 degrees.[112] Starting just inside the outer boundary of the fovea, the increasing density of rods already equals that of cones and after that increases rapidly, until just shy of 20 degrees when it reaches the previously cited maximum value, and after that the density starts decreasing. The much higher density of rods over most of the retina does not, however, translate into an increase in visual acuity. The higher density of rods does result in total rod count in the retina of each eye of between 110 and 125 million, as compared with a total cone count of only 6.8 million as determined by Oesterberg's investigation. In his discussion of this topic, Brown[113] reports as few as 75 million or as many as 150 million rods are distributed over the retina surface, but only 6 or 7 million cones, giving as his sources Davson*** and the same book by Polyak.

Wyszecki and Stiles, in Table 2.2 of their book Color Science, cited Polyak as the source for there being 25,000 cones in an area of 1.4 degrees in diameter, located in the center of the fovea that is termed the foveola, where cones reach their maximum length and highest densities. They also cite Polyak in stating that

---

* Oesterberg, G., "Topography of the Layer of Rods and Cones in the Human Retina," Acta Ophthal. Kbh., Suppl. Vol. 6, 1935, pp. 1-102.

** Polyak, S. The Retina, University of Chicago Press, Chicago, IL, 1941.

*** Davson, H., The Physiology of the Eye, Blakiston Co., Philadelphia, PA, 1949.

there are more than 4 million cone receptors within the retina and between 110 and 115 thousand cones in the nominal 5.2 degree diameter area of the fovea. Brown states that "on the basis of light microscopy, it is estimated that there are approximately one million fibers in the optic nerve."[114] Brown goes on to hypothesize that electron microscopy might reveal the existence of many more optic nerve fibers. Wyszecki and Stiles, in Table 2.2 of their book, cited Polyak as the source for there being only between 0.8 and 1 million optic nerve fibers. Given the preceding large numbers of cone and rod receptors in the retinas of each eye, the small number of optic nerve fibers available to transmit all of these signals to the brain signifies that most of these signals must be combined before being connected to a single optic nerve fiber.

Besides changes in the density of retinal receptors, and in visual acuity, as a function of position on the retina, other physical properties of the retinal receptors are also position dependent. Size and shape differences exist in cone receptors based on their physical locations within the retina. The same can be said for rod receptors, but the differences are limited to changes in their sizes. Table 3.11 relates the position of light receptors in the retina to the corresponding sizes of the cone and rod receptors. This table uses the data of Polyak adapted from Tables 2.1 and 2.2 of the book Color Science that were previously cited. The intent of Table 3.11 is limited to showing the size relationships between retinal light receptors. The original tables may be referred to for more detailed information, on related aspects of the physiology of the retina, including, but not limited to, the number and thicknesses of cell layers, within the retina, as a function of position on the retina. Table 3.11 shows that the diameters of both types of light receptors progressively increase in going, from foveal or parafoveal vision locations on the retina, outward to the limits of peripheral vision. Although Brown references Polyak's work, he describes the cone receptors in the fovea as having a cylindrical, rather than conical in shape, and a 1.5 micron diameter. Brown goes on to describe the shape of foveal cones as being more nearly similar in shape to rods than to the cones located elsewhere in the retina.

Another eye physiology factor capable of influencing the angular response characteristics of veiling luminance relates to the neural connections between retinal receptors and the individual optic nerve fiber pathways to the brain. As previously stated, individual optic nerve fibers are believed to collect stimuli from single cone receptors in the central foveal area, where there are no rod receptors. Beyond this nominal 2 degree diameter central foveal area, individual optic nerves are believed to be connected to spatial groupings of rod receptors. The descriptions of the neural interconnections of cone light receptors, in the literature reviewed for this report, are more ambiguous. Although it is implied that rods and cones are both ganged, starting with the foveal annular ring that surrounds the central fovea where electron micrograph evidence shows an increase in interconnectivity, no definitive experimental results to that effect were encountered for cone light receptors. The groupings of rods are described by Brown[115] as becoming progressively larger as the distance from the parafovea increases, and are reported to reach rod grouping sizes of 100 before stimulating a single optic nerve fiber, within the middle to the far periphery.* Based on the nominal density distributions of rods in the retina (i.e., these distributions are not the same along radials, extending from the center of the fovea, at different radial angles), groupings of 100 rods would range in size, from a minimum of approximately 4.4 minutes of arc in diameter, for a circular area at 20 degrees from the center of the fovea, in the middle periphery, to approximately 7.5 minutes of arc, at 50 degrees, in the far periphery. It should be noted that consistency between the preceding results requires that if there are indeed only one million fibers in each optic nerve bundle, then either there must be more than 100 rods in the largest rod groupings or there must be considerably fewer than 100,000 rod receptors in the retina of each eye. An undercount of the optic nerve fibers would be the most likely source of these contradictory results.

No specific information, beyond the grating pattern dark adaptation test previously described, was found in the literature reviewed concerning the visual acuity at night adaptation levels where only rod receptors are used. The limitation on visual acuity experienced under these conditions presumably occurs because of the increasingly larger numbers of rods ganged together before they stimulate an individual optic nerve fiber,

---

* Vitter, V., "Recherches Biometriques sur l'Organisation Synaptique de la Retine Humaine," C. R. Soc. Biol., Vol. 143, 1949, pp. 830-832.

Table 3.11. Location and Dimensions of Light Receptors on the Retina of the Eye.

Retinal Region	Approximate Outside Diameter on Retina in Microns	Corresponding Angular Diameter on Retina In Degrees	Diameter of Cones with the Taper from their Inner Segment → Outer Segment in Microns	Diameter of Rods in Microns
Central Fovea	500 - 600	1.7 - 2	1.5 - 1.0 → 1.0	No Rods
Fovea	1,500	5.2	3.5 - 4.0 → 1.3	1.0
Parafovea	2,500	8.6	4.5 → 1.5 -2.0	1.0 - 1.5
Parifovea	5,500	19.0	5.0 → 2.0	1.5
Near Periphery	8,500	29.0	5.0 - 6.0 → 2.5	1.5 - 2.0
Middle Periphery	14,500	50.0	6.0 - 7.5 → 2.5	1.5 - 2.0
Far Periphery	40,000		8.0 - 9.0 → 3.0	1.5 - 2.0

as the distance of the image from the central fovea increases. The strongest evidence for cone receptors located outside the central fovea being ganged, to stimulate an optic nerve fiber, is the fact that there are many more cone receptors in the retina than there are optic nerve fibers. Other indications of the ganging of cone receptors include the appearance of additional neural connections outside the central fovea, and the fact that daylight visual acuity continues to decrease as the angle from the center of vision increases beyond 20 degrees, where the density of cones becomes constant. No detailed data on the retinal position dependence of rod and cone receptor grouping sizes was found in the literature reviewed.

The purpose of the preceding descriptions was to present information, relevant to considering the role that the light receptor physiology of the eyes could potentially be expected to play in the observed decreases in image difference luminance thresholds, for image identification and detection tasks, as image critical detail dimensions and test images increase in size, respectively, and for the observed changes in the veiling luminance angular response characteristics, applicable to image identification and target detection tasks. The potential relationships of these observed experimental dependences on the light receptor physiology of the eyes will now be further explored.

The primary function of the groupings of rod receptors appears to be the spatial compression of signals, from the light receptors spatially distributed throughout the retina, to reduce the number of signals that must be concurrently transmitted to and monitored by the brain. In response to exposure of the retinal light receptors, by the spatially and spectrally distributed luminances received from throughout the human's instantaneous field of view, the retina's neural networks spatially compress the signals before retransmitting them to the brain for processing over the much smaller number of optic nerve fibers. To accomplish this successfully the combination of the light receptors, the neural networks, the optic nerve fibers and the brain must maintain spatially consistent scaling between the luminances and colors perceived and those contained in the sensed scene. In this context, consistent scaling of luminances and colors refers to the observer's perception of brightnesses, contrasts and colors, for large and small areas in the scene, being consistent with the corresponding luminances and colors obtained through direct photometric measurements of the scene luminances and colors.

Inevitably, constraints on the visual capabilities of the human visual system limit the fidelity of this transfer of information. For example, the image difference luminance levels of the visual scene, internal and external to the aircraft cockpit, must be at a sufficient level above the threshold of vision, for a particular light or dark

adaptation state of the observer (i.e., sometimes called super threshold levels), to make high fidelity perception of a visual scene possible. Also, the imaged areas of the scene being perceived must be at least as large as the eyes' light receptors or groupings thereof, which are used by the brain to sense the scene images, if the scene is to be perceived with consistent spatial scaling of its photometrically measurable luminances and colors. Another way of describing this limitation of visual perception is that the observer's perception of a visual scene can remain true to the luminance levels and colors present in the scene, only when the image critical detail dimensions, for the identification of images contained in the scene, or the image sizes, for detection of images contained in the scene, are not so small as to approach the respective perceptual thresholds, invoked by the visual acuity limitations of vision. Under the conditions required for consistent perceptual scaling of visual scene luminances and colors, no direct evidence could be found in the literature reviewed that the grouping (i.e., ganging) of light receptors causes any increase in the spectral stimulus to the brain, beyond that caused by smaller groupings of light receptors or even individual light receptors.

As visual scene luminance levels are progressively reduced from the mesopic through the scotopic range, at a rate slow enough to insure that the test subject is statically adapted to the scene, various parts of the retina reach their maximum sensitivity limits (i.e., the minimum image difference luminances they can be stimulated by and afterwards, in effect, become blind) at different threshold luminance levels. The central fovea, with its high density of cone receptors connected one on one to optic nerve fibers, reaches this limit first at or near the transition from mesopic to scotopic vision. At the other extreme, the last receptors to become ineffective are the rod receptor groupings between 20 and 30 degrees from the center of the fovea. The previously described increase in the number of rods contained in each receptor grouping, starting just outside the central fovea and culminating with 100 rods in each grouping in the middle to far periphery, when combined with the gradual reduction in rod density with increasing angle, from its maximum value at 20 degrees, would be a likely explanation for the assertion by Judd that the maximum sensitivity of vision occurs in the zone between 20 and 30 degrees from the center of the fovea.[116]

While the preceding facts make it likely that the ganging of rod receptors, in combination with the retinal spatial density variations of rod receptors, is responsible for the observed variations in the maximum absolute sensitivity limits of dark adapted vision, as a function of position on the retina, no analogous evidence that the ganging of cones, outside the central fovea, produces a corresponding increase in their absolute sensitivity was found in the literature reviewed. In fact, the previously mentioned results of Wald for parifoveal cones found no notable difference between their spectral sensitivity characteristics and those of central fovea cone receptors, other than a small, nominally uniform, overall reduction in spectral sensitivity.

3.7.3.7. Interpretation of Image Size or Critical Detail Dimension Dependence of Image Difference Luminance using Spatial Frequency Dependent Contrast Sensitivity Functions

The mental processing of visual stimuli produced by images viewed under photopic conditions and in sizes small enough to fit entirely within the central fovea, where no groupings of cone receptors are believed to occur, still produces image difference luminance requirements that are strongly dependent on image critical detail dimensions of the images to be identified or on target size of the images to be detected. Since there is no ganging of light receptors in this area of the retina, this result suggests that physiology variations in retinal receptors can at best play only a limited role in determining the large observed variations in the threshold image difference luminance requirements, in response to changes in image critical detail dimensions and target sizes. The dependence of the threshold image difference luminance requirements is instead shown in the literature to be primarily related to spatial frequency dependent contrast sensitivity functions, used by the mind to process the spatial features of the images a human perceives.

The first investigation of the human's contrast sensitivity dependence on the mentally synthesized spatial frequency content of display or real-world scene imagery being viewed by a human appears to have been conducted by Schade.[117] In the experiment conducted by Shade, which is considered to be most relevant to the present discussion, the contrast sensitivities of human vision as a function of spatial frequency were

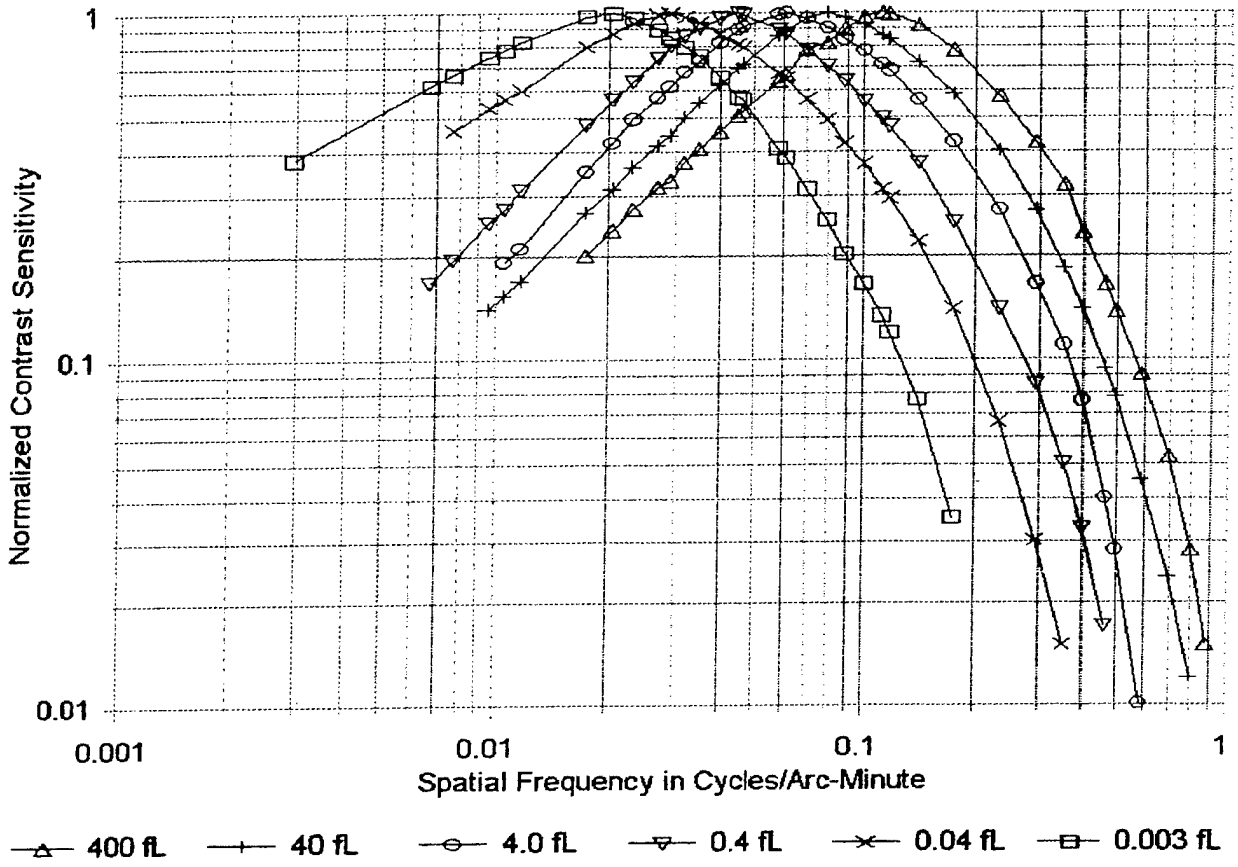


Figure 3.36. Schade Contrast Sensitivity Versus Spatial Frequency for a Linear One-Dimensional Sine Wave Pattern with the Mean Luminance of the Pattern as a Parameter and with the Maximum Sensitivity Normalized to Unity.

characterized by presenting test subjects with linear sine wave amplitude patterns, distributed in a single spatial dimension, on a cathode ray tube display. Holding the spatially averaged mean luminance of the pattern constant, the maximum to minimum luminance of the sine wave pattern (i.e., the image difference luminance) was varied to determine the value of threshold contrast between the peak to peak luminance levels just required to perceive the pattern at each of the different spatial frequencies tested.

Contrast sensitivity is the inverse of threshold contrast and is therefore also inversely proportional to the threshold image difference luminance. The contrast sensitivity was characterized by Schade at parameter values, for the spatially averaged mean luminance of the sinusoidal patterns, of 400, 40, 4, 0.4, 0.04 and 0.003 fL.[118] A plot of the experimental data, normalized to a maximum contrast sensitivity of unity, is shown in Figure 3.36. These characteristics show a significant shift in the normalized contrast sensitivity functions toward higher spatial frequencies as the mean luminance of the sine wave patterns is increased. If this result is translated from the spatial frequency domain to the spatial domain, it is equivalent to saying that an increase in the mean luminance (i.e., adaptation) level enables images with smaller critical detail dimensions to be identified, or smaller sizes of targets to be detected, which agrees with observations for the spatial domain. It should be noted that if these spatial frequency characteristics had not been normalized before graphing, the absolute contrast sensitivity characteristics for the sine-wave patterns with low mean luminance values would have higher maximum values for their contrast sensitivity characteristics than the characteristics for sine-wave patterns having higher mean luminance values.

Schade's research results were later confirmed and extended by De Palma and Lowery,[119] Campbell and Green,[120] and Campbell and Gubisch.[121] As the result of subsequent extensive research by Campbell and various other experimenters investigating the sine-wave response of the human visual system, it was determined that visual images are processed by the mind using information extracted from narrow spatial frequency channels of 1 to 2 octaves in bandwidth, with the frequency range examined based on the critical detail dimensions the observer selects to view. Although the spatial frequency bandwidth of the channels is narrow, the capability exists to control the position of the image identification channel on a sliding spatial frequency scale that allows the spatial frequency components of images of different sizes in a visual scene, and therefore in different channels, to be mentally processed, in time sequence, provided only that they are in part of the overall spatial frequency bandwidth range that human vision is capable of perceiving.

In accordance with Shannon's sampling theorem,[122] select spatial frequencies in a range of up to at least the critical frequency, v_c, given by the equation,

$$v_c = \frac{1}{2\alpha_c}, \tag{3.103}$$

must be perceptible in order to reconstruct (i.e., identify) an image (e.g., alphanumeric, graphic, video, real-world, etc.) having a minimum critical detail dimension, α_c. The critical spatial frequency location on the contrast sensitivity function is, therefore, directly dependent on the critical detail dimension of the feature of the image that must be discriminated, to make it identifiable, or the image size needed, to make it detectible. As the normalized contrast sensitivity characteristics of Shade show, even small changes in the critical frequency cause significant changes in the position of the spatial frequency identification channel, in the corresponding required contrast sensitivity and, hence, in the image difference luminance requirements. It is also noteworthy that the critical detail dimension parameter values on Jainski's characteristics, and the image sizes on Blackwell's characteristics, could be replaced using their equivalent critical frequency values, with no change in the meaning of the figures.

The ultimate limitation on the spatial discriminability of an image is the requirement that the spatial frequency content of the image to be perceived (i.e., the range from the critical spatial frequency, v_c, down to $v_c/4$), must occur at or below the maximum discriminable frequency, $v_m = 1/2\alpha_m$, where α_m is the minimum subtended angle that the eye's light receptors can resolve, under a particular set of viewing conditions. Based on the minimum separable acuity experiments of Aulhorn and Harms, and the spacing of cone receptors of nominally 0.4 minutes of arc, $\alpha_m \approx 0.4$ minutes of arc, the maximum spatial frequency is approximately 75 cycles per degree or 1.25 cycles per minute of arc. The commonly accepted value for the maximum spatial frequency is 50 to 60 cycles per degree or nominally one cycle per minute of arc. In practical terms, this spatial frequency discrimination limit translates into the well-known restriction on how small a real-world scene object or display image can become, before it can no longer be visually discriminated, or equivalently on the maximum distance that can separate an observer from a real-world scene object, or on the apparent distance to an image on a display.

An earlier article includes much of the preceding information on the spatial frequency dependence of vision.[123] The article's descriptions also go into additional depth on some practical aircraft cockpit display design implications of the spatial frequency dependence of contrast sensitivity, and of the spatial frequency channelization of the mental processing of visual scenes and display information. Since the information is not directly applicable to the subject matter considered in this section, the reader is referred to the article for a further discussion of this topic. A 1980 article[124] and 1981 report [125] by Ginsburg provide a good summary of the spatial frequency dependence of vision. These documents also provide useful figures and references to research conducted on the spatial frequency channels responsible for the overall contrast sensitivity functions.

3.7.3.8. Implications on Human Visual Capabilities of the Constraints Imposed by Retinal Cone and Rod Light Receptors

It is reported in the literature that central fovea cone receptors become blind for the combinations of image difference luminance thresholds and background luminance levels associated with dark adapted scotopic vision. Direct visual evidence of this limit on the sensitivity of the cone receptors is the reported appearance of a blank circular area in test images, where the central fovea cones are located, when the test image luminance levels become sufficiently low. This result implies that vision must shift from central fovea cone receptors to adjacent areas of the retina, populated with both rod and cone receptors, to be able to see images within the visual scene, which are focused upon the retina, at the scotopic or mesopic light levels where the cone receptors become limited by their maximum sensitivities or by the size of image being viewed. However, the results of Wald show that parifoveal cones do not exhibit enhanced sensitivity over their foveal counterparts. The preceding facts, when combined, therefore allow the following conclusions to be reached: first, cones outside the fovea do not extend the night vision sensitivity possible with foveal cones; second, cone receptors, which are ganged outside the fovea, do not lead to increased light sensitivity; and, finally, only rods operate at the luminance levels of scotopic vision.

Although the preceding descriptions are somewhat of an oversimplification, they do make two important points. The first is that, at scotopic ambient light levels, image detection requires a shift to using outer fovea or parafoveal rod receptors. The second point is that the need for an observer to resolve small image critical detail dimensions, to perform image identification tasks encountered within an aircraft cockpit, forces the mind to select stimuli received from central foveal cone receptors, rather than those received from rod receptors, and consequently requires the larger image difference luminance levels needed to stimulate cone receptors. The relative equivalence of the image difference luminance requirements obtained by Jainski, using test images of the same size and shape, but in different colors, confirms that Jainski's test subjects did use cone receptors throughout the image identification tests that Jainski conducted, just as a flight crew would have to do to be able to read the information displayed in a cockpit. Jainski's results, therefore, also show that for the largest critical detail dimension images tested, 19.6 minutes of arc, foveal cones remain sensitive, at least down to image difference luminance levels of approximately 0.004 fL, at display background luminance levels of about the same or lower values. Although the fact that the cones become blind, at sufficiently low light levels, is treated as a commonly accepted fact in the literature, information about the specific luminance levels and other test conditions, associated with this transition, was not found in the literature reviewed.

The reference above, to the discussion of the transitions between the use of cone and rod receptors to perform image identification and detection tasks, being oversimplified was in relation to the role that low image difference luminance and background luminance levels play in forcing the use of rod receptors. At the outset of this investigation, the detection and identification task related differences in the image difference luminance requirements, and later in the veiling luminance angular weighting functions, were expected to be due exclusively to differences in the ways rod and cone light receptors, respectively, respond to in the illumination conditions tested, which ranged from night to daylight levels for the different experimenters. In other words, the differences in the results were expected to be due to light sensitivity differences between the eye's rod and cone receptors during the mesopic transition between photopic and scotopic light levels. While the experimental evidence in the literature does not indicate that these expectations are entirely incorrect, it does show that they represent a significant oversimplification of the actual relationships. The extent to which these expectations are valid, and the additional factors that influence the transitions between retinal receptor types, is further explored below.

3.7.3.9. Implications of Image Size and Blackwell's Common Image Difference Luminance Inflection Point on the Transition Between the Use of Cone and Rod Light Receptors

Referring to Blackwell's image detection characteristics in Figures 3.31, 3.32 and 3.34, there are two features of the characteristics that require further consideration relative to the physiology of the eyes' retinal

receptors. One of these features is the inflection point that occurs at background luminances, in the vicinity of 0.001 to 0.002 fL, for all of the characteristics. The implications of this feature of Blackwell's image detection characteristics will be considered in the current subsection. The second feature of Blackwell's detection characteristics that requires further consideration is the plateau effect limitation, on the decrease in image difference luminance, as the background luminance is decreased through the mesopic vision range. The implications of this feature of Blackwell's data are treated in the next subsection.

Even though the inflection point feature is common to all of the Blackwell image detection characteristics, the figures also show that the image difference luminance values associated with that transition vary significantly in magnitude, depending on the size of the target. In fact, the image difference luminance levels, for the smallest target size of 0.595 minutes of arc, are so large that the characteristic may be seen in Figure 3.34 to overlap the Jainski image difference luminance level requirements for image identification and, therefore, the characteristic's entire length is in the range of image difference luminance levels generally associated with cone light reception. Furthermore, at 0.595 minutes of arc in diameter, Blackwell's smallest target size would only be large enough to stimulate three of the highest density central fovea cone or parifovea rod light receptors (i.e., ignoring the potential effects of saccadic eye motion). The limited stimulus area would also favor the target being detected by cone receptors, due to the likelihood that the area averaging by the larger area groupings of rods would reduce their sensitivity. In spite of this, however, the 0.595 minutes of arc characteristic still shows the signature increase in its slope below the background luminance transition region, of 0.001 to 0.002 fL, which is common, in varying degrees, to all of the image detection characteristics, and is associated by Blackwell with a transition, from viewing the target using foveal receptors to viewing it with parafoveal receptors, as the background luminance decreases. This result also appears to show that small areas having image difference luminance values within the mesopic range do not inhibit (i.e., desensitize) the retinal receptor's electrochemical transition to the scotopic state as the background luminance drops below 0.001 to 0.002 fL.

The strong dependence of the image difference luminance thresholds on the target size, for detection tasks, and on the critical detail dimensions of images, for identification tasks, was attributed, in the earlier discussion of the spatial frequency dependence of contrast sensitivity characteristics, to the mental processing of the stimuli sent to the brain by retinal receptors, rather than to the physiology of the eye or its different receptor types and configurations. Considering this dependence in the spatial domain, the large variations in the threshold image difference luminance that occurs as a function of target size appear to be attributable to a spatial summation of signal magnitudes received by the brain via the optic nerve fibers stimulated as the result of exposing the retina to targets of different sizes.

Target size data in the literature show that a strictly proportional dependence between target area and the image difference luminance sensitivity response only holds for targets less than 10 minutes of arc in diameter. For larger target sizes, the increase in sensitivity becomes nonlinear with increases in the test image area, producing progressively smaller differential improvements in sensitivity until eventually reaching a maximum sensitivity limit.

For target sizes even larger than those needed to reach the maximum sensitivity limit, the experimental evidence shows that sensitivity starts to decrease with increased target size. This latter behavior is entirely consistent with the channelization of the spatial frequency domain, since, as previously described, the spatial frequency dependence of sensitivity decreases below the maximum sensitivity spatial frequency (i.e., for larger target sizes), as is shown by the results of Schade in Figure 3.35. In contrast to this psychology-based explanation, the physiology-based explanation for the test image size dependence, described in the preceding paragraph in terms of the spatial domain, breaks down as the test image size becomes progressively larger, unless it is assumed that stimuli from the larger areas of a target start to be ignored by the mind, in favor of the smaller areas of a target, used to resolve the edge definition of a target to be detected or to more sharply define the critical detail dimensions of an image to be identified, as the size of the target continues to increase.

Another source of data regarding the mesopic to scotopic transition, and for the effects of target size and

placement on the retina, is provided by characteristics relating the time dependence of the human's dark adaptation. As examples of dark adaptation characteristics, Figures 3.37 and 3.38 show reproductions of Figures 17 and 18 of Bartley,[126] which depict dark adaptation data collected by Hecht, Haig, and Wald.* Based on the descriptions of both Bartley and Bartlett,[127] the intent of these experiments was to explore the time dependence of dark adaptation, by determining the threshold luminances, of test images of two degrees of arc or larger in diameter, and for different locations on the retina, as a function of time following the removal of a preadapting field luminance. This data differs from that of Blackwell, in that the test image is the only source of luminance in the test subject's field of view. By comparison, the values of Blackwell's dependent variable, the image difference luminance, are almost incidental to the independent variable, background luminance, which controls the dark adaptation of the test subjects. Although the image sizes, in Blackwell's investigations, overlap the smaller image sizes used in the dark adaptation tests, a large fraction of the observer's total field of view is exposed to the background luminance by the geometry of Blackwell's test configuration.

The human dark adaptation characteristics of Figures 3.37 and 3.38 show the threshold luminance, for each particular test image and retinal location, plotted as a function of elapsed time, after a preadapting light source of high luminance is turned off. These characteristics are dependent on many different experimental parameters, including the preadapting field luminance level, its duration, its size, its location on the retina and the colors of both the preadapting field and test images, besides the size of the test image and its location on the retina. Although a detailed discussion of the process of dark adaptation by the eyes is beyond the scope of this report, the time response characteristics associated with dark adaptation have been studied quite thoroughly in the literature and the general forms of their characteristics are relatively well known.

The characteristics showing the evolution of dark adaptation, with time, exhibit a two-phase dark adaptation process. In the first phase, the characteristics follow a rapid exponential-like adaptation down to a maximum sensitivity limit. This dark adaptation transition is typically associated with the response of cone receptors, or possibly both cone and rod receptors since it is pointed out in the literature that their responses cannot be readily distinguished in the mesopic range. The light receptor's threshold luminance versus time characteristics, for this phase of the dark adaptation process, exhibit very little variation in the decay durations to reach a fully adapted static state. The decay times to reach the fully adapted static state are about five minutes, however, all but about a final decade of the transition occurs within just a few seconds.

Following this first phase of the dark adaptation process, a second phase starts that is associated with an electrochemical change of the rod light receptors and possibly also in the neural network they stimulate in the eyes. In this second phase, a new and lower maximum sensitivity limit is exponentially approached, which again is dependent on the previously mentioned parameters, and in this case the duration is measured in tens of minutes and, for complete dark adaptation, can take as much as hours, depending on the preadaptive luminance conditions.

For centrally fixated targets of 2 degrees and smaller in diameter, which remain focused on the central fovea, the second phase of dark adaptation never begins. Conversely, for all of the test images larger than the nominal 2 degree diameter of the central fovea, and, for those test images focused on the retina at angular locations outside the central fovea, the second phase of dark adaptation occurs, for all of the dark adaptation characteristics, starting at about the same threshold luminance value, at least for the 3 to 20 degree range of centrally fixated circular targets and 2.5 to 10 degree target angular displacements tested.** A direct comparison of the preceding circular test image threshold luminance values, corresponding to the onset of the second phase of the dark adaptation time response characteristics (i.e., nominally 0.002 to 0.003 fL), with the

---

* Hecht, S., C. Haig, and G. Wald, "The Dark Adaptation of Retinal Fields of Different Size and Location," Journal of General Physiology, Vol. 19, 1935, pp. 321-339.

** Ibid., pp. 321 - 339.

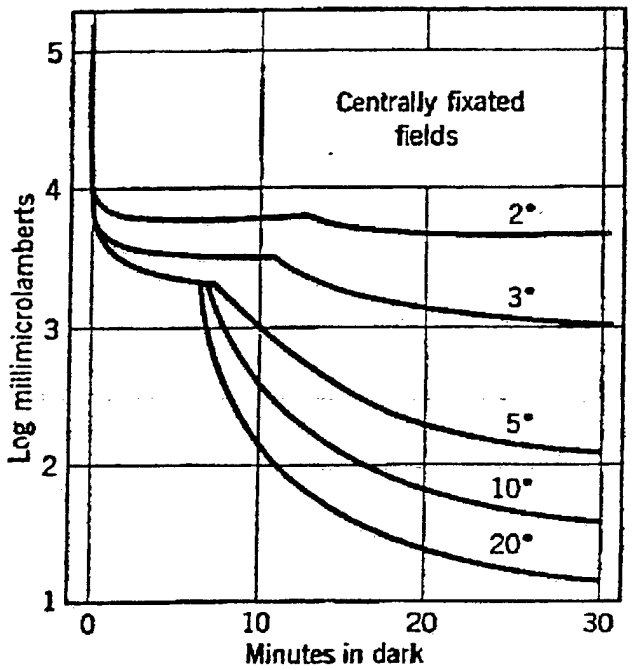


Figure 3.37. Dark Adaptation Following an Exposure to a Preadaptation Luminance of 300 mL and 2 Minutes Duration for Centrally Fixated Areas of Different Subtended Angles.*

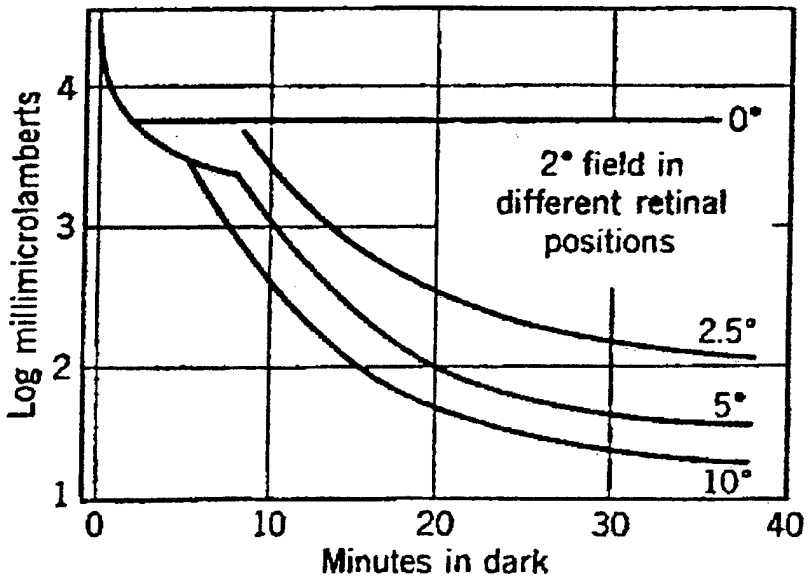


Figure 3.38. Dark Adaptation Following an Exposure to a Preadaptation Luminance of 300 mL and 2 Minutes Duration for a 2 Degree Field Area in Different Angular Displacements Relative to the Fixation Point.*

---

* Figures 17 and 18 of Bartley, Howard S., Handbook of Experimental Psychology, p. 947. Data from Hecht, S., C. Haig and G. Wald, 1935, pp. 321-339.

0.001 to 0.002 fL transition associated with Blackwell's background luminance inflection point data show they agree quite well with one another.

It should again be noted that the data, showing the time dependence of dark adaptation, are collected using the threshold luminance of a test image, in a viewing environment having essentially no background luminance present, and, hence, the dark adaptation is controlled by the size and position of the test image, within the observers field of view. By way of comparison, the data of Blackwell are collected using a background luminance that fills much of the observer's field of view, with a test image superimposed upon it, and where the image difference luminance of the test image is typically small by comparison to the magnitude of the background luminance. In effect, then, the large background luminance area used by Blackwell serves the same dark adaptation control role as does the large target areas in the time dependent dark adaptation characteristics of Figure 3.37. In other words, the onset of dark adaptation, predicted by Blackwell's background luminance inflection point, should be suitable for comparison with the threshold luminance values predicted by the onset of the second phase of the time dependent dark adaptation characteristics, for large area targets.

The validity of the time dependence of dark adaptation data, presented above, although collected using small numbers of subjects, and a 2.83 mm diameter artificial pupil, has been confirmed by a number of other experimenters. Blackwell's data, which is an average taken over many subjects and trials, with no pupil area constraints imposed on the test subject's vision, are also considered valid. In spite of the differences between these experiments, which causes their comparison to be somewhat tentative in nature, the close correspondence of the results indicates it is still safe to conclude that both types of tests reveal the same dark adaptation transition. In the literature, both the initiation of the second phase of dark adaptation, and the common inflection point, in the image difference luminance versus background luminance characteristics of Blackwell, are associated with the mesopic to scotopic transitions at nominally 0.001 to 0.002 fL, and with a corresponding physical transition from the use of retinal cone receptors, which are either approaching or have reached their maximum sensitivity, to the more sensitive dark adapted rod receptors.

3.7.3.10. Implications of Image Size on the Blackwell Image Difference Luminance Plateau Effect and on the Transition Between the Use of Cone and Rod Light Receptors

The second feature of the Blackwell characteristics that should be considered, relative to the cause and effect relationship to the eyes' retinal receptor physiology, is the plateau effect limitation on the decrease in image difference luminance or, equivalently, on the increase in the sensitivity of the retinal receptors, as the background luminance is reduced through the mesopic vision range. This behavior is most evident for the smaller target size characteristics shown in Figure 3.32, for Blackwell's minimum threshold legibility data, but also occurs for the 50% threshold legibility data shown in Figure 3.31. Because rod receptors are ganged, even in the fovea's outer annular ring of rods and cones closest to the central fovea, and are therefore unlikely to be sensitive to small test image sizes, the plateau effect for small test images is believed to be due to the sensitivity limits of central fovea cone receptors, rather than to the sensitivity limits of rod receptors that have not yet undergone the electrochemical transition to their dark adapted state.

For larger test images, the previously described spectral sensitivity results of Kinney, for a 2 degree diameter test image, located at 10 degrees from the center of the fovea in the near periphery, showed that the spectral sensitivity characteristics of the stimulated retinal receptors remained scotopic as the test image luminance was increased through mesopic range. The fact that these light receptors exhibited a maximum sensitivity near 510 nm, throughout the mesopic range, shows that the rod receptors remain operative up to test image luminance levels near the top of the mesopic vision range.[128] Like Kinney, the veiling luminance angular response results of Stiles were also obtained using a 2 degree diameter test image. However, for Stiles' test, the experimental design was intended to cause the test image be viewed foveally, and in the presence of various levels of background luminance. As previously discussed, the results of Stiles can also be interpreted as being attributable to rod receptors, from scotopic adaptation levels up to background

luminance levels near the top of the mesopic vision range, where a transition to the use of cone receptors occurs, presumably due to the light saturation of rods. While the preceding two results appear to confirm one another, it remains to explain why these experiments predict rods are operative up into the vicinity about 1 fL whereas the 2 degree test image data of Blackwell, for image difference luminance versus background luminance, and that of Hecht, Haig and Wald, for the time dependence of dark adaptation, show the mesopic to scotopic electrochemical transition to maximum dark adaptation occurs starting at nominally 0.002 fL.

An explanation that is consistent with the apparently conflicting results, summarized in the preceding paragraph, is that while rod receptors undergo an electrochemical transition to higher absolute sensitivity levels below the mesopic to scotopic transition (i.e., starting at nominally 0.001 to 0.002 fL), above this transition the mesopic adapted rod receptors continue to be operative, albeit with reduced sensitivity, and still possess the same, or nearly the same, relative spectral sensitivity characteristics as the scotopic adapted rod receptors. The previously described data of Kinney proves that this explanation for the operation of rods in the mesopic vision range is correct although not complete. It is not complete because the data of Kinney, while correct for a 2 degree test image size is not valid for all image sizes.

For a large enough test image size (i.e., 1 to 2 degrees in diameter and larger), the perception by the brain of the stimuli received from mesopic adapted rod receptors is apparently larger than that received from cone receptors. Since the combined effect of variations, in the groupings and densities of rod receptors, as a function of position on the retina, influence the ultimate sensitivity achievable with rod receptors, whereas cone receptor sensitivity appears to remain constant, a shift in vision toward the periphery would allow a test subject to take advantage of the elevated, mentally perceived, sensitivity of the rod receptors over that perceived for cone receptors in the mesopic range, if the test image is large enough to stimulate a sufficient number of rod groupings. Conversely, for small image sizes, the one-on-one coupling, of cone light receptors to optic nerve fibers, apparently causes the sensitivity of individual cone receptors to predominate over that of rod receptor groupings in the mesopic vision range. In fact, for small enough images, such as the 0.595 minute of arc subtended angle target size in Figure 3.32, the cone receptors can even reach their sensitivity limit, as evidenced by the image difference luminance plateau effect, before the background luminance becomes low enough to scotopically dark adapt the rod receptors, whereupon, the increased sensitivity of the rods allows them to provide the image detection visual stimulus to the brain. It also follows from this and the earlier examination of the figures containing Blackwell's characteristics for small test image sizes (e.g., of nominally 18 minutes of arc and smaller), that the luminous flux, which is associated with the combination of a small test image size and an image difference luminance large enough to use cone receptors for mesopic vision, is not of a sufficient magnitude to impede the electrochemical transition to scotopic vision as the background luminance is reduced through the 0.001 to 0.002 fL mesopic to scotopic transition.

Assuming the preceding conclusions, regarding the effect of test image size on the retinal receptors used by the brain to detect a test image, are correct, then the gradual disappearance of the plateau effect can be explained as a transition, from using primarily cone receptors to detect the 0.595 minute of arc test image size, to using primarily rod receptors, to detect test image sizes of 60 minutes of arc (i.e., 1 degree) and larger in the mesopic vision range. The intermediate size characteristics between these extremes can then be interpreted as a gradual transition from using mostly cones at small image sizes to using mostly rods at the larger test image sizes. More specifically, in the interval between the small and large image sizes described above, the differences in the comparative sensitivities of cones and rods, as a function of image size, would be expected to cause the transitions, from using foveal cones to parafoveal and parifoveal rods, to occur at progressively higher background luminance levels, between 0.001 fL and 1 fL, for the test image sizes subtending angles between the 18 minute of arc and 1 degree, respectively. Although the preceding descriptions, of the roles played by rod and cone light receptors, as the cause of the observed peculiarities in the shapes of the image difference luminance versus background luminance characteristics, adapted from contrast characteristic's format of Blackwell's image detection task data and shown in Figures 3.31 to 3.34, provide an explanation that is physically consistent with all of the previously described experimental evidence, the explanation must still be considered conjectural at this point, owing to the circumstantial nature of the evidence.

3.7.3.11. Dependence of Rod and Cone Receptor Usage Based on Experimental Design

Figure 3.33, which compares Blackwell's characteristics for test images of equal size, that is, for test images subtending 9.68, 18.2 and 121.0 minutes of arc, respectively, indicates the existence of some additional variable dependences, which could result from either psychological or physiological factors, or a combination of both factors. In the photopic vision range, above 3 fL, the literature reviewed consider rod receptors to be saturated, while the continued light sensitivity of cones causes them to be used to perform both image detection and image identification tasks. For the characteristic pairs, corresponding to the two smaller image sizes shown in Figure 3.33, the apparent continuities of the characteristics in the vicinity of 1 to 3 fL, that is, the lack of an inflection point in the characteristics, and the plateau effect in the mesopic vision range, provide further evidence that the cone light receptors continue to be responsible for image detection, on the lower of the top two pairs of image difference luminance characteristics. These characteristics are associated with the Blackwell detection data for minimum threshold legibility. In contrast to the lower characteristics, for each of these characteristic pairs, the upper image difference luminance level characteristics, which are associated with Blackwell's detection data for 50% threshold legibility, appear to exhibit a small inflection, indicative of a transition to the use of rods, at the top of the mesopic vision range, even for the smallest image size in Figure 3.33, that is, 9.68 minutes of arc. By way of comparison to the preceding results, the characteristic pairs corresponding to the largest image sizes compared in Figure 3.33, that is, for a target subtending an angle of 121 minutes of arc, both characteristics are similar, and exhibit evidence of transitioning from the use of cone to rod light receptors, as the background luminance decreases through the 1 to 3 fL photopic to scotopic transition.

The interpretations of Blackwell's results, in the preceding paragraph, are, as a minimum, contrary to what would be expected for physiology-based predictions for cone and rod light receptor sensitivities, based on the magnitudes of the threshold image difference luminance values shown in Figure 3.33. In particular, the higher image difference luminance levels, associated with the 50% threshold legibility characteristics, would be expected to invoke the use of cone light receptors before the use of rod light receptors is invoked, whereas the results for the two smaller image size characteristic pairs in the figure show that just the opposite is true. Nonetheless, these results are consistent with what might be expected from the experimental designs, for the tests Blackwell conducted. For example, Blackwell's minimum threshold legibility data were collected using test images centered on the central fovea. This would make the use of central fovea cone receptors, which the test images are focused upon, the preferred detection method. Likewise, in the case of Blackwell's 50% threshold legibility data, the fixation point for the test subjects was located in the center of the fovea, but the test images were placed randomly, at one of eight positions, on a three degree diameter circle. In other words, the location of the test images for the 50% threshold legibility data are inside the parafovea at a location just beyond the fovea, but beyond the nominal 1 degree radius of the rod-free area of the fovea. This means that either parafoveal cones or rods could be used for image detection, but since the density of rods is higher than that of cones at 3 degrees from the center of vision, this would make rods the preferred retinal receptor, all other factors being equal.

As noted above, both of the characteristics shown in Figure 3.33, for Blackwell's largest test image size (i.e., the 121 minute of arc diameter circles), show evidence of a transition from the use of cone receptors, to the use of rod receptors, at the photopic to mesopic vision transition. This result, for the minimum threshold detection task, requires the point visually fixated by the test subject's eyes, to be unconsciously shifted to a position outside the central fovea area of the retina, to allow the image of the target to be sensed by rod light receptors, and then transmitted to the brain for mental processing. A target subtending an angle of nominally 2 degrees, is equal to the diameter of the rod-free central fovea of the eyes, but the target is also sufficiently large, to encompass several hundred rod light receptor groupings, if imaged on the parafovea or other areas of the retina more distant from the fovea. The fact that rod, rather than cone, light receptors are used to detect the 2 degree target size, in the mesopic luminance range, was, as previously described, confirmed by several experimenters in different types of experiments. Detecting Blackwell's 2 degree target size, using rod light receptors, therefore, makes it likely that the signals transmitted to the brain, from multiple parafoveal rod light receptor groupings, produce higher spatial frequency dependent contrast sensitivities, than do the signals from

the more than one hundred thousand individual cone light receptors in the central fovea of the eyes. The latter observation is admittedly speculative, since the role played by higher mental processes in the performance of an image detection task are not known and, consequently, are not considered.

3.7.3.12. Veiling Luminance Angular Response Conclusions

Differences between the physical geometries, of foveal cone receptors and of rod receptors, would make it likely that a difference would also exist in the angular responsivity characteristics of these light receptors. It is also certain that an unconscious translation of the test image from the foveal cone to the parafoveal rod light receptors would be necessary to enable a test subject to perform image detection under fully scotopic viewing conditions. The fact that this transition occurs is not contestable due to the very low (i.e., scotopic) background luminance levels tested by Holladay and Stiles during their veiling luminance angular dependence experiments. As previously mentioned, the experimental results of Holladay and Stiles also show no indication of a change in the veiling luminance angular response characteristics, as a function of the background luminance levels, in the 0.001 to 0.002 fL transition range between mesopic and scotopic vision. Based on the preceding facts, the most likely candidate, for the sought after physiology-based explanation for the differences in the veiling luminance angular response characteristics determined experimentally for the Jainski and Nowakowski image identification task results, and the Holladay and Stiles image detection task results, is the change from using the cone light receptors to using rod light receptors.

When the experimentally determined differences between the veiling luminance angular weighting functions having narrow angular distributions and those having more gradual angular distributions were initially considered, the result seemed counterintuitive for a transition from rod to cone receptors. However, upon further consideration, the fact that rod light receptors are more densely packed than cone light receptors, in all areas of the retina that they share, except the outer annulus area of the fovea; and the fact that the shape and diameters of rod light receptors are very similar to those of central fovea cone receptors; makes it conceivable and, based on the angular response experimental data presented, likely, that rod receptors could have a more rapid decrease in sensitivity with increasing angles than do cone receptors. Beyond the preceding argument, no published results, comparable to the Stiles-Crawford effect for cone light receptors, nor any experiment dealing with the angular responsivity of rod receptors to incident light was encountered, in the literature reviewed, to validate this interpretation.

The fact that rod light receptors are ganged together into groupings, and, consequently, can function as enlarged light collective receptors, which, in turn, presumably produce the higher maximum sensitivities associated with rod light receptors, at night, as compared with those possible with cone light receptors, would explain, for the test images sizes used by Holladay and Stiles, the observed higher absolute values of veiling luminance obtained by Holladay and Stiles at small angles. However, the groupings of rod light receptors should not affect the angular cutoff in the veiling luminance angular response, since this should be determined solely by the angular sensitivity characteristics of the individual rod receptors contained within each light receptor grouping. If higher sensitivity rod light receptor groupings, coupled with a sharper angular cutoff by the angular response characteristics of rod light receptors, as compared with those for cone light receptors, is valid, this would be sufficient to produce the observed veiling luminance angular responses of Holladay and Stiles, at small glare source angles.

Irrespective of the correctness of the physiological explanations ascribed to the veiling luminance angular response characteristics of the different experimenters, described in this subsection, the composite results of the experiments show, convincingly, that it is the veiling luminance angular response characteristics of Jainski, which apply to image identification tasks, that is, to tasks requiring the extraction of information from aircraft cockpit instruments and panels, and that this is true under viewing conditions that extend from complete darkness to full daylight. Although different veiling luminance angular response characteristics have been shown to apply to visual tasks, which require detecting the presence or absence of images, these results are applicable to visual tasks performed external to the cockpit. Consequently, it is concluded that an automatic

legibility co[illegible] model, incorporating the angular response function derived from Jainski's data, can be applied under the f[illegible]ange of night to daylight illumination conditions experienced in an aircraft cockpit, not just to the conditions contained in the Jainski tests.

3.7.4. Influence of the Pupil Area of the Eyes on Veiling Luminance

The effect of changes in the eye's pupil diameter is another important variable dependence contained in the scattered luminous flux density equation introduced in Holladay's 1926 article. Holladay's theoretical equation, for the scattered luminous flux density incident on the fovea, includes the square of the pupil diameter (i.e., proportional to pupil area) as a direct proportionality term. Based on the earlier conclusion that veiling luminance is primarily attributable to light scattered by the optical media of the eyes into the retinal receptors being used at any instant in time to perceive the test image, Holladay's scattered luminous flux density equation allows the conclusion to be reached that veiling luminance must be dependent upon the pupil area of the eyes. The balance of this section is devoted to a description of the effect that changes in the eyes' pupil areas have on the induction of veiling luminance, and the manner in which this pupil area variable interacts with the discrete glare source empirical equation for veiling luminance, derived earlier from Jainski's test results.

The physical significance of the finding that the pupil area is dependent on the angular position of a glare source with respect to the observers line of site, as determined by the experiments of both Holladay and Crawford, could, at least potentially have had far reaching ramifications for the validity of the automatic legibility control model developed in this report. Up to this point it has been assumed that the angular and illuminance dependences of veiling luminance can be represented as the product of separable independent functions. When this functional relationship is satisfied, the angular weighting function dependence of veiling luminance would, for example, be unchanged when the illuminance of the glare source is changed, from a high to a low level, as when going from day to night viewing conditions or vice versa. Because light reaching the retina either directly, or after being scattered, is modulated by changes in the pupil diameter, this effect provides a potential physical mechanism for coupling the effects of the illuminance and angular position of a light source.

The empirical data of Jainski for the angular and illuminance dependences of veiling luminance already include the effect of the attendant pupil area changes, however, the angular weighting function data was collected at a fixed glare source illuminance of 371.6 fc, and the illuminance dependence data was collected at a fixed glare source angle of 15 degrees, both with the implicit assumption that the two dependences are functionally independent of one another. Fortunately, the pupil area test data, as represented in three equations, designated as Equation 1 of the 1936 article by Crawford,[129] show that the angular dependence term in each of the pupil diameter equations, corresponding to glare source illuminances of 0.00347, 0.102 and 4.37 fc, respectively, have the same exponential angle dependence, for subtended angles between the glare source and the test subject's fixation point, of 0, 7, 14, 28, 35, 42, 49 and 56 degrees. This result, in combination with the similarities between the veiling luminance angular dependence results of Nowakowski at low illuminance levels and those of Jainski at higher levels, neither of whom imposed constraints on their test subject's pupil areas during their tests, gave a clear indication, based on the experimental evidence, that the illuminance and angular dependences of both pupil area and veiling luminance are, at least to the first order of approximation, separable independent functions.

When considered from a theoretical perspective, a physical basis, sufficient to explain why the experimentally determined dependence of the pupil area, on the glare source illuminance and subtended angle independent variables, can be mathematically treated, using separable independent multiplicative functions, is less clear than it was for veiling luminance. For veiling luminance, if the scattering of light by imperfections within the eye's optical media is accepted as the origin of the veiling luminance induced in the eyes by a glare source, as has been previously concluded in this report, then the theory-based explanation described previously in Section 3.6.1.1 is sufficient to justify the separation of glare source illuminance and angle of incidence dependences of veiling luminance into separable functions. To elaborate on this veiling luminance theory further, the percentage of light scattered into the observer's line of sight, per unit volume of the eyes

optical media, is dependent only on the angle of incidence of the glare source light upon the eyes, which, in turn, determines the scattering angle necessary, for the light scattered to impinge upon the fovea, and consequently, the percentage of the glare source light scattered into the direction of the fovea. In other words, no physiological mechanism, is present within the eyes, that would permit the magnitude of the illuminance incident on the eyes to influence the percentage of light scattered into the direction of the fovea.

From a theoretical perspective, the dependence of the pupil area on the illuminance, and the angular displacement of the glare source, has to be physically determined solely by the physiological effect produced by the glare source being directly imaged onto the retina. In this context, the pupil area would be controlled by the total luminous flux incident on the retina, following exposure of the eyes to the incident glare source illuminance and after the mind has adjusted the pupil area, in a closed-loop feedback fashion, to the glare source illuminance incident on the eyes, at any particular angle. The previously described experimental results show that the only effect of the angular displacement of the glare source, from the observer's center of vision, is to apply an angle dependent multiplicative scaling factor, to the function that expresses the pupil area dependence on the glare source total luminous flux that is incident on the retina of eyes. Since the pupil area changes, observed in response to the angular displacement of the glare source, which are described in Section 3.6.3, are much larger than can be attributed to the optical effects, associated with the imaging of the glare source light as it enters the eyes at different angles, the observed angle dependences must be attributable to retinal position dependent sensitivity changes, and/or the retinal-mental signal sensing and processing feedback loop.

In concluding this discussion of the angular dependence of pupil area, it should be noted that while the empirical equation of Holladay for pupil area, Equation 3.84, is not separable into multiplicative angle and glare source illuminance dependent terms, this situation is the result of the method that Holladay used to formulate the empirical equation, rather than due to Holladay's experimental test data, which could have been used to formulate the equation in a separable format. Although a detailed theoretical explanation, for the experimentally established ability to separate the illuminance and glare source angle dependences, into a glare source angle dependent multiplier and an illuminance dependent function, consistent with Crawford and Holladay experimental results, cannot be offered, it can be concluded that this result is consistent with an angle invariant light sensing function of the retina, being physically distinct from the origin of the angle dependence. In other words, a glare source angle dependent multiplier that emulates the fraction of the light actually sensed, after reaching the retinal light receptors, in relationship to the light initially incident upon the eyes from a glare source, as a function of the glare source angle with respect to the line of sight, would satisfy the functional separability criteria.

Although speculative, one possible explanation, which is consistent with the observed pupil area angle dependences involves the combination of the previously described angle dependent physical-optics properties of the eyes, and the expected angular light sensitivity differences between foveal cone and rod light receptors, in analogy to the previously described Stiles-Crawford effect for foveal cone light receptors. Furthermore, the contributions of the angular sensitivities of retinal light receptors, to the pupil area angle dependence, could extend to a retinal position dependence of the angular sensitivities of retinal light receptors. Even though the variations in the sizes, shapes and densities of cone and rod light receptors, outside the fovea, make this type of dependence likely, no direct experimental evidence, supporting a retinal position dependence of the angular sensitivities of cone and rod light receptors, was encountered in the literature. Similarly, no experimental evidence was found, which would conflict with the existence of such angular sensitivity dependences.

Independent of whether or not the preceding eye physiology-based explanation for the origins of the experimentally observed pupil area angular dependences are correct, the only real requirement, which must be met to achieve separable illuminance and glare source angle functional dependences, is that a change in the illuminance level, incident on the eyes, cannot cause a change in the glare source angle dependence of the pupil area, or vice versa. In practice, no optical effect, or eye physiology phenomenon, is known that could cause a linkage of this type, between the illuminance and the angular function dependences, to occur.

The theoretical effect that the magnitude of glare source illuminance has on pupil area and, consequently, on veiling luminance is explored next. Unlike the angular dependence of veiling luminance, which, as previously described, is influenced by many different factors, the illuminance dependence of veiling luminance is less complex and therefore is more amenable to interpretation. The illuminance incident, at a point on the retina of the eye, is given by the integral sum over the attenuated values of luminance reaching the retina, along each possible path from a point on the object being viewed through the cornea of the eye, through the aperture defined by the pupil's area and finally through the lens, which focuses the luminance from each path through the pupil aperture onto the imaged point on the retina. In other words, the illuminance incident, at a point on the retina, is equal to the luminance reaching the retina, following the light's attenuation by passage through the various membranes and optical media within the eyes, integrated over the solid angle subtended, at the retina, by the pupil area. As previously mentioned, the human visual system does not, however, respond directly to the illuminance incident on the retina. Due to the Stiles-Crawford effect, which was previously discussed in relation to light scattering in the eyes, the angular receptivity of the retinal receptors must be accounted for, in any attempt to describe, quantitatively, the sensed/perceived response of the human visual system to either the intentionally focused images, in a real-world scene being viewed, or the unintentionally focused effects, of light scattered by the eye's optical membranes and optical media.

Since luminance passing through the pupil area at progressively larger angles, from the center of vision, has a progressively smaller effect in inducing a visual system response, a mathematical compensation for this effect must be included in any model intended to describe the response of the human visual system to pupil area changes on either directly viewed images or scattered light. A method described by Riggs[130] and used by Le Grand,* in an attempt to predict correct human visual system perceptual responses in the presence of pupil area changes, involved the definition of a quasi-retinal illuminance variable, to model the effect of pupil area changes linearly. As described by Riggs, this method employed the following rationale. To compensate for the Stiles-Crawford effect, it was reasoned that, as the pupil area enlarges, the visual system responds as it would to a uniform angular receptivity retina having a smaller effective pupil area. Although this is the extent of the detail provided by Riggs description, it can, in addition, be reasoned that field luminance exposure reductions (i.e., a change which causes an increase in the diameter of a natural pupil) can be compensated for the Stiles-Crawford effect by increasing the effective area of the pupil, at a reduced rate, in comparison to the rate of increase, in the area of a natural pupil (i.e., to compensate for the progressive reduction in receptivity of the retinal receptors to light added by the expansion of the pupil area, since the light added is located in an annular ring at the pupil's outer periphery). To evaluate the effect of applying this compensation rationale to scattered luminance within the eyes, the Riggs' pupil area rule of thumb approximation, Equation 3.82, can be used. In the context of applying the aforementioned mathematical compensation, the actual minimum pupil area would be reduced slightly and the exponent in the Riggs' equation, which is the slope of the pupil area versus field luminance relationship, when it is plotted on full logarithmic graph axes, would also be reduced.

The compensation of the pupil area described in the preceding paragraph can be expressed in mathematical terms by modifying Equation 3.82 for Riggs' pupil area rule of thumb approximation. Substituting for the actual pupil area parameter, A_{PI}, that corresponds to the field luminance parameter, L_{FI}, in the Riggs' equation, using an effective pupil area parameter, A_{PE1}, to represent the reduced area of the pupil, and replacing the fixed slope (i.e., - 0.1871) in the Riggs' equation with a constant, a, of smaller magnitude, Equation 3.82 can be rewritten as a retinal receptivity compensated effective area, A_{PE}, as follows:

$$A_{PE} = A_{PE1}\left(\frac{L_F}{L_{F1}}\right)^a = K_E L_F^a . \qquad (3.104)$$

The constant, K_E, in the equation is included to combine all of the constant parameters into a single term.

---

* Le Grand, Y., Light, Colour and Vision, Translated by R. W. G. Hunt, J. W. T. Walsh, and F. R. W. Hunt, Wiley, New York, 1957, pp. 1-512.

In the case of a discrete glare source of small size and uniform luminance, the field luminance can be replaced by the equation,

$$L_F = E_B / \Omega_B . \tag{3.105}$$

Since the solid angle, Ω_B, subtended by the glare source is a constant, Equation 3.104 can then be expressed as follows:

$$A_{PE} = K_E^{/} E_B^{a}, \tag{3.106}$$

where the constant, $K_E^{/}$, includes the solid angle from the previous equation.

In Holladay's theoretical equation for light scattered into the fovea, the glare source illuminance, E_B, and the pupil area, A_p, appear as product terms in the numerator of the equation. Consequently, if the scattered luminance sensed by the eyes' central fovea cone light receptors is assumed to be directly proportional to the perceived veiling luminance induced, then the veiling luminance can be expressed by the following relationship, involving the product of the effective pupil area and the illuminance incident on the eyes from the glare source:

$$L_V \propto A_{PE} E_B = K_E^{/} E_B^{a} E_B = K_E^{/} E_B^{1+a}. \tag{3.107}$$

In this equation, the value of the effective pupil area was substituted from Equation 3.106 and the result was then combined to provide the final expression in the equation.

The magnitude of the constant, a, that was applicable to pupil area predictions using the Riggs' rule of thumb, was $a = -0.1871$. If the magnitude of this constant is reduced, for the reasons described in the previous discussion, to a value of $a = -0.128$, which would not be an unreasonable reduction given the angular receptivity characteristics of the foveal receptors, then the illuminance dependence of veiling luminance predicted by Equation 3.107 would be as follows:

$$L_V \propto E_B^{0.872}. \tag{3.108}$$

The dependence of veiling luminance on the illuminance of a discrete glare source, as expressed in this equation, is by virtue of the choice of the exponent value for the constant, a, the same as the one determined when Jainski's data was empirically modeled. This result makes it likely that the nonlinear illuminance dependence indicated by the Jainski data is due entirely to the effect of pupil area changes.

If, as the preceding argument suggests, pupil area changes are actually responsible for the illuminance dependence of veiling luminance in Equation 3.108, then the exponent will remain at the value of 0.872 only as long as the pupil area is changing in approximate agreement with the Riggs rule of thumb, as represented by Equation 3.82. Once the pupil area starts to approach either its maximum or minimum size, asymptotically, the power on the illuminance term should continuously transition between the power of 0.872 and 1. A problem exists, however, in that the experimental data encountered in the literature reviewed is insufficient to allow a prediction of the spatial luminance distributions, glare source illuminance levels or the combinations of these conditions necessary, to cause the onset of the transition from the 0.872 to a unity exponent, in the illuminance term of Equation 3.108.

In the preceding context, Jainski's investigation is not particularly helpful, since the relationship between veiling luminance and the illuminance of the glare source was only tested for illuminance values from 1 lx (0.0929 fc) to 4000 lux (371.6 fc), as measured at the eyes. The data of Spring and Stiles, cited earlier, appear to show, at least at the lower pupil diameter limit, that the product of the field luminance and pupil area, which is proportional to the illuminance incident on the retina, produces a somewhat consistent prediction for the lower pupil area limit transition to the respective minimum pupil diameters applicable to their test subjects. Comparing the products of the field luminance and pupil area for the transition to the two millimeter pupil diameter predicted by the empirical equations of Crawford, Moon and Spencer, and De Groot and Gebhard, the transitions appear to start to occur around 30,000 Trolands (nt·mm^2), as was the case for Spring and Stiles experiment. Holladay's transition occurred at about a fifth of this level. The corresponding levels of field luminance were in the vicinity of 1,100 to 1,500 mL for the first three experimenters and at about 200 mL for

Holladay. The most probable explanation for this behavior of Holladay's data is explained below, however, the available experimental data are insufficient, either to allow the desired prediction of the conditions when Riggs' pupil area approximation starts to fail, or to confirm that the explanation proposed for the behavior of Holladay's data is correct.

In Holladay's test of pupil area as a function of field luminance, the field of view was filled with uniform luminance, whereas Spring and Stiles used a uniform luminance field area subtending only 52 degrees (by way of comparison, Crawford's experiment used a field area subtending 55 degrees). The exposure of the test subject's entire field of view to the same field luminance, during the pupil area tests of Holladay, could reasonably be expected to cause a reduction in the field luminance induced onset of the transition to the minimum pupil area limit. However, the only systematic investigation of the effect of field area on pupil size, encountered in the literature reviewed, was the investigation conducted by Holladay that was previously described.* Unfortunately, the investigation of field area by Holladay was restricted to small field areas and consequently does not provide the large field area dependences needed to reach any firm conclusions.

Holladay's previously described empirical equations for on-axis light sources gave predictions of pupil areas constricted from 50.27 mm^2, for a fully dark adapted pupil having a maximum diameter of 8 mm, down to only of 12.7 and 9.0 mm^2, for light sources whose diameters subtend 2.5 and 10.7 degrees, respectively, when evaluated at 1,000 mL of uniform field luminance. Furthermore, within the angle range of 2.5 to 10.7 degrees, Holladay's data show that the decrease in pupil area with increasing field area is rapid, for sources near the minimum 2.5 degree field size tested, but becomes progressively slower as the maximum 10.7 degree field size tested is approached. Due to the small sizes of these field luminance areas, the test data of Holladay is inadequate to project whether further increases in the field area reach a limiting value, beyond which no further decreases in the pupil area occurs, or, alternatively, as the comparison of the results of Holladay with those of the other experimenters would suggest, the pupil area continues to decrease as the field area continues to increase. Although the latter explanation is implied by the overall results of the preceding experimental data comparisons, the difference between Holladay's results and those of the other experimenters could, with equal validity, be attributed to the previously described extreme variability observed between the pupil area test results, for different test subjects, reported by all of the experimenters. The only firm conclusion that can be reached, based on the preceding experimental data, is that the data is inadequate to make detailed predictions regarding the dependence of pupil area on real-world environment illumination conditions.

In practical terms, it is doubtful that knowledge of the precise conditions that cause the veiling luminance equation to transition from an exponent 0.872 to unity, on the illuminance dependence term, would be meaningful, relative to the predictions of the automatic legibility control model, since Jainski's veiling luminance data show that this change has not yet started, for an illuminance as measured at the eyes, of 371.6 fc, with the glare source positioned at an angle of 15 degrees from the pilot's line of sight. Even if the illuminance exponent in the veiling luminance were to start to change, at as much as two decades below the illuminance produced by direct exposure to the sun (i.e., nominally 10,000 fc as experienced through an aircraft windscreen or canopy), the differential between the commanded image difference luminances on an aircraft head-down display would still be too small to justify modifying the automatic legibility control model. The high background luminances, associated with head-up and helmet mounted displays, under higher level daylight viewing conditions are already so high that the image difference luminance increments commanded to compensate

---

* Crawford, on Page 384 of his 1936 article, reported conducting a systematic investigation of pupil diameters, as a function of field areas of up to almost a steradian of subtended solid angle, with the luminance of the field held constant. Although this data would have been almost ideal for the present purposes, it could not be analyzed because the original data was not reported in a tabular form, and to the fact that Crawford converted the measured pupil areas into an "equivalent background brightness," before the data was graphed. Since the technique used to convert the data was not described, in sufficient detail to permit extracting the pupil area values, Crawford's results could not be analyzed.

for the presence of the sun would be nearly insignificant. The use of light-attenuative helmet mounted visors or sunglasses, to reduce the potential debilitating effects of exposure to the sun (e.g., eye discomfort or watering, for example), causes the legibility of helmet-mounted displays to be enhanced, but also causes the image difference luminance and background luminance levels of head-down and head-up displays, and the balance of the visual scene that the pilot views through them, to be attenuated by equal amounts and, consequently, does not alter their legibility control requirements.

Under night viewing conditions, it is also concluded that no need exists to compensate for the previously described changes in the exponent on the illuminance dependence term of the veiling luminance equation. The reason for this is that glare sources, having a sufficient illuminance magnitude to produce a perceptible level of veiling luminance, would also cause pupil area reductions to at, or near, the levels needed to invoke pupil areas that satisfy the Riggs' rule of thumb approximation.

3.7.5. Conclusions to the Theory of Veiling Luminance Induced by Discrete Glare Sources

The explanations of the theory of veiling luminance induced by discrete glare sources, as set forth this section, were presented for two purposes. The first and most obvious purpose was to describe the origin and operation of the veiling luminance phenomenon and the physical basis underlying its perception. A second and less obvious purpose was to describe some of the apparently contradictory experimental evidence published in the literature, and to attempt to resolve the apparent inconsistencies. The resolution of these inconsistencies, greatly reduces, but does not entirely eliminate, the potential that there are factors, not accounted for by the mathematical model developed, that could limit its applicability, for use in automatically controlling the legibility of electronic and other types of aircraft cockpit panels, controls and displays. The principal findings of the analysis performed are summarized below.

The first principal finding, presented in this section, is that veiling luminance is due to a real visual effect, not an illusion, and, for practical purposes, is attributable exclusively to the scattering of glare source light, into the pilot's line of sight to the display information being viewed, by imperfections in the optical media of each eye, its lens and its membranes. The importance of this result is associated with the fact that it allows the angular response characteristics of veiling luminance to be explained in theoretical terms, and because it permits the apparent conflicts between other published experimental data to be explained.

A second second principal finding, presented in this section, is that a mathematical model, formulated to describe the pilot's visual response to the environmental illumination conditions experienced in aircraft cockpits, only needs account for the image difference luminance requirements associated with the pilot performing image identification tasks, that is, tasks that require reading the information presented on aircraft cockpit displays, whether that information is presented in numeric, alphanumeric, graphic or video information formats. As an addendum to this finding, it is concluded that the same mathematical model for automatic legibility control, with adjusted parameter values, could be applied to image detection tasks, that is, tasks that require the perception of the presence or absence of a target, but only under photopic vision conditions, that is, for background luminances above nominally 1 to 3 fL, in daylight viewing conditions, or, without background luminance, for targets subtending angles of nominally one degree or larger, and satisfying the same luminance requirements. It can also be concluded with certainty that a different and more complex model would be needed to characterize pilot vision under dark adapted scotopic viewing conditions, for image detection tasks. Finally, it can be concluded that the literature reviewed provides inadequate information to formulate a mathematical model, suitable to account for the target size dependent transition from the cone light receptors, used for photopic vision, to parafoveal, parifoveal and peripheral rod receptors, used within the mesopic vision range, and, therefore, before the transition, from mesopic to scotopic vision, associated with the electrochemical transition to dark adapted vision, at 0.001 to 0.002 fL of background luminance or of target luminance when no background luminance present. It should be noted, however, that the initial efforts expended, to research the published image detection literature for information relevant to the mesopic vision

range, were curtailed, once it was concluded that this information was not nt to the control of the legibility of information presented to pilots within aircraft cockpits.

The third principal finding, of the analyses conducted in this section, is that the mathematical model for automatic legibility control is applicable, for all viewing conditions from full darkness to full daylight conditions, and for the glare sources, which can be present under any of these viewing conditions. A partial caveat must be added, with respect to the latter claim, in that the model, as implemented in this report, does not include an integral capability to adjust the response times of the image difference luminance levels controlled, for dynamically changing environmental illumination conditions. Because the visual requirements for image identification, within aircraft cockpits, limit vision to the use of the eyes' retinal cone light receptors, which respond rapidly, under all viewing conditions, excepting the lower end of the mesopic vision range, the very slow time responses to changing illumination conditions associated with scotopic vision do not become a factor in the model. This subject is dealt in greater detail in Chapter 8.

It should be noted that the effects of cockpit lighting, and of display image difference luminance settings, on the ability of the pilot to dark adapt to view visual scenes external to the cockpit, at scotopic background luminance levels, are not, in specific terms, dealt with by the automatic legibility mathematical model presented in this report. In those cases where the pilot must view external scenes at night, the attendant dark adaptation requirements come into direct conflict with the need for the image difference luminance levels, of the cockpit displays, to be high enough to permit viewing the smallest image critical detail dimensions of the imagery that has to be read by the pilot. For the present, the decision to dim the cockpit instruments from the legible levels commanded by the model, to the lower levels needed to improve the pilot's dark adaptation, to the external scene, must be left to the pilot's judgement, and the only effect on the model is that it must be implemented in a way that allows the pilot to easily and, quickly, make the necessary adjustments. These considerations are considered in greater detail later in the report.

The last principal finding of this section is that no special adjustments to the automatic legibility model are required, to include the effect of light or dark adaptation induced changes in the pupil area of the eyes, and that the illuminance and angular dependences of veiling luminance can be treated as separable variables. This latter result is important primarily with respect to the development of the distributed glare source version of the automatic legibility control mathematical model that follows.

3.8. Veiling Luminance Representations for Spatially Distributed Glare Sources

The purpose of this section is to develop, discuss and validate an empirically based mathematical model to represent the veiling luminance induced when the pilot's eyes are exposed to spatially distributed sources of glare. As a point of reference, for the development of the model, the physical and mathematical significance, of the discrete and distributed glare source formulations of veiling luminance, are introduced and then examined in considerable detail. This is done because, in theory, it should be possible derive the veiling luminance response induced by a discrete glare source from a valid mathematical model for the veiling luminance induced by a distributed glare source. The discussion in these subsections treats the general case of the veiling luminance, induced by discrete and distributed glare sources first, but, thereafter, follows the historical development perspective believed to have been first introduced by Holladay. This approach involves using the special case of distributed glare source equations that are linear in their respective illuminance or luminance dependence terms. A discussion of the general case of the nonlinear equations is deferred until later in this section, when the physical relationships involving veiling luminance have been more fully explored and developed.

In the third subsection, the distributed and discrete glare source formulations of veiling luminance are discussed, and compared with one another, in the context of how accurately the equations, and the experimental data that they represent, model the veiling luminance an observer would actually experience. As a check on the validity of the linear formulation of the discrete and distributed glare source induced veiling

luminance equations, a description of the derivation of the discrete glare source equation from the distributed glare source equation is provided. A similar derivation applicable to the nonlinear case of the general distributed glare source formulation of the veiling luminance equation is included for the theory-based version of the equation later in the section.

In the fourth subsection, the discrete glare source equation, previously derived from Jainski's data, is incorporated into an empirical based integral equation for the veiling luminance induced by a distributed glare source. An approximate calculation using this quasi-empirical equation is described in the fifth subsection. The application of the equation to the distributed glare source experimental data, published by Jainski, shows that the equation provides some reasonably accurate predictions.

The last two subsections approach the formulation of a mathematical model for the veiling luminance induced by distributed glare sources, based on the use of a better defined theoretical foundation, and from the practical perspective of causing the model to be compatible with aircraft cockpit applications of automatic legibility control. A means is introduced to circumvent the mathematical and physical contradictions associated with the nonlinear luminance term, contained in the first version of the distributed glare source veiling luminance empirical model, and, simultaneously, to make the model compatible with the implementation of automatic legibility control. The technique advanced, to accomplish this result, involved the use of lensed light sensors that concurrently optically integrate and apply a veiling luminance angular weighting function, to the spatial luminance distribution incident upon the aircraft cockpit, thereby producing a resultant output signal that is directly proportional to the luminance scattered into the fovea of the eyes. This approach provides reduced computation overhead by providing a directly measurable sensed light quantity, which when scaled and raised to a power yields a direct veiling luminance input for use in the automatic legibility control model.

To assure that the theory-based model, like the empirical-based model, can achieve the requisite compatibility with the automatic legibility control of aircraft cockpit instruments, controls and panel information displays, approximate calculations are described that correctly predict the experimental results of Jainski for a distributed glare source. As a check on this final version of the veiling luminance mathematical model, it is shown that the model can be used to predict the veiling luminance for the special case of discrete glare sources correctly.

3.8.1. General Case of the Discrete Glare Source Formulation of Veiling Luminance

While the veiling luminance equation formulation of Equation 3.58, for a discrete glare source, is accurate, with respect to its historical origin, the equation does not accurately represent the physical process involved in the stimulation of the veiling luminance induced by a glare source. The lenses of the eyes collect light, through the aperture of the iris constricted pupil area, and form a real image of the glare source, albeit, at times out of focus, onto the peripheral or parafoveal areas of the retina. A small fraction of the glare source luminance in transit, from the entry point on the cornea of the eyes, to the point of a retinal focus is scattered into the direction, followed by light from the test image, thereby qualifying as veiling luminance. Contrary to the implication given by the previously introduced discrete glare source veiling luminance equations, which feature an illuminance measure of the luminance distribution of the glare source, it is actually the cumulative effect of the scattering of the spatially distributed luminances entering the pupil areas of the eyes, from across the discrete glare source's surface area, that are responsible for stimulating the veiling luminance test results observed by Jainski, and the other experimenters, whose results were described earlier in this chapter.

As a starting point for developing a mathematical relationship valid for predicting the veiling luminance induced by a distributed glare source, the relationships that hold for discrete glare sources will first be considered in greater detail. By drawing an analogy with Equation 3.54, developed to describe Jainski's discrete glare source veiling luminance data, a general empirical relationship that describes all of the discrete glare source induced veiling luminance results of the experimenters previously cited in this report, can be summarized as follows:

$$L_V = K_D E_B^q f(\theta_B). \tag{3.109}$$

This empirical equation gives the veiling luminance response of the eyes to a single discrete glare source having finite angular dimensions. The equation consists of the product of a proportionality constant, K_D, the illuminance dependence of the veiling luminance, E_B^q, and the angular weighting function dependence of the veiling luminance, $f(\theta_B)$.

The glare source illuminance dependences determined by Holladay, Stiles, Fry and Alpern and Nowakowski all corresponded to a power of $q = 1$ for the illuminance term in Equation 3.109. Making this substitution yields the following simplified veiling luminance relationship for a discrete glare source:

$$L_V = K_D E_B f(\theta_B). \tag{3.110}$$

As previously described, the glare source illuminance range tested by these experimenters was quite small, which, may explain why a power of $q = 1$ was obtained for these results, whereas Jainski, whose data covered a much larger range of illuminance values, determined values for the illuminance exponents of $q = 0.88$ and $q = 0.95$, for the HDD and HUD test configurations, respectively, and ultimately settled on a value of $q = 0.92$ as a compromise value, applicable to both configurations. By comparison, based on the analysis of Jainski's data, described in Section 3.5, it was concluded that a power term of $q = 0.872$ would satisfy the glare source illuminance data of Jainski, for both the HDD and HUD test configurations. As discussed in the Section 3.6, the angular weighting function term in this equation differed for each of the cited experimenters.

As stated in the introductory discussion, at the beginning of this subsection, although all of the empirical data reported for discrete glare sources, used the illuminance incident on the eyes as the measure of the light level to which the test subjects were exposed, it is instead the luminance exposure of the test subjects' eyes that is responsible for inducing the veiling luminance response, even for discrete glare sources. To represent the general empirical equation, for the veiling luminance of a discrete glare source, explicitly in terms of the glare source luminance, rather than the illuminance incident on the eyes, the illuminance term in Equation 3.110 can be replaced by an equivalent integral expression, in which the luminance distribution of the discrete glare source is the principal variable.

The details of the relationship between illuminance and luminance, including the definitions of the terminology used in the equations that follow, are described in Appendix B. Substituting for the illuminance of the glare source, from Equation B.9 in Appendix B, into the discrete glare source veiling luminance equation, Equation 3.110, the following equivalent empirical veiling luminance relationships are obtained:

$$\begin{aligned} L_V &= K_D E_B f(\theta_B) \\ L_V &= \frac{10}{\pi} K_D \left[\oint_{\Omega_s} L_B(\theta,\phi)\, d\Omega_P \right] f(\theta_B) \\ L_V &= \frac{10}{\pi} K_D \left[\int_0^{2\pi} \int_0^{\theta_s/2} L_B(\theta,\phi) \cos\theta \sin\theta\, d\theta\, d\phi \right] f(\theta_B). \end{aligned} \tag{3.111}$$

It should be noted that the integral equations, substituted for the illuminance incident on the eyes from the glare source, and angular weighting function terms, in these equations, use two different spherical coordinate systems. The two systems have a common origin, at the location of the test subject's eyes, but have different z-axis orientations. For the illuminance equation, the z-axis from which the angle, θ, is measured originates at the eyes and goes to the center of the glare source and therefore may be regarded as the glare source coordinate system. For the veiling luminance equation as a whole and the angular weighting function, $f(\theta_B)$,

in particular, the glare source angle, θ_s, is measured with respect to a z-axis, aligned with the test subject's central vision axis, which extends from the test subject's eyes to the center of the test display. The latter spherical coordinate system, which also employs the position variable pair (θ,ϕ), will be referred to as the veiling luminance coordinate system.

Most of the terms used in Equation 3.111 have already been introduced. The projected differential solid angle, $d\Omega_p$, shown in the second equation above and its equivalent algebraic value, expressed in the glare source spherical coordinate system variables in the third equation above, is described in Appendix B. The solid angle, Ω_s, in the second equation above, is the angle subtended by the glare source with respect to a vertex at the test subject's eyes. The solid angle, Ω_s, integration limits, shown in the third equation above, correspond to glare sources, having circular surface areas, like those used in the previously described veiling luminance tests. A glare source with a circular shape, causes the solid angle, Ω_s, the glare source subtends to be conical in shape, with a central axis that passes through the center of the glare source, at the veiling luminance spherical coordinate system location, $(\theta,\phi)=(\theta_s,\phi_s)$, and at the glare source spherical coordinate system location, $(\theta,\phi)=(0,0)$. The zero radian lower integration limit on θ therefore corresponds to the central axis of the glare source and the upper integration limit, $\theta_s/2$, is the angular radius subtended by the discrete glare source as measured from its vertex at the test subject's eyes.

In Equation 3.111, the units of L_v and L_s are both expressed in millilamberts (mL) and E_s is expressed in lux. These are the units originally used by Holladay and since E_s was expressed in lux, that is, lumens per square meter (lm/m^2), the glare source luminance, L_s, within the integral would have to have units of nits, that is, lumens per square meter and steradian ($lm/sr \cdot m^2$). The application of the $10/\pi$ multiplier permits expressing L_s in millilamberts, rather than in nits. The use of this multiplier in the veiling luminance integral equation of Holladay, which is introduced and described in greater detail in sections that follow, is believed to have had its origins in the above equations.

3.8.2. Distributed Glare Source Formulation of Veiling Luminance

It has been shown by Luckiesch and Holladay,[131] Nowakowski,[132] Holladay,[133] Crawford[134] and Hartmann[135] that the effect of adding glare sources on circles concentric to a foveally viewed test symbol (i.e., at a fixed angle θ from the observer's line of sight) is equivalent to a single glare source at the same angle producing an illuminance at the eye equal to the sum of the illuminances of the individual glare sources. Luckiesch and Holladay, who appear to have been the first to report this relationship, generalized the result to a distributed glare source, by treating each differential solid angle element of the human's field of view as a differential glare source contribution to the total veiling luminance.[136]

Expressing the preceding thoughts in mathematical terms, and using a direct analogy to the light magnitude and angular dependences of the discrete glare source equation, the veiling luminance, L_v, can be represented in the most general terms by the following quasi-empirical equation:*

$$L_v = K_l \oint_{\Omega'_{FOV}} L_s(\theta,\phi)^q f_l(\theta)\, d\Omega . \qquad (3.112)$$

In Equation 3.112, K_l is a proportionality constant required to establish the correct veiling luminance magnitude. The distributed glare source luminance term, $L_s(\theta,\phi)$, is the spatial luminance distribution of the visual scene encompassed within the observer's total field of view, which may or may not also contain discrete

* The merits of using this equation to describe veiling luminance are further discussed in Sections 3.8.4 and 3.8.6.

high luminance sources such as the sun, moon, flares, lightning and so forth. The angular weighting function, $f_l(\theta)$, characterizes the proportion of the scene luminance that contributes to the veiling luminance as a function of the angle, θ. As written, this equation expresses the veiling luminance and distributed glare source luminance in terms of standard international (SI) units of nits (cd/m^2).

Utilizing Equation 3.112, an equation that was originally set forth by Holladay to account for the veiling luminance induced by a distributed glare source can be expressed in the following generalized form:

$$L_V = \frac{10}{\pi} K_l \oint_{\Omega'_{FOV}} L_B(\theta,\phi)\, f_l(\theta)\, d\Omega . \qquad (3.113)$$

Holladay expressed both the veiling luminance and distributed glare source luminance in units of milliLamberts (mL). As it was originally presented by Holladay, [137] the equation contained a value for the proportionality constant of $K_l = 4.3$, a power of $q = 1$ for the observer's response to the fraction of the glare source luminance scattered along the central vision axis and an angular weighting function of $f_l(\theta) = 1/\theta^2$. The subscript "l" on the angular weighting function is intended to make the distinction that an angular weighting function, corresponding to an infinitesimal solid angle, should be somewhat different from the angular weighting function, $f(\theta)$, determined experimentally, using a discrete glare source subtending a finite solid angle. The proportionality constant, K_l, is used to set the proper magnitude of the veiling luminance.

The $10/\pi$ multiplier, which appears in Equation 3.113 and in the equation in Holladay's original article, appears to have been inserted into the equation to enable the glare source luminance, $L_B(\theta,\phi)$, to be expressed in units of millilamberts (mL) rather than in nits (i.e., candela per square meter). This multiplier compensates for applying the conversion $L(mL) = \pi/10\, L(nit)$ to $L_B(\theta,\phi)$ and is believed to have been introduced by Holladay as a part of the process of emulating the discrete glare source equation, presented above, while deriving the integral equation for a distributed glare source. Other than as an indication that the veiling luminance integral equation had its origins in its discrete glare source counterpart, it is not clear why Holladay did not simply incorporate the units conversion factor into the constant, K_l. Units conversions, between the illuminance attributable to a glare source, and the luminance distribution of the glare source is further explored in Appendix B.

The luminance variable, $L_B(\theta,\phi)$, in Equations 3.112 and 3.113 characterizes the glare source luminance distribution throughout the observer's field of view (FOV). Except for a proportionality constant, the angular weighting function contribution of $L_B(\theta,\phi)$ (i.e., the fraction of $L_B(\theta,\phi)$ that is scattered) to the veiling luminance attributable to the differential solid angles, $d\Omega$, is given by the function $f_l(\theta)$, which is valid on concentric circles of radius, θ.

Holladay's original article did not stipulate specific integration limits, other than to say they should include the entire area of the distributed glare source. As used in this report, the solid angle integration limit, Ω'_{FOV}, applied to Equation 3.112 and 3.113, is intended to indicate that the integral summation, of the angle-weighted glare source luminance, is to be taken over the observer's entire field of view, with the prime sign on the solid angle integration limit indicating that the central 2.5° to 3° radius area of the foveal light receptors is to be excluded from the integration area. The central vision area is excluded in the case of a head-down display because it is at the symbol background luminance level, L_D, to which the eyes' foveal light receptors would be adapted in the absence of a glare inducing field, and therefore cannot induce a veiling luminance. For head-up or helmet-mounted displays, there is also no reason to include a veiling luminance contribution over the foveal area of the retina, because the luminance of the distributed glare source, $L_B(\theta,\phi)$, in that location, except for the transmittance loss of the image combiner, becomes indistinguishable from what has previously been defined as the display background luminance (i.e., the two luminances are approximately equal).

Substitution of the value of the differential solid angles, $d\Omega$, from Equation B.4 of Appendix B, into Equation 3.113 gives the following adaptation of Holladay's veiling luminance integral equation for a distributed glare source:

$$L_V = \frac{10}{\pi} K_H \int_0^{2\pi} \int_{\theta_F}^{\theta_L} L_B(\theta,\phi)\, f_I(\theta) \sin\theta\, d\theta\, d\phi\,. \qquad (3.114)$$

The lower integration limit on the angle, θ, on this equation corresponds to an approximate radius for the fovea of $\theta_F = 3°$ (i.e., 0.0524 radians) and is measured from an angle of zero degrees at the pilot's central vision axis. The upper integration limit, $\theta_L = g(\phi)$, corresponds to the function that defines the perimeter of vision for the human's instantaneous field of view and is illustrated in Figure 3.39.

3.8.3. Comparison of Discrete and Distributed Glare Source Formulations of Veiling Luminance

It is clear from a comparison of Equation 3.111, for the veiling luminance of a discrete glare source, and Equation 3.114, for a distributed glare source, that the two equations while similar in appearance are mathematically fundamentally different. If Equation 3.114 is a general equation for veiling luminance, applicable to any possible environmental illumination condition, as is claimed, then it should be possible to derive the same veiling luminance results, predicted by the empirical equation for a discrete glare source, using this equation. This calculation can be carried out by assigning the distributed glare source luminance, $L_B(\theta,\phi)$, in Equation 3.114, a value of zero throughout the observer's field of view, except those angles where the discrete glare source is located. This procedure should then yield approximately the same veiling luminance predicted by the empirical veiling luminance equation for a discrete glare source, Equation 3.111, if the two formulations are indeed equivalent.

Unfortunately, in the present circumstances, an exact comparison between the discrete and integral glare source equations cannot be expected to be achieved using the previously described technique. One reason an exact comparison cannot be achieved is that, while the measured illuminance of the glare source, E_B, was reported by all of the experimenters, they did not go on to report the spatial luminance distributions of their glare sources as a function of the spherical angles (θ, ϕ). Although an accurate calculation of the values of the veiling luminance, L_V, and of the illuminance at the eyes due to the glare source, E_B, is possible, using the respective integral equations for veiling luminance and illuminance if the spatial luminance distribution of the glare source, $L_B(\theta,\phi)$, is known, the reverse is not true. The best that can be achieved, where only the illuminance of a light source is known, is a calculation of an average value for the glare source luminance, L_B. Even this calculation can only be performed if it is first assumed that the luminance of the glare source, $L_B(\theta,\phi)$, is constant over the area of the glare source, and if the precise light emitting dimensions of the source are known.

A second factor, complicating the achievement of complete accuracy using Equation 3.114, is that the illuminance and angular dependence relationships, of all of the previously introduced test results, correspond to veiling luminance responses that are spatially averaged over the finite solid angle dimensions of the discrete glare source used as a stimulus, by virtue of the simultaneous exposure, of the test subject's eyes, to the complete spatial luminance pattern of the glare sources, used in the tests. The general discrete glare source empirical equations of Equations 3.109, 3.110 and 3.111, therefore already correspond to composite area averaged (i.e., integrated by the eyes) test results for glare sources having finite angular dimensions (i.e., Jainski's source, for example, subtended an angle of nearly eight degrees whereas Stile's source subtended an angle of 0.45 degrees). In effect, the available test data was all collected by sampling the veiling luminance responses of the test subjects' using glare sources having finite dimensions rather than the infinitesimal dimensions that would be needed to achieve complete accuracy using integral equations, such as Equation 3.114.

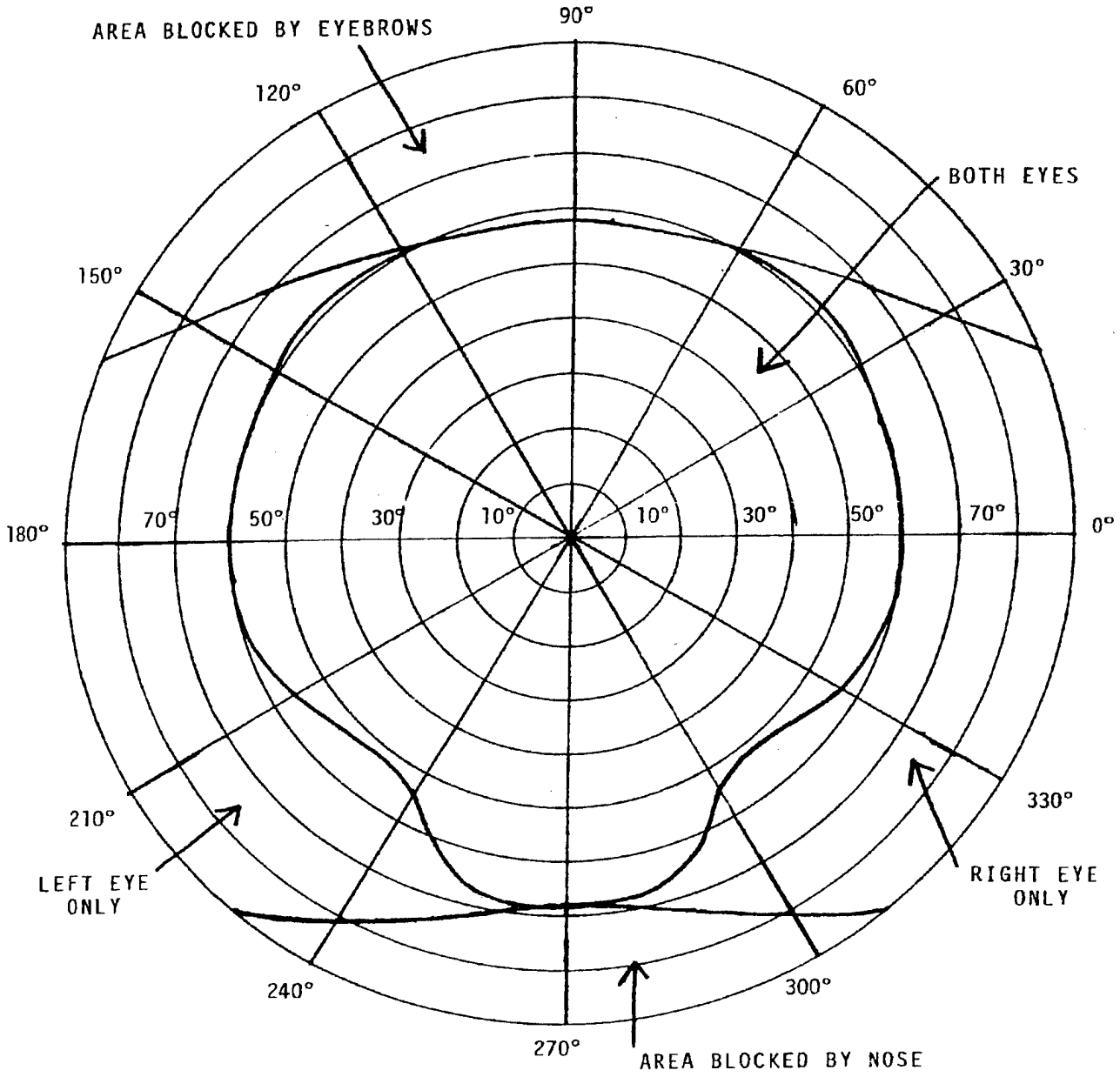


Figure 3.39. Human Visual Field of View.

Lacking a spatial luminance distribution for the glare sources, an alternative theoretical technique for making a comparison between Equations 3.114 and 3.111 is to use Dirac delta functions to represent the discrete glare source luminance functions that appear in both equations. The luminance excitation function representation for a discrete glare source can be expressed, in the veiling luminance coordinate system applicable to Equation 3.114, using a two dimensional Dirac delta function, converted to spherical coordinates as follows:

$$L_B(\theta,\phi) = L_B(\theta_B,\phi_B)\ \delta(\theta-\theta_B)\left(\frac{\delta(\phi-\phi_B)}{\sin\theta}\right). \tag{3.115}$$

In this expression, $L_B(\theta_B,\phi_B)$ is the luminance magnitude of a discrete glare source, located at the spherical angle coordinates (θ_B,ϕ_B), and $\delta(\theta-\theta_B)$ and $\delta(\phi-\phi_B)$ both satisfy the normal rules for Dirac delta functions. A concise summary of the more important properties of Dirac delta functions is contained in Appendix B of Davidson[138] and practical examples of its application may be found in Chapter 3 of Swartz and Friedland.[139]

The delta function property of interest for comparing the discrete and integral glare source equations, Equation 3.111 and 3.114, is given by the following general equation:

$$\int_{x_1}^{x_2} f(x)\,\delta(x-a)\,dx = f(a), \tag{3.116}$$

where the equation is defined only if the position coordinate, $x = a$, lies within the integration limit interval $x_1 \le a \le x_2$. By substituting Equation 3.115 for $L_B(\theta,\phi)$ into Equation 3.114 and applying the delta function integral property of Equation 3.116, to the integration over both θ and ϕ, the following equation is obtained:

$$L_V = \frac{10}{\pi} K_H \int_0^{2\pi}\int_{\theta_F}^{\theta_L} L_B(\theta_B,\phi_B)\ \delta(\theta-\theta_B)\left(\frac{\delta(\phi-\phi_B)}{\sin\theta}\right) f_l(\theta)\sin\theta\,d\theta\,d\phi \tag{3.117}$$

$$L_V = \frac{10}{\pi} K_H L_B(\theta_B,\phi_B)\, f_l(\theta_B).$$

This is the veiling luminance predicted for a discrete glare source, of luminance magnitude, L_B, at angular coordinates (θ_B,ϕ_B), with respect to the test subject's central vision axis, and where Holladay's units of millilamberts continue to be used for both of the luminance terms, as in Equation 3.114.

To evaluate Equation 3.111 in the same manner as Equation 3.114, the luminance excitation function of Equation 3.115 must be modified to accommodate the glare source coordinate system employed by the integral in Equation 3.111. Since the $(\theta,\phi) = (0,0)$ origin of the glare source coordinate system is centered on the glare source, the luminance excitation function representation for a discrete glare source can be expressed, in the glare source coordinate system applicable to Equation 3.111, using a two dimensional Dirac delta function, converted to spherical coordinates as follows:

$$L_B(\theta,\phi) = L_B(\theta_B,\phi_B)\ \delta(\theta-0)\left(\frac{\delta(\phi-0)}{\sin\theta}\right) = L_B(\theta_B,\phi_B)\ \delta(\theta)\left(\frac{\delta(\phi)}{\sin\theta}\right). \tag{3.118}$$

By substituting Equation 3.118 for $L_B(\theta,\phi)$, into Equation 3.111, and applying the delta function integral property of Equation 3.116 to the integration over both θ and ϕ, where with $a = 0$ radians, the $\cos\theta$ term becomes $\cos 0 = 1$ and the $\sin\theta$ terms in the numerator and denominator cancel. The resulting equation evaluates to yield the veiling luminance induced by a single discrete glare source as follows:

$$L_V = \frac{10}{\pi} K_D \left[\int_0^{2\pi}\int_0^{\theta_s/2} L_B(\theta_B,\phi_B)\ \delta(\theta)\left(\frac{\delta(\phi)}{\sin\theta}\right)\cos\theta\sin\theta\,d\theta\,d\phi\right] f(\theta_B) \tag{3.119}$$

$$L_V = \frac{10}{\pi} K_D L_B(\theta_B,\phi_B)\, f(\theta_B).$$

Like Equation 3.117, this equation predicts the veiling luminance for a discrete glare source of luminance magnitude, L_B, located at spherical angle coordinates (θ_B, ϕ_B), with respect to the test subject's central vision axis, and where the convention of Holladay to use units of millilamberts for both of the luminance terms continues to be used, as in Equation 3.111.

A comparison of Equations 3.117 and 3.119, shows these equations are very nearly the same. Since both equations were derived using a theoretical single valued luminance excitation function of infinitesimal angular subtense and of luminance magnitude, L_B, the angular weighting functions, $f(\theta_B)$, and, $f_I(\theta_B)$, represent the principal distinction between the two equations. The difference between these two functions is real and cannot be eliminated completely. The angular weighting function, $f_I(\theta_B)$, is a theoretical artifice, since its true angular relationship can only be approached through taking sample measurements using smaller and smaller glare sources. Consequently, an exact emulation of this ideal function, using conventional light sources and measurement techniques, is not an achievable goal, but, for sufficiently small real glare sources, the difference between the ideal angular weighting function and the one sampled using an actual glare source should become negligible.

In practice, the only comprehensive angular weighting function data available is that reported by Jainski. The veiling luminance data collected by Jainski, and modeled in this report, used a glare source subtending a solid angle of about eight degrees to sample the veiling luminance angular weighting function, $f(\theta_B)$. Because the ideal angular weighting function, $f_I(\theta_B)$, that Jainski sampled, represents a human visual response characteristic, it is realistic to expect it to be a continuously variable function (i.e., without discontinuities). Based on the premise this assumption is valid, then it can be shown that the nominal eight degree area-averaged angular weighting function, $f(\theta_B)$, measured by Jainski, would have been shifted to larger angles, from the path of the actual ideal angular weighting function, during the process of being measured.

A rudimentary analysis was conducted to learn the extent of the angular shift, in the ideal angular weighting function characteristic, to be expected from sampling this function using Jainski's nominal eight degree diameter glare source. The analysis of the shift in the angular weighting function characteristic was based on the known slopes of the empirical angular weighting function characteristic, $f(\theta_B)$, the circular shape of the glare source and an assumption that the spatial luminance distribution across the glare source surface was either uniform, or increased in going from its periphery to its center, which is realistic for the vast majority of light sources. Because of the decreasing values of veiling luminance with increasing glare source angles, the highest value of veiling luminance from within the sampled circular area, occurred at the smallest glare source angle. This sample was averaged with lowest value of veiling luminance, within the area subtended by the glare source, which occurred at the largest glare source angle. The mean of these values was then compared with the veiling luminance corresponding to the center of the glare source.

The empirical characteristic, given by Equation 3.58, was plotted, with the logarithm of veiling luminance on the vertical axis, and the glare source angle on the horizontal linear axis, as is shown in Figure 3.40. Figure 3.40 also shows that the graph of the empirical equation, representing Jainski's veiling luminance angular characteristics, can be approximated by a constant slope characteristic on a semi-logarithmic graph, with a maximum error of less than 4%, for glare source angles from ten to forty-five degrees. Because the decrease in the angular weighting function is approximately exponential with increasing values of the glare source angle, and, moreover, decreases more rapidly than predicted by the inverse of a linear increase in the angle, the contribution of veiling luminance on the small angle side of the glare source can always be expected to have greater angular weighting than the contribution from the large angle side, thereby, causing the mean luminance to be inflated, to some extent.

In accordance with the result predicted in the preceding paragraph, when Equation 3.58, the empirical equation for veiling luminance, is used to determine the veiling luminance samples, for the low and high angle areas of the glare source surface, the corresponding mean values of the veiling luminances calculated, were higher than the values of the veiling luminance determined by evaluating the empirical equation, for angles at

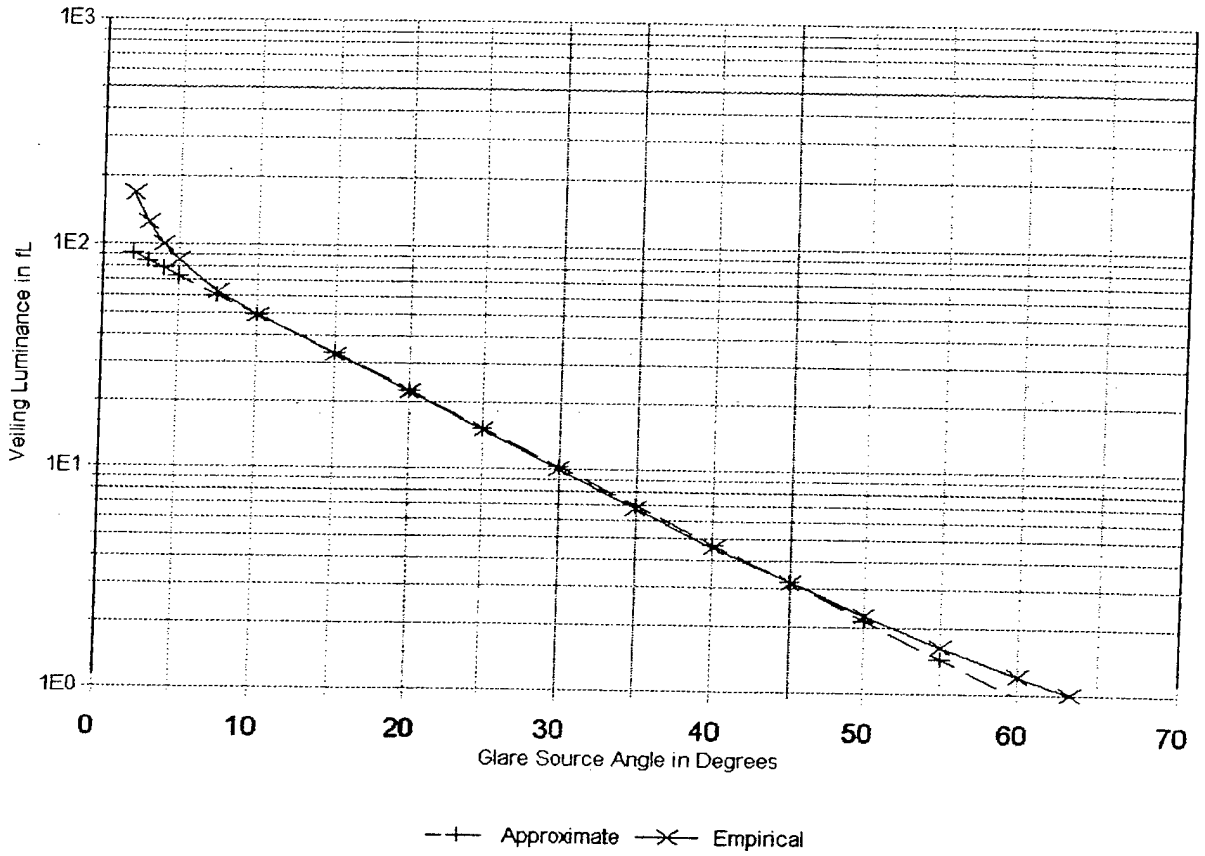


Figure 3.40. Semi-logarithmic Plot of the Empirical Veiling Luminance Equation for Jainski's Data for E_B = 371.6 fc and a Straight Line Approximation.

the center of the glare source surface area. For all of the glare source angles tested in this way, the predicted maximum value of the shift, in the veiling luminance angular weighting function characteristic, was by one degree toward larger angles, in the region of the characteristic described in the preceding paragraph. This analysis of the angular shift caused by Jainski's use of a large glare source to measure the human's ideal angular weighting function characteristic, shows that this measurement technique would have caused the measured characteristics to be displaced to higher angles, but, by at most, only one degree from the true position of the ideal characteristics. The limitation on Jainski's test data, to the range of nominally 5 to 50 degrees, and the nominal four degree radius of the glare source, prevented analyzing a greater range of angles using the above technique. It should be noted that the higher slope of the characteristic below ten degrees would predict larger shifts between the ideal and empirical characteristic positions.

Lacking the specific angular spatial luminance distribution for the glare source used by Jainski, a more accurate estimation of this source of measurement error cannot be derived. Based on the previously described errors, associated with the Jainski veiling luminance data, an error of one degree in the position of the empirical veiling luminance angular weighting function characteristic is, by comparison, considered negligible. It is known that Jainski's experimental techniques did reduce some additional potential sources of error. This was accomplished through Jainski's positioning of the glare source using a fixed radius rail system, and by using a set of neutral density filters in a filter holder attached to the front of the glare source, respectively, to move and dim the glare source, without causing a change to either its spatial or its spectral luminance distributions.

Since no better estimate of the ideal angular weighting function, $f_I(\theta_B)$, can be achieved under the present circumstances, and because this function is as accurate as is required for the present purposes, it shall hereafter be assumed that the angular weighting function modeled on Jainski's data, $f(\theta_B)$, is equal to the ideal angular weighting function, $f_I(\theta_B)$. With this condition satisfied, then the veiling luminances from Equations 3.117 and 3.119 can be equated. Doing so, the proportionality constants for the respective discrete and distributed glare source equations, Equations 3.111 and 3.114, can be considered to be equal to one another, that is,

$$K_D = K_I . \tag{3.120}$$

This means that the numerical multiplier values in the previously developed discrete glare source equations can also be used in the distributed glare source integral equations.

3.8.4. Empirical Model for Distributed Glare Source Veiling Luminance

Based on the previously introduced general empirical equation for the veiling luminance induced by a distributed glare source, Equation 3.112, the following quasi-empirical equation should be appropriate for modeling the distributed glare source data of Jainski:

$$L_V = \frac{K_I}{\pi^q} \oint_{\Omega'_{FOV}} L_B(\theta,\phi)^q \, f(\theta) \, d\Omega . \tag{3.121}$$

Furthermore, the introduction of the veiling luminance spherical coordinate system variables and constants into Equation 3.121, allows this equation to be transformed into the following more useful equivalent form:

$$L_V = \frac{K_I}{\pi^q} \int_0^{2\pi} \int_{\theta_F}^{\theta_L} L_B(\theta,\phi)^q \, f(\theta) \sin\theta \, d\theta \, d\phi . \tag{3.122}$$

These two equations are comparable to Equations 3.113 and 3.114, except that $L_B(\theta,\phi)$ is raised to the power of q and the units conversion multipliers have been changed to allow expressing both the luminance variables, L_V and L_B, either in apostilbs (asb), as Jainski did, or in foot-Lamberts (fL), the units of luminance used in this report. The illuminance units applicable to the corresponding discrete glare source veiling luminance equations, for these two systems of units, are the lux (lx) and foot-candle (fc), respectively. The angles in the equations are expressed in radians and the solid angles in steradians. The equations integrate the product of the distributed glare source luminance, $L_B(\theta,\phi)$, incident on the observer's eyes from the glare source, raised to the power of $q = 0.872$, and the angular weighting function, $f(\theta)$, derived from Jainski's discrete glare source tests, over the solid angle, Ω'_{FOV}. As previously described, the integration is taken over the observer's entire field of view (FOV), excluding only a central area that can be as small as the 2.5° to 3° radius of the fovea, or as large as the area of the display on which the eyes' light receptors are focused, to which they would be adapted in the absence of a glare inducing field. Both of these areas are assumed to be at the level of the display background luminance, L_D, and are therefore incapable of contributing to the veiling luminance induced. The latter fact is true, even for a HUD, since the glare source luminance, after attenuation by the windscreen and HUD optical combiner, becomes the background luminance of the imagery being projected using the HUD optics.

Based on the earlier data analysis of Jainski's discrete glare source veiling luminance data that culminated in Equation 3.58, the product of the constant, K_D, and the angular weighting function, $f(\theta)$, can be expressed as follows:

$$K_D f(\theta) = \frac{1.62\,\theta^{-0.74}}{1 + 4.764 \times 10^{-5}\,\theta^3} . \tag{3.123}$$

This equation applies for the case where the angle, θ, in the angular weighting function is expressed in units of degrees. To relate this equation to the integral equation for veiling luminance in Equation 3.122, the approximation described at the end of the preceding subsection, in which the empirical angular weighting function, for a discrete glare source, is used in place of the ideal angular weighting function, must be applied. Also, in analogy to Equation 3.120, but in this case only as an approximation, the integral constant, K_I, is equated to the discrete constant, K_D, from Equation 3.57 yielding:

$$K_I(\textit{degrees}) = K_D(\textit{degrees}) = 1.62\,. \tag{3.124}$$

which applies for the case where the angle, θ, in the angular weighting function is expressed in units of degrees.

To derive a relationship equivalent to Equation 3.123, where the angle, θ, is expressed in units of radians rather than in degrees, the following units conversion equation can be employed,

$$\theta(\text{deg}) = \frac{180}{\pi}\,\theta(\text{rad}) = 57.2958\,\theta(\text{rad}) \approx 57.3\,\theta(\text{rad})\,. \tag{3.125}$$

Substituting this conversion for θ into Equation 3.123 and carrying out the indicated mathematical operations, the equivalent relationship, with θ expressed in units of radians, rather than in degrees, is as follows:

$$K_D f(\theta) = \frac{1.62\,(57.3)^{-0.74}\,\theta^{-0.74}}{1 + 4.764 \times 10^{-5}\,(57.3)^3\,\theta^3}$$

$$K_D f(\theta) = \frac{0.081\,\theta^{-0.74}}{1 + 8.9626\,\theta^3}\,. \tag{3.126}$$

The constant, K_I, therefore, takes on the new value,

$$K_I(\textit{radians}) = K_D(\textit{radians}) = 0.081\,, \tag{3.127}$$

which applies for the case where the angle, θ, in the angular weighting function is expressed in units of radians.

Substituting Equation 3.126 into Equation 3.122 causes the general form of the veiling luminance equation to have its angular dependences expressed entirely in radians rather than degrees, thereby yielding the following general empirical equation for the veiling luminance of a distributed glare source:

$$L_V = \frac{0.081}{\pi^{0.872}} \int_0^{2\pi} \int_{\theta_F}^{\theta_L} \frac{L_B(\theta,\phi)^{0.872}\,\theta^{-0.74}}{1 + 8.9626\,\theta^3} \sin\theta\, d\theta\, d\phi\,. \tag{3.128}$$

As previously indicated, in relation to Holladay's version of this equation, the lower integration limit is the radius of the fovea, which will be approximated as $\theta_F = 0.05236$ radians (i.e., 3 degrees). As before, this integration limit can also be larger, provided that the enlarged area is at the display background luminance level, L_D. The upper integration limit, $\theta_L = g(\phi)$, as previously mentioned, is the field of view limit in the direction specified by the angle, ϕ, where $g(\phi)$ is the function defining the human's perimeter of vision, which is partially illustrated in Figure 3.39.

As an alternative to using the limits of the human's field of view, as the upper integration limit in Equation 3.128, a smaller angle can be used beyond which the integrated contribution, of the scene luminance multiplied by the angular weighting function, $f(\theta)$, can be considered negligible. Contributions to L_V for angles, $\theta_L > 60°$, are generally negligible. If the luminance of a discrete glare source such as the sun is known, it can be considered a part of the distributed glare source luminance and simply be integrated over using Equation 3.128. If the luminance of a discrete glare source is not known, but the illuminance incident on the eyes is known, then the contribution of the glare source to veiling luminance can be calculated separately, using discrete glare source veiling luminance equation, Equation 3.58, and then added to the distributed luminance

contribution from Equation 3.128. In either event, the total veiling luminance can be used with Equation 3.23 to establish the perceived image difference luminance, ΔL_P.

As an alternative to Equation 3.128, the veiling luminance equation for a distributed glare source can also be expressed either partially or completely in angular units of degrees, rather than radians. Expressing Equation 3.122 with the angle, θ, in degrees and the angle, ϕ, still in radians can be accomplished by substituting for $K_y f(\theta)$ from Equation 3.123 and converting the differential angle, $d\theta$, to degrees from radians by dividing by the conversion factor 57.3. The resulting general empirical equation for the veiling luminance induced by a distributed glare source, with the integration limits on the angle, θ, expressed in degrees, is as follows:

$$L_V = \frac{1.62}{57.3\,\pi^{0.872}} \int_0^{2\pi} \int_{\theta_F}^{\theta_L} \frac{L_B(\theta,\phi)^{0.872}\,\theta^{-0.74}}{1 + 4.764 \times 10^{-5}\,\theta^3} \sin\theta\, d\theta\, d\phi\,. \tag{3.129}$$

3.8.5. Validation of Empirical Model for Distributed Glare Source Veiling Luminance

If the mathematical model developed in the preceding subsection to predict the veiling luminance of a distributed glare source is correct, then the veiling luminances given by Equations 3.128 or 3.129 can be used to predict Jainski's distributed glare source test results. The distributed glare source test results of Jainski were collected by controlling the values of the surround-field luminance, L_U, and the panel or in-field luminances, $L_P = L_I$. A sample of these results was shown previously in Figure 3.13. This figure illustrates the effects on the perceived image difference luminance versus display background luminance characteristics, for different parameter values of the surround-field luminance, L_U, and the panel or in-field luminances, $L_P = L_I$.

To compare the mathematical model with Jainski's test results, the values of the surround-field luminance, L_U, and the panel or in-field luminances, $L_P = L_I$, shown in Figure 3.13 must be used to calculate the corresponding veiling luminances that are predicted using Equations 3.128 or 3.129. Once the veiling luminance is determined, it can then be substituted into Equation 3.23 to calculate the values of perceived image difference luminance to be compared with Figure 3.13. For convenience, Equation 3.23 is repeated here, as follows:

$$\Delta L_P = \Delta L_{PK}\left[1 + \left(\frac{L_D + L_V}{L_{DK}}\right)^m\right]. \tag{3.23}$$

The substitution into this equation of m = 0.926, the value for the perceived image difference luminance y-axis intercept, ΔL_{PK}, from Table 3.4, and the value for the corresponding luminance breakpoint, L_{DK}, that are applicable to the $\alpha_c = 8.8'$ critical detail dimension data of Figure 3.13, yields the following empirical equation for the perceived image difference luminance:

$$\Delta L_P = 0.0276\left[1 + \left(\frac{L_D + L_V}{0.1793}\right)^{0.926}\right]. \tag{3.130}$$

Because Jainski's report does not provide dimensions, for some parts of the simulated cockpit configurations illustrated, an approximate technique will be used to calculate the veiling luminance contribution to the perceived image difference luminance. Referring to Figure 3.39, radial lines will be taken as the boundaries between the constant surround-field luminance, in the upper part of the figure, and the constant in-field luminance in the lower part of the figure. The center of the display will be taken to be centered on the origin of the human's visual field of view. This means that the spherical coordinate system used to describe

the position of the glare source is the same as the one shown for the human visual system in Figure 3.39. The pilot's central vision axis passes through the center of the display, and is therefore coincident with the z-axis, where the test symbol in the Jainski tests was located. Increases in the spherical coordinate, θ, are shown in Figure 3.39 as concentric circles increasing from zero at the origin, which is coincident with the z axis. Increases in the spherical coordinate, ϕ, are shown in the Figure 3.39 as radial lines, and the angle increases in a counterclockwise direction, in the xy-plane, starting from zero, which coincides with the x axis.

Since L_U and $L_P = L_I$ are both constant within their respective areas of the human field of view, the distributed glare source luminance, $L_B(\theta,\phi)$, in the veiling luminance equations can be considered constant as a function of the angle, θ. Consequently, the general equation for the veiling luminance of a distributed glare source, which is given by Equation 3.122, and repeated here for convenience,

$$L_V = \frac{K_I}{\pi^q} \int_0^{2\pi} \int_{\theta_F}^{\theta_L} L_B(\phi)^q f(\theta) \sin\theta \, d\theta \, d\phi , \tag{3.122}$$

can be further simplified as follows:

$$L_V = \frac{K_I}{\pi^q} \int_0^{2\pi} L_B(\phi)^q d\phi \int_{\theta_F}^{\theta_L} f(\theta) \sin\theta \, d\theta$$

$$L_V = \frac{K_I K_\theta}{\pi^q} \int_0^{2\pi} L_B(\phi)^q d\phi , \tag{3.131}$$

where the constant, K_θ, is given by the equation,

$$K_\theta = \int_{\theta_F}^{\theta_L} f(\theta) \sin\theta \, d\theta . \tag{3.132}$$

The equation for K_θ was evaluated using Simpson's Rule for numerical integration, and a hand-held calculator. The value of K_θ was calculated with $f(\theta)$ expressed in degrees from Equation 3.123, after factoring out $K_I = 1.62$ and dividing by 57.3 to convert $d\theta$ from radians to degrees, using the following equation:

$$K_\theta = \frac{1}{57.3} \int_{3^\circ}^{60^\circ} \frac{\theta^{-0.74}}{1 + 4.764 \times 10^{-5} \, \theta^3} \sin\theta \, d\theta . \tag{3.133}$$

The use of the integration limits of $\theta_F = 3^\circ$ and $\theta_L = 60^\circ$, with a sampling interval of $\Delta\theta = 1.5^\circ$ resulted in integration by Simpson's Rule over a number of samples, $n + 1$, where n is given by the equation:

$$n = \frac{\theta_L - \theta_F}{\Delta\theta} = \frac{57}{1.5} = 38 . \tag{3.134}$$

The calculated value of K_θ using this technique was determined to be

$$K_\theta(\textit{degrees}) = 0.01706 . \tag{3.135}$$

No change in this result occurred when the sampling interval was reduced to 0.5 degrees.

The value of K_θ was also calculated with $f(\theta)$ expressed in radians from Equation 3.126, after factoring

out $K_I = 0.081$, using the equation:

$$K_\theta = \int_{0.05236}^{1.047} \frac{\theta^{-0.74}}{1 + 8.9626\,\theta^2} \sin\theta d\theta . \tag{3.136}$$

In this case, the same integration limits were used, but they were expressed in radians as $\theta_F = 0.05236$ and $\theta_L = 1.047$, rather than in degrees. When integration by Simpson's Rule was again employed, using the same total number of samples, $n + 1 = 39$, the resultant calculated value of the angle multiplier constant, K_θ, was as follows:

$$K_\theta(radians) = 0.3410 . \tag{3.137}$$

The boundary between the L_U and $L_P = L_I$ was taken as 20 degrees below the horizon for the case of the HUD and as 10 degrees below the horizon for the HDD. This adjustment in the integration boundary takes into account the fact that, even though the pilot's vision is centered on the display for each of these viewing conditions, the HUD is located higher in the cockpit than the HDD. The inaccuracy produced by this approximation can be expected to be most severe for the Jainski HDD test configuration, since the instrument panel, which is at a luminance level, $L_P = L_I$, extends 4 degrees above the display, whereas in the present approximation that area is at the luminance level, L_U.

To simplify the evaluation of Equation 3.131, the differential angle, $d\phi$, which is expressed in radians, was converted to a differential angular fraction of the field of view by multiplying the numerator and denominator of the equation by 2π and changing the integration limits to 0 to 1 from 0 to 2π. The converted equation can be written as is shown in the first equation below. A derivation, of an easily evaluated algebraic expression for the approximate veiling luminance equation, is shown in the second and third equations, below.

$$L_V = \frac{2\pi K_I K_\theta}{\pi^q} \int_0^1 L_B(\phi)^q \, d\phi_f$$

$$L_V = \frac{2\pi K_I K_\theta}{\pi^q} \left[L_U^q \int_0^{\phi_{Uf}} d\phi_f + L_I^q \int_0^{\phi_{If}} d\phi_f \right] \tag{3.138}$$

$$L_V = \frac{2\pi K_I K_\theta}{\pi^q} \left[\phi_{Uf} L_U^q + \phi_{If} L_I^q \right].$$

The simplification shown in the second equation is made possible by substituting the constant luminances L_U and L_I for $L_B(\phi)$, in the first equation, and the third equation follows directly from the second by evaluating the two integrals.

In the final equation, above, ϕ_{Uf} is the fraction of the circular field of view at the luminance level, L_U, and ϕ_{If} is the fraction of the balance of the circular field of view, at the luminance level, $L_P = L_I$. Because these two fractions, together, encompass the entire circular field of view, the two fractions must satisfy the equation,

$$\phi_{Uf} + \phi_{If} = 1 . \tag{3.139}$$

Substituting this relationship into Equation 3.138, an alternative final form of the approximate veiling luminance equation can be expressed as follows:

$$L_V = \frac{2\pi K_I K_\theta}{\pi^q} \left[\phi_{Uf} L_U^q + (1 - \phi_{Uf}) L_I^q \right]. \tag{3.140}$$

Equation 3.140, may be evaluated for Jainski's data by substituting $q = 0.872$ and consistent values of the constants K_l and K_θ. Specifically, the substitution involves $K_l = 1.62$ from Equation 3.124 and $K_\theta = 0.01706$ from Equation 3.135, for units of degrees, or $K_l = 0.081$ from Equation 3.127 and $K_\theta = 0.3410$ from Equation 3.137, for units of radians. As required, both sets of constants, when substituted into Equation 3.140 evaluate to give the same result, to three significant figures of accuracy, as follows:

$$L_V = 0.0640 \left[\phi_{Uf} L_U^{0.872} + (1 - \phi_{Uf}) L_l^{0.872} \right]. \tag{3.141}$$

To proceed further, with the evaluation of the preceding approximate equation for veiling luminance, the value of the fraction, ϕ_{Uf}, must be substituted into the equation. With the boundary radials, between the L_U and L_l luminance areas, located symmetrically on each side of the field of view, 20 degrees below the horizon, the fraction, ϕ_{Uf}, for the HUD test configuration can be calculated as

$$\phi_{Uf} = 220°/360° = 0.6111 . \tag{3.142}$$

Likewise, with the boundary radials, between L_U and L_l luminance areas of the field of view, located 10 degrees below the horizon, the fraction, ϕ_{Uf}, for the HDD test configuration can be calculated as

$$\phi_{Uf} = 200°/360° = 0.5556 . \tag{3.143}$$

Equation 3.141 can be used to calculate the veiling luminance by using the above values for ϕ_{Uf} and the values of L_U and L_l, from Jainski's distributed glare source tests. The latter values have been entered into Table 3.12, together with references to the Jainski figures in which they served as test parameters. The table also contains perceived image difference luminance values extracted from Jainski's HUD and HDD figures, for each combination of L_U and L_l tested, and the corresponding values the perceived image difference luminance, calculated using Equation 3.130.

Both the computed and test perceived image difference luminance values, contained in Table 3.12, correspond to the values referred to earlier in the report as the low display background luminance, y-axis intercept levels, ΔL_{PK}, and, consequently, were all extracted at the lowest display background luminance tested by Jainski, that is, for $L_D \approx 1 \times 10^{-6}$ fL. These points on the perceived image difference luminance versus display background luminance characteristics were chosen for this comparison, both because they are expected to give the most accurate results, in that they require only one coordinate axis intercept on Jainski's graphs to be read and compared, and because they were also used as one of the two parameters substituted into Equation 3.23 to obtain Equation 3.130, and, which, consequently, also serve as the baseline for the empirical model. Values of ΔL_P from the Jainski test characteristics that apply in the absence of veiling luminance are contained in Table 3.4.

Before comparing the test and computed perceived image difference luminance values, contained in Table 3.12, some comments need to be made about the test data of Jainski, contained in the table. The test methodology used by Jainski resulted in some of the same test conditions being evaluated multiple times. For example, in doing parametric assessments of the dependence of the perceived image difference luminance, first on the critical detail dimension of the test symbol, second on the in-field luminance and finally on the surround-field luminance, the same test was repeated three times and the results were reported in Figures 71, 75 and 84, respectively, of the Jainski report. The test results from these figures, corresponding to a display background luminance level of about 1×10^{-6} fL, are shown in the second HDD data grouping from the top of Table 3.12. Comparing the three values of ΔL_P , two of the values, 0.312 fL and 0.307 fL, are seen to be in good agreement, differing by only 1.6%, whereas the third value, 0.237, differs from 0.312 fL by 27.3%. The likely sources of these differences, were discussed previously in this chapter in Section 3.5.2.3 entitled "Assessment of the Accuracy of Jainski's Experimental Data," and the magnitudes of the errors are comparable to the values encountered in that section.

The value of 0.337 fL, predicted for the HDD configuration, for the distributed glare source veiling luminance model and shown in the last column of Table 3.12, is larger than the highest of the three test values

Table 3.12. Comparisons of Image Difference Luminance Requirements from Jainski's Tests with like Values Computed using the Empirical Veiling Luminance Integral, for Distributed Glare Source Viewing Conditions.

Test Conditions & Data from Jainski Figures [1]								Computed Values	
Display Type	Figure (Bild)	$L_P = L_I$ in asb	$L_P = L_I$ in fL	L_U in asb	L_U in fL	ΔL_P [3] in asb	ΔL_P [3] in fL	L_V [2] in fL	ΔL_P [3] in fL
HDD	84	920	85.5	92,000	8,547	47	4.4	96.8	9.38
HDD	71	920	85.5	530	49.2	2.55	0.237	2.44	0.337
	75	920	85.5	530	49.2	3.35	0.312		
	84	920	85.5	530	49.2	3.3	0.307		
HDD	78	920	85.5	1×10^{-5}	$\sim 1 \times 10^{-6}$	2.4	0.223	1.38	0.210
	84	920	85.5	1×10^{-5}	$\sim 1 \times 10^{-6}$	2.3	0.214		
HUD	57	1000	92.6	$L_U = 2L_D$		2.2	0.204	1.29	0.199
HDD	75	1×10^{-5}	$\sim 1 \times 10^{-6}$	530	49.2	1.81	0.168	1.06	0.171
HUD	57	$L_I = 0.003 L_D$		$L_U = 2L_D$		0.297	0.0276	~ 0	0.0276
HDD	78	1×10^{-5}	$\sim 1 \times 10^{-6}$	1×10^{-5}	$\sim 1 \times 10^{-6}$	0.286	0.0266	~ 0	0.0276
HDD	78	1	0.0926	1×10^{-5}	$\sim 1 \times 10^{-6}$	0.280	0.0260	0.00357	0.0283

Notes: 1. Test data corresponding to an image critical detail dimension of $\alpha_c = 8.8'$ (i.e., b = 0.4 mm, ℓ = 4b) was extracted from the cited Jainski figures.

2. Veiling luminance was computed using $\phi_{Uf} = 0.5556$ for the HDD test configuration and $\phi_{Uf} = 0.6111$ for the HUD test configuration.

3. The values of perceived image difference luminance, ΔL_P, were either extracted from Jainski's figures or computed for a display background luminance, L_D, of approximately 1×10^{-6} fL.

discussed in the previous paragraph, 0.312 fL, by 8%. By the standard of tests involving humans, and by virtue of the earlier assessment of the accuracy of Jainski's data, this 8% error magnitude can be considered small. In spite of this, the fact that L_U is less than L_I, in the veiling luminance calculation approximation used for the HDD, would tend to de-emphasize the true effect of L_I in comparison to its effect in the actual simulated cockpit test configuration experienced by a test subject, since the higher luminance panel area above, and on each side of the display, is not included in the approximate veiling luminance calculation. This situation would, at first glance, be expected to cause the mathematical model to predict values of ΔL_P lower than the values yielded by the experimental data, rather than to the higher value of 0.337 fL obtained. This result will, hereafter, be referred to as Analysis Point # 1.

In practice, the preceding analysis of the approximate veiling luminance calculation is oversimplified. The

lower integration limit used for both the HUD and the HDD was $\theta_F = 3°$. This is a fair approximation for the case of the HUD, since the 8°x 8° square background of the combiner is at half the surround field luminance, L_U. However, in the approximate veiling luminance calculation for the HDD, the 8°x 8° square display surface in Jainski's test is at a luminance of $L_D = 1 \times 10^{-6}$ fL, instead of at the $L_U = 49.2$ fL value used for the upper part of the display, and the $L_l = 85.5$ fL used for the lower part of the display. The use of these luminance values to calculate the veiling luminance, due to all but the central 3 degree radius area of the display excluded by the angular weighting function integral equation, leads to an increase in veiling luminance, which is not supported by the actual test configuration of the HDD. Since the highest values of the angular weighting function occur at smallest the glare source angles, the L_U contribution to the calculated veiling luminance is even further emphasized by the use of the approximate veiling luminance calculation technique. This result will, hereafter, be referred to as Analysis Point # 2.

In the third set of HDD data, from the top of Table 3.12, there are two sets of experimental test data, which, in concept, should be identical, but in practice have values for ΔL_P of 0.223 fL from Jainski's Figure 78 and 0.214 fL for Figure 84, a difference of 4.1%. The calculated value of the image difference luminance, for the corresponding glare source conditions, was $\Delta L_P = 0.210$ fL. Thus, for this comparison, the calculated veiling luminance was lower than the two values determined in Jainski's tests. This result is consistent with Analysis Point # 1, since $L_U = 1 \times 10^{-6}$ fL, was the same as the display background luminance for the HDD test, and therefore cannot contribute to the veiling luminance, via Analysis Point # 2.

The first data entry, for the HUD test configuration in the Table 3.12, occurs for the fourth data set from the top of the table. Since the HUD test configuration is a better match with the approximate calculation technique, used to determine the veiling luminance, little difference should be expected between the test and calculated values of the perceived image difference luminance. With the calculated value of the image difference luminance, 0.199 fL, only 2.5% lower than the test value of 0.204 fL this expectation appears to be satisfied.

The fifth data set from the top of Table 3.12 is again for the HDD test configuration. In this case, the in-field luminance at $L_l = 1 \times 10^{-6}$ fL is insignificant, in terms of inducing a veiling luminance response, and the surround-field luminance at $L_U = 49.2$ fL is at a low but significant luminance level, just the opposite of the conditions for the third HDD data set. The value of the calculated image difference luminance, 0.171 fL, is higher by 1.8% than the test value of 0.168 fL, which is consistent with Analysis Point # 2.

The sixth data set, for the HUD, and the seventh data set, for the HDD test configuration, have in-field and surround-field luminance conditions that are so low that no veiling luminance response should be expected. As previously described, in an earlier section of this chapter, the mathematical model uses the HUD characteristic, from which the ΔL_P data in the sixth data set was extracted, as its baseline.

The eight and final data set in the Table 3.12 is remarkable only because it has, over its length, the smallest image difference luminance values of any of the 8.8 minute of arc critical detail dimension characteristics recorded by Jainski, even though it has an in-field luminance of 0.0926 fL. Although it differs only by a small amount from the characteristic from which the data in the seventh column was taken, its predicted image difference luminance of 0.0283 fL is 2.5% higher than the 0.0276 fL value for the seventh data set and is 8.8% higher than the test value of the perceived image difference luminance value extracted from Jainski's characteristic. This experimental test result of Jainski is clearly contradictory with the theory of veiling luminance as set forth in this report and assumed to operate in the human's eyes. On the other hand, with the computed veiling luminance prediction of the perceived image difference luminance being only 8.8% higher the value predicted by Jainski's distributed glare source test result, the low value of the test result is well within the error range already demonstrated to exist for Jainski's test data and is therefore insufficient to prove that a contradiction actually exists. The Jainski report contained no duplicate experimental data for this test condition.

The first data set in Table 3.12 was saved until last to discuss because the calculated perceived image

difference luminance at 9.38 fL is 2.13 times the 4.4 fL of the corresponding Jainski test data. This difference is too large to be attributed to experimental or measurement error or even to the variability of test subjects. This error is, however, consistent with Analysis Point # 2. The actual Jainski HDD test configuration had the entire display area, excepting the test symbol, at a display background luminance level of $L_D = 1 \times 10^{-6}$ fL. Furthermore, the area above the display contains a four degree high panel area at a luminance of 85.5 fL, before the surround-field luminance area of 8,547 fL is reached. In contrast to Jainski's actual cockpit luminance test configuration, the integral computation of veiling luminance assumes the entire 200 degree wide area that is located above the boundary radials extending from the center of the display, between the two L_l and L_u boundaries, is assumed to be at the 8,547 fL level, except the three degree radius circle at the center of the display, which is excluded from the calculation. The inclusion of the low luminance display and panel surface areas, at a luminance of 8,547 fL, would cause the calculated value of veiling luminance to be increased above its true value. The veiling luminance predicted by Equation 3.130 is 42.6 fL, when the 4.4 fL test value from the first row in Table 3.12 is substituted for the perceived image difference luminance. The 96.8 fL calculated value for veiling luminance, shown in Table 3.12, is therefore a multiple of 2.27 higher than the value of the 42.6 fL experimental result.

Excluding the first data set in Table 3.12, all of the other calculated predictions for the perceived image difference luminance are within 9% of their corresponding values, determined through the experimental tests conducted by Jainski. This level of error is considered very good agreement, considering the ranges of variables involved and the previously described variations present in Jainski's test data.

3.8.6. Quasi-Theoretical Model for Distributed Glare Source Veiling Luminance

In concept, the task of carrying out the numerical integration of the previously introduced distributed glare source veiling luminance equations, that is, Equation 3.128 or 3.129, would be quite straightforward using a digital computer, if the spatial luminance distribution within the pilot's field of view is known. The most severe problems with this approach are related to the caveat that the spatial luminance distribution within the pilot's field of view is known. Owing to the extreme range of the luminance magnitudes encountered in an aircraft cockpit environment, existing spatially distributed sensors such as digital cameras are unsuitable to measure, and then convey to a computer, the time variant spatial luminance distribution, to which the aircrew members are visually exposed. In practical terms, it has to be concluded that this approach for the determination of veiling luminance is unnecessarily complex and difficult to implement.

Fortunately, optical integration provides an alternative technique for determining veiling luminance. Although, the previously introduced quasi-empirical equations, to calculate the veiling luminance for a distributed glare source, cannot be directly implemented using optical integration, this technique can be applied to an altered formulation of the equations. The balance of this section will be devoted to a description of this modification to the formulation of the veiling luminance equation, for a spatially distributed glare source.

In general terms, the approach involves the use of an optical lens designed to emulate a desired angular weighting function, when used in conjunction with a light sensor. This optical lens and light sensor combination allows the integral of the product of the spatial luminance distribution of the visual scene, to which the lensed sensor is exposed, and the desired angular weighting function to be automatically sensed. By designing the shape of the sensor lens so that its angular light reception characteristics are complementary with the angular sensitivity of the sensor, the angular dependence of the weighting function can be replicated. Since the light sensor can be designed to produce an output that represents the integral sum of all of the light that is incident on its surface, the result of the sensor-lens combination is the integral of the angle-weighted response to the luminance incident on the sensor, for spatially distributed luminance incident from anywhere within the sensor's instantaneous field of view. In this manner the design of the lensed sensor automatically accounts for the nonlinearity in the angular weighting function's dependence on the angle, θ, and opaque coatings can be used to block light from undesired angles that are beyond the eyes' total field of view. Orienting the lensed sensor so that its central optical axis is parallel to the pilot's central optic axis, when viewing a display to be controlled,

then gives the desired integrated response to the spatial luminance distribution seen by the pilot. Adding a spectral filter in the lens or over the sensor to give an approximately flat spectral luminance response across the human sensitivity range would complete the characteristics that the lensed sensor should possess.

A problem with the implementation of this optical integration approach occurs for the previously introduced distributed glare source mathematical models of Jainski's data. The nature of this problem and a way to overcome it is considered next. During the formulation of the distributed glare source integral equation, and based on the emulation of the empirical equations developed to model Jainski's discrete glare source veiling luminance test results, the luminance term in the integral equation was raised to a power of $q = 0.872$, thereby making it a nonlinear term. The lensed sensor, described above, can apply the veiling luminance angular weighting function to the visual scene luminance incident on its surface, and detect the integral of the resulting product, but it cannot raise the luminance to the power of q before performing the integration, as is required by the earlier quasi-empirical equations. To compensate for this problem, a different approach is needed for dealing with the nonlinear luminance term in the empirical equations, and the operation of human vision system provides guidance for formulating such an approach.

The scattering of light within the optical media of the eyes, like other forms of optical scattering, provides no inherent physical mechanism for a nonlinear response to the incident luminance, $L_s(\theta,\phi)$, or scattered luminance, L_{sc}. Instead, the nonlinearity of the veiling luminance response is considered to be an integral part of the overall operation of the human visual feedback system that senses light incident on the eyes' light receptors, and conveys the signals stimulated therein to the brain for processing and physical control over the eyes, including, but not restricted to, changes in their pupil areas. To accommodate the nonlinearities introduced by changes in the pupil areas of the eyes during the light reception and perception processes, rather than as a part of the scattering process, the veiling luminance can be expressed as follows:

$$L_v = L_{sc}^{q}. \tag{3.144}$$

In other words, the scattering process will be considered linear in the luminance variable, and only after scattering, into the direction from the pilot's line of sight to the test symbol, will the power of q be introduced to represent the human's response to the scattered luminance.

To be strictly correct, from a physical perspective, pupil aperture area changes do not control the luminance of an external visual scene imaged on the retina. Instead the pupil area controls the total incident luminous flux that enters the eyes, and, consequently, the illuminance incident upon the retinal light receptors. These results follow from the fact that luminance is defined as the illuminance incident per unit solid angle, and is, therefore, not influenced by a change in the light reception solid angle caused by a change in the pupil diameter.

The situation is different for the fraction of the incident glare source light scattered by the eyes' optical media into the direction of the fovea. Although the solid angle sensed by the foveal cone light receptors is fixed, the volume of the eyes optical media, contained within the light reception cone of each foveal light receptor that is illuminated by the incident light, is directly controlled by the size of the pupil area. Since increases or decreases in the pupil area change the illuminated volume of each of these light receptor cones, the number of scattering centers available to redirect light into the foveal light receptors is changed accordingly. Consequently, increases in the pupil area of the eyes cause a corresponding increase in the number of glare source photons scattered, within the conical light reception solid angles of the individual foveal light receptors, and, therefore, also cause an increase in both scattered luminance and illuminance, sensed by the foveal light receptors, and reducing the pupil area would have the opposite effect. Because changes in the pupil area do not occur until after a change in the luminance of the glare source image on the retinal has been sensed, and the visual system responds by changing the pupil area, it is considered physically accurate to treat this nonlinear effect as a part of the human's feedback response rather than as a part of the scattering process.

Since the preceding relationship is imposed by the human visual system, it follows that it must be compatible with the general empirical equation for a discrete glare source, Equation 3.109, introduced in

Section 3.8.1 to represent the discrete glare source test results of Jainski and the other experimenters discussed in this report. Based on this equivalence, the following relationship can be written:

$$L_V = K_J E_B^q f(\theta_B) = L_{SC}^q , \tag{3.145}$$

where since only Jainski's image identification task results show a power, q, other than unity, the constant, K_D, in Equation 3.109 was replaced by the constant, K_J, applicable to the Jainski data.

Treating the physical process responsible for the scattered luminance, L_{SC}, as linear in its dependence on the glare source illuminance, it can be represented as follows:

$$L_{SC} = K_{SC} E_B f_{SC}(\theta_B) . \tag{3.146}$$

This illuminance dependence is consistent with the empirical equations of all of the other experimenters, since the veiling luminance is equal to the scattered luminance, $L_V = L_{SC}$, in those cases. As pointed out earlier in this chapter, a possible exception exists for the target detection task data of Holladay, which was better fitted when the glare source illuminance is raised to the power of 0.872, determined for Jainski's data.

Substituting Equation 3.146 into Equation 3.145, the following relationship is obtained:

$$L_V = K_J E_B^q f(\theta_B) = K_{SC}^q E_B^q f_{SC}^q(\theta_B) . \tag{3.147}$$

When like terms in this relationship are equated, the values of the scattering constant, K_{SC}, and of the scattering angular weighting function, $f_{SC}(\theta_B)$, can be determined in terms of the previous empirical results of Jainski, as follows:

$$K_{SC} = K_J^{1/q} , \tag{3.148}$$

and

$$f_{SC}(\theta_B) = f(\theta_B)^{1/q} . \tag{3.149}$$

Figure 3.41 shows a visual comparison of the scattered luminance, predicted by solving Equation 3.144 for L_{SC}, with the veiling luminance obtained using Equation 3.58, with $q = 0.872$ and $E_B = 371.6$ fc, to represent Jainski's discrete glare source test results.

Because the published results of Holladay, and the other experimenters, were based on the glare source illuminance being raised to power of $q = 1$, and because the same physical process is being represented for both the veiling and scattered luminances, the distributed glare source integral equation, for the scattered luminance, L_{SC}, has to be the same as the generalized equation of Holladay for veiling luminance, Equation 3.114, introduced earlier in Section 3.8.2. Since the veiling and scattered luminances are equal, $L_V = L_{SC}$, when the veiling luminance is proportional to the glare source illuminance, it follows that the general equation for the scattered luminance can be written, in direct analogy Holladay's equation, as follows:

$$L_{SC} = \frac{K_{SC}}{\pi} \int_0^{2\pi} \int_{\theta_F}^{\theta_L} L_B(\theta,\phi)\, f_{SC}(\theta) \sin\theta \, d\theta \, d\phi . \tag{3.150}$$

The $1/\pi$ units conversion multiplier, used in this equation, permits the two luminance terms in the equation to be expressed either in units of apostilbs (asb), as employed by Jainski, or in units of foot-Lamberts (fL), as used in this report. The value of the integral constant, K_{SC}, should be the same as that given by Equation 3.148, for the discrete glare source case, since the Dirac delta function-based comparisons between the discrete and distributed glare source formulations of veiling luminance, presented in Section 3.8.3, should be equally applicable to the equations for the scattered luminance, L_{SC}.

Computations of scattered luminance, as represented in Equation 3.150, can be implemented using optical integration by a lensed sensor in the manner that was previously described. A computer accepting this

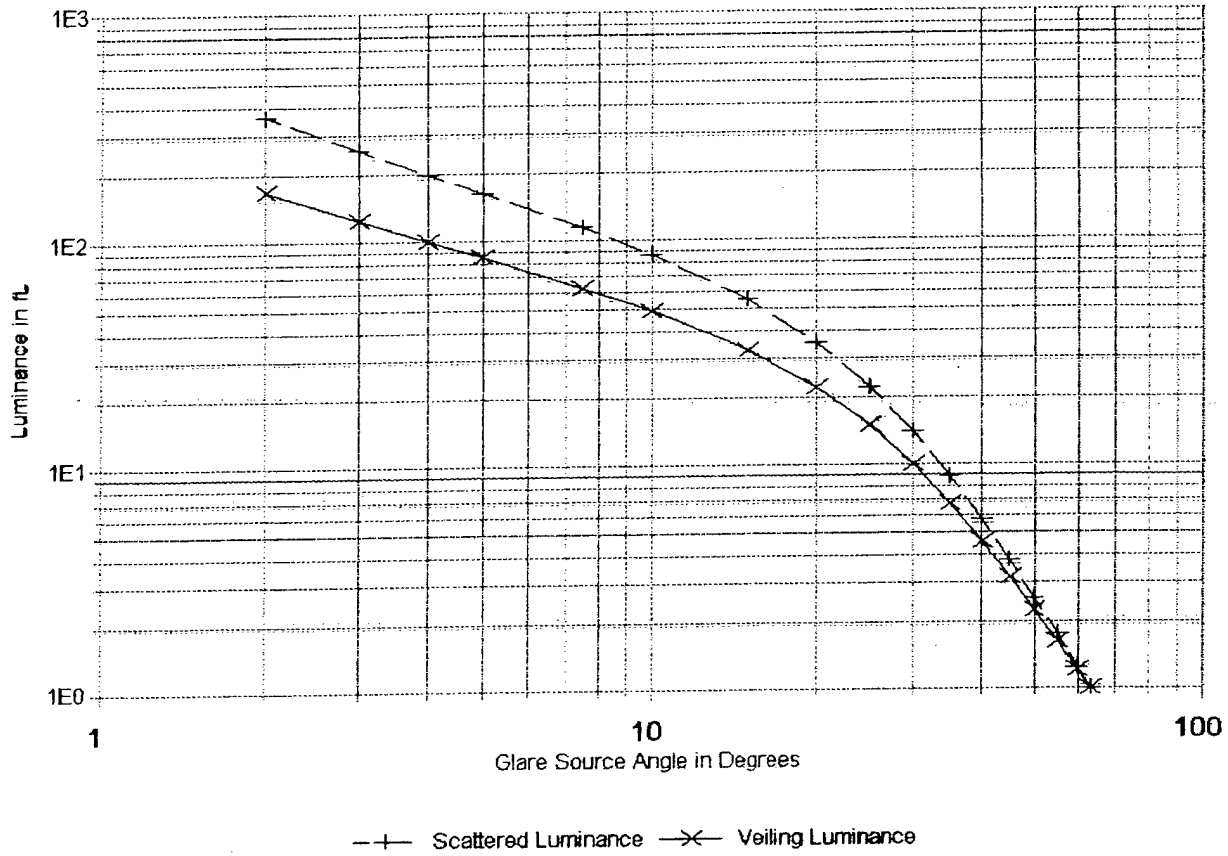


Figure 3.41. Comparison of Scattered and Veiling Luminance Angular Weighting Functions for Jainski Test Data for E_B = 371.6 fc.

input can then be used to calculate the veiling luminance, using Equation 3.144, and combine it with light-sensor-based readings of the display background luminance, to calculate the perceived image difference luminance, required to maintain the legibility of aircraft cockpit displays at a constant level, in changing cockpit incident ambient illumination and distributed glare source viewing conditions, using Equation 3.23.

3.8.7. Validation of the Quasi-Theoretical Model for Distributed Glare Source Veiling Luminance

The approach used in this subsection, to validate the theory-based model for determining the veiling luminance induced by distributed glare sources, is the same as the one used in Section 3.8.5, entitled "Validation of Empirical Model for Distributed Glare Source Veiling Luminance." For this reason, the description of the approximation used there will not be repeated, however, an indication of the modifications to some of the earlier equations to make them compatible with the scattered luminance equation will be described. Since the distributed glare source luminance, $L_B(\theta,\phi)$, is independent of the angle, θ, in the Section 3.8.5 example, Equation 3.150 for the scattered luminance can be expressed in the following simplified form:

$$L_{SC} = \frac{K_{SC}}{\pi} \int_0^{2\pi} L_B(\phi)\, d\phi \int_{\theta_F}^{\theta_L} f_{SC}(\theta) \sin\theta\, d\theta$$

$$L_{SC} = \frac{K_{SC} K_{\theta SC}}{\pi} \int_0^{2\pi} L_B(\phi)\, d\phi \,. \tag{3.151}$$

Evaluating the latter integral using the previously defined fractional parts of the pilot's field of view, an equation equivalent to Equation 3.140, but for the scattered luminance case, is obtained as follows:

$$L_{SC} = 2\, K_{SC} K_{\theta SC} \left[\phi_{Uf} L_U + (1 - \phi_{Uf}) L_I \right]. \tag{3.152}$$

As previously indicated in Section 3.8.5, the fractional parts of the pilot's field of view, occupied by L_U and L_I, are represented by ϕ_{Uf} and $\phi_{If} = 1 - \phi_{Uf}$, respectively, where for the HDD test configuration, $\phi_{Uf} = 0.5556$, and for the HUD, $\phi_{Uf} = 0.6111$.

The equation for the constant, K_{SC}, when $q = 0.872$ is substituted into Equation 3.148, can be expressed as

$$K_{SC} = K_J^{1/0.872} = K_J^{1.1468}, \tag{3.153}$$

Since, in conjunction with the formulation of Equation 3.145, the general discrete glare source constant, K_D, from Equation 3.109 was renamed, K_J, to indicate it applies specifically to the Jainski discrete glare source data, and, therefore, from Equation 3.124, has the value $K_J = 1.62$, when the angle, θ, is expressed in degrees, the value of the scattering constant calculated using Equation 3.153 is $K_{SC} = 1.7389$.

The constant $K_{\theta SC}$ is obtained through numerical integration of the equation

$$K_{\theta SC} = \frac{1}{57.3} \int_{\theta_F}^{\theta_L} f_{SC}(\theta) \sin\theta\, d\theta \,. \tag{3.154}$$

The denominator of 57.3 degrees per radian is included in this equation because the angle, θ, is expressed in units of degrees, rather than in radians. From Equation 3.149, with q = 0.872 substituted, the scattering angular weighting function, $f_{SC}(\theta)$, can be related to Jainski's discrete glare source angular weighting function, $f(\theta)$, by the following expression:

$$f_{SC}(\theta) = f(\theta)^{1/0.872} = f(\theta)^{1.1468}. \tag{3.155}$$

Finally, to permit an easy comparison of the predicted perceived image difference luminance requirements, Equation 3.154 is evaluated for same integration limits used to integrate the constant, K_θ, numerically, in the approximate calculation of Section 3.8.5, that is, $\theta_F = 3°$ and $\theta_L = 60°$. Substituting the angular weighting function for scattering from Equation 3.155 into Equation 3.154, the following relationship is obtained:

$$K_{\theta SC} = \frac{1}{57.3} \int_{3°}^{60°} \left(\frac{\theta^{-0.74}}{1 + 4.764 \times 10^{-5}\, \theta^3} \right)^{1.1468} \sin\theta\, d\theta \,. \tag{3.156}$$

Numerical integration of this equation using Simpson's Rule using either 1.5 degree or 0.5 degree sampling intervals, that is, with 39 or 115 samples, respectively, yielded the same value for the constant, namely, $K_{\theta SC} = 0.011577$.

Substitution of the preceding values of the constants, K_{sc} and $K_{\theta sc}$, into Equation 3.152, allows the approximate equation for the luminance scattered, when using the HDD configuration, to be written as follows:

$$L_{sc} = 2\,K_{sc}\,K_{\theta sc}\left[\Phi_{Uf} L_U + (1 - \Phi_{Uf})\,L_f\right]$$

$$L_{sc} = 2\,(1.7389)(0.011577)\,[\,0.5556\,L_U + 0.4444\,L_f\,] \qquad (3.157)$$

$$L_{sc} = 0.040262\,[\,0.5556\,L_U + 0.4444\,L_f\,]\ .$$

In a similar fashion, the approximate equation for the scattered luminance induced when using the HUD configuration can be written as follows:

$$L_{sc} = 0.040262\,[\,0.6111\,L_U + 0.3889\,L_f\,]\ . \qquad (3.158)$$

Once the scattered luminance is obtained for either of these test configurations, it is then a simple matter to calculate the veiling luminance using Equation 3.144 with 0.872 substituted for the power, q, as follows:

$$L_V = L_{sc}^{q} = L_{sc}^{0.872}\ . \qquad (3.159)$$

As a final step, the perceived image difference luminance, which is needed to permit comparisons to Jainski's test data, can be obtained using Equation 3.130 by substituting known values for the veiling luminance and image background luminance. As in Section 3.8.5, a display background luminance of effectively zero (i.e., 1×10^{-6} fL) is used for this calculation.

Values for the scattered luminance, veiling luminance and perceived image difference luminance, computed using the equations cited above, are shown in Table 3.13 for the same combinations of surround-field and in-field/panel luminances shown in the comparison table, Table 3.12, in Section 3.8.5. The experimental test data of Jainski shown in Table 3.13 are the same as those shown in the earlier table except that the duplicate luminance values expressed in units of apostilbs were removed.

The values of the perceived image difference luminance in the last column of the two tables do differ from one another and the differences are not consistent, that is, they do not simply differ by a constant multiplier. Nonetheless the differences are quite small, and the sets of computed image difference luminance results, from both Tables 3.12 and 3.13, are in reasonably good agreement with the Jainski test results. For this reason, the commentaries on the Jainski's experimental data, and on the differences between those results and the computed values given previously in relationship to Table 3.12, are also applicable to Table 3.13.

Comparing the computed luminances in the last two columns of Table 3.12 with those in Table 3.13, it may be seen that the values of both veiling luminance and of perceived image difference luminance are slightly larger in the second table, except for the values in second row, which are lower for both of these luminances. The inconsistency of the latter results stems from the fact that the two integral equations for veiling luminance are fundamentally different from one another. In the first integral equation of Section 3.8.4, the luminance term is raised to the power of q before integration occurs, whereas the second integral equation is raised to the power of q only after the integration that determines the scattered luminance. Because integration is in essence a sum of infinitesimal contributions of the quantity being integrated, the source of the inconsistency is due to the mathematical fact that the sum of individual numbers, each of which is raised to the same power before summing, is not equal to the sum of individual numbers raised to that same power.

3.8.8. Conclusions for Veiling Luminance Induced by Spatially Distributed Glare Sources

In concluding this section, it should be noted that veiling luminance, determined using the lensed sensor approach introduced in the previous section, and validated in this section, is not simply a convenient alternative to the earlier approach of Sections 3.8.4 and 3.8.5 for modeling Jainski's data. The lensed sensor model yields a more accurate representation of veiling luminance than did the earlier model, both physically and mathematically.

Table 3.13. Comparisons of Image Difference Luminance Requirements from Jainski's Tests with like Values Computed Using the Scattered Luminance Integral, for Distributed Glare Source Viewing Conditions.

Test Conditions and Jainski's Data [1]					Computed Values		
Display Type	Figure (Bild)	$L_P = L_I$ in fL	L_U in fL	ΔL_P [4] in fL	L_{sc} [2] in fL	L_V [3] in fL	ΔL_P [4] in fL
HDD	84	85.5	8,547	4 4	192.7	98.3	9.52
HDD	71	85.5	49.2	0.237	2.63	2.32	0.323
	75	85.5	49.2	0.312			
	84	85.5	49.2	0.307			
HDD	78	85.5	~ 1 x 10^{-6}	0.223	1.53	1.45	0.219
	84	85.5	~ 1 x 10^{-6}	0.214			
HUD	57	92.6	$L_U = 2L_D$	0.204	1.45	1.38	0.210
HDD	75	~ 1 x 10^{-6}	49.2	0.168	1.10	1.09	0.174
HUD	57	$L_I = 0.003 L_D$	$L_U = 2L_D$	0.0276	~ 0	~ 0	0.0276
HDD	78	~1 x 10^{-6}	~ 1 x 10^{-6}	0.0266	~ 0	~ 0	0.0276
HDD	78	0.0926	~ 1 x 10^{-6}	0.0260	0.00166	0.00376	0.0284

Notes: 1. Test data corresponding to an image critical detail dimension of $\alpha_c = 8.8'$ (i.e., b = 0.4 mm, ℓ = 4b) was extracted from the cited Jainski figures.

2. Scattered luminance was computed using $\phi_{Uf} = 0.5556$ for the HDD test configuration and $\phi_{Uf} = 0.6111$ for the HUD test configuration.

3. Veiling luminance was computed using $L_V = L_{sc}^{0.872}$.

4. The values of perceived image difference luminance, ΔL_P, were either extracted from Jainski's figures or computed for a display background luminance, L_D, of approximately 1 x 10^{-6} fL.

Physically, the lensed sensor model is more accurate because it accounts for the nonlinear dependence of veiling luminance, by associating it with the visual system's light reception and perceptual processes, rather than with the scattering of light in the eyes, where no physical basis exists for explaining a nonlinear luminance response. Mathematically, this model is more accurate because it predicts the same veiling luminance for a discrete glare source as does the experimentally derived discrete glare source veiling luminance equation, Equation 3.119.

The mathematical result claimed in the preceding paragraph can be demonstrated by substituting the discrete glare source excitation function from Equation 3.115,

$$L_B(\theta,\phi) = L_B(\theta_B,\phi_B)\ \delta(\theta - \theta_B)\left(\frac{\delta(\phi - \phi_B)}{\sin\theta}\right), \tag{3.115}$$

into the scattered luminance integral equation, Equation 3.150. Making this substitution gives a scattered luminance of

$$L_{SC} = \frac{K_{SC}}{\pi} L_B(\theta_B,\phi_B)\ f_{SC}(\theta_B). \tag{3.160}$$

Substituting this result into Equation 3.144, the following general equation for the veiling luminance induced by a discrete glare source is obtained:

$$L_V = L_{SC}^q = \left(\frac{K_{SC}}{\pi} L_B(\theta_B,\phi_B)\ f_{SC}(\theta_B)\right)^q = \frac{K_J}{\pi^q} L_B^q(\theta_B,\phi_B)\ f(\theta_B), \tag{3.161}$$

where the last term in the equation is obtained by substituting the values of K_{SC} from Equation 3.148 and $f_{SC}(\theta_B)$ from Equation 3.149.

This equation is directly applicable to Jainski's discrete glare source veiling luminance data, but it is equally applicable to the other experimenters' data, when q is set equal to one and the appropriate proportionality constants and adjustments for the differences in units have been taken into account. Expressing the equation in units of millilamberts, used by Holladay, rather than in units of foot-Lamberts and with the change of constants,

$$L_V = \frac{10\,K_H}{\pi} L_B(\theta_B,\phi_B)\, f(\theta_B) = L_{SC}. \tag{3.162}$$

The veiling luminance predicted for a discrete glare source, using the lensed sensor model of Equation 3.150, is therefore the same as that given by Equation 3.117, except that the equivalence of veiling luminance to the scattered luminance for these other experimenters' results has been added.

The earlier integral equations for the veiling luminance induced by a distributed glare source, Equations 3.121 and 3.122 (i.e., from Section 3.8.4), cannot be evaluated in the manner just described to predict the response to a discrete glare source because the integral of a Dirac delta function raised to a power is not mathematically defined. In spite of the fact that these earlier equations lack a solid theoretical foundation, based on the comparison of Tables 3.12 and 3.13, the predictions made using the equations are still quite accurate. The likely reason that the difference between the results of these two calculation techniques cannot be readily discerned is because the value of the power, q, on the visual scene distributed luminance term, $L_B(\theta,\phi)$, is so close to unity, for Jainski's data.

In conclusion, the comparison of the results of Tables 3.12 and 3.13 show that either of the two distributed glare source veiling luminance models described in this chapter could be employed without introducing a significant level of error. The lensed sensor model must be considered the preferred approach, however, since it is somewhat more accurate and is compatible with the implementation of automatic legibility controls.

3.9. Practical Aircraft Cockpit Display Legibility Requirements

As described in earlier sections of this chapter, the image difference luminance requirements needed to provide constant legibility on electronic displays in changing ambient illumination conditions were empirically modeled primarily based on the experimental results of Jainski, whose results were, in turn, judged to be valid through comparisons with the experimental data of a variety of experimenters. A feature common to all of these experiments was that they represented almost ideal viewing conditions and very austere test subject task loading environments. Thus, even though Jainski simulated an aircraft cockpit illumination environment, the visual, physical and mental task loading, that would be attendant to pilots performing normal mission scenarios, was absent during Jainski's tests, and those of all of the other experimental determinations of human image

difference luminance requirement characteristics, described earlier in this chapter, irrespective of the threshold legibility criteria employed. The practical significance of these differences, between the task loading of pilots and experimental test subjects, is that the numerical values of the image difference luminance requirements as determined by Jainski are much lower than those found to apply in actual aircraft. The purpose of this section is to discuss the validated operational military aircraft minimum legibility requirements of pilots and a method for applying them to the automatic legibility control model equations, developed earlier in this chapter.

3.9.1. General Legibility Equation as Formulated for Aircraft Cockpit Applications

The result of the previously conducted modeling was a family of characteristics, represented by Equation 3.23, which can be expressed in the following equivalent general form:

$$\Delta L_P = K(L_D + L_V)^m + \Delta L_N, \tag{3.163}$$

where $m = 0.926$ and ΔL_N is the image difference luminance limit that must be achieved or exceeded under night viewing conditions to make imagery of a specific critical detail dimension legible. The multiplier, K, is also dependent on the critical detail dimension of the imagery being viewed and is therefore functionally related to ΔL_N. In general, as the size of the critical detail dimension of the image being viewed is increased, the values of K and ΔL_N decrease and the reverse is true for smaller critical detail dimension imagery.

The relationship between the perceived image difference luminance, ΔL_P, the display reflected background luminance, L_D, and the glare induced veiling luminance, L_V, as given by Equation 3.163, is valid for all images, irrespective of their type, size and shape, provided only that the image critical detail dimensions are the same, and that the same viewing performance criteria (i.e., accuracy, speed of response, etc.) are employed. Stated in an alternative way, distinct equations, with different but related values of K and ΔL_N, are needed for each of a continuum of images having different critical detail dimensions.

To apply the general legibility requirements equation of Equation 3.163, to the automatic legibility control of aircraft cockpit displays, the appropriate values of the constant multiplier, K, and of the night image difference luminance level, ΔL_N, must be determined, which are applicable for satisfying the visual requirements of pilots while using information presented in cockpits to enable flying operational aircraft mission scenarios. The method used to do this is described in the next subsection.

3.9.2. Adaptation of General Legibility Equation to the Visual Requirements of Pilots

In the discussion that follows, an attempt will be made to describe the minimum image difference luminance requirements of pilots, in relation to the use of electronic displays in aircraft cockpits. These requirements have been determined and validated using two different methods. The first method involved using update specifications, for military aircraft cockpit electronic displays, where the legibility of the displays was subsequently validated through their acceptance by pilots, while in use during operational aircraft missions. The displays in question were absorption-bandpass filtered, P-43 phosphor, green-monochrome, cathode ray tube (CRT) electronic displays.

The second method used to establish the image difference luminance requirements was similar to the first, except that it involved the use of legibility requirements generalized to be applicable to both CRT and dot-matrix electronic displays. The latter requirements were developed through the adaption of the requirements determined, using the first method, and were subsequently applied for the development of multicolor active matrix liquid crystal displays (LCDs). Although the multicolor LCDs developed in this manner underwent a more limited flight testing, while being used to fly operational flight scenarios, the test results obtained validated the generalized legibility requirements.

The requirements information is presented from an evolutionary viewpoint because the minimum image

difference luminance requirements, needed to satisfy the pilots' needs in operational aircraft, can only be determined when the legibility of an operational display, such as a CRT, has just been increased to the point where the pilots finally judge the legibility of the displays to be adequate to meet their needs. A similar evolutionary point occurred for dot-matrix displays during a series of operational flight tests of multicolor LCDs, developed by Litton Systems Canada Limited, in the early 1990s, on a United States Air Force Military Airlift Command C-130 RAMTIP (Reliability and Maintainability Technology Insertion Program) aircraft, modified by Lockheed Aeronautical Systems Company specifically for the purpose.

Through technological advancements, made in the nineteen sixties and early seventies, monochrome CRT displays were eventually made sufficiently legible to be accepted for the first time by pilots, for the presentation of numeric, alphanumeric, graphic and video information, in the F-15 aircraft during the mid 1970's. Electronic displays, using the same technology and with similar viewing characteristics, were subsequently assessed to be satisfactory by pilots of F-16 and F-18 aircraft, in the years immediately following. The positive assessments by pilots, given that these early CRT displays only just exceeded the pilot's minimum visual requirements, provided a basis for establishing practical minimum legibility requirements for aircraft cockpit electronic displays. Performance information for the aforementioned displays was gathered in 1980 and an analysis was performed to permit converting the requirements established for these aircraft CRT displays into a form that could be applied to any type of display.[140] A summary of these finding and the methods used to arrive at them are summarized below.

As light emitting mode electronic displays, CRTs experience their greatest degradation in legibility under high ambient daylight viewing conditions. Some conditions known to severely degrade the legibility of these displays include the following: high illuminance diffuse surround conditions, such as those experienced near the top of sun illuminated white clouds; direct exposure of the display to light incident from the sun, in an otherwise blue sky illumination environment, or with the addition of illumination reflected from white clouds into the cockpit; and finally, sun glare conditions where the sun's location in the pilot's forward field of view creates a veil of luminance owing to scattering of the sun's light within the pilot's eyes. In the event that a display produces the image difference luminance output, or equivalently the image contrast, needed to make it legible under the preceding conditions, then it will also be at least as legible under all other lower illumination conditions that the pilot might experience.

It should be noted that the precise combinations of high ambient illumination conditions, which were responsible for causing F-15, F-16, and F-18 pilots to assess the green optical bandpass filtered P-43 phosphor CRT displays, used in these aircraft, to have adequate legibility, are not known. Consequently, the actual image contrasts being experienced by the pilots when the displays were judged to be acceptable are also not known. In spite of this shortcoming, the image difference luminance and contrast performance capabilities of these displays were characterized under standardized high ambient illumination test conditions, and this performance provides a valid basis for assessing the legibility performance capabilities of electronic displays intended for use in aircraft applications.

Two key legibility performance factors were common to the F-15, F-16 and F-18 aircraft P-43 phosphor monochrome CRT displays. The first was that all three displays were capable of producing image contrasts which permitted the presentation of six (6) video grey shades at a $\sqrt{2}$ grey shade separation, under the standardized illumination test conditions. The second legibility performance factor was that the three displays were all capable of producing a peak raster line luminance, as measured within a two mil diameter (i.e., 0.002 inch) spot area, of 200 fL or slightly greater. These two legibility criteria, together with the specification of the night image difference luminance requirements, provide a point of reference for establishing legibility requirements under different ambient illumination conditions. This is done by relating the satisfactory contrast and image difference luminance values determined for the F-15, F-16 and F-18 CRT displays, under the standard test conditions, to the families of equations for perceived image difference luminance requirements, which are described by Equation 3.163.

3.9.2.1. Minimum Contrast Requirement for Video Information in High Light Ambients

As a starting point for this derivation, it is necessary to first express the grey shade presentation requirement in terms of the equivalent minimum display contrast needed to permit the presentation of the six $\sqrt{2}$ separation grey shades. It should be noted that the $\sqrt{2}$ separation between grey shades has no direct physical relevance to the pilot's ability to perceive grey shades, or make use of the information they convey, but, rather, is simply a useful artifice adopted by the military to represent the luminance dynamic range a display must possess to render grey shades. A more in-depth treatment of grey shades, from the perspective of the human's perceptual and interpretive capabilities, is described in Chapter 5 and in an earlier article.[141]

Using the technique described above, the grey scale relationship between a measured symbol luminance, $L_s(n)$, at the nth grey shade level, and the measured reflected background luminance of the display, L_D, is expressed as follows:

$$L_s(n) = (GR)^{n-1} L_D \quad ; \quad n = 1, 2, 3, \ldots , \tag{3.164}$$

where GR is the grey scale ratio between adjacent levels, and the first grey shade level, $n = 1$, is the off background reflected luminance of the display, that is,

$$L_s(n = 1) = (GR)^0 L_D = L_D . \tag{3.165}$$

Expressing the grey shade levels in terms of the image difference luminance, $\Delta L(n)$, as follows:

$$\Delta L(n) = L_s(n) - L_D = [(GR)^{n-1} - 1] L_D , \tag{3.166}$$

the contrast of any grey shade level can be expressed as follows:

$$C(n) = \frac{\Delta L(n)}{L_D} = (GR)^{n-1} - 1 . \tag{3.167}$$

A display portraying six grey shades with a grey shade separation of GR = $\sqrt{2}$, would, therefore, have a minimum contrast requirement (i.e., that is, a minimum grey scale range), above the background luminance level, corresponding to

$$C = (\sqrt{2})^5 - 1 = 4.65685 \cong 4.66 . \tag{3.168}$$

This minimum contrast requirement, in combination with the minimum 200 fL CRT peak raster line luminance requirement, provides a set of minimum legibility requirements for video information presented on aircraft CRT displays, under the worst-case viewing conditions experienced by pilots in the F-15, F-16 and F-18 aircraft cockpits.

3.9.2.2. Minimum Image Difference Luminance Requirements for Video Information in High Light Ambients

A 200 fL luminance level, for a 2 mil (0.002 inches) measurement spot diameter positioned at the peak of a CRT display's raster or stroke written lines, when viewed from a 28 - 30 inch cockpit viewing distance, would not be perceptible by the pilot at the peak measured value but instead as a reduced area averaged value, due to the gaussian spatial luminance distribution of the CRT lines. Because of the superposition of the luminance from adjacent Gaussian CRT raster lines, as the lines are moved closer together or the CRT spot is increased in size, the 200 fL peak line luminance can be achieved as a flat field luminance. However, since information is conveyed to the pilot, by virtue of the spatially modulated changes in the grey scale levels or colors within the video picture, the luminance of the CRT spot, as area averaged by the human visual system between its half intensity points, provides a more accurate representation of the CRT display picture element (pixel) luminance, which is effective in spatially rendering the small critical detail dimensions needed to legibility convey the information encoded in the video picture to the pilot. The comparable area on a dot-matrix display

is the total area of its pixel, which involves area averaging over all of the activated monochrome or primary color display elements, and the inoperative areas surrounding them, within each pixel.

For CRT displays, the area averaged luminance of the CRT spot (i.e., pixel) is determined by integrating between the half intensity points of the Gaussian spatial luminance profile, as measured transverse to the scanned or stroke written CRT lines formed by the passage of the electron beam. The integration limits are based on a need for the half intensity points of activated lines to be separated, by at least a half intensity line width (i.e., an off line), to avoid the Gaussian luminance tails, which extend beyond the half power points of the activated lines, from blending (i.e., mixing) excessively with the information presented on adjacent activated lines, and thereby interfering with or degrading the ability to render the desired image with perceptible spatial features. The intent of this choice of integration limits was to define a CRT pixel that exhibits a low level of coupling approaching the virtual lack of coupling typically associated with dot matrix display pixels. This decoupling of the CRT pixels is essential if images of limited spatial extent and their critical detail dimensions are to be accurately rendered and perceived. The extent of this blending of information between adjacent lines on CRT displays is not a generally recognized limitation of monochrome CRT image rendition capabilities, but can be readily illustrated by using a color CRT display to write adjacent lines in different colors and observing the blending of colors in the resulting lines.

The equation for a Gaussian spatial luminance profile can be represented by the following equation:

$$\Delta L(x) = \Delta L \exp\left[-\frac{x^2}{2\sigma^2}\right], \tag{3.169}$$

where ΔL is the peak line luminance and σ is the standard deviation of the Gaussian distribution. At $\Delta L(x)/\Delta L = 0.5$ and $x/\sigma = 1.1774$, the integration between the half luminance points can be expressed as follows:

$$\Delta L_p = \frac{1}{2.3548\sigma} \int_{-1.1774\sigma}^{+1.1774\sigma} \Delta L \exp\left[-\frac{x^2}{2\sigma^2}\right] dx$$

$$\Delta L_p = \frac{\sqrt{2\pi}\Delta L}{2.3548} \int_{-1.1774}^{+1.1774} \frac{1}{\sqrt{2\pi}} \exp\left[-\frac{u^2}{2}\right] du, \tag{3.170}$$

where $u = x/\sigma$, and the integral equation is expressed in standard normalized form, for the Gaussian probability density function. From mathematical tables,[142] the value of the integral can be determined as 0.76096, therefore

$$\Delta L_p = \frac{\sqrt{2\pi}}{2.3548} \Delta L\ (0.76096)$$

$$\Delta L_p = 0.81002\ \Delta L. \tag{3.171}$$

Thus, for a CRT, with a peak raster line image difference luminance of ΔL = 200 fL, the perceptible line image difference luminance, ΔL_p, would be 162 fL. This minimum area-averaged perceived image difference luminance requirement, after rounding to

$$\Delta L_p = 160\ fL \tag{3.172}$$

was used as the minimum luminance requirement, for grey shade encoded sunlight readable video displays, in MIL-L-85762, where luminance and contrast are expressed in terms of area averaged rather than raster line peak luminance values. Although the two methods of CRT measurement, corresponding to the 200 and 160 fL requirements, produce equivalent legibility results for CRT displays, the transition to area averaged luminance measurements permits the image difference luminance values of different displays to be directly compared with one another, on an equal basis, whatever the display technology employed.

3.9.2.3. Image Difference Luminance Requirements for Video and Multicolor Information in Night Light Ambients

The setting of the night image difference luminance level, ΔL_N, for use in the general legibility control equation, Equation 3.163, represents a compromise for a pilot between good display image legibility for multicolor graphics and monochrome video image presentations at night and the need to set displays at low enough levels to be compatible with allowing the pilot to achieve the best possible dark adapted night vision external to the cockpit. Unfortunately, no test data corresponding to setting the image difference luminance level of aircraft displays at night for this specific operational condition could be found. As an alternative, it was decided to derive the value of this night image difference luminance requirement from available legibility requirements for alphanumeric display information that had been verified through operational use in aircraft cockpits.

During a USAF development of yellowish-green dot-matrix light emitting diode (LED) displays starting in the early 1970s, a design requirement to allow portraying alphanumeric characters down to at least 0.05 fL at night was established by the author based on a variety of test data and earlier flight test results.[143] As a spinoff of this program, the contractor, Litton Systems Canada Limited, used the technology to develop a LED display, called the Data Entry Display (DED) and designed to portray alphanumeric information. This electronic display was installed and flown in large quantities in operational F-16 aircraft.

The validity of the 0.05 fL requirement was subsequently questioned and then confirmed as the result of a problem reported by pilots engaged in operational F-16 aircraft missions. The problem reported by the pilots involved the inability to adjust the minimum night luminance level settings of these displays to a sufficiently low level during night flights. As a part of tests conducted in the early 1980s to evaluate whether this was a specification or an equipment problem, and to resolve this problem, it was determined that a control problem, external to the displays, had prevented the pilots' from operating them down to their minimum luminance design limit. Following this correction, the displays have been flown operationally to the satisfaction of F-16 pilots for more than 15 years.

The image difference luminance requirements for video and multicolor graphics presentations at night, ΔL_N, can be obtained from the 0.05 fL legibility baseline for reading alphanumeric characters at night, by making an adjustment, using the image difference luminance and contrast relationships of Table 3.14, and then adjusting for differences between the F-16 application and the table, for both character heights and viewing distances. A multiplier for making the adjustment between alphanumeric characters and video portrayals can be obtained by taking the ratio of 10.3 from Table 3.14, for the contrast requirement for the eight $\sqrt{2}$ grey shade luminance dynamic range that, as a minimum, is desired by pilots, when no display imposed capability constraints limit the legibility of the display presentations, to the contrast requirement of 2.0 for alphanumeric characters. Applying this adjustment yields a compensated value for the night image difference luminance, of ΔL_N = 0.26 fL. The second adjustment involves compensating the nominal 0.15 inch height of the F-16 display characters to the 0.2 inch character height in the table, applicable to the contrast of 2.0. The final adjustment was to compensate for the reduction in the display viewing distance, due to its location flush with the edge of the F-16's glare shield rather than being at the larger distance of the instrument panel, which is assumed for the values in the Table 3.14. When all of the compensations described above are applied, the result is a final requirement, for the night image difference luminance, of ΔL_N = 0.2 fL, for an eight $\sqrt{2}$ grey shade luminance dynamic range, contrast of 10.3, display presentation.

Displays having different luminance dynamic ranges, or image contrast requirements, would have correspondingly increased or decreased night image difference luminance requirements. For example, the night image difference luminance requirement, corresponding to a display that is only capable of depicting video pictures, presented using a six $\sqrt{2}$ grey shade luminance dynamic range, that is, for a maximum contrast in the picture of 4.66, would, therefore, be ΔL_N = 0.09 fL (i.e., 0.2(4.66/10.3)). The origins of the contents of Table 3.14 are described in Section 3.9.4.

Table 3.14. Alternative Table II for Use in MIL-L-85762A

TABLE II. High Ambient Daylight Luminance and Contrast Requirements

Types of Information to be Displayed	Required Contrast (C_L and C_1)	Required Difference Luminance (ΔL_{21} and ΔL_{23})	Luminance and Contrast Compensations for other character heights and stroke widths
Numeric Only	≥ 1.5 for h = 0.2 inch and 0.12h ≤ SW ≤ 0.2h	≥ 50 fL for h = 0.2 inch and 0.12h ≤ SW ≤ 0.2h	Multiply Required Luminance and Contrast by 0.2/h for 0.1 ≤ h ≤ 0.3 and by 0.12h/SW for 0.01h ≤ SW ≤ 0.12h
Alphanumeric	≥ 2.0 for h = 0.2 inch and 0.12h ≤ SW ≤ 0.2h	≥ 66.7 fL for h = 0.2 inch and 0.12h ≤ SW ≤ 0.2h	
Graphic symbols and alphanumerics	≥ 3.0	≥ 100 fL	
Video a. Worst-case ambient condition	≥ 4.66, to make at least six $\sqrt{2}$ gray scale ratio shades visible (counting "off" as one)	≥ 160 fL	
b. Otherwise	≥ 10.3, to make at least eight $\sqrt{2}$ gray scale ratio shades visible under other than worst-case ambient conditions		

Definitions:

$\Delta L_{21} = L_2 - L_1$ = difference luminance between the average luminance of activated display image elements and the average background luminance of the display surface in areas adjacent to and therefore visually contrasted with activated display image elements.

$\Delta L_{23} = L_2 - L_3$ = difference luminance between the average luminance of activated display image elements and the average luminance of deactivated display image elements.

3.9.3. Minimum Image Legibility Requirements Equation for Aircraft Cockpit Displays

To evaluate Equation 3.163, to obtain the specific image difference luminance versus background luminance legibility control requirement characteristic that provides the minimum legibility considered to be satisfactory by F-15, F-16 and F-18 pilots, under worst-case daylight viewing conditions, the image legibility equation must simultaneously satisfy the minimum 200 fL peak, or 160 fL area-averaged, CRT line luminance, the minimum contrast of 4.66 (i.e., six grey shade $\sqrt{2}$ spacing requirements for video information) and the night image difference luminance of ΔL_N = 0.09 fL. The value of the combined display reflected background luminance, L_B, and the veiling luminance, L_V, that satisfies both the minimum perceived image difference luminance requirement, ΔL_P = 160 fL, and the minimum perceived contrast requirement, C_P = 4.66, in the presence of veiling luminance, can be calculated using the equation for display perceived image contrast introduced previously, Equation 3.24. The display reflected background luminance that permits six grey shades to be displayed with a $\sqrt{2}$ multiple grey shade ratio between levels is, therefore, given by the following equation:

$$L_D + L_V = \frac{\Delta L_P}{C_P} = \frac{160\ fL}{4.66} = 34.33\ fL\ . \tag{3.173}$$

The remaining unspecified term in the legibility control characteristic equation, ΔL_N, is the luminance needed to depict monochrome video or multicolor graphics information at night, when the display reflected background luminance, L_D, and the veiling luminance, L_V, induced by glare sources are negligible, that is, when

$$\Delta L_P \cong \Delta L_N\ . \tag{3.174}$$

As previously described, the value assigned for this night display image difference luminance, corresponding to a contrast requirement of C = 4.66, is

$$\Delta L_N = 0.09\ fL\ . \tag{3.175}$$

Substituting the known terms into Equation 3.163, the following relationship is obtained,

$$160 = K(34.33)^{0.926} + 0.09\ , \tag{3.176}$$

which when solved for K yields a value of

$$K = 6.051\ . \tag{3.177}$$

The image difference luminance requirement for making video imagery with six $\sqrt{2}$ grey shade ratio levels legible under all ambient illumination conditions from full daylight to complete darkness can therefore be expressed as

$$\Delta L_P(C_L\ \&\ C_I = 4.66) = 6.051\ (L_D + L_V)^{0.926} + 0.09\ . \tag{3.178}$$

All of the luminance terms in this equation are in units of foot-Lamberts (fL). The contrasts C_L and C_I are defined in Formulas 15 and 16 of MIL-L-85762A. These contrasts are essentially the same as the contrast definition for C used in this report for the higher resolution displays (i.e., nominally 60 pixels per inch and greater) that are suitable to depict graphics and video information. For the lower resolution displays, used only to depict numeric and alphanumeric information, a distinction had to be made in the specification to account for displays with individual pixels, whose shapes are clearly discernable to the pilot at the specified viewing distance for the display. The latter situation requires that the background luminance surrounding a pixel, and the image difference luminance of the pixel active area, be accounted for separately, rather than being treated as a single area-averaged pixel, when calculating the minimum contrast that must be exceeded to assure that a depicted image will be legible.

3.9.4. Generalized Image Legibility Equation for Aircraft Cockpit Displays

Other image difference luminance requirement characteristics can be related to the one given by Equation 3.178, if their respective contrast requirements are known for high ambient daylight illumination viewing conditions, relative to the corresponding reflected background luminance of the display. Table II of MIL-L-85762A gives a listing of such contrast requirements for the following types of information to be displayed: numeric, alphanumeric, graphic and video. A modified version of this table is included here as Table 3.14. The information from the Table II of MIL-L-85762A is contained in the first, second and fourth columns of Table 3.14. The third column of Table 3.14 has been added to incorporate the minimum image difference luminance requirements, originally included in the text of the requirements section of the MIL-L-85762A specification into the table for easier reference. Table 3.14 contains a correction to the original table in the fourth column, and other improvements on the accuracy and the applicability of the requirements, in the third column, and in the title of the fourth column.

When the author of the current report originally wrote the "Daylight Legibility and Readability" requirements and test procedures that appear in MIL-L-85762 and MIL-L-85762A, it was intended that the compensations listed in the fourth column of Table 3.14, under the titles "Numerics only" and "Alphanumerics," would also apply to the information types listed in the first column of the table as "Graphic symbols and alphanumerics." In addition, those responsible for the formulation of the specification felt the breakout of minimum image difference luminance requirements, for the "Numerics only" and "Alphanumerics" categories of information types, added unnecessary complexity to the specification. In particular, the image difference luminance reductions, from the 100 fL requirement for the "Graphic symbols and alphanumerics" category, were considered unnecessary and possibly misleading, since they are only applicable to displays intended for the exclusive presentation of "Numerics only" and "Alphanumerics only" information, that is, because it is the smaller size of character sets, associated with these information types, that make the reductions possible. The only other change in the table is the addition of image difference luminance, to the image attributes that can be compensated, in the fourth column of Table 3.14.

In concluding the discussion of Table 3.14, it should be noted that the minimum contrast and image difference luminance requirements in the table are proportional to one another. This allows expressing the image difference luminance requirements of Equation 3.178 in terms of the high ambient contrast requirements from Table 3.14 in the following more general form,

$$\Delta L_P(C) = 1.30C\,(L_D + L_V)^{0.926} + \Delta L_N . \qquad (3.179)$$

where 1.30C was substituted for 6.051 in Equation 3.178, to allow the contrasts for image types other than the minimum contrast for video imagery, C = 4.66, to be substituted into the equation from Table 3.14. The last term in Equation 3.179 is the night image difference luminance, ΔL_N, from Equation 3.163. To make Equation 3.179, completely consistent with Equation 3.178 the night image difference luminance, ΔL_N, can be expressed as follows:

$$\Delta L_N = 0.0193\,C . \qquad (3.180)$$

This relationship for the night image difference luminance, ΔL_N, makes Equation 3.179 compatible with the following: a 0.09 fL night luminance setting in Equation 3.178, for a display operating at the minimum sunlight readable video contrast level of 4.66; a 0.2 fL night luminance setting, for the minimum contrast level of 10.3 considered by pilots to be desirable for the presentation of video information; or any night image difference luminance level setting that satisfies Equation 3.180, for a specified value of the electronic display contrast capability, C.

An equivalent alternative formulation of Equation 3.179 can be obtained by expressing the night image difference luminance, ΔL_N, as follows:

$$\Delta L_N = 0.0193\,N_L\,C . \qquad (3.181)$$

The substitution of this relationship, for the night image difference luminance, ΔL_N, into Equation 3.179, allows

a separate coordi ·1 control, by the pilot, over both the legibility level of a display portrayal, by setting the value of the contra and of the value of the night luminance level setting, ΔL_N, by controlling the value of the multiplier N_L. ituting this value for ΔL_N from 3.181 into Equation 3.179 yields the following still more general equation:

$$\Delta L_P(C) = 1.30C\,(L_D + L_V)^{0.926} + 0.0193\,N_L C\,, \tag{3.182}$$

where it is intended that N_L would initially have a value of

$$N_L = 1.0 \tag{3.183}$$

until the pilot has adjusted it to a new level.

Equation 3.179 is applicable to the minimum legibility requirements for video, graphics, alphanumerics only, and numerics only information presentations, when the appropriate value of high ambient contrast is substituted for the C parameter in the equation from Table 3.14. Equation 3.182 differs from Equation 3.179 only in the technique used to implement the pilot's ability to adjust both the high ambient contrast and the night image difference luminance levels, to meet the needs of different mission segments and scenarios. It is intended that the pilot trim adjustment inputs to the automatic legibility control would afford the pilot coordinated independent control over both the contrast setting, C, and of the night image difference luminance level setting of the display, ΔL_N, in both Equation 3.179 and 3.182.

Although the constants in the preceding equations were established for aircraft displays using specific minimum requirements for a perceived image difference luminance of ΔL_P = 160 fL, for a contrast C = 4.66 and at a display background luminance of L_D = 34.33 fL, the resulting family of image difference luminance control requirement characteristics, because they were derived from Equation 3.163, should be valid over the entire range of L_D values that can be experienced in an aircraft from nominally 10^{-6} to 10^{+4} fL, and should apply equally to any display including head-down, head-up and helmet-mounted displays, when the appropriate value of the contrast, C, is substituted. For head-up and helmet-mounted displays, pilots exhibit a willingness to accept lower contrast levels, C, for graphic information formats than is the case for essentially the same information when it is presented head-down, however, this may only reflect the fact that the angles subtended by the head-up and helmet-mounted presentations are typically much larger than they are when presented on head-down displays, in which case the contrast requirements, C, substituted into the equation from Table 3.14 would be expected to be reduced.

The general equations for the control of image difference luminance can also be used to satisfy legibility requirements in excess of those corresponding to the minimum legibility requirement values given in Table 3.14, for each type of information. By substituting the appropriate values of the contrast, C, into Equation 3.179 or Equation 3.182, the higher image difference luminance requirement levels, for example, corresponding to comfort levels of legibility, or other "super contrast" legibility criteria, can be commanded and maintained over the full range of display background luminance or veiling luminance conditions experienced in a cockpit.

Aircraft cockpti displays operated at contrast levels above the 4.66 minimum contrast requirement of Table 3.14, for example, to present video information with eight, ten, or more, $\sqrt{2}$ grey shade dynamic ranges, would, at high enough background luminance levels, have to be capable of exceeding the 160 fL minimum area-averaged luminance requirement, to maintain the legibility of the information presentation at a constant level. Alternatively, high contrast displays, whose designs or technologies limit them to imagery portrayed at 160 fL, or less, would reach this image difference luminance limit, as the illuminance incident on the display or the veiling luminance induced in the eyes continues to increase, and, thereafter, the imagery displayed would experience a degradation in its contrast until, with an acceptable design, a contrast level of not less than 4.66 is reached, under the worst-case viewing conditions a pilot can experience in an aircraft cockpit. An important example of a display application that requires the ability initially to depict, and afterwards maintain, high constant levels of displayed information legibility, is for the rendition of full color information presentations, so that the colors depicted remain perceptually invariant, and, consequently, reproducible, under the full range

of incident ambient illumination and glare source viewing conditions that can be experienced by pilots in aircraft cockpits.

3.9.5. Interpretation of the Image Difference Luminance Requirements Equation

The dependence of the image difference luminance requirements equation on the grey shade level and on other visually discernable properties of graphic, alphanumeric, and numeric information, is implicit in the high ambient viewing environment contrast requirements contained in Table 3.14. These contrast requirements, and the adjustments to contrast, for differing character sizes and stroke widths, were originally developed and incorporated into MIL-L-85762 to specify the minimum legibility requirements monochrome and multicolor display imagery should satisfy under high ambient illumination daylight viewing conditions. The stated intent of including sunlight readability requirements in MIL-L-85762, by the government personnel responsible for its preparation, was to assure the displays would not only be compliant with the primary night vision purpose of the specification, but, would also satisfy an aircrew's minimum legibility requirements, under high ambient illumination daylight viewing conditions. The perceived image difference luminance requirements equation presented in this chapter, extend the requirements in Table 3.14 to displays with different reflection characteristics and to any ambient illumination viewing condition from night to full daylight.

Because the perceived image difference luminance requirements of the pilot, ΔL_p, depend directly on the background reflected luminance of the display, L_D, rather than directly on the ambient illumination responsible for stimulating the display reflected luminance, electronic displays having low reflectance viewing surfaces require lower image difference luminance levels than do higher reflectance displays, to achieve the same level of displayed image legibility under the same ambient illumination viewing conditions. This relationship has been used for many years in military aircraft cockpits, first with emissive and more recently with transmissive operating mode electronic displays, to improve their power efficiency, through the application of optical filters. Applying optical filtering to these displays allows a power efficiency advantage to be achieved because the luminance reflected by the display surfaces is reduced at a faster rate than the reduction in image difference luminance, emanating from the filtered displays, as the transmittance of the optical filter is reduced. However, two human visual effects limit the legibility advantage that can be gained by lowering the reflectance of the display to reduce its image difference luminance requirements.

The first limiting effect is the image difference luminance plateau effect, shown in Figure 3.10 and associated with the human's image difference luminance versus background luminance requirement characteristics, at low reflected background luminance levels. This effect imposes a constraint on how small the image difference luminance of an electronic display can be made, through optical filtering, and still remain effective for conveying information to an aircrew member.

Glare source induced veiling luminance is the second effect that limits the legibility advantage that can be gained by lowering the reflectance of a display to reduce its image difference luminance requirements. Veiling luminance, imposes a minimum perceived background luminance level against which the display image difference luminance is contrasted, and in so doing limits how far the image difference luminance of the display can be reduced without degrading the legibility of the information portrayed in a glare source viewing environment.

In comparison to the preceding description, of the effect of veiling luminance on displays having low viewing surface reflectances and low image difference luminance outputs, displays with inherently high image difference luminance outputs are not strongly influenced by the presence of veiling luminance. For example, conventional transmissive mode signal indicator and reflective mode electromechanical displays, which have high reflected background luminance levels, but also have correspondingly higher image difference luminance levels, to make them legible in high ambient daylight viewing conditions, with illuminance from the sun directly incident on their viewing surfaces, are not significantly influenced by glare source induced veiling luminance conditions, since the veiling luminance induced in the eyes is comparable to or smaller than the reflected

background luminance of these displays.

Each of the display visual effects, described in this subsection, are known to be valid from prior aircraft cockpit experience gained during the development and test of conventional and electronic displays. One purpose of the interpretation of the image difference luminance requirements equation, described in this subsection, was to show that this equation correctly predicts each of these effects. Another purpose was to point out that the presence of veiling luminance places a limitation on the minimum image difference luminance needed to make displays legible. The implications of this prediction of the image difference luminance requirements equation are explored further below. Finally, as described near the beginning of this chapter, and as considered in greater detail later in this report, when the image difference luminance requirements equation is properly implemented, in terms of the luminances reflected from different displays and the veiling luminance induced in an aircrew member's eyes, it can be used as an automatic legibility control algorithm with any type of display.

3.9.6. Origin of Aircraft Electronic Display Minimum Image Difference Luminance Requirements

Based on the interpretation of the image difference luminance requirements of the preceding subsection and the assessment that follows, it is concluded that the 200 fL peak, or 160 fL area averaged, minimum image difference luminance requirement, for the F-15, F-16 and F-18 CRT displays, stems from the need to overcome the legibility degrading effects of the veiling luminance experienced by the pilots of these aircraft under worst-case viewing conditions, rather than the need to overcome the legibility degrading effects of increases in the background luminance reflected by the display, L_D, when, for example, the sun is incident on the display from directly over one of the pilot's shoulders. The principal reason for reaching this conclusion is that the contrast requirements in Table 3.14, which were established for ambient illuminance directly incident on the display being assessed with no glare sources present, lack any physical basis to support the existence of a minimum image difference luminance requirement for displays. Since, for any specific contrast requirement from Table 3.14, the corresponding image difference luminance requirements, for any particular high ambient illuminance viewing condition, are variable, that is, they can range from much more to much less than an area-averaged image difference luminance of 160 fL, depending on the reflectance of a particular displays viewing surface, this image difference luminance requirement is not compatible with being the origin of the fixed 200 fL peak, or 160 fL area-averaged, minimum image difference luminance requirement for the F-15, F-16 and F-18 CRT displays.

The veiling luminance term, L_V, in the image difference luminance requirement equation is always present, but its contribution is typically small, when compared with the reflected display background luminance, L_D, unless the sun, or an intense distributed source of glare, is visible in the pilot's field of view when reading a display. Furthermore, when an aircrew member is attempting to read information presented on aircraft instruments, and the sun is positioned so that it acts as a glare source within the aircrew member's field of view, then the sun's light cannot simultaneously be directly incident on the display being read. Consequently the display reflected background luminance, L_D, is typically low when the veiling luminance, L_V, is high and vice versa. Based on this fact, the display reflected luminance, in high incident ambient illumination environments, and the veiling luminance induced in the eyes, in high glare source exposure conditions, can be expected to produce different worst-case display legibility requirements.

As described previously in this chapter, a veil of luminance induced in the pilot's eyes is equivalent to the addition of a fixed level of background luminance, which is dependent on the glare source luminance magnitude and spatial distribution, to the background luminance already being reflected from display, as the result of its exposure to ambient illumination directly or indirectly incident on the display, at its installed location in the cockpit. To make each particular type of information in Table 3.14 legible, with respect to this composite value of reflected background and glare source induced veiling luminance, the minimum perceived image contrast requirements of Table 3.14 must still be satisfied. It is therefore concluded that it is the combination of this contrast requirement, with the fixed level of veiling luminance induced by a worst-case glare source

exposure of the aircrew, which is the origin of the minimum image difference luminance requirements imposed in Table 3.14 for military aircraft CRT displays, just as the minimum contrast requirements in the table are based on the background luminance reflected from the display, in the absence of glare effects. The image difference luminance requirement equations, Equations 3.179 and 3.182, incorporate both of these requirements into a single equation, valid for any aircraft illumination environment.

As a partial confirmation of the conclusions reached above, measurements of the reflected luminance on a 1979-1980's vintage five inch square active area F-18 monochrome CRT, using the standard test conditions specified in MIL-L-85762A, yielded a combined specular and diffuse reflected luminance value of 30.36 fL. Comparing this background luminance with the combined veiling and reflected background luminance of 34.33 fL, predicted by the need to make six $\sqrt{2}$ ratio grey shades legible on a display required to provide a 160 fL or larger minimum image luminance output, shows that the veiling luminance requirement is the more stringent of the two requirements, at least for displays having low levels of reflected background luminance.

3.9.7. Predicting the Veiling Luminances Experienced in Operational Aircraft Cockpits

As described earlier in this chapter, the glare source light scattered within the optical media of the eyes of a pilot, or other aircrew member, is an absolute physical quantity, analogous to the background luminance reflected from a display's viewing surface. In turn, the veiling luminance induced by the light scattered within an aircrew member's eyes depends only on the spatial luminance distribution of the light incident on the eyes, and on whether retinal rod or cone light receptors are used to perceive the visual scene on which the veiling luminance is superimposed. It was also previously shown that it is the veiling luminance response of foveal cone light receptors, which applies to the display image identification tasks, performed when reading the information presented on cockpit displays within an aircraft cockpit. Because this is true, and veiling luminance is also an absolute physical quantity, any validly collected values of veiling luminance must, therefore, be directly comparable and consistent with one another, after accounting for differences in glare exposure geometries. Stating this result in a different way, it can be concluded that the veiling luminance induced, when a pilot is exposed to a glare source viewing environment, is independent of the techniques, used by the different experimenters reported herein, to collect veiling luminance data, including differences in the test images used, the test subject task loading, and, in general, any psychological factors. It is for the foregoing reasons that the respective veiling luminance values collected, and described earlier in this chapter, should be directly comparable and consistent, in absolute terms, with veiling luminance values determined, using any other valid means.

In the first subsection that follows, the predictions of the veiling luminance equations, developed earlier in this chapter, as represented by the distributed glare source veiling luminance test results of Jainski, are compared with the predictions of the veiling luminance experienced in operational aircraft cockpits under worst-case veiling luminance conditions, as described above. As a part of this discussion, a more in-depth exploration of what constitutes worst-case glare source conditions, in operational aircraft cockpits, is considered, since, as previously stated, the precise conditions responsible for the minimum contrast and image difference luminance requirements of military aircraft cockpit electronic displays, contained in Table 3.14, are not known.

In the second, and final, subsection that follows, the effects of applying an approximate veiling luminance sensing technique that does not conform to the precise requirements for an accurate measurement of veiling luminance, as described earlier in this chapter, are considered. As presented in Chapter 7, some automatic legibility control design strategies benefit from the use of light sensors with angular weighting functions that do not conform to the optically integrated narrow angular response associated with the direct measurement of veiling luminance. One light measurement technique of interest, due to its simplicity, is to use a light sensor with a cosine receptor angular response characteristic. This approximate technique for making veiling luminance measurements is described as an alternative to using the more precise, but also more complex, veiling luminance model, introduced earlier in this chapter.

3.9.7.1. Comparison of Operational Aircraft and Veiling Luminance Model Predictions

As previously indicated, one technique that can be used to predict the magnitude of the worst-case veiling luminance, experienced by pilots in operational aircraft, is to use the minimum image difference luminance and contrast requirements, as stipulated in Table 3.14, to permit the pilot to perceive video image portrayals. In this context, the conditions associated with using a display under worst-case veiling luminance conditions include the minimum 160 fL image difference luminance, and 4.66 contrast requirements, which together predict a combined display background and veiling luminance of 34.33 fL as shown in Equation 3.173. The principal limitation of this approach is that while several indications exist that veiling luminance is the origin of the minimum image difference luminance requirements, for operational aircraft displays, in Table 3.14, no definitive proof exits that this is true. The choice of video as the type of display information to be used to find the associated veiling luminance was arbitrary, since any of the information types could have been used to produce nominally the same veiling luminance result.

Since, as previously described, glare source viewing conditions that induce large veiling luminances in the eyes, typically also cause the corresponding value of a display's reflected background luminance to be reduced, all but a few tenths of a foot-Lambert of the predicted combined display background and veiling luminance in operational aircraft cockpits can be attributed to veiling luminance, under worst-case veiling luminance conditions. For example, if the combined specular and diffuse reflected luminance value of 30.36 fL, for the F-18 display described earlier, were to be scaled down, from a nominal 10,000 fc direct incident illuminance exposure condition to a 200 fc indirect incident illuminance exposure condition, when sunlight is incident from just over the glare shield into the pilot's eyes, rather than directly incident on the displays, then the reflected background luminance would be reduced to about 0.6 fL. Since the light reflective properties of the F-15 and F-16 CRT displays are similar to those of the F-18 display, cited above, the predicted value of veiling luminance in these operational aircraft would therefore also be expected to be about 33.7 fL, under worst-case glare source viewing conditions.

Subject to the normal variations between individuals, the physical optics of the eyes and the scattering of light within them can be expected to be nominally the same, in both operational aircraft and experimental test environments. Because of this, the prediction of 33.7 fL, for the veiling luminances experienced by the pilots in operation aircraft, should be directly comparable to and consistent with the experimental results presented earlier in this chapter. Although the latter statement is correct, the method used in this section to arrive at a prediction of the veiling luminance experienced by pilots in operational aircraft, under worst-case glare source viewing conditions, namely, a luminance dynamic range of 4.66, for compressed grey shade video pictures, and the minimum image difference luminance of 160 fL, both of which are accepted as minimal requirements for electronic displays installed in military aircraft cockpits, is still somewhat speculative. More specifically, while this approach is logically consistent with the established aircraft cockpit image contrast and luminance requirements, shown in Table 3.14, since nominally the same veiling luminance value is predicted for each type of information in the table, this result has not been validated through measurements of veiling luminance in operational military aircraft cockpits.

Based on the preceding considerations, if the 33.7 fL prediction for the veiling luminance experienced by pilots, under the worst-case glare source viewing conditions in operational aircraft using head-down displays, is correct, then this veiling luminance can be directly compared with the value of 42.6 fL, reported in Section 3.8.5 to be applicable to the distributed glare source test configuration of Jainski, illustrated on the left-hand side of Figure 3.3, for a uniform surround luminance of 8,547 fL, a panel luminance of 85.5 fL, and a test image having a critical detail dimension of 21 minutes of arc. When these veiling luminances are compared, however, the result raises an apparent contradiction. In particular, the predicted worst-case veiling luminance of 33.7 fL in military aircraft cockpits is less than the 42.6 fL experimental result of Jainski. Moreover, this is true in spite of the fact that the image legibility conditions for the operational aircraft cockpit displays are more severe, that is, for spatially distributed glare luminance of 10,000 fL, or 10,000 fc of incident sun and blue sky illuminance, and for image critical detail dimensions of nominally one third the 21 minutes of arc value for the Jainski test symbol. Despite this apparent inconsistency, arguments are presented below to show that the

predicted worst-case veiling luminance of 33.7 fL in operational aircraft cockpits, and the 42.6 fL experimental result of Jainski, are reasonably consistent with one another, when the differences in the cockpit glare source exposure geometries, applicable to each of these veiling luminance values, are taken into account.

The origin of the difference in the veiling luminances, noted above, is attributed to the fact that the Jainski head-down display is installed in the middle of the instrument panel, with its center positioned eight degrees below the glare shield, in a location occupied by the head-up display control panel and the box containing the HUD's internal optics and CRT image generator, in the F-15, F-16 and F-18 aircraft. This location of the HUD, in the F-15, F-16 and F-18 aircraft, causes the head-down CRT displays to be installed lower on the instrument panel, as shown in the cockpit panel illustration of Figure 3.2. The result of installing the head-down displays, further down inside the cockpit, is to limit the magnitudes of the veiling luminances that can be induced by either discrete or spatially distributed glare sources, in these aircraft cockpits. Because the fraction of the pilot's field of view, containing the sun and/or high luminance sky or cloud areas, is more restricted for the operational aircraft cockpit head-down display installations, than it is for the Jainski test configuration, due to being blocked by the instrument panel and cockpit structure out to larger angles, from the line of sight to the center of the head-down displays, the 33.7 fL veiling luminance prediction for operational aircraft cockpits is considered consistent with the predictions expected for the previously introduced veiling luminance equations, even though, this veiling luminance initially seems inconsistent with the higher, 42.6 fL, veiling luminance value of the Jainski test.

Based, in part, on the previously described theory of veiling luminance, and, in part, on the confirmation of the preceding comparative analysis, it is concluded that the methods described in the veiling luminance sections of this chapter for the determination of veiling luminance, are suitable both for the direct calculation of veiling luminance and for use as an integral part of an automatic legibility control subsystem, for use in controlling aircraft cockpit displays.

3.9.7.2. Assessment of Using a Rough Approximation to Represent Veiling Luminance

As an alternative to the more accurate veiling luminance relationships introduced in earlier sections of this chapter, the following equation can be considered as an approximate relationship for determining veiling luminance:

$$L_V = \frac{33.7\ fL}{10{,}000\ fc} E_E = 0.00337\ E_E \qquad (3.184)$$

In this equation, E_E is the illuminance incident on the pilot's eyes from discrete and distributed glare sources within a hemispheric field of view centered on the line of sight to the display information being read, and as such includes light from both the internal and external parts of the cockpit visual scene. It should be noted that the illuminance incident on the eyes, E_E, is not equal to the illuminance of a discrete glare source, E_D, incident on the eyes and measured along a line from the glare source to the eyes, which was referred to earlier in this chapter, but, instead, includes the angle weighted effects of spatially distributed luminances incident on the eyes, including those of any discrete glare sources that happen to be present in the pilot's field of view, as measured along the pilot's line of sight to the display. In other words the illuminance, E_E, is equal to the illuminance employed in the Jainski discrete glare source equations, cited and described earlier in this chapter, to characterize the light incident on the eyes, from glare sources within the observer's field of view. To establish the magnitude of the veiling luminance predicted by this equation, the 33.7 fL worst-case veiling luminance, previously associated with reading the information presented on displays in operational aircraft, has been related to the exposure of the pilot to 10,000 fc of illuminance, following the light's attenuation by the aircraft transparency.

Several sources of inaccuracy are associated with using Equation 3.184 to approximate the veiling luminance induced in a pilot's eyes by a glare source. The principal source of inaccuracy associated with using this veiling luminance equation, stems from the fact that the illuminance term, E_E, depends on the cosine

of the angle, θ_v, between a point in the scene of luminance, L_v, and the pilot's line of sight to the display, whereas the actual angular weighting function dependence of the eyes drops off much more rapidly, as a function of the angle, θ_v. One practical consequence of this difference, in actual cockpits, would be to cause an illuminance sensor, with its central optic axis oriented parallel to the pilot's line of sight to the display, to overemphasize the effect of high luminance areas, including discrete glare sources such as the sun, located at large angles with respect to the pilot's line of sight. Since higher than necessary veiling luminance levels translate into higher than necessary image difference luminance levels, for displays operated using automatic legibility controls, this would simply cause the imagery depicted on the display to be as or more legible than it would be, if an accurate veiling luminance was used.

A second source of inaccuracy associated with using Equation 3.184 involves the relationship between the 33.7 fL worst-case veiling luminance and a glare source exposure of 10,000 fc. As previously stated, this association is not exact because the illumination conditions pilots are exposed to, and which result in the worst-case display viewing conditions, are not known precisely. The 10,000 fc glare source illuminance exposure of the eyes is based on the pilot or other aircrew member being exposed to the sun and a blue sky background of 12,500 fc, through a highly transparent aircraft canopy or windscreen of 80% transmittance. While aircraft transparencies with visible light transmittances in the range of 70 to 80% are common, the precise values applicable to the F-15, F-16 and F-18 aircraft canopies, upon which the legibility requirements of Table 3.14 were based, are not known, nor are the corresponding illuminance levels that were actually experienced by the pilots' of these aircraft. Appendix B may be referred to for a more detailed description of potential sun exposure conditions.

As previously described, the 33.7 fL worst-case value of veiling luminance applies to head-down displays, which are installed at fairly large distances below the glare shield in military aircraft cockpits. Based on the earlier arguments, it can be inferred that either higher or lower values of veiling luminance would apply at different display installation locations in the cockpit, for the same worst-case spatial distribution of glare source luminance external to the cockpit. For example, for head-down displays installed on or just below the glare shield, Equation 3.184 would be expected to underestimate the veiling luminance, because the operational aircraft displays used to derive the 33.7 fL worst-case value of veiling luminance are installed lower down in the cockpit instrument panels. Corrected values of veiling luminance, suitable for substitution into Equation 3.184, in place of the 33.7 fL value, can be calculated using the previously introduced veiling luminance equations, for any installed display location, cockpit configuration and worst-case spatial distribution of glare source luminance external to the cockpit.

As an alternative to the preceding approach, a single worst-case veiling luminance, applicable to a display installed on the glare shield could be used for all of the displays in the cockpit, since this would cause displays installed in positions, where the veiling luminance is less severe, to operate at a higher than required level of legibility. Due to the cosine angular dependence of the illuminance term in Equation 3.184, the adjustments in the calculated value of veiling luminance, caused by the orientations of the cosine receptors being coordinated with each of the different installed display locations in the cockpit, would only cause small image difference luminance reductions, even for displays at large vertical angles with respect to the glare shield. The likely disadvantage of operating electronic displays in this way, over an extended period of time, would be a reduction in their useful operating lifetimes.

The veiling luminance approximation of Equation 3.184 would also appear to pose a significant problem for the accurate prediction of the veiling luminance for head-up and helmet-mounted displays, where the sun can reach an angle of $\theta_v = 0°$, that is, directly behind the imagery the pilot is attempting to view. However, several factors relegate veiling luminance to a secondary role for HUD and HMD applications. For example, the background luminances of the imagery presented on these displays would be expected to by very large, in comparison to the veiling luminances for daylight sky or cloud backgrounds, thereby causing the veiling luminance, whether correct or in error, to be negligible in comparison to the display background luminance in the image difference luminance requirements equation. Likewise, for viewing conditions, where the sun is either directly behind the information presented on these displays, or in very close proximity to the pilot's line

of sight, the effects of debilitating glare would tend to make the display imagery unreadable, no matter how the legibility of the displayed information is controlled.

Although the cosine receptor light sensor angular response characteristic, associated with the veiling luminance approximation of Equation 3.184, does not provide an accurate representation of veiling luminance, it has been considered in this subsection for two reasons. The first reason for considering cosine receptor light sensors, as an approximate veiling luminance measurement technique, was to explore the limitations and/or inaccuracies associated with their use, since they are often used to make light measurements, even when their use is not fully justified, because of the beneficial properties they offer. Among the benefits offered by cosine receptor light sensors are the following: the ease of fabricating and applying Lambertian light diffusing translucent lenses to light sensors; the known sensitivity and reproducibility of light measurements made using this method; the ability to create a small light sensor footprints, by light-piping the sensed illuminance to larger remote sensors; and the insensitivity of the light measurements to misalignments in the orientations of the cosine receptor surfaces.

A second and more important reason cosine receptor light sensors were considered in this subsection, as an approximate veiling luminance measurement technique, is because automatic legibility control implementation strategies are described in Chapter 7 that can benefit from the use of light receptors having a cosine light receptor angular response characteristic. For automatic legibility controls, examples of the advantages of using a cosine receptor to sense light from discrete and distributed glare sources include the following: potential reductions in the number of sensors needed to implement automatic legibility control throughout a cockpit, greater flexibility in the placement and orientation of sensors, and slower time responses for the image difference luminances commanded by the automatic legibility controls, in response to aircraft attitude changes.

It should be noted that while valid reasons can exist for using the veiling luminance approximation described in this subsection, or possibly a different more appropriate approximation, in place of the more accurate and, admittedly more complex, veiling luminance model presented earlier in this chapter, doing so, without careful consideration and good cause, is not recommended. To aid in this consideration, the topics described in this subsection are discussed in greater detail in Chapter 7, in relationship to the use of light sensors, for practical implementations of automatic legibility controls. Other advantages and disadvantages of using veiling luminance approximations are also described in Chapter 7.

3.10. Conclusions

The overall result of the analyses performed in this chapter is a comprehensive image difference luminance requirements model, valid for ideal display imagery in time changing ambient illumination and spatially distributed or discrete glare source viewing conditions. In using the image difference luminance requirements model, it should be born in mind that many variables in Table 3.1 that influence pilot performance, which were formerly considered to have ideal constant values during the model development in this chapter, are nonetheless very important. The form of the model presented in Section 3.9, indirectly accounts for many of the variables in Table 3.1, by virtue of casting the model in terms of legibility requirements that are already applicable to operational aircraft cockpits, and therefore do not require further compensation. The variable time, is an example of a variable that is not automatically compensated for in the model presented in Section 3.9. This variable is particularly important under night adaptation conditions, where external targets can potentially be obscured by the combined effects of slow eye adaptation time constants, and the veiling luminance caused by cockpit lighting acting as a distributed glare source. Controlling the image difference luminance levels of displayed information, as a function of time, whether the control inputs are made manually by the pilot or another aircrew member, or by automatic legibility control, is also important. In these cases, response time filtering must be applied to avoid the potential negative impacts of simply slaving the control response to the effectively instantaneous response times of the ambient illumination and glare source light sensors. These and other factors that influence the application of automatic legibility controls in aircraft

cockpits are considered in greater depth in later chapters of this report.

Although the effects of image colors were tested by Jainski, the threshold luminance levels would have produced desaturated color symbols, when superimposed on a white background, except under the lowest background luminance conditions tested. This is the likely reason that the test symbols of Jainski, depicted in colors other than white, were shown to be no more legible than white symbols on a white background. The color purity is greatly reduced for test symbols, of a particular hue, which only produce a small differential in their threshold image difference luminance, ΔL, above the background luminance, L_D. Reduced test symbol color purity, in the Jainski tests, is caused by the mixing of the symbol and background colors that occurs when the color symbol is superimposed over a white light background, which in relative terms, is of much higher luminance.

The preceding limitation of the Jainski color tests, points to the need to first achieve adequate absolute image luminance contrasts, for the information presented on displays, before it can be expected that the color coding of the displayed information will become effective as a technique for conveying information to aircrew members. In this context, the image difference luminance requirement equations in Section 3.9, for the general legibility model for aircraft cockpit display information, have been modified to allow the control of up to full color display pictures, provided that suitable values of the contrast multiplier are substituted into the equations. As a practical matter, currently available display technologies, suitable for use in aircraft cockpit applications, lack the capability to generate the high image difference luminance levels required to maintain the legibility of the information they present at a constant level, under the highest ambient illumination and glare source viewing conditions encountered in aircraft cockpits, except for the minimum video contrast, and lower contrast requirement values, listed in Table 3.14. Similarly, maintaining accurate color renditions is only possible, for the same low contrast information types listed in Table 3.14, under these severe viewing conditions. Because of the high luminance contrasts needed to portray full color display information, it follows that the currently available aircraft cockpit display technologies do not permit maintaining constant perceived colors in pictures rendered on these displays, under the worst-case daylight viewing conditions. Strategies for taking maximum advantage of the available electronic display technologies, in spite of this information presentation limitation, are introduced near the end of the report.

In the balance of this report, the image difference luminance requirements model developed in this chapter, and issues associated with the application of automatic legibility controls to aircraft cockpits are dealt with in greater depth. Time dependence, color and other factors that, either directly or indirectly, influence the legibility of display information presentations are also considered, in greater detail, in later chapters of this report.

CHAPTER 4

Historical Perspective of Automatic Brightness Controls (ABCs) and Automatic Legibility Controls (ALCs)

Historically, the use of automatic brightness controls to set the output image difference luminance levels of electronic displays operated in changing ambient illumination conditions during daylight missions in military aircraft cockpits has been rather unpopular with pilots. A valid reason for the strong aversion of military pilots to the use of ABCs is described in the first section below, together with the historic context in which these initial versions of automatic brightness control were experienced. The second section is devoted to an introductory description of the automatic brightness control used in Boeing's more recent commercial aircraft, which airline pilots have judged to be satisfactory due to an ABC design improvement first incorporated by Boeing. In the third section, the application of the general automatic legibility control law, described in Section 3.9, to the Lockheed ATF aircraft is described in an overview fashion. This application is described, even though it was only flown in the test aircraft, because it involved the first known use of a light transmissive backlighted color active matrix liquid crystal displays, rather than cathode ray tube displays, in a fighter type aircraft. Finally, in the fourth section, a summary is provided of the features shared by the Boeing ABC and the General ALC. A more in-depth comparison of the ABC and ALC is contained in Chapter 5, where it is shown that these two control techniques, in spite of their apparent differences, can be used interchangeably to produce essentially the same results, provided the corresponding correct values for their respective parameters are employed.

4.1. Initial Versions of Automatic Brightness Controls

Even some very early sunlight readable monochrome cathode ray tube (CRT) displays used in military cockpits incorporated some form of automatic brightness control. Under the most adverse ambient illumination viewing conditions experienced in fighter aircraft cockpits, these displays were only just capable of exceeding a pilot's minimum legibility requirements. Because of this, the introduction of the first automatic brightness controls was not related to the pilot's legibility needs. Rather, the intended purpose of the automatic brightness control was to prolong the life of the CRT displays, by operating them, whenever possible, at less than their maximum emitted luminance level output capabilities.

The preliminary automatic brightness controls employed illuminance sensors, typically installed in the bezel of the CRT display. As the light sensed, by these bezel mounted illuminance sensors, decreased, the display would be automatically dimmed from its maximum imaged difference luminance level, typically following a straight line full logarithmic dimming characteristic. These automatic brightness controls were only designed to operate from the maximum illuminance levels sensed down to about 100 fc of illuminance and, thereafter dimming was accomplished using the display's manual luminance control. Furthermore, these automatic brightness control characteristics were designed to cause the image difference luminance of the displays to decrease progressively, as the sensed ambient illumination incident on the displays becomes lower, rather than, for example, to hold the image difference luminance level constant until a fully adequate level of legibility is first achieved, as the illumination incident on the displays decreases, and then attempt to maintain the legibility of the display information portrayals at a constant level, as the illumination incident on the display continues to decrease even further. At the time that the original ABCs were installed in military aircraft in the early 1970s, the information available on the pilot's legibility requirements was insufficient to permit the latter type of legibility control to be implemented.

The principal shortcoming of the original ABC equipped aircraft displays occurred under high ambient conditions, when the sun or other high luminance sources of illumination, such as reflections from white clouds, are directly incident on the pilot's eyes rather than on the displays and their respective light sensors. Under these conditions, the illumination incident on the display's light sensors would be reduced and, therefore, cause the displays to be dimmed by the ABC, at a time when the light incident on the pilot's eyes is producing a veiling

luminance condition that would make the displays difficult to read, if set to provide maximum legibility, or extremely difficult to impossible to read at legibility levels dimmed by the ABC.

The opinions expressed by military pilots concerning their experience with the performance of early ABCs were almost universally negative, that is, they considered use of ABCs to be unacceptable. This experience appears to have created a lingering aversion among military pilots to the idea of using any form of automatic brightness or legibility control, with military aircraft displays, an opinion that continues to surface anytime the possibility of automatically controlling the legibility of displays is mentioned. Based on the first-hand accounts of military pilots, the method adopted to deal with the original ABCs was to switch to the manual luminance control mode and thereafter not use the ABC.

Boeing was the first aircraft manufacturer to account both for the direct incidence of ambient illumination on the displays, and glare source viewing conditions incident on a crew member's eyes, by including both display and glare shield mounted sensors in their commercial aircraft automatic brightness control systems. These ABCs were initially installed on the Boeing 757 and 767 aircraft. Boeing has reported commercial airline pilot satisfaction with this advanced ABC design during operational usage and it has continued to be installed in newer Boeing commercial aircraft.

The first USAF aircraft to use both display and glare shield mounted light sensors with an automatic brightness control design was the Lockheed Advanced Tactical Fighter (ATF) aircraft, the prototype for the F-22 aircraft. Even though, the design for the ATF automatic control differed from the Boeing design in several important ways, from a practical standpoint, the control algorithms developed were very similar, in terms of the light quantities sensed and the overall control, capable of being achieved. Differences in the control philosophies employed during the derivation of the two control algorithms are responsible for the noticeable differences in their formulations. These apparent differences are related to the constant legibility control philosophy originally used to derive the algorithms applied to ATF automatic brightness control and the pilot preference control philosophy employed by Merrifield and Silverstein in their derivation of the Boeing automatic brightness control algorithms. In the ATF design, a requirement was also imposed to make the control algorithms compatible with the control of multiple displays using a common digital legibility control.

4.2. Boeing Automatic Brightness Control

The most advanced automatic brightness control (ABC) implemented to date on operational aircraft was developed by Boeing and was first deployed on the Boeing 757 and 767 commercial aircraft. The description of the experimental program, conducted by Boeing in preparation for the development of their ABC system, was reported in 1988, many years after the fact, by Merrifield and Silverstein.[144] In the conclusion to this paper, Merrifield and Silverstein made the following statement: "An Automatic Brightness Control system conforming to the basic characteristics discussed" in their paper "has received extensive operational validation during both flight test and airline service of Boeing 737/757/767 aircraft."

The preceding quotation has been singled out to emphasize the fact that an ABC system conforming to the "basic characteristics" of the ABC control algorithm derived in the Merrifield and Silverstein experiments was implemented by Boeing in their aircraft rather than the explicit numerical parameters derived through the experiments. This distinction is important because, while the ABC system "basic characteristics" should translate between different cockpit geometric configurations, display types, aircraft missions, display information presentation objectives, and so forth, the explicit numerical parameter values would be expected to change. The recognition of this fact was expressed by Merrifield and Silverstein in the following quotation, which was taken from the Conclusions section of their paper: "Refinement and modifications of the system described in this paper will undoubtedly be necessary to meet the diverse requirements of the varied cockpit environments."

The balance of this section is devoted to an introduction of the "basic characteristics" of the ABC system

control law algorithm developed by Merrifield and Silverstein.

4.2.1. Boeing ABC System Control Law Algorithm

The ABC system control law algorithm formulated by Boeing, when mathematically represented in terms of its basic characteristics, can be expressed in summary form using the following three equations:

$$\log B_d = a + b \log B_e , \tag{4.1}$$

and

$$B_{out} = G B_d , \qquad \text{for } G \geq 1 , \tag{4.2}$$

where

$$G = d + e \log \frac{B_f}{B_d} . \tag{4.3}$$

An explanation of the terms used in these equations and of their physical significance is described below.

The variables B_d, B_e, B_f, G and B_{out} used in these equations were defined by Merrifield and Silverstein as follows:

B_d = display luminance

B_e = cockpit ambient

B_f = FFOV (forward field of view) luminance

G = luminance gain function (to compensate for B_f / B_d mismatch)

B_{out} = gain compensated display luminance.

The literature research conducted by Boeing, to enable them to describe a pilot's display luminance requirements, combined with the experimentally derived laboratory data collected using test subjects, led them to apply numerical values, to the three equation ABC system luminance control law algorithm, as follows:

$$\log B_d = 0.833 + 0.276 \log B_e , \tag{4.4}$$

and

$$B_{out} = G B_d , \tag{4.2}$$

where

$$G = 0.298 + 1.126 \log \frac{B_f}{B_d} . \tag{4.5}$$

Although this formulation of the Boeing automatic brightness control law appears to be quite straightforward, this impression of the control law is misleading, since it glosses over several underlying issues that require better definition if the control law is to be applied to other aircraft cockpits, electronic displays and aircraft mission requirements.

The interpretation of the equations that constitute the ABC system control law algorithm formulated by Merrifield and Silverstein, which were introduced in this subsection, will be considered in the next subsection.

4.2.2. Interpretation of Boeing ABC System Control Law Algorithm

To be able to use the Boeing ABC system control law algorithm correctly, or to compare it with alternative algorithms, further consideration should be given to the significance of the terms used in the equations and to their interrelationships.

4.2.2.1. Display Brightness Control Equation

The first equation in the set of equations that constitute the Boeing ABC system control law algorithm, Equations 4.1 through 4.3, relates the "display luminance," B_d, necessary to satisfy the pilot's display viewing preferences and requirements, to a term defined by Boeing as the "cockpit ambient," B_a. The "display luminance," B_d, is, by its definition and its usage by Boeing, the same as the display image difference luminance, ΔL, employed elsewhere in the present report to represent the modulated luminance emanating from the images displayed on light reflective, transflective, emissive or transmissive mode displays. As a result, the relationship between the two variables may be expressed, as follows:

$$B_d = \Delta L . \tag{4.6}$$

The "cockpit ambient," B_a, is described by Merrifield and Silverstein in the following quotation: "First, the bezel-mounted light sensor used to measure the level of ambient illumination incident on the display must have a sufficient field of view to measure all incident angles of ambient illumination that significantly affect the amount of light reflected back from the display surface. Because the percentage of ambient illumination reflected from a display is a function of the angle of incidence, the bezel-mounted light sensor must have a lens that attenuates illumination as a function of the angle of incidence. The lens off-angle transmissivity characteristics must roughly match the off-angle reflectivity characteristics of the display surface." If the light sensor used to measure B_a is implemented as just described, the quantity measured will be equal to the display reflected background luminance, except for a constant scaling factor. The display ambient, B_a, as used by Boeing is, therefore, equal to a scaling constant, k_a, multiplied by the display reflected background luminance term, L_D, used elsewhere in the present report, and can be expressed as follows:

$$B_a = k_a L_D . \tag{4.7}$$

In considering the preceding relationships, Equation 4.1 may be interpreted as the basic relationship between the luminance requirement for a displayed image, and the display reflected background luminance against which the displayed image is contrasted, when glare effects either are not present in the display observer's field of view, or can be treated as negligible. This equation can also be expressed in the alternative exponential form, which was also introduced by Merrifield and Silverstein, by substituting log MC for "a" in Equation 4.1. Making this substitution, then the alternative equation can be derived as follows:

$$\begin{aligned} \log B_d &= \log MC + b \log B_a \\ \log B_d &= \log MC + \log B_a^{\,b} \\ \log B_d &= \log [MC\ B_a^{\,b}] . \end{aligned} \tag{4.8}$$

The resultant equation, expressed in exponential form, can then be expressed, as it was in the article by Merrifield and Silverstein, as follows:

$$B_d = MC\ B_a^{\,b} , \tag{4.9}$$

where MC stands for a parameter value suitable for "Manual Compensation" by the air crew. Alternatively, making the substitutions indicated by Equations 4.6, for B_d, and Equation 4.7, for B_a, Equation 4.9 can be expressed as follows:

$$\Delta L = MC\, k_e^{\,b}\, L_D^{\,b}, \tag{4.10}$$

in terms of the terminology used in the present report.

Like Equation 4.1, Equations 4.9 and 4.10 plot as straight lines on a full logarithmic graphing media having a slope "b." The legibility characteristic produced by any of these equations can be translated to higher or lower legibility levels, by increasing or decreasing the value of either "a" (in Equation 4.1) or "*MC*" (in Equations 4.9 and 4.10), respectively. In the Boeing implementation of their luminance control, the transition to the manual night operation of the control is initiated automatically when the sensed level of B_e drops below a lower limit corresponding to 1 fc of incident illuminance. Below the 1 fc limit, the variable B_e in the control law equation is set to a constant value, and after that the display luminance is adjustable using the manual compensation control. This method of control, in effect, creates an operator adjustable electronic display image difference luminance level setting capability, which is consistent with the manual control capabilities available historically in night lighted aircraft cockpits.

4.2.2.2. Compensation of Display Image Difference Luminance Requirements for Glare

Equation 4.2 is the adaptation mismatch luminance compensation equation. The equation is set forth in the block diagram presented in Figure 5 of the previously cited article by Merrifield and Silverstein. The display image luminance glare gain compensation multiplier, *G*, used in the equation, is intended to increase the electronic display image difference luminance automatically, to a level, B_{out}, that will permit the pilot to read the display, with glare present, as well as it could be read, at a display image luminance level, B_d, in the absence of a glare source.

Using the terminology employed elsewhere in this report, Equation 4.2 can be expressed as follows:

$$\Delta L = B_{out} = G\, B_d = G\, MC\, k_e^{\,b}\, L_D^{\,b}, \qquad \text{for } G \geq 1, \tag{4.11}$$

The image difference luminance is represented in this report using the terminology, ΔL, whether the gain compensation multiplier is equal to unity, when no glare source is present, or is equal to a higher value, when a glare source is present within the pilot's forward field of view.

4.2.2.3. Image Difference Luminance Forward Field of View Glare Gain Compensation Multiplier

The final formulation of the Boeing ABC system control law algorithm, shown in Equation 4.11, incorporates the effect of exposure to a glare source by applying the luminance gain compensation multiplier, *G*, to the display image difference luminance requirement in the absence of glare. Equation 4.3 calculates the value of the glare gain compensation multiplier, based on the ratio of the sensed values of the forward field of view luminance, B_f, and of the "cockpit ambient," B_e, where the latter term is proportional to the luminance reflected by the surface of the display, L_D, as given by Equation 4.7. The compensated luminance of the display, B_{out}, obtained in this manner is simply the image difference luminance output of the display, B_d, adjusted to a higher value of image difference luminance by the application of the glare gain compensation multiplier. An auxiliary condition on the validity of applying the glare gain compensation multiplier is that it can only take on values of $G \geq 1$. The value of the gain, *G*, given by Equation 4.3, evaluates to one or greater, only if the "adaptation mismatches," between the FFOV luminance, B_f, and the display background luminance, L_D, are sufficiently large in magnitude. For smaller ratios, the value of *G* is set equal to unity.

In introducing the glare gain compensation multiplier function, G, in Figure 3 of their paper, Merrifield and Silverstein referenced an earlier article by the author[145] as the source of the glare gain compensation multiplier function. The original gain compensation function was presented in a graphical format, rather than as an equation, and showed the display luminance gain compensation multiplier, G, plotted versus the ratio of "surround luminance," B_f, using the terminology of Merrifield and Silverstein, or as L_U, using the terminology

of this report, to "display background luminance," L_D. The original figure from the author's article is shown in Figure 3.9, where the gain compensation function is included as an inset.

In adopting this glare gain compensation multiplier function, Merrifield and Silverstein substituted the display luminance, B_d, for the display reflected background luminance, L_D. Although the reason that it was decided to make this change is not stated in their paper, the following quotation describes the fact that the change was made intentionally, and of their assessment of the results that the change would produce: "The discrepancies between the low-ratio segments of present and previous correction functions may be explained by the fact that the denominators of the ratios that determine the two functions differ. Display luminance will always be higher than, but proportional to, background luminance for a display with an acceptable level of contrast."

The gain equation that Merrifield and Silverstein used to represent the high gain end of the glare gain compensation multiplier function is a straight line when plotted on a semilogarithmic graph of G versus B_f/B_d. Since the high gain end of the G versus B_f/L_D function can also be represented as a straight line on a semilogarithmic graph, the difference between the two functions can be derived from the original G versus B_f/L_D graphical representation of this relationship, illustrated in the inset to Figure 3.9, using the following equation:

$$G = d' + e' \log \frac{B_f}{L_D}. \tag{4.12}$$

If the numerator and denominator of the B_f/L_D ratio are both multiplied by the display image contrast, C, as follows:

$$G = d' + e' \log \frac{CB_f}{CL_D}, \tag{4.13}$$

then the values of the required luminance compensation gain returned by the equation for any stipulated B_f/L_D ratio would be unchanged. Using the laws of logarithms for product terms, this equation can also be expressed in the following equivalent revised form:

$$G = d' + e' \left(\log C + \log \frac{B_f}{CL_D} \right). \tag{4.14}$$

After performing the multiplication operation indicated and substituting the display image difference luminance emanated by the display, $B_d = C\,L_D$, for the product of the display image contrast, C, and the display surface reflected background luminance, L_D, Equation 4.12 can be expressed in the following completely equivalent form:

$$G = d' + e' \log C + e' \log \frac{B_f}{B_d}. \tag{4.15}$$

Based on the preceding derivation, it can be concluded that the gain equation, Equation 4.15, is completely equivalent to Equation 4.12 from which it was derived, except that Equation 4.15 is expressed in terms of the same variable ratio, B_f/B_d, employed by Merrifield and Silverstein in their representation of the image difference luminance gain compensation equation, Equation 4.3. Equating Equation 4.15 first with Equation 4.3 and then with the equation of Merrifield and Silverstein, following the substitution of their experimentally determined constant values, Equation 4.5, yields the following equalities:

$$d = d' + e' \log C = 0.298, \tag{4.16}$$

and

$$e = e' = 1.126. \tag{4.17}$$

Since d' and e' are constants, changing the value of the display image contrast parameter, C, creates a family of G versus B_f/B_d characteristics, in place of the single G versus B_f/L_D luminance compensation gain

function. In other words, the constant d in Equation 4.3, whose value was found experimentally by Merrifield and Silverstein to be $d = 0.298$, is strictly valid only for the CRT displays and image contrast used in their experiment.

The display image contrast, C, like the display image difference luminance, B_d, in Equation 4.1, refer to the values required by a display when no adaptation mismatch exists, that is, the uncompensated values of display image contrast and image difference luminance. As the value of the forward field of view (FFOV) luminance, B_f, increases with respect to the value of L_D or B_d, the application of the required gain multiplier establishes new higher values of contrast, C', and of display image difference luminance, B_d', such that

$$C' = GC \tag{4.18}$$

and

$$B_d' = C'L_D = GCL_D = GB_d = B_{out} \tag{4.19}$$

The latter equation provides the physical basis underlying the formulation of Equation 4.2 by Merrifield and Silverstein.

The empirical gain relationships used to compensate for the presence of glare, as represented by Equations 4.3 and 4.12, were either verified experimentally, or determined directly from experimental test data, using surround fields of approximately uniform luminance. While some ambient illumination conditions encountered in an aircraft are consistent with the uniform surround field luminance assumption used in the preceding experiments, most are not. Furthermore, as described in Chapter 3, it is known that the effects of glare sources, whether they are point sources or spatially distributed, are highly dependent on the angle subtended between the position of a glare source, within the pilot's field of view, and the line of sight direction to the cockpit display, from which the pilot is attempting to extract information. Recognition of the existence of this angular relationship by Merrifield and Silverstein was shown in the following admonition in their 1988 article:[146] "...The sensor used to measure the luminance of the FFOV must have approximately the same field of view as the cockpit geometry affords the pilot." They immediately follow this with the following additional clarification: "The forward-facing light sensor should have a lens that attenuates incident light as a function of the square of the cosine of the angle of incidence of the light to the sensor."*

Based on the preceding description, the forward field of view brightness, B_f, that Merrifield and Silverstein recommend be measured by the FFOV sensor is equal to a $\cos^2\theta$ angle weighted integration over the spatially distributed luminance of the visual scene within the pilot's forward field of view. As such, the operation of this FFOV sensor is very similar to the light sensor measurement of veiling luminance described in Chapter 3. Two distinctions should be noted. The first distinction between the two light measurement approaches is that the angular dependence of a $\cos^2\theta$ angular weighting function decreases much less rapidly, as a function of increases in the angle, θ, than do any of the human veiling luminance angular distributions described in Chapter 3. The second distinction worth noting is that the magnitude of the veiling luminance, L_V, induced in the pilot's eyes, can be expected to be much less than the magnitude of the forward field of view brightness, B_f, that would be measured with a FFOV sensor, since only a small fraction of the incident scene luminance is scattered into the pilot's line of sight to the display being read.

In spite of the aforementioned distinctions, it has to be concluded that, except for the choice of a different angular weighting function, and the need for a much more attenuative scaling factor to provide veiling luminance, the Merrifield and Silverstein FFOV sensor measurement technique is consistent with the sensor measurement technique described previously in detail in Chapter 3 of this report, and as originally proposed in the author's earlier 1979 article on this subject.[147] It should be noted that Chapter 7 of this report describes practical cockpit design considerations, where choosing light sensors having angular weighting functions with

---

* Reference cited by quotation: Silverstein, L. D. and R. M. Merrifield, The Development and Evaluation of Color Systems for Airborne Applications, DOT/FAA/PM-85-19, 1985, pp. 157-165.

broad angular response distributions, like the one described by Merrifield and Silverstein, could be preferable to using the narrower distributions associated with human vision.

A more in-depth comparison of the original adaptation mismatch gain compensation multiplier, as represented by Equation 4.12, and the one used by Merrifield and Silverstein, Equation 4.3, is warranted to provide further insight into the significance of the latter equation. Doing so at this point would provide little in the way of additional interpretive advantage, and consequently this comparison is deferred until Chapter 5.

4.3. General Automatic Legibility/Brightness Control

The automatic legibility/brightness control algorithm selected for use in controlling the electronic displays in the Lockheed Advanced Tactical Fighter (ATF) aircraft was designed to have very general capabilities. The intent of Lockheed was to permit a broad selection of different luminance control characteristics to be flight tested, which, for example, could be caused to match the empirically derived constant automatic legibility control (ALC) requirements, described in Chapter 3, or to match the Boeing pilot-preference derived automatic brightness control (ABC) characteristics. The design choice flexibility was a Lockheed requirement, intended to permit experimentation to determine the optimal performance characteristics for a fighter type aircraft. A manual trim control adjustment capability was also required to permit the pilot to set the desired level of legibility based on personal preference or visual needs.

In this section, the application of the general automatic legibility/brightness control law algorithm designed for the General Electric Company, for use with their color liquid crystal displays in the Lockheed ATF aircraft, is considered only in generic terms. Because these displays utilize the transmissive operating mode, the relative image difference luminance and contrast relationships, portrayed on the display viewing surface at any point in time, are electronically controlled by modulating the transmittance of the picture elements using a display image generation computer. The absolute image difference luminance levels and image contrasts at which the display information is portrayed are controlled separately by adjusting the display backlight's luminance output.

4.3.1. Composite Display Grey Shade and Image Difference Luminance Control

A complete description of the image difference luminance output, $\Delta L(n)$, of a color liquid crystal display, including both grey shade and backlighting control, can be expressed as follows:

$$\Delta L(n) = Y(n)\,\Delta L(W) \tag{4.20}$$

In this equation, the function $Y(n)$ is the relative luminance transmitted by a specific LCD pixel at a specific instant of time. As formulated in Equation 4.20, the relative luminance function represents time changing fractional values between zero and unity, of the grey shade encoded signal inputs for each picture element in the display surface, which are transferred to the display from an aircraft image generation computer. The function $\Delta L(W)$ is the maximum white grey shade image difference luminance level of the activated display surface when the display picture elements are operated at their maximum transmittance while being illuminated from the rear by the display's backlight source. This image difference luminance variable is therefore equal to the emitted luminance level of the backlight, as attenuated by the maximum transmittance of the display viewing surface, and can be controlled between the maximum and minimum levels to which it can be driven by the backlight.

Although the automatic brightness or luminance control of the white image difference luminance level, $\Delta L(W)$, is of principal interest in this paper, the grey scale control function Y(n) will be briefly described here, and in greater detail in Chapters 5 and 6, to distinguish clearly between the separate legibility control roles of these two variables.

4.3.2. Grey Scale Relative Luminance Function

For a transmissive mode liquid crystal display, the relative luminance function $Y(n)$ takes on fractional values from the minimum display grey shade level of $n = 1$, produced when the liquid crystal light value attenuation is a maximum, up to a maximum value of unity at a grey scale level $n = n_{max}$. Because of the light leakage through the liquid crystal structure at maximum attenuation, the minimum perceptible grey scale level is $n = 1$ rather than $n = 0$ since a true off, that is, a zero image difference luminance, cannot be achieved due to a finite level of backlight transmittance that is always present. In other words, the reflected background luminance of the display surface, corresponding to $n = 0$, can only be seen and measured if the backlight is turned entirely off.

For any given setting of the white image highlight luminance level, $\Delta L(W)$, between the minimum and the maximum levels established by setting the luminance level of the white backlight source, a further reduction in display emitted luminance levels can be achieved by separately controlling LCD grey shades using the relative luminance control function Y(n). If for example, the ratio between the white $\Delta L(n=n_{max})$ level and the black $\Delta L(n=1)$ level is 50, as measured in the dark, then $Y(n=n_{max}) = 1$ and $Y(n=1) = 1/50 = 0.02$. The use of the Munsell Value scale was recommended to select the discrete digitally generated grey scale levels to be presented on the GE color liquid crystal displays. The image difference luminance of the display white level control function is not, therefore, directly related to the minimum "off" transmitted luminance of the LCD, except through the pixel modulated values of $Y(n)$ that can be displayed, which, in turn, is controlled by the grey shade encoded input signals from a computer, video sensor, or video storage media, and the display technology dependent limitations on the minimum light leakage the display is capable of achieving.

4.3.3. White Image Difference Luminance Level Control Function

The control law function, for the image difference luminance level of the highlight white, recommended for implementing the GE color LCDs on the Lockheed ATF aircraft is given by the following equation:

$$\Delta L(W) = K(L_D + L_V)^m + \Delta L_N . \qquad (4.21)$$

This control law gives the image difference luminance level, corresponding to the white grey shade, that the display should be set to as a function of the reflected display luminance, L_D, and the glare source induced veiling luminance, L_V. Equation 4.21 is the same as the general legibility requirement equation, derived in the Chapter 3 and presented in Equation 3.163, except that the use of the "W" in the image difference luminance variable is intended to show that the values of K and ΔL_N must be selected to make the display's white color legible, at a level that causes the balance of the color information rendered on the display to be legibly portrayed. The physical significance of these equations, and of the terms used in them, is described in Section 3.9 and further expanded upon in later chapters.

To enable Lockheed to conduct the pilot preference and legibility requirement tests of the GE color LCD backlight luminance, under automatic control, the parameters K, ΔL_N and m, in Equation 4.21 were designated for treatment as experimentally alterable test variables. The effect of changing the value of the parameter K is to alter the contrast of the information displayed. Changing the value of ΔL_N alters the night image difference luminance of the information presented on the display. Finally, the value selected for the power parameter, m, changes the slope of the display's image difference luminance output response to the sensed variables L_D and L_V.

To produce display pictures that the pilot would perceive to be of constant legibility, independent of changing ambient illumination environment viewing conditions, a value of m = 0.926 would be used in Equation 4.21. When presenting grey shade encoded information, constant legibility has the advantage of causing the display to be equally effective in presenting information under any arbitrary incident ambient illuminance and veiling luminance viewing condition. The constant automatic legibility control feature should yield the greatest benefit for pilot information display tasks, where a premium exists on achieving consistent objective rather than

subjective performance. A sampling of military display information presentation tasks, which would benefit from this facilitation of the pilot's objective visual perception capabilities, include the following: sensor-video grey shade encoded information, relative color coded navigation map information and flight-safety critical absolute color coded information. By way of comparison, reducing the value of the power parameter, m, from a slope of 0.926, for constant legibility, to the slope of 0.276, that was experimentally determined by Merrifield and Silverstein as the slope preferred by airline pilots, would cause the display's legibility to increase rather than remaining constant, as the ambient illumination incident on the display or the veiling luminance induced in the pilot's eyes, become smaller. The effects of each of these parameters, on the general legibility requirement equation, are described in greater detail in Chapter 5.

4.4. Summary of Features Shared by Boeing ABC and General ALC

Features of the Boeing ABC and of the General ALC that are common elements of both control techniques were pointed out in the earlier sections of this chapter. In the preceding section, it was furthermore asserted without proof that Equation 4.21, a version of the general legibility control law, could, with the substitution of the appropriate parameter values, be used to emulate the response of the Boeing automatic brightness control law. In this section, these common elements will be further explored as a prelude to Chapter 5, where the equivalence of the two control laws will be demonstrated. Four critical points of commonality between the features of the Boeing automatic brightness control law and the general automatic legibility control law, which are regarded as significant, are summarized in the balance of this section.

The first shared feature of the Boeing ABC and the General ALC is the display light sensor. Although the measured light quantity, B_a, is designated by Merrifield and Silverstein as the "cockpit ambient," the description of how the sensor should be designed to operate actually corresponds to B_a being directly proportional to the luminance reflected from the display viewing surface, which is designated elsewhere in this report by the nomenclature, L_D. This is the baseline luminance level to which the pilot's eyes are adapted when attempting to read information portrayed on an electronic display at an image difference luminance, ΔL (i.e., referred to as B_d by Merrifield and Silverstein), above the level of the reflected background luminance level of the display surface. Because the "cockpit ambient," measured by Merrifield and Silverstein, is directly proportional to the display background luminance, which, as described elsewhere in this report, is the key factor in determining the image difference luminance level needed to legibility portray the information presented on a display, when the ambient illumination environment incident on a display is changing, it is considered significant that both models share this variable.

The second significant shared feature of the Boeing ABC and the General ALC is their forward field of view (FFOV) light sensors. Again, although the light quantity the Merrifield and Silverstein sensor measures, B_f, is designated as the FFOV luminance, the description of how the sensor should be designed to operate instead corresponds to an optical integration of an approximation for the angular sensitivity weighted response of the pilot's eyes to the spatial luminance distribution that exists, external to the aircraft, with the additional constraint imposed that the sensors field of view be restricted to the cockpit imposed light exposure solid angles the pilot would experience when flying a specified type of aircraft. The forward field of view light quantity recommended for measurement by Merrifield and Silverstein is, therefore, significant in that it gives an approximate measure of the glare source exposure the pilot actually experiences. An additional provision that the central optic axis, of this light sensor, be oriented parallel to the pilot's line of sight to the display being viewed is not specifically mentioned in the Merrifield and Silverstein paper, however, it is implied. This method of treating the FFOV sensor is the same one proposed by the author in the 1979 article cited earlier and recommended for use on the Lockheed Advanced Tactical Fighter predecessor to the F-22.

The third significant shared feature, by the Boeing ABC and the General ALC, is the basic display image difference luminance control algorithm, Equation 4.1. This algorithm applies to daylight viewing requirements and is equivalent in form to the general automatic legibility control algorithm, shown in Equation 4.21 and

described elsewhere in this report, when the night image difference luminance is negligible and if compatible equation parameter values are employed. A practical difference is that Boeing's test goal was not to develop a constant legibility control law, but was instead to satisfy the personal preferences of commercial airline pilots for display legibility. The result of this difference in design objectives is that the parameter values substituted into the Boeing control law by Merrifield and Silverstein produce increasing display legibility as the ambient illumination level in the cockpit decreases, rather than causing the legibility to be held constant, a result that either control law can achieve with the correct choice of equation parameter values. Both control laws follow logarithmic image difference luminance response characteristics under high ambients, with a transition to a constant difference luminance level, which is adjustable by the pilot under night viewing conditions. It should be noted that because the Boeing ABC law was implemented to switch automatically to the manual control mode below one foot-candle of illuminance, neither their experiment, nor the Boeing commercial aircraft implementation of the ABC, tested automatic control below this cockpit ambient illumination limit.

The fourth, and last, significant feature, shared by the Boeing ABC and the General ALC, is the effect of the gain compensation multiplier of Equation 4.3, in the presence of a glare source, on the image difference luminance of a controlled display. This equation generates a compensation multiplier that automatically adjusts the image difference luminance of a display for the effect of spatially distributed or discrete glare sources, located external to the aircraft cockpit. Properly designed outside looking cockpit sensors, individually positioned to sense the glare exposure the pilot receives while looking at different instruments, should make it possible to generate a gain compensation multiplier that can account for the effects of the glare source exposures. Unlike the earlier features of the Boeing ABC compared with the General ALC, the gain compensation multiplier employed by Boeing to compensate for the effects of glare exposures is not directly comparable to the glare source induced veiling luminance formulation of the General ALC. Nonetheless, the overall results obtained by using these two methods of compensating for the presence of distributed and discrete glare sources in the pilot's forward field of view are very similar.

A more in-depth comparison of the Boeing ABC and the General ALC is presented in Chapter 5. The comparison shows that, when properly implemented, the Boeing ABC and the General ALC produce essentially the same electronic display legibility control results.

CHAPTER 5

General Automatic Legibility Control (ALC) Law

The most flexible form of the general automatic legibility control law appears in Equation 3.163, which is repeated here for convenience, as follows:

$$\Delta L_P = K(L_D + L_V)^m + \Delta L_N . \qquad (3.163)$$

This equation includes two constant terms, K and ΔL_N, which can be used to permit the pilot to intervene in the legibility settings of the displays being controlled by making trim control adjustments to the legibility of the display. The equation also includes a third constant term, m, in the exponent of the equation that determines the legibility response of the display to changing incident illuminance and glare source exposure conditions, through the implementation of properly designed light sensors to measure quantities directly proportional to the display reflected background luminance, L_D, and to the veiling luminance, L_V, induced by exposure to discrete or distributed glare sources, such as the sun or sun illuminated white clouds, respectively.

In this chapter, the practical implications of the choice of the values for the aforementioned constants in Equation 3.163 will be described. The major emphasis of this description will be on the effect of the choice of the exponent constant, m, on the legibility control achieved. The other two constants, K and ΔL_N, have been previously described in Section 3.9 but are also of interest in this chapter. This interest is due, in part, to the potential interactions of these two constant parameter values with the value chosen for the exponent, m, in the general case, before a specific value is assigned to this constant, m, but is also due to the physical significance of these two constants with respect to the human's image difference luminance requirements, once a specific value is assigned to this constant, m.

To illustrate the flexibility of the general automatic legibility control law equation, the first section below considers the equation in the context of an implementation that would permit an electronic display to respond to incident ambient illumination in the same manner as conventional electromechanical displays. Since conventional aircraft display techniques possess legibility properties known to be satisfactory in aircraft cockpit applications, this approach to the interpretation of the general automatic legibility control law has the added advantage that it provides a well-established baseline, to which alternative implementations of the control law using different constant parameter values can be compared. The result of this comparison in the first section is that the night image difference luminance term, ΔL_N, has the same meaning in both control laws, the exponent, m, takes a value of unity, the veiling luminance term is dropped and the constant K takes on the value of the contrast, C, of the conventional instrument.

In the second section of this chapter, a detailed comparison is made between the General Automatic Legibility Control (ALC) law and the Automatic Brightness Control (ABC) law developed by Merrifield and Silverstein. This comparison is carried out in two stages. First, the general legibility control law equation is cast in the same form as the Boeing control law to demonstrate the commonality between the two formulations. Next, using the modified form of the general legibility control law equation, the equivalence of the two glare source gain compensation equations is evaluated. Although this comparison is rather involved, the results show that the general automatic legibility control law is roughly equivalent to the Boeing automatic brightness control law, when the appropriate parameter values are used in the respective equations.

The third section introduces background information and mathematical tools to permit describing the control exercised by the human visual system over the legibility of information contained in electronically displayed and directly viewed visual scenes. These results are introduced for use in the interpretation, application and use of the general automatic legibility control law and, its special case, the constant legibility control law, in the fourth and fifth sections of this chapter and, ultimately, throughout the balance of the report. The section starts by quantifying the legibilities of different types of aircraft display information using historic legibility measures. This is followed by descriptions of the use of relative luminance levels to quantify the

legibility of visual information and the compatibility of this technique with the Munsell system for characterizing color and grey shade perception. Next, visual perception capabilities of humans and image rendition capabilities of existing aircraft displays are compared in an effort to determine the capabilities that the electronic displays need to possess to satisfy a pilot's visual requirements. This is followed by a description of the grey shade perception capabilities made possible using electronic displays and then by a more involved subsection in which mathematical relationships are developed to relate the image rendition requirements needed to replicate the visual perception of grey shades and colors in real-world scenes in electronic display presentations. The final two subsections describe the electronic display presentation implications of the constant legibility control capability of the human visual system and the ability of this system to extend the range of perceptible grey shades through the spatially selective adaptation of the eyes light receptors.

The fourth section of the chapter deals with the practical implications of configuring the general automatic legibility control law in different ways, through the choice of the exponent, m, and the other control law parameters in Equation 3.163. The choice of the value of the constant power parameter, m, is primarily responsible for determining the image difference luminance control characteristic followed by aircraft cockpit displays in response to changes in the display background luminance and veiling luminance. The practical significance of whether the election is made to operate aircraft electronic displays using an automatic brightness or a constant legibility control law is also considered. As previously described, when $m = 0.926$ is substituted for the exponent in this equation, the resultant equation,

$$\Delta L_P = K(L_D + L_V)^{0.926} + \Delta L_N, \tag{5.1}$$

produces control characteristics, under changing ambient illumination and glare source exposure conditions, that cause the controlled display imagery to be perceived by aircrew members at different constant legibility levels, subject to the values selected for K and ΔL_N. The effect of choosing different values for the slope parameter, m, including values of unity, zero, the value determined by Merrifield and Silverstein, using a legibility criterion intended to satisfy the subjective preferences of airline pilots, and the value corresponding to the constant legibility criterion, are described. Interactions between the slope of the control law and aircrew settings of the night image difference luminance level are described in the last subsection.

The final section in the chapter deals with possible implementations of the aircrew adjustable legibility trim controls that would be used by pilots or other aircrew members to adjust the control characteristics of electronic displays, operated using automatic legibility controls. Control law equations using either single legibility trim controls, for both day and night legibility adjustments, or dual legibility trim controls, to permit separate day and night legibility settings, are described. This section concludes with an introduction to the factors that influence the choice of the parameters used in the constant legibility control law equation, a subject considered in greater detail in subsequent chapters.

5.1. Emulation of Conventional Electromechanical Aircraft Instrument Legibility using Electronic Displays

Under very low light levels, at night, and in the absence of either discrete or distributed glare sources, the terms L_D and L_V are very low and the night image difference luminance, ΔL_N, acts as a floor on how low the image difference luminance levels of electronic displays are allowed to decrease at night under automatic legibility control. If ΔL_N is made controllable by the pilot, say between 1.5 fL and 0.05 fL or less, then ΔL_N would introduce the same pilot control capability as that possessed by conventionally illuminated electromechanical instruments, and existing electronic displays under manual control at night. The performance distinction introduced by using automatic legibility control with electronic displays occurs as the ambient illumination incident on the display increases. Under this condition, the perceived image difference luminance, ΔL_P, of electronic display imagery is automatically increased, which allows the legibility of the display to be maintained at a fixed level if the proper control characteristic (i.e., $m = 0.926$) is followed during the transition from darkness to daylight or vice versa.

As the ambient illumination incident on conventional electromechanical instruments increases, the night

lighted luminance of the display imagery is automatically augmented, because of the increased luminance reflected from the image and background areas on the instrument's faceplate. This performance is roughly emulated by an electronic display operated by an automatic legibility control (i.e., ALC). Likewise, the use of an automatic brightness control (i.e., ABC), with the proper control characteristics, also allows electronic displays to emulate the legibility performance of conventional reflective operating mode instruments in natural ambient light. To achieve complete legibility equivalence with conventional electromechanical instruments, the automatic brightness control characteristic would have to be selected so that it provides the electronic display with the image difference luminance levels and constant contrasts, equal to those associated with the reflective painted faceplate imagery depicted on electromechanical displays being emulated.

The control characteristic for conventional electromechanical instruments can be expressed mathematically as follows:

$$\Delta L = K_{EM} L_D + \Delta L_N . \tag{5.2}$$

Comparing the preceding equation with the general constant legibility control law of Equation 5.1, it may be seen that the night image difference luminance levels of the electromechanical and electronic displays have already been equated in writing Equation 5.2. Continuing the comparison, the slope of the full logarithmic plot of this conventional instrument control characteristic is m = 1, rather than m = 0.926, and the veiling luminance compensation term, L_V, is absent. In higher ambient illumination conditions, where the night image difference luminance term, ΔL_N, is negligible in comparison to the reflected luminance term, $K_{EM} L_D$, Equation 5.2 can be expressed, with negligible error, as follows:

$$\Delta L = K_{EM} L_D , \tag{5.3}$$

Solving this equation for the constant, K_{EM}, the constant is found to be equal to the contrast, C, of either the conventional instrument or electronically generated display imagery, that is,

$$K_{EM} = \frac{\Delta L}{L_D} = C . \tag{5.4}$$

Making this substitution into Equation 5.2, yields the following legibility control equation:

$$\Delta L = C L_D + \Delta L_N . \tag{5.5}$$

Electronic displays designed to satisfy this automatic brightness control equation would, therefore, match the constant contrast legibility characteristics of a conventional electromechanical instrument's painted faceplate imagery.

Carrying the comparison of the general constant legibility control law of Equation 5.1, to the natural control law of an electromechanical instrument, Equation 5.5, one step further, it may be concluded that two displays, which follow control characteristics with initial slopes of m = 0.926 and m = 1, respectively, and that start at the same high ambient perceived image difference luminance and contrast values will, due to dimming at different rates, result in the electronic display that follows the general constant legibility control law characteristic, having a progressively higher image difference luminance and contrast, than its conventional display counterpart, as the background luminance continues to be reduced. This difference between the dimming characteristics of the two displays continues to exist, as the incident ambient illumination is reduced, down to the common night image difference luminance level setting requirements of the displays, which limit any further perceptible decreases in the display image difference luminance levels. Because of the different dimming characteristics the two displays follow, the conventional display would reach this limit at a higher display reflected background luminance level than the electronic display that follows the general constant legibility control law characteristic.

The progressively higher perceived image difference luminances and contrasts, which occur when electronic display portrayals are dimmed following the general constant legibility control law, is necessary to compensate for the gradual decrease in the pilot's visual acuity, as ambient light levels decrease below the optimal conditions present during high ambient daylight viewing conditions. As described in Chapter 3, this decrease in visual acuity is, in part, associated with the gradual increase in the eyes' pupil areas, as the light

levels that the eyes are adapted to decrease in magnitude, and, in part, due to a gradual loss of cone light receptor sensitivity, as the image difference luminance levels decrease.

5.2. Comparison of the General and the Boeing Automatic Brightness Control Laws

The Boeing automatic brightness control (ABC) system algorithm, described in the previous chapter, and the more general automatic legibility control (ALC) system algorithm, described in Chapter 3, are both consistent with their respective empirical test data, and, moreover, should both be suitable for the automatic control of the image difference luminance levels of electronic displays in aircraft cockpits. Based on the analyses of the prior chapters, it is known that the light sensors of both systems measure essentially the same light quantities. In this section, the degree to which the two systems can be considered equivalent will be explored in greater detail.

5.2.1. Commonality Between General and Boeing Control Laws

The mathematical formulation of the general legibility control law, as previously introduced in Equation 3.163 of Chapter 3 and in Equation 5.1, is repeated here for convenience as follows:

$$\Delta L_P = K(L_D + L_V)^m + \Delta L_N , \tag{3.163}$$

where

$$m = 0.926 \tag{5.6}$$

for constant legibility characteristics. As previously described, the constant multiplier, K, can be interpreted as a daylight legibility multiplier and ΔL_N as the night image difference luminance level setting of the display.

Although the inclusion of a term to represent the night image difference luminance level setting of the display, ΔL_N, was discussed in the Merrifield and Silverstein article, the term was not included in their mathematical representation of their automatic brightness control law. For this reason, and to facilitate a comparison between the general automatic legibility control law, Equation 3.163, and the Boeing automatic brightness control law, it is necessary to revise the formulation of the general ALC law to include only the daylight portion of the equation, as follows:

$$\begin{aligned} \Delta L &= K(L_D + L_V)^m \\ &= K\left[L_D\left(1 + \frac{L_V}{L_D}\right)\right]^m \\ &= K L_D^m \left(1 + \frac{L_V}{L_D}\right)^m . \end{aligned} \tag{5.7}$$

The elimination of the night image difference luminance level setting of the display, ΔL_N, makes it necessary to place a lower limit on the image difference luminance, ΔL, and hence on the display background luminance, L_D, for which the equation is approximately valid. This constraint is comparable to the one applied by Merrifield and Silverstein to the Boeing ABC law, namely, that the control equation only applies when ambient illuminance levels of one foot-candle and larger are incident on the display light sensors. Another constraint, which is implicit when using the ABC law, is that the logarithmic slope of the Merrifield and Silverstein brightness control characteristic, b, must be small enough so that, when the 1 fc day to night incident ambient illuminance transition is reached, the smallest display image difference luminance commanded by the ABC is greater than or equal to the largest image difference luminance level requirement of the aircrew, immediately after switching the display from the daylight automatic control mode to night manual control mode of operation.

To make the final expression in Equation 5.7 equivalent in mathematical form to the Boeing automatic

brightness control algorithm, it can be represented in the following alternative form:

$$\Delta L = K L_D^m G', \tag{5.8}$$

where

$$G' = \left(1 + \frac{L_V}{L_D}\right)^m. \tag{5.9}$$

The gain, G', given by Equation 5.9, can be interpreted as a gain compensation multiplier, for the image difference luminance of a display, whose purpose is to account for the effect of the veiling luminance induced by a glare source. In this equation, when no glare source is present, the veiling luminance is zero and the gain is equal to unity.

The daylight portion of the general legibility control law, as expressed by Equation 5.8, may be seen to be equivalent in form to the Boeing automatic brightness control law, when Equation 4.9,

$$B_d = MC\, B_s^b, \tag{4.9}$$

is substituted into Equation 4.2,

$$B_{out} = G\, B_d, \tag{4.2}$$

yielding the following composite form of the Merrifield and Silverstein legibility equation:

$$B_{out} = MC\, B_s^b\, G. \tag{5.10}$$

The equivalence of the general legibility control law with the Boeing automatic brightness control law is made even more evident, if the sensed Merrifield and Silverstein "cockpit ambient" term, B_s, is replaced by the previously introduced proportionality relationship between B_s and L_D, as expressed by Equation 4.7,

$$B_s = k_s L_D. \tag{4.7}$$

In this equation, L_D is the luminance reflected by the surface of the display, when it is exposed to incident ambient illumination, and k_s is a constant scaling factor. As pointed out in Chapter 4, this latter relationship is a mathematical representation of the way Merrifield and Silverstein described the operation of the B_s sensor in their article. Substitution of B_s from Equation 4.7 into Equation 5.10 yields the following equivalent form of the Boeing automatic brightness control law:

$$\Delta L = MC\, k_s^b L_D^b\, G, \tag{5.11}$$

where the gain-compensated image difference luminance of a display is being represented by the term ΔL, rather the B_{out} nomenclature used in the previously cited article of Merrifield and Silverstein. Except that the order of the terms is rearranged, Equation 5.11 is the same as Equation 4.11. It may be seen to have the same mathematical form as the modified version of the general legibility control law equation, introduced in Equation 5.8.

Although Equations 5.8 and 5.11 are of the same mathematical form, full equality would require that the slopes of the two equations b and m be equal, that is,

$$m = b \tag{5.12}$$

and that

$$KG' = MC\, k_s^b G. \tag{5.13}$$

From a purely mathematical standpoint, the first condition on the equality between the two control law equations, Equation 5.12, can be satisfied by simply choosing to make the constants, m and b, equal to one another. Satisfying the equality shown in Equation 5.13 is another matter, since, as will be shown later, the gain terms, G' and G, previously introduced in Equations 5.9 and 4.12, respectively, cannot be reformulated so as to differ only by a constant multiplier.

Even though the two control laws are not equal, it remains to determine the extent to which Equations 5.8 and 5.11 can be considered equivalent representations. When no glare source is present, it is a basic premise of both the general and Boeing control laws, as represented by Equations 5.8 and 5.11, respectively, that the gain condition expressed by the equation

$$G = G' = 1, \tag{5.14}$$

must be satisfied. Under this gain condition, Equation 5.13 should be satisfied and, consequently, a single equation, recognizing the equality of the two control laws and expressed as follows:

$$\Delta L = K L_D^m = MC\, k_s^b L_D^b, \quad \text{for } m = b, \tag{5.15}$$

can be used to control the image difference luminance output of a display, ΔL, under moderate to high levels of daylight illumination incident on the display light sensor. It can, therefore, be concluded that in the absence of a glare source, both control laws predict the same image difference luminance requirements under daylight viewing conditions, except for differing constant multipliers to account for the difference in the legibility criteria used in Section 3.9 and those employed by Boeing.

More generally, even when a source of glare is present, it can be concluded that the two control laws are of the same form under daylight viewing conditions, that is, both equations can be expressed by the single equation, as follows:

$$\Delta L = K L_D^m G', \tag{5.16}$$

where K and m are interpreted as they were previously in Section 3.9, for the general control law, and G' is given by Equation 5.9. To use Equation 5.16 to represent the Merrifield and Silverstein control law, the parameters, $K = MC\, k_s^b$, $m = b$, and G, as given by Equation 4.3, can be substituted into Equation 5.16 for G'.

In the subsection that follows, the gain compensation equation for the general control law, Equation 5.9, and the equation of Merrifield and Silverstein, Equation 4.3, will be compared and the extent to which they can be considered equivalent to one another will be explored.

5.2.2. Evaluation of Equivalence of Gain Compensation Equations

The unity gain condition, that must be satisfied in the absence of glare, and that leads to the valid application of Equation 5.16, is computed using Equations 5.9 and 4.3 with differing degrees of difficulty. A gain of unity can be obtained, using the general gain compensation equation of image difference luminance, Equation 5.9, by simply substituting the induced veiling luminance value of, $L_v = 0$ fL, into the equation. In other words, a unity gain is obtained as a natural consequence of evaluating Equation 5.9, when no glare is present in the pilot's field of view, and hence no veiling luminance is induced. The simplicity of using this equation is based on the fact it is valid for any values of its independent variables that can be physically realized in an aircraft cockpit.

For the Boeing gain compensation equation of image difference luminance, Equation 4.3, which for convenience is repeated here as follows:

$$G = d + e \log \frac{B_f}{B_d}, \tag{4.3}$$

the interpretation of the equation and its use is more complex. For starters, this equation is valid only for B_f/B_d ratios that cause the gain equation to satisfy the supplemental constraint, $G \geq 1$. As previously described, Equation 4.5 is Boeing's version of Equation 4.3, following the substitution of the numerical values for its parameters that were experimentally determined by Merrifield and Silverstein. For convenience, the equation is repeated here, as follows:

$$G = 0.298 + 1.126 \log \frac{B_f}{B_d} . \tag{4.5}$$

The evaluation of this equation, with the gain set equal to unity or larger, causes the luminance ratio B_f/B_d to yield values of 4.2 or larger. For values of the ratio B_f/B_d smaller than 4.2, the gain, G, is by definition equal to unity rather than the values to which Equation 4.5 evaluates under this condition.

Equation 4.12 was introduced in Chapter 4 to represent the experimental data shown in the inset to Figure 3.9 that Merrifield and Silverstein cited as the origin of their gain equation. For convenience, the equation is repeated here, as follows:

$$G' = d' + e' \log \frac{B_f}{L_D} . \tag{4.12}$$

The differences between this equation and the one adopted for modeling the data in the inset to Figure 3.9 by Merrifield and Silverstein, Equation 4.3, were described in Chapter 4. It should be noted, however, that Equation 4.12 is still not in the exact form of the empirical equation that would be needed mathematically to represent the data shown in the inset to Figure 3.9, since the forward field of view brightness variable, B_f, of Merrifield and Silverstein, is a viewing-angle-weighted function of the uniform measurable surround field luminance, L_U, that was actually tested to produce the result shown in the inset to Figure 3.9.

As described by Merrifield and Silverstein, the FFOV brightness is the $\cos^2\theta$ angle-weighted integral of the surround field luminance, L_U, over the pilot's field of view. Since L_U is a constant, as a function of the spherical angles, θ, and, ϕ, it can be factored out of the integral. Based on these facts, an equation for the forward field of view brightness (i.e., actually a luminance), B_f, in terms of surround field luminance, L_U, can be expressed as the product of a fractional multiplier constant, k_B, and the surround luminance, as follows:

$$B_f = k_B L_U , \tag{5.17}$$

where the constant can take on different fractional values close to unity. The value of the constant, k_B, would be dependent on the angular limits placed on the pilot's field of view (i.e., the size of the uniform surround luminance field) by the test environment, or by the different cockpit geometry limitations on the pilot's field of view in operational aircraft cockpits. Making this substitution into Equation 4.12, the gain equation, suited for modeling the data in the inset of Figure 3.9, can be derived, using the product law of logarithms, as follows:

$$\begin{aligned} G' &= d' + e' \log k_B + e' \log \frac{L_U}{L_D} \\ G' &= d'' + e' \log \frac{L_U}{L_D} . \end{aligned} \tag{5.18}$$

Choosing numerical values of G' and L_U/L_D for two points on the high luminance ratio portion of the characteristic, shown in the inset to Figure 3.9, and substituting these values into Equation 5.18 provides two simultaneous equations that can be solved for the unknown parameters d'' and e'. The application of this approach to the data represented in the inset of Figure 3.9 yielded the following numerically evaluated mathematical model for the high luminance ratio portion of the characteristics:

$$G' = 0.359 + 1.028 \log \frac{L_U}{L_D} . \tag{5.19}$$

A direct comparison of this result, to the one reported by Merrifield and Silverstein in Equation 4.5 (i.e., which was repeated above), presents a problem, however, since the independent variables in the luminance ratio are expressed using different variables in the two equations. The Merrifield and Silverstein article described their viewing geometry as corresponding to a Boeing 767 flight deck with the external FFOV luminance levels varied between 150 and 10,000 fL. Although this information, and the location of the pilot's eye point of regard in the cockpit, would permit calculating the value of k_B, the vertical and horizontal angle constraints on the

pilot's exposure to the FFOV luminance through the windscreen, coupled with the slow angular variation of the $\cos^2\theta$ angular weighting function, mean that the value of this constant would evaluate to very nearly unity and, for the present purposes, the constant can therefore be approximated as $k_B \approx 1$. Making this substitution into Equation 5.17, allows the forward field luminance to be expressed approximately in terms of the surround field luminance of the inset to Figure 3.9, as follows:

$$B_f \approx L_U \tag{5.20}$$

Substituting $k_B \approx 1$ into Equation 4.12, or the substitution of Equation 5.20 into Equation 5.18, allows both gain equations to be approximately represented as follows:

$$G' = d' + e' \log \frac{L_U}{L_D} . \tag{5.21}$$

Comparing this approximately equivalent form of Equation 4.12 to Equations 5.18 and 5.19, the values of the constants in Equation 5.21 can be expressed as $d'=d''=0.359$ and $e'= 1.028$.

The reason for presenting Equation 5.21 and giving its parameter values is that these values do not satisfy the compatibility relationships of Equations 4.16 and 4.17, developed in Chapter 4 to relate Equation 4.12 and Boeing's Equations 4.3 and 4.5. However, the unity gain intercept of the high luminance ratio portion of the gain characteristic shown in the inset to Figure 3.9, that is, the luminance ratio predicted by Equation 5.19, for $G' = 1$, and the unity gain intercept of the Merrifield and Silverstein Equation 4.5, for $G = 1$, are both nominally equal to 4.2 to three significant places of accuracy. In other words, the unity gain values of the luminance ratio B_f/B_d for Equation 4.5, of Merrifield and Silverstein, and the luminance ratio L_U/L_D, for Equation 5.19, are both equal to 4.2. To satisfy the compatibility relationships of Equations 4.16 and 4.17, the only way these two equations could evaluate to the same value of the luminance ratio, for a gain of unity, without causing a contradiction, is if the image contrast used by Merrifield and Silverstein was set to approximately unity during their experiment, and, in addition, for either or both of the 1.126 and 1.028 slopes of Equations 4.5 and 5.19, respectively, to be slightly in error.

The substitution of a contrast of unity into Equation 4.16 causes the logarithm of the contrast term to evaluate to zero. Consequently, for a contrast of unity, Equations 4.16 and 4.17 predict that the following equalities between the equation constants, $d = d'$ and $e = e'$, should be satisfied. Subject to the approximations made, it should, therefore, be possible to conclude that if no error had been introduced when the values of the constants in Equations 4.5 and 5.19 were derived from Figure 3.9, they should have been nominally equal to one another. The fact that these constants do not agree more closely cannot be explained with any degree of certainty using the available evidence. If Merrifield and Silverstein used the small inset to Figure 3.9 to determine the slope of their gain characteristic, rather than referring to the original reference[148] or to another source of the same information,[149] that provided the graph in an expanded size, then a small error in determining its value would be reasonable. However, this argument is just conjecture.

Merrifield and Silverstein elected to ignore the low luminance ratio portion of the characteristic shown in the inset to Figure 3.9. No direct mention of this choice was made in their article, however, experimental data points that validate the extrapolation of the high luminance ratio portion of the characteristic down to a gain of unity were presented in Figure 3 of that article. The validity of the decision to ignore this part of the characteristic is also confirmed by the data of Jainski described in Chapter 3, which shows that surround or panel luminance values from slightly greater than the display background luminance level down to the lowest measurable values of these luminances does not affect the required image difference luminance level.

To be able to make a direct comparison of the gains given by Equations 4.3, 4.12 and 5.21 with Equation 5.9, the independent variables of the equations need to be the same. The same logic used to relate the FFOV brightness to the surround field luminance, also applies for relating the induced veiling luminance to the surround field luminance. Even though the angular weighting function for veiling luminance is more complex than the angular weighting function used by Merrifield and Silverstein, the fact that the surround field luminance is constant allows it to be factored out of the integral over the pilot's forward field of view. This, as before,

causes the integral to evaluate to a constant multiplier, which in this case will be designated as k_V, a constant whose value is dependent on the total field of view encompassed by the solid angle integration limits, but for veiling luminance is further reduced by the small fraction of incident light scattered into the pilot's line of sight. Thus, whereas $k_B \approx 1$, the constant k_V can be expected to satisfy the inequality $k_V \ll 1$. Based on the preceding analogy, the expression relating the veiling luminance, L_V, and the surround field luminance, L_U, can be written as follows:

$$L_V = k_V L_U . \tag{5.22}$$

Substituting the value L_U, given by this equation, into Equation 5.18, and then using the law of logarithms for division, allows Equation 5.18 to be expressed in the following equivalent forms:

$$G' = d'' - e' \log k_V + e' \log \frac{L_V}{L_D} \tag{5.23}$$

$$G' = d''' + e' \log \frac{L_V}{L_D} . \tag{5.24}$$

Comparing this equivalent form of the Merrifield and Silverstein gain equation to the general control law equation for gain, given by Equation 5.9, shows that the functional dependences of gain, on the independent variable luminance ratio L_V / L_D, for these two equations, are fundamentally different from one another, even though the independent variables of the original gain equations, subject to the experimental conditions they were used to model, are directly proportional.

In spite of the differences in the functional dependences of the two gain equations, both predict increasing gain compensations, G and G', as the ratio between the FFOV luminance, veiling luminance or surround field luminance and the display background luminance increases. Due to the unknowns involved in determining the values of the previously introduced proportionality constants, making an objective numerical comparison of the predictions of the gain equations is not possible. By taking some liberties in establishing comparison conditions, a subjective comparison of the functional dependence predictions of the equations is possible. Using Equation 4.5 of Merrifield and Silverstein and Equation 5.9 of the general legibility control law to make the gain comparison, with the exponent m set equal to the slope of the Merrifield and Silverstein legibility equation, $b = 0.276$, Equation 4.5 predicts a gain compensation of 2.55 for a luminance ratio, B_f / B_d, of 100 and Equation 5.9 predicts the same gain at a luminance ratio, L_V / L_D, of 29.71. Preserving the ratio between the B_f / B_d and the L_V / L_D luminance ratios, that is, 100/29.71 = 3.366 as the luminance ratio B_f / B_d is reduced, the comparable values of gain shown in Table 5.1 are obtained.

As expected, the comparison of the gains, G and G', in Table 5.1 shows they are not equal. Nonetheless, the values of the two gains are in relatively good agreement for B_f / B_d luminance ratios of 10 or more and even below this luminance ratio the maximum error is only 25%. The small size of the ratio between the B_f / B_d and the L_V / L_D luminance ratios, 3.366, in Table 5.1 is attributed to the dependence of the Merrifield and Silverstein gain compensation equation, through its B_f / B_d luminance ratio, on the contrast of the display image under test. As previously described in Chapter 4, the image difference luminance relationship, $B_d = C L_D$, in the denominator of the gain compensation equation luminance ratio causes the gain predicted by the equation to be dependent on the contrast of the imagery presented on the specific display being controlled by the ABC.

The point of the preceding comparison is that in spite of the two gain functions being mathematically different from one another, for practical purposes they can be evaluated to provide gain values that are nominally numerically equivalent to one another in their ability to compensate for the veiling luminance induced by an exposure to a glare source. Because the respective luminance ratios of the two gain equations were shown above to be directly proportional, the comparison of Table 5.1 makes it possible to conclude that the general control law gain compensation versus luminance ratio results, predicted by Equation 5.9, are in good agreement with the gain compensation versus luminance ratio results of the Merrifield and Silverstein gain

Table 5.1. Comparison of Gain Compensation Using Equations 4.5 and 5.9.

G	B_f/B_d	G'	L_V/L_D
2.550	100	2.550	29.71
2.300	60	2.248	17.83
1.961	30	1.883	8.913
1.698	17.5	1.655	5.199
1.424	10	1.463	2.971
1.174	6	1.326	1.783
1.0	4.2	1.251	1.248
1.0	3	1.192	0.891
1.0	1.75	1.123	0.520
1.0	1	1.074	0.297
1.0	0.1	1.008	0.0297

compensation equation, Equation 4.3. Owing to the previously cited lack of objective information concerning the gain comparison, the most definitive claim of equivalence that can be made for the two gain equations is to say that, under the right conditions, the general control law gain equation can produce nominally equivalent results to the Merrifield and Silverstein gain compensation equation, or vice versa.

5.3. Human Visual System Control over the Legibility of Perceived Visual Scenes

Before proceeding with a discussion of the general legibility control law, a description of the innate legibility control mechanisms of the human visual system used to provide "natural" control over the legibility of perceived visual scenes, including the electronic and conventional aircraft cockpit displays contained in those scenes, would be beneficial. In the present chapter, Equation 5.1, the image difference luminance requirements equation described in Chapter 3, takes on the added significance of serving as a constant legibility requirements control law, and also provides a rational foundation for introducing and discussing the topic of natural legibility control. In particular, the expression of the image difference luminance requirements equation, in the form given by Equation 3.182, which is repeated here for convenience as follows:

$$\Delta L_P(C) = 1.30C\,(L_D + L_V)^{0.920} + 0.0193\,N_L\,C\,, \tag{5.25}$$

provides a foundation for describing a form of automatic legibility control inherent to the operation of the human visual system. The contrast requirement, C, is included in the perceived image difference luminance control term, $\Delta L_P(C)$, to show the equation's dependence on the type of imagery being portrayed.

Previous descriptions of the image difference luminance requirements equation, as expressed by Equation 5.25, emphasized its origin in threshold image difference luminance requirements and its extension to cover effects of maintaining constant display legibility in changing ambient illumination conditions for super-threshold image contrasts. This was adequate for the intended purpose of describing the application of the automatic legibility control equation to higher contrast electronic display imagery, but the description neglected to mention the practical constraints imposed by the human visual system on the benefits that can be derived

from continued increases in the contrasts of electronic display pictures. The limitation on the benefits of using high contrasts is due to a form of automatic legibility control that is an inherent part of the operation of the human visual system, provided that the correct conditions to make it operative are satisfied. A direct practical consequence of this feature of vision is a natural imposition of a saturation limit, on the legibility improvements possible with any type of display, as the contrast of the information portrayed is increased, with respect to the reflected background luminance of the display. Another consequence of this feature of vision, is that when the contrast of the information portrayed on a display exceeds this legibility saturation limit, no other form of active control, whether manual or automatic, is needed.

To be able to explain the natural legibility control capability of the human visual system, it is first necessary to provide historic information as a background, for use in conveying an understanding of the legibility of displayed information, in both subjective and objective terms, and to introduce metrics and techniques that permit characterizing the legibility of information portrayed on displays, to serve as both a qualitative and quantitative framework for describing this subject. The initial subsection below endeavors to establish the practical significance of the legibility of information, as experienced by aircrew members viewing electronic displays in aircraft cockpits, through a description of the adequacy of the legibility requirements applied to current and past aircraft displays, and through comparisons with the legibility requirements of commercial television and conventional aircraft displays. This is done by relating the maximum contrast levels of displayed picture grey scale information in both historical and automatic legibility control contexts. In the second subsection, a distinction is made between the absolute and the relative luminance and contrast levels in a display picture. Based on this distinction, a technique for representing the legibility of monochrome and color display information, from the perspective of the relative luminance levels present in display pictures, and the luminance dynamic range capability of the electronic display, is considered. Following this, the characterization of color and grey shade perception using the Munsell System, which also uses relative luminance levels to express the human's perceptual requirements, is discussed in the third subsection. To provide a basis for considering the extent to which human legibility requirements can be satisfied using electronic displays, human perceptual capabilities and display image rendition capabilities are considered in the fourth subsection. As a follow-up to this topic, the fifth subsection introduces and explains the practical constraints on the ability of aircrew members to perceive grey shades present either in real-world scenes or as rendered by electronic displays. Based on the human's perceptual capabilities, the sixth subsection tries to describe and provide a means to characterize the image rendition requirements needed for the presentation of real-world scenes as sensor-video information portrayals on electronic displays, in the context of the viewing environments experienced in aircraft cockpits. Using the previous information on human capabilities and limitations, the constant legibility control capability associated with the human visual system is presented in the seventh subsection. In the eighth and final subsection, this capability is then interpreted in terms of the extension of the human's perceptible grey scale range, through the spatially selective adaptation capability of the eyes' light receptors.

5.3.1. Historic Context for Considering the Adequacy of Aircraft Display Legibility

As previously described in Section 3.9, the contrast, C, in the constant legibility image difference luminance requirements equation of Equation 5.25, defines a family of constant legibility requirements characteristics, where minimum values of the contrast term in this equation are specified in Table 3.14 for different types of display information. Because the substitutions, of these minimum values of contrast, cause this equation to define the minimum constant legibility characteristics, for each type of information to be displayed, the resulting portrayals, while adequate to convey the information to the pilot, are not likely to impart a legibility to the display presentations that a pilot would prefer, if given a choice. For example, on a video display having a luminance dynamic range that can depict only six $\sqrt{2}$ grey shades, that is, for the minimum high ambient contrast of $C = 4.66$ that pilots have judged to be minimally acceptable under worst case ambient illumination conditions, the grey scale in the resulting picture depicted by the display would be perceived as compressed (i.e., can be read only with difficulty) and, if color encoded, the picture colors depicted would also be perceived as desaturated. The only benefit of constant legibility control, in this instance, is that the

appearance of the information presented on electronic displays would remain unchanged, as the levels of the background luminance reflected from the display and the veiling luminance induced in the pilot's eyes increases and decreases, because of the compensation of the image difference luminance levels of the displays by the automatic legibility control, in response to its light sensor inputs.

Increasing the number of $\sqrt{2}$ grey shades used to display video information from six to eight, that is, to a contrast of $C = 10.31$, which is the minimum luminance dynamic range preferred by pilots and is also the minimum required for all but the "worst case ambient conditions" by Table 3.14, would expand the separation between actual picture grey shades and provide more saturated colors. This increase in the luminance dynamic range of the picture being presented would also make the display subjectively more acceptable to the pilot, but still falls short of the previously calculated, white on black, contrast of $C = 22$, for conventional electromechanical display information formats, and the minimum contrast of $C = 29$ (i.e., a maximum to minimum range of screen luminances of 30) considered necessary by the National Association of Broadcasters to assure that commercial color television pictures will be subjectively pleasing to a viewer.[150]

Due to the image difference luminance limitations of existing light emissive and light transmissive mode electronic display technologies, achieving the higher picture contrasts, cited above for worst case ambient illumination and glare source viewing conditions experienced by aircrew members in aircraft cockpits, is not feasible at this time. It follows from these limitations, on the ability to display of information legibly, that none of the methods used to control the image difference luminance levels of these displays can produce picture legibility that is entirely satisfactory to aircrew members, under all viewing conditions. To achieve display legibility performance, overall, which would be assessed as adequate by pilots and is also effective conveying information, throughout the range of viewing conditions experienced in aircraft cockpits, the limitations on the image difference luminances of existing aircraft cockpit displays make it necessary to consider tradeoffs among the different available control strategies, based on the task loading of pilots, their ability to perceive display information and the useful operating lifetimes of the displays. Since several factors that influence the choice of the best control strategy will not be introduced until later in this chapter, the discussion of this topic will be deferred, other than to outline some of the considerations involved.

Manual control of the image difference luminance outputs, of existing operational military aircraft cockpit cathode ray tube and color liquid crystal displays by the pilot, is, for example, at one extreme of the possible strategies for legibility control. This control approach permits existing aircraft cockpit displays to be operated at their maximum luminance, under daylight viewing conditions, or, alternatively, imposes a requirement for active manual dimming control of the displays, to maintain the pilot's personal preferences or needs for legibility, as ambient illumination and glare source viewing conditions change over time.

At the opposite extreme of legibility control strategies, an automatic legibility control would permit a pilot to manually trim adjust a display to follow the eight grey shade, 10.3 contrast, constant legibility requirements characteristic of the earlier example, in response to the combined effects of changes in the background and veiling luminance. This strategy eliminates the need for the pilot to control the display actively, but the display would still experience the same fundamental image difference luminance limitation. For increasing ambient illumination conditions, the constant legibility characteristic would be followed until the display reaches its maximum saturated or design limited image difference luminance output. At still higher combinations of display background and veiling luminance, up to the maximum illumination conditions experienced in a cockpit, the imagery would be presented at the maximum image difference luminance limit imposed by the display, and the legibility of the imagery would continue to decrease.

Up to the point where the technology used to implement an electronic display limits its legibility, an automatic legibility control can be configured to allow aircrew member's to select different constant legibility characteristics in accordance with their personal preference for the legibility of a particular display presentation, rather than the minimum preferred contrast example chosen above. Independent of how an electronic display is controlled, it is still required to support a minimum six $\sqrt{2}$ grey shade video presentation under worst case viewing conditions, when aircraft cockpit displays are typically at their minimum level of legibility. These and

other display legibility control strategies are considered in the next section of this chapter and, in greater detail, in Chapter 7.

5.3.2. Quantifying Electronic Display Picture Legibility in Terms of Relative Luminance

Before proceeding with a description of the perceptual capabilities of the human visual system, it is useful to emphasize a distinction between the following: (1) the absolute contrast of symbolic or pictorial elements of a display information presentation format, with respect to the luminance reflected from the display's surface; and (2) the relative contrasts that exist between the symbolic, or pictorial elements, within a display picture. This distinction is probably most clearly indicated by the previously introduced equation for color transmissive mode liquid crystal displays, Equation 4.20, which, after modifying its terminology to suit the needs of the present description, can be expressed by the following general equation:

$$\Delta L_p(Y) = \Delta L_p(Y, x_p, y_p) = Y(x_p, y_p)\, \Delta L_p(C)\,. \tag{5.26}$$

The minimum required backlight image difference luminance, $\Delta L_p(C)$, that must emanate from the viewing surface of a display to make display information, with a minimum absolute contrast requirement, C, legible in any particular viewing environment is given by Equation 5.25. This absolute image difference luminance corresponds to the maximum luminance, capable of being depicted in a picture portrayed by an electronic display (i.e., the highlight white light emissions, from a color display picture, or the highlight single color light emissions, from a monochrome display picture), and, in combination with the relative luminance independent variable, $Y(x_p, y_p)$, sets the absolute image difference luminance, $\Delta L_p(Y)$, of each pixel on the display, where (x_p, y_p) are the display surface coordinates of each pixel in the display surface. With the relative luminance of each pixel and the highlight image difference luminance level of the display specified, Equation 5.26 establishes the composite legibility of the complete picture portrayal.

Video signals, encoded with the grey shade and chromaticity information needed to assemble a complete picture frame of information, are transmitted to the display by its image generation computer. When decoded, these signals provide the relative luminance levels, $Y(x_p, y_p)$, and, if required, the chromaticity coordinate pairs, (x, y) or (u, v), that are to be displayed at each of the display surface monochrome or color pixel coordinate locations (x_p, y_p). In other words the fixed fractional values, of the relative luminance levels, $Y(x_p, y_p)$, of each picture element on the display surface, convey the fixed information content of a display picture frame, and the value of the highlight image difference luminance, $\Delta L_p(C)$, determines the legibility of that information when depicted on the display in different ambient illumination and glare source viewing environments.

For a transmissive mode color liquid crystal displays, $Y(x_p, y_p)$ values range from unity, for the white highlight luminance, to a low but finite fractional value corresponding to the lowest "off" grey shade level of the display pixels. This "off" state light leakage, which cannot be electronically controlled, would be expected to be present for any transmissive mode display panel. For liquid crystal display panels, capable of producing sufficiently low light transmittance values, the light leakage could in concept be so low in the relative luminance range that it becomes imperceptible. The "off" state light leakage of existing liquid crystal display panels is perceptible, when a blank screen is displayed, particularly when viewed from outside the design solid angle for viewing the display, but is neither noticeable nor sufficient to interfere with viewing the types of information currently presented on these displays in aircraft cockpits. A true "off" state on existing color LCDs can only be achieved with the display backlight turned off. It should be noted that light emissive operating mode displays can also be represented using Equation 5.26 with equal validity, however, such displays lack the clear physical separation between the mechanizations used by light transmissive mode displays to control the image difference luminance levels and the grey scale compositions of their pictures. Most light emissive displays do permit the $Y(x_p, y_p)$ values in Equation 5.26 to be controlled from unity to zero.

To aid in the conceptualization of the interactions between the display highlight image difference luminance and grey shade control variables, Equation 5.26 can be expressed using a slightly modified form of Equation 3.24, the equation previously introduced in Chapter 3 for perceived image contrast, as follows:

$$C_P = \frac{\Delta L_P(Y)}{L_D + L_V} = Y(x_p, y_p)\,\frac{\Delta L_P(C)}{L_D + L_V}, \tag{5.27}$$

where, as previously, $\Delta L_P(C)$ is given by Equation 5.25, the minimum absolute highlight image difference luminance level of the display needed to render the grey shades and chromaticities in the scene to be depicted. Equivalently, this equation can also be expressed as

$$C_P = Y(x_p, y_p)\, LDR_E(C), \tag{5.28}$$

where $LDR_E(C)$, given by the equation,

$$LDR_E(C) = \frac{\Delta L_P(C)}{L_D + L_V}, \tag{5.29}$$

is an abbreviation for the effective luminance dynamic range that a display must be able to produce to legibly render the relative luminance values, $Y(x_p, y_p)$, depicted by each of the display's picture elements, in the presence of the combined effects of the display background luminance and the veiling luminance induced when a glare source is illuminating the pilot's eyes. As indicated by Equation 5.28, the combination of the relative luminance values, for each pixel used to assemble a complete picture frame, with the magnitude of the effective luminance dynamic range of the display, determine the legibility of the information presented on the display.

Although the values of the effective luminance dynamic range term, $LDR_E(C)$, calculated from the highlight image difference luminance, $\Delta L_P(C)$, using Equation 5.29, and the relative luminances, $Y(x_p, y_p)$, of Equation 5.28, are controlled independently in practical display implementations, their values do need to be coordinated to achieve adequate legibility for each particular type of display information presentation. The incorporation of the maximum value of contrast that is to appear on a display, C, into the image difference luminance requirements equation in Section 3.9, as represented by Equation 5.25 in this section, allows this equation to be used to set the corresponding minimum highlight image difference luminance level needed to portray picture information having grey shade contrasts of up to the value of contrast stipulated in the equation legibly on a display. Values of $Y(x_p, y_p)$ between unity and zero then relate the absolute image difference luminances and contrasts of pixels, or of uniform images displayed at reduced grey shade levels with respect to the highlight image difference luminance and contrast, which must be rendered by the display, for any particular set of display reflected and veiling luminance viewing conditions. In general, the values of the maximum, or highlight, grey shade contrasts, C, used in Equation 5.25, and of the relative luminances, $Y(x_p, y_p)$, used in Equations 5.26 and 5.28, are interrelated, both being dependent on the complement of different types information to be depicted on a display. It is instructive to consider this relationship in terms of everyday experience when viewing real-world visual scenes. This will be done later in this section, after first considering the human's legibility response to colors and, consequently, to grey shades and chromaticities in greater detail.

It should be noted that in a completely general equation for the luminance dynamic range (LDR) of an electronic display, the range of highlight image difference luminances, ΔL_H, that a display is capable of modulating simultaneously with grey shades would appear in the numerator of the equation and the absolute luminance of the lowest controllable grey shade level of the display, that is, the luminance, L_0, corresponding to $Y(x_p, y_p) = 0$, would be in the denominator. Therefore, unlike the effective luminance dynamic range given by Equation 5.29, the luminance dynamic range characterization of an electronic display is customarily a specification of a display's image generation capabilities, carried out without regard to ambient light environments in which it could be used. Since this measure of the luminance dynamic range of an electronic display typically remains nominally fixed, when the highlight image difference luminance of the display is changed, increasing the brightness of the picture by increasing the value of ΔL_H also causes a directly proportional increase in the lowest controllable grey shade level of the display. Consequently, the absolute luminance of the lowest controllable grey shade level of a display, L_0, would usually not be equal to the reflected background luminance of the display, L_D.

In comparison to the general case for the luminance dynamic range (LDR) of an electronic display, just described, the perceptual luminance dynamic range, $LDR(C)$, of an electronic display, is obtained from Equation 5.29, when the veiling luminance is equal to zero. Making this substitution into Equation 5.29 leads to the following equation:

$$LDR(C) = \frac{\Delta L_P(C)}{L_D}. \tag{5.30}$$

As in the case of the effective luminance dynamic range, given by Equation 5.29, the perceptual luminance dynamic range, $LDR(C)$, given by Equation 5.30, is predicated on having highlight image difference luminance levels, $\Delta L_P(C)$, which are coordinated with the maximum grey shade image contrast, C, and the relative luminance range, that is to be portrayed by the display. Like the general equation for the luminance dynamic range of a display, Equation 5.30 is expressed entirely in terms of measurable physical properties of the display. This equation is a special case of the general luminance dynamic range equation. This special case is invoked when the highlight image difference luminance is controlled so that it satisfies the relationship, $\Delta L_H = \Delta L_P(C)$, in changing reflected background and veiling luminance conditions, that is, so that the maximum grey scale contrast, C, that the display is capable of modulating is matched to the range of relative luminance levels, $Y(x_p, y_p)$, to be depicted on the display. Under this special case, and where, as previously, $\Delta L_P(C)$ is given by Equation 5.25, the following background luminance relationships: $L_0 = L_D$, when veiling luminance is absent, or $L_0 = L_D + L_V$, when veiling luminance is present, would also be satisfied. The general case is discussed further in Section 5.3.6. Since Equation 5.30 does not include the effect of the veiling luminance, it fails to predict correctly the perceived luminance dynamic range, which is effective in making a display presentation legible.

If the display highlight image difference luminance, $\Delta L_H = \Delta L_P(C)$, in Equations 5.29 and 5.30, is not automatically compensated to a higher value when veiling luminance is induced in an aircrew member's eyes, that is, if a manual control is being used to adjust the display highlight image difference luminance, ΔL_H, rather than the automatic legibility control law of Equation 5.25, then the effective luminance dynamic range of the display would be reduced from the value given by Equation 5.30, when no glare is present. The effective luminance dynamic range that results when a glare source induced veiling luminance, L_V, is introduced into the pilot's field of view can therefore also be expressed in terms of Equation 5.30, the luminance dynamic range with no glare present, using following equation:

$$LDR_E(C) = \frac{L_D}{L_D + L_V} LDR(C). \tag{5.31}$$

Considering the effect of the introduction of veiling luminance into the aircrew's field of view, the highlight image difference luminance, $\Delta L_P(C)$, and, hence, the perceived luminance dynamic range of the display, $LDR(C)$, given by Equation 5.30, would have to be increased, either manually or by automatic legibility control, by the inverse of the luminance ratio in Equation 5.31 to be able to compensate the display picture so that it would appear as legible in the presence of a glare source exposure as it did formerly in the absence of such an exposure. Stated in another way, for the legibility of the display information to remain unchanged when glare is introduced into the pilot's field of view, it is required that the effective luminance dynamic range of the display, Equation 5.29, with glare present, be numerically equal to the original luminance dynamic range of the display, Equation 5.30, when no glare was present.

It should be noted that the luminance compensation ratio, described in the previous paragraph as accounting for the introduction of veiling luminance into the field of view, evaluates to $1 + L_V/L_D$. This ratio is therefore the same as the independent variable in the gain compensation equation for glare exposure, Equation 5.9, discussed earlier in this chapter, and is, moreover, intended to perform the same function, that is, to adjust the image difference luminance requirement for the presence of veiling luminance. Since the power dependence of the gain compensation relationship in Equation 5.9, when set to m = 0.926, is thought to be due to the effects of pupil area and retinal cone light receptor changes, in response to the veiling luminance exposure of the eyes, and because this factor was not considered during the formulation of the

luminance dynamic range equations, these results are considered reasonably consistent.

5.3.3. Munsell System Characterization of Color and Grey Shade Perception

The most accurate and complete system for characterizing colors perceptually is one developed by A. H. Munsell for standardizing color notation.[151] This system uses three variables Hue, Chroma and Value to characterize the reflective colors encountered in real-world viewing environments. A particularly useful feature of the Munsell Color system is that each of its variables is characterized in terms of equally perceptible steps. Furthermore, the Munsell color notation system Hue and Chroma variable pairs can be related to corresponding CIE chromaticity coordinates and the Value variable can be related to luminous reflectance or relative luminance, $Y_M(V)$, of the color using appropriate standard illumination test conditions. Table 5.2 relates the linear Munsell value scale's equally perceptible grey shade steps to the corresponding relative luminances or luminous reflectances, expressed in percent. The table appears at the end of Munsell's book on a page entitled "A Color Notation, Table of Luminous Reflectances for Munsell Values." This table, was adopted in 1943, by the Optical Society of America Subcommittee on Spacing of the Munsell Colors, to relate Munsell values of 10.0 down to 0.1, in 0.1 increment steps, to equivalent luminous reflectances of 102.57% down to 0.120%, respectively.

In Table 5.2, the luminous reflectance or relative luminance quantities are all expressed relative to the luminance reflected by a standard white magnesium oxide, MgO, reference surface. This surface is accorded a 100% reflectance but in absolute terms only has a reflectance of 97.5%. Because an actual physical surface with a 100% absolute luminance reflectance white surface is physically unrealizable, as is also true for a 0% luminous reflectance black surface, measurements of luminous reflectance and calibrations of luminance are typically characterized with respect to a realizable standard white reference surface, rather than directly as absolute quantities. Using this method of characterizing luminous reflectance causes the absolute luminous reflectance of 100% to correspond to a Munsell Value of 10.0, and to a luminance reflectance of 102.57%, which allows the MgO standard reference surface to assume a luminance reflectance of 100% at the practical top of the Munsell value scale. The rationale used to arrive at the preceding method for characterizing the Munsell value scale relationship to luminous reflectance or relative luminance is described below.

The luminance, $L_M(V)$, reflected by the opaque diffuse reflecting (i.e., Lambertian) surfaces of the Munsell value scale standard paint swatches, when uniformly illuminated by an incident ambient illuminance, E_A, can be expressed mathematically as follows:

$$L_M(V) = R(V)E_A, \tag{5.32}$$

where $R(V)$ is the absolute reflectance of the Munsell grey scale swatches of Munsell value, V. Multiplying the numerator and denominator of this equation by the same reference surface absolute reflectance, R_R, leaves the equation unchanged but allows it to be expressed in the following equivalent form:

$$L_M(V) = \left(\frac{R(V)}{R_R}\right)(R_R E_A) = Y_M(V)L_R. \tag{5.33}$$

This alternative form of Equation 5.32 shows that the luminance reflected by a grey scale swatch can, with equal validity, be expressed as the product of the luminous reflectance, or relative luminance term, $Y_M(V)$, defined as follows:

$$Y_M(V) \doteq \frac{R(V)}{R_R}, \tag{5.34}$$

and the reference luminance, L_R, reflected from a reference surface of absolute reflectance, R_R, where the reference luminance is defined as follows:

$$L_R \doteq R_R E_A. \tag{5.35}$$

A practical advantage of the formulation of the reflected luminance equation in Equation 5.33 is that errors are

Table 5.2. Munsell Value Scale.

Munsell Value V	Luminous Reflectance $Y_M(V)$ in %	Munsell Value V	Luminous Reflectance $Y_M(V)$ in %	Munsell Value V	Luminous Reflectance $Y_M(V)$ in %	Munsell Value V	Luminous Reflectance $Y_M(V)$ in %
0.0	.000						
.1	.120	2.6	4.964	5.1	20.68	7.6	52.30
.2	.237	2.7	5.332	5.2	21.62	7.7	53.94
.3	.352	2.8	5.720	5.3	22.58	7.8	55.63
.4	.467	2.9	6.128	5.4	23.57	7.9	57.35
.5	.581	3.0	6.555	5.5	24.58	8.0	59.10
.6	.699			5.6	25.62		
.7	.819	3.1	7.002	5.7	26.69	8.1	60.88
.8	.943	3.2	7.471	5.8	27.78	8.2	62.71
.9	1.074	3.3	7.960	5.9	28.90	8.3	64.57
1.0	1.210	3.4	8.471	6.0	30.05	8.4	66.46
		3.5	9.003			8.5	68.40
1.1	1.353	3.6	9.557	6.1	31.23	8.6	70.37
1.2	1.506	3.7	10.134	6.2	32.43	8.7	72.38
1.3	1.667	3.8	10.734	6.3	33.66	8.8	74.44
1.4	1.838	3.9	11.355	6.4	34.92	8.9	76.53
1.5	2.021	4.0	12.001	6.5	36.20	9.0	78.66
1.6	2.216			6.6	37.52		
1.7	2.422	4.1	12.66	6.7	38.86	9.1	80.84
1.8	2.642	4.2	13.35	6.8	40.23	9.2	83.07
1.9	2.877	4.3	14.07	6.9	41.63	9.3	85.33
2.0	3.126	4.4	14.81	7.0	43.06	9.4	87.65
		4.5	15.57			9.5	90.01
2.1	3.391	4.6	16.37	7.1	44.52	9.6	92.42
2.2	3.671	4.7	17.18	7.2	46.02	9.7	94.88
2.3	3.968	4.8	18.02	7.3	47.54	9.8	97.39
2.4	4.282	4.9	18.88	7.4	49.09	9.9	99.95
2.5	4.614	5.0	19.77	7.5	50.68	10.0	102.57

Note: $Y = 1.2219V - 0.23111V^2 + 0.23951V^3 - 0.021009V^4 + 0.0008404V^5$, where V is the Munsell Value.
Reference: Newhall, S. M., D. Nickerson, and D. B. Judd, "Final Report of the O.S.A. Subcommittee on Spacing of the Munsell Colors", Journal of Optical Society of America, Vol. 33, No. 7, July 1943, pp. 385-418.

reduced and the relative luminance, $Y_M(V)$, is more easily determined when the luminance, $L_M(V)$, reflected from a Munsell color swatch or real-world diffuse reflecting surface, and the reference luminance, L_R, reflected

from a reference surface, can be directly compared through measurements made using the same uniform source of illuminance.

The reference reflectance, chosen by the Optical Society of America Subcommittee on Spacing of the Munsell Colors to define the Munsell value scale, was a white MgO surface of absolute reflectance $R_R = 97.5\%$. This choice for a white reference surface provides a reproducible high absolute reflectance surface, which permits paints, dyes and colors found in nature to be expressed as fractional values, or as percentages, through convenient comparative measurements with respect to the reference luminance reflected by its white standard surface. Substituting the absolute reflectance of $R(V = 10.0) = 100\%$, corresponding to a Munsell value of $V = 10.0$, into Equation 5.34, together with the reference reflectance of $R_R = 97.5\%$, yields the previously described luminous reflectance of $Y_M(V = 10.0) = 102.57\%$ at the top of the Munsell value scale.

Using grey shades, conforming to the original 1915 Munsell value scale, Munsell, Sloan and Godlove[152] showed through experiment that the human's perception of a reflective grey scale remains invariant, as a function of the incident ambient illuminance, in the range from 10,000 down to 22.8 fc. This result is very important since it shows that if the same relative luminance level relationship is maintained between the colors in a picture, as the overall absolute luminance level of the picture changes, then, except for changes in brightness, the picture appearance remains perceptually invariant for picture highlight reflected luminance levels in the range from 10,000 down to 22.8 fL, that is, for the vast majority of daylight viewing conditions. No experimental grey scale perception data, comparable to that of Munsell, Sloan and Godlove, was found for lower levels of daylight, dusk or night viewing conditions that occur for picture highlight luminance levels below 22.8 fL.

The characterization of the Munsell value scale in terms of the relative luminance, $Y_M(V)$, permits a correct representation of the observable fact that a grey scale chart, when exposed to a changing photopic illuminance level, remains invariant in its appearance, even though the absolute luminances reflected by each of the grey shade areas on the chart, $L_M(V)$, change in direct proportion to the incident illuminance, E_A, and the reflected reference luminance, L_R. Another equivalent method for describing the human's perception of a grey scale chart is to consider the relative luminance range of the grey scale as moving up and down an absolute luminance scale, in response to changes in the ambient illumination and reference luminance levels. This latter method of describing the human's grey scale perception capabilities emphasizes both the finite extent of the perceptible relative luminance range and the fact that maximum and minimum absolute grey shade luminance levels change as the relative luminance range moves with respect to the absolute luminance scale. It should be noted that the luminous reflectance of zero assigned in Table 5.2 to a Munsell value of zero ties the lower end of the Munsell value scale to an absolute luminance of zero, and is, therefore, inconsistent with the observed human perception of grey scales.

Although the Munsell color perception results were characterized using light reflective mode media, these results apply, with equal validity, to the light emanated by light emissive, transmissive and transflective mode displays and to any other information presentation techniques that produce the same luminance levels as measured at the eyes. As described previously near the beginning of Chapter 3, the human's perception of light depends solely on the spatial, spectral and temporal distributions of the light entering the eyes and not on how it was generated and/or modulated before reaching the eyes. It can therefore be concluded that the Munsell color perception results for grey shades and chromaticities are fundamental human color perception relationships, which can be interpreted in the context of any display operating mode, provided that the light emanating from the reflective media and the viewing conditions applicable to the Munsell results can be matched using the alternative display techniques.

It should be noted that the small differences between the 1915, and the latest 1943 version of the Munsell value scale, involve the luminous reflectances assigned to the equally perceptible grey shade step Munsell value scale. These differences have been attributed to a change from using a white to a standard medium grey background, having Munsell value of five and a nominally 20% luminous reflectance, when visually comparing color swatches.[153] Much of the preceding information, and also the information that follows, on grey scales and

the perception of grey shades, is base[d] [o]n an earlier investigation and analysis of the subject in the 1980s.[154] [155] The inform[a]tion o[n] color percep[tion] [a]nd the Munsell System for specifying color, is covered in greater detail in a 1984 article [a]nd its referer[nces].[156]

5.3.4. Comparison of Human Visual Perception and Display Image Rendition Capabilities

The purpose of this section is to compare human visual perception capabilities with the image rendition capabilities of electronic displays and to determine from this comparison realistic electronic display image rendition objectives. This information is needed to serve as a partial basis for understanding the control exercised by the human visual system over the legibility of perceived visual scenes, as is described in later subsections.

The gamut of brightnesses and colors that can be perceived by a human is much larger than the corresponding ranges of luminances, grey shades and chromaticities that can be accurately generated to render those brightnesses and colors using practical electronic displays, or, for that matter, using virtually any other type of information presentation technique. To render the brightnesses a human can perceive, using an electronic display, would require the control of the luminances, associated with the portrayal of a color picture grey scale range, from slightly less than 10^{-6} to somewhat greater than 10^{4} fL. To render the relative luminance or luminous reflectance perception range that Table 5.2 shows a human is capable of perceiving, simultaneously, on a grey shade encoded electronic display, would translate into having to satisfy a minimum luminance dynamic range of about 854 (i.e., (102.51 - 0.12)/0.12 = 853.75). In other words, a display would have to be able to generate controlled image difference luminance levels having grey shades, with image contrasts between them, of up to 854. While an absolute contrast of this magnitude, with respect to the background luminance reflected from the viewing surface of a display, is readily achieved by several existing electronic display technologies, at least under reduced daylight and night ambient illumination viewing conditions, available electronic displays are not designed to generate controllable relative luminance levels with contrasts, and hence luminance dynamic ranges, of this magnitude. Furthermore, and as previously described, the generation of either of these contrasts is not yet feasible, using any of the existing electronic display technologies, under worst case daylight ambient viewing conditions.

As is true for grey shade perception, the human's ability to perceive colors greatly exceeds the color image rendition capabilities of electronic displays. To enable an electronic display to make essentially full use of the pilot's chromaticity perception capabilities would require a significant change in the primary colors used by current electronic displays to generate color picture presentations. More specifically, the red, green and blue primary colors of an electronic display would have to be confined to narrow spectral bandwidth colors having chromaticity coordinates that are on, or very near to, the spectral color locus. In addition, the red and blue primaries would have to be near the opposite extremes of the visible light spectrum, and the green primary would have to be separated, into deep-green and yellow-green spectral primaries, to be able to generate mixed colors that encompass most but still not all of the human's chromaticity perception capability.

The principal advantage that would be offered by electronic displays, if they could meet, or nearly meet, the limits of the human's visual perception capabilities, is a significant increase in the number of colors, that is, the number of grey shades and particularly the number of different chromaticities, which could be assigned to present information, while tasks that utilize comparative and absolute color discrimination are being performed. Electronic map displays probably provide the best example, where an increase in the number of comparatively discriminable colors would benefit both the performance attainable by the aircrew using the color encoded presentations, and the clarity and comp[lex]ity of the information that is capable of being conveyed to the aircrew members. The ability to increase t[he] color separations between small sets of color encoded graphic symbols, characters and lines, on a variety [of] graphically generated display formats, would also lead to performance improvements, primarily through decreased instrument scan times.

An example of the advantage offered by absolute color discrimination would be the ability to depict aircrew

station signal indicator colors and brightness levels on electronic displays. To be effective for the presentation of warning, caution and advisory signals, a luminance dynamic range of nominally 100:1, or greater, would be probably be needed in each of the primary colors. In addition, the primary colors would probably have to include a spectral red of 625 nm wavelength or greater, to provide both Aviation and Identification Red, and a spectral yellow-green between 540 and 555 nm wavelength to mix with the red primary to obtain Aviation Yellow. A blue primary satisfying the chromaticity requirements of Aviation Blue would in concept be capable of being mixed with the aforementioned spectral green primary to produce Aviation Green, but a fourth spectral primary, preferably in the range of 505 to 515 nm, would be required to produce Identification Green.*

Fortunately, the realistic limits on the colors (i.e., grey shade and chromaticity combinations) that suffice to satisfy the human's visual perceptual needs for an accurate electronic display representation of typical sensed visual scenes, do not require the image rendition capability of the display to match the human's visual perception capabilities limits. Likewise, the colors used in computer-generated graphical information formats can be selected to satisfy most information presentation needs, while still complying with the color image rendition limitations of existing electronic displays. In this context, the practical limits on the Munsell values and chromas (i.e., color saturation or purity) that can be represented using reflective color swatches act as realistic upper and lower limits on the colors that are likely to be encountered in either natural or manmade settings.

Consistent with the practical limitations on the permanent materials, used to make the standardized reflective color swatches used in the Munsell Color System, the Munsell Neutral Value Scale, Matte Finish, 32-Step Scale includes 32 grey shades from a Munsell value of 9.5 to 1.75, in 0.5 value step increments. As a practical matter, this range of grey shades exceeds the range of grey shades associated with the reflective colors found in real-world scenes. Thus, to render the upper and lower limits of the Munsell value scale corresponding to the luminances reflected by practical real-world scene materials requires only the ability to render luminous reflectances, or relative luminances, in the range from 90% to 2.5%, instead of the full Munsell value scale. On this 32-step scale, the color name "white" has been experimentally associated with Munsell values, V, of 8.75 ($Y_M(V)$ = 73.4%) to 9.5 ($Y_M(V)$ = 90%), where 8.5 ($Y_M(V)$ = 68.4%) is associated with the transition from light gray to white, and the name "black" has been experimentally associated with Munsell values, V, of 1.75 ($Y_M(V)$ = 2.5%) to 2.25 ($Y_M(V)$ = 3.8%), where 2.5 ($Y_M(V)$ = 4.6%) is associated with that transition from dark gray to black.**

No easy method exists to relate the practical numerical limits on the chromas achievable using Munsell color swatches, which is comparable to the method cited above to describe the practical limits for the Munsell Value Scale. The problem describing the practical Munsell chroma scale limits is that, although the minimum chromas are easy to describe because they all correspond to chromas or excitation purities of zero and, therefore, are all coincident with the central Munsell neutral value axis, the maximum chroma limits change significantly as a function of the individual color hues. As an alternative, albeit subjective, means of comparing reduced chromas, which are acceptable in everyday experience, to the perceptual limits of human color vision capabilities, consider the color space defined by the red, green and blue primary colors specified by the NTSC (National Television Standard Committee) standard for color television receivers. These electronic displays produce color saturations (chromas) that consumer television viewers subjectively assess as satisfactory, yet the maximum color chroma limits, capable of being displayed, are of lower color purity than even the practical chroma limits achievable with Munsell color swatches. Existing aircraft cockpit color displays produce color saturations that are comparable to or slightly less saturated than those of television receivers that meet the NTSC standard.

The commonly accepted practical limits on the human's perception of luminous reflectances cover a

---

* Aviation and Identification Colors are specified in MIL-C-25050.

** Munsell Neutral Value Scale Matte Finish 32-Step Scale, 1970 Edition, Published by Munsell Color, Macbeth Division, Kollmorgen Corporation, 2441 N. Calvert Street, Baltimore, Maryland, 21218.

range from slightly greater than 100% down to the luminous reflectance of black velvet at 1%. Even this grey scale range exceeds the practical upper and lower limits described above for the nominal 90 to 3% luminous reflectance range encountered in both natural visual scenes and for most manmade objects. Consequently, sensor-video imagery sensed by a color television camera, for example, could be faithfully rendered using the 90 to 3% luminous reflectance range, rather than the entire range a human can perceive. The only evident shortcoming of this image rendition capability is that intense light sources within the visual scene, or computer generated aircrew station signals, would be rendered at the maximum relative luminance that the aircraft display can produce, rather than being faithfully rendered at a scaled value of the maximum image difference luminance output of these light sources.

As a final comparison of the uses of restricted grey scales, the Electronic Industries Association (EIA) Logarithmic and Linear Reflectance Charts employ two grey scales, each with nine grey shades, extending in opposite directions, from a luminous reflectance of 60% to 3%, and with a 1% black velvet swatch centered between the scales on the chart, to measure and adjust the grey shade rendition of television receivers and studio monitors. It should be noted, however, that this luminous reflectance test range is deceptive, owing to an ability to adjust the luminous reflectances, perceived to be associated with a grey scale range, when the grey scale is depicted on an electronic display. This perceptual capability will be further discussed in the next subsection.

5.3.5. Perception of Grey Shades on Electronic Displays

Home color television (TV) sets provide an easily confirmable example of the human's relative luminance and grey shade perception capabilities in operation. With the television turned "off," the viewing screen appears to be a medium to light-gray in color depending on the make and model of the TV. Matching the color to other grays exposed to the same illumination environment and measuring their reflected luminances, it would be found that they are about equal in luminance, suggesting that the display and its surroundings are part of the same spatial luminance adaptation region. Turning the television "on" produces a color picture with a relative luminance grey scale range, which has a minimum absolute luminance level that can be no less than the luminance reflected by the "off" display viewing surface that appeared grey before the TV was turned "on." In spite of this, a TV with a luminance dynamic range of about 30 produces a picture that appears to range from black to white, with corresponding Munsell Values between 2.0 and 9.5 and luminous reflectances (relative luminances) between 3% for black and 90% for white, respectively.

The example of the preceding paragraph makes two important points. The first point is that when the television is turned "on," it produces a perceived black on its viewing screen that replaces the previous gray appearance of the "off" screen and yet this occurs exclusively as the result of adding luminance to the existing reflected background luminance of the display's viewing screen. It can therefore be concluded that the perception of black in place of the gray of the "off" TV screen is due solely to the fact that a new relative luminance adaptation range has been established, by virtue of the human visual system's spatially selective adaptation to the higher absolute luminance levels of the relative luminance grey scale range being portrayed on the TV viewing screen. This ability by the eyes' light receptors to adapt, on a spatially selective basis, will be revisited later in this section in a slightly different, but perceptually equivalent, context. The second important point is that the selective adaptation of the eye's receptors to the TV picture portrayal does not perceptibly influence the appearance of the real-world visual environment surrounding the display.

The preceding example of using electronic displays to render television pictures, indirectly illustrates the fact that such displays can portray real-world imagery in a way that causes the observer to subjectively perceive the pictures rendered to be accurate reproductions of the real-world visual scenes they depict. Consistent with the limitations imposed by color television video signal encoding and the image rendition limitations of the displays, or of their image projection systems, if used, these displays can also provide accurate objective reproductions of the real-world visual scenes imaged on their viewing surfaces. As indicated above, to realize this perceptual result requires the television display be able to render a picture grey

shade range that the observer will interpret as luminous reflectances (relative luminances) between 3% for black and 90% for white. Some additional reasons why electronic display renderings of real-world visual scenes, or of graphic information formats, using less than the full range of a human's grey scale and chromaticity perception capabilities, suffice to provide display presentations that the viewer judges to be accurate reproductions of the original sensed visual scenes or adequate grey shade encoded graphics information depictions, respectively, are considered below.

At the low end of the relative luminance range, the differences between the 1% luminous reflectance of the black velvet swatch, located at the center of an Electronic Industries Association (EIA) Logarithmic Reflectance Chart, or for that matter the much lower 0.12% luminous reflectance, corresponding to a Munsell Value of 0.1 in Table 5.2, and the 3% luminous reflectance of the black end of each of the two grey scales on the EIA reflectance chart, are perceptible only as various gradations of black. Even though the spacings between these three black grey shades can be readily perceived, gradations of black are usually not particularly useful in electronic display presentations and, consequently, little is gained by rendering these black grey shades even if they were to be present in the sensed signal, at least for commercial television purposes. Conversely, pilots could derive some advantage by being able to perceive these black grey shades on military aircraft displays, where they could be used to show large dynamic range sensor-video signals, although alternative means, for achieving this objective, are described in Chapter 6 using displays with more restricted luminance dynamic ranges.

To be able to predict the perceptual result of increasing the highlight image difference luminance, ΔL_H, of displayed imagery, under a fixed ambient illumination and veiling luminance viewing condition, a distinction must be made between two different information presentation possibilities, which could be invoked along with such an increase. One of the information presentation possibilities involves increasing the display's luminance dynamic range along with the increase in the overall highlight image difference luminance level of the display presentation. Invoking this option allows the range of relative luminance levels, $Y(x_p, y_p)$, that are available to portray a picture to be extended. The other information presentation possibility involves making no change in the luminance dynamic range of the picture portrayed, when the overall highlight image difference luminance level is increased. This option can result in increasing the overall highlight image difference luminance level, ΔL_H, above the minimum required highlight image difference luminance level, $\Delta L_p(C)$, needed to portray a display picture legibly, for a particular display reflected background luminance and veiling luminance viewing condition.

At the high end of the relative luminance range, light emissive and transmissive mode electronic displays can be designed to permit them to portray information at or excess of the 102.57% luminous reflectance limit of the Munsell value scale. The perceptual effects produced by electronic display imagery operated at the high end of this expanded relative luminance range depends on whether or not the full extent of the expanded grey scale range can actually be displayed. Under high ambient viewing conditions, the limitations on the maximum image difference luminance output capabilities of both emissive and transmissive electronic display technologies has the effect of severely restricting the grey shades and chromaticities that can be portrayed. Conversely, under night and lower level daylight ambient illumination viewing conditions, the expansion of the grey scale rendition range of electronic displays permits images to be displayed within video picture, or graphic, information formats, that aircrew members would perceive as light emissive sources, with no perceptible change in the remainder of the display format. Electronic displays possessing this image rendition capability would permit the incorporation of signal indications into electronic display presentation formats, having the requisite capability to attract the attention of aircrew members, by virtue of their higher relative, and absolute, image difference luminance levels in comparison to the other information being presented. This feature, along with the ability to present larger dynamic ranges of sensor-video information, would be the primary advantage gained by extending the relative luminance range of electronic displays used in aircraft cockpits.

The perceptual effects caused by either manually or automatically controlling electronic displays so that they operate at highlight image difference luminance levels, ΔL_H, higher than the $\Delta L_p(C)$ levels predicted by Equation 5.25, for any particular set of ambient illuminance and veiling luminance viewing conditions, and with

no change in the relative luminance levels of the picture grey shades, depend on the size of the display area activated. Electronic displays, operated as just described, cause each of the absolute image difference luminance levels of the grey shade encoded imagery portrayed to operate at proportionally higher levels than the corresponding minimum absolute image difference luminance levels required by Equation 5.26 to portray the grey shade encoded imagery legibly. For electronic display information formats having a small percentage of their surface areas operating at the high end of the relative luminance grey scale range, such as graphic symbols intended to depict aircrew station signals, for example, the small areas can be perceived as light emissive sources, if the remainder of the display format area is portrayed using imagery and background features operated at proportionately reduced relative luminance levels. Examples of this type of image presentation on television displays include pictures containing stars in a night sky, street lights in night settings, or depictions of fireworks. While the subjective impressions conveyed to a television viewer using this approach can be useful, they are not completely satisfactory even in subjective terms. For example, the muting of the luminances, and the desaturation of the chromaticities, of fireworks are quite evident when depicted on television displays. Attaining satisfactory objective performance results, would most often require an expansion of the luminance dynamic range of the electronic display, as described in the preceding paragraph. Due to the practical instantaneous limitations on the relative luminance range of vision, previously described, the amount by which the luminance dynamic range of television displays must be increased, to create accurate renditions of light sources in displayed pictures, are quite modest.

If the image difference luminance levels of the grey shades and chromaticities throughout an entire display picture format are concurrently shifted to higher levels, relative to the fixed reflected background luminance level of the display, L_D, with no change in the picture grey scale and luminance dynamic range, for example, by increasing the contrast, C, in Equation 5.25 to a higher level than is required to display a picture legibly using either a manual or automatic legibility control, the light receptors of the human visual system, used to view the display, simply readapt to the increased absolute luminance level of the display format. One perceptual effect, of this increase in the absolute luminance levels of the displayed picture grey shades and chromaticities, would be to cause the reflected background luminance of the display to become less perceptible and, for sufficient large increases in the highlight image difference luminance, would cause the reflected background luminance to become imperceptible. The important perceptual effect of this increase in the display's image difference luminance level is that the appearance of the grey shade and chromaticity encoded information being portrayed on the display remains essentially unchanged, except that the picture being displayed appears to increase in brightness. This lack of a perceptual response, beyond the increase in the brightness of the picture displayed, to increases in the display's highlight image difference luminance level once full legibility is achieved is discussed in greater detail in Section 5.3.7.

5.3.6. Image Rendition Requirements for Video Portrayals on Electronic Displays

To enable an electronic display to make essentially full use of the pilot's grey shade perception capabilities would require that the display be capable of achieving a luminance dynamic range (i.e., highlight white on black picture contrast) of greater than 100:1 with respect to the combination of the background luminances reflected from the display surfaces and the veiling luminance induced in the pilot's eyes by a glare source, under any viewing condition that can be experienced by an aircrew in an aircraft cockpit. However, as previously described, the accurate perception of grey shades, whether observed directly on a grey scale chart or as a part of a video picture portrayal of the grey scale chart imaged on an electronic display, does not require that the full grey scale range that a human is capable of perceiving to be displayed. To be accurately perceived, the precise range and spacing of grey shades (i.e., relative luminances), conveyed by the luminous reflectances in a grey scale chart, in a real-world scene or in a computer generated graphic presentation, need to be faithfully reproduced by an electronic display. Stated in objective terms, an electronic display viewing surface must be capable of providing a faithful rendition (i.e., a linear transformation) of the portion of the Munsell color space needed to characterize the sensed color scene, or computer-generated information, if the colors (i.e., Munsell values, hues and chromas) in the display presentation are to be perceived as accurate reproductions of the original colors. In this context, the primary advantage of the Munsell color space occurs

for the encoding of computer-generated display presentations, and in the event that sensor-video grey shade and chromaticity information, to be transmitted to the display, are to be digitally encoded. In this instance, the equally perceptible steps of the Munsell color space allow minimizing the number of samples of grey shades and chromaticities required to accurately render sensed color scenes or computer generated information. This subject is discussed further in Chapter 7.

An accurate sensor-video rendition of the Munsell Neutral Value Scale, the EIA Logarithmic Reflectance Chart or of any alternative white to black grey scale on a reflective or transflective mode electronic display, can be created using two different approaches. The first approach involves a replication of the natural reflectances of real-world scenes, or of standard reflectance charts, using the display viewing surface media. In this case, the electronic display would have to be able to depict an image of each of the grey scale swatches, at the same area-averaged absolute luminous reflectance values of the original grey shades on the respective charts. As an example of this display implementation requirement, if it were necessary to depict a white grey shade swatch, with a luminous reflectance of 90%, on a reflective or transflective mode electronic display, then the display viewing surface would have to be able to diffusely reflect 90% of the ambient illuminance incident on the display viewing surface, as measured relative to the previously described white 100% luminous reflectance reference surface. Practical implementations of reflective and transflective mode electronic displays have, to date, had great difficulty creating pixels, with high enough area-averaged luminous reflectances, to satisfy this image rendition requirement. The description of the second approach for the implementation of reflective and transflective mode electronic displays, involving the use of scaled luminous reflectances, is deferred until Section 5.3.8, where the principles it is based upon are described.

Light emissive and light transmissive operating mode displays both use control over their image difference luminance outputs to achieve an accurate sensor-video rendition of the grey shades and chromaticities depicted on their viewing surfaces. As previously mentioned, to accommodate the differences in the techniques used to implement these two display operating modes, namely, to account for the separation of the light modulation and luminance control mechanisms and the light leakage inherent to transmissive mode display surfaces, slight differences in the interpretation of grey scales produced are necessary. Light emissive and transmissive mode electronic displays, by virtue of the direct ability to control their highlight image difference luminance values, offer greater control flexibility over the legibility of their picture portrayals, than do light reflective and transflective mode electronic displays, but, to achieve optimal objective effectiveness of the information transferred to the user by the displays, the image renditions and luminances of the pictures portrayed on these displays must be carefully controlled.

The ability to control the image difference luminance of light emissive and transmissive mode displays, and, hence, the absolute contrasts of their grey shade encoded pictures, independent of the ambient illumination incident on the display is the fundamental difference between light emissive and transmissive mode displays and their reflective and transflective mode counterparts. Optimal renditions of real-world and computer generated colors is achieved on light emissive and transmissive operating mode displays, when the displays are controlled to emulate accurately the relative luminances of the real-world scenes or computer generated pictorial information that the displays are intended to portray, while using an absolute highlight image difference luminance level that is sufficient to make the range of colors, in the display picture, legible when superimposed on the display's background luminance. In other words, the chromaticities, the luminous reflectances, and the effect of the illumination present in the real-world scenes, to be rendered in the display presentation, must be accurately emulated by the chromaticities, grey shades and the appropriately scaled image difference luminances, when depicted on light emissive and transmissive operating mode displays.

5.3.6.1. Relationships to Replicate Real-World Scenes in Electronic Display Pictures

For any arbitrarily selected choice of the Munsell Value, V, Equation 5.33 defines the corresponding Munsell absolute luminance level, $L_M(V)$, as the product of the Munsell value scale relative luminance, $Y_M(V)$, from Table 5.2, and reference luminance, L_R. As indicated by Equation 5.35, the value reference luminance

is completely determined by the ambient illuminance incident on the real-world scene to be imaged on a display, by virtue of the fixed reflectance of the white reference standard surface. Likewise the relative luminances, given by Equation 5.34, are completely determined by the Munsell Value of the color to be displayed because of the fixed relationship between the Munsell values and their corresponding luminous reflectances, as specified in Table 5.2. In other words, once the ambient illumination viewing condition is known, the Munsell absolute luminance levels, $L_M(V)$, of all of the colors in a real-world scene can be completely and uniquely specified using measurable Munsell color space descriptive variables. This grey shade and chromaticity descriptive approach is also directly applicable to the previously described implementation of light reflective and light transflective operating mode electronic displays.

To achieve a match between the portion of the Munsell value scale contained in a real-world scene, on a level per level basis, to the reproduced grey scale encoded picture of the scene depicted on emissive or transmissive operating mode electronic displays, requires that the displays' produce measurable display image luminance levels, $L_m(V)$, that are linearly scaled (i.e., attenuated or amplified) copies of the corresponding directly measurable Munsell luminance levels, $L_M(V)$, satisfying the following equation:

$$L_m(V) = k L_M(V), \tag{5.36}$$

where k is a linear luminance scaling multiplier constant, the value of which depends on the ambient illumination conditions present both when viewing the scene and the display. The total luminance, $L_m(V)$, of a grey shade on the electronic display is equal to the image difference luminance output for that grey shade, $\Delta L_P(V)$, added to the reflected background luminance of the display's viewing surface, L_D. In the real-world scene, the luminance level, $L_M(V)$, corresponding to the Munsell value. V, to be rendered on the electronic display can also be expressed as shown in Equation 5.33. Making these substitutions into Equation 5.36, produces the following grey shade requirement equation:

$$\Delta L_P(V) + L_D = k\, Y_M(V) L_R. \tag{5.37}$$

This equation is entirely general, and when satisfied should produce grey shades on the electronic display that are visually equivalent to those of equal Munsell value in real-world visual scenes.

The validity of Equation 5.37, for predicting the image difference luminance levels required to produce a faithful rendition of colors, as perceived by a user of an electronic display, is dependent on the relationships established between the display background luminance, L_D, and the Munsell value system independent variables, $Y_M(V)$ and L_R, and the linear scaling constant, k. As a practical matter, several additional conditions must be satisfied to enable Equation 5.37 to serve the intended purpose of producing a linear translation of a real-world scene, into a faithfully rendered picture of the real-world scene, on the electronic display's viewing surface. When the correct conditions are satisfied, this equation does permit a perceptual match between the grey scales of displayed pictures and the Munsell value scale representations of real-world scenes, on a value per value (i.e., grey shade per grey shade) basis, however, the equation does not usually cause the rendered picture to be perceived at the same brightness level as the real-world scene being rendered.

Although Equation 5.37 is mathematically quite straightforward, the equation is also quite complex. The complexity stems from the difficulty in physically interpreting and applying the equation, because virtually every term in the equation is an independent variable or a constant that can be assigned different values. As mentioned above, the relative luminance term, $Y_M(V)$, is determined by the real-world scene and the range of Munsell Values needed to render the scene, while the reference luminance, L_R, is determined by the ambient illuminance incident on the scene. Although, the linear luminance scaling constant, k, is in concept arbitrary, there are practical visual adaptation constraints on its magnitude.

On the other side of Equation 5.37, the magnitude of the display reflected background luminance, L_D, is unrelated to the reference luminance, L_R, applicable to the real-world scene, since it is determined by the combination of the diffuse and specular reflectances of a particular display's viewing surface, and by a combination of the ambient illuminance level incident on the display viewing surface and the luminance incident on the display surface, from a specular reflection angle, with respect to the pilot's line of sight, to the display

in the cockpit. For light emissive and transmissive operating mode displays, the image difference luminance, $\Delta L_P(V)$, which differs from the $\Delta L_P(Y)$ term used in Equation 3.26 only in its use of the Munsell Value, V, in place of the corresponding relative luminance, Y, is typically completely independent of the ambient illumination environment in which the display is situated, and, in general, depends only upon the highlight image difference luminance setting of the display.

The explanation of Equation 5.37 will start with a discussion of some of the previously mentioned conditions, on its application to individual displays. For each particular implementation of light emissive and light transmissive electronic displays, two fundamental relationships have to be established between the two sides of this equation. One of these is the relationship between the reflected background luminance of the electronic display viewing surface, L_D, and the minimum luminance of the real-world scene that is to be rendered on the electronic display viewing surface. The other relationship is between the display and real-world scene luminance dynamic ranges.

As mentioned above, different equally valid interpretations can be applied to Equation 5.37 for emissive and transmissive mode electronic displays. One interpretation of the equation assumes that the range of driven grey shade levels, $\Delta L_P(V)$, on emissive and transmissive mode electronic displays are unrestricted in the sense that while the driven levels are linearly translated replicas of the real-world scene relative luminance levels, $Y_M(V)\,L_R$, they are not directly coordinated with the background luminance reflected by the display viewing surface, L_D. This situation typically occurs when the display's highlight image difference luminance, ΔL_H, is manually controlled, however, aircrew initiated trim control adjustments to an automatic legibility control level $\Delta L_P(C)$, described in Section 5.5 and Chapter 7, can cause the same results.

As an example, assume that the highlight image difference luminance level of the electronic display, ΔL_H, is initially set to the lowest level, capable of providing a faithful rendition of the real-world scene it is being used to portray, for the ambient illumination present at the time, $\Delta L_P(C)$. This setting is the same as the one described previously in Section 5.3.2 that caused the display luminance dynamic range to satisfy Equation 5.30. If the highlight image difference luminance level setting of the display is then increased, to a higher level than $\Delta L_P(C)$, this would shift the grey scale modulation range that the display capable of rendering, and the luminance dynamic range it is capable of modulating, to proportionately higher absolute luminance levels. Doing this, does not change the relative luminance spacings between grey shades, but, because the display reflected background luminance remains unchanged, it causes an increase the relative luminance spacing between the lowest driven grey shade and the reflected background luminance of the display.

Although increases in a display's highlight image difference luminance, ΔL_H, above the minimum level, $\Delta L_P(C)$, needed to portray imagery having up to a maximum contrast of C legibly, with no change in the ambient illuminance or veiling luminance conditions, do alter the relative luminance relationship between the display's grey scale range and the fixed display reflected background luminance, the increases do not cause the luminance dynamic range to change in magnitude. An explanation for the visual effects described in the last subsection, in association with increases in a display's highlight image difference luminance, is that the correspondence between the display reflected background luminance, L_D, and the lowest relative luminance level being rendered in the real-world scene, that is, $Y_M(V_{min})\,L_R$, from the right-hand side of Equation 5.37, is responsible for the picture brightness attribute, of low image difference luminance electronic displays. The rationale used to reach this conclusion follows. As the display highlight image difference luminance, ΔL_H, increases, the higher absolute image difference luminance levels of the displayed picture cause it to be perceived as becoming progressively brighter. This increase in the absolute image difference luminance and brightness of a displayed picture cause the background of the display to appear to the viewer in progressively deeper shades of black. Because the relative luminance relationships in the displayed picture do not change, when its luminance is increased, the luminance increase is interpreted by the human visual system, in relationship to the fixed relative luminance range of vision described by the Munsell system, as an expansion of the grey scale range, caused by a reduction in the lowest grey shade level, that is, in the lowest displayed Munsell Value, which is perceptible on the Munsell relative luminance scale, rather than only as an increase in the picture brightness. Increasing the absolute image difference luminance and brightness of an electronic

display, depicting, for example, a picture of a real-world scene, therefore, causes the reflected background luminance level of the display to correspond to progressively to lower values of the minimum Munsell Value, V_{min}, on the Munsell luminous reflectance scale.

If in the preceding example the display highlight image difference luminance, ΔL_H, is set to levels lower than $\Delta L_P(C)$, instead of being increased, this causes the displayed grey scale to shift to a lower absolute luminance range. In this case, however, because the display reflected background luminance level does not change, and because the resultant reduced individual grey shade luminance levels, $\Delta L_P(V)$, are added to the reflected background luminance level of the display, the electronic display's grey scale range is compressed. Because of this compression, the relative luminance spacing between adjacent grey shades is reduced throughout the grey scale range, the picture depicted by the display becomes less legible and the linear transfer of scene grey shades to the display picture, represented by Equation 5.37 can no longer be achieved without reducing the range of scene grey shades to be displayed. These relationships are considered further in Chapter 6.

In the other interpretation of Equation 5.37, it is assumed that electronic displays use the reflected background luminance, L_D, as their lowest "off" grey shade level and that this level is coordinated in a natural grey shade progression, with the higher image difference luminance levels, $\Delta L_P(V)$, of the driven display grey shades, by establishing and maintaining a correspondence to the lowest Munsell Value, V_{min}, in the real-world scene relative luminance levels, $Y_M(V_{min})\,L_R$, that are to be displayed. Relating the electronic display and Munsell grey scales in this way, produces a faithful rendition of real-world scene grey scale luminance levels, while using the smallest setting of the display highlight image difference luminance, $\Delta L_H = \Delta L_P(C)$, needed to provide a fully legible display picture presentation. For reasons that are described later in this section, little if any display legibility control advantage can be gained, by using the higher settings of the display image difference luminance levels, described in the preceding two paragraphs, although signal conditioning control techniques described in Chapter 6 provide a means of taking advantage of the ability to lower or increase the brightness of a displayed picture. It is the interpretation of Equation 5.37, described in this paragraph, that is employed in the balance of this report, unless otherwise stated.

Since, as previously described, the pictures presented on emissive and transmissive mode electronic displays are created by adding grey shade encoded image difference luminance levels, of the same or differing chromaticities, to the reflected background luminance level of the display viewing surface, the starting point for establishing a mathematical relationship between the two sides of Equation 3.37 corresponds to the condition on the electronic display where the perceived image difference luminance in is equal to zero, that is,

$$\Delta L_P(V = V_{min}) = 0\,, \tag{5.38}$$

and the electronic display luminance, $L_m(V)$, becomes equal to the display surface reflected background luminance, L_D. The corresponding luminance within the real-world scene is established by the minimum Munsell value, $V = V_{min}$, that has to be rendered on the electronic display. This minimum luminance level can therefore be represented by the scene luminance level, $L_M(V = V_{min})$. With the condition in Equation 5.38 satisfied, making the appropriate substitutions into Equation 5.37 yields the following general display background luminance requirements equation:

$$L_D = k\,L_M(V_{min}) = k\,Y_M(V_{min})\,L_R\,. \tag{5.39}$$

Solving this equation yields a general relationship for the linear luminance scaling constant, k, as follows:

$$k = \frac{L_D}{L_M(V_{min})} = \frac{L_D}{Y_M(V_{min})\,L_R}\,. \tag{5.40}$$

This equation expresses a variable relationship, which in an aircraft cockpit could change as a function of time, due, for example, to relative changes between the ambient illuminance levels incident upon the display and upon the scene, or as the result of mission dependent changes in the type of information a particular display depicts. The implementation of automatic legibility control would compensate for changes in the display viewing environment and methods for dealing with the other changes mentioned are described in Chapter 6.

Upon substituting the constant, k, from Equation 5.40 into Equation 5.37, the following modified version of the luminance requirements equation is obtained for matching the grey shades on an electronic display with those in the real-world scene being imaged:

$$\Delta L_P(V) + L_D = \frac{L_D}{L_M(V_{min})} Y_M(V) L_R = \frac{Y_M(V)}{Y_M(V_{min})} L_D . \tag{5.41}$$

This equation is valid for numerical magnitudes of the constant, k, that range from daylight viewing conditions, where the picture displayed is an attenuated version of the grey scale luminance levels present in the real-world scene, to night viewing conditions where the real-world scene as sensed by a low light level television camera or other type of night vision imaging system results in display picture luminance levels that are amplified versions of the sensed real-world scene. As a special case, for $k = 1$, the luminance levels of the display and of the real-world scene are matched to one another, for each luminance level displayed.

Owing to the use of the variable scaling factor in Equation 5.37 and 5.41, the relationship between the luminance dynamic ranges of the display picture and that of the real-world scene, that needs to be rendered by the display, is not self-evident. Equation 5.41 gives the displayed image difference luminance corresponding to each Munsell value in the real-world scene, as follows:

$$\Delta L_P(V) = \frac{Y_M(V)}{Y_M(V_{min})} L_D - L_D = \frac{Y_M(V) - Y_M(V_{min})}{Y_M(V_{min})} L_D . \tag{5.42}$$

Using Equation 5.30 for the display luminance dynamic range, but changing the independent variable nomenclature from the maximum contrast the display must portray to the maximum Munsell value grey shade, $V = V_{max}$, the display must portray, the luminance dynamic range of the real-world scene, as presented on the electronic display, LDR_D, can be expressed by the following equation:

$$LDR_D = \frac{\Delta L_P(V_{max})}{L_D} = \frac{Y_M(V_{max}) - Y_M(V_{min})}{Y_M(V_{min})} . \tag{5.43}$$

The luminance dynamic range of the scene before being rendered on the display, LDR_S, can be represented by the difference between the maximum Munsell value scene luminance, $L_M(V_{max})$, and the minimum Munsell value scene luminance, $L_M(V_{min})$, divided by the scene background luminance, which is the luminance corresponding to the lowest Munsell value grey shade, from the scene that is to be rendered on the display, that is, $L_M(V_{min})$, as follows:

$$LDR_S = \frac{L_M(V_{max}) - L_M(V_{min})}{L_M(V_{min})} = \frac{Y_M(V_{max})L_R - Y_M(V_{min})L_R}{Y_M(V_{min})L_R}$$

$$LDR_S = \frac{Y_M(V_{max}) - Y_M(V_{min})}{Y_M(V_{min})} . \tag{5.44}$$

This result shows that the perceived luminance dynamic range of the real-world scene depends only on the maximum and minimum luminous reflectances of the grey scale range contained in the scene, and does not depend on the magnitudes of the reference luminance levels that are present, due to the illumination that must be incident on the real-world scene to make it legible.

Comparing the luminance dynamic ranges from Equation 5.44 for the scene with that of Equation 5.43 for the rendition of the scene on the display shows they are equal to one another, that is,

$$LDR_D = LDR_S . \tag{5.45}$$

This finding demonstrates that the previously derived equations for the rendition of display pictures and visual scenes correctly predict the known grey shade requirements of the human visual system. More specifically, if the display rendition of a real-world scene is to be perceived as a faithful rendition of the scene itself, then their luminance dynamic ranges must be matched, since, as has been previously described, the human visual system is indifferent to the means used to generate the grey shades and depends only on the relationships

present in the light being sensed by the eyes.

5.3.6.2. Equating Munsell Value Scale and Electronic Display Relative Luminance Levels

Another important relationship that must be established relates to the faithful rendition of real-world grey shade levels on an electronic display presentation. Earlier in this section, Equation 5.26 was introduced to represent the image difference luminance of the grey shades rendered by each of the electronic display pixels, $\Delta L_P(Y)$, in terms of the relative luminance of each pixel, $Y(x_p, y_p)$, and the perceived image difference luminance, $\Delta L_P(C)$, needed to render faithfully the maximum highlight white (or another color in monochrome display presentations) grey shade in a real-world scene. For convenience, the equation is repeated here, as follows:

$$\Delta L_P(Y) = Y(x_p, y_p)\, \Delta L_P(C) \tag{5.26}$$

To make this equation consistent with the rendition of real-world grey shades on electronic displays, it remains to relate the terms in Equation 5.26 to the equations already developed that characterize such scenes using the Munsell luminous reflectances.

The definition of the perceived image difference luminance, $\Delta L_P(C)$, used in Equation 5.26, is the same as the definition of the perceived image difference luminance, $\Delta L_P(V_{max})$, used in Equation 5.43, to define the required display luminance dynamic range, LDR_D, in terms of Munsell luminous reflectances, that is,

$$\Delta L_P(C) = \Delta L_P(V_{max}). \tag{5.46}$$

Stated in another way, the only difference between these two perceived image difference luminance variables is the nomenclature, C and V_{max}, used to characterize the image difference luminance of the maximum grey shade to be displayed.

When Equation 5.26 was originally introduced, it was pointed out that the perceived image difference luminance, $\Delta L_P(C)$, could be substituted from Equation 5.25 to implement automatic legibility control of the grey shade luminances, $\Delta L_P(Y)$, of Equation 5.26, under changing reflected background and veiling luminance viewing conditions. In order for these equations to render a real-world scene faithfully, or any other particular type of information defined by the grey scale rendition limits of an electronic display, the minimum contrast, C (i.e., which has the same defining equations as do the luminance dynamic ranges given by Equations 5.30 and 5.43), is required to satisfy the following relationship:

$$C = \frac{\Delta L_P(C)}{L_D} = \frac{\Delta L_P(V_{max})}{L_D} = LDR(C) = LDR_D = LDR_S. \tag{5.47}$$

The other term in Equation 5.26 that has to be defined in relation to the Munsell characterization of a real-world scene is the relative luminance. As previously described in the subsection on relative luminance, $Y(x_p, y_p)$, which takes on values between zero and unity, can also be represented as $Y(V)$ by dropping the explicit reference to the location on the display surface of the pixel being addressed and by adding a reference to the Munsell value, V, represented by the relative luminance. By making appropriate substitutions of equivalent nomenclature in Equation 5.26, this equation can be expressed in the following form:

$$\Delta L_P(V) = Y(V)\, \Delta L_P(V_{max}). \tag{5.48}$$

Substituting for the two image difference luminance terms in this equation, using Equation 5.42, allows Equation 5.48 to be expressed in terms of the corresponding Munsell luminous reflectances, as follows:

$$\frac{Y_M(V) - Y_M(V_{min})}{Y_M(V_{min})} L_D = Y(V) \frac{Y_M(V_{max}) - Y_M(V_{min})}{Y_M(V_{min})} L_D. \tag{5.49}$$

Solving this equation for the relative luminances, $Y(V)$, of the electronic display depiction of the scene grey

shades, yields the following relationship between the display relative luminances and the scene relative luminances, as expressed in terms of the limiting values of the scene Munsell Value scale:

$$Y(V) = \frac{Y_M(V) - Y_M(V_{min})}{Y_M(V_{max}) - Y_M(V_{min})}. \quad (5.50)$$

This equation provides a means of translating relative luminance levels corresponding to Munsell Values in a real-world scene, $Y_M(V)$, into the relative luminance levels, $Y(V)$, compatible with the portrayal of the scene on emissive and transmissive electronic display viewing surfaces. Relative luminances determined using Equation 5.50 are also numerically compatible with the signal encoding typically associated with such displays. When the Munsell values of $V = V_{max}$ and $V = V_{min}$ are substituted into the $Y_M(V)$ term in this equation, the equation yields relative luminances of $Y(V_{max}) = 1$ and $Y(V_{min}) = 0$, respectively. The relative luminance, $Y(V)$, and the upper and lower limits on its range of magnitudes are therefore compatible with the intended usage of this variable in Equation 5.26, for controlling the grey shade image difference luminance levels in an electronic display picture presentation.

5.3.6.3. Electronic Display Image Rendition Requirement Conclusions

The preceding discussion of electronic display image rendition requirements was confined to establishing the legibility requirements for achieving a faithful rendition of real-world scenes having upper and lower Munsell value limits of $V = V_{max}$ and $V = V_{min}$, respectively, on the information in the scene that is to be displayed. Unlike the legibility levels described earlier in this report, where the intent was to determine the threshold of legibility needed to achieve a 99% plus accuracy of reading displayed information, or the higher legibility levels necessary to satisfy a pilot's minimum legibility requirements in an operational aircraft cockpit environment, the legibility level sought in this section is to meet the pilot's information presentation needs fully, a condition illustrated by using the faithful rendition of real-world scenes on electronic displays, as an example. To achieve this optimal level of legibility, through the faithful rendition of real-world scenes, having Munsell-Value-limit constrained image rendition requirements, it was determined that the image difference luminance levels of grey shades in an electronic display picture would have to satisfy Equation 5.26, with the relative luminance levels satisfying Equation 5.50 and the highlight image difference luminance being able to support a luminance dynamic range satisfying Equation 5.43.

It should be noted, that although the preceding discussions have been restricted to the rendition of real-world scenes that would be sensed and encoded for presentation on a display using a television camera, to aid in visualizing the relationships, the results obtained can be adapted for application to displayed renditions of radar, forward looking infrared, low light level television, night vision imaging systems or other types of sensor-video information.

5.3.7. Constant Legibility Control Capability of the Human Visual System

In an earlier example, a television display having luminance dynamic range of nominally 30, and depicting a picture with a grey scale perceptible as ranging from white to black, when the display is turned "on," was compared with the gray color appearance of its viewing screen, when the display was turned "off." If instead of simply turning the TV on, the luminance dynamic range of the TV had been slowly increased from zero, then the picture would initially be of low contrast. Under this condition, all of the grey shades spacings in the display presentation would be compressed by equal amounts throughout the picture's grey scale range. The resultant picture would then be perceived as having no blacks or whites, only darker and lighter shades of grey. A continued increase in the display luminance dynamic range would further expand the relative luminance range and simultaneously cause the spacing between picture grey shades to expand by an equal amount until the maximum and minimum grey shades in the picture become perceptible as a low brightness white and a high brightness black. This result is achieved for a maximum grey shade contrast or luminance dynamic range of about 10, the minimum wanted by pilots for aircraft display grey shade presentations. For luminance dynamic

ranges above 10 the display picture becomes subjectively more pleasing until the Munsell value range contained in the scene is faithfully rendered by the display, as specified in the previous subsection. Using a scene consisting of real-world reflected luminances, as an example, unless the scene to be displayed contains information encoded to represent luminous reflectance imagery lower than 3% or greater than 90%, little in the way of legibility improvement, in the imagery being rendered, is gained by increasing the luminance dynamic range of the display beyond, LDR(C) = 29. The ability to limit the luminance dynamic range to 29, for this example, occurs because the grey scale range and spacings of the portrayal of the real-world scene in the display picture match the human's objective requirements for accurate color (i.e., grey shade and chromaticity) perception, by virtue of satisfying the image rendition requirements of the real-world scene Munsell value scale.

Continuing the preceding example of an electronic display, which is intended to portray the information content of a real-world scene characterized by Munsell Values between 2.0 and 9.5 and having corresponding luminous reflectances between 3% for black and 90% for white, respectively, it can be concluded that further increases in the display highlight image difference luminance, ΔL_H, and the corresponding display luminance dynamic range, beyond the value of LDR(C) = 29, given by Equation 5.30 and 5.47, which is needed to render the real-world scene colors in the display picture optimally, would, as previously described, simply cause the eyes light receptors to adapt to the higher luminance levels contained in the picture. While the increased luminance of the picture with respect to the combined display reflected background and veiling luminance does cause the picture to be perceived correctly as increasing in brightness, the perception of the colors within the picture rendered by the display remains essentially invariant. The only known limitations on this ability by the human visual system to control legibility automatically, as a function of the magnitude of the luminance dynamic range, are imposed when image difference luminance levels are sufficiently in excess 10,000 fL to cause physical discomfort to the eyes, and when contrast levels become so large that they are sufficient to cause imperfections within the optical media of the eyes to produce perceptible visual artifacts. Although this visual system legibility control effect has been described in terms of increasing the display luminance in a constant viewing environment, its importance in aircraft cockpits is related to the legibility of emissive and transmissive mode displays during periods when the image difference luminance remains unchanged and the ambient illumination conditions in the cockpit are decreasing.

The invariance of the legibility of display image grey shade and color relationships, when depicted on displays using sufficiently high luminance dynamic ranges, is a feature of vision that has in the past and continues to play a very important role in gaining pilot acceptance for most types of light emissive and light transmissive mode aircraft cockpit displays. Historically, the electronic displays used in aircraft cockpits have been CRT displays or other light emissive display technologies including, for example, the light emitting diode data entry display used in the F-16, and incandescent filament alphanumeric readouts often used for the presentation of navigation coordinates, radio frequencies and so forth. More recently color active matrix liquid crystal displays, which depend on the transmissive operating mode, have been applied in increasing numbers to aircraft cockpit display applications. The advantage possessed by these display operating modes is that if they can be made sunlight readable, then the legibility of the displays is assured under any lower ambient illumination viewing condition, provided only that the display can be dimmed to the appropriate lower emitted luminance and contrast levels for night operation. The latter assertion is made because existing aircraft cockpit emissive or transmissive mode displays, set to portray graphics at a contrast of 3 in a 10,000 fc illuminance test environment, would produce a contrast of 30 in 1,000 fc, 300 in 100 fc, 3,000 in 10 fc, and so forth.

For sensor-video image presentations, the equalization of brightness between emissive and transmissive electronic displays, and the real-world scenes they depict, appears to occur for highlight image difference luminance levels somewhat higher than those needed to render real-world visual scenes faithfully, and, therefore, at levels well below the luminance dynamic range needed to encounter the limits of the human's grey scale perception capabilities. The luminance dynamic range (i.e., minimum contrast) thresholds, necessary to initiate this form of human automatic legibility control, for the low grey shade rendition requirements of numeric, alphanumeric and graphic presentations, is not known with any degree of precision. Like the full grey shade sensor-video image presentations, the thresholds, for an invariant appearance of these lower contrast requirement display presentations, are related to matching or exceeding the luminance dynamic range required

to render the displayed colors accurately, at their scaled Munsell luminous reflectance values on the display's viewing surface. This luminance dynamic range is consistent with the level needed to cause the backgrounds of these display presentations to be perceived as black under high ambient incident illuminance viewing conditions, and the luminance dynamic ranges are, consequently, much higher than the levels required to make the display information legible at the minimum levels, specified by MIL-L-85762 and presented in Section 3.9.

The perceived brightness of light emissive and light transmissive operating mode electronic display pictures can be made to appear the same as those of real-world scenes by causing the effective display luminance dynamic range given by Equation 5.29, to match or exceed the level needed to achieve a faithful image rendition of the real-world scene. No experiments were found in the literature, which systematically investigated or even explicitly recognized the existence of this spatially selective adaptation effect. This topic is discussed further near the end of the next subsection.

5.3.8. Extension of Perceptible Grey Scale Range Through Spatially Selective Adaptation

Although the experimentally derived Munsell value scale shows that the human's ability to perceive grey shades on a display, or in a particular area of a visual scene, is limited to a nominal relative luminance range of 100:1, an ability by the light receptors in the pilot's eyes to adapt simultaneously, on a spatially selective basis, to light received from different areas of the field of view, greatly extends this range. The practical effect of this spatially selective adaptation capability of the eyes' light receptors is to allow display picture presentations, and other parts of the internal and external cockpit visual scenes, which have very different absolute luminance level limits on their grey scale ranges, to be perceived simultaneously. This aspect of relative luminance perception is very important, since without it most electronic display information presentations in aircraft cockpits would not be legible.

As a practical aircraft cockpit example, of this selective spatial adaptation capability, by the human visual system, portrayals of grey scales on green monochrome cockpit CRT and color liquid crystal displays, in a 10,000 fc incident illuminance viewing environment, are perceived as light green to black, and white to black, respectively, despite the fact that the absolute image difference luminance level limits, on the grey shades presented by these displays, range from nominally 250 to 25 fL, where 250 fL is less than the luminance reflected from the black bezels of the displays. The point is that, in a nominal 10,000 fc ambient illuminance environment, and without the benefit of spatially selective adaptation of the eyes' light receptors, these electronic display image difference luminance levels would appear as shades of between black and very black, if perceived as a part of a reflective grey scale chart extending from 10,000 fL to 25 fL in the same field of view.

It is the very low reflected background luminances of these aircraft cockpit electronic displays that enables the eye's light receptors to adapt, on a spatially selective basis, to their viewing surfaces, and to enable the creation of new relative luminance ranges of perceptible grey shades when the display's are activated. This aspect of relative luminance perception is not unique to electronic displays. Instead, the ability to adapt, on a spatially selective basis, is just a part of the natural vision process, since the same result is obtained when a person is inside a building, and the observer's field of view simultaneously encompasses both a high luminance external visual scene, viewed through a window, and a low luminance scene, internal to the building. This capability, by the human visual system, to adapt to vastly different scene background luminance levels, in different areas of the pilot's instantaneous field of view, explains the pilot's ability to perceive the grey scales and chromaticities in light emissive and light transmissive mode electronic display picture portrayals, and in real-world scenes, with essentially equal ease, even when large differences exist between the upper and lower limits, on the absolute luminance levels of the internal display pictures and the external visual scenes visible simultaneously in a cockpit. As an incidental feature, this example also demonstrates the rapid response times with which the individual light receptors within the eyes can adapt to new absolute luminance level limits of different relative luminance ranges in the visual scene, as the head and eyes are moved to permit the fovea of the eyes to focus on spatial details contained in different parts of the daylight visual scene being viewed.

An ability of pilots to perform rapid instrument crosschecks, in operational aircraft cockpits, which have historically included a complement of both electronic and conventional displays, provides a direct confirmation of the ability of the eyes to adapt quickly in daylight viewing environments.

For the example, described above, of viewing an external scene through a window in a building, the internal and external scene colors would be perceived to be the same, provided the spectral distribution of the illumination present both inside and outside is nominally the same, however, the external scene would be perceived to be brighter. Even this difference can be eliminated, when using electronic displays, by increasing the image difference luminance, and hence the maximum grey shade contrast range of the picture presented on the display, to a level slightly above that needed to render the grey scale range of the imagery presented on the display faithfully, and in so doing overcome the effects of veiling luminance. This can be easily demonstrated by comparing a visual scene as seen through a window with a television display presentation of the same external scene generated using a video camera. At display luminance levels well below those of the external scene imaged on the display, but for a display luminance dynamic range slightly greater than those present for the external scene being rendered, the display picture and the external scenes can be made to appear identical both in brightness and color. As previously shown, a larger display highlight image difference luminance and grey shade contrast is needed to produce equal perceived brightness for the display presentation and for the external scene imaged on the display, if the effects of veiling luminance must also be overcome.

The spatially selective adaptation of the eyes, which, as described above, is known to permit emissive and transmissive operating mode electronic displays to be perceived in aircraft cockpits, should also allow reflective and transflective operating mode electronic displays, having comparable low background reflected luminance levels, to be perceived in a manner similar to their emissive and transmissive electronic display counterparts. Again, because it is the light perceived by the eyes that determines the legibility of a display presentation, and not the operating mode or modulation technique implemented to portray information on the display surface, the rendition of real-world scene grey shades and chromaticities, scaled to reduced luminous reflectances and having the same luminance dynamic range as the real-world scene depicted, should make it possible to achieve optimal legibility pictures using reflective or transflective operating mode electronic displays. The problem is that reflective and transflective mode displays implemented, to date, have not included an integral means of augmenting the reference luminance level of their display presentations, beyond that resulting from the daylight ambient illumination that happens to be incident on the display at the time it has to be viewed. In other words, these displays possess no inherent means to compensate for the presence of veiling luminance, or to increase the image difference luminance of the display presentations, to compensate for the reduced reflectances typically associated with these electronic display operating modes. As formerly described in Chapter 2, to use these electronic display operating modes in aircraft cockpits, requires the incorporation of integral illumination sources, to enable achieving and maintaining control over the legibility of the display presentations, under both daylight and night viewing conditions. Head-up and helmet-mounted displays, with low absolute reflectance image projection sources, indirectly demonstrate the validity of this display technique.

5.4. General Automatic Legibility Control Law Application Considerations

The daylight portion of the image difference luminance requirements equation can, as was previously described at the beginning of this Chapter, be expressed as shown in Equation 5.16, irrespective of the specific technique chosen to implement the gain compensation equation. Adding the night image difference luminance, ΔL_N, to the daylight portion of the image difference luminance requirements equation, Equation 5.16, the complete general automatic legibility control law, applicable for both day and night control, can be expressed either in the following gain compensated format:

$$\Delta L_P = K L_D^m G' + \Delta L_N , \tag{5.51}$$

where

$$G' = \left(1 + \frac{L_V}{L_D}\right)^m, \tag{5.9}$$

or in the equivalent format of Equation 3.163 as follows:

$$\Delta L_P = K(L_D + L_V)^m + \Delta L_N. \tag{3.163}$$

Practical consequences of using different values of the power term, m, in the general automatic legibility control law, as represented by the preceding equations, are considered in the balance of this section.

The values of the constants m and b that have been previously introduced for use in the General and Boeing legibility control laws, respectively, were determined based on quite different display legibility performance criteria. For the general legibility control law, the legibility performance criteria selected corresponds to controlling the display image difference luminance so that the imagery remains at a constant level of legibility under all of the ambient illumination and glare source viewing conditions experienced in aircraft cockpits. As previously indicated a value for the exponent of $m = 0.926$ was necessary for the control law to satisfy this condition. For the Boeing control law, the legibility performance criterion is intended to correspond to controlling the display image difference luminance so that the display imagery suits the personal preference of airline pilots for legibility under the daylight ambient illumination conditions experienced in commercial aircraft cockpits. As previously indicated, Merrifield and Silverstein experimentally determined that a value of the exponent of $m = b = 0.276$ would cause their control law to satisfy this condition. The factors that influence the choice of value of the exponent for use in the legibility control law are considered in greater detail below.

Although the 0.926 and 0.276 slopes produce very different legibility response characteristics for the image difference luminance control law, even more extreme slope values have been used in military aircraft cockpits. It has been pointed out in Section 5.1 that conventional electromechanical instruments have for many years produced satisfactory legibility performance, under daylight ambient illumination viewing conditions, using an inherent automatic brightness control characteristic having a slope of $m = 1$. As described in that section, the general automatic legibility control law, when configured to follow a constant legibility control characteristic of slope, $m = 0.926$, is very similar to the control characteristic of conventional instruments under daylight viewing conditions. The difference is that the constant legibility control characteristics produce image difference luminance levels somewhat higher than those produced by the constant contrast conventional instruments in lower illuminance daylight ambients. This somewhat higher image difference luminance characteristic produces constant legibility by compensating for the decrease in the eyes' visual acuity under reduced daylight ambient illumination conditions.

At the opposite control law slope extreme, from the inherent legibility control characteristics of conventional instruments, are the control characteristics that correspond to electronic displays that are manually set by the pilot to operate at a fixed maximum image difference luminance level under daylight viewing conditions. This control law extreme, corresponds to operating the emitted or transmitted image difference luminances of operational aircraft CRT or LCD displays at their respective maximum levels. In the context of the general automatic legibility control equation, this would correspond to using a control characteristic slope of $m = 0$, that is, a straight horizontal line that does not change the image difference luminance of a display as a function of the display background luminance. The automatic brightness control characteristics of Merrifield and Silverstein, and the constant legibility control law characteristics of this report, fall between the zero and unity slope extremes, with the Merrifield and Silverstein characteristics more closely approximating the zero slope characteristic and the constant legibility control law being very similar to the unity slope characteristic of conventional reflective operating mode electromechanical instruments.

Excepting the unity slope characteristic of conventional reflective operating mode instruments, which has been previously described in Chapter 2, and in Section 5.1, the consequences to be expected from employing each of the preceding legibility control characteristics on the pilot's visual performance will be described in greater detail in the subsections that follow.

5.4.1. Context for Assessing the Legibility of Electronic Displays on Aircrew Performance

Before proceeding with the discussion of the different legibility control strategies described later in this chapter, it is desirable to place the effects of electronic display legibility, on pilot performance, into the context of operational military aircraft cockpits. In particular possible caveats exist to the ability by pilots to read information presented at or above the minimum legibility requirement levels specified in MIL-L-85762A and stipulated in Table 3.14, in a accurate and timely fashion. These caveats relate to the complement of conventional and electronic displays used within a cockpit, the design of the information formats, the control-display tasks being performed by the pilot, and the task loadings that were applicable, when the original minimum legibility requirements of Table 3.14 were established for fighter type aircraft. The potential relevance of these factors, on the performance to be expected from pilots, is considered below.

The premise upon which the following discussion is based is that an interaction exists between the time available for pilots to read cockpit displays, and the pilots' minimum legibility requirements. This premise is based on two observations. The first observation is that the minimum legibility requirements for information displayed in aircraft cockpits are greatly in excess of the threshold legibility requirements determined in laboratory tests, even when aircraft illumination conditions are accurately replicated in the laboratory test environment. Higher stress, in actual aircraft environments, and a more benign task loading, in the laboratory test environment, are believed to be the source of the differences in the display legibility requirements. The second observation is that, as the legibility of display presentations transition from being optimal, to satisfactory, and then to marginal, the degree of difficulty experienced by pilots reading the displayed information increases. The increase in reading difficulty translates into more time being required to read the less legible information at the same level of reading accuracy (i.e., some information will no longer be legible at a glance). Provided that the pilot's task loading allows the scan time for the instrument cross-check to be maintained at or below a critical duration, necessary to track the changes in time dependent information, or, alternatively, to be extended by a sufficient amount to permit accurate readings of all necessary information to be achieved, changing legibilities under different viewing conditions should not produce a problem.

To the extent that changes in the operational mission-related-factors, experienced in military aircraft, such as stress and task loading, can occasionally increase the time required for a pilot to perform the instrument crosscheck in a cockpit, a potential exists for causing display presentations, which would originally have met the pilot's minimum legibility requirements, to become only marginally legible. Since the circumstances responsible for increasing the time required for a pilot to perform the instrument crosscheck are not predictable, they cannot be included in an automatic legibility control algorithm. Increasing the display legibility above the pilots' minimum legibility requirements allows the instrument crosscheck to be performed more rapidly and, thereby, provides a means for the aircrew to compensate for changes in factors that would otherwise increase the duration of the instrument crosscheck, through the use of aircrew-adjustable legibility trim controls. No investigations were found that explore the details of the interrelationship, between improving the legibility of electronic display presentations, in aircraft cockpits, and the decrease in the time duration of an instrument crosscheck, however, an increase in the image difference luminance of displayed information, beyond the point where optimum legibility is achieved, can reasonably be expected to serve as a practical limit on how much, the time needed to perform the instrument crosscheck, can be reduced.

The original minimum legibility requirements for aircraft cockpit electronic displays were determined for fighter aircraft flown operationally in the late 1970s. In recent years, the mix, of high legibility conventional displays and of lower legibility electronic displays, installed in fighter type aircraft cockpits, has shifted toward the use of a higher percentage electronic displays. This shift, to a larger proportion of displays that can exhibit lower legibilities while flying daylight missions, raises the prospect that the time required to perform the instrument crosscheck would increase and that pilot performance would decrease, due to the larger percentage of lower legibility display information that must be read. No experimental evidence gathered in an aircraft could be found, either to support or to dispel this hypothesis. Operational aircraft cockpit experience, which is typically assessed based on aircrew complaints, would suggest the changing mix of conventional and

electronic displays, with differing image legibility capabilities, has not affected the performance of aircrew members. This conclusion cannot be confirmed, however, since changes in other cockpit information display design factors have occurred that could have provided the compensation needed to produce this result. Considerations involving some of these design factors are described in the following paragraphs.

The majority of aircraft cockpit displays, whether implemented using conventional or electronic display techniques, use numerics, alphanumerics and graphics, either alone, or more typically in combination, to construct the information formats used to convey information to the aircrew. These information formats are usually designed to be highly resistant to the effects that legibility changes could have on the interpretation of the information they convey. This is accomplished, for example, by using simple uniform luminance symbols and vector-graphic constructions, using lines, geometric figures and scales, which can be shown against a black or low relative luminance background of a different color. These displays typically do not use grey shades to encode information. Avoiding grey shades, when encoding aircraft cockpit graphic information presentations, provides a means of circumventing the effects of expanding and contracting grey scales, as the legibility of the information portrayed on the displays is altered by changing ambient illumination and glare source viewing conditions. Furthermore, the use of color in these display presentations, to convey information to the pilot, is quite restricted and, in designs that are more resistant to legibility changes, color is used as a redundant coding technique with other forms of information encoding, usually shape coding.

Three primary objective performance improvement goals are typically sought when color coding is used on existing aircraft electronic displays. The first goal is to make it easier for aircrew members to discriminate visually between dynamic symbology, which that can at times overlap. The second goal is to group related display information so that it can be more rapidly found. The third goal is to encode a connotation of advisory, caution and warning information to specified ranges of variables, typically using a small number of absolutely discriminable colors, such as green, red and amber (orange). In those instances, where creating a resistance to the effect of legibility changes on reading accuracy and speed is an objective of a format design, the use of absolutely discriminable colors is typically restricted to display formats, or portions thereof, where, except for low luminance background colors, only those colors are used. This approach to color coding reduces the possibility that colors, which must be absolutely discriminated, will be erroneously interpreted as different colors. Exclusive of the aforementioned purposes, the primary goal of using of color in existing military aircraft display information presentation formats, is to add aesthetic appeal to the appearance of the display presentations.

The extraction of radar or other grey shade or color encoded sensor-video information from electronic display presentations is the perceptual task in which an aircrew member's performance would be expected to be most significantly degraded or enhanced by changes in the legibility of existing electronic displays. Even in this instance, changes in legibility caused by the compression and expansion of the grey shades in a rendered picture can sometimes be avoided. For example, the conversion of weather-radar information to a color encoded graphics format avoids the need to display grey shades, and also eliminates the need for the pilot to interpret the storm intensity information, by encoding it in green, orange and red colors, interpretable as advisory, caution and warning information, respectively. Unfortunately, unlike the weather-radar data, which is directly dependent on the intensity of the radar signals returned by a storm, the information content, encoded into most of the sensor-video signals needed by aircrew members, is, as yet, still too complex to permit it to be graphically displayed, using only computer processing to allow the signal information content to be recognized, identified and interpreted. Two applications of electronic displays in operational aircraft, which would benefit in a significant way from holding the grey shade and chromaticities relationships of display imagery constant, are the presentations of monochrome sensor-video information and full color map information.

Many operational military aircraft, including fighter type aircraft, have now been upgraded with a variety of monochrome and color electronic displays. Under high ambient illumination viewing conditions, these displays operate at or near the previously established minimum levels needed to satisfy a pilot's legibility requirements (i.e., as specified in MIL-L-85762A and stipulated in Table 3.14). Due to the acceptance of these

displays by the pilots of existing operational military aircraft, a conclusion can be reached that the legibility levels, of the electronic display portrayals used in these aircraft, is sufficient to convey the information needed by pilots, within the time available to perform instrument crosschecks. It can also be concluded, at least for these aircraft cockpits, that the effect of the changing percentage mix of low and high legibility displays has been compensated, through the combination of the small improvements that have occurred over the years in the legibilities of aircraft electronic displays, and the changes that have occurred in the information presentation techniques being employed.

The preceding operational aircraft experience could also be interpreted as suggesting that the specific legibility levels, at which electronic displays are operated, between the minimum required legibility needed to present numeric, alphanumeric and graphics information, and the nearly optimum legibility levels, at which this information is portrayed in high ambient viewing conditions by conventional displays, may not be as important as was previously inferred in this section. However, beyond the general conclusions of the preceding paragraph, little information, which is definitive in nature can be garnered reliably from a pilot's experience with operational aircraft cockpits, due to the complexity of the task environment and the consequential difficulties associated with correctly attributing cause to effect, in that environment. Although the experiences of pilots in operational aircraft, would seem to be a fertile ground for gathering information, and for developing requirements that are directly relevant to the conditions experienced by pilots in aircraft cockpits, very few systematic investigations involving operational aircraft have been conducted. The high cost of instrumenting and conducting in-flight tests appears to be the principal reason this is true, but does not explain why so few structured analyses using pilot interviews and questionnaires have been employed.

5.4.2. Fixed Maximum Display Luminance Control Law

The preferred manual legibility control strategy of most military pilots simply involves setting a display information presentation to the maximum image difference luminance level the display is capable of achieving and then leaving it set to that fixed level under all daylight ambient illumination viewing conditions. From the perspective of a pilot using the displays, no obvious penalty is incurred by using this control strategy and, in fact, two significant advantages are gained. The first advantage is that the displays are always maintained at the maximum image presentation legibility that they can achieve. The second advantage is that the pilot does not have to take time away from doing mission-related tasks to adjust the legibility of the information presented on the displays.

5.4.2.1. Legibility Expectations for Displays Operated at Maximum Luminance in Daylight

To appreciate this manual control strategy better and to provide a comparison with the automatic control techniques that are subsequently described, the legibility results that would be experienced by pilots for an electronic display operated at its maximum image difference luminance under daylight viewing conditions will be described. A military aircraft electronic display, set to depict a picture that can just meet the pilot's minimum legibility requirements, under high ambient illumination conditions, will be postulated as a realistic starting point for this description. A reduction in the reflected background luminance of this display, while maintaining its image difference luminance output at a fixed level, causes the picture grey shades to become more legible and the colors depicted to become more saturated. As described in the last section, this improvement in legibility continues as the display background luminance is further reduced, but only up to the point that the renditions of the grey shades and chromaticities in the picture on the display fully match the requirements of the human's perceptual color space, as characterized for example by the Munsell color system. This match of the grey shades and colors corresponds to the condition previously referred to as optimum legibility and occurs when reductions in the display background luminance cause the luminance dynamic range of the display imagery to increase to the point where it is equal to or greater than the luminance dynamic range of a directly viewed real-world scene.

For still further reductions in the display background luminance level, the legibility, and with it, the appearance of the display becomes essentially fixed. This condition occurs when the maximum grey shade contrast, of the imagery presented on a display, equals or exceeds the level needed to activate the human's color perception capabilities fully. In the last section, it was explained that as the contrast of the displayed imagery increases beyond this point, a process of spatially selective light adaption of the eye's light receptors is initiated. In the present context of a decreasing display background reflected luminance, rather than in the previously described context of an increasing highlight image difference luminance, this spatially selective adaptation effect by the human visual system can be interpreted as occurring either because the eyes' light receptors adapt to the progressively higher image difference luminances and absolute contrasts of the grey shade encoded display pictures, by, in effect, becoming saturated, or because the human visual system's need for information has been fully met. Independent of the actual physiological processes at work, and as suggested in the previous section, this response of vision can be considered a form of automatic legibility control. This light adaptation response is a partial explanation for why no obvious penalty is incurred by a pilot electing to use the control strategy of holding the display at its fixed maximum image difference luminance level under daylight viewing conditions. The remainder of the explanation, for why this control strategy is effective, concerns legibilities that are less than the optimal, but are greater than or equal to the minimum legibility requirements, for the information presented on electronic displays in aircraft cockpits.

Up to the point where the legibility becomes fixed at the optimum legibility of the information presented, the legibility of the display information presentation and with it the perceived grey shades and colors depicted by the display change. It can therefore be concluded that owing to the limitation on the maximum image difference luminance output capability of existing flight-worthy electronic displays, there is no practical way to both provide optimum legibility, when the ambient illumination viewing conditions are low enough, and also avoid the legibility degradation that occurs under high ambient illumination daylight viewing conditions. Moreover, this is true irrespective of the technique that is implemented to control the legibility of these displays, be it manual or automatic. As a practical matter, it can, therefore, be concluded that the slope of the display legibility control characteristics can be set to any value which prevents the display image difference luminance and contrast levels of display imagery from dropping below the minimum legibility control characteristic requirements for acceptable legibility.

5.4.2.2. Conclusions for Displays Operated at Maximum Luminance in Daylight

As indicated in the preceding subsection, the limitations on the maximum image difference luminance output capability of existing flight-worthy electronic displays can be expected to cause the information presentations these displays portray to undergo considerable changes in their visual appearance and image legibility under changing ambient illumination conditions. Owing to the fact that the information presentations on these displays meet or exceed the pilot's minimum legibility requirements, the impact on pilot performance of changes in visual appearance and image legibility of the information presented on these displays is not obvious and, as previously described, have not been the subject of any systematic investigations. The operational cockpit experience of fighter pilots with electronic displays in high ambient illumination environments was used to establish the original daylight minimum legibility requirements specified in MIL-L-85762, and that experience indicates that display presentations, meeting the minimum legibility requirements, should be capable of being read at a glance by pilots, subject to the caveats described in Section 5.4.1.

Based on the preceding analyses, it can be concluded that the daylight manual legibility control strategy of setting the image difference luminance of a display to a fixed maximum level has only two significant disadvantages. The first disadvantage is that the operation the display for prolonged periods at its maximum luminance output can be expected to increase the frequency of required maintenance. A second disadvantage associated with this type of operation arises due to the potential that the effects of heating on the displays components will significantly reduce the operating life of the display.

Although the compression of grey scales and changes in perceived colors, under worst-case viewing

conditions, could also be listed as disadvantages of this control strategy, this disadvantage is shared by the automatic control strategies, still to be discussed. The only exception to this would occur if the legibility of the cockpit electronic displays were to be automatically controlled at a constant level that the display can achieve under all ambient illumination viewing conditions, that is, to a level that is less than the optimal legibility the display can achieve under reduced ambient illumination viewing conditions. Automatic legibility control can, of course, also be used to maintain the legibility of a particular display presentation constant at the optimum level, under reduced ambient illumination and glare source viewing conditions, and like the constant luminance control strategy only experience a decrease in legibility under worst-case viewing conditions. This latter approach is consistent with the main historic impetus for automatically controlling the image difference luminance of electronic displays used in operational military aircraft, that is, to reduce maintenance and to extend the useful life of the electronic displays, by decreasing the amount of time the displays are operated at maximum luminance, rather than for either maintaining a constant level of display image legibility, or for satisfying a pilot's legibility control preferences.

As previously described, the problem with earlier automatic brightness controls was not with the slope of their image difference luminance versus display reflected background luminance control characteristics. Instead, the problem was due to the lack of a corresponding automatic adjustment to compensate for the effect of veiling luminance induced in the pilot's eyes by glare from the sun, at times when the display panel light sensors are commanding the image difference luminances of the displays to operate at reduced levels, because the sun is in the pilot's field of view rather than illuminating the display.

5.4.3. Merrifield and Silverstein Brightness Control Law

The performance criterion employed by Merrifield and Silverstein, to establish their control law parameter values experimentally, was directed at satisfying the personal preferences of commercial airline pilots for display image legibility. Following the inherent legibility control of conventional aircraft displays, described in Section 5.1, and the fixed maximum display luminance control law, just described, the implementation of the Boeing automatic brightness control law in airliners has logged the greatest number of hours of operational flight experience by pilots. For this reason, the merits of this control technique and the validity of the information that is available to assess it will be considered in as much detail as is possible.

To assess the merits of the pilot preference control strategy used by Boeing, it is desirable to first clarify the context in which the validity of their results should be interpreted. In particular, it should be born in mind that the 0.276 slope of the control characteristic that was experimentally determined by Merrifield and Silverstein to meet their pilot performance criteria is unlikely to be the same as the magnitude of the slope used in the actual application of the control law on the Boeing 757, 767 and 737 commercial aircraft. As was described earlier in this chapter, the Merrifield and Silverstein article states that the form of their control law was implemented on the Boeing aircraft but not the specific experimentally determined values of the constant parameters. Stated in another way, the automatic brightness control characteristic parameters that airline pilots have judged to be acceptable in operational airliner applications of the Boeing's color CRT displays are not known.

The choice by Boeing to use a pilot preference criterion to implement their automatic brightness control means that the Boeing legibility control law is based on a subjective, rather than an objective, performance criterion. The practical consequence of this choice of a legibility control criterion is that factors that can influence the pilot's subjective preference for good legibility will cause different control law results to be obtained depending on the control objectives of different pilots. The factors that can influence a pilot's legibility objectives and control strategies can be quite diverse, and the slopes of the control characteristics could reasonably be expected to vary between the previously described legibility characteristics, for conventional aircraft instruments, and the horizontal control characteristics, of the displays operated at their fixed maximum image difference luminance level, under daylight ambient illumination conditions. The pilot's preference can be expected to vary, depending on the nature of the display information-assisted tasks, being performed, and

whether those tasks require fine or course visual acuity, rapid or slow response times and so forth. The workload pilots are subjected to, while performing visual tasks, and issues such as prior training and experience, can also play a role.

One factor involving prior training and experience, which appears to have been operative during the Boeing experiment, is reduced expectations by the aircrew members tested, with respect to the legibility that electronic displays can achieve under high ambient daylight viewing conditions. This conditioning factor appears to have resulted in the acceptance of legibility levels, for high ambient illumination viewing conditions, which are quite low, when compared with the high legibility levels the same pilots preferred under lower daylight ambient illumination conditions. Under high ambient illumination conditions, the maximum image difference luminance capabilities of the color CRT displays, used in the Boeing aircraft, offer virtually no flexibility for the pilot to control the legibility of the displays, since they must be set to their maximum luminance output level to achieve adequate legibility under this viewing condition. Conversely, under lower level daylight ambient illumination conditions, the same displays place essentially no limitations on the pilot's ability to set the display's legibility to any desired level, between the minimum and optimal levels, and, under this viewing condition, the control law parameters determined by Merrifield and Silverstein cause the displays to operate at legibility levels previously described as optimal. The existence of this apparent contradiction raises a question about whether the control law of Merrifield and Silverstein, Equation 4.4, truly represents the legibility preferences of the commercial airline pilots tested.

Although the image difference luminances and contrasts, predicted by the Merrifield and Silverstein automatic brightness control law of Equation 4.4 in high ambient illumination viewing conditions, are greater than the minimum levels associated with the threshold of legibility, they are still inconsistent with achieving the minimum image legibility requirements of military fighter type aircraft, under high ambient viewing conditions. For this reason, it can also be concluded that this numerical parameter value implemention of the Merrifield and Silverstein automatic brightness control law, if used with the Boeing color CRT displays, would not be compatible with the still higher contrast settings, determined by Merrifield and Silverstein to be preferred by airline pilots under lower level daylight ambient illumination test conditions, or with maintaining saturated display image colors, under high ambient illumination conditions.

The legibility assessment, in the preceding paragraph, of the merits of the Merrifield and Silverstein automatic brightness control law, when applied for use with the Boeing color CRT displays, is based on a maximum image difference luminance level of 86 fL (i.e., or less depending on the interpretation of the "cockpit ambient," B_a), predicted by the Merrifield and Silverstein legibility control law equation, Equation 4.4, with an illuminance of 10,000 fc incident on the display. This image difference luminance is assessed as insufficient to provide adequate color graphics legibility, for even the small number of colors used in the Boeing Electronic Flight Instrument System (EFIS), electronic attitude director indicator (EADI) and electronic horizontal situation indicator (EHSI), display formats, based on a background display surface diffuse reflectance of 1.25 fL/ fc, reported in an earlier report.[157] It should also be noted that the presence of the sun in the FFOV, at angles near the glare shield, is a much more severe veiling luminance condition than the maximum 10,000 fL FFOV uniform glare source luminance level tested by Merrifield and Silverstein and would cause imagery rendered with the image difference luminance level of 86 fL to be within a legibility range of from marginal to unacceptable. It is not known if the gain control could drive the color CRT displays, used by Boeing, to the emitted luminance levels of 100 fL or greater, called for by MIL-L-85762 for graphics presentations. However, unlike military aircraft pilots, commercial airline pilots also have the option of using window shades, attached to the side windows of the cockpit to block the direct incidence of the sun on their cockpit displays, and low light transmittance movable sun visors, that make it possible to reduce the veiling luminance induced in the eyes by a factor of at least ten. The role that these pilot controllable light blocking and attenuation devices have played in gaining airline pilot acceptance of the Boeing color electronic displays, operated using automatic brightness controls is unknown.

In general, the choice by Merrifield and Silverstein to use the preferences of pilots, as a legibility performance criteria for establishing the response characteristics for their automatic brightness control law,

is, in concept, as valid as any of the other legibility control strategies described in this section. Furthermore, when properly implemented, this control law sho provide display legibility as good as that achieved using the maximum daylight image difference luminan tting, described in the previous subsection, for daylight control characteristic slopes of greater than zero . ss than or equal to 0.926. As previously indicated, the primary benefit of an automatic brightness, or gibility, control is that the reliability of the display should increase, roughly in proportion to the magnitude of the control characteristic slope, by virtue of the limitation this slope places on the time the display is operated at or near its maximum drive level.

5.4.4. Rationale for Using the Constant Legibility Control Law

The preferred method of automatically controlling the legibility of electronic displays in aircraft cockpits, under changing ambient illumination and glare source conditions, is to cause the image difference luminances of the imagery rendered by these displays to conform to a constant legibility control law. By configuring the automatic legibility control so that the electronic display image difference luminance conforms to a constant legibility control law, as the magnitude of ambient light reflected by the display surface or incident on the pilots eyes changes, the relationship between image grey shades and colors will be perceived to be invariant.

Lacking constant legibility control over the perceived image difference luminance levels produced by a display, the picture grey shades are compressed as the ambient illumination incident on the display or on the pilot's eyes increases. This compression of the grey shades makes adjacent grey shades more difficult to discriminate, and colors displayed become more desaturated, that is, the colors in the information format being displayed actually change, as the ambient illumination conditions change. Conversely, a decrease in the ambient light incident on the display, or on the pilot's eyes, causes the spacing between adjacent grey shades to expand, and the colors depicted in the information format being displayed to change as they become more saturated. Whether these changes are important from a mission performance perspective, or not, depends on the tasks the pilot must perform using the display and the relevance of its grey shade and color encoding to its information presentation design. To achieve consistent objective pilot visual performance for image recognition, identification and interpretation tasks, or to be assured of attaining accurate discrimination of both relative and absolute color presentations of, for example, color maps and signal indications, respectively, under changing ambient illumination conditions, the legibility of electronic display presentations need to be maintained at a constant level.

In spite of the aforementioned advantages of automatically controlling the legibility of aircraft cockpit display presentations at a constant level, in changing ambient and glare source illumination environments, the previously described practical limitations of the legibility capabilities of existing electronic displays, which are suitable for use in operational aircraft cockpits, precludes the possibility of retaining constant legibility at any desired level, under all viewing conditions, except legibility levels that just meet or slightly exceed the aircrew's minimum requirements. The best legibility control strategy that can presently be implemented, using constant automatic legibility control, is to allow the legibility of a display presentation to be set by the pilot at the level deemed to be satisfactory, and then cause that level to be maintained in changing day and night, ambient and glare source illumination viewing conditions, up to the point where the limitations of the electronic display technology prevent holding the legibility constant. This control strategy permits the desired display legibility performance set by an aircrew member to be achieved, under most of the viewing conditions experienced in the cockpit, and provides the additional advantage of extending the useful operating lifetime of the display, without having to resort to maintenance or replacement.

5.4.5. Control Law Slope and Night Image Difference Luminance Level Interactions

The inclusion of the night image difference luminance term, ΔL_N, in the general legibility control law, as expressed above in Equations 5.51 or 3.163, in concept, allows continuous automatic control to be maintained over the legibility of a display, independent of the ambient illumination conditions the pilot experiences in the

cockpit. In practice, however, the ability to achieve continuous perceived image difference luminance control characteristics that are consistent with the pilot's legibility requirements for both day and night operation imposes constraints on the value of the exponent *m* that can be used to implement the control law.

The problem occurs for control characteristics that can command displays to high enough perceived image difference luminance levels, ΔL_p, to make them legible at reflected background luminance levels, L_D, corresponding to 10,000 fc of incident ambient illuminance but having small slopes, *m*. As the ambient illumination decreases to the point where the cockpit lighting would normally be switched from day to night operation, the control characteristic continues to command perceived image difference luminance levels that are higher than, and possibly much higher than, the night image difference luminance level, ΔL_N, needed by the pilot for use in night missions. The resultant discontinuity in the image difference luminance control characteristics at the day to night transition was briefly noted by Merrifield and Silverstein in their article,* but no explanation was offered for why such a large difference in pilot preference should occur at a transition where a smooth transition would normally be expected.

Because the Merrifield and Silverstein control law is only intended to apply to daylight viewing conditions, in preparation for switching to the night operating mode, the image difference luminance is set to a constant value equal to the last image difference luminance level commanded by the automatic brightness control, when the illuminance incident on the display reaches 1 fc. For still lower incident illuminance levels, it is left up to the pilot to decide when the cockpit viewing conditions merit switching to the conventional manual control techniques that have historically been used to satisfy the image difference luminance requirements of the pilot for display legibility while conducting night operations.

As the slope of the general legibility control characteristics increase in magnitude, the discontinuity between the day to night image difference luminance levels is progressively reduced until for slopes approaching $m = 0.926$ the discontinuity is eliminated. Using this slope, to cause the image difference luminance of displays to follow constant legibility control characteristics, produces no discontinuities in the automatically controlled transition from day to night cockpit legibility conditions and, in so doing, also provides a smooth transition that accounts for the effects of both the ambient illuminance incident on the cockpit displays and the veiling luminance induced in the pilot's eyes by a setting sun.

5.5. Automatic Legibility Control Implementation and Adjustment Considerations

The constant legibility form of the general legibility control law, as expressed by Equation 5.1, contains two control terms, the night image difference luminance, ΔL_N , and daylight contrast control multiplier, *K*, that are available for use by the pilot to make legibility trim control adjustments. This choice of pilot trim controls, or the previously described variants of it, would give the pilot the greatest legibility control flexibility. Unfortunately, this choice of trim controls would also impose a requirement for each display, or each functional grouping of displays, to have two different pilot trim controls. Since the use of an automatic legibility control (ALC) is intended to simplify the cockpit configuration and reduce the pilot's task loading, a more in-depth look at the methods used to implement the pilot's ability to exercise control over the legibility of the display presentations the ALC controls are merited.

The discussion of how best to implement a pilot or aircrew member adjustable trim control, for use with a constant legibility ALC, starts with an assessment of why pilots need a legibility trim control adjustment capability at all, when the legibility is presumably to be controlled automatically. Next, a method to permit aircrew members to adjust the legibility of displayed information, using a single trim control is introduced, and a potentially important limitation of this control approach is considered. The other legibility trim control

---

* This problem was discussed by Merrifield and Silverstein in conjunction with Figure 2 on Page 179 of their 1988 Society for Information Display article, cited previously in this report.

approach to be introduced requires the pilot to use two controls. Because one control would be for use only at night, and the other would be for use during the day, this dual control approach should not cause any increase in pilots' task loading over that associated with the single control approach. Of these two approaches the dual control is favored because it should give the aircrew greater flexibility in initially setting, and then maintaining the day and night legibility level adjustments of the display information presentations. In particular, the control that sets the contrast of the display presentations, produces a legibility level setting that is valid under both day and night viewing conditions and yet allows the night image difference luminance level to be independently adjusted by the night trim adjustment control. The primary advantage of dual trim controls is that they are expected to result in a reduction in task loading, in comparison to the single control approach, after some experience has been gained by pilots', using the controls to meet their personal preferences or needs for legibility. Having considered the legibility trim control adjustment techniques, the final topic discussed in this section is the choice of settings for the constant legibility control law equation parameters.

The control of legibility of the information presented on electronic displays, described in this chapter, is closely related to another display information presentation control topic, namely, the control of the information content presented by a display. This topic is concerned with the capabilities that should be made available to aircrew members to permit them to exercise control over sensor-video signals, and their transformation for depiction as spatially distributed grey shade or color encoded pictures, on monochrome or color electronic displays, respectively. The reason this topic is mentioned here is because the effect of a change in the information content presented in a display picture is generally interpreted as directly influencing the legibility of the information presented on the display, even when it is the information content of the picture and not its legibility that is being controlled. Because the information content of an electronic display picture should be controlled separately from the display picture's image difference luminance by the ALC, and its legibility trim controls, this topic considered in Chapter 6.

5.5.1. Circumstances Requiring Aircrew Trim Control Adjustments to Display Legibility

Starting with fundamentals, a reasonable question to ask is why the pilot would require access to any legibility control, if the ambient light sensing is adequate, and the luminance control settings needed to satisfy the pilot's visual requirements are known, for any given sensed illumination environment and veiling luminance condition. A partial answer to this question is that the pilot's legibility requirements depend on the visual task being performed, the aircraft mission, the tactics being employed and the fact that different pilots have differing requirements and/or preferences (i.e., it is not clear which) for the legibility of information presented on aircraft cockpit conventional and electronic displays. The remainder of the answer to the preceding question is that the condition on the question, namely that the pilot's visual requirements are known, is not currently satisfied to the degree necessary to make complete automatic control of display legibility feasible, under all of the possible ambient illumination conditions that a pilot can experience in an aircraft cockpit.

The greatest variability in pilot legibility settings occurs during night flights. Missions that require good external night vision, typically cause pilots to set the internal night lighting to levels so low that they are only just able to read the most critical information on their flight instruments. Stated in another way, to satisfy this objective, the pilot has to reduce the image difference luminance levels in the cockpit intentionally, to levels below those that would be commanded by a constant legibility ALC, initially set under daylight viewing conditions. Conversely, when flying high-level navigation routes that do not require acquiring visual reference to ground way points or external threats, the instrument image difference luminance settings can be set as high as is wanted by the aircrew, and in so doing provide comfort level reading of the display information. This is the condition that most frequently applies to night flights in commercial airliners, where the use of onboard navigation aids, the lights at airports and the lights on other aircraft make it unnecessary for the pilot to dark adapt to the lower light levels external to the aircraft.

The preceding examples illustrate the fact that the aircraft mission requirements can play a role in setting the desired instrument luminance levels; something an ALC, responding only to light sensor inputs, could not

be expected to anticipate in selecting the correct control response characteristic. Similarly, and as previously described, the image difference luminance levels of displays trim adjusted to permit the aircrew to extract information effectively, from grey shade encoded sensor-video pictures, is much higher than the settings needed, as a minimum, on the same display when it is used to portray graphics imagery such as an EADI or EHSI format. Thus, unless the ALC incorporates task-selective control logic, and the corresponding input information (e.g., a mission mode control input), which permits it to adjust automatically for how a pilot is using a display, at a particular point in time, a luminance trim adjustment would have to be provided to permit the pilot to make the necessary legibility adjustments.

Although, the preceding types of adjustment capabilities were described in the context of night flight operations, display image difference luminance, and, hence, absolute contrast, adjustments can also be required of the aircrew during daylight flight operations. The need for aircrew members to make trim adjustments from a constant optimum legibility control characteristic is not as obvious during daylight operations. An increase in the legibility setting to portray sensor-video information on a display initially adjusted to display graphics, could occur, however, no mission-related reasons exist, for example, to set the displays to the lowest level that provides adequate legibility during daylight operations, as there are, at times, during night operations. In other words, and as previously mentioned, simply controlling the displays automatically, at sufficiently high constant legibility levels, allows the aircrew's daylight viewing requirements, to be satisfied.

Even though the life expectancy of an electronic display would be extended, and maintenance would by reduced, by operating it at less than the optimal legible levels needed to make sensor-video information fully satisfactory to aircrew members (i.e., comfort reading level), the improvement would be marginal in comparison to the effect achieved by adding automatic legibility control. Furthermore, it is doubtful aircrew members would or should use a legibility trim control for this purpose. The primary purpose for a legibility trim control adjustment capability, under daylight viewing conditions, is to satisfy the legibility requirement and/or preference differences between individual aircrew members. A secondary purpose would be to allow compensating for differences in the luminance decay rates of different electronic displays or displays installed at different times during the lifetime of an aircraft. Even if legibility trim control adjustment capability, under daylight and night viewing conditions, were not needed for any other reasons, satisfying the differences between the legibility requirements and/or preferences of individual aircrew members would still be necessary.

Still another display viewing condition that merits consideration, particularly under changing daylight viewing conditions, is the constancy of the colors being used to portray graphics and video picture presentations encoded in color. Whether this consideration is important or not depends on the role color plays in relation to the information presentation function the display is intended to perform. Electronic attitude director indicators (EADIs) and electronic horizontal situation indicators (EHSIs), for example, have historically been portrayed in black and white in military aircraft and, therefore, the use of color in the new electronic versions adds primarily to their aesthetic appeal, rather than being an image rendition requirement to achieve good pilot performance. As described previously, however, even in this application some objective legibility advantages accrue from color coding portions of the display symbology, for instance, to improve the discriminability of symbology that can from time to time overlap, and to permit the grouping of related functions to make them easier to find and control. If the misidentification of a displayed color can change the interpretation of the information being conveyed, then a means of holding colors constant in the presence of changing ambient illumination and veiling luminance viewing environments becomes a necessity.

5.5.2. Implementation of Single Aircrew Adjustable Legibility Trim Controls

Based on the perceived image difference luminance requirements equation, first described in Section 3.9, and subsequently in later chapters, an image difference luminance control law of the following form would be best suited to satisfy the pilot's display legibility control requirements, if the pilot is to have access to only one legibility trim control:

$$\Delta L_P = P_C \left[1.30\, C\, (L_D + L_V)^{0.926} + 0.0193\, C \right]. \tag{5.52}$$

or equivalently as

$$\Delta L_P = P_C \left[1.30\, C\, L_D^{0.926}\, G' + 0.0193\, C \right], \tag{5.53}$$

where

$$G' = \left(1 + \frac{L_V}{L_D} \right)^{0.926}. \tag{5.54}$$

The quantity inside the brackets in Equation 5.52 is the previously derived perceived image difference luminance requirement equation, Equation 3.179, with Equation 3.180 substituted for ΔL_N. Likewise, the quantity inside the bracket in Equation 5.53 is the previously derived perceived image difference luminance requirement equation, expressed in the equivalent veiling luminance gain multiplier format of Equation 5.51, after substituting the same values for the parameters K and ΔL_N, used in Equation 5.52.

The multiplicative constant, P_C, has been added to this equation to represent the effect of a pilot adjustable perceived contrast (i.e., display luminance dynamic range) legibility trim control. The purpose of this trim control is to permit pilots to adjust a display to a fixed multiple above or below the minimum image difference luminance requirements characteristic (e.g., $0.1 < P_C < 10.0$) controlled by the ALC, in order to suit their personal preferences or requirements for image legibility and to, thereafter, have the display image legibility remain fixed, day or night, in changing ambient illumination conditions, until changing visual task requirements cause the pilot to adjust the legibility to a more appropriate level for a new task to be performed. Although changes in the contrast, C, would have the same effect as making changes in the contrast multiplier trim control, P_C, introduced in the above control law equations, adding this multiplier emphasizes the different usages of these two parameters by the ALC. This distinction in the usage of these parameters is further clarified in Section 5.5.4, which discusses the factors that influence the values of the contrast, C, that are appropriate for use in aircraft applications of the ALC.

The use of a single legibility trim control approach, as represented by either Equation 5.52 or Equations 5.53 and 5.54, poses a problem with being able to track the human's experimentally derived image difference luminance versus background luminance legibility requirement characteristics accurately. These characteristics are illustrated, mathematically modeled and described in Chapter 3, for all possible ambient illumination and veiling luminance viewing conditions. The problem with the representational accuracy of Equations 5.52 and 5.53 stems from the fact that the breakpoint between the low and high slope asymptotes of the experimentally determined image difference luminance requirement characteristics shifts to higher or lower values of display background luminance as the level of the night image difference luminance is increased or decreased, respectively. By way of comparison, when the contrast multiplier, P_C, is changed, the shape of the constant image difference luminance requirements characteristics of Equation 5.52 or 5.53 remain invariant and the locations of their breakpoints, with respect to the display background luminance axis, remain unchanged. In other words, the result of this change in contrast multiplier, P_C, in Equation 5.52 or 5.53, is to cause the constant image difference luminance requirement characteristics to move, by fixed multiplicative amounts, to higher or lower values with respect to the image difference luminance axis, over the entire range of the background luminance axis, as the contrast multiplier is increased or decreased, respectively. If an aircrew member were, for example, to use the contrast multiplier trim control to reduce the night image difference luminance, with respect to a legibility control level formerly set under daylight viewing conditions, the new reduced legibility level setting would be retained when flying from darkness into daylight, thereby causing the controlled display to follow a suboptimal legibility characteristic, if no further adjustments are made to the trim control setting by an aircrew member.

The point being made in the previous paragraph is that changes made to the contrast multiplier settings of Equations 5.52 and 5.53 cause a coordinated change to occur in the legibility of the display picture portrayal under both day and night viewing conditions. As previously explained, a variety of reasons exist for why a pilot

might want to change the night image difference luminance level controlled by the ALC, while retaining daylight legibility ALC characteristic previously established for use under daylight viewing conditions. The use of the single legibility trim control approach forecloses the possibility of maintaining different day and night legibility settings. It should be noted that the constant legibility control law equations, Equations 5.52 and 5.53, above, do account for the background luminance shifts in the image difference luminance requirement characteristics caused by changes in the veiling luminance sensed, so the practical effect of the limitation of the single legibility trim control approach just described is restricted to causing the pilot to have to readjust the contrast control setting for some transitions from day to night or night to day viewing conditions.

5.5.3. Implementation of Dual Aircrew Adjustable Legibility Trim Controls

Based on the image difference luminance requirements equation, previously described in Sections 3.9 and 5.3, and shown in Equations 3.182 and 5.25, respectively, an image difference luminance control law of the following form would be best suited to satisfy the pilot's display legibility control requirements if the pilot is to have access to two legibility trim controls:

$$\Delta L_P = P_C \left[1.30 C \left(L_D + L_V \right)^{0.926} + 0.0193 N_L C \right]. \tag{5.55}$$

This equation is a modified version of Equations 3.182 and 5.25. It is essentially the same as Equation 5.52, except that a multiplicative constant, N_L, has been added to the equation to represent the effect of a pilot adjustable image difference luminance trim control suitable for use at night. As was true for the single trim control equation, this equation can also be expressed in the equivalent veiling luminance gain control format, as follows:

$$\Delta L_P = P_C \left[1.30 \, C \, L_D^{0.926} \, G' + 0.0193 N_L C \right], \tag{5.56}$$

where the veiling luminance gain compensation term is given by Equation 5.54, as before.

The purpose of this night trim control is to permit pilots to adjust the image difference luminance levels of displayed information, to suit their personal preferences for image legibility at night. The control permits the night image difference level to be set to a fixed multiple, for example, between $0.1 < N_L < 10.0$, below or above the night image difference luminance level commanded by the constant legibility ALC characteristic, which would have been previously set by the pilot under daylight viewing conditions using the contrast trim control, P_C. Once this trim control has been adjusted to the night image difference luminance preferred by an aircrew member, the ALC would cause the image legibility of a display to remain fixed, in changing night through dusk through daylight ambient illumination conditions, until changing visual task requirements cause the pilot to readjust the legibility setting, to a more appropriate level for a new task to be performed. Because the magnitude of the night image difference luminance, ΔL_N, would typically be less than 2 fL, but, as a maximum, possibly as high as 5 fL for the display of sensor-video information, the setting of this night viewing preference would have no noticeable effect on the perceived legibility of the display, except for the lowest daylight viewing conditions. Since the contrast multiplier control setting, P_C, also alters the night image difference luminance level setting of the display, the intent of the night image difference luminance trim control setting N_L is to give aircrew members the ability to adjust the night image difference luminance level of the display, without significantly altering the daylight legibility preference setting.

The dual control approach to day and night legibility trim control, therefore permits the ALC, to compensate for differences between the pilot's day and night preferences, and/or requirements, for display legibility and, moreover, would have the added benefit of not requiring further legibility control trim adjustments by a particular pilot, unless the pilot is required to do so, due to a change in the visual tasks being performed. By way of comparison, the single trim control approach would typically require that an adjustment be made each time a day to night or night to day ambient illumination viewing condition transition occurs. This is the basis for the assertion, in the introduction to this section, that the use of two controls, to effect separate day and night legibility trim control adjustments of displayed information, could reduce the workload of pilots, as compared with the use of the single legibility trim control approach. The judicious use of common pilot legibility

trim controls, applied to control multiple display installations, should further reduce the impact of the task loading, imposed by the need to control the legibility of displays in aircraft cockpits, for implementations where automatic legibility control is used in conjunction with each display installed in an aircraft cockpit. This topic is discussed in greater detail in Chapter 7.

5.5.4. Choice of Settings for the Constant Legibility Control Law Equation Parameters

The value of the contrast term, *C*, in the preceding equations is determined by the type of information that is being displayed. The minimum requirements for the contrast, C, are described in Section 3.9 and their corresponding values for different types of display information are summarized in Table 3.14. An electronic display intended to present highlight white or monochrome video information, at a contrast of C = 10.31 (i.e., an eight $\sqrt{2}$ dynamic range) or higher, would, therefore, be expected to operate using a higher image difference luminance control characteristic than a display that is never intended to portray anything more than monochrome graphics, at a contrast of C = 3.0, for example. The disadvantage of this control approach is that the ALC used to control the image difference luminance of a display, would have to be dedicated to the operation of that particular display, once the value of the contrast in the automatic legibility control law is set to make its output control signal compatible with the display being controlled.

An alternative approach, which appears to provide a means of avoiding the need to custom-tailor the control signals generated by the automatic legibility controls, by setting the value of the contrast of the information, the display is intended to convey to the aircrew, to make the ALC compatible with the specific information presentation capabilities of each electronic display, used in an aircraft cockpit, involves having the display manufacturer or aircraft system integrator assume the responsibility for interpreting the signal generated by the ALC. For example, to operate displays that can only portray graphic, alphanumeric or numeric information, a standardized ALC signal, say for video information, would have to be interpreted (i.e., the equivalent of scaling to a lower value image difference luminance using a constant multiplier) to make it consistent with the lower image difference luminance response characteristics of displays that can only generate the image difference luminance levels needed to depict of graphic, alphanumeric or numeric information.

For multipurpose video displays, which can portray graphic, alphanumeric and numeric information, besides sensor-video information, a single ALC signal corresponding to the highlight luminance level in the video picture would be provided to control the display legibility. The video signal modulation then determines the grey shade or color relative luminance level, below the maximum image difference luminance level commanded by the ALC, at which graphic, alphanumeric or numeric information that is to be presented on the display is portrayed. The actual absolute magnitude of the image difference luminance generated by a display in response to an automatic legibility control input would consequently be expected to be determined by three distinct factors: (1) the automatic legibility control signal; (2) the sensor-video or computer generated video, graphic, alphanumeric, or numeric signal modulation applied to the display media; and finally (3) by the maximum absolute image difference luminance and luminance dynamic range capability limit, imposed by the current state-of-the-art of display technology, which is designed into the display system by its manufacturer.

Although the interchangeability of the outputs of the ALCs, offered by customizing the displays to allow them to interpret the common ALC output signals differently for each specific display being operated, would be quite desirable, the factors influencing the choice between the two control approaches described in this subsection, are both much more involved and, moreover, also more complex than has been described up to this point. In practice, the choice of methods used to implement automatic legibility controls in aircraft cockpits, involve a variety of design factors and potential tradeoffs, not yet considered in this report. Since these design factors can influence the legibility control accuracies that can be achieved in significant ways, these tradeoffs, and the factors influencing them, are considered separately in Chapter 7. Most of the other issues considered in this section are explored in greater detail in Chapters 6 and 7.

CHAPTER 6

Sensor-Video Signal Conditioning

In Chapter 5, the ability to achieve a faithful rendition of a real-world visual scene on a display was conditioned upon being able to achieve both a linear signal transformation between the real-world scene and the picture presented on the display, and a displayed picture having a luminance dynamic range equal to that of the visual scene being sensed. The display renditions of real-world scenes sensed using radar, infrared and a variety of other sensors, do not have a direct visually perceptible counterpart. Consequently, a faithful rendition of a real-world scene with one of these sensors is not well defined. For the purposes of this report, a faithful rendition of a real-world scene will arbitrarily be taken as a linear signal transformation between the sensed signals received from, or returned by, a real-world scene, and the image difference luminances used to render the signals as a picture presented on an electronic display, set to produce optimal legibility for a person viewing the picture, as previously defined in Chapter 5.

Because sensor signals are conventionally expressed in terms of electromagnetic variables, which have visually perceptible counterparts, for example, radiance and luminance, and irradiance and illuminance, these variables are often used to relate sensed scene variables to the variables used to characterize human visual responses to displays portraying the sensed signals. When this is done, the radiance dynamic ranges, of the signals detected by sensors, are frequently found to be much larger than the instantaneous luminance dynamic ranges of the displays, used to portray the signals. It should be noted, however, that since the sensor signal has no visual counterpart, the relationship between the dynamic range of the sensor signal and the luminance dynamic range of the electronic display is in reality arbitrary. For this reason, the signals sensed could with equal validity be scaled in amplitude, that is, compressed to permit the signal sensed to be displayed using the entire luminance dynamic range of the electronic display, or, alternatively, expanded to permit only a small portion of the sensor range to be depicted using the entire luminance dynamic range of the electronic display. In practice, the precise nature of this relationship is unimportant, if the information content the pilot needs to acquire, which is encoded within the signal sensed, can be controlled in a way that permits the pilot to extract the information successfully, when it is legibly displayed.

Achieving a faithful image rendition of the entire amplitude range of a real-world scene is often a valid objective for depicting sensor-video information on an aircraft cockpit display and, moreover, is a prerequisite if the pilot is to be given the capability to perceive the imaged presentation on the display as an accurate grey shade and color (i.e., if applicable) reproduction of the real-world scene, as sensed. Many situations exist, however, where the aircrew member's objective when using a display is not simply to see a replica of the real-world scene, as detected by a video sensor but instead is to extract the maximum amount of information, that is relevant to the mission segment being flown, from the sensed scene signals.

In this chapter, different signal conditioning methods are described that can be used to aid the aircrew in perceiving and extracting the grey shade encoded information contained in the sensor-video signals derived from real-world scenes. The approach used to attain this objective involves giving aircrew members the ability to enhance the legibility of the grey shade and, if present, the color encoded sensor-video information presented within a display picture, based on allowing the aircrew to exercise control over the sensor-video signals that are available for display. It is the capability of the human visual system to perceive any grey scale, of up to nominally a 100:1 luminance dynamic range, that allows this approach to be implemented. This visual capability, makes it beneficial for aircrew members to be given the ability to select and amplify small portions of the overall signal dynamic range sensed, and, in so doing, enhance the perceived contrasts between the resultant grey shades during their rendition on an electronic display.

The reason that military pilots need to be able selectively to enhance and control the information content presented, via the grey shade encoded images contained in pictures of real-world scenes rendered by cathode ray tube or other types of electronic displays in aircraft cockpits, is that the intensity modulated sensor-video

signals generated by radars, FLIRs, IR sensors, low light level TV sensors, CCD cameras and other imaging sensors, generally contains much more information than a pilot is capable of recognizing, identifying, and interpreting in a single complete dynamic range rendering of the information on the electronic display. As previously mentioned, the dynamic range of the signals returned by most video sensors are much greater than the instantaneous luminance dynamic range of both aircraft cockpit electronic displays and of the human visual system. Consequently, the scaled linear transformation of the sensor data results in a compression of the grey scale data being displayed. This result, in combination with the progressively more important role played by the human's ability to perceive grey shades, in visual tasks involving the recognition, identification and significance of grey shade encoded imagery, causes some information encoded in the sensor signal to be unusable by a pilot, even when viewing a faithful rendition of a real-world scene on electronic displays adjusted to provide optimum legibility. When properly implemented, signal conditioning can be used to compensate for the combined limitations of existing displays and of the human visual system. Even in reduced ambient illumination conditions, when the image contrasts of emissive and transmissive operating mode electronic displays can become very large, causing presentations of sensor-video pictures on these displays to be very legible, the luminance dynamic ranges over which grey shade relative luminances can be spread are still quite restricted in comparison to those of the sensor-video signal being displayed. The practical 100:1 upper usable limit for the luminance dynamic range of the human visual system (i.e., 20 dB) also makes it worthwhile to employ signal conditioning to enhance the transfer of information to the aircrew.

Providing the pilot and other aircrew members with signal conditioning controls that permit altering the displayed grey shade and/or color relationships contained in sensor-video signal information, to make the information easier to perceive and interpret, is most effective when implemented independently of the previously described techniques for controlling the legibility of an electronic display's image portrayals. Historically, the controls provided, for use with operational aircraft cathode ray tube (CRT) displays, have not separated the signal conditioning and legibility control functions. In spite of this, both manual legibility control, and automatic legibility control with manual legibility trim control settings by the aircrew, are more effective, when they are implemented to permit aircrew members to exercise separate control over the conditioning of sensed signal intensities and over the image difference luminance, and, hence, the luminance dynamic range of the displayed picture. This separation of these control functions permits the selection of the sensor signal grey shades and colors that are to be rendered on the display viewing surface to be accomplished independently of the settings of the legibility of that information when it is presented by the display.

Even though the preceding discussion was implicitly framed in terms of analog sensor to display signal transformations, signal conditioning can be applied with equal validity to sensor-video subsystems or display image generator computers that create digitized sensor-video signals and, consequently, display presentations rendered using quantized grey shades. In the event the information provided for display is in a digital format, additional consideration is required to account for the subjective and objective constraints the human visual system imposes on the number and spacing of grey shade levels encoded in the digitized sensor signals and rendered on the electronic display. This is particularly true in those situations where the output signals from sensor subsystems are digitized and must be compatible with the input requirements of electronic display subsystems interfaced through a digital computer.

Two factors tend to make sensor-video signal intensity conditioning more important now than has been the case in the past. The first factor is the trend toward the replacement of monochrome CRTs with color active matrix liquid crystal displays (AMLCDs) in both new and retrofit military aircraft cockpit installations. The second factor is the trend toward digitizing the intensity of sensor-video signals before display. Both factors, if not compensated for, can degrade the ability of aircrew members to control sensor-video information, in comparison to the historic control capability available using analog signals and the inherent information conditioning and presentation capabilities of CRT displays. Conversely, by compensating for these factors, significant improvements in the sensor-video information, made available for use by the aircrew, become possible.

The preceding considerations are explored in further detail in the discussion of sensor-video signal conditioning, and control techniques, in the balance of this chapter. In the first section below, the control of the information content contained in the sensor-video signals depicted on electronic displays is considered. This discussion is divided into subsections, which consider the effects of signal conditioning implemented first as an integral part of displaying the information, and, then when implemented to carry out signal conditioning before the information is displayed. Following this, the second section describes the appropriate signal conditioning for use with digitally encoded sensor-video signals. This section is further subdivided into the following three parts: the human's ability to perceive and extract information from pictures presented on digital displays; the digital processing and conditioning of sensed video signals before display; and special information processing considerations for color digital displays. In the third and final section, the legibility control and signal conditioning techniques for different types of electronic displays are compared.

6.1. Control of the Sensor-Video Information Content Depicted on Electronic Displays

Pilots, having experience using CRTs to display sensor-video information, expect to have access to brightness and contrast controls, not only to control the display legibility under night or changing daylight ambient illumination viewing conditions, but also to enable them to exercise control over how the information content of the sensor-video signal is displayed. Unlike the CRT display, which allows manipulation of the picture grey shade relationships after the video signal is processed for display, neither color LCDs, nor any of the other electronic display technologies that are potentially capable of depicting sensor-video signal information, possess this inherent grey shade control mechanism. Although the origin of this capability in the CRT display causes its effectiveness to be limited, this inherent grey shade control mechanism has nonetheless been very useful to aircrews seeking to enhance the information they can extract from video picture presentations, depicted on CRT displays.

The discussion of signal conditioning control and implementation techniques that follows is divided into two parts. In the first part, the concern is with the conditioning of the sensor-video signal, using control features that are inherent to the proper application of the display being used to render the sensor-video information. As an alternative approach to achieving effective signal conditioning, the second part of this section is concerned with applying conditioning to sensor-video signals, prior to their application to the video input terminals of the display. The first signal conditioning approach applies primarily to CRT displays, whereas the second approach applies to any type of electronic displays including the CRT.

6.1.1. Conditioning Sensor-Video Signals During Display

Adjustments to brightness and contrast controls represent the primary means, made available to aircrew members, for use in conditioning the information content of sensor-video signals, during their display on raster scanned CRT displays in aircraft cockpits. In the discussion of CRT display sensor-video signal conditioning that follows, the origin of the nonlinear effects, upon which the signal conditioning is based, is described, namely the incomplete Gamma compensation of CRT video displays. Next, the method used to condition sensor-video signals using CRT display brightness and contrast controls is described. Finally, an overview of CRT display signal conditioning capabilities and limitations is described.

6.1.1.1. Gamma Compensation of CRT Video Displays

An amplified sensor-video signal voltage, applied between the grid and cathode terminals of a CRT, is translated into a luminance emission from the CRT viewing surface, by the inherent nonlinear signal transfer characteristic between this signal voltage and the electron beam current that stimulates the phosphors in the CRT viewing surface to emit light. The resulting relationship is symbolically represented in the literature by an equation, which can be mathematically expressed in the following form:

$$\Delta L_e = K_{ge} v_g^{\gamma}. \tag{6.1}$$

In this equation ΔL_e is the emitted luminance of the CRT display, v_g is the amplified sensor-video signal voltage applied to the control grid, when it is negatively biased to the electron beam current cutoff point, K_{ge} is a grid voltage to emitted luminance conversion constant, for a particular CRT anode voltage setting, and γ is the power to which the grid voltage is raised to represent the nonlinear relationship between the CRT display's grid voltage input to emitted luminance output transfer characteristic.

To produce the linear transfer characteristic needed to render real-world scenes faithfully, a nonlinear compensation is applied to the sensor signal, before applying it as a grid voltage to the CRT, which can be symbolically expressed as follows:

$$v_g = (A\, v_s)^{\gamma_c}, \tag{6.2}$$

where A is the total amplification applied to the sensed signal, v_s is an analog voltage proportional to the sensed signal, and γ_c is the nonlinear compensation applied to the amplified analog voltage signal. Once this grid voltage signal is applied, the CRT emitted luminance can be symbolically represented, in equation form, as follows:

$$\Delta L_e = K_{ge}\left((A\, v_s)^{\gamma_c}\right)^{\gamma} = K_{ge}\,(A\, v_s)^{\gamma_c \gamma}. \tag{6.3}$$

If the value of the nonlinear compensation term, γ_c, is selected to satisfy the following inverse relationship, with respect to the grid voltage power term, γ, used to model CRTs nonlinear characteristic:

$$\gamma_c = 1/\gamma, \tag{6.4}$$

then the result is an approximately linear relationship between the luminance emission from the CRT viewing surface and the original sensed analog signal voltage. The final relationship, between the CRT emitted luminance and the sensor-generated analog voltage signal, can, therefore, be expressed as follows:

$$\Delta L_e = K_{ge}\left((A\, v_s)^{1/\gamma}\right)^{\gamma} = K_{ge} A\, v_s. \tag{6.5}$$

Linearizing the signal transfer characteristic of a CRT, in the manner just described, is referred to as applying a Gamma correction, where gamma, γ, is the power used to characterize the CRTs nonlinear transfer characteristic and the gamma correction, γ_c, is the power to which the amplified signal voltage is raised before applying it to the control grid. Numerical values of the parameter Gamma for CRT displays are typically in the range of less than two to more than two and a half.

To avoid introducing undue complexity into the presentation of the basic principles involved in Gamma correction, the specific details associated with the many types of interfaces between practical video sensors and electronic displays have been omitted or are greatly simplified in this chapter. This point is illustrated in the treatment of the preceding equations, which, while accurate relative to the overall input to output variable relationships of real sensor-video systems, gloss over the intermediate signal processing, transmission and signal adjustment steps needed to achieve a linear signal transfer characteristic between the sensed signals and the CRT display emitted luminance output. To be more specific, the preceding equations ignore the modulation or digital encoding of signals, their amplification in preparation for transmission, and the diverse means used to transmit the gamma compensated video signals from the sensor to display subsystems. In addition, following transmission to the display subsystem, the signal received can undergo several stages of amplification during the process of demodulating the signal, in preparation for its presentation on a display, or, if digitized, the signal could also be routed to an image processing computer for decoding before being sent to the display. Furthermore, for analog video signals, a variety of video interface standards exist, having the common feature of requiring that the video signals be incorporated into standard normalized formats, which permit the transmitted signals to be correctly interpreted when received by the display subsystems for display. The intricacies of determining the values of the Gamma corrections, and applying them to CRT displays, are also beyond the scope of this report, but are dealt with in detail in the literature, for example by Loughlin.[158]

Because nonlinear Gamma compensation characteristics initially rise quite rapidly and then rise more

slowly as the signal amplitude continues to increase, this causes a shift in lower amplitude portions of the signals to higher levels, a process called signal emphasis. Emphasizing the lower signal levels of sensed signals in this way gives the compensated signal a degree of noise immunity not shared by the original signal. For this reason, gamma compensations typically occur in the sensor rather than in the display subsystem, and as close to signal detection as possible.

Assuming the signal transmission path is linear, except for the CRT and its Gamma compensation in the sensor subsystem, the key to achieving an overall linear transformation between the original sensed signal and the emitted luminance displayed by the CRT is that each of the absolute voltage levels of the Gamma corrected signal must be aligned with the corresponding amplified absolute voltage levels on the nonlinear characteristic of the CRT, upon which the Gamma correction is based. This requirement, to achieve linearity, can also be stated in the following alternative equivalent forms: the minimum and maximum absolute voltage levels of the Gamma corrected signal must coincide with the corresponding minimum and maximum signal voltage levels on the CRT's nonlinear characteristic, or, the mean values of both the sensor and CRT signals must occur at corresponding points on both nonlinear characteristics, and the signals must span the same relative ranges on the two characteristics. In other words, only one value of the overall signal amplification and of the grid bias voltage applied to the grid to cathode terminals of the CRT can cause the voltage levels of the gamma corrected sensor signal, and the voltage levels applied to the CRT, to be aligned with the corresponding points on the matched set of nonlinear Gamma compensation and CRT characteristics, to produce an overall input to output response, which is linear, as represented symbolically by Equation 6.5.

Although, in special circumstances, a sensor and display that are directly connected could be designed to couple the direct current component of sensor signals through, the amplification, the gamma correction, the signal transmission and the application the signal voltage between the grid and cathode terminals of the CRT, this approach is difficult to implement in practice, and, consequently, is usually not used. The alternative is to transfer only the time variant portion of the signal. This approach results in stripping the direct current (dc) component from the total analog sensor-video signal, leaving the time variant portion of the alternating current (ac) signal voltage, which is, therefore, distributed about the mean value of the Gamma compensated sensor signals, including any synchronization pulses added at the blanking level of the signal. It is this ac voltage form of the signal that is typically transmitted to the display subsystem. Applying the correctly amplified Gamma compensated ac sensor signal voltage, and the correct dc bias voltage to the grid of the CRT, restores the proportionate dc voltage component and the proportionate signal amplitude scaling, present in the original Gamma's compensated sensor signal, and allows a linear translation between the original sensed signal and the emitted luminance output of the display to be achieved.

6.1.1.2. Conventional Aircraft CRT Display Conditioning of Sensor-Video Signals

The ability to use a CRT display to condition the relationships between sensor-video signal grey shades and those actually displayed, results from the fact that the linearization of the CRT's signal transfer characteristic is strictly valid at only the one grid bias voltage, and total sensed signal amplification, for which the Gamma correction is applicable. Because of this limitation on controlling the linearity of the CRT's signal transfer characteristic, each different setting of the grid bias voltage, and of the signal amplification, using the CRT brightness and contrast controls, respectively, produces a somewhat altered nonlinear signal transfer characteristic. This limitation is of little consequence for computer monitors and televisions, which are typically viewed in nearly constant low ambient illumination viewing conditions, but the need for aircrew members to control brightness and contrast to overcome the effect of CRT display legibility changes, with changing environmental conditions in aircraft cockpits, means these display controls are virtually never set to provide linear signal transfer characteristics. Although the application of different Gamma corrections to the signal voltage, to maintain a linear signal transfer characteristic, whenever the brightness or contrast settings are changed, would be possible, historically, this additional refinement would have been difficult to implement and does not appear to have been employed on televisions, computer monitors or military aircraft CRT displays.

Although the nonlinear effects introduced by the brightness control can be expected to be more pronounced than those caused by contrast control adjustments, the individual settings of the linear signal gain (contrast) control also produce nonlinear effects, even for brightness control settings that are equal to the Gamma compensated linearized transfer characteristic setting. This nonlinear effect is most easily described if it is considered as occurring in two phases, namely, the linear amplification of the gamma compensated sensor signals, prior to its application to the CRT as a grid voltage, and the nonlinear effect that the amplified grid voltage produces in the luminance emitted by CRT displays. In the linear amplification phase, the gain setting of the CRT establishes the amplification applied to the gamma compensated sensed signal voltage and, therefore, determines the upper and lower limits on the deviation of the amplified signal with respect to the grid voltage bias point. As the amplification is changed, the spacings between the adjacent signal grey shade levels change proportionately. Finally, the settings of the CRT gain control also play a key, but not an exclusive, role in establishing the luminance dynamic range of the picture displayed by the CRT.

In the second nonlinear signal transformation phase, increases or decreases in the peak to peak magnitude of the amplified video signal cause the individual grey shade levels, contained within that amplified sensed signal range, to translate (i.e., to move) to new locations on the CRT's nonlinear signal transfer characteristic. As the gain control settings change the spacings between the amplified sensor-video signal grey shade levels, this causes the spacings between the corresponding picture emitted luminance grey shade levels displayed by the CRT to experience different nonlinear deformations along the length of the Gamma compensated grid voltage to emitted luminance transfer characteristic. Due to the uncompensated nonlinearity of the signal transfer characteristic, some parts of the displayed grey scale range exhibit increased grey shade spacings, relative to the equivalent spacings in the sensed signal, whereas other parts of the grey scale range exhibit decreases in the relative spacings.

The saturation and cutoff points of the CRTs light emission imposes practical upper and lower limits, respectively, on the control that can be exercised over the emitted luminance grey scale contained within a display picture, and over the associated spacings of grey shades, using the brightness and contrast controls. Although the emitted luminance of a CRT can be controlled from cutoff to saturation, using the brightness control to adjust the grid bias voltage, the optimal setting of this control would in concept occur when the grid voltage bias point allows the gain control to be used to cause the highlight luminance of the sensed signal to reach the saturation point just as the black level of the signal reaches the cutoff point. This setting would allow the maximum legibility of the displayed picture grey scale to be achieved without compression of the grey shades through either saturation or cutoff of the emitted luminance. In practice, design constraints imposed on the amplification applied by the gain control would limit the excursions of the sensor-video signal to the grey scale range the display is intended to portray.

For television and most other CRT displays intended to depict sensor-video information, illuminated test charts containing standard grey scales, are used to set the gain applied to the sensor-video signal in preparation for displaying grey shade and chromaticity encoded information. Following this procedure, causes an upper limit to be imposed on the contrast control settings, which permits the relative luminance levels, that is, the grey shade levels, of the grey scale charts rendered in the CRT picture, to be controlled from very low levels of signal amplification, where essentially none of the displayed information is visually discriminable, up to values somewhat greater than those needed to cause a match between the displayed grey shades and the relative luminance levels of the Electronic Industries Association standard grey shade charts, sensed by the video camera. As described in Section 5.3, the grey shade levels on the EIA chart range from a maximum of 60%, to a minimum of 3%. Matching these grey shades to those rendered on the displays establishes a correct gain setting to render real-world scenes sensed by the video camera accurately, and typically allows the required 90 to 3% relative luminance range of real-world grey shades to be correctly rendered on a display having a maximum contrast of about 29. While this setting of the displayed grey scale required using most of the limited emitted luminance control ranges of early televisions, severely restricting the range of useful brightness control possible, this is not true for existing aircraft cockpit CRT displays, which exhibit larger ranges of emitted luminance control. The need to use the brightness control on aircraft CRT displays to control the emitted luminance range in which the display grey shades are portrayed, to make them legible, is the principal

origin of the problem of achieving and maintaining adequate gamma compensation for aircraft cockpit CRTs, however, as stated above, this is also the reason brightness and contrast controls can be used for conditioning the sensor signals portrayed by these displays.

6.1.1.3. An overview of Conventional Aircraft CRT Display Signal Conditioning

Because the contrast control of the CRT display simultaneously sets both the sensor-video signal amplification and the luminance dynamic range of the display, it not only controls the maximum perceived contrast of a displayed grey scale but also the highlight image difference luminance level that can be rendered in a displayed picture, subject to the setting of the brightness control and for a particular setting of the CRT anode voltage. Unrestricted increases in the contrast control would eventually cause the excursions of the amplified sensor-video signal about the grid bias point to reach either the emitted luminance saturation or cutoff limits of the CRT. Whether the upper or lower emitted luminance limit of the CRT would be reached first as the gain control setting is increased is dependent on the setting of the grid bias voltage (brightness) control. If still further increases in the signal amplification using the gain control were permitted, first one end and then the other end of the signal grey shade range would not be displayed, however, the spacings between the grey shade levels in the balance of the range displayed would continue to increase, making the grey shade encoded information depicted there more legible. Although the interdependence of the signal conditioning and legibility control features of CRT displays, make it impractical to use CRT contrast and brightness controls in this way, creating these signal display capabilities in the pictures depicted on CRT displays is possible, by controlling the sensor-video signal information content encoded into the composite video signal transmitted from the sensor to the CRT for display, as is described in Section 6.3. These capabilities aside, the combined effect of changing the settings of the brightness and contrast controls on existing aircraft cockpit CRT displays, still allow different regions of the signal intensity range to be emphasized or de-emphasized, and their corresponding displayed grey shade spacings to be expanded or compressed, respectively.

The combined effect of the CRT's brightness and contrast controls, on the image difference luminance levels of sensor-video information displayed, is often difficult for the person using a CRT display to visualize. A convenient analogy occurs for the magnification and demagnification of image scenes using optical lenses. By using zoom magnification, a smaller area of a large area scene can be viewed in greater detail. The disadvantage of this linear spatial transformation is that only the magnified portion of the visual scene remains visible and the balance of the field of view can only be viewed by moving the magnified area with respect to the complete scene that was being viewed before magnification. This disadvantage can, in part, be overcome by using a lens that magnifies at its center, demagnifies at its edges and leaves the total field of view unchanged. The result of this nonlinear transformation is that some parts of the visual field are spatially distorted in comparison to others, making the imagery portrayed in distorted areas of the scene potentially more difficult to recognize, identify and interpret correctly. Some wide angle (fish-eye) lenses for cameras utilize this technique. This nonlinear spatial transformation technique is directly analogous to the effect that CRT brightness and contrast controls can create, with respect to the total dynamic range of the intensities displayed on a CRT. For the CRT, the top, center or bottom of the signal intensity dynamic range can be amplified (emphasized) with the balance of the range compressed (de-emphasized), so that the total dynamic range of the signal remains unchanged.

Aircrews are familiar with adjusting the contrast and brightness controls of CRT displays to enhance the grey shade perceptibility of the imagery portrayed on electronic displays depicting sensor-video input signals. Unfortunately, the results obtained by operating these two controls is not predictable. This is true because the process, for achieving the desired enhancement of the picture, involves trial and error, keyed to making the portion of the displayed signal intensity range containing the picture information of interest, more legible and interpretable, at the expense of a compression of the balance of the displayed signal range. A limitation on the ability of the aircrew to use this control technique successfully is its dependence on the ambient illumination incident on the display, or on the glare source luminance incident on the aircrew member's eyes, being at low enough levels so that the manual brightness and contrast controls do not have to be used for their intended

purpose, under high ambient illumination viewing conditions, that is, to keep the display information legible.

Based on the preceding assessment, it can be concluded that adjustments by the aircrew to the CRT's brightness and contrast controls can be used to produce selective enhancements in the legibility and, therefore, the recognizability, identifiability, and interpretability of sensed scene pictures, rendered on a CRT display under sufficiently low ambient daylight and night viewing conditions. Unfortunately, due to the unpredictable nature of the grid bias (average brightness) controlled interaction between the gamma correction applied to the sensor signal and the nonlinear transfer characteristic between the CRT's grid-cathode voltage and its anode current, the signal grey shade enhancement achievable by aircrew members using brightness and contrast control settings of the CRT are neither predictable nor reproducible by the aircrew. Because of this latter limitation, the times required to condition signals can often be excessive to the point of not lending themselves to being used, by a single pilot performing high workload mission segments.

Even though the methods used to generate sensor-video picture information on CRT displays provide an inherent signal intensity conditioning capability, other electronic displays, and in particular the color AMLCDs being installed in new and retrofit military aircraft display installations, do not possess this inherent capability to condition the grey shade encoded sensor-video signals depicted in pictures presented on these aircraft cockpit displays. Thus, while the single manual or automatic control used to adjust luminance emitted by a LCD backlight, and, consequently, the highlight white image difference luminance of the display, does, for example, perform essentially the same dimming function as a CRT's brightness control, it does so without introducing the nonlinear signal transfer function, used by the CRT to permit signal conditioning. In other words, the methods described previously in this report to control the legibility of electronic displays do not include a signal conditioning capability. For this reason, an alternative means to provide signal conditioning for electronic display picture portrayals should be provided, when electronic displays other than CRTs are used. This subject is considered in greater detail below.

6.1.2. Conditioning Sensor-Video Signals Prior to Display

A more effective technique for implementing the signal conditioning, needed to permit aircrew members to make controlled enhancements to information content presented on a display, is to use a separate means to control the amplification, or attenuation, and voltage offset of the sensor-video signal amplitude sensed. Moreover, the insertion of this control capability in the sensor should occur before standardizing the signal and applying any necessary nonlinear compensation to linearize the overall transmission and display of the information, and should be independent of the controls used to adjust the CRT or other electronic display for optimum picture legibility. As previously described, to achieve and maintain optimum picture legibility when using an automatic legibility control, a minimum of one, but preferably two, legibility trim controls are needed by aircrew members to adjust the image difference luminance, if the legibility of an electronic display is to be maintained at a constant level, independent of the ambient illumination incident on the display and glare source luminance exposure of the pilot's eyes. Irrespective of whether the legibility of the display is implemented using an automatic or manual control technique, electronic displays only require a single control input to perform the legibility control function.

If properly designed and temperature compensated, liquid crystal and other electronic displays (i.e., including the CRT, under restricted operating conditions) can have fixed linear input sensor-video signal voltage to output image difference luminance transfer characteristics. These transfer characteristics make it possible to condition the sensor-video input signal, prior to its transmission to the display, in a variety of ways, to satisfy the display information presentation objectives of aircrews. The two major categories of signal conditioning control can be categorized as linear and nonlinear transformations. Linear transformations correspond to the aircrew selecting a grey shade intensity range, from the total dynamic range of the sensor signal, and then linearly amplifying that range, to cause it to match either the full black to white luminance dynamic range that the electronic display can render, or a controlled fraction of that dynamic range. The nonlinear transformations of interest would be similar to the linear transformations just described, but would

allow an aircrew selected amplitude range, to be amplified and displayed, along with a correspondingly compressed version of the balance of the full dynamic range of the sensor. This approach permits the full signal range capability of the sensor to be visually monitored, while still allowing a selected range of signal grey shade amplitudes to be expanded for examination in greater detail.

In the event that an aircrew member can see that only part of a sensor's signal grey scale range contains the information being sought, then this fraction of the sensor's total dynamic range capability can be selected and linearly scaled (i.e., amplified), to permit full utilization of the entire white to black luminance dynamic range rendition capability of the display. The advantage of this approach is that the aircrew could learn target signatures more easily, and, afterwards, should be able repetitively adjust the display to achieve recognizable target signatures, since the signal gray shade relationships are not distorted by the linear signal amplitude scaling transformation process. As an example of a signal that would benefit from this type of conditioning, the video signals generated by infrared sensors, detecting an external scene during the summer, would not contain signal intensities corresponding to the lower temperatures of winter, and, therefore, part of the signal range that the sensor can detect is not needed. It should also be noted, that the linear amplification of real-world visual scene signal amplitudes does not require any adjustments to the legibility settings of the display and still results in the portrayed display images being perceived by aircrew members as faithful renditions of previously learned target signatures. For example, the result of signal amplitude scaling could be to restore the grey shade signatures of mist, fog, haze or glare enshrouded targets, to the range of grey shades associated with the same target, when viewed under higher visibility conditions.

As an alternative to direct manual control of the sensed signal amplification and offset, a comparative grey scale legend with markers that can be adjusted by the aircrew to the upper and lower limits on the grey scale range in the picture, which the aircrew wants to have amplified, could, for example, be provided to limit the workload of the aircrew, when using this manual signal conditioning technique. A method of automatically determining the range of sensor grey shade intensity levels that are useful to an aircrew member, and of and linearly scaling the selected sensor signal amplitude range to the corresponding emitted luminance range for display, would be preferable to manual control. However, even if the grey scale range to be amplified is to be determined automatically using computer processing of the sensed signal, controls would still have to be provided, to permit aircrew members to make trim control adjustments to the range of signal intensities to be displayed. A control capability, to permit an aircrew member to toggle quickly between the full dynamic range of the sensor, and the reduced range of signal amplitude scaling, set by the aircrew, would also probably be needed. The design of an effective, efficient and intuitive method of effecting aircrew control over the sensor signal amplitude range being displayed would be a very important element in the development of any type of sensor-video signal conditioner.

Methods of achieving truly nonlinear sensor-video signal intensity to display luminance transformations, which are both useful and easily controllable by the aircrew, would be much more difficult to achieve than would be the linear signal transformation techniques, just described. The automatic detection of the sensed signal intensity range, or ranges, that are to be expanded, to limit the aircrew's manual control adjustment requirements, would also be desirable for nonlinear signal intensity to display luminance transformations. For nonlinear transformations, not only must the signal intensity range, which includes the information of interest to the aircrew, be detected and amplified (i.e., intensity scaled) for display, but the sensed signal ranges both above and below the amplified range would have to be condensed to permit their simultaneous display. The principal advantage of this nonlinear approach to signal conditioning, as compared with the nonlinear conditioning described previously for CRT displays, is that the nonlinear transformations of the sensor signal amplitudes, carried out for the purpose of signal conditioning in preparation for display, are subject to control by the designer, solely to enhance the information content being displayed, rather than being integrally related to the control of the brightness and contrast of CRT displays.

For nonlinear signal conditioning, an assessment is also necessary to determine whether the nonlinear transformations should be piecewise-linear, that is, with different linear signal amplifications and attenuations in different ranges of the sensed signal intensity dynamic range, or whether the amplification and attenuation

changes should be continuously variable, as a function of the sensed signal amplitude, within the total signal amplitude dynamic range. Like the display of linearly transformed sensor signal outputs levels, consideration would have to be given to devising intuitive control techniques, which would permit the aircrew to learn how to use the signal conditioning controls to achieve the same scene grey shade enhancement effects, both predictively and repetitively.

A significant advantage for either linear or nonlinear conditioning of sensor signals prior to display, in comparison to the composite legibility and signal conditioning control of CRT displays, is that the signal conditioning and the legibility of the displayed grey shade information can be separately and independently controlled. The signal conditioning controls allow the sensor-video signal grey shades, rendered on a display's viewing surface, to be changed by the aircrew by showing either more, or less, of the sensor-video signal range. These controls, therefore, cause the information contained in the displayed picture to be changed to suit the aircrew member's needs for information. As an indirect consequence of the changes made in the signal information being rendered on the display, and as a direct result of changes in the relative luminances and contrasts between grey shades depicted in the pictures displayed, the information being displayed could also be characterized as undergoing a change in legibility. This "information legibility" must be distinguished, and treated separately, from the image legibility of the display picture's grey scale range portrayal capability (i.e., the legibility with respect to the background luminance reflected from the display surface or with respect to the veiling luminance induced in the pilot's eyes, described elsewhere in this report), which is not altered by changes made to the information depicted within the display picture, by using signal conditioning.

6.2. Signal Conditioning for Digitally Encoded Sensor-Video Signals

The principal advantage of converting sensor-video signals from an analog to a digital format is that doing so provides a level of immunity to the pickup of noise, as the signals are transmitted and processed for display, which is not achievable with analog sensor-video signals. A potential disadvantage of digitizing these signals is the possible loss of information between the sampled signal grey shade levels. This disadvantage can be minimized and effectively eliminated by displaying a sufficiently large number of sampled grey shade levels from the sensed signal amplitude dynamic range. Practical limitations on the variations in the video signal intensities that are capable of conveying useful information, places limits the number of discrete grey shade levels that have to be digitally encoded. In addition, the combined effect of the perceptual capabilities of the human visual system and the cognitive processing capabilities of the mind, further limit the number of discrete grey shades needed to render a picture on a display, so that a digitally sampled rendition of the sensed real-world scene cannot be visually distinguished from a continuous rendition of the original sensed scene. While the digitization of sensor signals adds no new noise after the signal is encoded, it does not eliminate the need to provide compensation for displays having nonlinear response characteristics.

Digitally encoded electronic displays, capable of depicting graphic and sensor-video information, typically display information stored in refresh memories, containing a memory-mapped picture frame of the information to be displayed. While the display picture is being refreshed, new information to be displayed is being stored in an identical picture frame update memory. When the storage of a new picture frame is complete, the two memories are swapped, and the updated information is displayed while a new picture frame of information is stored. Because each of these picture frame memories must store the grey shade information for each pixel in the display surface, and for each of the display's primary colors for a color display, an analog to digital conversion process that encodes many signal levels and chromaticities usually costs much more than one that encodes a smaller number of levels. To reduce this cost, sensor-video display systems tend to be built using the fewest number of digital sampling levels possible, to achieve a result that is subjectively acceptable to the pilot. This section is devoted to a generalized description of methods of manipulating and digitally encoding sensor-video signals to reduce the number of digitized grey shade levels the system is designed to use, without degrading the signal intensity information that can be conveyed to an aircrew member in a picture, depicted using a digitally encoded electronic display.

As previously indicated, the success of the aircrew's signal conditioning control adjustments to enhance the presentation of the scene information being portrayed by an electronic display, depends on the availability of an input sensor-video signal, which is either analog, a signal that is continuous in the sensed signal amplitude range, or digital, a signal that has a sufficiently large number of sampled amplitude levels to convey the same information as its analog counterpart. When the signals, sensed or processed for display, are digitized, this raises two important issues not shared by analog display presentations of sensor-video information. The first issue involves the cognitive processing of visual information by a human and a determination of how few discrete grey shades are required by a human viewing a digitally rendered scene to be able to achieve, as a minimum, objective performance as good as can be achieved when viewing an analog rendered scene or, as a maximum, to create a subjective appearance of grey shade continuity. The second issue relates to how to digitize the sensor, or processed display, signals so that the resultant display presentations are both accurate representations of the sensed signals, and so that the signal conditioning remains as effective as it is for analog rendered scenes.

6.2.1. Human Perception and Extraction of Information from Pictures on Digital Displays

The limitation of either the sensor's video output signals or the electronic display's video input signals to discrete samples, causes the imagery to be rendered using discrete grey shades, rather than as continuous analog presentation of the sensed signals. This raises the possibility that important signal information will not be displayed, and, moreover, causes the scenes rendered to take on the subjective appearance of a terraced terrain landscape, due to the often quite noticeable stepped differences between adjacent picture grey shades. This issue is, therefore, concerned with how well a human perceives and can cognitively extract and process useful information from displays that render their video picture information using visibly discrete digitized grey shades.

Although visible discrete grey shade steps are commonly interpreted as detracting from a user's ability to extract useful information from a display's video image presentations, this impression is not born out either by the theory of vision, as it relates to the electrophysiology of the visual system's operation, or by experimental investigations conducted using discrete grey shade encoded sensor-video information. Viewing real-world scenes gives the impression that vision is continuous in the distribution of the temporal, spatial and color variable dependences of the luminance functional that characterizes the viewed scene. Contrary to the impression that visual perception is continuous, the theory of vision, that is, the accumulative result of physiology-based experimental evidence and its interpretation, assembled over many years, shows these dimensions of vision are discretely sampled by the light receptors in the eyes and then cognitively reconstructed by the brain, so as to create the impression of continuity.

From a psychology-based experimental standpoint, the most directly applicable results encountered in the literature were those obtained by Rogers and Carel. Their target recognition study investigated the number of discrete equally perceptible grey shade levels that are needed to take full advantage of the human's ability to perform image detection and recognition tasks on targets, such as a straight bed truck, a two and a half ton truck, a semi-tractor, a jeep, an armored personnel carrier, a tracked howitzer and a helicopter, when the targets were presented from an aerial perspective as an integral part of real-world scene depictions. Rogers and Carel used a raster-scanned CRT display, to depict a sequence of television camera sensed pictures of military target scenes, rendered using progressively larger numbers of digitally encoded grey shades that were adjusted until they were perceived as equally distributed, over the full luminance dynamic range of the display. The test results showed that the increase in test subjects' objective performance reached a maximum plateau level, while depicting only a few discrete grey shades for target detection, and with no more than eleven, and possible as few as eight, discrete grey shades for target recognition.[159]

Care must be taken, not to read too much into the preceding Rogers and Carel result, and, in so doing, cause the significance of the result to be misinterpreted. While it is true that the result shows that the human only requires a small number of clearly legible stepped grey shades to recognize targets, and even a smaller

number to detect them, the conditions tested by Rogers and Carel represent only a subset of those experienced by aircrew members under operational mission conditions. The simplest way to illustrate this point is to describe some of the discrete grey shade presentation issues not addressed by the Rogers and Carel investigation.

The first grey shade presentation issue, not adequately considered by the tests conducted by Rogers and Carel, is a practical limitation placed on the visual tasks that had to be performed by their test subjects. Although the historic uses of electronic display presentations of sensor-video information in aircraft cockpits have typically been restricted to the conduct target detection and recognition tasks, and, therefore, are consistent with the testing performed by Rogers and Carel, this limitation is predicated on the relatively low spatial rendition capabilities of historic aircraft CRT displays. The higher image quality and spatial image rendition capabilities of dot-matrix displays make it more likely that these displays would, in addition, be used for the higher level mental information processing tasks of image identification and interpretation. Image identification involves, for example, the friend or foe identification of a vehicle, which has already been recognized as a tank. To make the identification of the type of tank possible requires the discrimination of smaller spatial visual features of the tank, such as the configuration and number of track wheels or other target signature features and markings. Image interpretation involves, for example, the threat status posed by the target, which often requires resolving even smaller spatial features of the target. The point is that if these higher level tasks had been investigated they would likely have produced a requirement for a larger number of discrete grey shades to be displayed. It is known that as the size of the critical detail dimensions of targets that must be discriminated becomes smaller, the need to be able discern smaller gradations in grey shades also becomes more important, and this is particularly true for military targets, which use camouflage to hide or disguise the signature features of visual targets.

The second grey shade presentation issue not considered by the tests conducted by Rogers and Carel is less than ideal viewing conditions or reductions in target visibility due to other causes. Ideal viewing conditions, as employed here, refer to the use of the full luminance dynamic range of the CRT display to render the high legibility target scenes used in their investigation. While the tests conducted by Rogers and Carel shows that only a small number (i.e., eight to eleven) of equally spaced discrete grey shades are necessary, for example, to perform their image recognition task, the study did not investigate how much smaller discrete grey shade spacings could become before the number of grey shades required to render a target scene, at the same level of image recognition performance, changes.

Direct observations of real-world scenes, and experimental investigations of the perceptibility of much more closely spaced grey shades, would suggest that targets, of the same size and legibility, but rendered on electronic displays using reduced grey scale spacings, would produce similar target recognition test results. In real-world viewing conditions, humans' learn to detect, recognize, identify, and interpret familiar targets having progressively reduced grey shade spacings through experience gained when viewing the targets in the presence of glare, haze, mist, fog, rain and snow. Each of these reduced visibility viewing conditions alters the legibility of a target scene. All of them compress the perceived grey scale range of the target. Some of them also attenuate the grey shade luminance levels emanating from the target. Still others scatter light emanating from the target into the eyes, causing the target also to appear progressively more blurred as the visibility decreases. A common source of legibility degradation, in each of these examples, and the only legibility degradation effect of interest, in this instance, is the compression of the target grey scale. In each case, the compression of the target grey scale is caused by the interposition of light reflections between the retina of the eyes and the target. This superposition of reflected light between the target and the eye's light receptors results in the perceived background luminance being increased, the image difference luminance of each grey shade being reduced and the respective perceived contrasts and grey shade spacings of the target being correspondingly reduced. Even with relatively high visibility conditions, this effect is responsible for the faded appearance of targets viewed at large ranges and becomes more pronounced when the humidity level is high.

The final grey shade presentation issue not considered by the experimental investigation Rogers and

Carel is the size of the set of targets used for the test. While the number of different targets investigated by Rogers and Carel was reasonable, for the purposes of their test, that number was still quite small in the context of the targets that could be experienced by operational aircraft pilots and aircrews. Larger target sets, including both military and civilian vehicles, could add to number of discrete grey shades required to recognize a target, due to the larger size of the set of target signatures the aircrew must be able to recognize. Adding additional vehicles, to permit friend or foe identity distinctions to be made, could also lead to an increase in the number of grey shades needed for target recognition, due to the further increase in the size of the target set the observer must distinguish among to identify targets correctly. The point is that even for ideal viewing conditions, the number of grey shades needed to permit targets to be correctly recognized is not all that definitive and could vary somewhat from the Rogers and Carel findings.

To eliminate visually perceptible steps between grey shade levels, that is, to cause the stepped variations in luminance be perceived as continuous, would require a much larger number of equally spaced steps than would be necessary to meet the needs of aircrews for the detection, recognition, identification or to interpret the significance of target imagery. Luminance steps of nominally 1-2% of the display pictures maximum emitted luminance are adequate to reduce this effect to the point it is not noticeable in practical electronic display applications in aircraft cockpits.

6.2.2. Digital Processing and Conditioning of Sensed Video Signals Prior to Display

Factors influencing the digitization of sensor signals either directly, or indirectly, while they are being processed for display, are considered in this subsection. The objective of the digitization and information processing of sensor signals is to cause displayed presentations of discrete grey shades that provide accurate representations of the analog signal amplitudes sensed, and also convey the information the aircrew needs to perform their mission. The issue of applying signal conditioning to a digitized sensor signal, so that the resulting rendition of the scene remains as effective as it is for an analog rendered scene, is also considered.

Although the experimental results of Rogers and Carel show that as few as eight and no more than eleven equally perceptible digitized grey shades should typically be adequate to make a target recognizable, as was alluded to above, a variety of reasons exist for expecting that additional grey shades could be required to render sensor-video display presentations of real-world scenes accurately. One way to minimize the number of discrete grey shades that need to be displayed is to convey information to the aircrew using grey shades distributed with perceptually equal spacings over the dynamic ranges of the sensor and the display. The small number of grey shades found by Rogers and Carel investigation, to be associated with target recognition, is attributable to the fact that they adjusted the discrete grey shade levels, used to render their video pictures, until each of the grey scales tested was perceived to be equally spaced.

To define an accurate equally perceptible grey scale, would require the use of Table 5.2 to determine the luminous reflectance values that correspond to equal 1943 Munsell Value scale steps. Equation 5.50 would then be used to convert the luminous reflectance sampling limits from the table, for each grey scale level, into the relative luminance level ranges to be used for sampling. For example, using a 1943 Munsell value scale that spans the range from 2 to 9.5, a difference of 7.5 and a luminous reflectance range from 3 to 90%, a grey scale with 16 equally perceptible levels, and having Munsell value spacings of 0.5 between each of the discrete grey shades to be displayed, could be encoded with a 4 bit binary code word. Signal intensities in the range of from ± 0.25 from the discrete grey shade level to be displayed would be encoded at the corresponding luminous reflectance level.

If only a few equally perceptible grey shades are to be displayed, such as the sixteen in the previous example, then the inclusion of provisions to avoid the display of visually perceptible fluctuations between adjacent grey shade levels also becomes necessary. These fluctuations can be produced by even very small variations in the signal intensity, which happen to occur at the transition between grey shade signal encoding ranges and, therefore, at the transition boundaries between displayed grey shades. To avoid this distracting

visual effect, signal intensity hysteresis would have to be incorporated into the analog to digital conversion process at the grey shade transition boundaries. In the event this problem is not eliminated it can cause a perceived movement of image edges similar to the image jitter sometimes seen in CRT imagery. With a sufficient increase in the number of displayed grey shades, and with the corresponding decrease in the spacings between adjacent grey shades that this causes, this effect becomes imperceptible, thereby eliminating the need for signal intensity hysteresis processing of the sampled signal.

To implement an approach for sampling signals, so that it is consistent with the presentation of equally perceptible grey shades, would require the design of a special purpose analog to digital converter, capable of sampling the sensor-video signals at spacings scaled to match the nonlinear relative luminance level spacings corresponding to the equally perceptible grey shades to be displayed. Such an A/D converter would have to perform the following functions: sample the sensor signal amplitude; assign the sampled signal to the appropriate equally perceptible grey scale step level; encode the grey shade number that represents the signal from the sampled range; and transmit the code for the grey shade level to the display image generation computer. A typical display image generation computer using this approach, would, upon receipt of the coded grey shade levels, store the respective grey shade codes or display drive level in the picture frame update memory locations, corresponding to each pixel in the display surface, and in three or more memory locations for each pixel in color displays. When the complete picture frame of pixel information has been stored, then the refresh and update memories would have to be interchanged. The information stored in what has now become the refresh memory would be used to apply appropriate drive levels, to cause a scaled match between the displayed relative luminance levels and the originally encoded signal levels. The accuracy of this approach is limited primarily by the step spacings of the sensor signal sampling employed and the repeatability of the display drive levels. Because the grey shade step spacings decrease with the addition of sampled grey shade levels, this also causes an increase the accuracy of the grey scale rendition of the sensor signal. The higher accuracy of the signal amplitude display rendition is, however, achieved at the cost of larger code word and memory storage bit capacities.

Although the sampling of the sensor signals, to provide display presentations using equally perceptible discrete grey shades, allows minimizing the size of the encoded pixel bit codes and, therefore, of the bit storage capacities of the interchangeable memories used to store the display picture frame refresh and update information, several alternatives exist to this approach, which are only slightly less accurate. Some of these possibilities will be briefly considered but, as for the equally perceptible grey shade case, not in detail.

Using a linear analog to digital (A/D) converter produces grey shade steps that are numerically equal in magnitude throughout the grey scale range, rather than being perceptually equally spaced. To be able to match the small numerical magnitude of the equally perceptible grey shade steps that occur at low signal amplitudes and display luminous reflectance levels, to the numerically equal grey shade steps, produced using a linear A/D converter to sample the sensor signals, forces all of the linear grey scale steps to be of the same small size. By comparison, a sensor signal sampled to display equally perceptible grey scale steps has progressively larger sensor signal and luminous reflectance step sizes as the signal amplitude increases. The result of linear A/D conversion is, therefore, many more grey shade levels than are required using the equally perceptible grey shade spacing criteria.

Much of the basic grey scale information presented in this subsection was taken from an earlier report[160] and the article,[161] previously cited in Chapter 5, in relation to the rendition of grey scales. Figure 2 of the article compares an eight-shade grey scale, which uses the 1943 Munsell Value scale as the basis for its perceptually equally spacings, with the grey scale steps that would be produced by 3, 4 and 5 bit linear analog to digital converters. This comparison shows that the 32 level, 5 bit, A/D converted linear grey scale is the minimum required, to provide grey shade steps equal to or smaller in signal intensity or luminous reflectance than the lowest step of the eight level equally perceptible grey scale. Because of the progressively larger numerical step sizes of the eight shade equally perceptible grey scale, the 32 level linear grey scale provides eight steps, within the highest signal amplitude or luminous reflectance step of the equally perceptible Munsell grey scale. It should be noted that while displaying the 24 extra A/D converted grey shade levels of the preceding example

could potentially convey additional information from the video signal, the extra levels would be more effective if they were perceptually equally spaced rather than being concentrated near the top of the linear grey scale.

A method of producing an approximately perceptually equally spaced grey scale, while also reducing the display system memory requirements needed to display the information, can be described in terms of the linear A/D converter grey scale example of the preceding paragraphs. This method involves encoding the signal using a linear analog to digital converter, as before, but then assigning new code values to the numerically equally spaced grey shades that most nearly match the equally perceptible levels of the sensed signal using a digital computer. Using this method would require the remaining 24 of the 32 levels produced by the A/D converter to be assigned the same codes as the nearest approximately perceptually equally spaced grey shade levels. By causing the display to produce grey shades that are proportional to the eight sensor signal levels sampled, which most closely match the corresponding equally perceptible levels, then the grey shades would only be approximately equally spaced, however, each level would be an accurate representation of the sampled sensor signal and could be represented using only a three bit code word, rather than the 5 bits needed to encode the 32 output levels of the A/D converter. Except for the fact that the eight levels are only approximately equally spaced, this method has all of the advantages, and produces results, equivalent to the perceptually equally spaced grey scale method previously described, except that the earlier example was for a four bit code word, sixteen level grey scale, rather than for a three bit, eight level grey scale.

As an alternative to increasing the bit encoding level of a linear A/D converter to make the digitization more effective, a nonlinear transformation could be applied to the signal, which is similar to the previously described Gamma function correction applied to the sensor signal to linearize the transfer function of a CRT display. The purpose of this nonlinear transformation is to expand the lower end of the sensor signal range selectively, to cause equally perceptible sensor signal voltage levels to produce approximately equal magnitude voltage levels for sampling, that is, voltage levels that are directly analogous to the equal steps of the Munsell value scale. Stated in another way, the transformation is intended to approximately align the equally spaced voltage sampling levels, v_s, of a linear analog to digital converter with the corresponding relative sensed signal levels, represented by the analog voltage, v_a, that correspond to equally perceptible sensor signal grey shades.

One viable candidate equation for carrying out this approximate nonlinear transformation presents itself in the form of the 1915 Munsell value scale, which can be represented by the following equation:

$$V = 10\left(\frac{Y}{100}\right)^{1/2}. \tag{6.6}$$

This equation expresses the relationship between the Munsell Value, V, and the luminous reflectance, Y, expressed as a percent. Plotting this equation with the logarithm of V as the ordinate, and with the logarithm of Y as the abscissa, the graph is a straight line with a slope of one half. In comparison, the 1943 Munsell value scale does not plot as a straight line when graphed against full logarithmic axes. It does, however, produce results similar to those for the 1915 Munsell value scale for luminous reflectances between 1 and 100%. Equal Munsell value steps for the 1943 scale produce slightly larger steps between the grey shades, for relative luminances above about 20%, about the same sizes steps between 20% and 5%, and slightly smaller step sizes between about 5% and 1%. For equal Munsell value steps below a luminous reflectance of 1%, the 1943 Munsell value scale has progressively smaller grey scale spacings, than is the case for the 1915 Munsell value scale, and in this range the latter grey scale is no longer a reasonable approximation for the former.

By direct analogy to the above equation for the 1915 Munsell value scale, the desired signal transformation equation can be expressed, using an equation similar to the previously introduced nonlinear Gamma correction equation, as follows:

$$v_s = A\, v_a^{\gamma_c}, \tag{6.7}$$

where setting the Gamma correction term, γ_c, equal to

$$Y_c = 1/2\,, \tag{6.8}$$

completes the analogy. The application of the transformed sampling voltage, v_s, to the input of a linear analog to digital converter, with the amplifier gain, A, set to provide the required input signal voltage range to the A/D converter, allows a binary coded word to be directly generated for each equally perceptible grey shade level sensed. A display image generation computer, upon receiving the grey shade level encoded words, would have to cause the appropriate display pixels to be activated, at discrete relative luminance drive levels preselected to be consistent with the respective relative grey shade levels of the original sampled sensor signal levels. To achieve an accurate display rendition of the discrete grey shade encoded signals using this technique, requires that the displayed grey shade drive levels be selected, to cause the image difference luminance levels to match the relative luminance levels obtained, by converting the perceptually equally spaced luminous reflectance values predicted by the 1915 Munsell value scale, using Equation 5.50. It is unlikely that the small deviations from equally perceptible spacing that result from the use of the 1915 rather than the 1943 Munsell value scale would suffice to alter the aircrew's performance.

The linear and nonlinear signal conditioning techniques for analog signals, described earlier in this section, are dependent on being able to take advantage of the fact that the sensor signal contains signal intensity variations that, while visually discernable in the display video presentation, are only capable of causing the video imagery they depict to become recognizable, identifiable and interpretable by the aircrew when the range of signal intensities containing the variations has been further amplified. For a digitized signal to produce comparable results, small but usable variations of the sensor-video signal must be sampled at a sampling rate of at least twice that of the variation in the signal intensity, that is, based on using the Nyquist Criterion, if the information contained therein is to be displayed.

If an aircrew member is to know, from viewing the sensor-video scene picture rendered on a display, that a very small signal intensity anomaly is available for amplification (i.e., signal conditioning), that anomaly would have to be visually perceptible to permit further information to be acquired, from the sensor-video scene being presented, through the use of signal conditioning. Applying the Nyquist sampling rate to the situation just described would, in effect, require that signal intensity sampling be applied to produce grey shade level spacings at or very near to the limits of perceptibility. The literature is not, however, forthcoming in providing guidance on the question of how faded a target can become and still represent a valid candidate for further amplification. From a practical standpoint, and using CRT displays as guidance for the degree of signal enhancement that is feasible, it is likely that a real target would have to present a relatively noticeable signature, rather than a just perceptible one, before an aircrew member would consider applying signal conditioning to enhance a potential target image, portrayed by a display. The earlier example of a grey scale with sixteen equally perceptible levels would allow the latter criteria to be satisfied. However, once noticed a sensor-video picture rendered with a sixteen level grey scale would be inadequate to provide additional information, through signal conditioning.

One instance where the information content of digitally encoded sensor signals can potentially be masked, is when a small usable information range exists within the large dynamic range of a sensor, as could be true for infrared (IR) or forward looking infrared (FLIR) sensors. To illustrate this point, a FLIR sensor scene that, due to environmental conditions, contains only a 10-20 degree range of temperatures would occupy only a small fraction of the total sensed dynamic range of the FLIR. If, for example, the analog to digital converter is only able to render sixteen equally perceptible grey shades and these are set to span the entire range of the sensor, the portion of the display's dynamic range that contains the useful image information would be conveyed by only a few discrete grey shades, making it difficult or impossible for an aircrew member to perceive and interpret the displayed information correctly. This situation requires either that many more grey shades be sampled, to be available for signal conditioning, or that the means provided to digitize the grey shades must allow the aircrew to align the sampling of the signal, to select only that portion of the total sensor signal range that needs to be displayed. Due to the small number of grey shades available to render the complete dynamic range of the sensor, it is also possible that information of interest in the sensed scene would not become legible on the display until the signal conditioning controls are actually used. While this is less than

an ideal situation, from the perspective of an aircrew member trying to use the displayed sensor information, the situation would be essentially the same using an analog display such as a CRT, if the useful display information occupied only a limited portion of the display's luminance dynamic range. The author is unfamiliar with the manual and/or automatic signal conditioning controls that are currently made available to permit aircrews to exercise control over the display of aircraft IR and FLIR sensor information.

To be at their most legible, and presumably also to create the most effective aircrew performance, both analog and digitized grey shades must be capable of being presented so that they span the entire useable luminance dynamic range of a display. This grey scale presentation range is initially needed to permit a preview of the scope of the image information contained in the sensed scene. Thereafter, this grey scale presentation range would sometimes also be needed to portray sensor signal intensity ranges that involve only part of the entire dynamic range that the sensor can receive. In this latter context, a strategy that allows a closer examination of only part of the sensor signal's dynamic range, while still permitting the number of discrete grey shades encoded for display to be minimized, is to only digitize the signal range that is to appear on the display. For the FLIR example, where the limited range of useful signals can be anticipated, the useful range of signals could be set up ahead of the mission segment, in which the sensor is to be used and, thereby, avoid the inadvertent loss of information.

Giving the aircrew a means of conditioning the analog sensor signal before analog to digital conversion, such as the previously described signal offset and gain control, and the grey shade marker legend, used to define the signal intensity boundaries of the sensor signal grey scale range to be examined in greater detail, allows only that portion of the signal dynamic range to be sampled and encoded for display. Using this fixed sampling approach, dictated by the spacings of the display grey shades, therefore, permits a digital display that can only render a small number of equally perceptible grey shades, for example, possibly as few as sixteen, to be used to render the full dynamic range of the sensed signal, or, alternatively, only that portion of the range, in which the relevant scene image information is contained. As indicated in earlier examples, this approach reinforces the requirement that coordination be maintained between the sampling of the sensed scene signal and the display's discrete grey shade levels. The use of the same number of grey shade samples by both the sensor and the display, in the manner previously described for equally perceptible grey shade steps, would permit an accurate scaled match between the sensor and video display grey shades to be achieved using the smallest number of grey scale levels. Although, as previously shown, the use of equally perceptible grey shade steps permits the most efficient sampling and display rendition of the sensor signal, a variety of other approaches are also feasible. In addition, as the number of grey shade levels increases, the benefits of equally perceptible grey shade spacing are reduced.

6.2.3. Special Considerations for Color Digital Displays

Before closing this discussion of digital processing and conditioning of sensed video signals, the role of color in digital display presentations should be briefly mentioned. This subject will be approached by making comparisons between the image rendition requirements of monochrome and color displays. Most often, a four bit code word and sixteen nominally equally spaced grey shades per pixel are adequate for the presentation of sensor-video information in a monochrome color. This number of grey shades is also adequate for driving the individual primary color elements that form each of the electronic display's color pixels, when mixing the small number of colors employed in existing color graphic display information formats in aircraft cockpits. To achieve color display presentations that can render true full color pictures would, however, require additional grey shades. The need to be able to exercise perceptually continuous control over the colors mixed using the primary colors elements contained within each of the electronic display's color pixels is reason these additional grey shades are needed.

A simple example of the additional image rendition requirements imposed on color electronic displays, in comparison to their single color counterparts, occurs when attempting to mix neutral colors to cause the mixed primary color grey shade levels of the display pictures to be perceived as whites, grays and blacks.

For instance, a color display, with the capability to control each of its primary colors at only sixteen equally perceptible grey shade levels, is, in general, insufficient to permit mixing the primary colors to achieve neutral color grey shades that are perceptible either as sixteen equally spaced levels or as specifically designated constant chromaticity neutral colors. In this general case, the small number of discrete grey shade drive levels for each primary color is only adequate to achieve chromaticities that are perceptible as variants of the desired neutral colors, with most of the mixed grey shade levels being perceptible as different desaturated color hues rather than as the desired neutral colors. Existing aircraft AMLCDs avoid this display limitation by rendering grey shade encoded sensor-video information using only the green primary color elements in the display pixels. The small number of colors used to display color graphic information can then be selected from the total number of mixed colors the display can render, which is limited to the product of the primary color grey shade drive levels, that is, 16 x 16 x 16 = 4,096. In operational usage, only a small fraction of these mixed colors are of practical value for display, since legibility considerations restrict the display presentations to the use of high relative luminance colors, to depict the graphic images, and low relative luminance colors, to depict background colors.

If the design of the electronic display technology implemented, permits the image difference luminances of the primary colors to be preset so that when mixed, using the same relative luminance grey shade drive levels for each of the primary colors, they provide the desired neutral color, then the display in the preceding example would be able to render sixteen equally perceptible and approximately constant chromaticity grey shade levels, but only for the chromaticity coordinate of the preset neutral value scale. For other mixtures of the primary colors, holding the grey shade constant, while changing the chromaticity, or vice versa, would not be possible. Of the existing color electronic display technologies, suitable for use in aircraft cockpits, only the CRT display has internal trim controls that permit individual adjustments to the image difference luminance levels of its primary colors, to satisfy the preceding special case. Color AMLCDs specifically designed to satisfy this special case are feasible, but due to practical technology constraints would be quite difficult to implement.

Extensive past experience, with the digital memory storage requirements for CRT display primary color picture frames, has shown that an eight bit, 256 level, grey scale, having linear grey shade spacings, with luminous reflectance steps equal to 0.341%, is adequate to provide the perceptually continuous color mixing needed to provide satisfactory full color display picture presentations of real-world color scenes, for the luminous reflectance range from 3 to 90%. Based on an assessment of the spacings of a seven bit, 128 level, equally perceptible grey scale, it is concluded that this grey scale would provide better color mixing and overall image rendition performance than the 256 numerically equal spaced levels of the linear grey scale.

The preceding conclusion was reached for two reasons. The first reason is that the largest step, among the 128 levels of the equally perceptible grey scale, never exceeds a luminous reflectance 1.2%, even at the top of the scale, where the largest numerical luminous reflectance steps occur. Since this grey shade step size would only just become perceptible, for a display depicting large uniform areas that are directly adjacent to one another, and because this is an unlikely spatial image configuration, for aircraft sensor-video or color map presentations that are depicting useful information, the display image portrayals rendered using the 128 level equally perceptible grey scale should be perceived as continuously variable, throughout its range. The second reason this conclusion was reached, is that the 128 level equally perceptible scale has smaller grey shade spacings, over somewhat more than one fourth of the lower end of the grey scale, than does the 256 level linear grey scale. Although this would produce an improved color mixing capability for the 128 level equally perceptible grey shade presentations, at the low end of the grey scale range, the larger spacings of the 256 level linear scale are already known to be adequate for color mixing, in this part of the grey scale range. Since the 128 level grey scale is equally perceptible, and because the grey scale it provides is definitely adequate to mix colors at the low end of the grey scale, it follows that this grey scale must also be adequate to mix satisfactory colors throughout the 128 level equally perceptible grey scale range.

Using the preceding argument, and because the lower end of a six bit, 64 level, equally perceptible grey scale has grey shade luminous reflectance spacings of 0.318%, that is, smaller than the 0.341% of the 256

level linear scale, this equally perceptible grey scale would provide color aircraft cockpit display performance commensurate with that of 256 level linear scale color CRT displays. A display picture encoded at 64 equally perceptible grey shades per primary color would, therefore, provide nearly perceptually continuous grey scale and chromaticity renditions, at least for the small image sizes typical of aircraft display information presentations. In larger areas of 64 level equally perceptible grey shade presentations, grey shade steps would continue to be capable of being perceived in background areas, at both low and high relative luminance levels if the display picture is carefully examined, but should not detract from the objective performance of aircrew members or provide visual effects perceived to be distracting. The primary aircraft cockpit application, for the rendition of picture information in full color on an electronic display, is the presentation of computer-generated or previously stored color electronic moving maps. This full color display image rendition capability would, for example, allow perceptually-exact replicas of paper aviation maps to be presented in an electronic display format.

6.3. Comparison of Legibility Control and Signal Conditioning Techniques for Different Types of Electronic Displays

To conclude the discussion of signal conditioning in this chapter, the legibility and signal conditioning functions performed by the brightness and contrast controls of CRT displays will be considered in relation to the analogous functions performed by other types of electronic displays. The purpose of this comparison is to show how the respective controls would have to be implemented and used with different electronic display techniques to achieve as good or better display legibility and sensor-video signal picture renditions than those achievable using aircraft cockpit CRT displays. As the first topic to be considered in this section, color active matrix liquid crystal displays, suitable for use in aircraft cockpits, will again be used as the basis for this comparison, because of the clear separation the LCD offers between the imagery generated on transmissive liquid crystal display panels and the emitted luminance of illuminated backlight used to make that imagery legible. Next, the perceived legibility effects associated with the application of signal conditioning are considered. Finally, the limitations imposed by the choice of display technology on the signal conditioning and legibility control of electronic display pictures are described.

6.3.1. Applying Signal Conditioning to Active Matrix Liquid Crystal Displays

The grey shades and chromaticities, in the pictures rendered by existing aircraft color AMLCD panels, are established by controlling the transmittances of the primary color elements contained in each of the panel's tricolor picture elements, which, in turn, are based on preestablished drive levels for the number and spacing of discrete grey shade levels and chromaticities the display is designed to portray, when commanded by an image generation computer. To render the signals produced by a video sensor faithfully, the digitized sampling of the sensor signals must be carefully coordinated (i.e., the digital equivalent to Gamma compensation) to maintain a direct linear correspondence between the discrete grey shade levels of the sensed signal and the discrete grey shade levels the display is designed to portray.

The primary purpose, of the aircraft cockpit AMLCDs designed and implemented to date, is to portray color graphics, with the display of sensor-video information taking a secondary role. These digital displays employ a fixed scaling between the sensed signal amplitudes and the corresponding image difference luminance levels that render the signals in the picture displayed, so that the entire range of the video signals sensed is permanently scaled for display using the entire relative luminance grey scale range of the display picture. With no means of signal conditioning currently being provided for use with these displays, the aircrew cannot exercise the control needed to permit parts of the sensor-video signal range to be more closely examined. Testing performed on operational C-130 in the early 1990s, using color AMLCDs and color CRTs, installed at the navigator's station, and while displaying the same ground mapping radar information, showed that parts of the sensor signal range, which conveyed image information that could be displayed on the CRT, by adjusting the brightness and contrast controls, could not be seen on the AMLCD.

Although the grey shades and chromaticities of the light transmitted by AMLCD panels, operated as described above, are fixed by the sampled sensor or computer-generated signals applied to the AMLCD panels, the presence of ambient light reflected from the display surface causes the emitted and reflected light to mix, thereby reducing the relative spacings of the grey shades and causing a desaturation of the colors emitted by the AMLCD panels. The perceived legibilities of the grey shades and chromaticities, contained within the pictures displayed by the AMLCD panels, are not controlled by the AMLCD panel, but, instead, by aircrew member or automatic legibility control settings of the luminance emitted by the backlight, which, in turn, controls the absolute image difference luminance and contrast levels of the various grey shades and chromaticities transmitted by the AMLCD panel, with respect to the background luminance reflected from the display viewing surface.

Applying signal conditioning to sensor-video signals before transmitting the signals, from the sensor, for display on an AMLCD displays, would allow linear signal gain and offset control adjustments to be made by the aircrew, to permit them to select the signal information to be presented using the displays' discrete grey shade levels, by maintaining the fixed relationship between the sensor-video signal levels sampled and the grey shade levels displayed. Despite the digital sampling of the sensor signals and their display rendition using discrete grey shades, the linearity of this signal conditioning control capability has the advantage of permitting aircrew members to more readily predict the results of making changes in their signal conditioning control settings, than is possible using the brightness and contrast control settings of CRT displays. As previously mentioned, a distinction between the implementations of these two types of signal conditioning controls is that the gain and offset controls applied in the signal path of an AMLCD do not directly influence the legibility of the display, although they can make the information content available in the video signal easier to perceive, and in that sense more legible, whereas the CRT contrast and brightness controls influence both the legibility of the display and the information content it portrays simultaneously.

As described earlier in this chapter, the image difference luminance levels transmitted by the AMLCD panels, for a particular control setting of the emitted luminance of the backlight, are responsible for the subjective brightness attribute of the absolute image difference luminance levels of the displayed picture. Furthermore, when the ratio of the maximum image difference luminance that the LCD panel can transmit, for a particular emitted luminance setting of the backlight, is taken with respect to the reflected background luminance of the display viewing surface, the resulting display performance metric can be described, with equal validity, as either of the following: (1) the luminance dynamic range of the information, the LCD display is capable of depicting; or (2) the maximum contrast the display is capable of depicting. Consequently, the LCD backlight luminance control establishes both the perceived brightness and luminance dynamic range (i.e., or maximum contrast), of the picture grey shades and chromaticities displayed. Because of this, it is the setting of the LCD backlight luminance control that is responsible for establishing the legibility of the picture presented by a display. Although the relative luminance relationships between the grey shades and chromaticities, within the picture transmitted by the AMLCD panel pixels, are controlled by the drive levels applied to the panel pixels, in response to the grey shades present in the conditioned sensor-video signal received from the sensor or image generation computer, it is the luminance dynamic range and contrast of this imagery, which is established by the settings of the backlight, that is responsible for making the sensor-video imagery legible, in changing ambient illumination induced reflected display background luminance and glare source induced veiling luminance viewing conditions.

6.3.2. Perceived Legibility Effects Associated with the Application of Signal Conditioning

Comparing the AMLCD backlight luminance control, with the control functions of the CRT, it may be seen that the single LCD control does not perform precisely the same function as either the CRT contrast or brightness controls. The CRT contrast control, in setting the gain applied to the sensed signal, does set the spacings between the signal grey shades. In this respect, the CRT gain control is, therefore, nearly equivalent to the signal conditioner gain control, which, as previously described, could be used to control the amplification of sensor signals, before displaying them on LCDs. A difference between these control functions is that the

CRT gain control also simultaneously controls the luminance dynamic range, and, therefore, the legibility of the information that can be rendered by the CRT display, whereas this function is controlled independently by the LCD backlight luminance control, as stated above.

To complete the control comparison, if the CRT contrast control is first set to a fixed level of gain that provides a faithful rendition of a real-world scene, then the CRT brightness control would provide a control function, analogous to the one described earlier for the single LCD backlight emitted luminance control. A caveat associated with this control condition, is that changes in the brightness control settings, from the Gamma compensated grid bias point of the CRT, also introduces nonlinearities into the sensor signal to emitted luminance transfer characteristics of the CRT, thereby causing the grey shade spacing relationships between the sensed signal and its displayed counterpart to be unpredictably altered, whereas changes in the LCD luminance control do not affect the signal transfer characteristics.

For the preceding reasons, no complete analogy between the operation of liquid crystal and CRT displays is possible, due to the inherent differences between the design techniques necessary to implement these transmissive and emissive operating mode displays. The closest analogy is obtained by setting the brightness and contrast controls of the CRT display, to the fixed Gamma compensated levels needed to provide a linearized signal transfer characteristic, and also the full luminance dynamic range and maximum contrast that the CRT display can achieve for a particular setting of its anode voltage. To complete this analogy, the average brightness and grey scale contrasts of the information content of the picture displayed by the CRT could be controlled using a signal conditioning offset and amplifier gain adjustment of the sensor signal, before the application of Gamma compensation to the sensor signal. Since this approach allows the grid to cathode voltage bias level setting (brightness), and gain setting (contrast), of the CRT to remain fixed, these adjustments would not alter the linearity of the display's presentation of the sensor signals.

The preceding method, of controlling the brightness of a CRT picture is currently used to cause pictures depicted by televisions to be perceived as occurring at night, in bright daylight or for intermediate ambient illumination conditions, under fixed ambient illumination exposure conditions. Changing the illuminance or irradiance levels incident on a real-world scene only causes changes in the absolute levels of the reflected luminances or radiances. The spatially distributed reflected relative luminance or radiance levels, that is, the grey shades associated with the reflected real-world scene signals available to be sensed, remain unchanged. Consequently, the brightness appearance of the real-world scenes, rendered in the electronic displays pictures, can be changed by altering the absolute levels of the sensor-video signals generated by a video camera or other sensor, before transmitting them for presentation on an electronic display. The methods used to achieve this result could involve something as simple as sensing real-world scenes in different natural ambient illumination environments or setting the scene lighting in a controlled television studio environment. Alternatively, signal conditioning can be employed to amplify and offset the grey shade encoded sensor-video signals, acquired by sensing real-world scenes, using controls on the television cameras or by processing the signals using TV studio video editing equipment. Making these adjustments to the sensed video signals, before Gamma compensation is applied to the signals, retains the linear transformation between the conditioned signals and the emitted luminance rendition of the signals on studio monitors and the television receiver of home viewers.

Setting the percieved brightnesses of a transmitted television picture is typically accomplished by changing the black level setup of the picture, that is, the difference between the blanking level and video picture black level, at the time that the composite video signal is created, by adding the synchronization pulses to the sensed signal amplitudes produced by the TV camera. The range of signal amplitudes contained within the normalized standard video signal is not altered by this process, unless the signal is also attenuated or amplified while conditioning the sensed video signal. Instead the picture transmitted is shifted by modest amounts, to lower or higher average luminance levels, within the confines of the total grey scale range, capable of being encoded into the transmitted signal, and presented on the television display. Using this method to control the brightness and contrast of the information content of the pictures presented on CRT displays, allows the linearity of the transformation between the sensed signal and the display emitted luminance to be maintained,

as the brightness and contrast of the displayed picture are changed using sensor gain and voltage offset controls, since the grid voltage (brightness) and gain (contrast) settings of the CRT, and, consequently, the Gamma compensated linearity of the CRT remain fixed. Since CRT brightness and contrast controls are not needed to use this signal conditioning approach, an advantage of this approach, for use in controlling the information content of CRT display pictures, is that the signal conditioning adjustments, made by aircrew members, produce predictable linear responses that can be learned.

6.3.3. Display Technology Limitations on the Signal Conditioning and Legibility Control of Electronic Display Pictures

Televisions are designed to take advantage of the inherent automatic legibility control capabilities of the human visual system, which were described near the end of Section 5.3. Under most television viewing conditions, the display is much more legible than, as a minimum, would be necessary to produce satisfactory picture portrayals on the display. Television viewers have come to accept the fact these displays must be operated in low ambient daylight and night illumination environments, and, consequently, it is only in rare instances that a viewer will even attempt to adjust their brightness and contrast controls for changing ambient illumination conditions. Unfortunately, the option of controlling the environment in which the display is viewed is not available to military aircrew members viewing cockpit displays.

To compensate for changes in the legibility of light emissive operating mode displays, in response to changes in the luminance reflected from the display surface or the veiling luminance induced in the aircrews' eyes, not only must it be possible to change the absolute image difference luminance and brightness, as described above, but this has to be accomplished over the entire range of luminances the display can produce. Although controlling the image difference luminance and contrast of a display picture portrayal, by amplifying and offsetting the input signal intensity range is a valid approach for any type of electronic display, picture presentation constraints, inherent to making displays legible in changing ambient illumination environments, limit the practical application of this control capability to the conditioning of signals, that is, to changes in the information content and the appearance of scenes being portrayed on displays.

The principal constraint on using this technique for controlling the legibility of display information, in changing ambient illumination environments, is related to the limitations on the relative luminance levels, that is, the instantaneous grey scale range, which can be achieved using existing display technologies. For example, a display that can present grey shades and chromaticities in a relative luminance range from 90 to 3%, would require a luminance dynamic range of 29 (i.e., (90 - 3)/3) and an emitted luminance of nominally 1,250 fL (i.e., 200 fL x 29/4.66) to make it legible, under worst-case daylight viewing conditions in an aircraft cockpit. If the 90% white, or monochrome color, highlight luminance is 1,250 fL, then the absolute luminance corresponding to the 3% grey shade level would be about 43 fL. In other words, to use signal conditioning for legibility control, the luminance dynamic range of the display would have to be much larger than 29. In fact, to permit dimming the display to the point where night lighted cockpit luminance control is manually activated, a luminance dynamic range of about 1,250 x 29 = 36,250 would be needed to use a conditioned signal to dim the highlight luminance level to 1 fL and still be able to show a 90 to 3% grey scale range. For the same display to depict a highlight white level dimmed to 0.5 fL, which is near the minimum suitable for making a contrast of 29 grey scale display pictures usable by aircrew members, would therefore require a luminance dynamic range of about (1/0.5) x 36,250 = 72,500. It can therefore be concluded that the implementation of signal conditioning to compensate for the changes in the image difference luminance requirements that occur over the very large ranges in ambient illumination and glare source conditions encountered in aircraft cockpits would be very difficult, if not impossible, to achieve using the control techniques available for use with existing emissive operating mode display technologies, such as the CRT or LED. In spite of this practical limitation of this control technique for brightness and contrast control, the technique remains valid for achieving the previously described purposes of signal conditioning using emissive operating mode displays. Control of the picture image difference luminances, using only the transmittances, reflectances or transflectances of the display viewing surface, has an even more problematic potential for capitalizing on this control technique for

legibility control.

A method for controlling the brightness of LCD display pictures that is comparable to the signal offset technique described above for CRT displays could be achieved by changing the transmittances of all of the picture pixels in unison, to dim or brighten the picture. The physical restrictions on the range of transmittances that are feasible, using AMLCDs or other transmissive operating mode displays, are currently too limited to permit using an offset of the input signal intensity range to compensate for changes in the display legibility over the complete range of ambient illumination conditions experienced in aircraft cockpits. However, since the same results can be achieved by changing the emitted luminance of transmissive operating mode display backlights, little can be gained through the implementation of this type of brightness control, on AMLCDs or other types of transmissive operating mode displays. The technique remains valid when used with transmissive operating mode displays, for purposes of conditioning signals to enhance the aircrew member's ability to control the information content of the sensor signals being displayed.

For reflective and transflective mode displays, viewed under daylight ambient illumination conditions, the changes of display surface reflectances required to realize constant legibility control, as the ambient illuminance incident on the display changes, are quite small, when compared to those required for emissive and transmissive mode displays. The problem encountered in this case is that the absolute luminous reflectances of these display surfaces are currently too low to make them legible in daylight viewing conditions, without employing auxiliary sources of illumination to increase the reflected image difference luminance levels, to high enough values to satisfy the aircrew's image difference luminance requirements and to overcome the effects of veiling luminance induced in the crew members eyes by discrete or distributed glare sources. As described in Chapters 2 and 5, if a means of providing an adequate auxiliary source of illumination can be found, then the small reflectance changes needed to maintain the display picture portrayals at a constant legibility level, under direct incidence daylight ambient illumination viewing conditions, could be satisfied. The methods previously described for conditioning sensor-video signals prior to display would be directly applicable to light reflective and transflective mode electronic displays, if they can first be made legible using another means.

CHAPTER 7

Practical Aircraft Manual and Automatic Legibility Control Implementation Considerations

The intent of this chapter is to provide closure to the earlier descriptions of manual and automatic legibility control by describing several implementation considerations that would be expected to influence the effectiveness of the information portrayed using electronic displays to satisfy an aircrew member's legibility requirements under operational flight conditions in aircraft cockpits. These practical considerations were reserved for presentation until near the end of this report so that they would not become unduly enmeshed with the more fundamental information presented earlier. As has been true throughout this report, the intent of the present chapter is to provide sufficient information to permit the reader to make practical judgements, in those situations where additional application information concerning the details of a particular aircraft's mission and flight control capabilities would be necessary to reach a final conclusion.

In the first section that follows, the influence on automatic legibility control caused by accounting for the specular as well as the diffuse component of the background luminance reflected by electronic displays is considered. Although the existence of the specular component of the background luminance reflected by electronic displays has been consistently mentioned in earlier chapters, its contribution to the reflected background luminance of an electronic display is often negligible, except under a narrowly defined set of ambient illumination exposure conditions occurring in aircraft cockpits. For this reason, and to avoid unnecessarily complicating the earlier descriptions, the effects of taking specular reflections into account have been deferred until the present chapter. The limited set of illumination conditions that do produce legibility degradation is described in this section. Methods used to determine the luminance specularly reflected by electronic displays, and to account for this contribution to the total reflected luminance, using measurement results obtained from light sensors installed in the cockpit, are also described.

The second section considers the implications of the human's image difference luminance requirements characteristics, developed in Chapter 3, on the legibility control requirements of electronic displays, based on their locations in the cockpit and on their light reflection properties. In the section, separate legibility controls are shown to be needed, to produce the differing image difference luminance levels required, for electronic displays placed at different locations in the cockpit, to reconcile the legibility control requirements of aircrew members accurately. Furthermore, this is true irrespective of whether the electronic displays have different light reflective properties or are identical, and on whether the displays are adjusted manually, by aircrew members, or automatically, using automatic legibility controls.

In the third section, implementation techniques and requirements associated with electronic display legibility controls operated by aircrew members are considered, starting with the relationship that should exist between an electronic display's image difference luminance output and an aircrew member's manual control input. Next, considerations related to interfacing display image difference luminance controllers with both manual and automatic legibility controls are described. Thereafter, the merits of dedicating aircrew controls to each individual display are discussed, followed by the ramifications of using a common shared control to adjust the legibility of multiple displays concurrently. The latter topic is addressed from two perspectives. First, the common control approach is considered in terms of the constraints that its application can impose on the legibility control accuracy that is achievable for multiple cockpit electronic displays, when the same control signal is applied simultaneously to all or a portion of the cockpit electronic display image difference luminance controllers. This common control approach is considered both from the standpoints of manual and automatic legibility control. The second perspective involves the application of a common legibility trim control signal when it is applied as an input to multiple dedicated ALCs, each of which is tailored to suit the electronic display to be controlled. Finally, the integration of manual with automatic control techniques needed for practical applications of automatic legibility control in aircraft cockpits are considered.

The implementation considerations considered in the fourth section involve the coordination of multiple light sensors, automatic legibility controls and electronic displays, to achieve and maintain adequate electronic display legibility, under either static spatially variant illumination conditions or dynamically changing illumination and/or veiling luminance conditions. Under static spatially variant illumination conditions, the two primary implementation considerations considered are the placement of light sensors in the cockpit and the criteria for selecting the light sensor signals used, to assure that the legibility of the electronic displays is maintained at a constant level whether the displays are located in fully illuminated or in shadowed areas within the cockpit. The other implementation consideration dealt with in the fourth section concerns the time dependent response that electronic displays should exhibit during times when the aircraft is being maneuvered. Maneuvering an aircraft in daylight produces dynamic movements of illuminated and shadowed areas in the cockpit both with respect to the electronic displays and their respective light sensors. Aircraft maneuvers also produce time dependent changes in the exposure of the veiling luminance sensors with respect to glare sources such as the sun. Control options are considered for dealing with the potentially rapid changes that could occur in the image difference luminances of electronic displays commanded by the automatic luminance controls receiving these time changing light sensor signals.

In the fifth section and final section of the chapter, implementation considerations concerned with making digitized sensor signals, automatic legibility controls and display luminance controllers compatible with the pilot's image difference luminance control and discrete luminance control increment requirements are described. The primary emphasis of the section is on the derivation of the sensor signal magnitude ranges and sampling intervals required to provide electronic display luminance control over the full range of night through daylight ambient illumination and veiling luminance conditions, while also providing stepped luminance increments that are acceptable to an aircrew member.

7.1. Specular Reflection Component of the Background Luminance of Electronic Displays

In this section the methods used to implement the reflected background luminance variable term in the automatic legibility control (ALC) law algorithm will be considered in relationship to the measurable light quantities that can be expected to influence the effectiveness of any type of automatic brightness or legibility control implementation. Up to this point in this report, only the implementation of display or display panel illuminance sensors to permit calculating the diffuse reflectance component of the display reflected background luminance term in the ALC equation has been described. The effect of specular (mirror-like) reflections, as an integral part of the display reflected background luminance term, L_D, of the ALC equation has, where appropriate, been mentioned but no means of measuring its contribution to the display background luminance in a cockpit environment has been considered nor has the extent of the error encountered by ignoring its contribution been described. The primary reasons this topic was not introduced earlier in this report are as follows: first, the contribution of specular reflected luminance to the display background luminance term is generally small; and, second, the inclusion of this term is considered a practical implementation issue, which does not directly influence the validity of the derivation of the pilot's image difference luminance requirements or the interpretation of the automatic legibility control law. It is presumed that these reasons, combined with the greater difficulty associated with carrying out the measurement of the specularly reflected component of the background luminance of an aircraft cockpit display, are the reasons that Boeing chose to ignore this legibility degradation variable when implementing their automatic brightness control design.

7.1.1. Conditions under Which the Legibility of Electronic Displays is Influenced by Specularly Reflected Luminance

Before discussing possible methods for measuring the specularly reflected component of an electronic display's background luminance, its relevance to electronic display image legibility in an aircraft cockpit will be briefly considered. In particular, the relevance of the luminance specularly reflected into an aircrew member's eyes will be considered in terms of the viewing conditions that need to be present in an aircraft cockpit to make

this contribution to the display reflected background luminance important as a source of legibility degradation. For well designed electronic displays, the specular reflectance contribution to the total background reflected luminance of the display is usually quite small. Stated in another way the diffuse reflectance contribution is typically much higher than the specular reflectance contribution. This is usually true because aircraft cockpits are designed so that the orientations of the displays, mounted in their instrument panels, cause the areas viewed by aircrew members, via specular reflections from display surfaces, to be limited to highly attenuated mirror reflections (i.e., typically less than 0.5%) of ambient light that has already been attenuated by one or more reflections from interior cockpit surfaces, such as the pilot's clothing, seats, instrument panels, consoles, and so forth. Although the diffuse reflectances of sunlight readable aircraft displays are comparable to the magnitudes of the specular reflectances, the sources of illumination for diffuse reflections from electronic displays are the much higher luminance areas of sky and clouds located external to the cockpit. In other words, the sources of the luminances, that are specularly reflected by the cockpit display surfaces into the pilots' eyes, are already attenuated through prior reflections from interior surfaces within the cockpit, as the result of direct and indirect exposures to external ambient light and, to a much lesser degree, by their exposure to light emissions generated luminous cockpit signals, controls, integrally illuminated panels and displays within the cockpit.

Typically, in daylight, it is only when interior cockpit surfaces, which are located at mirror reflection angles with respect to the eyes, are directly illuminated by the sun that these surfaces are raised to high enough luminance levels, to cause specular reflections from the display viewing surfaces that can degrade the legibility of cockpit displays. As a somewhat more remote possibility, a pilot flying a bubble canopy cockpit type aircraft below a sun illuminated diffuse high luminance surround condition, such as white clouds or sun illuminated haze or mist, could also experience a masking of the imagery depicted by instrument panel mounted electronic displays due to specular reflections. Despite the infrequency in the incidence of legibility degradations caused by specular reflections, because this problem can be experienced in any operational aircraft, the effect needs to be taken into account if electronic display legibility is to be maintained under all possible atmospheric illumination flight conditions. The conditions that must be satisfied for specular reflected luminance to create legibility problems are discussed in greater detail below.

As a consequence of cockpit structures limiting the illumination exposure of displays and, in particular, for covered canopy type aircraft, the illuminance levels incident on the displays and instrument panel mounted ALC light sensors can be quite low (e.g., 60-100 fc) even on a clear day. Under such conditions, the instrument panel mounted light sensors will cause the image difference luminance levels of automatic legibility controlled displays to be significantly reduced. This result occurs because the instrument panel light sensors are exposed to illuminance levels that can be from 20 (i.e., fighter type aircraft) to 100 times (i.e., cargo type aircraft) less than those attributable to the same external-looking sensors receiving direct exposure from the sun. If under this condition, the sun is located anywhere between two arcs that define a spherical zone, extending from overhead to either side of the aircraft and for forward angles from overhead to those that just clear the glare shield but still illuminate the specular reflection surface areas of the cockpit, then the sun can directly illuminate interior cockpit surfaces that are at a specular angle with respect to the pilots line of sight to one or more of the cockpit electronic displays, while leaving the ALC sensors for those displays in the shadow cast by the glare shield. The combination of the displays the pilot is reading being exposed to reduced illumination, and the specular reflected luminance being enhanced due to the illumination of the internal cockpit surfaces by direct exposure to the sun, is the condition that can be expected to cause the most severe display legibility degradation, as the result of specular reflections from the displays into the pilot's eyes.

7.1.2. Techniques for Measuring the Luminance Specularly Reflected from Electronic Display Surfaces

The most accurate method of measuring the luminance specularly reflected by the surfaces of aircraft cockpit electronic displays would involve using lensed luminance sensors oriented with their major optical axes coincident with the pilot's line of sight to the displays and focused upon the display viewing surface, just as the pilot's eyes would be when viewing the displays. Since the preceding direct measurement approach is

impractical, an alternative indirect approach is necessary to derive the luminance specularly reflected from the cockpit displays into the pilot's eyes. Probably the most straightforward method of doing this involves placing illuminance sensors at various locations on the cockpit interior surfaces, from which the luminances specularly reflected by the electronic display surfaces into the pilot's eyes emanate. In order for the preceding indirect measurement approach to be effective, careful consideration has to be given to the placement of the illuminance measurement sensors on the interior cockpit surfaces, both to reduce the number of sensors required and also to assure that any illuminated area that moves into the region of the cockpit that contains the specular reflection, light reception fields of the displays, is measured in adequate time to increase the legibility of the correspondingly affected display or displays accordingly.

To complete the preceding specular luminance determination, the luminance emanating toward the display surface can be calculated by multiplying the sensed illuminance values by the respective diffuse reflectances that characterize the interior cockpit surfaces surrounding each of the illuminance sensors. Using these calculated luminance values, a relatively good estimate of the specularly reflected component of each display's background luminance can be obtained by multiplying the luminance incident on the display by the specular reflectance of the display surface that is applicable to the specular angle at which the luminance is reflected into the pilot's eyes. The highest of the calculated values of the specular reflected luminance, determined in this way, for a particular display, a grouping of displays or all of the displays, dependent on the design philosophy adopted, would be added to the diffuse reflectance component of the background luminance term before being substituted into the automatic legibility control equation.

A problem with the preceding indirect approach for determining the specular reflection component of a display's reflected background luminance occurs for specular reflection angles where placing an illuminance sensor on the cockpit surface that would be seen reflected in the display surface by an aircrew member is not feasible. More specifically, it is not reasonable to use illuminance sensors to measure, for example, the light incident on an aircrew member's clothing, exposed skin or the seat on which that person is sitting. The luminances of the cockpit surfaces that cannot be measured using illuminance sensors can, as an alternative, be measured using luminance sensors installed in the cockpit, forward of the pilot, or in the instrument panel. Due to the large distances between the luminance sensors and the cockpit interior surfaces to be measured, these sensors should exhibit a large depth of field so that they would not have to be refocused to provide accurate results, when, for example, the positions of the seats are adjusted. These sensors would also benefit from the use of large luminance measurement spot sizes, to permit area averaging the luminance reflected from cockpit interior surfaces such as clothing. Because the luminances reflected by diffusely reflecting surfaces radiate approximately equally in all directions, the angular orientation of these luminance sensors with respect to the surfaces they measure is not critical, provided they can monitor the surface areas specularly reflected by the displays. The problem with the use of luminance sensors is that very little room is available in cockpits, and particularly behind instrument panels, for devices requiring lenses to focus their detector areas at a distance. Although the inclusion of luminance sensors to measure cockpit surfaces that cannot otherwise be measured would be required to produce the most accurate results, the need for the high degree of accuracy this would achieve is not a clear requirement.

Since the luminance specularly reflected from instrument panel mounted electronic displays into the pilot's eyes should usually be negligible, when compared with the diffuse reflected component of a display's background luminance, it is reasonable to question whether a less accurate technique could not be used to estimate the specular reflected component of the display background luminance. Since external ambient light that illuminates a crew member cannot do so without also illuminating the areas to the crew member's left, or right or simultaneously on both sides, illuminance sensors located on cockpit side walls, center and side consoles, panels or other fixed structures can be polled and, based on the illuminance measurement results obtained, be used to predict when the surfaces that are not directly measurable are likely to be illuminated. The illuminance levels, measured in this way, can also be used to calculate accurate estimates for the specular reflected luminances corresponding to the cockpit surface areas where placing illuminance sensors is not practical. This would involve applying the products of the diffuse reflectances of the actual cockpit surfaces and the specular reflectances of the actual displays, which are applicable to pilot reading the information

displayed at the correct viewing angle, to the selected illuminance values. While the adoption of this approach would at times lead to displays being operated at a somewhat higher legibility level than would occur if all of the necessary illuminance sensors could be properly positioned, the approach would assure that the displays are always operated at either the correct level or, if not, at a higher than needed level of legibility. To illustrate this point, if for example only one side of the cockpit is illuminated at a higher illuminance level, with the balance being in shadows, then, as a worst case, electronic displays that are reflecting shadowed areas that cannot be measured would be caused to operate at a higher legibility level, as if they were specularly reflecting the same interior cockpit surfaces, but at a time when those surfaces are exposed to the higher illumination level.

7.2. Legibility Requirement Dependence on the Types and the Locations of Cockpit Displays

To simplify the control of electronic displays in aircraft cockpits, using either manual or automatic legibility control, it would be convenient to be able to generate a single universal control signal that, except for a luminance multiplier to adjust for displays with different image difference luminance requirements, can be used to operate any display, independent of its type or location in the cockpit. As a practical matter, it is, in general, not feasible to set the image difference luminances of different types of displays, or even displays of the same type, at different locations in the cockpit, so that they are equally legible, and afterwards expect to maintain equal legibility using a universal automatic legibility control signal to adjust for subsequent changes in the veiling luminance induced in the aircrew member's eyes, or in the ambient illumination exposures of the electronic displays. The reasons why this is true are described in the balance of this section.

The image difference luminance requirements equation, as it is represented in any of the several different forms presented earlier in this report, shows that the aircrew's legibility requirements depend on the combined effect of the veiling luminance, L_V, induced in an aircrew member's eyes, as the result of being exposed to glare sources, such as the sun, while viewing a display at a particular location in the cockpit, and the background luminance reflected by the surface of the same display, L_D. Moreover, the equation shows that the relationship between pilots' image difference luminance requirements and the equation's independent sensed luminance variables, L_V and L_D, is nonlinear.

The significance of the nonlinearity in the pilot's image difference luminance versus background luminance requirement characteristic to the present discussion is that two displays with different reflectance characteristics, or identical displays in different locations in the cockpit (i.e., since such displays are typically exposed to different levels of incident illuminance), would be represented by different operating points on the pilot's image difference luminance requirement characteristic, for the same cockpit ambient illumination or glare source exposure viewing conditions. This would, in turn, cause the two displays to operate within different ranges on the pilot's image difference luminance requirement characteristic, as the cockpit ambient illumination or glare source viewing conditions change over time. Because the characteristic is nonlinear, a change to a new operating range, upon the pilot's image difference luminance characteristic, is equivalent to operating on an entirely different image difference luminance characteristic and, therefore, cannot be compensated by simply applying a constant luminance multiplier to one display to match the image difference luminance requirements of the other display, under different viewing conditions. To illustrate this point with an example, consider one display having a low enough reflectance to operate in the zero slope portion of the requirements characteristic and another display having a higher reflectance and operating above the knee of the characteristic. Decreasing the illuminance incident on both displays simultaneously will not change the image difference luminance requirement for the first display but will decrease that requirement for the second display. Consequently, a single control signal, whether controlled manually or automatically, is not adequate to control both displays. Some practical implementation implications stemming from this difference in display control requirements are explored in greater detail below.

While the glare source veiling luminance induced in the aircrew member's eyes is dependent on the position of a display in a cockpit, by virtue of the angle subtended, between the line of sight to the display and the direction of the glare source, the magnitude of the veiling luminance induced in the aircrew member's eyes

is independent of the properties of the display being read. In comparison, while the display background luminances diffusely and specularly reflected toward the crew member's eyes are dependent on the position of a display in a cockpit, by virtue of the spatial distribution of external ambient illumination environment that illuminates the cockpit, the differences between the diffuse and specular reflectances of individual displays also have a significant effect on the image difference luminance requirements of otherwise similar electronic displays exposed to the same incident illuminance viewing conditions.

An example in which installation locations, of electronic displays in a cockpit, result in particularly different control requirements, occurs for identical displays, where one is used for primary flight control tasks and is installed in the instrument panel, roughly in front of the pilot, and the other is used for communications, mission segment mode control, or navigation, and is installed in the center console, in a side by side cockpit configuration. As described the previous subsection, the background luminance reflected by the display mounted in the instrument panel would be dominated by diffuse reflections, with a small additional intermittent specular reflectance component. In comparison, the reflected background luminance of the display installed in the center console, while having a somewhat comparable diffuse reflected luminance component, could also contain a large specularly reflected luminance component, due to the specular reflection of sky or clouds through the cockpit's side windows or a bubble canopy. Owing to the potential for the pilot to have to read the display on an intermittent basis both in the presence and absence of large specular reflections, a separate manual or automatic luminance control signal would be required to be able to compensate the center console display for the intermittently higher background luminance, if the legibility is to be maintained at the same level as for the display mounted in the instrument panel.

Although the preceding example represents an extreme case, it shows that the need for the individualization of display legibility control, in varying degrees, applies to any difference in the locations of electronic displays in a cockpit, even without including the effects of veiling luminance. It should be noted that a forward placement of an electronic display in the center console of a side by side dual seat cockpit, in combination with orienting the panel that the display is mounted on, can be used to cause internal cockpit surfaces to be located at the specular reflection angle, with respect to the pilot's line of sight to the display surface, rather than the sky. Since the sun can be imaged in any display surface, which specularly reflects the sky, display locations that produce this possibility should be reserved for displays that can retain legibility under this condition, such as diffuse reflecting sunlight readable push-button switches, signal indicators and many conventional controls and panels.

The practical importance of the reflective properties of individual electronic displays can be illustrated by comparing the image difference luminance requirements, which are needed to make electronic displays having different surface reflectances equally legible. For example, and as described in earlier chapters, for displays having very low reflectance viewing surfaces, veiling luminance viewing conditions establish the minimum highlight image difference luminance levels, the displays must achieve, to cause the pictures depicted by a display to be perceived as being legible. When the minimum requirements to depict highlight image difference luminance levels in the presence of sun induced veiling luminance are satisfied, for these low reflected background luminance displays, then the luminance dynamic ranges produced by these displays are already greater than the minimum values required to portray display pictures legibly, when sunlight is directly incident on the displays. Conversely, for high reflectance displays that can achieve legibility equal to that of the low surface reflectance displays, the image difference luminance levels needed to make the display legible, when sunlight is directly incident on the display, can greatly exceed the previously cited image difference luminance levels needed to make the display legible under sun induced veiling luminance conditions.

To complete the preceding comparison, of the effects of different display surface reflectances on the image difference luminance control requirements of electronic displays, night viewing conditions will be briefly considered. At night, electronic displays presenting identical information have the same image difference luminance requirements, despite the differences that may exist between the light reflectance properties of the individual displays. This result stems from the very low level of reflected display background luminances at night, even for displays having a viewing surface that is highly light reflective.

The effect of veiling luminance, under night viewing conditions, is display independent, just as it is for daylight viewing conditions. As concluded previously in this report, the day and night image difference luminance requirements both depend, in the same way, on the effects of veiling luminance. In turn, the veiling luminance induced depends on the angular separation between the aircrew member's line of sight, to the display, and the direction to the glare source. Consequently, the effect of veiling luminance depends primarily on the location where the display is mounted in the cockpit, and on the luminance magnitude and spatial distribution of the discrete or distributed glare source, to which the aircrew is exposed.

In summary, because the veiling luminance depends on the position of a display on the cockpit instrument panel or consoles, and the reflected background luminance depends on both the position of the display and the combination of the diffuse and specular reflectances of the display surface, manual or automatically controlled signals applied directly to the display luminance controller, used to control the legibility of the displays, cannot be universal but instead must be tailored to each particular display and to the location where it is to be viewed. Since, each display technology, and even different implementations of the same technology, can have different reflectances, each produces different reflected background luminances for the same incident ambient illumination viewing condition. The differences in the veiling luminances induced, due to the different locations of displays in a cockpit, and the differences in the background luminances reflected by electronic display surfaces upon which ambient illuminance is incident, either due to differences in the displays or due to their locations in a cockpit, means that these displays must be operated at different background luminance (i.e., and veiling luminance) operating points on the aircrew member's image difference luminance requirement characteristic, if the different displays and their installed locations are all to provide the same image legibility. In the context of automatic legibility control, differences in the locations of displays in a cockpit, and in display surface reflectances, translate into a need simultaneously to provide individualized control signals to each of the electronic displays in an aircraft cockpit, so that they can be operated in the respective legibility control ranges, appropriate to satisfy the image difference luminance requirement characteristics of the aircrew.

On the basis on the preceding analysis, it can be concluded that although the image difference luminance requirements for electronic displays, at different cockpit locations or having different light reflectances, must all satisfy the same human legibility requirements equation, the required image difference luminance, applicable to each specific display and display location, must be determined independently for the applicable veiling luminance and display reflected background luminance conditions present. It can also be concluded that to concurrently achieve equal legibility on all of the electronic displays in a cockpit, under any arbitrary set of ambient illumination and veiling luminance conditions, each display requires a separate legibility control, whether that control is exercised by an aircrew member using manual control or by an aircrew adjustable automatic legibility control.

A broader range of legibility control options, implemented by controlling the image difference luminance of electronic displays, including both precise and approximate control techniques, are described and further discussed in the sections that follow.

7.3. Aircrew Control Over Electronic Display Legibility

To provide a display legibility baseline, for discussing the information presented later in this section, information about the legibility of conventional and electronic displays, which is described elsewhere in this report, is reviewed as an introduction to the topic of aircrew control over electronic display legibility described in this section. Because the legibility of conventional electromechanical instruments is an accepted fact, the legibility control properties of these displays are reviewed first, followed by the different types of electronic displays. The purpose of summarizing this information is to point out the legibility control needs of each of these types of display.

Conventional electromechanical displays rely on the ambient illumination entering the cockpit, and being reflected from the static and moving parts of the surfaces of their face plates, tapes and pointers, to make the

information they convey legible, under daylight viewing conditions. Because the reflected image difference luminances and colors rendered by reflective operating mode presentations track the ambient illumination incident on these displays, they possess an inherent automatic legibility control capability that makes it unnecessary for the aircrew to control their image difference luminances under changing daylight ambient illumination conditions. While the image legibility, achieved by these constant contrast aircraft instrument presentations, does not remain entirely constant in changing ambient illumination conditions, the high contrasts of the imprinted images continue to provide legibility that exceeds the pilot's minimum requirements, even under the worst case viewing condition for the types of information presented on these displays, that is, when the sun is in the pilot's field of view, causing it to act as a glare source. This is the worst case viewing condition for conventional electromechanical displays because the sun, when located in the pilot's forward field of view, cannot also directly illuminate the cockpit displays. Consequently, at a time when the direct exposure of the pilot's eyes to the sun causes high veiling luminance levels to be induced, which, in turn, imposes minimum reflected image difference luminance requirements that must be exceeded if the displays are to remain legible, the illuminance levels that are directly incident through the cockpit canopy or windows onto the displays are greatly reduced, thereby also reducing the image difference luminance levels reflected by the display's imagery.

Currently, no light reflective or transflective operating mode electronic displays can produce a range of electronically controllable luminous reflectances that are comparable in magnitude to the range of reflectances associated with the information presentations of conventional electromechanical displays. Consequently, these displays are unable to satisfy a pilot's legibility requirements automatically by using only the daylight ambient illumination available within a cockpit to render the imagery the displays portray. The existing electronic displays that can satisfy an aircrew member's legibility requirements use either the emissive or transmissive modes of operation to depict the information they present. Because these displays rely on internally generated light, to render displayed information, they must employ either manual or automatic legibility control to permit their use in the ambient illumination and veiling luminance conditions experienced in aircraft cockpits, under daylight viewing conditions. At night, the image difference luminance of both electronic displays and their conventional display counterparts must be controlled either manually or automatically to permit adequate legibility to be maintained. The balance of the present section is devoted to a discussion of practical methods that can be used to effect control over the image difference luminance levels and the resultant legibilities of electronic displays in aircraft cockpits.

In the first subsection that follows, the control characteristics that aircrew operated electronic displays should possess, to cause their image difference luminance levels to be perceived as changing in direct proportion to the manual control inputs made by members of the aircrew, are introduced. Next, this overall image difference luminance control characteristic for electronic displays is separated into two parts, consisting of the control characteristics that should be possessed by the aircrew operated manual luminance controls, and display image difference luminance controllers. Finally, two different methods, of achieving the same overall image difference luminance control characteristic for electronic displays, are presented and their pros and cons discussed.

In the second subsection, the requirements that should be met by an interface between an electronic display image difference luminance controller and aircrew manual and automatic legibility controls are considered. The first topic considered involves the criteria that should be met, to make aircrew controls used to operate electronic displays, interchangeable. Next, the criteria are expanded to include achieving compatibility at the control interface for the control signal information content, as well as for the electrical hardware. Two protocols are described, which are referred to as the standard and relative control interface protocols. The discussion is concluded with a comparison of the relative merits of the standard and relative control interface protocols.

In the third subsection, electronic display manual legibility control options are discussed in two parts, individual electronic displays operated using dedicated manual controls and multiple individual electronic displays operated in unison using a common manual control. To ease the added workload burden on aircrew

members, introduced by the need to control the legibility of electronic displays in daylight using separate individual controls, a further level of control can be provided. This further level of control consists of a common control that can be used by the aircrew members to change the legibility of all of the electronic displays in unison. This latter topic is discussed in some depth since it is the currently favored control technique in military aircraft cockpits using multiple electronic displays.

The fourth subsection deals with electronic display automatic legibility control options. It is only with the addition of automatic legibility controls dedicated to the operation individual electronic displays that the workload of aircrews can be reduced, under daylight viewing conditions, to the same level present in a cockpit equipped with conventional electromechanical instruments. In addition, to meet the individual legibility control needs and preferences of aircrew members, the methods used to achieve control over the image difference luminance of electronic displays, should take into account the extent to which the crew is to be afforded the ability to exercise control over both the luminance of individual displays and of displays controlled in unison, via a common control.

The automatic legibility control information provided in this subsection is further elaborated upon in terms of three different automatic legibility control options. Multiple individual electronic displays operated using dedicated ALCs is the first option described. This is followed with the considerations involved in the implementation of multiple electronic displays operated in unison using a single ALC. The latter topic is included as a second option because it is preferable to using manual control and would be satisfactory for aircraft whose missions do not require optimum display legibility control. Finally, the third option described involves multiple individual electronic displays, operated using dedicated ALCs and a common legibility trim control, to permit legibility adjustments to be made in unison. It was shown in Section 7.2 that optimum legibility cannot be achieved by directly applying a common manual or automatic control signal to the luminance controller inputs of multiple electronic displays. Although this is true, applying a common control is still possible, while achieving optimum legibility on multiple displays, if each display is operated from a dedicated automatic legibility control that, in turn, receives a common signal inputted as trim control adjustment by an aircrew member.

The fifth and final subsection describes the integration of manual with automatic legibility control techniques. Reasons for carrying out this integration of manual and automatic legibility control are described along with some considerations involved in its implementation.

7.3.1. Electronic Display Image Difference Luminance Manual Control Characteristics

In general, some means of control is required to permit members of an aircrew to set the image difference luminance of an electronic display, to any desired level between its minimum value at night and its maximum value in full daylight viewing conditions. Once this setting has been made, it is expected that the display will remain at the image difference luminance value set, without fluctuating in value, until the control position is again changed by a crew member.

To enhance the aircrew's ability to learn to gauge the effect of a change in the luminance control knob position, it is desirable for a clockwise angular rotation of the control knob between its minimum and maximum rotation angles to cause a directly proportional increase in the logarithm of the display image difference luminance from its minimum to maximum values. The use of this image difference luminance control algorithm causes the attribute of the display perceived as brightness to change in direct proportion to the rotation angle of the control knob. Implementing this type of control characteristic enhances an aircrew member's ability to gauge the effect of control adjustments. A mathematical representation of the control characteristic relationship between the image difference luminance of a display and the rotation angle of a control knob is presented in the first subsection below.

The overall image difference luminance control characteristic just described relates the output of the

display to the control input made by a pilot or other member of the aircrew. In practice, the control characteristic relationship between the control input by the aircrew member and the electronic display image difference luminance output is typically divided into two separate control characteristics. One characteristic applies to the control operated by the aircrew member and the other applies to the display image difference luminance controller. Two different configurations of the manual control and display controller characteristics are considered in the second subsection.

7.3.1.1. Image Difference Luminance Versus Control Knob Rotation Angle Characteristic

The previously described luminance control algorithm can be represented by a control law of the form,

$$\alpha = k_1 \log_{10}(k_2 \Delta L), \tag{7.1}$$

where the angle through which the control knob is rotated, α, has been normalized to a fraction between 0 and 1 of the full rotation angle of the control. The values of k_1 and k_2 are selected so that

$$\begin{aligned} \alpha = \theta_{min} = 0 \quad @ \quad \Delta L = \Delta L_{min} \quad \text{and} \\ \alpha = \theta_{max} = 1 \quad @ \quad \Delta L = \Delta L_{max}. \end{aligned} \tag{7.2}$$

If $\Delta L = \Delta L_{min}$ is substituted into the control algorithm, Equation 7.1, for a rotation angle of $\alpha = 0$, then

$$0 = k_1 \log_{10} k_2 \Delta L_{min}, \tag{7.3}$$

which yields

$$k_2 = \frac{1}{\Delta L_{min}}. \tag{7.4}$$

Likewise, if $\Delta L = \Delta L_{max}$ is substituted into the control algorithm, Equation 7.1, for a maximum rotation angle, $\alpha = 1$, then

$$1 = k_1 \log_{10} \frac{\Delta L_{max}}{\Delta L_{min}}, \tag{7.5}$$

which yields

$$k_1 = \frac{1}{\log \frac{\Delta L_{max}}{\Delta L_{min}}}. \tag{7.6}$$

Substituting the values of k_1 and k_2 into the control law, Equation 7.1, and solving for ΔL yields

$$\Delta L = \Delta L_{min}\, 10^{\alpha \, Log \frac{\Delta L_{max}}{\Delta L_{min}}} \tag{7.7}$$

as the desired control law relationship between the image difference luminance and the rotation angle of the brightness control knob.

7.3.1.2. Separation of Aircrew Manual Control and Display Controller Characteristics

In a practical application, the setting of the control knob rotation angle, by the aircrew member, would be translated into a voltage that is measurable at the output of the control. This control voltage output would then be used as an input to the display image difference luminance controller. By establishing a standard interface protocol specification for this control voltage, then, in concept, it becomes possible to use any installed control with any electronic display, or to control multiple electronic displays in unison by interfacing them to a compatible common control. Such a specification would have to include, but not necessarily be restricted to, stipulating the following provisions: the polarity of the control voltage; the transfer characteristic between the aircrew manual control input and the absolute voltages at the control output; and the transfer characteristic that

the display's image difference luminance controller must satisfy, when translating the control voltage inputs into absolute image difference luminance levels emanated from the viewing surface of the display.

To illustrate the effect of the control law of Equation 7.7, if for example ΔL_{min} is taken as 0.02 fL and ΔL_{max} is taken as 200 fL then a 50% ($\alpha = 0.5$) rotation of the control knob would, as required, predict a ΔL setting of $\Delta L = 2$ fL, which is the half way point in the logarithmic luminance control range. Two methods of implementing the overall control characteristic of Equation 7.7, while still using a standard interface between the manual luminance control and the display image difference luminance controller, are summarized below.

The control characteristic shown in Equation 7.7 could, for example, be implemented using a control that produces an exponential voltage output in response to the rotation angle of the control knob by an aircrew member, in combination with a display controller that produces a linear image difference luminance output in response to its voltage input. This luminance controller characteristic implementation of Equation 7.7 can be expressed mathematically, as follows:

$$\Delta L = \Delta L_{min} V/V_s, \tag{7.8}$$

where the relationship between the manual rotation angle inputs by the aircrew and the absolute voltages output of the voltage control would then be expressed by the equation

$$V/V_s = 10^{\alpha Log \frac{\Delta L_{max}}{\Delta L_{min}}}. \tag{7.9}$$

Applying the values from the above example and arbitrarily choosing a 0 to 5 Volt range for a standard interface voltage, V, the right side of Equation 7.9 evaluates to 10,000, for a full rotation of the control knob to $\alpha = 1$. The corresponding value of voltage scaling factor, V_s, would have to be equal to 1/2,000 or 0.5 mV for a full scale rotation to result in a 5 Volt maximum control voltage. A disadvantage of this manual control implementation is that the display controller must accurately respond to a very large range of input voltages and produce a correspondingly large range of image difference luminance levels.

Alternatively, the control characteristic of Equation 7.7 could be implemented using an aircrew operated control that produces a linear output voltage in response to the rotation of the control knob, in combination with a display controller that produces an exponential image difference luminance output in response to its voltage input. This control characteristic implementation of Equation 7.7 can be expressed mathematically as follows:

$$\Delta L = \Delta L_{min} 10^{V/V_s}, \tag{7.10}$$

where

$$V/V_s = \alpha Log \frac{\Delta L_{max}}{\Delta L_{min}}. \tag{7.11}$$

Continuing to use the values from the earlier electronic display example, the right side of Equation 7.11 would evaluate to four, for a full rotation of the control knob to $\alpha = 1$, and the scaling voltage, V_s, would have to be equal to 5/4 or 1.25 V for a full scale rotation to result in a 5 Volt maximum control voltage. Since a human's response to the display's image difference luminance output is nominally proportional to the logarithm of the image difference luminance, ΔL, Equation 7.10 shows that this control implementation causes the human's response to be directly proportional to the display controller's input voltage, V, and Equation 7.11 shows that it is also directly proportional to the rotation angle, α, of the manual control knob. Although the combination of Equations 7.8 and 7.9 produces the same overall result as does the combination of Equations 7.10 and 7.11, voltage sensitivity and selectivity problems at low control voltages would make the earlier image difference luminance controller more difficult to implement.

Examination of Equations 7.8 to 7.11, shows that to make the same fixed (e.g., 0 to 5 Volt) standard control voltage range compatible with electronic displays having either smaller or larger image difference luminance control ranges than the ΔL_{min} = 0.02 fL to ΔL_{max} = 200 fL range, used in the preceding example, would require that the voltage scaling factors used by the display image difference luminance controllers be

personalized to each individual electronic display to be controlled. The image difference luminance controller designs for different displays must include not only the effect of the range of the display image difference luminance outputs but, in addition, must produce the appropriate absolute values of a particular display's image difference luminance outputs, by also accounting for the effect of differences in the ΔL_{min} term in Equations 7.8 and 7.10.

For the initial application of color active matrix liquid crystal displays to military aircraft cockpits, the control voltage range applied at the display luminance controller input was varied from 0 to 5 Volts, using the precautions described in the succeeding two paragraphs. In these instances, the manual controls used were linear in their voltage output to control knob rotation angle input, and the display luminance controllers produced an exponential image difference luminance output in response to the control voltage input. In other words, these applications used the control interface implementation technique represented by Equations 7.10 and 7.11.

To enhance the fault tolerance of the preceding manual control, the voltage level translation was selected to cause the minimum luminance to be commanded by the maximum control voltage of + 5 Volts dc, and the maximum luminance was commanded by the minimum control voltage of zero. The rationale for this inversion of the control voltage is that an open or shorted control line would command the display to its maximum rather than its minimum display luminance. The relationship between the rotation angle of the control knob and the control voltage, using this control algorithm, can, therefore, be represented, as follows:

$$\alpha = 1 - \frac{1}{5}V, \tag{7.12}$$

or as

$$V = 5(1 - \alpha), \tag{7.13}$$

where as before the angle, α, has been normalized to values between zero and one (i.e., between 0% and 100% rotation).

Essentially the same image difference luminance control technique can be applied in a slightly modified form that, besides providing fault tolerance, also enhances the capability to monitor for a failure of the controls to operate as required. To permit distinguishing a faulted signal line from a commanded control level, the voltage control range can, for example, be reduced to 0.1 Volts to 4.9 Volts, thereby permitting a 0 or 5 Volt open or short condition to be distinguished from a commanded control voltage level.

7.3.2. Interfacing Aircrew Legibility Controls with Image Difference Luminance Controllers for Electronic Displays

The idea that aircrew controls can be used interchangeably and that a common control voltage can be used to adjust the legibilities of multiple cockpit displays, in unison, stems from the historic use of such controls in operational aircraft to set the night lighting levels of various groupings of conventional reflective operating mode displays, such as integrally illuminated ADIs, HSIs, and engine instruments, and integrally illuminated panels and switches. In practice these control implementations are not as straightforward, as at first impression, they might seem. For example, to achieve coordinated uniform lighting between different integrally illuminated conventional instruments in a control group, as the brightness control variac voltage is changed, not only must the number and placement of incandescent lamps be carefully controlled to achieve uniform luminance information depictions across each display's viewing surface, but all of the instruments in a controlled group must use the same wheat lamps and light bulb color adjustment filters to implement their integral illumination. This latter requirement is necessitated because different types of lamps have different illumination versus alternating current (AC) voltage control characteristics.

The differences between the incandescent lamp control characteristics become particularly noticeable

at low AC voltage levels, when using a common variac to control the power applied to instruments illuminated by different types of lamps. In this case, the differences between the luminance versus voltage control characteristics, of the different types of lamps that can be used with integrally illuminated aircraft instruments, are sufficient to cause one instrument to be illuminated when another is still off, with the same AC voltage applied to both instruments. Assigning different variacs to control the night lighting of distinct groupings of instruments or panels, which individually have matched control characteristics, but which have differing control characteristics between the groupings, provides a means to enlist the aid of aircrew members to bypass this control problem. The point of introducing the preceding information is that the potential differences in the control characteristics between individual electronic displays are vastly greater than those of the integrally illuminated instrument and panel displays that are used in conventionally equipped cockpits, and can even differ significantly for implementations of the same electronic display technology by different manufacturers.

Historically, manual legibility controls for use with individual electronic displays have been implemented by causing the extremes of their voltage control ranges to coincide nominally with the image difference luminance range, established by the minimum and maximum absolute image difference luminance output limits of the individual electronic displays, they are intended to control. The limits on the absolute image difference luminance ranges of electronic displays are, in turn, typically imposed by a combination of the differing legibility requirements of the information to be displayed and of technology related capabilities and limitations of the displays, and of their image difference luminance controllers. These differences cause the maximum image difference luminances of electronic displays, designed to depict different types of information or having different background surface reflectances, to differ from one another.

For example, this historic manual legibility control technique envisions two electronic displays, having the same background surface reflectances and their respective manual voltage controls set to their maximum luminance settings, causing the image difference luminance of an electronic display that only presents alphanumerics to match the image difference luminance of alphanumeric information presented on a video display, and therefore achieve equal legibility for the two display presentations, even though this requires the maximum image difference luminance of the video display to be much higher than that of the display designed only to present alphanumerics. Likewise, two displays, which produce equal legibilities when presenting the same information, and that have their respective manual voltage controls set to their maximum luminance settings, would have to operate at different image difference luminance levels, if they have different background surface reflectances.

It is also assumed, when using this historic control strategy, that if each controlled electronic display has the same overall normalized image difference luminance versus control voltage characteristic, then as their control voltages are manually adjusted between their minimum and maximum values, for example, by applying the 0 to 5 Volt of the earlier example, or any other standard, fixed control voltage range, the response of the individual electronic displays to the image difference luminance controllers would cause the legibilities of the displays to remain nominally in balance, even though image difference luminance levels for the same information presented on different displays could differ. The overall manual luminance control characteristics, expressed by Equation 7.7 and through the manual control and luminance controller combinations of Equations 7.8 and 7.9 or Equations 7.10 and 7.11, would provide manual control characteristics, consistent with this historic control technique, since, as required, these control equations are predicated on the fact that different electronic displays frequently require image difference luminance control ranges, with differing ΔL_{min} and ΔL_{max} values, if the imagery they portray are to be perceived as equally legible.

Although the image difference luminance control strategy assumed in the preceding paragraph is valid for electronic displays, with equal surface reflectances, and when viewed, with each display exposed to the same incident ambient illumination conditions, the assumption is invalid when either of these two conditions is not satisfied. As described in Section 7.2, electronic displays with different surface reflectances or identical displays exposed to different incident illuminance levels, cause the displays to operate at different points on the human's nonlinear image difference luminance requirements characteristics. This is equivalent to the human's visual requirements following different nonlinear control characteristics, and the result is that

proportional changes in the image difference luminances of displays, controlled as described in the preceding paragraph, does not maintain the sought after legibility balance between the displays, as coordinated changes are made in their control voltages. As a practical matter, this imbalance between the legibilities of electronic displays only becomes a problem when the displays are operated using common rather than individual manual luminance controls, and, even then, need not always create a problem, as is described later in this chapter.

The automatic legibility control law equations, introduced earlier in this report to permit the human's image difference luminance requirements to be satisfied, when information is presented on electronic displays, predict the absolute image difference luminance levels of the imagery to be portrayed on the individual electronic displays these ALC outputs are intended to control. Therefore, like the manual luminance control techniques, described in the preceding paragraphs, the automatic legibility control generates absolute image difference luminance requirements, a display must meet. If a control interface, with a fixed voltage range is used, the control voltage must be capable of being interpreted by a display luminance controller, as the absolute image difference luminance level, at which the display should be operated.

Based on the preceding information, it can be concluded that the standard output control voltage produced by any particular setting of a manual luminance control, or commanded by an automatic legibility control in response to any sensed aircraft cockpit ambient illumination and veiling luminance environment, must be capable of being interpreted and directly translated, by the image difference luminance controller associated with each electronic display, into the absolute image difference luminance value encoded into each display's standard output control voltage. In other words, a direct correspondence must exist between the absolute image difference luminance output of the electronic display and the standardized voltage applied at the input to the image difference luminance controller, and, furthermore, the standardized voltage output of the control must unambiguously encode the aircrew member's image difference luminance requirement, whether it is set manually by an aircrew member or established by an automatic legibility control.

In the balance of this subsection, the subject of interfacing aircrew legibility controls with image difference luminance controllers suitable for use with electronic displays is examined in greater detail. The specific topics considered include the following: the interchangeability criteria for aircrew manual controls; an absolute control interface protocol; a relative control interface protocol; and a comparison of the advantages and disadvantages of the absolute and relative control interface protocols.

To establish a control interface protocol standard, which would be compatible with using interchangeable common aircrew manual luminance controls, and automatic legibility controls, with image difference luminance controllers operating multiple electronic displays, would require not only that the properties of the control interface voltage be defined, as described above, but that the input versus output control characteristics, applicable to the image difference luminance controllers, for any electronic display, and to any aircrew manual and automatic legibility controls, to be interfaced, also be coordinated and standardized. For the reasons described above and in Section 7.2, even taking these precautions does not provide a reasonable expectation that the application of a common control signal to multiple electronic display controllers, implemented using this historic control strategy, would produce a legibility match between different displays, unless the displays are essentially identical and are viewed under essentially identical incident illuminance viewing conditions. It should be noted that while the display equivalence and commonality of viewing conditions, of the latter caveat, would not be satisfied in typical applications where common manual or automatic legibility controls would be used to adjust the legibilities of electronic displays in operational military aircraft, the practical effect of these legibility control inaccuracies can be restricted to causing some displays to be more legible than they would otherwise have to be if they were precisely controlled.

The topic of applying common manual luminance control and automatic legibility control to aircraft cockpit displays is considered in greater detail later in this chapter. In that discussion some tradeoffs and implications of achieving less than ideal legibility control, for electronic displays installed in aircraft cockpits, are considered. Furthermore, a method is described that does allow the use of common aircrew legibility controls to allow precise legibility to be maintained on all of the electronic displays in an aircraft cockpit concurrently.

7.3.2.1. Interchangeability Criteria for Aircrew Manual Controls

Establishing a standard control interface protocol, which stipulates a fixed control voltage range, such as the 0 to 5 Volt voltage range of the earlier example, is sufficient to assure that aircrew controls will be interchangeable, at least from the perspective of the compatibility of voltage magnitudes, at the interface between the outputs of the controls and the inputs to the image difference luminance controllers. For manual controls, interchangeability also implies that all of the controls must use the same input to output control characteristics (e.g., linear or exponential). This requirement is necessary, for manual control interchangeability, if any display image difference luminance controller is to be able to interpret the input control voltage setting of an aircrew member in the same way, for any manual control. Satisfying the preceding requirements is both a necessary and sufficient condition to make it possible to interchange manual controls between individually controlled displays without causing the legibility control characteristics of the displays to be altered. Dedicated manual controls, implemented in aircraft cockpits to satisfy the criteria just described, would allow individual members of the aircrew to adjust any electronic display to meet their personal preferences or needs for legibility, subject only to the stipulation that the individual display controllers can use the full image difference luminance output range of each of the individual displays controlled, using the standard manual control voltages as inputs.

Because aircrew members, when provided with dedicated manual controls, can be relied upon to be able to adjust the legibilities of individual electronic displays, the interface protocol requirements of the previous paragraph did not have to include the specific control characteristics that different displays and their respective image difference luminance controllers should possess, when operated using the standard control voltage. When individual displays are to be operated, using dedicated automatic legibility controls, or when multiple displays are to be operated, using either a single common manual control or a single automatic legibility control, then a more completely defined control interface protocol becomes necessary. Although it is not essential for different display image difference luminance controllers to produce the same perceived changes in legibility, as a function of the rotation angle of their respective manual luminance controls, a coordinated legibility response of electronic displays across the cockpit would lead to the aircrew learning to make adjustments that meet their legibility needs more rapidly, thereby, leaving more time to perform other more important tasks.

7.3.2.2. Absolute Control Interface Protocol

As previously described, a complete standard control interface protocol would have to incorporate image difference luminance controllers for electronic displays, designed to produce absolute image difference luminance output values that are fully consistent with the respective inferred absolute image difference luminance levels, encoded in control signals applied at their inputs. Thus, to achieve complete interface standardization would require full coordination of both the control characteristics and signal level relationships, of manual and automatic legibility controls, and the corresponding control characteristics and signal level relationships, of the different electronic displays and their respective image difference luminance controllers. The objective of complete interface standardization is to achieve coordination between the control characteristics of the different electronic displays installed in the cockpit, so that the image difference luminance levels depicted, when the different display image difference luminance controllers are presented with a succession of equal input control voltage levels, result in the correct inter-display legibility levels, at each control voltage level and when viewed under identical illumination conditions.

In practical terms, the implementation of a complete absolute control interface protocol means that an electronic display intended to only present alphanumeric information and another intended to present sensor-video information would receive differing absolute voltage control levels, consistent with the difference in the image difference luminance requirements needed to portray alphanumeric and video information presentations legibly. Because the ranges of the control voltages and controlled image difference luminances are absolute,

display information presentations that achieve legibility at reduced image difference luminance levels would also have correspondingly lower voltage control levels and the display controller would have to be designed to be compatible with interpreting and translating this reduced control voltage range into a correspondingly reduced image difference luminance output range for the display. The implementation of this control protocol should cause alphanumeric information presented on an alphanumeric display, at a reduced absolute image difference luminance level, to have essentially the same legibility as alphanumeric information presented on a multipurpose video display, which, though controlled to operate at a much higher absolute image difference luminance level, presents alphanumeric information at a reduced modulation and image difference luminance level befitting the information being presented.

If automatic legibility control is implemented using this absolute voltage control interface protocol, then differences in the absolute voltage control levels, consistent with the image difference luminance requirements of displays having different light reflectance properties, or having cockpit location dependent differences in their exposures to ambient illuminance or to the veiling luminance induced in the pilot's eyes, can also be taken into account. As alluded to earlier, and as described later in this section, these differences cannot be completely taken into account using a common manual luminance control to operate multiple displays in unison, even if the complete absolute voltage control interface protocol is implemented. In spite of this inherent limitation, using the complete absolute control interface protocol does provide a degree of coordination between the legibilities of like information presented on different displays that is not otherwise attainable using manually adjusted aircrew controls. As described in Section 7.2, and later in this section, optimum legibility control is still only possible for the case of individual displays operated using dedicated automatic legibility controls, equipped with individually adjustable aircrew trim controls.

The ability to map absolute control voltages into absolute display image difference luminance levels unambiguously, is both the primary advantage and disadvantage of this control technique. The advantages have already been described. The disadvantage is the need to provide an expanded range of control voltages, and of image difference luminance controller levels, to provide for compatibility with the retrofit of higher image difference luminance displays, as they become available in the future.

7.3.2.3. Relative Control Interface Protocol

Although the complete absolute control interface protocol appears to provide the ability to make aircrew controls interchangeable between any electronic displays, this in fact only applies to manual aircrew controls. As described in Section 7.2, and as covered in greater detail later in this section, automatic legibility controls must be individualized through the incorporation into the reflected background luminance term of the diffuse and specular reflectance properties of the specific electronic displays they control. Thus, while the control voltages generated are physically compatible with any display, the interpretation of the control levels is specific to each display unless the reflectance properties of the displays are the same.

Since the control lines from individual automatic legibility controls cannot be interchanged, even for the absolute control interface protocol described in the previous section, this opens the possibility of using other tailored signal interface techniques that still use a standard voltage with a fixed range voltage interface at the input to the display image difference luminance controllers. A viable alternative to the absolute control interface protocol uses a technique that will be called relative control. Relative control as defined here, refers to mapping the image difference luminance values, calculated using the automatic legibility control algorithm for a particular electronic display, onto a control voltage range that encompasses all, or nearly all, of the fixed range of control interface voltages. The coordinated display image difference luminance controller is then designed to read the image difference luminance levels encoded into the mapped voltages presented at the control interface and operate the display at the commanded output levels. The technique is called relative because each display, whether having a large or small image difference luminance control range would map its image difference luminance requirements onto the same interface control voltage range. In spite of the name, this control technique still involves relating absolute image difference luminance values from the automatic legibility control

to the display image difference luminance controller.

In practical terms, the relative control technique is just an extension to automatic legibility controls of the current practice, described in the introduction to this section, of historic technique of matching the fixed range of voltages associated with manually adjustable aircrew controls to the full image difference luminance range of the electronic display to be controlled.

7.3.2.4. Comparison of Absolute and Relative Control Interface Protocols

The primary advantages of the relative versus the absolute control interface techniques relate to the increased accu of control that is potentially available when relative control is used. Unlike the absolute control interface p ol, the relative control protocol does not require reserving portions of the control voltage range that are on sed by some displays. The recovery of these portions of the interface control voltage range by using the ve control technique, at least potentially, can lead to an increase the control sensitivity that is achievable. ne display controller side of the interface, being able to map the entire control voltage range into image c ence luminance drive levels should also lead to an improvement in control accuracy. A specification using the latter approach to map interface control voltage levels into displayed image difference luminance levels would also be easier to specify, and less prone to misinterpretation. The only noteworthy disadvantage of the relative control interface technique, when compared with the absolute control interface technique, is that the control characteristics of the individual display image difference luminance controllers, having once been designed to be compatible with control signals that span the entire fixed range of the control interface voltages, cannot, except by chance, or by restricting common manual control to electronic displays having matched surface reflectance properties, afterwards produce any close semblance of coordination between the legibilities of electronic displays that are operated using common manual controls.

In comparisons between the relative and absolute control interface techniques, there also are some relative merits of the two techniques that appear to either be closely matched or tend to counterbalance each another. For example, dedicated manual aircrew controls are interchangeable between different types of electronic displays for both of these control interface techniques. Likewise, while the relative control interface technique requires the range of output image difference luminance values, generated by the automatic legibility control algorithms, for each of the dedicated electronic displays controlled, to be scaled to span the entire fixed voltage range of the control interface, the absolute control interface technique also requires scaling of the automatic luminance control output signals, but to a smaller portion of the fixed voltage range of the control interface.

Because the legibility control performance capabilities of electronic displays using dedicated automatic legibility controls are not affected by a choice between the relative and absolute control techniques, the greater potential accuracy offered by the relative control interface technique causes this technique to be preferable to the absolute control interface technique. The reduced ability to coordinate the legibility of different electronic displays, when using the relative control interface technique and a common manual control to adjust the legibility of multiple displays, in unison, is not a significant factor in the choice of a preferred control technique. The reasons this reduction in the ability to coordinate the legibility of different electronic displays is not significant, in the choice of a preferred control technique, are related to the way that aircrew members would have to approach the use of common controls to be able to achieve and maintain adequate display legibility, under the typical ambient illumination and veiling luminance viewing conditions, experienced by aircrew members in operational military aircraft cockpits. The ability of aircrew members to adjust the legibilities of multiple displays using a common manual control is considered in greater depth later in this section.

7.3.3. Electronic Display Manual Legibility Control Options

At one control capability extreme, the provision of a dedicated manual legibility control for each individual

electronic display gives the aircrew member the flexibility to set each display to suit that crew member's individual legibility preferences and needs, but, due to the multiple controls, this approach also imposes a significant added workload requirement that is not present for conventional light reflective mode displays, at least when viewed under daylight ambient illumination conditions. At the other extreme, a common manual control reduces the workload associated with individual controls but, as indicated in the Section 7.2, does not allow optimum legibility to be achieved for most of the cockpit electronic displays being controlled, even if the displays are physically identical.

7.3.3.1. Individual Electronic Displays Operated Using Dedicated Manual Controls

The difference between the control requirements of conventional and electronic displays occur under daylight viewing conditions. As indicated in the introduction to this section, conventional reflective operating mode displays already possess an inherent form of automatic legibility control, which accounts for any changes in ambient illumination conditions incident on the displays in the cockpit, and that makes it unnecessary for their legibility to be controlled by members of the flight crew, except at night. In comparison, the legibility of existing electronic displays that are suitable for use in aircraft cockpits must be controlled by the flight crew under both day and night viewing conditions, unless they are initially set to operate at their maximum image luminance levels and, afterwards, are not controlled under daylight viewing conditions, as was previously described in Chapter 5.

While the control of display legibility is a necessary task, if the flight crew is to be able acquire the information needed to carry out a mission, it is nonetheless an ancillary task that adds nothing to mission performance and, in fact, can only serve to degrade the performance of the aircrew by using time that could otherwise be spent conducting primary mission-related tasks. In the event the aircrew member cannot divert the time needed to control the legibility of the electronic displays manually, then the information these displays portray can potentially become illegible, if the ambient illumination or glare source viewing conditions subsequently increases. In spite of its limitations, the use of dedicated manual controls is the predominant electronic display legibility control technique currently in use in operational military aircraft cockpits.

7.3.3.2. Multiple Electronic Displays Operated in Unison Using a Common Manual Control

If the image difference luminances of electronic displays are to be manually controlled, then a means should also be provided to allow aircrew members to change the luminances of these displays rapidly in unison, as the need for adjustments to maintain information legibility demands. As described in Section 7.2, this control approach has some shortcomings, but it is still preferable to forcing the aircrew to adjust the legibilities of multiple electronic displays, on an individual basis, during periods when mission requirements place constraints on the time available to attend to ancillary tasks.

When a common control is employed to permit the image difference luminances of multiple electronic displays to be set in unison, individual display image difference luminance controls continue to perform a useful function by allowing the aircrew to set the relative luminance levels on the different displayed instrument information presentations. Under this control scheme, the common control takes over the function of setting the absolute luminance levels of the individual displays, the idea being to provide a means for the aircrew quickly to adjust the image difference luminances of all of the displays in unison by using the common control. In this case, the dedicated individual display controls, provide a means for aircrew members to balance the legibilities of the different displays relative to the nominal value set by the common control.

As described in Section 7.2, a common control signal poses a problem when used to operate multiple electronic displays unless the displays have almost the same light reflectance properties, and, even then, equal legibility cannot be maintained with different time changing ambient illumination and veiling luminance viewing conditions incident simultaneously on different display positions in an aircraft cockpit. To reiterate the

conclusions reached earlier in Section 7.2, electronic displays, which present the same information but have different light reflectances, or are installed at different locations in the cockpit, must be operated at different image difference luminance levels, if equal legibility is to be achieved for all of the displays. Furthermore, electronic displays, having different reflectances, or exposed simultaneously to different incident illuminance and veiling luminance conditions, operate at different points on the pilot's nonlinear image difference luminance versus background luminance requirement characteristic. In other words, the image difference luminance controllers, for each individual electronic display in the cockpit, must be designed to track simultaneously different parts of the human image difference luminance control characteristic, if equal legibility is to be maintained. However, this poses a problem for displays controlled using a common manual image difference luminance controls.

The significance of the preceding result is that knowing the image difference luminance requirements for one display and the luminance multiplier relationship between that display and a second display, at one background luminance level, is insufficient to permit the prediction of the image difference luminance requirement for the second display, at a different background luminance level. Moreover, when electronic displays are controlled in unison using the same common manual control signal, and the individual dedicated manual controls are initially set to provide equal legibility, changes in the incident ambient illumination or glare source condition of the display viewing environment also alters the legibility relationships between the displays. Because of the preceding facts, it can be concluded that a common control signal cannot simultaneously encode the control requirements needed to compensate for the time variant incident illuminance and veiling luminance conditions, for electronic displays installed at different locations in a cockpit. Moreover, for the reasons previously explained, this conclusion remains valid even if the electronic displays are identical.

A completely different situation exists, if the individual dedicated legibility controls, for the electronic displays in a cockpit, are adjusted at night to provide equally legible information format portrayals. Under this viewing condition, information format designs having similar character and symbol font sizes, would be perceived as equally legible when the imagery presented on the electronic displays operates at closely matched image difference luminance levels, essentially independent of the background reflectances of the electronic display viewing surfaces or of the image difference luminance level settings of the displays. Even if differing image difference luminance requirements exist for information presented on the different diplays, to compensate for imagery having different image critical detail dimensions, maintaining a fixed ratio between the image difference luminance levels portrayed would maintain constant legibility when the luminance levels of the displays are changed in unison. Therefore, under night viewing conditions, it can be concluded that electronic displays, operated by luminance controllers designed to produce equal luminances for the same imagery, are amenable to being controlled in unison. This type of control would produce no greater legibility discrepancies between displays than those that already apply to the common control of conventional displays at night. To be more specific, the only shortcoming of using a common manual legibility control with either conventional or electronic displays at night would be the inability to account for the directional effect of the veiling luminance induced by night glare sources on the legibilities of the displays.

As previously described, although significant differences between the reflectances, of the individual electronic displays installed in a cockpit, do not influence their night legibility settings, under daylight viewing conditions, differences in the display reflectances translate into differences in the image difference luminance levels needed to achieve equally legible presentations. Furthermore, this is true even if identical ambient illumination exposure conditions are incident concurrently on each display during day viewing conditions. Consequently, unless the display reflectances are nearly matched, the use of a common legibility control to adjust the legibility of these display presentations, in unison, following a transition from night to daylight viewing conditions, would require the image difference luminance levels of the individual displays to be readjusted from their night settings, just to cause them again to be of equal legibility under the specific daylight viewing conditions being experienced at that particular point in time.

Because of the differences between the image difference luminance control requirements of electronic displays operated at night rather than during the day, probably the best strategy for implementing a common

manual image difference luminance control with electronic displays, would involve initially designing the individual electronic display controllers to provide equal legibility at night. Aircrew members could then use the common control signal to adjust the image difference luminances of the electronic displays in unison to achieve the desired level of legibility on the cockpit display that is the least legible, for the glare source and ambient illumination conditions being experienced at any given point in time under daylight viewing conditions. This control strategy causes the remainder of the cockpit electronic displays to more legible that would be required, but this situation already exists without causing problems in aircraft cockpits equipped with a mixture of electronic and conventional electromechanical displays. The constraints previously described on the use of a common manual control and, in particular, the need for the displays to have essentially the same light reflectance properties, become a mute point when using this control strategy.

The principal disadvantage of even a properly implemented common manual luminance control adjustment strategy, in comparison to using automatic legibility control, is that maneuvering an aircraft can rapidly cause changes to occur in the individual electronic displays that are experiencing the greatest legibility degradation. This introduces the potential for repeated adjustments to the common control setting, unless the control is simply set to its maximum setting under such conditions. In spite of this disadvantage of common manual luminance controls, in comparison to the precision possible using automatic legibility controls, dedicated for use with individual electronic displays, from an aircrew workload perspective, the addition of common manual controls to permit the aircrew to adjust the legibility of groupings of electronic displays, in unison, is still a significant improvement over the workload associated with the adjustment of each individual display using only dedicated manual controls.

7.3.4. Electronic Display Automatic Legibility Control Options

Control prerogatives that should be provided to the aircrew, in the event that automatic legibility control is to be implemented, include the following:

1. The ability to choose between manual and automatic legibility/brightness control.

2. The ability, when under the manual control mode of operation, to control the luminance of individual displays both alone and, if so equipped, also in unison.

3. The ability, when the automatic control mode of operation is selected, to make trim adjustments to the luminance of individual displays, and to make trim adjustments in unison, using a common legibility trim control, to displays already being controlled with independent automatic legibility controls, in response to changes in the ambient illumination conditions in the cockpit and in the glare field luminances, if present in the aircrew's field of view.

In the subsections that follow, the pros and cons of adopting three different electronic display legibility control approaches are presented. The approaches described include the following: (1) multiple individual electronic displays operated using dedicated ALCs; (2) multiple electronic displays operated in unison using a single ALC; and (3) multiple individual electronic displays operated using dedicated ALCs and legibility trim controls, with a common legibility trim control to permit legibility adjustments to be made in unison.

7.3.4.1. Multiple Individual Electronic Displays Operated Using Dedicated ALCs

If automatic legibility control is implemented so that the diffuse and specular surface reflectance components of the reflected background luminance term of each individual electronic display are programmable, then an ALC output tailored for each type of display to be controlled in an aircraft could be generated. In this case, each automatic control line would, in general, be encoded with a different control signal, just as they would if a pilot had individually set manual luminance controls to provide equal legibility.

However, because each signal is already tailored to the needs of the display receiving it (i.e., the signal encodes the specific image difference luminance the display is supposed to produce), there should be no confusion by the display manufacturer with respect to the design requirements for their display luminance controller to cause it to satisfy the aircrew's legibility needs fully, under any combination of incident and glare source ambient illumination conditions. The principal advantage of the dedicated ALC control approach is that it produces the most precise level of electronic display legibility control possible, with the least amount of legibility control intervention by aircrew members, provided only that a consistent complement of light sensors is installed in the aircraft cockpit to insure effective operation of the dedicated automatic legibility controls. The appropriate integration of light sensors with multiple displays and dedicated automatic legibility controls is the topic considered in the next section of this chapter.

The disadvantages of controlling individual electronic display using the dedicated ALC control approach may be summarized as follows: (1) ALC signal lines are not interchangeable between electronic displays of different types (i.e., with different reflected luminance responses) or for the same displays in different locations in the cockpit; (2) each control output must be capable of being generated using ALC algorithms with different programmed reflectance terms, operating in parallel; and (3) display upgrades, possibly using different display types or manufacturers' displays, would almost certainly require reprogramming the reflectance component in the background luminance term in the ALC algorithm applicable to the cockpit display position where the upgrade occurs.

7.3.4.2. Multiple Electronic Displays Operated in Unison Using a Single ALC

Many information presentations depicted on existing electronic displays in operational aircraft cockpits do not require maintaining precise display legibility control to allow the aircrew to achieve satisfactory aircraft mission performance. Under such circumstances, a question naturally arises whether it is worth the extra development time and cost to provide an automatic legibility control capability that permits the best possible display legibility performance to be achieved, where a more easily implemented solution would suffice to satisfy the aircrew's legibility requirements. This question cannot be answered definitively, except by its intended user and developer, and then only in the context of the mission capability requirements of a specific aircraft. It is for this reason that this section has been included to describe the implications of choosing the option of using multiple electronic displays operated in unison using a single ALC.

If the same control signal is sent to every electronic display in the cockpit, whether it is an automatic or manually controlled signal, then a considerable compromise in the control accuracy that is achievable must be accepted as a necessary consequence of adopting this control approach. The extent of the error encountered, and the ambient illumination conditions for which the error is most severe, depends on several implementation options and constraints, which are considered below only in general terms.

As previously described, the ALC algorithm parameter that must be altered to achieve accurate legibility control performance is the reflective response of the display to incident ambient illuminance, for diffuse reflectance, and for incident luminance, for specular reflectance. The assignment of specific reflectances, to establish a single ALC algorithm, results in causing displays to be precisely controlled only when they have diffuse and specular reflectances that match the ones programmed into the ALC algorithm, whereas displays with other reflectances will incur image difference luminance control errors. To achieve a reasonable degree of control accuracy using a single ALC signal would, therefore, require that the displays employed be chosen to have approximately the same diffuse and specular reflectance values, and, consequently, the same image difference luminance outputs, for any given set of ambient illumination environment conditions present in an aircraft cockpit.

One reason the single ALC approach is being discussed here is that most of the existing electronic display technologies that can be designed and fully implemented to achieve adequate daylight legibility have remarkably similar diffuse and specular light reflectance characteristics. In particular, this applies to

monochrome cathode ray tube, light emitting diode and back lighted color liquid crystal displays that have been properly designed and optically filtered to make them legible in aircraft cockpit operating environments. Since sunlight readable versions of all of these displays operate in essentially the same reflected background luminance range of the aircrew member's image difference luminance requirement characteristics, applying a single automatic legibility control signal applicable to the highest surface reflectance display technology in use, would cause all of the displays to operate, at or slightly above, the image difference luminance level needed to make that technology legible. A second reason that the single ALC approach is being discussed here is that it produces the same legibility control problems for the aircrew as a single common manual control, when it is used to provide the aircrew with control over multiple electronic displays, in unison.

The application of either a single ALC or manual control signal, to different electronic display technologies that have nominally matched display surface reflectances, as described above, or even to identical displays, would, however, require further potentially significant compromises. Using a single ALC control signal infers that all of the displays will ultimately be controlled using a single set of incident ambient illuminance and veiling luminance sensor signals. In order for all of the displays to be legible, the use of a single control signal further infers that it is the sensed values of these light measurement variables, which cause the highest image difference luminance level to be commanded, that would have to be used to operate the full complement of electronic displays installed in the cockpit. Consequently, electronic displays, which are in shadows or that are located on the opposite side of the cockpit from the veiling luminance sensor receiving the highest reading, will be commanded by the ALC to operate at legibility levels that are higher than those of the displays to which the light measurements would apply if they were receiving individualized ALC output signals. The single ALC control signal implementation approach would, therefore, require that the light measurement signals from throughout the cockpit be monitored and that a voting process occur to select the combination of these values needed to provide satisfactory legibility for the display experiencing the most severe combined ambient illumination and glare source exposure conditions. The combination of sensor values selected in this manner, from the cockpit's incident illuminance and veiling luminance sensor measurements, would then have to be used to control all of the displays simultaneously. When a single common manual control signal is used to control the legibility of multiple displays, instead of using a single ALC signal, aircrew members would have to perform the previously described monitoring and control functions to satisfy their legibility needs.

7.3.4.3. Multiple Individual Electronic Displays Operated Using Dedicated ALCs and Both Individual and Common Legibility Trim Controls

A significant advantage of the automatic legibility control adjustment strategy occurs if both individual and common aircrew trim controls are implemented to permit trim adjustments to the legibilities of automatically controlled electronic displays both individually and in unison. The ability to use individual ALC trim controls, in combination with a common ALC trim control, permits aircrew members to adjust the relative legibilities of individual electronic displays, and afterwards to control their overall legibilities, in unison, to suit the aircrew's personal needs or preferences for the legibility of display information portrayals, using the common trim control. Since the automatic legibility control maintains the legibilities of the individual displays at a constant level, under time changing day or night ambient illumination viewing environments, the trim control settings are made with respect to the sensor commanded level established by each of the respective automatic legibility controls and, consequently, they also should remain at the relative levels set by the aircrew members. An example of the legibility adjustment flexibility benefits offered by providing individual display and common trim adjustments of image difference luminance levels would be the ability for aircrew members selectively to reduce the interference caused by individual color electronic displays, when using night vision devices in the cockpit. Another example of these benefits, would be the ability selectively to reduce the effects on aircrew dark adaptation of the image difference luminances emanating from individual cockpit displays that are located close to the pilot's line of sight to exterior night scene objects of interest.

7.3.5. Integration of Manual with Automatic Control Techniques

To assure that the overall image difference luminance and automatic legibility control subsystem used to adjust the image difference luminance levels of electronic displays are fail-safe, automatic legibility control should be treated as an adjunct to manual control. If any part of the automatic legibility control system fails, or provides performance that does not fully meet the aircrew's needs, it should be possible for individual aircrew members to switch from the automatic to the manual control mode of operation. In those instances where the use of automatic brightness control has been stipulated in the past, it has typically also been required that a failure of the automatic control would not prevent the continued operation of the electronic displays, using manual controls to set their image difference luminance levels. An additional advantage of this composite control strategy, if properly implemented, is that it provides an inherent level of redundancy, if there is a fault in the common control, in one of the individual display controls or in the automatic brightness or legibility controls. Like any other integral part of the electronic display subsystems in aircraft cockpits, including its image generators and processors, and the electronic circuitry used to implement the aircrew's capability to control the image difference luminance levels of electronic displays manually, any potential sources of single point failures associated with the implementation of automatic legibility controls, which have the potential of causing one or more displays to become unusable, should be carefully analyzed and eliminated. The capability to operate in a backup control mode should still be provided.

Considerations involved in the implementation of display legibility trim controls, to permit aircrew members to adjust the legibilities of individual electronic displays, in relationship to the level commanded by the automatic legibility control, so that the crew's personal preferences or needs for the legibility of displayed information portrayals can be satisfied, were described previously in Chapter 5. The act of switching from the automatic to manual control mode would provide a means of allowing the legibility trim control(s) described in Chapter 5 to serve the dual functions of being able to make trim adjustments, to the legibility levels set by the automatic legibility controls, and to serve as manual controls, for the adjustment of the image difference luminance levels of the electronic displays, when functioning in the manual control mode.

To permit manual controls to serve in the dual function role, just described, requires that some additional constraints be satisfied. In Section 7.3.1.2, two implementations of the overall manual control characteristic described in Section 7.3.2.1 were considered. One implementation consisted of a manual control, with an exponential input to output control characteristic, interfaced to a display luminance controller with a linear input to output control characteristic. The other implementation consisted of a manual control, with a linear input to output control characteristic, interfaced to a display controller with an exponential input to output control characteristic.

The first of these implementations, involving the exponential control and linear luminance controller, allows direct switching back and forth, between the automatic and manual control modes. The reason direct switching is possible is because the output response of the automatic legibility control algorithm is already proportional to the desired image difference luminance output from the display and therefore can be linearly scaled to create the applicable absolute or relative control voltage range, previously described in Sections 7.3.2.2 through 7.3.2.4, that is directly compatible with being used as an input to a linear display image difference luminance controller. This means that, when properly scaled, this ALC output can be directly interchanged with an output from a manual control having an exponential input to output angular position versus voltage characteristic, since both controls produce image difference luminance changes, the viewer perceives as changing linearly, in response to exponential changes in the control voltage signals, at the input to the image difference luminance controller. In this instance, the exponential response characteristic of the manual control should also be suitable for implementing the individual display and common legibility trim control functions of automatic legibility controls, when the manual control's output voltage is linearly scaled and used to set the values of the contrast and night image difference trim controls.

In the second control implementation, a display image difference luminance controller having an exponential input to output control characteristic, and operated by a linear manual control, requires that the

logarithm of the output of the automatic luminance control algorithm be taken before it is scaled to match the applicable absolute or relative interface control voltage range. Since the output of the ALC algorithm is already proportional to the image difference luminance the display is intended to operate at, the logarithm of the output of the ALC algorithm must be used as the input to the exponential display image difference luminance controller. The display image difference luminance controller's exponential input to output control transfer characteristic, when operating on the logarithm of the ALC's output value, takes the antilogarithm of the scaled input voltage, and in so doing restores the necessary direct proportionality between the image difference luminance level commanded by the ALC and the image difference luminance at the output of the electronic display. It follows directly from this result that taking the logarithm of the ALC output is an essential signal processing step, if interchangeability between the linear manual and automatic legibility controls is to be achieved, at the input to display image difference luminance controllers having exponential input to output control characteristics.

To enable a linear manual control to be used as an input to a display image difference luminance controller having an exponential input to output control characteristic, and, interchangeably, as a legibility trim control input to an automatic legibility control, an input to output transfer characteristic, analogous to the exponential characteristic described in Section 7.3.1.1, has to be implemented to serve as an interface between the linear manual voltage control and the input voltage to the automatic legibility control algorithm. The introduction of an exponential output from the legibility trim control, to serve as a contrast or night image difference trim control input at the interface to the automatic legibility control algorithm, is necessary, if the image difference luminance response, and, consequently, the legibility response, of the controlled electronic displays are to be perceived by aircrew members to change in direct proportion to the rotation angle of the legibility trim control knob, when using a linear manual control.

7.4. Coordination of Multiple Light Sensors, Automatic Legibility Controls and Displays

In cockpit configurations involving multiple light sensors, controls and displays, there are many viable automatic legibility control implementation possibilities, dependent on the light sensing and control strategy adopted and the degree of legibility control precision required to satisfy the aircraft mission objectives. Because of this, and the lack of flight test data to validate the different possible implementations, considering specific control configurations in detail is neither appropriate nor practical. Instead, this section will attempt to describe some factors that should be considered to coordinate the legibilities of multiple displays operated from multiple light sensors when using automatic legibility control.

In the earlier chapters of this report, the descriptions of automatic legibility control have made an implicit assumption that each electronic display would have its own automatic legibility controller, legibility trim control or controls, and incident illuminance and veiling luminance sensors available to permit controlling its legibility automatically. Individualizing the light sensing and image difference luminance control to each display, is, at least in concept, one way to assure that the respective constant legibility levels can be maintained for individual electronic displays, installed at different locations in the cockpit and under all possible ambient illumination and glare source viewing conditions. The caveat is added to the preceding statement in recognition of the fact that a display's luminance controller may not be capable of faithfully tracking the signals measured by the light sensors.

The use of light sensors, dedicated to automatically controlling the legibility of individual electronic displays, as described above, could lead to a cumbersome, and possibly also impractical, overall ALC system installation in a cockpit having more than just a few displays. Concurrently, consideration also must be given to how such a system would interact with the aircrew under both spatially variant static and dynamic flight conditions, experienced in operational military aircraft. The types of legibility problems that could potentially arise using this ALC configuration will be described using examples involving individually controlled displays.

7.4.1. The Effect of Static Illuminated and Shadowed Areas on ALC Controlled Displays

An important potential legibility problem with individual electronic displays, controlled by dedicated ALCs, is caused by the existence of static shadowed and illuminated areas in the cockpit, and the relationship of the shadow boundaries, with respect to the light sensors and the displays that they control. Whether an actual problem exists or not is related to the placements, orientations and the manner in which the measurement data acquired from the display light sensors is used to control the image difference luminance levels of the individual displays. Even when these design factors are properly taken into account, the existence of static shadowed and fully illuminated areas within the cockpit will cause the individually controlled electronic displays to exhibit quite different image difference luminance outputs, depending on whether they are enveloped in shadows or in sunlight, when the legibility of the displays are set to a constant level throughout the cockpit. Likewise, individual displays installed at different positions in an aircraft cockpit, will also exhibit quite different image difference luminance outputs, based on the exposure of their individual veiling luminance sensors, to different glare source luminance conditions present within the total field of view visible from the cockpit, when the legibilities of the displays are set to a constant level throughout the cockpit.

The differences between the image difference luminances of electronic displays under the conditions described in the preceding paragraph would produce perceptible brightness differences between displays located within shadowed areas and those fully exposed to the sun. This viewing situation is not, however, any different than the one experienced by aircrew members using conventional reflective mode electromechanical displays in operational aircraft cockpits. These displays also appear brighter when fully illuminated and dimmer when enveloped in a shadow, and in spite of the differences retain adequate, though not constant, legibility under these two viewing conditions.

In cases where the sun is positioned so that it induces veiling luminance in the pilot's eyes, no means is available to adjust the luminance of conventional instrument panel mounted displays to compensate for the reduced reflected luminances that occur when shadows are cast on the instruments, due to the sun being in the pilot's forward field of view. As a result, conventional displays become somewhat less legible under this viewing condition. Under the same conditions, for electronic displays controlled to maintain constant legibility by an ALC, the display image difference luminance level would be increased to compensate for the glare caused by the sun, even though the displays and their light sensors are enveloped in shadows. Since electronic displays have been found through many years of operational aircraft experience in daylight to be able to coexist with the much brighter conventional displays that share the same cockpits, the relative increase in the image difference luminance levels of the electronic display under the veiling luminance condition should not produce a viewing problem for aircrew members. Based on the preceding comparison, it can be concluded that the electronic displays controlled with individualized automatic legibility controls and dedicated light sensors would not create viewing problems for the aircrew, under either directly illuminated or veiling luminance conditions.

In the preceding discussion, it was implicitly assumed that the viewing areas of the individual electronic displays, and, by implication, their light sensors were either fully illuminated or entirely in a shadow. When only a part of an electronic display's viewing surface is fully illuminated and the balance is in a shadow, or when the light sensor is in a shadow and the display surface is fully illuminated, the use of only a single illuminance sensor to control the image difference luminance of an electronic display is shown to be inadequate. In this case, the display must actually be operated so that it will be legible in the higher incident ambient illuminance condition and a question arises as to how light sensing should be implemented to meet this requirement.

To accommodate shadows that only partially cover the viewing surfaces of individually controlled electronic displays, it would be necessary to place illuminance sensors at or near the four corners of each display. Polling the illuminance measurement results of the four sensors would then permit the highest measurement result to be used as the input to the display's ALC. Doing this, would assure that the display image difference luminance output is set to be consistent with the highest illuminance level present, under which the display information has to be perceived.

A variety of alternatives to the preceding ALC-sensor coordination approach exist. For example, polling the outputs of light sensors associated with individual electronic displays that are distributed across the instrument panel would allow fewer strategically placed shared light sensors to be employed. This approach requires the implementation of a computational technique to predict the locations of shadows and to assign the correct light sensor outputs to the correct automatically controlled individual displays. As still another alternative, the highest illuminance measurement result, from anywhere in the cockpit could be used as the light sensor input, to the ALCs used to control each display. This approach would result in displays enveloped in shadows being more legible than those receiving full illumination, but would assure that all of the information portrayed on electronic displays located anywhere on the cockpit instrument panels would remain legible. Time dependent changes in display image difference luminance levels caused by moving shadows would also be reduced by using this approach.

The polling and voting to select the specific light sensor outputs to be applied to the individual electronic display ALCs, which was described in the preceding paragraph, should also be extended to the interpretation of veiling luminance sensor measurement results. The control options are the same for both sets of light sensors and, therefore, the veiling luminance sensor case does not require further elaboration.

7.4.2. The Effect of Dynamic Flight Maneuvers on ALC Controlled Displays

Another potentially important legibility problem with individually controlled electronic displays relates to the temporal control of the image difference luminance of the individual electronic displays, in response to illuminated and shadowed areas moving across the cockpit instrument panel or to the sun moving with respect to the veiling luminance light sensors, as the result of the pilot maneuvering the aircraft. Shadows moving with respect to the individually controlled electronic displays distributed throughout the cockpit would be expected to cause the display incident illuminance sensors to experience a rapid succession of changing ambient illumination conditions. In response to these sensed ambient illumination changes, the image difference luminance outputs of the displays, associated with the sensors, would also be expected to change in rapid succession. In an analogous fashion, changes in the aircraft's attitude with respect to the sun or another source of glare, such as sun illuminated white clouds, would be expected to cause the veiling luminance sensors associated with the individual displays to be exposed to a rapid succession of changing forward field of view veiling luminance conditions. These sensed veiling luminance changes would, in turn, also cause the image difference luminance outputs of the individual displays to change in rapid succession, in response to the control signals generated by the ALCs that are tracking the light sensor changes.

The human legibility requirements model presented in Chapter 3 was intentionally restricted to static viewing conditions to avoid adding unnecessary complexity to the discussion. Consequently, the automatic legibility control law algorithms, developed earlier in this report, do not contain provisions to take into account the time dependence of a pilot's legibility requirements. The principal reasons the inclusion of the pilot's time dependent legibility requirements has been deferred is a lack of information in the literature about the needs of a pilot, for real-time legibility control in an operational aircraft setting, and the potential limitations of current electronic display control technologies to respond as rapidly as published human response time data would suggest is necessary.

The full impact on a pilot's performance, of the visual effects produced by changes in the image difference luminances of electronic displays, occurring in real-time, in response to dynamically changing ALC control inputs, during banked turns, aileron rolls, immelmann turns and other aircraft maneuvers, is not easy to anticipate. It would be reasonable to expect that the image difference luminance changes occurring on head-down displays during such maneuvers could be distracting, when perceived peripherally, during a period when the pilot is using a head-up display to acquire primary flight control information. Nonetheless, very similar changes already occur in cockpits equipped with conventional electromechanical displays, due to changing illumination exposures of the cockpit, with respect to the external ambient illumination environment (i.e., a succession of exposures to sun, clouds, sky, ground, etc.), as the aircraft performs flight maneuvers in

response to the pilot's control inputs. Based on the latter analogy, it is possible to conclude that provided the ALCs, and the displays they control, accurately track the changes in incident light caused by moving shadows or glare sources, in real-time, the ALC controlled displays should cause no greater distraction for the pilot than would be caused by shadows moving across the displays in a conventionally equipped cockpit.

7.4.2.1. The Implications of Control Technology Limitations

Electronic displays, due to being operated by image generation and processing computers, are updated at the typical maximum rate of 30 picture frames per second. Consequently, for portrayals of an attitude director indicator (EADI) and a horizontal situation indicator (EHSI) information formats, during snap rolls at roll rates approaching two revolutions per second in fighter aircraft, the horizon line and pitch ladder would be depicted in only 15 angular orientations on the EADI during a complete roll, and, assuming the direction the aircraft is pointing does not change during the maneuver, the compass rose would appear essentially static on the surface of the EHSI. Results similar to those of the EADI just described, have also occurred on EHSIs when an aircraft inadvertently enters a flat spin. In both cases the limited update rate of the displays makes unusual attitude recovery cues more difficult for a pilot to interpret. Since the sensed external ambient changes from high to low illuminance, and back again to high, during a complete roll of the aircraft, the limited number of light sensor samples per revolution of the aircraft, and the one picture frame delay in depicting a change dictated by a light sensor, would prevent controlling the image difference luminance levels of displays used in highly maneuverable aircraft by changing the luminance levels between successive picture frames. Even for less maneuverable aircraft, this technique would cause noticeable luminance step increments between samples that could potentially be perceived as flicker or be incorrectly interpreted as flash rate coding, when the display is viewed peripherally.

In direct analogy to the separate control of the information portrayed by AMLCD panels and the luminance levels of their backlights, existing electronic displays can be implemented so that their picture information is independent of the control over the absolute image difference luminance levels of their presentations. This approach can also be compromised, however, if the display luminance controller and the light sensors are for technological reasons unable to respond in real-time to the rapid changes in the illumination conditions attendant to operational flight maneuvers in military aircraft.

It should be noted that on electronic displays having image difference luminance decay time constants in the low milliseconds such as P-43 phosphor CRTs, or for the much shorter time constants of LED displays, the dynamic horizon and pitch ladder lines of the EADI format depicted during the snap roll maneuver, are displayed only momentary, one at a time, before the successive format frame is drawn at a new angle. By way of comparison, a succession of the EADI format horizon and pitch ladder lines are shown at the different angles on AMLCDs, with the most recent format being the brightest and previously drawn formats appearing at progressively lower image difference luminance described above, these effects are typically not noticeable for electronic display presentations during less extreme instances of the flight maneuvers. Additional situation awareness cues are used to compensate for these electronic display presentation shortcomings in highly maneuverable military aircraft.

7.4.2.2. The Implications of Aircrew Visual Response Time Limitations

When the snap roll of the preceding example is considered from the perspective of the 200 - 250 ms time exposures required by the pilot to perceive the full image difference luminance of a display image, it would be expected that the pitch ladder and horizon line would be perceived at a reduced luminance level, rather than the actual image difference luminance being commanded by the ALC, and being depicted by the electronic display. Assuming the EHSI format remains essentially stationary during the snap roll, this format would be perceived as a time average of many frames of information and would therefore be perceived to be at the full displayed image difference luminance level.

The preceding example points out a previously mentioned limitation of the human image difference luminance requirements model developed in Chapter 3. Namely, the equation does not account for the response time limitations of the human visual system and, consequently, it does not accurately predict the legibility of dynamic display imagery that is translating or rotating at a high speed on the display surface, or the legibility of static display imagery when the luminance of the imagery is being rapidly changed. Although the practical effects of this limitation of the human visual system can be aggravated by the periodic update of display information formats on electronic displays, the result is also applicable to rapidly moving conventional electromechanical display presentations.

7.4.2.3. Compensation for Aircrew Visual Response Time Limitations

The limitations of the human's ability to respond to rapidly changing image difference luminance levels, coupled with the aforementioned technology limitations, raises a question about whether the display image difference luminance should not be maintained at the highest level required to make the display imagery legible during dynamic flight maneuvers rather than being allowed to track rapid changes in the values being measured by the light sensors.

The uncertainty as to whether the previously described problems are real and need to be taken seriously stems from the lack of laboratory tests or of operational aircraft experience with ALCs. As previously described, military aircraft pilots have historically disabled display automatic brightness controls and as a result no known guidance is provided through this potential source of operational experience. As described in Chapters 4 and 5, electronic display automatic brightness controls are used on several Boeing commercial aircraft, however, these displays are operated over both very limited luminance control ranges, and the dynamics associated with flight maneuvers by the aircraft are very restricted. From an intuitive standpoint, it seems likely that individually controlled electronic displays could create visual distractions for the pilot and any other aircrew members, however, no evidence exists to support this hypothesis. Moreover, comparisons with conventional displays under the same viewing conditions would result in the conclusion that there should be essentially no difference between a pilot's experience with conventional and ALC controlled electronic displays, provided that the image difference luminances of the electronic displays can be controlled so that they can accurately track the cockpit ambient illumination and veiling luminance conditions as commanded by their respective light sensors.

Because it is critical that image difference luminance levels of electronic displays are controlled so that the display information always remains legible, irrespective of the time dependent changes in the environmental illumination conditions that the aircrew is exposed to as the aircraft is maneuvered to perform a mission, increases in sensed incident illuminance and veiling luminance levels must be faithfully tracked using appropriate increases in a display's image difference luminance levels, to maintain the legibility of the display at a constant level. Conversely, when sensed incident illuminance and veiling luminance levels decrease, it is not essential that a display's image difference luminance levels be decreased (i.e., other than to maintain legibility at a constant level), since the display should still be capable of being easily read. The extent to which increases in a display's legibility would be noticeable, under this circumstance, depends on whether the display is operating near the threshold of just adequate legibility, where changes could be quite noticeable, or near the optimum display legibility level, previously described, where the changes would not be noticeable.

7.5. Digital Control Signal Compatibility Considerations

Digital control of the image difference luminance output of electronic displays, or the digitization of signals obtained from light measurements using external field of view veiling luminance sensors and display or panel mounted light sensors, impose additional requirements on the implementation of an automatic legibility control system. The use of digitized sensor or manual control signals with a digital display controller to adjust the

image difference luminance outputs of electronic displays, rather than analog signals and display controllers, means that as the image difference luminance of the display portrayals are changed by an automatic legibility control or by an aircrew member, the luminance change will occur in discrete steps rather than continuously. If these time dependent discrete step changes in a display's image difference luminance level are large enough, they can potentially serve as a source of distraction to aircrew members, both while using the display as it is controlled and while viewing other displays.

The likelihood of image difference luminance changes that occur in discrete steps creating a visual effect that could distract a pilot is enhanced when the image difference luminances of electronic displays are controlled automatically in an aircraft cockpit. The reason for this is that onset of any visual effects stimulated, when an ALC is actively adjusting the image difference luminance of a display, cannot be anticipated by an aircrew member, as happens when the visual effect coincides with manual control inputs by the aircrew member. The likelihood image difference luminance adjustments, made by an ALC, or even those made by a manual legibility control, will cause the discretely stepped changes in a display's image difference luminance level to create a distracting visual effect is also enhanced during night cockpit operations, when the controlled display is located in the crew member's peripheral field of view, where the changes can be perceived as flicker or even flash rate coding, depending on the rate of change of the display image difference luminance. Since electronic displays will occupy parts of a crew member's peripheral field of view, anytime a task is performed that requires the use of external cockpit vision or even the use of other cockpit controls and displays, the likelihood that time dependent discrete changes in a display's luminance would cause a distraction cannot be considered a remote possibility.

The possibility that time dependent discrete changes in the image difference luminance output levels of electronic displays will distract an aircrew member can be reduced or even eliminated by making the luminance step sizes sufficiently small. Because the display image difference luminance steps can have different origins, the methods needed to deal with them differ. For a digital display controller, the origin of the luminance step sizes is directly attributable to the design of the controller. Digitized sensor signals, used as inputs to an automatic legibility control, serve as an indirect origin of steps in a display's luminance output, as does the least significant bit size associated with using the automatic legibility control algorithm. The step size is also influenced when the preceding digital devices and signals are interfaced. For digitized sensor signals, two considerations must be addressed. The first concerns how close together the digital samples of a sensor signal should be, to cause the display to operate in a way that members of an aircrew would consider to be satisfactory. The second concern, which is easier to overlook, is how low or high the sampling of the background luminances incident on the display light sensors and the glare source luminances sensed by the veiling luminances sensors, must extend, to be able to provide a full range of display automatic legibility control.

A straightforward approach for dealing with these questions is to make the digital step sizes of the display's image difference luminance controller and the sampling intervals of the sensor signals so small that discrete changes in the image difference luminance levels of the electronic displays would be perceived to be continuously variable, that is, make the step size changes in going between adjacent levels so small that they become imperceptible. An alternative approach is to make the step sizes just small enough that the time dependent changes in the display luminance, while still perceptible, are not large enough to be distracting. The practical difficulty encountered with either of these implementations, stems from the very large number of discrete control levels needed. The large number of control levels results from the fact that the veiling luminance and display incident illuminance variables, which must be sensed and digitally processed to command the correct highlight image difference luminance level on an electronic display, cover a ten-decade range. More specifically, the illuminance incident on the display surface can vary between somewhat greater than 10^4 fc, under a direct sunlight incident illuminance condition, to nearly 10^{-6} fc on heavy overcast dark nights with no stars, although, in practice, cockpit lighting prevents pilots from being able to adapt to the 10^{-6} fc level. When both day and night glare source conditions are to be considered, the sensor signal range for veiling luminance is only slightly smaller than the one for incident ambient illuminance. Further design complications arise when it is necessity to make digitized sensor signals compatible with a display controller, which uses a digital design and can also have a four decade or larger image difference luminance control

range.

It is not the intent of this section to describe all of the possible combinations of analog and digital designs that can be used to produce feasible image difference luminance control implementations for use with aircraft cockpit electronic displays. Instead, the intent of this section is to consider the previously mentioned design factors in relationship to their capability to influence the legibility and visual artifacts associated with the presentation of information by digitally controlled electronic displays.

7.5.1. Display Image Difference Luminance Controller Step Size Criteria

In Section 6.2, the discrete grey scale step sizes needed to cause a digitally encoded picture to appear continuously variable, rather than as grey shade stepped terrain maps, were considered. The perceptibility threshold for time dependent changes in the luminance of a displayed picture frame, when the picture is incremented by one grey shade step between two successive picture frames during a time sequence of otherwise identical picture frames, is about the same as it is for a one grey shade spatial step between two sides of an otherwise uniform luminance display surface. Based on this equivalence, the earlier discussion of the perceptibility of static spatially distributed grey shades can be applied to setting the limits on discrete temporal changes in a display's image difference luminance control levels.

The minimum digital step size needed to control the image difference luminance of an electronic display can probably be best illustrated using an example. For this purpose, an active matrix liquid crystal display (AMLCD) having a display area of nominally five inches on a side, a highlight white image difference luminance control range from nominally 200 fL to 0.1 fL and that meets or exceed the minimum legibility requirements for aircraft cockpit displays, will be used. To increase the image difference luminance from 0.1 to 200 fL, increments of between 1 and 2% of the highlight luminance level of the display, before each step increase is added, should typically suffice to make the steps imperceptible, under normal aircraft cockpit utilization conditions. The 2% increment is appropriate for use with the five inch display size cited above, or smaller, provided the display is used to depict the types of information that are typically found useful in aircraft cockpits. Somewhat lower thresholds would apply to the large uniform luminance areas typically used for testing. Smaller increments would also apply for use with larger display active area displays. Alternatively, luminance increments or decrements between nominally 3 and 4% of the highlight white luminance level, while being perceptible, should not be distracting. The preceding descriptions are left intentionally vague, due to multivariate dependence of the perceptibility of these step thresholds.

To minimize the number of steps needed to control the image difference luminance between 0.1 and 200 fL, the luminance can be changed in approximately equally perceptible steps by using a logarithmic-linear relationship between the luminance levels and the control levels. For example, using an eight bit digital word to control 256 level discrete image difference luminance levels between the example display's maximum, $\Delta L_{Max} = 200$ fL, and minimum, $\Delta L_{Min} = 0.1$ fL, image difference luminance limits, the relationship between the intermediate controlled levels, ΔL_j, and the luminance step index number, j, can be calculated using the following equation:

$$\log \Delta L_j - \log \Delta L_{Min} = j[\log \Delta L_{Max} - \log \Delta L_{Min}]/255 , \tag{7.14}$$

or equivalently as

$$\log \Delta L_j/\Delta L_{Min} = j[\log \Delta L_{Max}/\Delta L_{Min}]/255 . \tag{7.15}$$

Substituting the values of the image difference luminance from the above example into the right-hand side of this equation, it evaluates to give the following relationship:

$$\log \Delta L_j/\Delta L_{Min} = j[\log 2000]/255 = j3.3010/255 = j0.012945 . \tag{7.16}$$

Next, taking the antilogarithm of this equation, the image difference luminance control equation can be expressed in the following equivalent form:

$$\Delta L_j/\Delta L_{Min} = 10^{0.012945\,j} = (10^{0.012945})^j, \tag{7.17}$$

where evaluation of the term in the parenthesis on the right yields the final image difference luminance control relationship as follows:

$$\Delta L_j/\Delta L_{Min} = (1.03026)^j \quad \text{for } j = 0,1,2,...255\,. \tag{7.18}$$

The eight bit binary coding therefore produces a geometric progression with a 3.026% luminance ratio between its successive stepped luminance control levels. For comparison, a ten bit binary code would allow setting the luminance to any one of 1024 levels rather than 256 and would permit a geometric progression with a 0.745% ratio, somewhat less than the 1% required to assure that the steps would be imperceptible even on cockpit electronic displays having large active areas of eight to ten inches on a side.

An equivalent linearly stepped control would need the same initial step size, that is, from 0.1 fL to (1.03026)0.1 = .103026 fL, a step of 0.003026 fL or less, and would require nominally 200/0.003026 = 66,094 steps to control the display highlight image difference luminance level from 0.1 to 200 fL. In other words, somewhat more than a 16 bit word (i.e., 65,536 control levels) would be needed to provide the same step size control.

7.5.2. Sampling Criteria for Automatic Legibility Control Light Sensor Signals

If the background reflected luminance, L_D, and veiling luminance, L_V, input signals to the automatic legibility control are digitally sampled and encoded, rather than being continuous analog signals, then the absolute luminance magnitudes of the samples and the interval between samples of the background and the veiling luminance signals must be compatible with the analog or digital input requirements of a display's image difference luminance controller, after these signals have been operated upon by the ALC. In practice, since the requirements on the discretely stepped luminance outputs of the display's image difference luminance controller, and the control requirements of the automatic legibility control, are each established by capabilities and limitations of the human visual system, as described previously in this report, it is the combined effect of these two sets of requirements that determine how the light sensor signals must be sampled to produce controlled image difference luminance levels that meet the visual needs of aircrews.

If the sensor signals are undersampled, that is, the discrete steps are too large, then the resultant discrete ALC output step sizes would cause a display using an analog image difference luminance controller to produce output image difference luminance step sizes that could range from being just perceptible to extremely noticeable, depending on the degree to which the sensor signals are undersampled. For a display using a digital image difference luminance controller, undersampled sensed signals would cause the discrete ALC output step sizes to exceed the minimum input step sizes of the display's digital controller. The lack of alignment between the ALC output step transitions and the input step transitions of the display's digital luminance controller, besides producing displayed output image difference luminance step sizes that could range from being just perceptible to extremely noticeable, depending on the degree of undersampling, would also cause the display to exhibit unpredictable fluctuations in the luminance step sizes, in response to changes in the magnitudes of the sensed signals. Furthermore, if the sensors being used are unable to respond either to low or to high enough values of the light variables sensed, then the useful control range of the display would not be fully utilized.

Based on the preceding considerations, it can be concluded that the maximum step sizes between the samples of the sensed display background and veiling luminance, that is, the maximum intervals between samples of these sensed variables, can be determined by working backwards from the values of the display image difference luminance levels required to meet the aircrew's visual requirements, and from the minimum step sizes in these luminances, needed to make stepped changes in the luminance level of a display acceptable to the aircrew. Sampling intervals equal to this maximum step size, or alternatively any smaller sampling interval, should produce acceptable changes in the display luminance output. As stated above,

samples of the combined sensed background reflected luminance, L_D, and veiling luminance, L_V, input signals to an automatic legibility control that are not consistently aligned with the same level of each of the input step intervals of the image difference luminance controller, say for example their centers, when incrementally increasing or decreasing the luminance of a display, would cause a timing error in the onset of the step change in the display's luminance, and thereby cause luminance changes in response to a sensor signal, commanding a temporally continuous increase in the display image difference luminance, to be perceived as erratic, rather than smooth. For luminance increments smaller than the maximum step size, this variability in the sampling should not cause a noticeable visual effect, if the nominally equally perceptible increments in the display luminance, corresponding to the maximum step size, are not noticeable.

As described earlier in this report, the image difference luminance requirements of a display, and the maximum step size permissible when its luminance is incrementally increased or decreased, can be dependent on legibility that must be achieved to portray a particular type of display information, that is, whether the information portrayed is numeric, alphanumeric, graphic, video or in color, and, therefore, on the corresponding contrast, C, in the ALC control law, or the aircrew's adjustments of the contrast, P_C, and night image difference luminance, N_L, trim controls, in Equation 5.55, which is repeated below for convenience. Examples are presented in the following two subsections to illustrate the role that the human's discrete luminance increment and image difference luminance requirements play in establishing the requirements on sensor signal sampling. As described in Chapter 2, depending on the operating mode and technologies chosen to implement an electronic display, the designs of the image difference luminance controllers needed to present a particular type of display information, while meeting these incremented luminance step requirements, will differ significantly from one another.

7.5.2.1. Light Sensor Range and Step Size for Minimum Legibility Video Displays

This subsection is devoted to considering the light sensor ranges and step sizes, needed to operate a video display, at the minimum legibility level considered suitable by pilots for use in an aircraft cockpit viewing environment. The automatic legibility control law can be used to relate the image difference luminances and minimum step sizes to the sizes of the steps required by the digitally encoded sensor signals. Equation 3.182, which is derived and described in Section 3.9 or, alternatively, Equation 5.55,

$$\Delta L_P = P_C \left[1.30C\,(L_D + L_V)^{0.926} + 0.0193\,N_L C \right], \tag{5.55}$$

with the aircrew's contrast trim control set to $P_C = 1$, can be used to represent the automatic legibility control law, as follows:

$$\Delta L_P = 1.30C(L_D + L_V)^{0.926} + 0.0193 N_L C\,, \tag{3.182}$$

where the equation is expressed in units of foot-Lamberts. To control a display so that it can depict an eight $\sqrt{2}$ grey shade luminance dynamic range picture, the minimum desirable for aircraft cockpit use (i.e., see Section 3.9), a highlight white (or monochrome) contrast setting of C = 10.3 needs to be used in Equation 3.182. Making this substitution yields the following control law equation:

$$\Delta L_P(C = 10.3) = 13.4(L_D + L_V)^{0.926} + 0.2 N_L\,. \tag{7.19}$$

When the values of the sensed background and veiling luminance are sufficiently small, to cause the $L_D + L_V$ term to approach zero, Equation 7.19 reduces to the following relationship for the display image difference luminance requirement under night viewing conditions:

$$\Delta L_P(C = 10.3,\, L_D + L_V \to 0) = 0.2 N_L\,. \tag{7.20}$$

To use these equations with the earlier example of a display that is controllable from 0.1 to 200 fL, the pilot or other aircrew member would have to set the night trim control adjustment to $N_L = 0.5$ to cause the highlight white luminance to be reduced to the minimum luminance, ΔL_P= 0.1 fL. Using this trim control setting, the complete control law can be expressed as follows:

$$\Delta L_P\,(C = 10.3) = 13.4\,(L_D + L_V)^{0.926} + 0.1\,. \tag{7.21}$$

The display reflected background luminance term, L_D, that appears in Equation 7.21 is linearly related to the measured ambient illuminance, E_P, incident on the instrument panel or display light sensors, and to the specular reflection source of luminance, L_{SRS}, by the respective diffuse and specular reflectances, R_D and R_S,

$$\begin{aligned} L_D &= R_D\,E_P + R_S\,L_{SRS} \\ &= K_D\,S_P + K_S\,S_{SRS}\,. \end{aligned} \tag{7.22}$$

of the display viewing surface using the following equation:
To enable incorporating this value of the display reflected background luminance, L_D, into the image difference luminance control law, for an actual installation, the reflected luminance terms shown on the right-hand side, in the first line of Equation 7.22, would have to be related, one on one, to the equivalent sensed voltages, S_P and S_{SRS}, and their corresponding calibration constant scaling factors, K_D, and, K_S, respectively, in the second line of the equation. In other words the values of the calibration constant scaling factors, K_D, and, K_S, must be chosen to cause the correct absolute values for the luminances diffusely and specularly reflected by the display viewing surface in response to the measurement of the light sensor voltages, S_P and S_{SRS}, to provide the absolute value of the display reflected background luminance needed as an input to the automatic luminance control algorithm. Likewise, the veiling luminance, L_V, is related to the voltage sensed by the angle-weighted veiling luminance optical integration sensor, S_V, by the calibration constant scaling factors, K_V, using the following equation:

$$L_V = K_V\,S_V\,. \tag{7.23}$$

As is true for the diffuse and specular reflectance source constants, the value of the calibration constant, K_V, must be chosen to cause the correct absolute value of the veiling luminance, L_V, which would be perceived by an aircrew member, when applied to the voltage output of the veiling luminance sensor, S_V, using Equation 7.23, to be compatible as an input to the automatic luminance control algorithm.

Continuing the earlier example of a display luminance controller, designed to increase or decrease the image difference luminance of a display in 255 nominally equally perceptible steps between 0.1 and 200 fL, the combined level of the display background and veiling luminance, $L_D + L_V$, needed to raise the image difference luminance of the display by one 3% step above the ΔL_P= 0.1 fL night level setting of Equation 7.21 can be calculated by the substituting a value of ΔL_P= (1.03)0.1 = 0.103 fL into the equation and solving, which yields $L_D + L_V$ = 0.0001144 fL. Increasing the image difference luminance by an additional 3% step to ΔL_P= (1.03)0.103 = 0.10609 fL, and again solving for the value of $L_D + L_V$, the new level is 0.0002457 fL, and the difference between the two successive levels is 0.0001313 fL.

The background luminance reflected by a 200 fL maximum image difference luminance display, which can depict aircraft sensor-video information with a minimum of a six $\sqrt{2}$ grey shade luminance dynamic range, that is, at a contrast of 4.66 under a worst-case incident ambient illuminance viewing condition, would have to be nominally 43 fL. Consequently, assuming the MIL-L-85762 worst-case of 10,000 fc, incident on the display over the pilot's shoulder, gives an estimate for the diffuse reflectance of the example display as 0.0043 fL/fc. For a display having this level of diffuse reflectance, it can be inferred that the reflected background luminance levels of 0.0001144 fL and 0.0002457 fL, determined above, roughly translate into the need to be able to sense an increase in the incident ambient illuminance level from nominally 0 fc (i.e., actually any sensed value less than 0.0266 fc that can be reliably discriminated, say 0.01 fc, or less) to 0.0266 fc, to increase the display image difference luminance from 0.1 to 0.103 fL, and sense a subsequent increase from 0.0266 fc to 0.0571 fc, to increase the display image difference luminance from 0.103 to 0.10609 fL. The corresponding intervals, between samples of the incident ambient illuminance, are therefore a maximum of 0.0266 fc between the first (i.e., the null sample) and second sample, and 0.0305 fc between the second and third samples. This example is presented to make two related points. The first point is that the relevant absolute magnitudes of the display background and veiling luminances, which must be taken into account to use automatic legibility controls, can become quite small. The second point is that while the spacings between the discrete sampling levels of the

sensed light measurement variables for perceptually equally display luminance steps are very small, in absolute terms, they increase in magnitude as the sensed illuminance increases, even though they decrease in magnitude when considered as a ratio between successive incident illuminance sampling levels.

If the preceding calculation procedure could be extended to the entire 0.1 to 200 fL range of the display, it would produce samples of the sensor signal levels that are precisely coordinated with the 256 equally spaced discrete display luminance controller output levels, and would, therefore, not only produce the minimum possible number of samples of the sensor signal needed to control the display's image difference luminance output levels, but would also permit a single look-up table to be implemented, to coordinate between the discrete display luminance controller levels and the sensor sampling levels.
In effect, this would allow the look-up table to serve as the automatic legibility control algorithm, however, the current example of the light sensor sampling intervals involved setting the values of several automatic legibility control parameters, which should not be set to fixed values in an actual aircraft cockpit application of the ALC.

Although the implementation of a display image difference luminance controller using 256 equally perceptible luminance levels, with an eight bit digital code word to set the levels, is still feasible, to be effective in practical applications, the light sensor signals sampled to serve as inputs to the automatic legibility control, cannot conveniently be restricted to range of sensor signal magnitudes predicted by working backwards from the display's luminance control range as described in the preceding example. The reason for this is that although the maximum image difference luminance control range of the display remains invariant (e.g., between 0.1 and 200 fL), its relationship to the sensed signals, and, hence, to the discrete samples of the sensed signals, depends on both the aircrew settings of the contrast trim and night image difference luminance controls.

For example, an increase in the contrast trim control setting, P_c, in Equation 5.55, shown above, to values greater than unity, would cause the entire control characteristic, including the night image difference luminance level, to be shifted to higher image difference luminance levels, by the value of the constant multiplier, P_c, applied by an aircrew member using the contrast trim control. However, because of the luminance saturation limitation imposed by the maximum image difference luminance of practical electronic displays (i.e., 200 fL for the current example), the effect of this contrast increase is to cause the sloped part of the image difference luminance characteristic of a display to appear to shift in unison to lower background luminance levels. For a particular display image difference luminance level on the control characteristic, the practical effect of increasing the value of P_c is to cause the corresponding background luminance level to be reduced, whereas reducing the value of P_c causes the corresponding background luminance level to be increased.

A change in the value of the night image difference luminance control by an aircrew member increases or decreases the image difference luminance level corresponding to the zero slope portion of the control characteristic, while making only a negligible change to the daylight portion of the characteristic. The practical effect of increasing the night image difference luminance level is to reduce the range over which sampling of the light sensor signals is required, whereas, reducing the luminance setting of this control has the opposite effect.

An alternative sampling technique, which does not appreciably increase the number of samples, involves using the automatic legibility control requirements equation to match the display luminance controller step sizes to corresponding discrete sensor signal samples, at high image difference luminance levels. The slope of the automatic legibility control characteristic is a maximum at high image difference luminance levels, and, consequently, the ratio between successive background and veiling luminance samples is at a minimum value for this evaluation position on the control characteristic. Using the 3% geometric progression between the discrete image difference luminance levels of the earlier 256 level equally perceptible luminance step example, the first discrete level down from 200 fL would be 200/1.03 = 194 fL. The corresponding minimum luminance discrete sample spacings can then be found by evaluating the $L_D + L_V$ values determined for image difference luminances of 200 fL and 194 fL using Equation 7.21 and calculating the value of the ratio between these two

luminance levels. Using this approach, the ratio between the $L_D + L_V$ values for 200 fL and for 194 fL was calculated to be 1.033.

Since the minimum sampling ratio, determined using the above procedure, results in the smallest sampling interval between adjacent sampled $L_D + L_V$ signal levels, that occurs within the control range of a display luminance controller, designed to produce equally perceptible step sizes, the use of this ratio to sample lower sensor signal levels assures that the sensor signals will either be sampled adequately or oversampled. As described at the end of the previous subsection, the use of a fixed minimum sampling ratio would not result in light sensor sampling levels, after processing by the ALC, that are aligned with the encoding levels of the equally perceptible image difference luminance steps of the earlier 256 level image difference luminance controller. The sampled sensor signals would, therefore, result in discrete luminance steps that are less than or equal to the sought after 3% step size of the earlier example, if an analog image difference luminance display controller were used to drive the display. Since smaller sampling intervals would simply cause a larger number of smaller size luminance steps as the luminance of the display is changed this method of sampling would not create a problem when used with an analog image difference luminance display controller.

For the digital image difference luminance display controller of the earlier example, using 256 equally perceptible luminance control levels, to be compatible, then after the discretely sampled light sensor signals are processed by the ALC, they would have to be interpreted and assigned to the correct input signal encoding level of the digital image difference luminance display controller. The mismatch that would exist between the discrete sampling intervals of the oversampled light sensor signals and the larger intervals of the encoding levels of the digital controller would not, however, be noticeable, for the reasons previously described. Oversampling of the light sensor signals, using the preceding method, has the advantage of not requiring the sampling and the design of the digital image difference luminance display controller to be coordinated, beyond assuring that oversampling and not undersampling of the light signals is achieved. This topic is considered in greater detail in the next subsection.

7.5.2.2. Light Sensor Range and Step Size for Optimum Legibility Video Displays

The light sensor range and step size needed to operate a video display at an optimum legibility level, suitable for use in an aircraft cockpit viewing environment, is considered in this subsection. Increasing the grey scale luminance dynamic range from the value of 10.3, of the preceding eight $\sqrt{2}$ grey shade example, to 29, which corresponds to a luminance dynamic range just shy of eleven $\sqrt{2}$ grey shades, permits the display of the 3 to 90% range of luminous reflectances, needed for the full monochrome grey scale or color display picture portrayal of a real-world visual scene. The corresponding image difference luminance control equation is obtained by substituting $C = 29$ into Equation 3.182, shown previously in this section, which yields the following equation:

$$\Delta L_P(C = 29) = 37.7\,(L_D + L_V)^{0.926} + 0.56N_L$$
$$\Delta L_P(C = 29) = 37.7\,(L_D + L_V)^{0.926} + 0.1\,. \qquad (7.24)$$

The second image difference luminance equation follows from the first when a night trim control adjustment is set to $N_L = 0.178$ to cause the night highlight image difference luminance, ΔL_N, to equal 0.1 fL.

To give a comparison the earlier example of a luminance control range divided into 256 equally perceptible levels, controllable with an eight bit word input to the image difference luminance digital display controller, the sampling intervals corresponding to equally perceptible luminance levels, are calculated by working backwards using the automatic legibility control algorithm of Equation 7.24, for display presentations depicted at a contrast of 29 instead of 10.3. Using the same procedure, described in the previous subsection for the eight $\sqrt{2}$ grey shade, contrast of 10.3 example, leads to smaller values of $L_D + L_V$ that must be sensed. In particular, a $L_D + L_V$ value of 0.0000374 fL is calculated for the sensor sample corresponding to $\Delta L_P = 0.103$ fL, a value of 0.0000804 fL is calculated for $\Delta L_P = 1.03(.103) = 0.10609$ fL and the interval between these

samples is 0.000043 fL. The corresponding incident ambient illuminance levels are 0.0087 and 0.0187 fc, respectively, yielding a maximum incident ambient illuminance sampling interval size of 0.01 fc.

As for the display with the contrast setting of its automatic legibility control adjusted to depict eight $\sqrt{2}$ grey shades, the ratio between the $L_D + L_V$ values for 200 fL and for 194 fL is also calculated to be 1.033 using Equation 7.24, where the luminance dynamic range has been increased from 10.3 to 29. Since this higher grey shade luminance dynamic range (i.e., contrast) can be made legible using existing aircraft cockpit electronic displays, under all but the highest daylight ambient illumination conditions, the minimum absolute background and veiling luminance values, for the contrast of 29 example, would be the most appropriate for use in determining the lowest sensor signal levels that need to be digitized. Moreover, because the ratios between the discrete samples of the sensed luminance are based on the slope of the human's image difference luminance requirement characteristics at high image difference luminance levels, and not the legibility characteristics of a particular display, the ratios between light sensor sampling levels should have general applicability to the sampling of sensor signals for use with any display.

To span a range of sensed ambient illuminance values that are incident on a display from, for example, 0.0087 to 10,000 fc using a log-linear analog to digital conversion with a 3.3% spacing between samples, the minimum required number of samples, n_{min}, can be calculated as follows:

$$(1.033)^{(n_{min}-1)}\,0.0087 = 10{,}000$$

$$(n_{min} - 1)\log(1.033) = \log(1.149 \times 10^6) \qquad (7.25)$$

$$n_{min} = 430\,.$$

A nine bit binary word, which can encode 512 levels could, therefore, be used to provide acceptably sampled discrete sensor signals for use with an automatic luminance control algorithm. Retaining the multiple of 1.033 for the sensor signal sample spacing and arbitrarily choosing 0.001 fc as the lowest sample level, 512 encoding levels would permit sampling up to 16,042 fc. The use of a ten, rather than an eight, bit binary word to encode 1024 equally perceptible display image difference luminance levels, at a ratio of 1.015 between the sampling levels, would allow an illuminance range from 0.003 to 12,356 fc to be sampled, with a maximum error of less than half the display controller luminance step size. For purposes of comparison, a linear analog to digital converter, scaled to give a sample spacing of 0.01 fc, would require one million samples to cover the 0.01 to 10,000 fc range and a 20 bit A/D converter.

7.5.3. Interface Compatibility for Digital Control Signals

In this subsection, considerations involving the interface compatibility of digital control signals are briefly discussed. The digital signal interfaces of particular interest occur between the light sensors and the automatic legibility control, and between the automatic legibility control and the display image difference luminance controllers.

Since the calculation of image difference luminance values using the automatic legibility control algorithm requires calibrated background and veiling luminance inputs to provide valid calibrated image difference luminance output values, analog sensor signals would have to be analog to digital (A/D) converted and scaled before being used by the ALC algorithm. Likewise, digital sensor signals encoded as numbered step levels would have to be converted to calibrated numerical luminance values to provide the necessary discrete background and veiling luminance values to be used by the ALC algorithm. In both cases, calibrated input values are needed to permit the ALC algorithm to be used to calculate valid calibrated image difference luminance output values.

In Section 7.3, interface options between display image difference luminance controllers and either manual or automatic controls were discussed. It was assumed, for purposes of discussion throughout most of Section 7.3, that the display image difference luminance controller is designed to operate on the analog

signals that manual controls are typically configured to produce. In that case, the image difference luminance levels supplied by the ALC would have to be digital to analog (D/A) converted before being supplied to the controller.

As an alternative to an analog control interface to the image difference luminance controller, the design could instead use a digital interface protocol or, to enhance redundancy, use both techniques. Whether the control interface is analog or digital the same control characteristic considerations and options described in Section 7.3 would apply to the digital interface. Aircrew adjustments made using manual controls would have to be A/D converted before being applied to a digital image difference luminance controller interface. In the event the interface to the display image difference luminance controller is digital then additional signal processing, comparable to the scaling needed to implement the analog control interface would be needed, to make the ALC output levels compatible with the digital input requirements of the controller. Interface standardization would also be needed to achieve compatibility between different manufacturers' products, if digital interfaces are used, but that topic is beyond the scope of the present report.

Although digital interface standardization will not be treated here, it should be observed that the considerations are in many respects comparable to those already described for the analog interface, however, the specification of the interface protocol is more complex due to the much larger number of design variables to be stipulated. It should also be noted that an interface protocol specification, which transfers information from the ALC to the image difference luminance controller using the absolute values of the image difference luminance values calculated by the automatic luminance control, would provide the benefit of a digital interface that would be difficult for different manufacturers to misinterpret. For standardization purposes, such an interface protocol should use a standard bit length digital word, with the values of least and most significant bit specified.

CHAPTER 8

General Conclusions Regarding the Applicability of Automatic Legibility Controls to Aircraft Cockpit Displays

This chapter endeavors to summarize the general conclusions reached, regarding the applicability of automatic legibility controls to aircraft cockpit conventional and electronic displays, resulting from the conduct of the analyses of aircrew legibility requirements described in this report, and of the features that automatic legibility controls should possess to satisfy these requirements, when used to control the image difference luminance levels, and, consequently, the legibilities of aircraft cockpit displays. The first section in this chapter summarizes the principal conclusion, substantiated by the information and analyses presented in earlier chapters of this report, namely, that effective control of the legibilities of aircraft cockpit displays, suitable to meet the information legibility needs of pilots and other aircrew members, can be achieved through an appropriate application of automatic legibility controls. The balance of the chapter deals with various considerations that could potentially influence the effectiveness of automatic legibility control, if not properly taken into account.

Besides these general conclusions, the chapter also introduces and attempts to provide analyses of potential constraints on the ability of aircrews to use displays operated by automatic legibility controls, during both day and night flight operations, without having to resort to making manual adjustments to the legibilities of the displays. The potential constraints involve the need to take into account changes in the legibility requirements of the information presented on aircraft cockpit displays during different mission segments, and to adjust the legibility of displayed information to compensate for the effects of aircrew light and dark adaptation. These potential constraints are considered in this chapter rather than elsewhere in the report due to the lack of applicable quantitative information in the literature to permit a definitive model of vision to be formulated that, with certainty, would allow compensating the output of automatic legibility controls for these potential constraints. Due to the inability to find adequate published information on the subject, the descriptions provided occasionally resort to an anecdotal treatment of the nature of the constraints imposed on the application automatic legibility controls and of the means for dealing with these constraints. This is done for the sake of completeness, and because of the need to enhance the description of the effect of automatic legibility controls, on an aircrew member's night vision, in operational cockpit settings. Conditions that could cause these two exceptions to "hands-free" automatic legibility control to occur are described in greater detail Sections 8.2 and 8.3, respectively.

The remaining four sections in this chapter are concerned with additional areas where it is considered appropriate to draw general conclusions regarding the application of automatic legibility control to aircraft cockpit displays. Section 8.4 describes the conclusion reached with respect to an effective strategy for using automatic legibility controls to adjust the legibility settings of existing electronic displays. Section 8.5 describes the importance of using automatic legibility controls from the perspective of aircrews. Section 8.6 describes the conclusion reached for an effective strategy to implement a common automatic legibility trim control that permits aircrew members to adjust the legibilities of multiple displays concurrently. The final section, provides an overall conclusion regarding the application of automatic legibility controls, to all of the displays in aircraft cockpits, rather than just to the electronic displays.

8.1. Principal Conclusion Reached Regarding the Applicability of Automatic Legibility Control to Aircraft Cockpit Displays

The principal conclusion to be presented in this chapter is that the pilot legibility requirements information assembled, analyzed and developed in Chapter 3, and further considered and developed in Chapters 4, 5, 6, and 7, for use in the application of automatic legibility controls, to electronic displays in aircraft cockpits, is sufficient to permit achieving an effective implementation of automatic legibility controls in both commercial and

military aircraft cockpits, and under both day and night viewing conditions. As a corollary to this conclusion, the analysis of the information presented also shows that when an automatic legibility control is properly configured and implemented it should permit the legibility of the cockpit electronic displays to be maintained at a constant level with little or no intervention by the pilot, despite the ambient illumination conditions present in the cockpit and the exposure of the pilot's eyes to discrete and distributed glare sources.

The only evident exceptions to the adequacy of the "hands-free" constant display automatic legibility control capability summarized in the preceding paragraph occur when a logical assessment of the operational conditions encountered by the pilot or other aircrew member is necessary to adjust the legibilities of electronic displays in aircraft cockpits correctly. The need for such aircrew legibility adjustments can, for example, be associated with either of the following two types of events: (1) the need to make changes in the information presentation techniques to perform different mission segments, where the changes in legibility preferences and needs of pilots that often accompany transitions between day and night ambient illumination viewing conditions are a special case; or (2) the potential needs to adjust the image difference luminance levels of displays during night operations to compensate for inadequacies in the time dependent adjustments made to the outputs of automatic legibility controls, while experiencing and following exposures to time-variant glare sources, such as flares or lightning. These two exceptions to the "hands-free" display automatic legibility control capability are described in greater detail in the following two sections.

8.2. Constraints on the Automatic Control of Display Legibility, Imposed by Changes in Aircrew Information Requirements, for Different Mission Segments

As described earlier in this report, changes in the legibility adjustment settings of electronic display information can be required, when transitions are made between mission segments, to support the differences in the mental information processing and decision making requirements, imposed on the aircrew members. This would most typically occur, when changes in the types of information portrayals to be displayed are required, to perform the new mission segment tasks, such as a change between a graphic and a sensor video information presentation on a particular display, or, as a special case, between day and night viewing conditions.

Because the knowledge needed to permit accurate theoretical emulations, of the preferences, logical analyses and other decision making processes of pilots and other aircrew members is not yet available, the legibility adjustment settings associated with the foregoing transitions are not particularly conducive to being automated. As an alternative to this theoretical predictive modeling approach, if it could be determined through the observation of pilots, questionnaires, interviews and in-flight experiments that the legibility setting strategies of different pilots agree, for the tasks performed during a particular mission segment, and the number of controlled legibility levels is not too great, then the preceding legibility adjustments could, for example, be integrated with an aircraft's mode control switching. Since neither of these types of information is presently available, it is concluded that automating these types of functions is not currently feasible, and a means must therefore be provided to allow the aircrew members to make the necessary legibility adjustments.

The balance of this section is devoted to a description of the special case of the legibility adjustments made by aircrew members between day and night viewing conditions. This special case of the legibility changes made by aircrew members, with or without a change in mission segment tasks, is described both because information about this transition is available in the literature and because it may be indicative of other legibility changes made when changing to a new mission segment. Whether the image difference luminance settings of a display operated by an automatic legibility control is modified by the aircrew or not during this transition, would depend on the day and night missions of the aircraft. If no requirement to become dark adapted to the night visual scene external to the aircraft exists, as is typically true for commercial aircraft, then no adjustment to the daylight settings of the automatic legibility control would be needed. Alternatively, aircraft missions that require the pilot to view and extract information from external night visual scenes depend on achieving and maintaining the best possible dark adaptation of the pilot's eyes. Because the luminance level

settings of cockpit displays can potentially cause the pilot's ability to dark adapt, to be limited to a luminance dark adaptation floor that exceeds the lowest luminance levels present in the external scene to be viewed, cockpit displays are generally operated at the lowest luminance levels a pilot can tolerate, and still permit reading the cockpit display information considered essential to perform the tasks to be carried out. Consequently, it can be anticipated that the pilot or another aircrew member would reduce the legibility level settings of the display automatic legibility controls, from the legibility levels preferred for daylight viewing, to perform missions requiring good external night vision. Still another aircrew member legibility setting alternative occurs for aircraft missions that use a night vision imaging system (NVIS). In this instance, the image difference luminance levels set by aircrew members are typically intermediate between the low levels used to achieve good external night vision, and the high levels used during takeoffs, landings and, more generally, for any missions flown using instrument flight rules where no external night vision requirement for dark adaptation exists throughout the duration of the mission.

Two conditions typically impede the pilot's ability to achieve dark adaptation sufficient to perform missions involving the use of external night vision. One of these conditions is the need to provide information to the pilot using cockpit displays. As noted previously above, this is a special case of the changes in the image difference luminance level settings of cockpit displays that must be initiated by pilots or other aircrew members when a transition between mission segments occurs. The other condition is the exposure of the pilot's eyes to a glare source. This condition is described in the next section.

Excepting aircrew exposures to glare sources, the image difference luminance levels required to make the information portrayed by displays readable in a cockpit at night has probably the greatest degrading influence on the ability to dark adapt to exterior visual scenes at night. No experimental data could be found in the literature that is directly applicable to answering the question of the extent to which external night vision is degraded by transitioning back and forth between reading information from cockpit displays and then reading information contained in the external night visual scenes. However, data for transitions, from a temporary exposure to higher luminance levels than those present in a night-lighted cockpit, to a fully dark adapted state, appear to be sufficient to allow the results to be inferred. It is known, for example, that the manual luminance level settings of pilots under this viewing condition are typically of the order of a factor of five to ten lower than the levels the pilot would set for missions that do not require dark adapted vision. Consequently, an automatic legibility control configured to provide constant legibility control and set by the pilot to provide adequate legibility under daylight viewing conditions would typically have to be manually trim adjusted to a lower luminance level by the pilot to permit performing night missions requiring dark adapted vision. This manual control adjustment by the pilot to the automatic legibility control setting of the cockpit display luminance levels is of course no different from the manual luminance setting requirements of conventional cockpit displays intended for use in a mission requiring dark adaptation or, for that matter, from the luminance setting requirements of any electronic display that is manually controlled.

As indicated above, the quantitative improvements in the pilot's dark adaptation to external visual scenes caused by the reductions in the cockpit display luminance levels is unknown. Nevertheless, it can be expected that the origin of a luminance dark adaptation floor is in part due to veiling luminance induced in the pilot's eyes by their peripheral vision exposure to the cockpit display luminance level settings, while the external scene is being viewed, and in part due to the degradation in the dark adaptation of the eyes' rod receptors caused when the pilot reads information from the cockpit displays and then transitions to read information from the night visual scene. As considered in greater detail in the following section, the light receptors used by the eyes to read information from the cockpit displays are foveal cone light receptors, and those used to read information from external night scenes are cone light receptors, if the scene's reflect luminances is in the mesopic vision range, and are rod light receptors, if the scene's reflect luminances in the scotopic vision range. For the reasons described in Section 3.7.3, the high spatial discrimination capabilities of the central foveal cone light receptors are responsible for their use in perceiving the information presented on cockpit displays and the small image critical detail dimensions typically involved in identifying the focused images of distant external scene objects. The cone and rod light receptors distributed throughout the balance of the eye's retina, beyond the central fovea, are jointly responsible for the lower spatial resolving capabilities of the eyes, throughout most

of the human's field of view. Only the rod light receptors appear to operate in the night scotopic vision range, whereas only cone light receptors appear to operate in the daylight photopic vision range.

Based on the investigation by DeBruine and Milligan, described previously in Section 3.3.3 of this report, concerning the display luminance level settings of pilots at night,[162] it is concluded that the formulation of a theoretical or empirical algorithm to emulate the logic employed by pilots to set the luminance levels of the cockpit display information at night is probably not feasible, because the variability of the image difference luminance level settings of individual aircrew members would cause this type of legibility control adjustment to be unsuitable for being automated. Due to the preceding constraints, it is concluded that a means must be provided to permit aircrew members to make manual trim control adjustments to the legibilities of displays being operated by automatic legibility controls. Moreover, this must be done not only due to the aforementioned lack of information to permit automating these legibility control tasks, but also because permitting aircrew members to satisfy their personal preferences and needs, for the legibility of the information being displayed, and to account for any unforseen circumstances encountered while flying a mission, is deemed to be essential.

Even though this legibility level setting function of the aircrew cannot be automated, the inclusion of a legibility trim control to allow pilots to adjust the image difference luminance of the displayed information, to the reduced automatic legibility control levels needed for missions that require night scenes to be viewed external to the cockpit, would be essentially the same as the current requirement to perform this task manually. If all of the cockpit's displays, including conventional displays, integrally illuminated panels, signal indicator light panels and so forth, were to be subject to automatic legibility control, then attaining both constant legibility control and a reduced workload would be possible by setting only a single common legibility control, rather than using the multiple manual controls, as is required to reduce the display legibility settings in existing military aircraft cockpits. It remains to consider these legibility control techniques in the context of the adaptation effects on the eyes caused by exposures to glare sources.

8.3. Constraints on the Automatic Control of Display Legibility, Imposed by the Time Dependence of Changes in Aircrew Light and Dark Adaptation

The ability to develop an algorithm that can automatically adjust the output of automatic legibility controls to compensate the legibility of aircraft cockpit displays for the time dependence of the aircrew's light and dark adaptation, in response to time changing ambient illumination and glare source exposures during both day and night viewing conditions, is hampered by a lack of published light and dark adaptation data that is directly relevant to the conditions aircrew members experience in aircraft cockpits. In spite of a considerable body of published basic research, the relationships between the legibility of information displayed in an aircraft cockpit and the dependences of the light and dark adaption time responses of aircrew members on the ambient illumination and glare source exposure conditions experienced in aircraft cockpits remain, in quantitative terms, ill-defined. This modeling of the aircrew's legibility requirements, to permit the legibility degrading effects of light and dark adaptation to be compensated, is also hampered by a lack of published data, about the strategies pilots and other aircrew members' employ to deal with changes in night illumination and glare source viewing conditions experienced during operational missions. The preceding uncertainties, along with other considerations that would be expected to have an influence on the capabilities automatic legibility controls should possess in aircraft cockpits under either daylight or night viewing conditions, are described and further elaborated upon in the subsections that follow.

In lieu of the explicit information described above, and to aid in considering the effects of the light and dark adaptation response times of a pilot or other aircrew member eyes on the legibility of aircraft cockpit displays operated using automatic legibility controls, this section attempts to provide relevant background information, aircraft cockpit contextual information and data analyses to support the conclusions reached. The modifications to the output of the automatic legibility control law, beyond the time dependent control requirements needed for daylight flight operations that were previously described in Section 7.4, are projected

to be relatively minor in nature, based on the results of the analyses described in the balance of this section. In considering the results presented, and as previously indicated in the introductory remarks to this chapter, it should be born in mind that, insofar as the information available in the literature is insufficient to a permit a full direct validation of all of the conclusions reached, some of these conclusions must be considered speculative. In other words, it is left to the reader to make an informed judgement as to the validity of the conclusions presented, based on the merits of the information, interpretations and arguments used to arrive at the conclusions.

The first subsection below, Section 8.3.1, describes the two phase process of dark adaptation. This is done to provide general background information, for use in considering the effects of dark and light adaptation, on the legibility of information presented on aircraft cockpit displays in changing ambient illumination and glare source viewing conditions, which is the primary emphasis of the balance of the section. In Section 8.3.2, the legibility effects light and dark adaptation responses of aircrew members, under daylight viewing conditions where the effects are better documented, are described. This is intended to provide a basis for the comparison of the legibility effects attributable to the light and dark adaptation responses of aircrew members, under night viewing conditions. From a perceptual standpoint, a pilot's light adaptation visual response to being exposed to a glare source at night and the subsequent recovery of dark adaptation, following the extinction of the glare source, can be most readily understood if considered in two parts. The first part, is concerned with the display legibility effects experienced by pilots and other aircrew members during exposure to a glare source up until the time that it extinguishes, and is described in Section 8.3.3. The second part is concerned with the display legibility effects experienced during the recovery period after an exposure to a glare source that either extinguishes, or is no longer visible within the pilot's field of view, due to a change in the attitude or location of the aircraft, and is described in Section 8.3.4. These two subsections are the primary emphasis of this section. This section concludes with Section 8.3.5, which gives an abbreviated description of the effects of different choices of night automatic legibility control options, discussed previously for daylight viewing condition in Section 7.3, and Section 8.3.6, which presents conclusions, concerning the compensation of automatic legibility controls for the effects of light and dark adaptation.

8.3.1. General Background Information on the Two Phase Process of Dark Adaptation

To serve as a background for considering how the outputs of automatic legibility controls should be altered to respond to the time dependent changes in the night visual scene luminances and glare source exposures experienced by aircrew members under night viewing conditions, the response time implications of the two phase process of dark adaptation, previously described Sections 3.7.3.3 and 3.7.3.9, will be briefly considered. The first phase of dark adaptation applies to a pilot or other aircrew member reading information either on displays within an aircraft cockpit or in visual scenes external to the cockpit, where in both cases the threshold luminance levels of the areas being adapted to are in the photopic or mesopic luminance ranges of vision. Photopic dark and light adaptation are characterized by visual response changes that are very rapid. Response times, for adapting to photopic luminance levels, are typically in the low seconds to fractions of seconds depending on the magnitude and direction of the luminance change. Presumably, it is for this reason that the dark and light adaptation component of the response times required by humans to perceive information visually under photopic viewing conditions are typically not identified and treated separately in the literature.

When a threshold luminance level, to be adapted to, is in the mesopic range of vision, which corresponds to luminance levels in the approximately three-decade transition from photopic daylight to scotopic night vision, the times required to dark adapt to a steady state viewing condition, for a specific visual scene, are still quite short but in relative terms are much longer than the times to dark adapt to photopic luminance levels. Dark adaptation times, to reach a steady state mesopic luminance threshold, are dependent on the luminance, duration, and color of the preadapting light, with lower preadapting luminance levels, shorter exposure durations and red preadapting light producing shorter times to reach the fully dark adapted state. Typical elapsed times to dark adapt from a fully light adapted photopic luminance level to a mesopic luminance level can be up to about five to ten minutes long but the adaptation times also depend on the visual properties of the

images to be perceived. Circular test fields subtending angular dimensions of about three degrees or smaller and centered on the fovea of the eyes result in progressively more rapid dark adaptation times as the size of the circular area becomes smaller, whereas angles larger than nominally three degrees do not appear to extend the times required to achieve mesopic dark adaptation further (e.g., see Figure 3.37). Moreover, for a particular preadaptation test field size (i.e., not specified) and luminance (i.e., 1,500 mL or 1,394 fL), the elapsed times to dark adapt the eyes, from photopic levels to mesopic levels, do not change appreciably, as the critical detail dimensions of line grating imagery to be perceived become larger (e.g., see Figure 3.35), and the threshold luminance levels required to perceive the line grating images become progressively lower in the range from nominally 3 fL to 0.003 fL.

No experiments dealing with mesopic dark adaptation, where dark adaptation started from mesopic, rather than photopic preadaptation luminance levels, were found in the literature, however, based on the trend for decreasing photopic preadaptation luminance levels, described later, dark adaptation should occur in seconds rather than minutes for such transitions. Another practical issue not considered in the dark adaptation literature is the effect of preadaptation luminance exposures, to the glare source viewing conditions experienced in the real-world, where the sizes, or subtended solid angles, of the glare sources with respect to the pilot's total field of view can be quite small (e.g., the sun and moon subtend angles of about one half degree). Glare sources that do not fill the observer's field of view are considered in the literature only in terms of the veiling luminance they induce, but not in terms of their potential effects on dark adaptation.

Owing to the lack of directly applicable experimental data, the effects of the size of a glare source on mesopic dark adaptation are dealt with, in the subsections on dark adaptation that follow, from a theoretical perspective. In particular, exposures to glare sources subtending small angles would be expected to result in preadapting only the retinal light receptors exposed to the focused image of the glare source. Based on the demonstrated spatially selective adaptation capabilities of the eyes, the dark adaptation data cited above, which are applicable to preadaptation exposures of the complete field of view, are used to interpret limited area glare source exposures of the light receptor within the viewers' eyes.

Experimental results, demonstrating that preadaptation to red light produces faster dark adaptation times, were the factual basis for using red lighting to illuminate military aircraft cockpits at night over a period of many years. This benefit of using red night lighting is generally attributed to two factors. The first benefit is that a spectrally selective desensitization of the cone and rod light receptors in the eyes, during a full field of view exposure to red light, retains the higher level preexposure sensitivity of the light receptors to other colors present within a white test image or in external night scenes, where the color red occurs with a low frequency. Incidentally, this result also serves an example of selective dark adaptation of the eyes light receptors in the spectral domain. The other benefit of being preadapted to red light is generally attributed to the fact that red light of a particular luminance level has less effect than other preadaptation color spectrums in bleaching, that is, in reversing the scotopic dark adaptation of rod receptors.

In the late 1960s, the USAF started to convert from the use of red to white night lighted cockpits, when it was found that a pilot's abilities to dark adapt received little real benefit, from using red over white cockpit lighting, when viewing night scenes from the cockpit. As a practical matter, the experiments cited above used wide field of view preadaptation luminance sources, operated at more than one thousand foot-Lamberts, whereas the spatially distributed discrete image luminances, associated with night lighted cockpits, are spatially dispersed throughout the cockpit, rather than being a uniform luminous area, and their imagery typically operates in the mesopic luminance range of vision, from 0.02 to 1.5 fL, a multiple of a thousand to more than ten thousand less than the preadaptation luminances applicable to the experiments. As discussed in greater detail later, the available evidence suggests that the USAF finding for white lighting is due to the combination of these lower luminance level exposures, and the fact that the exposure periods, experienced after transitioning vision into the cockpit to view sensor-video displays or to perform instrument crosschecks, are insufficient to reverse the dark adaptation of the scotopically adapted rod light receptors, when vision is again transitioned back out of the cockpit to perform mission scenarios that require viewing external night scenes.

The image difference luminance level that display information is set to operate at in a cockpit by aircrew members, relative to the threshold luminance for the same image, is another factor that influences the elapsed time to reach the state of dark adaptation necessary to perceive the imagery being presented. As the ratio between the aircrew's setting of the image difference luminance levels increases, relative to the threshold image difference luminance, the elapsed times required to dark adapt to the level that permits perceiving the imagery quickly decrease. While the effect of this relationship is applicable in any ambient illumination viewing environment, its effect is most pronounced under night viewing conditions, where the elapsed times to dark adapt are inherently longer. This relative luminance or contrast relationship does not play a meaningful role in external night vision because night scene luminance levels are usually not controllable. An exception would be for the moon or a flare illuminating an external night vision scene. In this special case, the moon or a flare would produce an effect for an external night scene that is comparable to increasing the image difference luminance levels of displays in a cockpit. In the literature, this subject is treated as a contrast rather than a dark adaptation effect.

The preceding visual response time characteristics for adapting to mesopic luminance levels apply to both the pilot's foveal and peripheral fields of view and are based on the use of cone light receptors, which are involved in the performance of cockpit display and external visual tasks requiring good visual acuity in both the photopic and mesopic luminance adaptation ranges. In the mesopic luminance adaptation range, the time dependent dark adaptation responses of rod receptors appear to be very similar to those of cone receptors, except that they are reported to be less light sensitive, in this range of vision. As previously described in Section 3.7, the rod light receptors do not appear to play any role in the photopic luminance adaptation range and very little information was found in the literature that describes their role in the mesopic range.

The second phase of dark adaptation involves scotopic adaptation and primarily applies to a pilot or other aircrew member acquiring information from visual scenes located external to the aircraft cockpit. In the scotopic range of vision, which starts at the lower end of the mesopic vision range and extends down to the lowest levels of night vision, the times required to dark adapt to a steady state viewing condition increase to between tens of minutes and hours, as the threshold luminance levels of the visual scene information to be perceived, become progressively lower in the range from nominally 0.002 fL down to less than 1×10^{-6} fL. The actual adaptation response times vary significantly based on factors, such as, the luminance of the preadapting field, its spatial extent, its duration, and its color. Rod receptors, found outside the central fovea of the eyes, are responsible for scotopic vision, with cone receptors and, consequently, the entire central fovea of the eyes playing no apparent role. The degradation in visual acuity accompanying the adaptation to scotopic vision, and the use of rod light receptors to perceive visual information, causes the luminance levels associated with this type of vision to be unsuitable for perceiving small external scene images or for reading the information presented on cockpit displays.

8.3.2. Legibility Considerations Attributable to the Light and Dark Adaptation Responses of Pilots under Daylight Viewing Conditions

Under daylight viewing conditions, the cone light receptors in an aircrew member's eyes can be expected to adapt very rapidly following a transition from viewing cockpit displays, to perform an instrument crosscheck, for example, to viewing an external visual scene, where the sun or another source of glare may be present. In contrast to the light adaptation process just described, a transition from viewing an external visual scene back into the cockpit to read display information involves the dark adaptation of the cone light receptors. This process, while still very fast compared with dark adaptation at night luminance levels, can be expected to be somewhat slower than light adaptation, because the adaptation is not being driven by an exposure to higher luminance levels, but instead involves a relaxation to the reduced luminance levels within the cockpit.

The ability of a pilot or other aircrew members to light and dark adapt rapidly, in a daylight illuminated cockpit viewing environment that includes possible exposures to a glare source of extreme luminance, such as the sun, is expected for at least two reasons. One reason is that pilots avert their eyes to avoid the visual

discomfort caused by focusing these light receptors directly on the sun. The result of this often unconscious behavior by pilots is that the foveal cone light receptors, which are used to acquire most of the information acquired from both external visual scenes and cockpit displays, are never exposed directly to the luminance level of the sun, but, instead, are adapted to the luminance levels present in the external scene or in the cockpit, as augmented by the veiling luminance induced by exposures to discrete or distributed sources of glare elsewhere in the instantaneous field of view.

Although averting the eyes prevents the foveal cone light receptors from receiving more than very brief direct exposures to the sun's luminance, more peripheral cone and rod sensors are exposed to a direct focused image of the sun. Voluntary eye and head movements, along with saccadic movements of the eyes, are generally thought to be responsible for preventing the overexposure of these light receptors and, yet, do not impede the light or dark adaptation of the foveal light receptors used to acquire cockpit or exterior scene information, due to the ability of the eyes to adapt, simultaneously, on a spatially selective basis, to different luminance levels in different areas of the retina. The capability of the eyes light receptors to adapt spatially to vastly different luminance levels and the veiling luminance induced by exposures to discrete or distributed sources of glare, including their dependence on the angular separation between the sun and the pilot's line of sight, are described in detail in Sections 3.5 through 3.8.

The second reason for the rapid light and dark adaptation capability of the eyes, under daylight viewing conditions, is, in part, simply due to the nearly real-time adaptation response of cone light receptors at daylight luminance levels, but is also enhanced by the restricted range of luminances over which the light or dark adaptation has to occur, during visual transitions between reading the information in scenes located outside the cockpit and information depicted on displays located inside the cockpit. This change in luminance between the image difference luminances emanating from objects in the external visual scene and those emanating from imagery depicted on cockpit displays is frequently less than a multiple of ten and only under special circumstances does it exceed a multiple of one hundred for any particular object or image color being viewed. The latter circumstances can include visual transitions to and from the imagery depicted on both conventional displays and on some lower image difference luminance optically filtered electronic displays. Even for the largest of these luminance level transitions, practical aircraft experience shows the dark and light adaptation elapsed times of aircrew members for visual transitions into and out of the cockpit, respectively, are still very rapid, that is, not long enough to be interpreted as causing a legibility problem by the aircrew members.

As a practical matter, the previously described visual transitions between inside and outside the cockpit, would be no different for cockpits equipped with conventional and manually controlled electronic displays, and those equipped with displays that are operated using automatic luminance controls. The only exception to this equivalence would occur if a peripheral glare source were to be visible in the daylight illuminated external visual scene. In this instance, automatically compensated displays could be more legible than their manually controlled counterparts, dependent on the settings of the aircrew legibility trim controls.

The point being made, albeit indirectly, in the previous discussion is that while the automatic legibility control law presented in this report does not possess a capability to sense aircrew visual transitions into and out of the cockpit and, therefore, cannot make legibility adjustments for the effects of light and dark adaptation response times during these transitions, this is no different from aircraft cockpits of the past, equipped with a mix of conventional and manually controlled electronic displays. Furthermore, based on aircraft experience, under daylight viewing conditions, the dark adaptation response to visual transitions from outside to inside the cockpit would result in at most a very temporary degradation in the visual perception performance of pilots, viewing either conventional or electronic displays. The light adaptation responses to visual transitions from inside to outside the cockpit, under daylight viewing conditions, occur in fractions of a second and do not create noticeable legibility problems.

Although the implementation of the automatic legibility controls described in this report intentionally ignore the visual transitions of aircrew members into and out of the cockpit, the times required for aircrew members to light and dark adapt, in response to changes in the luminances reflected within the cockpit viewing

environment and the veiling luminance induced in the eyes, can be taken into account by making time dependent adjustments to the outputs of automatic legibility controls and in so doing to control the time dependence of the image difference luminance levels of the information presented on electronic displays in aircraft cockpits. The real-time changes that occur in the luminances reflected from conventional displays, in response to reductions in the ambient illuminance, incident on the cockpit displays, in going from a full sunlight exposure of the displays to shadows, during an aircraft maneuver, for example, are known to produce a perceptible reduction in the legibility of the information portrayed, due to the reduction in the image difference luminance levels (i.e., brightness reductions) of the display presentations, caused by the presence of shadows on the displays. It is not, however, clear under this circumstance whether this evident reduction in the image difference luminance and legibility of the displays serves to mask a much smaller temporary degradation in the visual perception performance of pilots viewing the displays, attributable to the time required to dark adapt. Since these conventional displays are considered to provide satisfactory legibility under this condition, it is inferred that electronic displays would, similarly, not require any compensation for the time to dark adapt, under this viewing condition.

Unlike conventional displays, which lack the ability to be compensated for the temporary reductions in their legibility under changing ambient illumination and glare source viewing conditions, electronic displays can be compensated with relative ease under such conditions using an automatic legibility control. To make this adjustment to electronic displays operated under daylight viewing conditions, for the effect of light adaptation of the eyes, a time constant that allows controlling the electronic display to the new higher image difference luminance level, commanded by a display illuminance or veiling luminance sensor, in nominally 100 milliseconds or less would insure that satisfactory legibility levels are maintained throughout a transition between ambient illumination and glare source exposure levels. A similar adjustment to the image difference luminance levels of electronic displays to insure uninterrupted legibility of the information being displayed, for dark adaptation under daylight viewing conditions, could be satisfied by applying a decay time constant to the output of the automatic legibility control of only a few seconds. The inclusion of rise and decay time constants to achieve other purposes when operating electronic displays using automatic legibility controls under daylight viewing conditions is discussed in Section 7.4.

8.3.3. Legibility Considerations During Aircrew Exposures to Glare Sources at Night

When a pilot is flying an aircraft at night, the effects on information legibility caused by being exposed to a glare source are most strongly influenced by where the pilot's vision is directed in relationship to the location of the glare source when the exposure occurs. Although other glare source exposure parameters, such as its luminance, color, subtended solid angle, exposure duration, and the luminance level to which the pilot is adapted before exposure to the glare source, also influence the cockpit display and external night scene information legibility, the discussion in this subsection and in the subsection that follows it, dealing with the effect of exposure to a glare source following its extinction, will be subdivided into two fields of vision, broadly based on the angle between the pilot's line of sight and the glare source at the time the pilot is exposed. For this purpose, the pilot's field of vision and the attendant visual tasks will be subdivided into the glare source effects associated with reading information contained in the night visual scene external to the cockpit and reading information from displays located within the cockpit. Lightning and flare exposures will be used as examples to illustrate the effects that glare source exposures have on the legibility of information in night visual scenes and in the cockpit.

8.3.3.1. Legibility of External Night Scenes While Being Exposed to a Glare Source

If a glare source exposure occurs while an aircrew member is attempting to perceive information from night illuminated real-world scenes through the windscreen or canopy, then the effects of the exposure would be expected to be similar, in some respects and fundamentally different in others, to the effects experienced while viewing daylight illuminated real-world scenes. The extent of the difference in the effects experienced,

between night and day glare source exposures, is dependent on the spatial extent, luminance and temporal dependence of the glare source exposure of the eyes' light receptors, and on the cockpit and visual scene luminances to which the affected light receptors in the eyes are initially preadapted.

In spite of the extremely high luminance of a lightning strike, which is listed as nominally 2.34×10^{10} fL in Table B.1 of Appendix B, the luminance exposure is limited to a small portion of retinal receptors directly illuminated by the focused image of the lightning strike on the retina, with the balance of the light receptors in the eyes being exposed to the luminance reflected by the night visual scene illuminated by the lightning strike and the veiling luminance induced by the lightning strike. Each of these sources of the luminance exposure occurs over the same very short period, of the order of microseconds, although the perceived legibility effects extend over a period of up to a few hundred milliseconds.

As a worst case scenario, that is, for a nearby lightning strike, the spatially selective exposure of the retinal light receptors to the focused image of the lightning can lead to temporary blindness for those retinal receptors that are directly illuminated. For lessor exposures to more distant lightning strikes, the light receptors would start to adapt to the luminance level of the exposure to the lightning received. In either of these cases, the very short duration of the lightning strike, which is typically composed of multiple discharges, does not permit the eyes to move, even saccadically, during the exposure of the retinal receptors and, consequently, no image motion induced blur is associated with the perception of a lightning strike. Because it is an electrochemical change within the individual retinal rod receptors that is responsible for dark adaptation into the scotopic luminance range, exposure to lightning would reverse this process to varying degrees and cause responses that range of from a prolongation of normal dark adaptation recoveries down to very rapid recoveries, depending on the product of the luminance and the elapsed-time of the exposure of the affected rod light receptors. The topic of recovery of dark adaptation, following exposure to a glare source is considered in greater detail in Section 8.3.4.

During a lightning strike at night, the dark adapted state of the retinal light receptors not directly exposed to the focused image of the lightning on the retina of the eyes, would theoretically only be modified by their exposure to the general illumination created by the lightning strike and by the veiling luminance induced in the eyes by the lightning strike. No experimental investigations were found in the literature that explore the effect of a temporary exposure to a glare source on the sensitivity of dark adapted light receptors, in areas of the retina away from the exposed receptors. Nevertheless, the known spatially selective adaptation capability of retinal receptors under photopic and mesopic viewing conditions lends indirect support for extending the validity of spatially selective dark and light adaptations of the eyes' light receptors into the scotopic luminance range.

Based on subjective personal observations, the retinal receptors located outside the area of the retina on which the focused image of the lightning impinges are not noticeably influenced by a lightning strike. Moreover, this is true independent of whether the retinal receptor area exposed to the lightning is temporarily blinded or simply experiences a loss of dark adaptation. In particular, a lightning strike does not appear to affect the legibility of the information depicted on illuminated reflective mode displays and has only a marginal effect on degrading the legibility of external night scenes, immediately following such a lightning strike. Because of the lack of published test data, the extent of the degradation to external night vision caused by a lightning strike, in those portions of the retina not directly exposed to the lightning, cannot be quantified at this time.

Based on theory, the effects caused by a lightning strike should include the induction of veiling luminance in the eyes, as described in Chapter 3, and a temporary increase in the general illumination of the external night visual scene and of the cockpit viewing surfaces. The predicted result of a lightning strike would, therefore, be a temporary increase in the luminances reflected from the night visual scene and from the cockpit display and panel surfaces. This, in turn, should produce a temporary increase in the legibilities of the night visual scene information and of the reflective and transflective operating mode portions of the information displayed in the cockpit, temporized to some extent by the veiling luminance induced by the lightning.

Concurrently, the temporary additional illumination in the cockpit, in combination with the lightning induced veiling luminance, would reduce the legibility of emissive and transmissive operating mode displays unless they were to be compensated using automatic legibility controls.

If the direct glare source exposure of the light receptors in the pilot's eyes is caused by one or more flares rather than lightning, then the direct luminance level exposure to the flare is greatly reduced in comparison to lightning, but the period of exposure is greatly extended. Whereas lightning produces an essentially instantaneous freeze frame exposure, similar to taking a picture using a camera with, for example, a 1/1,000 second shutter speed, the eyes can be averted from the light emanating directly from a flare to prevent prolonged exposures of the same light receptors to the luminance of the flare, in the same way direct exposure to the sun is dealt with when viewing external scenes at photopic luminance levels. A problem that the persistence of the light emanating from a flare creates, which is not caused by lightning, is the exposure of many more of the eyes' retinal receptors to the flare's luminance, due to movements of the head and eyes during the longer period that the flare is active.

Prolonged exposures of retinal light receptors to the luminance of a flare would be expected to cause a progressively more severe degradation to initially dark adapted cone and rod light receptors, if the same light receptors are directly exposed throughout the exposure to the flare. In real aircraft missions involving exposures to flares, anything more that a very brief direct exposure of the same peripheral rod and cone light receptors would be extremely unlikely, due to head and eye movements and the motion of the flair. The same would be true for the foveal cone light receptors in the eyes because no reason exists for an aircrew member to track a flare visually and, thereby, cause this extreme form of exposure. Consequently, neither cone nor rod light receptors would be expected to receive more than very brief direct exposures to the luminance of a flare during operational night flights. For these reasons, the primary exposure of cone and rod light receptors in a flare environment would be due to the elevated reflected luminance levels in both the cockpit and the external night scene caused by the illumination from the flare.

The immediate effect of a flare when it fires would be to increase the luminance levels reflected from the night scene being viewed and to induce veiling luminance in the eyes of pilots and other aircrew members. Assuming the eyes' light receptors are initially dark adapted to scotopic luminance levels, when the flare illumination of the night scene occurs, the immediate effect of the flare illumination would be to light adapt the foveal and more peripheral cone receptors in the eyes, enabling them to extract information from areas of the night scene raised to mesopic reflected luminance levels. The time required for the cone light receptors to respond sufficiently to allow the scene information to be perceived is quite rapid, in the order of fractions of seconds to seconds. Other than the fact that the rod light receptors, exposed to the mesopic luminance levels of this viewing condition, would retain their dark adapted state for some time during their exposure to the flare illuminated visual scene, the literature does not provide a clear indication of the role the rod light receptors play in perceiving information, at the elevated mesopic reflected luminance levels of a night visual scene.

The legibility of information in portions of a night scene that remain at scotopic luminance levels when a flare is activated is much more difficult to assess. Although the increase in the luminances reflected from the night scene would make the scene easier to perceive using the scotopic adapted rod light receptors, the spatially variant veiling luminance induced in the eyes by the flare would in higher veiling luminance areas act to mask and, therefore, to counteract the improvement in the legibility of areas of the external night scene that are still only reflecting scotopic luminance levels during their exposure to the illumination produced by the flare. As the night scene reflected luminance levels, due to the illumination from a flare, become progressively higher during visual transitions into night scene areas that are in the mesopic luminance range, the effect of veiling luminance induced in the eyes by the flare on the legibility of the flare illuminated night scene becomes progressively less important. On average, the illumination of night scenes by flares does greatly improve the legibility of the night scenes they illuminate.

While the reflected luminance levels of a flare illuminated night scene would be expected to be quite low, that is, within the mesopic luminance range, exposures to these luminance levels over a sustained period

would be expected eventually to reverse the initially scotopic dark adaptation state of the rod light receptors used to extract information from night scenes. More specific information, concerning the dependence of the reversal of the scotopic dark adaptation of rod light receptors, on the combined effects of the luminance and duration of a light source exposure, is considered in Section 8.3.4, as is the recovery of scotopic dark adaptation following the extinction of a glare source. For other than a prolonged direct exposure of the foveal sensors, the effect of transitioning back into the cockpit to read information on the displays, during an exposure to elevated general scene illumination caused by a flare, would be expected to be entirely compensated, for displays operated using automatic legibility controls.

8.3.3.2. Legibility of Cockpit Display Information While Being Exposed to a Glare Source

In the event an exposure of the pilot's eyes to a glare source, such as a flare or lightning flash, occurs at night while the pilot is reading information from a cockpit display, then the effect of the exposure on the legibility of the information portrayed would be expected to be the same as it is during daylight. More specifically, while the pilot is reading the display, the cone and rod receptors in the peripheral area of the eyes where the defocused shape of the glare source is imaged would experience a spatially selective degradation in their dark adaptation. Simultaneously, the foveal cone receptors, which are focused on the display surface to read information depicted there, would be exposed to an increase in the cockpit illumination attributable to the flare and to the effect of the veiling luminance induced by the glare source superimposed over the displayed information being read. To be able to maintain constant legibility, under this viewing condition, the image difference luminance requirements level of the information being portrayed on any type of cockpit display must be increased, but only by the amount needed to compensate for the effect of the additional cockpit illumination and the induced veiling luminance. An automatic legibility control could satisfy this portion of a pilot's visual response to a glare source at night, with no alteration to the way it operates under daylight viewing conditions, provided only that the veiling luminance sensors are sufficiently sensitive to measure the angle-weighted luminance emanating from the glare source.

While an increase in the display image difference luminance levels commanded by automatic legibility controls, to compensate for the increased cockpit illumination and the veiling luminance induced by the exposure to glare sources, would assure that the legibility of the displayed information is not degraded, information concerning what a pilot's legibility control strategy would be under this viewing condition could not be found in the literature. It is not known, for example, whether pilots would decide to increase the manual brightness settings of conventional and electronic displays under this viewing condition to maintain the legibility of the information, or alternatively would decide to leave these control settings unchanged. Some possible reasons why the manual brightness settings could be left unchanged by a pilot, even though this could cause the legibility of the information depicted on cockpit displays to be degraded, include the following: to avoid a further degradation to the state of the pilot's external dark adaptation, due to the increase in luminance levels of the cockpit displays needed to maintain their legibility; the anticipation that the effects of the glare source exposure would only be temporary and because of this it would not worth the pilot's time to alter the luminance level settings of the displays; and personal experience with glare source exposures that either cause the pilot to compensate the display luminances for such exposures in advance, or the knowledge that the degradation of the legibility the displays during and/or following such an exposure do not require compensation.

8.3.4. Legibility Considerations Following Aircrew Exposures to Glare Sources at Night

The dark adaptation recovery from a temporary exposure to a glare source at night is the other part of a pilot's visual response to a glare source that must be considered, and, in this instance, experimental evidence exists to suggest the night response can differ significantly from the response experienced during daylight viewing conditions. Although the automatic legibility control law was developed to predict the veiling luminance induced by glare source exposures under daylight though night viewing conditions accurately, night exposures to glare source viewing conditions still poses two important potential constraints on the direct application of an

automatic legibility control law configured for use in daylight. The reason for this is that the formulation of the automatic legibility control law did not consider the time dependent effects of light and dark adaptation of the eyes, due to an exposure to a glare source, on the legibility of cockpit displays.

The first potential constraint is concerned with the legibility of external night scenes after an exposure to a glare source. This constraint involves two possible exposure scenarios. One exposure scenario is concerned with the mitigating effects, on dark adaptation recoveries from exposures to night glare sources, caused by the veiling luminance induced in the aircrew member's eyes by the image difference luminances emanating from cockpit displays acting as a glare source, while aircrew members are trying to extract information from the external night scene, following the extinction of the glare source. The second scenario concerns the effect that the light adaptation of the eyes, caused by an initial task of acquiring information depicted on cockpit displays operated using automatic legibility controls rather than manual legibility controls, has on the ability to perform a subsequent task of acquiring information when vision is redirected to an external night scene. Neither of these exposure scenarios is specifically dealt with by the present formulation of the automatic legibility control law.

A second potential constraint is concerned with the legibility of cockpit display information after an exposure to a glare source. This potential constraint also involves two possible exposure scenarios. One of these scenarios concerns the time response of the automatic legibility controls needed to reduce the image difference luminance levels of cockpit displays that were being viewed at the time when the glare source extinguished. The second scenario concerns the display legibility control needed to achieve and then maintain satisfactory display legibility when vision is redirected into the cockpit following a glare source exposure received while viewing the external night scene. Again, neither of these exposure scenarios is specifically dealt with by the present formulation of the automatic legibility control law.

The dark and light adaptation constraints, on the ability of the automatic legibility control law to provide satisfactory control over the legibility of cockpit displays, are considered only potential constraints, for the exposure scenarios described above, because, as the discussion that follows endeavors to show, the constraints either can be compensated, by making only minor modifications to the daylight response time characteristics of the automatic legibility controls, discussed in Chapter 7, or are unavoidable, that is, the constraints are incurred, independent of whether the legibilities of the cockpit displays are controlled manually or automatically.

8.3.4.1. Legibility of External Night Scenes after an Exposure to a Glare Source

The first potential constraint on automatic legibility control is concerned with the extent to which a pilot's dark adaptation is degraded, owing to the exposure of the light receptors in the eyes to a glare source, while viewing an external visual scene at night. In comparison to the situation experienced under daylight viewing conditions, which was described near the beginning of this section, aircrew members viewing night scenes external to the cockpit and who received a direct exposure of the eyes' retina to the focused image of a glare source are commonly expected to have the state of their dark adaptation either moderately degraded, for the exposure of mesopically adapted retinal receptors, or severely degraded, for the exposure of scotopically adapted retinal receptors. The extent to which this commonly held expectation is fulfilled in practice will be considered below, based on a sampling of the available experimental evidence published in the literature, beyond that described earlier in Sections 3.7.3.5 and 3.7.3.9.

Many experimental investigations intended to characterize the time progression of the human's dark adaptation from an initial high luminance preadaptation level have been reported in the literature. The common results of experimental investigations into the progression of dark adaptation through the mesopic and scotopic luminance ranges, as a function of the visual acuity of a grating pattern test image, were described earlier in the report in Section 3.7.3.5 and shown in Figure 3.35. Likewise, the progression of dark adaptation through the mesopic and scotopic luminance ranges, as a function of the angular dimensions and positions of the

luminance test field on the retina, was briefly summarized in Section 3.7.3.9 and shown in Figures 3.37 and 3.38, respectively.

An investigation that explores the effect on a pilot's dark adaptation caused by a using different preadaptation exposure durations and luminance levels, under night adapted viewing conditions, was conducted by Haig.* In this investigation, the progression of the time dependent dark adaptation responses of the eye's rod light receptors, for a test subject initially dark adapted to a scotopic level of nominally 10^{-5} fL, to recover to a fully dark adapted state, following exposure to a 415 fL luminance light adapting field for periods of 0.1, 0.4, 1, 2, 4, 6, and 10 minutes were characterized. In addition, for the four minute exposure period, light adapting field luminances of 3.7, 18.6, 41, 415, 1,070, 1,940, and 4,370 fL were also tested. The analysis of Haig's results performed for the present investigation used descriptions of Haig's data and graphs, labeled Figures 106 and 107, respectively, in a report by Semple, Heapy, Conway and Burnette,[163] which are reproduced in Figures 8.1 and 8.2.

The dar adaptation recovery results of Haig are very similar to those of Mote and Riopelle,** who, according t mple, et al,[164] found that a 2.5 minute (150 second) or longer exposure to a relatively high luminance le will produce an essentially steady state adaptation of the eyes light receptors to the luminance level, with shorter exposures producing a reduced loss of dark adaptation and a faster recovery of the exposed retinal light receptors to the fully scotopic dark adapted state. In their description of these results, Semple, et al, presented, as Figure 105 of their report, a graph adapted from the Mote and Riopelle investigation. This graph showed a directly proportional relationship between "Sensitivity Loss (Loss of Dark Adaptation) in Percent," scaled from 0 to 100%, as the ordinate, and "Exposure Time To Higher Brightnesses (Seconds)," scaled from 0 to 150 seconds, as the abscissa. Subsequently, in an example of how to use the graph Semple, et al, asserted that the same dark adaptation recovery response times should be obtained, any time that the product of the preadaptation luminance levels and exposure elapsed times is a constant, that is for constant energy density exposures of the initially scotopically adapted rod receptors in the retina. The example provided cited exposures of 200 mL (i.e.,186 fL) for 150 seconds and 2,000 mL (i.e., 1,860 fL) for 15 seconds, that is, 30,000 mL·sec (i.e., 27,900 fL·sec), as causing essentially equal dark adaptation recovery response time characteristics.

In the second set of test results attributed to Haig, and shown in Figure 107 of the report by Semple, et al, and in Figure 8.2 of the present report, the scotopic dark adaptation recovery characteristics, shown for a parametric set of four minute (240 second) time duration preadaptation exposure's, exhibit the distinctive two phase mesopic and scotopic dark adaptation recovery responses for luminance field exposures of 415 fL or higher (i.e., 99,600 fL·sec or higher), whereas for 41 fL (i.e., 9,840 fL·sec) or less there is only a single scotopic dark adaptation characteristic. By way of comparison, the first set of Haig test results, illustrated in Figure 8.1, shows that the distinctive two phase mesopic and scotopic dark adaptation response recovery characteristics occur for a field luminance of 415 fL at exposure time of two minutes (i.e., 49,800 fL·sec) and more, whereas for 415 fL exposures of one minute (i.e., 24,900 fL·sec) and less, the recovery characteristics to full dark adaptation are much more rapid and lack the inflection point indicative of the mesopic dark adaptation phase at the start of the scotopic dark adaptation.

The 27,900 fL·sec preadaptation exposure constant, for the product of the exposure luminance and time duration, used by Semple, et al, to illustrate the results of the Mote and Riopelle investigation, also appears to provide a value for this constant that is approximately valid for predicting the transition between single and

---

* Haig, C., "The Course of Rod Dark Adaptation as Influenced by Intensity and Duration of Pre-Adapting to Light," Journal of General Psychology, Vol. 24, 1941, pp. 735-751.

** Mote, F. A. and A. J. Riopelle, "The Effect of Varying the Intensity and the Duration of Pre-Exposure Upon Subsequent Dark Adaptation in the Human Eye," Journal of Comparative Physiological Psychology, Vol. 46, 1953, pp. 49-55.

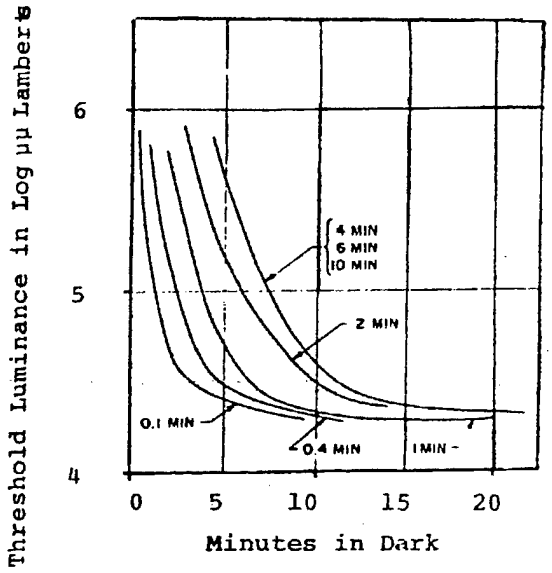


Figure 8.1. Dark Adaptation as a Function of Exposure Time for a 447 mL Preadaptation Luminance (Figure 106 of Semple, et al, p. 269. Data of Haig, 1941).

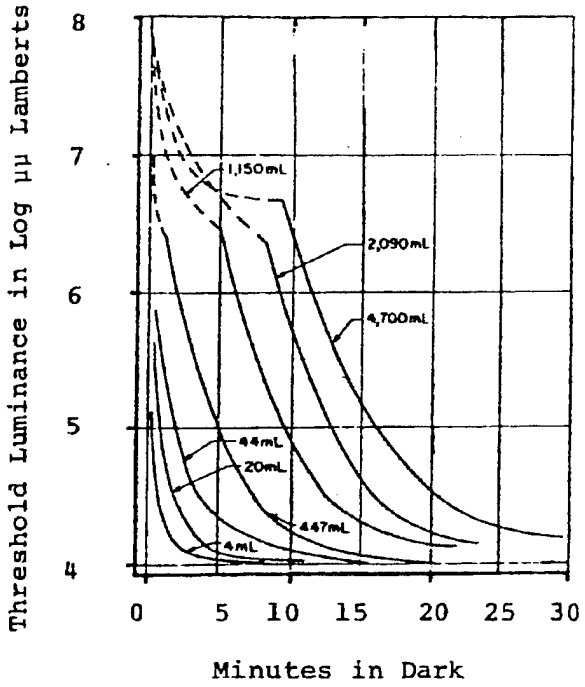


Figure 8.2. Dark Adaptation as a Function of Preadaptation Luminance for a 4 Minute Exposure Time (Figure 106 of Semple, et al, p. 269. Data of Haig, 1941).

two phase dark adaptation recovery characteristics. In particular, for values of the constant larger than 27,900 fL-sec, the recovery occurs in two phases and becomes progressively slower as the value of the constant increases, whereas, for smaller values of this constant the recovery follows a single characteristic and becomes progressively faster as the value of the constant decreases. The implication of this result is that low energy density glare source exposures of rod light receptors are insufficient to reverse the electrochemical process responsible for causing dark adaptation to scotopic luminance levels.

The experimental results of Mote and Riopelle are also described by Bartlett in a chapter of the book "Vision and Visual Perception" entitled "Dark Adaptation and Light Adaptation."[165] Figure 8.4 of that chapter is reproduced here in Figure 8.3. This figure shows the progress of scotopic rod dark adaption recovery following the preadaptation exposure of an initially dark adapted test subject for periods 0.5, 5, 50 and 500 seconds in four graphs corresponding, respectively, to preadaptation field luminances of 6,170, 617, 61.7 and 6.17 fL. These depictions of threshold luminance as a function of time show that the transition from the slower two phase mesopic to scotopic dark adaptation characteristics to the faster single phase characteristics occurs when the product of the preadaptation luminance and the elapsed exposure time is roughly 30,800 fL-sec or less. This result supports increasing the value of the Mote and Riopelle constant to 30,800 fL-sec.

In the graph of Figure 8.1, corresponding to the first set of Haig's test data introduced earlier, the dark adaptation recovery response time characteristics for 4, 6 and 10 minutes of exposure to 415 fL were all coincident with one another, with still shorter exposure times resulting in progressively faster recoveries to full dark adaptation. Bartlett, in Figure 8.3 of the book Vision and Visual Perception, presents comparable data from an earlier experimental investigation by Wald and Clark.* Bartlett's Figure 8.3 was attributed to Bartley[166] and is reproduced here in Figure 8.4. This figure shows the dark adaptation responses of initially dark adapted test subjects, for a preadapting field luminance of 309 fL and exposure times of 10 seconds, 1, 2, 5, 10 and 20 minutes.[167] In this case, the 10 and 20 minute exposure characteristics are separate, for the portion of the characteristics normally associated with mesopic adaptation, and only coalesce into a single recovery characteristic, just below the inflection point, normally associated with the transition from mesopic to scotopic dark adaptation. The coalescence of these recovery characteristics into single characteristics for both the Haig and Wald and Clark experimental data is interpreted as resulting from the test subjects having been exposed for long enough times to reach a state of full light adaptation to the preadaptation source luminance.

Both the Haig and the Wald and Clark experimental data also exhibit one or more additional dark adaptation response characteristics, which have lower luminance thresholds than the characteristics that coalesce, as dark adaptation progresses, but which still have luminance exposure-time products that exceed the Mote and Riopelle constant. This was true for the 2 minute exposure characteristic, for the Haig data, and the 2 and 5 minute exposure characteristics, for the Wald and Clark data. Each of these intermediate characteristics follow separate recovery characteristics until, following a period of dark adaptation in the vicinity of 20 minutes, all of the threshold luminance characteristics start very slowly to approach the fully dark adapted state. These additional characteristics are mentioned because they appear to exhibit both progressively longer recovery times and a more pronounced mesopic adaptation phase before the start of the scotopic dark adaptation phase, as the value of the product of the preadaptation luminance and the exposure-time increases above the 30,800 fL-sec value of the Mote and Riopelle constant. This behavior is interpreted, as resulting from a progressive transition between the fully dark adapted state and the lowest level of mesopic dark adaptation, caused by the reversal of the electrochemical processes, which occurs during the process of the rod light receptors becoming scotopically dark adapted. If this is true, then the faster recoveries to scotopic adaptation levels that occur for values of the product of preadaptation luminance and elapsed time up to the Mote and Riopelle constant can be attributed to the exposure energy density being insufficient to reverse the slow electrochemical changes in the rod light receptors that is responsible for the very low luminance levels of scotopic dark adaptation. The Haig and the Wald and Clark experimental data also lend further support for

---

* Wald, George and A. B. Clark, "Visual Adaptation and Chemistry of the Rods," Journal of General Physiology, Vol. 21, 1937, pp. 93-105.

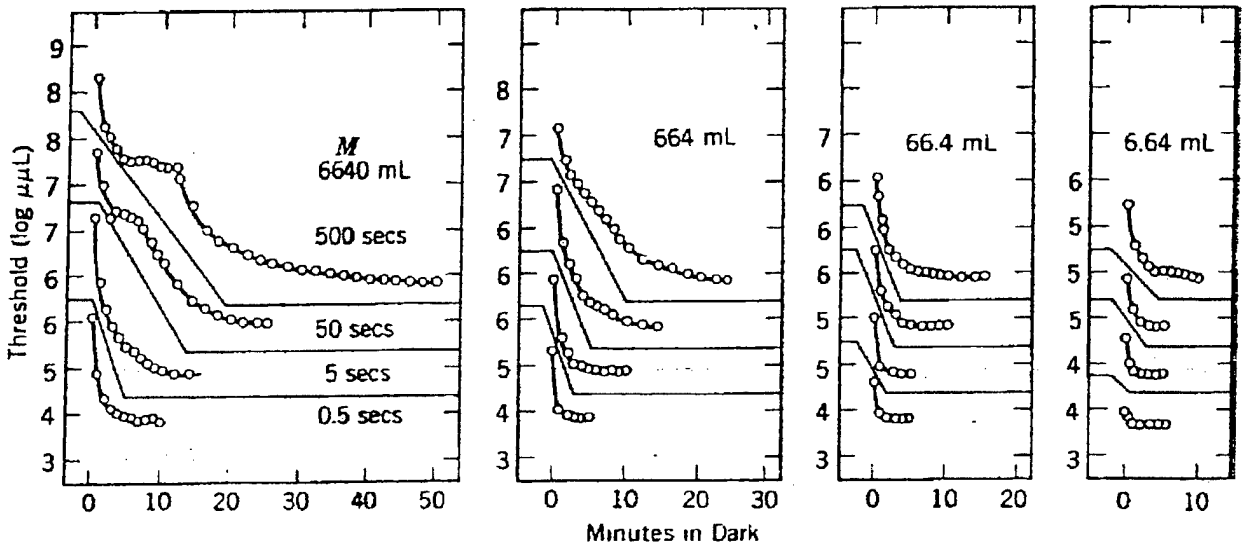


Figure 8.3. Dark Adaptation Following the Preadaptation Luminance Exposures, Shown at the Top of Each Graph, for the Exposure Durations Shown in the Left Most Graph (Figure 8.4 of Bartlett, N.R., Vision and Visual Perception, 1966, p.189. Data from Mote and Riopelle, 1953).

the value of the Mote and Riopelle constant, in that it is bounded by slow and fast dark adaptation recovery characteristics corresponding to values of 49,800 fL·sec, for a 2 minute exposure, and 24,900 fL·sec, for a 1 minute exposure, for the Haig recovery characteristics, and by values of 37,100 fL·sec, for a 2 minute exposure, and 18,500 fL·sec, for a 1 minute exposure, for the Wald and Clark recovery characteristics.

The preceding analysis used a limiting process as a criterion for determining the value of the Mote and Riopelle constant. This criterion involved determining the approximate upper limit on the value of the products of preadaptation times and luminances, for which the ensuing recovery time responses to the scotopic dark adapted state follow similar single characteristics having no inflection point indicative of a mesopic to scotopic transition. As values of the products of preadaptation times and luminances increase up to the upper limit, given by the Mote and Riopelle constant, the dark adaptation recovery elapsed times become progressively longer. While small enough preadaptation exposures can result in dark adaptation recoveries of seconds or even fractions of seconds, exposures equal to the Mote and Riopelle constant require about 15 minutes to reach full dark adaptation. The single phase dark adaptation recovery characteristics are interpreted to be the result of there being insufficient energy density in a preadaptation exposure, that is, less than or equal to the energy densities corresponding to the Mote and Riopelle constant, to reverse the slower electrochemical changes, which occur when achieving full dark adaptation. For still larger exposures, the electrochemical process is reversed to the point that the recovery delay associated with the mesopic to scotopic transition is encountered in the recovery characteristics, and the times to reach full dark adaptation are extended to nominally 25 minutes and beyond.

Bartlett's commentary on the results of the Mote and Riopelle investigation, employed a different criterion for establishing a maximum value for the Mote and Riopelle constant. Bartlett states this criterion as follows: "Within the conditions tested, when the product of the preadaptation time and luminance remained below 3,320 mL·sec, Mote and Riopelle's results show time of preadaptation to be compensable with luminance, and the product (energy) as approximately fixing the threshold at the outset of adaptation. As long as the product does not exceed 3,320 mL·sec, a single recovery function, displaced variously along the time axis depending on the energy, describes dark adaptation."

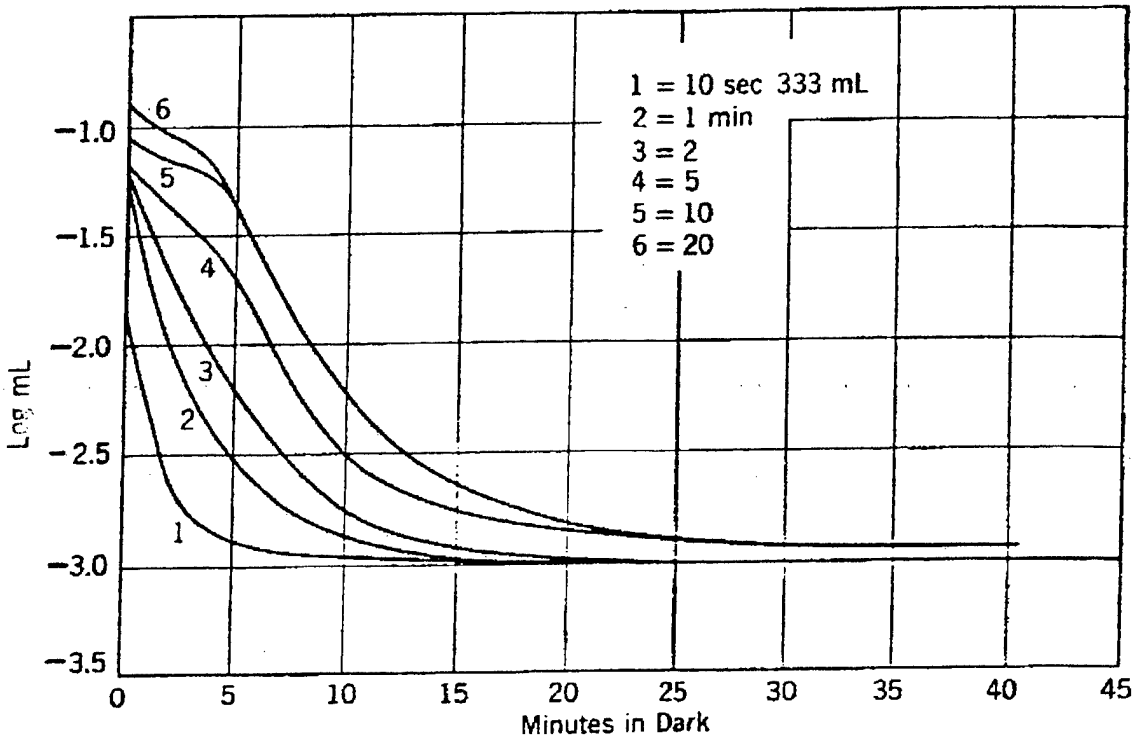


Figure 8.4. Dark Adaptation Following a Preadaptation Luminance of 333 mL and for the Exposure Durations Shown (Figure 8.3 of Bartlett, N. R., Vision and Visual Perception, 1966, p. 189. Data from Wald and Clark, 1937).

In describing the rationale for choosing this criterion Bartlett went on to state the following: "When the product of time and luminance of preadaptation is very large, the single recovery function no longer suffices as a description, and, moreover, luminance has more of an effect than duration in retarding recovery. The experiments were not designed to determine the upper limits of flash luminance or duration at which a single function applies, nor where reciprocity breaks down; they merely demonstrated such effects. They showed, for example, that 66.4 mL exposed for 500 sec required less recovery than the same energy spread over a shorter time, and so likewise did 664 mL exposed for 50 sec."[168]

To reconcile the observations and conclusions of Bartlett, quoted above, with the Mote and Riopelle data shown in Bartlett's Figure 8.4, and here in Figure 8.3, it was necessary to use the luminance difference between the data point corresponding to the luminance described by Bartlett as the "threshold at the outset of adaptation" and shown at zero minutes on each of the Mote and Riopelle dark adaptation characteristics, and the fully dark adapted luminance level, which was about 7×10^{-6} fL for each of the characteristics, as the metric for assessing the dark adaptation recovery. In comparison to Bartlett's evaluation of the Mote and Riopelle data, the assessment of the dark adaption recovery described above used the elapsed time to reach full dark adaption as the metric, that is, the change along the abscissa rather than along the ordinate. Using the elapsed time to reach full dark adaptation as a metric, the 33,200 mL·sec (30,800 fL·sec) examples of 66.4 mL exposed for 500 seconds and the 664 mL exposed for 50 seconds, chosen by Bartlett to demonstrate differences in the response characteristics for higher preadaptation exposure energy densities, produce essentially the same recovery times, as does the last characteristic for this energy density, a 6,640 mL exposure for five seconds. At the next lower energy density exposure level, the four recovery characteristics corresponding to 3,320 mL·sec (3,080 fL·sec) also have approximately the same adaptation recovery times, and, consistent with theory, the elapsed recovery times are shorter than for the higher energy density

preadaptation exposures. Finally, the individual characteristics, corresponding to 308, 30.8 and 3.08 fL·sec, each have approximately equal response times, which become progressively shorter as the energy density of the preadapting luminance becomes smaller.

The distinction between the conclusions reached, using these two dark adaptation recovery metrics, is assessed as resulting from Bartlett's use of the first data point collected, for each of the dark adaptation recovery characteristics and referring to the point as the luminance "threshold at the outset of adaptation." Since the luminance a test subject is light adapted to at the outset of dark adaptation is the luminance of the preadapting light source, the luminance threshold at the outset of adaptation, which is also referred to as the instantaneous threshold in the literature, should be about one grey shade range, that is, a factor of about one hundred, below the luminance of the preadapting light source just after it is extinguished. Although, as previously described, the initial dark adaptation is very fast, it does not occur instantaneously after the preadaptation luminance is extinguished. Instead, a finite number of seconds or fractions of a second elapse before the first data point can be collected. During this initial dark adaptation recovery time, the rate of change of the threshold luminance is very high, with short high luminance preadaptation light exposure pulses exhibiting the higher rates of change. It is, therefore, to be expected that the luminance corresponding to the first data point collected could vary significantly, due to slight variations in elapsed times at which it is collected, and could even correspond to a sample during the high rate of change transient period, rather than representing the start of the much slower recovery period that Bartlett appears to have intended to serve as the "outset of adaptation."

The predominance of large luminance spacings and short time intervals between the first and second data points on the sixteen Mote and Riopelle dark adaptation recovery characteristics in Figure 8.3 (i.e., Bartlett's Figure 8.4), with much smaller changes in luminance occurring between succeeding sample points, bears out the interpretation that the first data points on the characteristics are part of the initial high rate of change transient dark adaptation recovery, rather than the much slower recovery period that follows. By ignoring the first data point on each of the Mote and Riopelle recovery characteristics, when using the luminance difference metric, the revised luminance differences were found to produce the same adaptation recovery interpretation ascribed earlier to the use of the elapsed time metric. Because the elapsed time metric is not sensitive to the small time differences between collection times of the first data point nor is the result altered by the elimination of the first data point on each of the adaptation recovery characteristics, ignoring the first data point on each of the characteristics produces no change in the earlier interpretation, using the elapsed time metric. It is therefore concluded that assigning a value to the Mote and Riopelle constant of 30,800 fL·sec, both as the approximate preadaptation exposure boundary between single and two phase dark adaptation recovery characteristics and for Bartlett's upper limit on the reciprocity of the products of the preadaptation luminances and exposure times, would be reasonable.

The most significant result of the preceding experiments, for the present investigation, is the fact that dark adaptation recovery times rapidly decrease as the value of the product of the glare source luminance and exposure time becomes smaller. As previously described, the small angles subtended by flares, as seen by pilots from a cockpit at night, would result in only very brief direct exposures of individual retinal receptors to the luminance of the flare. Consequently, the degradation in retinal light receptor dark adaptation would be expected to be due to the elapsed time of the exposure to the combined effect of the flare illumination reflected by the night scene and the veiling luminance induced by the flare, rather than the very brief exposures of a spatially confined group of the eyes' retinal light receptors to the flare itself. Recovery of dark adaptation from the light adaptation to the mesopic luminance levels associated with these exposures would, therefore, be expected to occur rapidly in comparison to even the briefest exposures of the experiments described above. Possible exceptions to this conclusion would include situations where the pilot is exposed to a multiple flare environment over an extended period of time.

Although the particular details for lightning exposures differ from those for flare exposures, the results should be similar in many respects. For lightning, the exposure is effectively instantaneous and cannot be either unconsciously or intentionally avoided by a pilot. However, unlike the test subjects of the preceding

experiments, where the entire field of view was preadapted to the same high luminance level, pilots and other aircrew members are not restricted to using the small percentage of retinal receptors directly exposed to the lightning to view the night visual scene following an exposure. For the light receptors not directly exposed to the lightning, the degradation in the dark adaptation, of the initially scotopically dark adapted light receptors used to view an external night scene at scotopic luminance levels, would be expected to result from their brief exposure to the combined effect of the lightning illumination reflected by the night scene and the veiling luminance induced by the lightning. Recovery of dark adaptation following the partial light adaptation of the retinal receptors caused by these secondary light adaptation effects of lightning is more difficult to assess.

The time averaged light adaptation effect of being exposed to the combined scene reflected luminance and veiling luminance induced by a single nearby lightning strike, is assessed as equivalent to being light adapted by the lightning to steady state luminance levels in the mesopic range of vision. This assessment is consistent with the perceived night scene reflected luminance levels caused by such lightning strikes. Typical dark adaptation recoveries of rod light receptors from these secondary lightning exposure effects would be expected, as for secondary effects of flare exposures, to occur rapidly in comparison to even the briefest exposures of the experimental test results described above. Recovery of dark adaptation following even extreme exposures of this type would be expected, therefore, to occur in seconds or even in fractions of a second, rather than in minutes or longer. This result, for secondary exposure effects of a lightning strike, does not minimize the fact that the areas of the retina, temporarily blinded by a direct focused exposure to a lightning strike, could require tens of minutes, and possibly much more time, to recover to the mesopic or scotopic luminance level, of the dark adapted state of the eyes light receptors, before the lightning exposure occurred. The effect of a pilot being exposed to multiple lightning strikes over an extended period is unpredictable, owing to the uncertain impact on vision caused by the accumulation of temporarily blinded areas on different parts of the retina caused by the light adapting effects of multiple direct lightning exposures.

Because the dark adapted foveal cone light receptors, used to read cockpit display and external scene information at mesopic luminance levels at night, occupy only a small fraction of the retinal area, and are also in a different location on the retina than the rod light receptors, used to extract useful information from night visual scenes when dark adapted to the scotopic luminance levels, it would be unlikely that foveal cones would be exposed to a direct image of a glare source during night operations. However, in the event the foveal cones are directly exposed to lightning, or in the more unlikely event they receive prolonged direct focused exposures to the light of flares, then the affected light receptors would become light adapted. Under this circumstance, periods of up to ten minutes, and possibly much more for lightning, could be required to readapt to the lowest mesopic luminance levels of external night visual scenes, although the higher image difference luminance levels setting of information displayed in a cockpit would be expected to reduce these recovery times greatly, as has been previously described. For flare exposures, the degradation to dark adaptation can be minimized, if aircrew members pursue a strategy to focus the foveal cone light receptors of the eyes upon the night scene areas illuminated by the flares, rather than on following the movement of the flares.

The overall effect of the preceding factors, which can influence a pilot's dark adaptation while viewing external night scenes, is that the glare source exposures that are likely to be experienced by aircrew members at night are less than is generally thought to be the case and, moreover, the degradations caused by the exposures to the aircrew's dark adaptation are likely to be less serious than is commonly believed. It should be noted, however, that because the secondary illumination and veiling luminance effects of glare sources on scotopic night vision are unavoidable, and, moreover, should not appreciably affect the image difference luminance control requirements for information presentations on cockpit displays, this topic was considered beyond the scope of the present investigation. Consequently, the exploration of this dependence, including the comparison, analysis and attempts to model different experimenters' data, was quite limited during the present investigation.

The preceding descriptions of dark adaptation recoveries from exposures to lightning or flare exposures at night were aimed primarily at providing a background context for the exposure scenarios described in introducing the present subsection. These scenarios involve the potential effects on the previously described

dark adaptation recoveries from glare source exposures resulting from the use of displays operated with automatic legibility controls versus those controlled manually. The first exposure scenario is concerned with the mitigating effects on dark adaptation recoveries, from exposures to night glare sources, caused by the veiling luminance induced in the aircrew member's eyes by the image difference luminances emanating from cockpit displays acting as a glare source, while they are trying to extract information from the external night scene following the extinction of the glare source.

Whether operated using automatic or manual legibility controls, cockpit displays do induce veiling luminance into the eyes of pilots and other crew members while they are viewing an external night scene. This veiling luminance adds to the veiling luminance and reflected night scene luminances produced when the night glare sources are active and the veiling luminance attributable to the cockpit displays remains when a glare source extinguishes. The effect of the cockpit displays operated by an automatic legibility control is to cause a small increase in the veiling luminance attributable to the cockpit displays while the glare source is active that returns to the former level following the extinction of the glare source. Because of the low image difference luminance levels of the cockpit displays, before and even during such glare source exposures, and the limited percentage of the total visible cockpit area that emanate light, the veiling luminance levels induced would be quite small to start with, that is, at luminance levels within the scotopic luminance range, and would be only slightly increased by the automatic adjustment to the image difference luminance levels of the information displayed in the cockpit during the exposure to the glare source.

Since the veiling luminance levels induced by the cockpit displays, would represent only a very small fraction of the luminance levels attributable to the glare sources in the night scene being viewed, it can be concluded that the veiling luminance contribution from the cockpit displays can be ignored, except, possibly, in areas of the visual scene receiving very little illumination or veiling luminance from the glare source. When the glare source extinguishes, the longer recovery times, associated with dark adaptation recovery from the higher mesopic luminance levels attributable to the preadaptation of the eyes' retinal receptors, which, in turn, is caused by the composite exposure to the glare source illuminated night scene and the veiling luminance induced by the glare source, would predominate the recovery. Again, the veiling luminance attributable to the cockpit displays are too small to play a role. This situation changes, however, near the end of the dark adaptation recovery, where the veiling luminance attributable to the cockpit displays serves as a mask with respect to the scotopic luminance levels associated with the night scene, which must be perceived to permit information to be visually extracted. At this juncture, the veiling luminance induced in the eyes by the cockpit displays becomes the predominant source of legibility degradation to the night visual scene being viewed by the scotopically adapted aircrew members.

The small increases in the image difference luminance levels of cockpit displays operated using automatic legibility controls, over those operated using manual legibility controls (i.e., assuming there is no control intervention by the aircrew), disappear when the glare source extinguishes, as would the small extra amount of veiling luminance induced by the automatically controlled cockpit displays, while viewing an external night scene, before the glare source extinguished. Whether the higher veiling luminance induced by the automatically controlled cockpit displays, while an external glare source is operative, would be perceptible or not, after the glare source extinguishes, would depend on the luminance decay response characteristics of the individual automatic legibility controlled displays. Controlling the image difference luminance of the automatic legibility controlled displays so they decay more slowly than the aircrew's dark adaptation recovery, from the exposure to the glare source, to the nominal 0.02 to 0.1 fL image difference luminance levels that either manual or automatic legibility controlled cockpit displays would have been set to by the aircrew, before the glare source exposure was sensed, would cause a temporary degradation in night scene legibility, due to the brief added veiling luminance exposure caused by the slower decay of the image difference luminance of the automatic legibility controlled displays. Alternatively, allowing the reduction in the veiling luminance sensor signal to reduce the display luminance in real-time, or using larger intermediate response time constants to control the luminance decay of the automatic legibility controlled displays, should cause the effect of the higher veiling luminances induced by the luminances emanating from displays, operated by automatic legibility controls, to be negligible during the dark adaptation recovery from the glare source.

In the period following the extinction of the glare source that is the primary focus of this subsection, the preadaptation of the retinal light receptors to the higher image difference luminances of cockpit displays operated by automatic legibility controls would be expected to have, at most, only a brief effect on the aircrew member's ability to extract information from the night scene, and even then only for scenes at the lowest scotopic luminance levels. This effect of preadapting the retinal receptors while reading information from cockpit displays is part of the second scenario described in introducing the present subsection. In particular this scenario is concerned with the comparative effect that the light adaptation of the eyes, caused by an initial task of acquiring information depicted on cockpit displays operated using automatic legibility controls, versus those controlled manually, has on the ability to perform a subsequent task of acquiring information when vision is redirected to an external night scene.

Exposure of the eyes to the luminance levels of night lighted cockpit displays, adjusted to optimize external night vision, would result in luminance and exposure time products a factor of a hundred or less than the lowest values tested in the previously described experiments, for the typical exposure periods needed to perform an instrument crosscheck. It can be concluded from the preceding facts, and the response time trends predicted by the experimental results of Mote and Riopelle, that recovery of dark adaptation after periodic scanning of the information presented on cockpit displays, would occur in elapsed times of just a few seconds, and possibly less, after transitioning to acquire information from the external night visual scene for either manually or automatically controlled displays. Furthermore, the differences in dark adaptation recovery times for displays controlled automatically versus those controlled manually, following the visual transition back to view a night scene, should in theory be shorter for manually controlled displays that are not adjusted by the members of the aircrew to compensate for glare source exposures, but in practical terms the difference should be nearly imperceptible, due to the small differences between the image difference luminance levels of displays controlled using these two techniques.

8.3.4.2. Legibility of Cockpit Display Information after an Exposure to a Glare Source

The second potential constraint on the applicability of automatic legibility controls is concerned with the legibility of cockpit display information during the dark adaptation recovery of aircrew members who are attempting to read information from cockpit displays immediately following an exposure to a glare source. In particular, the concern is with the compatibility of the light sensor commanded output of the automatic legibility control with the dark adaptation recovery response of the aircrew members starting at the time the glare source extinguishes. Following the extinction of the glare source, automatic legibility controls configured for daylight flight operations would directly respond to the reduction in the light measured by the cockpit illuminance and veiling luminance light sensors, by returning the image difference luminance level of the information displayed in the cockpit to the levels they were at before the light sensors were exposed to the glare source in a very short interval of time. The modifications to the daylight time responses of automatic legibility controls to make them suitable for use under this night viewing condition are considered in the discussion that follows. Before proceeding with this discussion, the light and dark adaptation conditions applicable to the night viewing conditions dealt with in this subsection will be considered in greater detail.

As previously described in Section 8.3.1, cone light receptors are typically considered responsible for the first phase of dark adaptation, that is, up to the inflection point where the transition between the mesopic and scotopic regions of vision occurs in the dark adaptation threshold luminance versus elapsed time characteristics. If any further dark adaptation occurs, beyond this inflection point, it is attributed to rod light receptors, since cone light receptors do not appear to adapt to scotopic luminance levels, and, as previously described in Section 3.7.3.4, leave a blind spot at the center of vision where the foveal cones are located. Following Bartlett's commentary on the Mote and Riopelle dark adaptation recovery characteristics, described in the previous subsection, in relation to the dark adaptation of rod light receptors to scotopic adaptation luminance levels, Bartlett also briefly described an earlier article by Mote and Riopelle presenting experimental

data applicable to the dark adaptation recovery of foveal cone receptors.* In referring to this article, Bartlett stated the following: "An account essentially similar to the foregoing applies to Mote and Riopelle's data (1951) for the fovea. After exposure to high preadapting luminances, the dark adaptation is retarded. As the luminance, duration, or product of the two increases, the initial threshold increases and the time to reach a final steady threshold becomes greater; and again (although the authors did not stress the point) with high luminances the effect of luminance is more pronounced than that of duration."

In published descriptions of either the dark adaptation that occurs, following a prolonged exposure to a high field luminance level, or the recovery of dark adaptation, from a temporary exposure to a high luminance level, the very large luminance difference between the preadaptation field luminance level, to which the observer is initially light adapted, and the first recorded level of threshold luminance, shown for zero time after the preadaptation light source is extinguished, is seldom emphasized. During this dark adaptation time interval, the published experimental data show luminance differences approaching five orders of magnitude can occur over elapsed times of only seconds or fractions of seconds. Uncertainty in the duration of this initial period of dark adaptation, where the observer transitions between being light adapted to the luminance of the preadaptation light source, and the threshold luminance point, from which the much lower rates of dark adaptation proceed, stems from the fact that the progress of dark adaptation in this very short time interval has historically been difficult to evaluate experimentally and, consequently, very little information concerning this dark adaptation period is available in the published literature. The emphasis of published dark adaptation descriptions, whether the dark adaptation is from a fully light adapted state or represents a recovery from a temporary exposure to a preadaptation field luminance, is typically directed at the relatively slow process of dark adaptation that proceeds from the first recorded level of threshold luminance after the preadaptation light source is extinguished.

The preceding general information concerning dark adaptation recovery times is presented because experimental dark adaptation recovery time response characteristics that are directly applicable to cone light receptors, which are mesopically adapted before, during and after exposure to a glare source was not found in the published literature. Based on this general information and by drawing parallels to the scotopic rod dark adaptation characteristics described in the preceding subsection, it can be inferred that aircrew members should recover to the dark adaptation level required to read information from cockpit displays very rapidly, whether they are viewing the cockpit displays or the external night visual scene during their exposure to a glare source.

As previously described in the introduction to Section 8.3.4, the potential constraints imposed by using automatic legibility controls, configured for daylight flight operations at night, following an exposure to a glare source, involve two possible exposure scenarios. The first dark adaptation recovery scenario, following a glare source exposure, concerns the time responses that automatic legibility controls should employ to reduce the image difference luminance levels of the cockpit display information being viewed, at the time the glare source extinguished, to provide satisfactory legibility during the dark adaptation period that follows the extinction of the glare source. Exposure of a pilot or other aircrew members to a glare source in the peripheral field of view, while viewing information presented on cockpit displays, would cause the image difference luminance levels of displays operated by automatic legibility controls to be increased. These increases would occur in response to the increases in the light sensed by the veiling luminance and cockpit illuminance sensors, and would compensate for the degradation in the legibility of the displays that would otherwise be caused by the increase in the veiling luminance levels induced in the eyes and in the ambient illumination levels in the cockpit caused by the glare source. The combined effect of the veiling luminance and the increases in the display and cockpit reflected luminance levels would, in turn, cause the foveal light receptors in the eyes to light adapt to the new composite image difference luminance levels perceived when reading information from the cockpit displays.

---

* Mote, F. A. and A. J. Riopelle, "The Effect of Varying the Intensity and the Duration of Pre-Exposure Upon Foveal Dark Adaptation in the Human Eye," Journal of General Physiology, Vol. 46, No. 5, 1951, pp. 657-674.

Following the extinction of the glare source, the automatic legibility control would, as stated earlier, return the display image difference luminance quickly to the level it was at before the glare source exposure, unless the output of the automatic legibility control is modified to cause the image difference luminance levels of the controlled displays to be decreased at slower approximately exponential decay rates, consistent with the dark adaptation decay rates of the aircrew member's eyes.

Based on the dark adaptation recovery information presented in the previous subsection, the values of the display luminance decay time constants, used to control the time decays of the image difference luminances of cockpit displays operated using automatic legibility controls, should be determined based upon the product of the composite image difference luminance exposure, described in the preceding paragraph, and the exposure time of the foveal cone light receptors used to view the cockpit displays, where progressively smaller values of this product should cause the outputs of the automatic legibility controls and the corresponding image difference luminances of the displays to decay using progressively shorter time constants. A precise implementation of this control technique, for application to cockpit displays being viewed both before and following an exposure to an external night glare source, would require the use of a look-up table to assign the correct luminance decay time constants based on the computed values of a luminance and exposure time metric. To determine the value of this exposure history metric involves taking the integral convolution of the composite image difference luminance exposures received while reading the displays. An integration exposure window of sufficient duration to allow the time dependent variations in the night glare source exposures experienced in aircraft cockpits to be contained within the duration of the window is needed. Because of the movements of aircraft in relation to night glare sources and the scenes they illuminate, it is likely that a duration for the integration exposure window that includes the preceding five to fifteen minutes, depending on the type of aircraft, would be adequate for this purpose. The values of this exposure history metric would have to be calculated on a nearly continuous basis to be able to extract and update the display luminance decay time constants from the look-up table that are both accurate and timely, at the cessation of a night glare source exposure. Moreover, each display in the cockpit operated by an automatic legibility control would require the calculation of a different exposure history metric and the output of each automatic legibility control would require the application of a different decay time constant, due to differences that exist in the composite image difference luminance exposures that occur during night glare source exposures. As a practical matter, the published dark adaptation response time data is presently considered insufficient to permit specifying the contents of such a look-up table.

Despite the lack of information needed to match the image difference luminance decay of cockpit display information presentations to the dark adaptation decay of the aircrew precisely, theory would predict that this level of control accuracy and complexity is probably not necessary to maintain satisfactory cockpit display legibility following the extinction of a glare source that is located in the aircrew member's peripheral field of vision. The reason for this is that the dark adaptation recovery response times are expected to be too rapid for the cockpit display legibilities to benefit significantly from having the time constants applicable to the output of the automatic legibility control fine tuned in the manner described above. This conclusion rests on several different practical factors that influence the time dependent control that must be exercised over the legibility of displayed information in night lighted cockpits.

The first and most important of the factors influencing the extent of the time dependent control that must be exercised over the legibility of displayed information in a night lighted cockpits is that the magnitude of induced veiling luminance, attributable to night glare sources, should be only a very small fraction of the nominal value of 34.3 fL, which is applicable to head-down cockpit displays under worst-case daylight viewing conditions (see Section 3.6.9). This result is expected for the veiling luminance induced by lightning, in spite of the fact that the instantaneous luminance of a lightning flash is much higher than the luminance of the sun, for two reasons. One reason is that the short duration of the lightning strokes cause the perceived time-averaged luminance of lightning to be much less than that of the sun. The second reason is that the very small total solid angle subtended by a lightning flash, in combination with the balance of the solid angle sensed by the veiling luminance sensors being at low to very low night luminance levels, causes lightning to induce much less veiling luminance than the sun. The overall validity of this theoretical prediction is demonstrated by the

fact that the perceived scene reflected luminances due to the illumination provided by a lightning strike at night is very much less than that due to the daylight illumination provided by the sun.

In comparison to a nearby lightning strike, flares produce both much smaller veiling luminance exposures and much lower time-averaged reflected luminances from night visual scenes than does lightning. The effect on dark adaptation recovery, following a typical flare exposure, would, therefore, be expected to be much less than for a nearby lightning exposure. Because the illumination due to a flare occurs over a much longer time than for lightning, the flare illumination is nonetheless more effective for viewing a night scene, even though it produces lower instantaneous reflected luminance levels.

A second factor that reduces the time required for an aircrew member's dark adaptation to recover to the same image difference luminance levels that permitted reading the cockpit displays prior to a night glare source exposure is the fact that, even when displays are operated at reduced luminance levels for good external night vision, their image difference luminance levels are still about a factor of ten, or greater, than their corresponding mesopic threshold luminance values. As previously described, dark adaptation recovery from lower photopic and mesopic preadaptation luminance levels occurs very rapidly, often in a matter of seconds or fractions of a second, respectively, until within a decade or so of the mesopic threshold luminance levels. Consequently, only having to dark adapt to an image difference luminance level a factor of ten or more above the threshold luminance level required to read a display, should greatly enhance the speed of dark adaptation recovery to the image difference luminance levels at which cockpit displays are operated by aircrews at night in the absence of glare sources.

A third, and probably the most important factor, speeding the recovery of dark adaptation from the increased image difference luminance levels, set by the automatic legibility control to compensate for the elevated levels of illumination and the veiling luminance levels induced in an aircrew member's eyes by a glare source in a cockpit at night, is the small magnitude of the image difference luminance decrease needed to recover to the dark adapted image difference luminance levels the cockpit displays would be set to before the glare source exposure. Maximum image difference luminance levels, in night lighted cockpits using conventional displays, are set by pilots in range from about 1.5 fL to about 0.02 fL, for critical information that must be read to fly the aircraft, with lower values for background areas of displays and higher values up to 15 fL for master caution and warning signal indicators. The point of presenting this information is that, except the signal indicators and possibly some electronic displays, none of the luminance levels in the night lighted cockpit reach the nominal 3 fL level of photopic vision, and the change in the image difference luminance levels of the cockpit displays, between the maximum and minimum luminance level settings for the imagery portrayed in night lighted cockpits, is less than a factor of one hundred. Consequently, even if the cockpit displays are increased to their maximum luminance settings at night, the changes in luminance, while making the information displayed more legible, are insufficient to produce a light adaptation response by the eyes' cone light receptors that exceeds the dimming range of the displays. It follows from this that, while returning cockpit display luminance settings to the minimum levels needed to aid external night vision would cause the information displayed to become less legible, the operation the cone light receptors at the maximum luminance levels, followed by their operation at the reduced luminance levels, would not impose a dark adaptation time response delay on the ability to extract information from the displays. By analogy, it can be concluded that the increases in display image difference luminance levels caused by automatic luminance control sensing of glare source exposures should also allow cockpit display legibility to be maintained during a rapid return of the image difference luminance levels of the displays to their preexposure image difference luminance levels, following the extinction of a night glare source.

A further consideration that infers there is no need to implement different display luminance decay rates at night, than for daylight missions, is the fact that displays operated by automatic legibility controls, which can change their image difference luminance levels in real-time, and that lack a capability to control luminance decay time constants selectively, would be no different from existing manually controlled conventional and electronic displays, operating under the same night viewing conditions, except that the former displays would be temporarily compensated by the automatic legibility controls for the veiling luminance induced by night glare

sources. Overall, the effect of the preceding factors, in combination, should produce adaptation response times that are quite rapid. It is, therefore, not certain that a need exists to extend the luminance decay time constants beyond their daylight values, to maintain the legibility of the displays at acceptable levels during either the increases or decreases in the image difference luminance levels of cockpit displays, introduced by using automatic legibility controls at night, at least while performing tasks that only require reading head-down display information.

The second dark adaptation recovery scenario, following a glare source exposure, concerns the time response that the display automatic legibility control should employ to achieve and then maintain satisfactory display legibility when a glare source extinguishes, while a pilot or other aircrew member is viewing an external night scene, and the pilot's line of sight is then redirected to read information displayed within the cockpit. As previously described for daylight applications of automatic legibility controls, the automatic legibility control law, as currently formulated, does not have a capability designed-in to sense and, therefore, make it possible to compensate for the adaptation effects resulting from visual transitions into and out of the cockpit by aircrew members. Consequently, if a transition is made back into the cockpit following exposure to a glare source, any adjustment needed to maintain satisfactory display legibility would have to be accomplished using an aircrew legibility trim control. This, of course, is no different from the current situation in night lighted cockpits, where manual controls would have to be used to adjust the legibility of cockpit displays under similar circumstances, if the aircrew thought such an adjustment was necessary.

As a practical matter, and for the reasons described previously in this section, it is unlikely that any manual trim control adjustment by the aircrew would be necessary to compensate for the loss of dark adaptation caused by an exposure to a glare source experienced while viewing a night visual scene, after transitioning back into the cockpit, unless the foveal cone light receptors were by chance to be directly exposed to the focused image of the glare source. The use of a luminance decay time constant, to recover from the small increase in the image difference luminance levels of cockpit displays, made automatically by the automatic legibility controls in response to the sensed changes in the cockpit illuminance and veiling luminance levels caused by an exposure to a glare source at night, would provide a slight legibility advantage for transitions from viewing the external night scene back to the cockpit displays, which occurs during or happens to be coincident with the extinction of the glare source.

8.3.5. Effects of Different Choices of Automatic Legibility Control Options at Night

A question raised in Section 7.4 concerning the best method of controlling the legibilities of multiple cockpit displays, under daylight viewing conditions, is also of potential concern for night viewing conditions. Although several control techniques were described in Section 7.4, for the purposes of the present discussion the question is restricted to whether each display and its individual automatic legibility control should be assigned dedicated light sensors, or whether the veiling luminance sensor, having the largest response to the glare source exposure, should have its output applied to all of the display automatic legibility controls in unison. In the former case, the display image difference luminances will respond to the respective sensed light levels measured by the different veiling luminance sensors, which, in turn, depend on their individual exposures to the glare source, based on its orientation with respect to the cockpit. This implementation would make it possible for the information portrayals on all of the automatically controlled displays in a cockpit to be set at the minimum image difference luminance levels needed to satisfy the pilot's preferences or needs for display legibility at night and, thereafter, automatically maintain the legibilities of the information portrayals at the levels set by the pilot, as the orientation of the aircraft with respect to the glare source changes with time. At night, while viewing external visual scenes, this control strategy would minimize the veiling luminance induced in the eyes by the luminances emanating from cockpit displays. Furthermore, if all the displays in the cockpit, including conventional instruments, panels, signal indicators and so forth, were to be operated by automatic legibility controls, as is described later in this chapter, then the veiling luminance induced when viewing an external night scene would be reduced in comparison to the minimum veiling luminance levels achievable with displays operated using manual legibility controls in existing aircraft cockpits. The specific image difference

luminance control techniques that make it possible to reduce the veiling luminance induced by cockpit displays when they are being operated by automatic legibility controls, as opposed to manually, are described in Section 8.7.

If the light sensor signal corresponding to the worst-case glare source exposure condition, measured at any given point in time in the cockpit, is applied simultaneously to the automatic legibility controls of all of the displays in the cockpit, then the display information portrayals would be perceived to have different legibilities. Furthermore, because this control technique causes most of the cockpit displays to operate at higher image difference luminance levels than those operated using the dedicated light sensor control technique, the cockpit displays would induce somewhat higher veiling luminance levels while the pilot is attempting to view external visual scenes. Based on the distributed glare source equation, described in Section 3.8, this increase in the induced veiling luminance can be approximated as being directly proportional to the increase in the image difference luminance levels of the cockpit displays. Consequently, the increase in the display induced veiling luminance over that due to the dedicated light sensor control technique would be quite small, and dependent on the pilot's line of sight with respect to the glare source, when the glare source is emitting light, and would be no different from the dedicated light sensor control technique when the glare source extinguishes.

According to the analyses of dark adaptation discussed earlier in this section, the increase in the veiling and reflected luminance levels in the night scene caused by the light emitted by the glare source, would usually be much larger than the veiling luminance induced by the automatic luminance control adjusted image difference luminance levels of the cockpit displays. It is concluded, therefore, that while the difference between the veiling luminances induced by the two control techniques would be quite small, both veiling luminances would be very nearly negligible in comparison to the veiling and reflected luminance levels perceived in a night scene when the glare source is active. Following the extinction of the glare source, the effect of the difference in these control techniques on the legibility of external night scenes, should be very nearly negligible if the aircrew was viewing the external scene during the glare source exposure, and should be negligible if the aircrew was viewing the cockpit displays during the exposures. The overall conclusion is that both techniques would produce very nearly equal aircrew night vision perception capabilities, both internal and external to the aircraft cockpit, with a slight advantage going to the displays operated by automatic legibility controls using the independent veiling luminance sensor signals, described earlier in this section.

8.3.6. Conclusions Regarding the Constraints Imposed by Aircrew Light and Dark Adaptation on the Legibility of Automatically Controlled Displays

To match the range of different dark adaptation recoveries experienced by aircrew members under night viewing conditions precisely, the implementation techniques described in Section 7.4, for controlling the daylight time responses of electronic displays operated by automatic legibility controls, would have to be modified at night to permit the time constants that control the transient response characteristics of the image difference luminance levels of the displays to be selectively changed. The implementation of this control technique would require a method of both measuring the light exposure history of the aircrew and assigning appropriate time constants for controlling the outputs of the automatic legibility controls that operates in near-real-time. In addition, and as described previously in Section 8.3.4.2, the quantitative relationships between the light exposure histories, experienced by aircrew members in an aircraft cockpit viewing environment at night, and their respective dark adaptation recovery time responses, which are needed to assign the correct time constants to control the image difference luminance decays of cockpit displays following a glare source exposure, are not presently available in the literature.

Although the preceding obstacles could pose a severe impediment to the implementation of automatic legibility controls that are effective during night missions, the analysis of dark adaptation recoveries in Section 8.3.4.2 shows that the magnitudes of the changes in the image difference luminance levels of cockpit displays, encountered while viewing cockpit displays at night, are insufficient to invoke light and dark adaptation responses by the aircrew. In other words, the adjustments made to the image difference luminance levels of

cockpit displays at night, whether the displays are under manual or automatic control, are not large enough to cause the aircrew to benefit from the implementation of automatic legibility controls using the precise treatment of response times described in the previous paragraph. Contrary to this result for the effects of light and dark adaptation with respect to the legibility of cockpit displays night, it was shown above that the glare source exposures experienced by aircrews, when viewing external night scenes, are sufficient to invoke light and dark adaptation responses by the aircrew. However, the resulting degradation in the legibilities of the night scenes being viewed by the aircrew cannot be altered or otherwise compensated by either manually or automatically controlling the image difference luminance levels settings of the cockpit displays.

Since the precise control technique, referred to in the preceding two paragraphs is not needed, and based on the light and dark adaptation response time findings previously described in Sections 8.3.3 and 8.3.4, it is concluded that no noticeable degradation to the legibility of the information presented on the cockpit displays or of the information contained in external night scenes should be incurred by using fixed rise and decay time constants to control the image difference luminance transient responses of cockpit displays. It is further concluded that this approximate approach for controlling the transient responses of cockpit displays operated using automatic legibility controls could be implemented by causing the image difference luminance levels of the displays to respond with a fixed rise time constant of 7.5 milliseconds (ms) or less and a fixed decay time constant of nominally ten seconds or less. The reasons for reaching these conclusions are described in greater detail below.

As previously described in Section 7.4, the preferred time response of cockpit displays under daylight viewing conditions is for the image difference luminance of the displays to track the increase in the outputs of the respective ambient illumination and veiling luminance sensors in real-time. This conclusion is also valid for displays operated under night viewing conditions. The reason this is true is because cockpit displays, operated by automatic legibility controls, that can respond in near-real-time, to the abrupt elevation of ambient illumination and veiling luminance levels caused by a glare source, would allow the image difference luminance to be rapidly increased to the levels needed to display the information being portrayed legibly, and, in so doing, reduce the time it takes for an aircrew member to read the information being presented on the displays accurately.

Since the time responses of practical electronic displays, their automatic legibility controls and their light sensors are not instantaneous, but, instead, involve time delays and exponential time responses, a need exists to explore the effect these response time constraints have on the legibility of displays operated by automatic legibility controls. The effects of these response time constraints will be considered first in the context of aircraft cockpit scenarios and then with respect to the legibility responses to be expected of pilots and other aircrew members when the image difference luminance levels of displayed information increases. The effect of the difference between the temporal responses of practical displays, and responses in real-time, is treated below for daylight and then night viewing conditions in the context of relevant aircraft cockpit scenarios, by making comparisons between manually controlled conventional and electronic displays and displays operated using automatic legibility controls. This discussion is followed by a description of published experimental data about the prediction of the temporal legibility responses to be expected from pilots and other aircrew members, due to different transient increases in the luminance levels of displayed information.

As described in Chapter 7, conventional reflective mode flight instruments do respond instantaneously, that is, in real-time, to changes in the illumination incident on their surfaces. During daylight flight maneuvers, the legibilities of conventional displays change (i.e., in effect are automatically adjusted) in real-time, in response to the movement of shadows and exposures to glare sources, although the changes do not necessarily result in improved legibility. For example, during a change in the attitude of an aircraft that causes the sun or a distributed source of glare to appear in a pilot's field of view, shadows would be likely to be cast on the instrument panel, while veiling luminance is concurrently being induced in the eyes by their exposure to the glare source. This viewing condition would produce a reduction in the legibility of the information displayed within the cockpit. By comparison, an electronic display controlled by an automatic legibility control under the same circumstances would respond by increasing the image difference luminance of the display to

compensate for the veiling luminance, but would not do so in real-time. The point of this example is that the delay in reaching the new legibility level, caused by the transient response of electronic displays, operated using automatic legibility controls, is associated with the time it takes to compensate the legibility of the automatically controlled electronic displays for the exposure to the glare source, a compensation that does not occur for conventional reflective operating mode displays and would occur for existing electronic displays that are manually controlled only after an adjustment of the image difference luminance of the displays by an aircrew member.

Alternatively, in a transition from shadows to a full sunlight ambient illumination exposure of both conventional and existing electronic displays that are manually controlled, the legibility of the conventional display would increase abruptly as the sunlight illuminates the display viewing surface whereas the legibility of an existing electronic display would be reduced and remain at the new level until its image difference luminance setting is manually increased. In this case, cockpit displays controlled by automatic legibility controls would experience a temporary legibility disadvantage, in comparison to the real-time response of a conventional reflective mode display, and a legibility advantage, in comparison to an electronic display using a manual luminance control to adjust its legibility.

At night, the legibility of conventional reflective mode displays is controlled by the settings of their integral lighting and the legibility of electronic displays is controlled by the image difference luminance levels they emit. In the absence of night glare sources, changes in the ambient illumination incident on cockpit displays, due to changes in the illuminance incident from the external night environment, for example, when maneuvering the aircraft, are too small to cause the luminances reflected by the displays to change by amounts that are sufficient to influence the legibility of either of these types of displays. This result is inferred from the image difference luminance requirements equation of Section 3.4 and the corresponding visual requirement characteristics of humans shown in the figures of Section 3.3. The result is based on the near constant image difference luminance level portions of the characteristics that are applicable when changes occur in the reflected background luminance levels of cockpit displays at night.

When a glare source is present at night, conventional and manually controlled electronic displays are not compensated for the changing levels of veiling luminance induced in the eyes, while making aircraft maneuvers or when a glare source activates or extinguishes, unless an aircrew member decides to make an adjustment. Under this circumstance, the fact that the automatic adjustments to the image difference luminance levels of cockpit displays, operated by automatic legibility controls, does not occur in real-time simply means that the increase in their image difference luminance level with respect to the luminances of their manually controlled conventional and electronic display counterparts is not immediate, but instead requires a small response time. Since a manual control adjustment of the legibility of conventional or manually controlled electronic displays would, as a minimum, involve typical aircrew response time delays of nominally 0.3 to 0.6 seconds, before the adjustments could begin, total response times of less than this amount by displays operated using automatic legibility controls would still provide a legibility advantage.

An improvement in legibility, caused by an increase in the image difference luminance level of displayed information, also depends on the human's perceptual response to the increase in the image difference luminance levels of the automatically controlled displays. According to the experimental test results of Graham and Kemp*, as described by Brown and Mueller, and presented in their Figure 9.3 of the book Vision and Visual Perception,[169] for an increase in the image difference luminance levels of information presented on a cockpit display to be perceived at the new higher image difference luminance level would require the aircrew to be exposed to the imagery for a minimum "critical duration, t_c," that becomes progressively shorter between approximately 100 ms, for an adapting luminance of 0.00173 fL, down to 30 ms, for an adapting luminance of 186 fL, before the imagery will be perceived at its new increased image difference luminance level. Shorter

---

* Graham, C. H. and E. H. Kemp, "Brightness Discrimination as a Function of the Duration of the increment in Intensity," Journal of General Psychology, Vol. 21, 1938, pp. 635-650.

exposure durations than the respective minimum critical durations, required to perceive the full increase in the image difference luminance, result in a proportionate reduction in the increase in image difference luminance perceived. Brown and Mueller noted that the preceding critical durations are also considered applicable, when the luminance levels of displayed information are reduced. To achieve a valid application of these human time response design criteria, the image difference luminance changes involved must be insufficient to cause a light or dark adaptation response by the light receptors in the eyes. As previously described, image difference luminance level increases of less than a multiple of nominally one hundred, that is, one grey scale perception range, would satisfy this requirement.

Brown and Mueller, as well as others, have attributed the preceding result to the human responding to the energy sensed by the eyes up to the critical exposure duration. The perceived image difference luminance, $\Delta L_P(t = t_c)$, at the end of this critical time interval can, therefore, be mathematically represented in terms of the initial constant perceived imaged difference luminance level, $\Delta L_P(t = 0)$, and the time dependent increase in the image difference luminance of the information presented on a display, $\delta L(t)$, by the following integral equation:

$$\Delta L_P(t = t_c) = \Delta L_P(t = 0) + \frac{1}{t_c}\int_0^{t_c} \delta L(t)\, dt, \tag{8.1}$$

where the second term on the right-hand side of this equation is the mean value of the luminance increase during the critical duration. The significance of this finding is that the human is unable to perceive the form of the luminance variations that occur during the critical duration, but instead responds to the time-averaged luminance increase over the critical duration interval. For example, if an immediate increase in luminance of magnitude δL is held and perceived for the critical duration, t_c, producing a product $\delta L\, t_c$, proportional to the increase in the light energy sensed, then at the end of the critical duration, a luminance increase equal to δL would be perceived. The same result would be obtained for one or more pulses of light, with proportionately reduced durations and increased amplitudes, provided only that their amplitudes and durations produce a time-averaged luminance increase of δL at the end of the critical duration, as calculated using Equation 8.1. The preceding interpretations of a human's perceptual response to being exposed to image difference luminance increases, having durations shorter than the critical duration, are confirmed by experiments reported in the literature.

Returning to the purpose of the present discussion, Equation 8.1 also allows predicting the perceptual effects of the response time limitations on the legibility responses of the pilot or other aircrew members viewing increases in the image difference luminance levels of information being presented on practical displays operated by automatic legibility controls. Used in this way, Equation 8.1 predicts, for example, that a linear increase in the image difference luminance of a display presentation to a value of δL, during the period from a time of zero to the critical duration, would result in an increase in luminance of 1/2 $\delta L(t)$ being perceived at $t = t_c$. To carry this example to observation times, t, that extend beyond the critical duration, t_c, the image difference luminance perceived at any point in time, t, would have to be expressed by the following more general equation:

$$\Delta L_P(t) = \Delta L_P(t = 0) + \frac{1}{t_c}\int_{t-t_c}^{t} \delta L(t)\, dt, \tag{8.2}$$

where the second term on the right-hand side of this equation is still the mean value of the luminance increase that occurs during the critical duration leading up to the time, t, when the perceived effect of the exposure to the display luminance increase is recognized. If it is assumed that the linear increase in the display image difference luminance becomes constant after reaching the value of δL, at an elapsed time, $t = t_c$, then Equation 8.2 shows that for the displayed information to be perceived at the final δL level, the luminance increase, $\delta L(t)$, would have to remain constant at the value of δL for, as a minimum, another critical duration while it is being perceived. Consequently, this assessment shows that the minimum elapsed time before the display imagery is perceived to have reached its full luminance after starting its linear increase at zero time would be

$t = 2\,t_c$, for this example. It should be noted that the relationships described here, for the critical durations of luminance exposures required to perceive an increase in luminance, are also applicable for absolute image difference luminance thresholds,[170] not just the relative changes in image difference luminance described in the last two paragraphs.

Because a change in the image difference luminance level of displayed information, which follows an exponential rise time characteristic, can be considered essentially complete after a period of four time constants, a display with the previously cited maximum rise time constant of 7.5 ms would cause the display to approach the new luminance control level in 30 ms, the critical duration previously cited as required for an aircrew member to respond fully to the new luminance level if adapted to a background luminance level of 186 fL. However, according to Equations 8.1 and 8.2, the aircrew members would actually perceive the change in the display luminance to be only 75% complete at 30 ms of exposure, 90% complete at 37.5 ms of exposure and would not perceive the full luminance change until more than a 60 ms exposure time had passed, due to the exponential rather than abrupt rise in the luminance of the display.

Although the preceding results show that the use of the shortest possible rise times for the image difference luminances of the displays would be preferable, even the rapid response times of pilots for continuous pursuit tasks would be unlikely to be influenced by displays having image difference luminance rise time constant of 7.5 ms and less. In closing this discussion, it should be noted that transient response characteristics designed to cause the image difference luminance of displays to overshoot the final intended increase in the image difference luminance level of information being displayed could be used to reduce the time needed to perceive the displayed information at the new luminance level, provided that the overshoot of the luminance transient and its return to the new luminance level is complete in less than the critical duration and is, therefore, not perceptible.

Although luminance decay time constants of less than ten seconds in duration should be acceptable under all day and many night viewing conditions, if the times required for an aircrew member to recovery dark adaptation were to be less than the display image difference luminance decays this would simply cause the information displayed to be more legible, for a short period, than it would otherwise be, were the image difference luminance levels of the cockpit display presentations to track the faster recovery of an aircrew member's dark adaptation exactly. From the perspective of the image difference luminance levels of the cockpit displays, acting as a preadapting light source, following the transition to view external night scenes, the information presented previously in this section allows a conclusion to be reached that a short-duration extension to the period of exposure to the glare-source-elevated levels of the image difference luminance levels of the cockpit displays, attributable to using an automatic legibility control with up to a 10 second luminance decay time at night, versus using manual control, should not noticeably affect the scotopic dark adaptation recovery of rod light receptors to the luminance levels of an external night scene.

Similarly, while viewing an external night scene, the short extension of the period of display induced veiling luminance exposure in the external night scene resulting from use of up to a 10 second time constant to control the transient recovery of the cockpit display image difference luminances to the levels they were at before the glare source exposure, should not noticeably affect the scotopic dark adaptation recovery of rod light receptors to the luminance levels of an external night scene. The reason for reaching this latter conclusion is that the veiling luminance induced by the cockpit displays would be very small in comparison to the veiling luminance induced by the night glare source and, consequently, the recovery of dark adaptation, following an exposure to a glare source at night would be dominated by the energy density exposure history that the rod light receptors have experienced, due either to their direct exposure to the glare source or to the product of the exposure time and the combined night scene reflected luminances and glare source induced veiling luminances.

After the dark adaptation recovery of an aircrew is complete, following a glare source exposure, veiling luminances induced by light emissions from either manually or automatically controlled cockpit displays are still induced in the eyes whenever the external night scene is being viewed. Because the veiling luminance

levels induced by the luminance level settings of cockpit displays, and the night scene scotopic luminance levels they are visually superimposed over, are of about the same order of magnitude, the result is that the induced veiling luminances and the scene luminances are a part of the same scotopic grey scale range. Consequently, the veiling luminance becomes an integral part of the night scene and, in so doing, creates a visual effect similar to that of fog or haze, that is, the veiling luminance simply reduces the legibility of the night scene imagery, rather than affecting the aircrew's scotopic dark adaptation. For veiling luminance or another source of light to raise the luminance threshold of fully scotopically adapted aircrew members, would probably require luminances within the mesopic range, or, as a minimum, greater than one grey scale range, that is, a factor of nominally more than one hundred, greater than the minimum scotopic luminance threshold level of the aircrew that permits extracting information from the external night scene.

Based on the preceding arguments it is concluded that whether cockpit displays are controlled manually or automatically, the veiling luminance they induce in the aircrew's eyes, while night scenes are being viewed, will not restrict the scotopic luminance level to which the aircrew can dark adapt nor increase the times involved in recovering dark adaptation following an exposure to a glare source at night. The ability to achieve full scotopic dark adaptation, in the presence of the veiling luminances induced by either manually or automatically controlled luminance emissions from cockpit display acting as glare sources, does not, however, alter the legibility degrading effect that the superposition of veiling luminances over a night scene has on the aircrew's ability to extract useful information from that scene.

As a final item, it should be noted that aircrew luminance control inputs, whether implemented using manual luminance controls or using the legibility trim controls associated with automatic legibility controls, should be designed to produce predictable display image difference luminance changes that closely track the control inputs being made by the aircrew members, as described in Section 7.3. In particular, responses to aircrew legibility control adjustments should not exhibit the rise and decay time constants described above, when the legibility of the displays is being controlled automatically. To instill confidence in an aircrew member that a manual luminance control or an automatic legibility trim control is working properly, it was concluded in Section 7.3 that the control should produce legibility changes in the information presented on cockpit displays that are both predictable and directly responsive to the inputs made by aircrew members.

8.4. Automatic Legibility Control Adjustment Strategy for Use with Existing Electronic Displays

Existing multipurpose electronic displays that are suitable for use in aircraft cockpit viewing conditions all share technology limitations that restrict the maximum image difference luminance capabilities of these displays. The effect of this limitation on the maximum image difference luminance a display can produce is to impose a constraint on the maximum picture contrasts that can be rendered on manually controlled displays, under worst-case daylight viewing conditions. In the event the same displays are operated using automatic legibility controls, the same maximum picture contrast and maximum image difference luminance limitations are encountered, but an additional effect of this limitation is to restrict the range of legibilities that can be portrayed at a constant legibility level. If the legibilities of the electronic display portrayals are to be maintained at a constant level throughout their incident illuminance and veiling luminance ranges by automatic legibility controls, it follows that these displays would have to be controlled so that they are never more legible than they are under their respective worst-case viewing conditions.

Using automatic legibility controls to adjust the legibilities of the information presented on existing aircraft cockpit electronic displays so that the legibilities remain constant at the maximum legibility levels achievable under worst case daylight viewing conditions, for all viewing conditions, would cause the pictures rendered by the displays to be judged as having inadequate grey shades and desaturated colors in lower daylight ambient illumination environments. Alternatively, holding the legibility of the displays constant, at or near the optimum legibility levels for the type of information being presented, in reduced daylight and night ambient illumination viewing conditions, and only allowing their legibility to degrade under worst case daylight viewing conditions, would cause the pictures rendered by the displays to be judged as having fully acceptable grey shades and

saturated colors, except under the worst-case viewing conditions. The optimum legibility results for this automatic legibility control strategy are essentially the same as those obtained under daylight viewing conditions, when pilots elect to set the electronic displays to operate at their maximum image difference luminance levels (see Section 5.4). The practical advantage of operating electronic displays, at the constant optimum automatic legibility control level, is that they are only operated at their maximum image difference luminance levels under the worst-case daylight viewing conditions. For the technologies used to implement existing aircraft cockpit electronic displays, the use of automatic legibility control would lead to a reduction in the required maintenance of the displays and to an extension of their operating lifetimes.

8.5. Importance of Using Automatic Legibility Controls from the Perspective of the Aircrew

The implementation of automatic legibility control is important from a user perspective for two reasons. The first reason is that the task of manually controlling the legibility's of electronic displays in a cockpit is an ancillary task for aircrew members, which only serves to detract from the limited time available for an aircrew member to perform direct mission related tasks, such as flying the aircraft, acquiring targets and so forth. Although the workload reduction benefits of implementing automatic legibility controls are most important in cockpits employing multiple electronic displays, the ability of aircrew members to preset the legibilities of cockpit displays to suit their personal preferences or needs, and afterwards to avoid the need for further legibility control inputs, would represent an important improvement over the current manual control approach to electronic display legibility control, even for a cockpit with only a single electronic display.

The second reason that implementing automatic legibility control is important from a user perspective is that it is only by this means that the legibility of displays can be held constant in changing ambient illumination and veiling luminance viewing conditions, while still being able to maintain the image difference luminance levels of information presented on the displays at minimum levels, consistent with satisfying an aircrew member's needs or preferences for legibility. As described in Section 7.2, whether a display is controlled manually, or automatically tracks the inputs from cockpit illuminance and veiling luminance light sensors, each display must be individually controlled under daylight viewing conditions, if the legibilities of all of the displays are to be initially set and then maintained at the same level. The need for continuous control stems from the fact that differing time dependent illuminances would typically be incident upon each individual electronic display location in the cockpit, thereby causing differences to develop over time in the legibilities of individual displays, even though they may, for example, be initially set to provide equal legibilities. Moreover, this is true even when all the electronic displays have the same display reflective properties, and therefore can be considered identical. The presence of a glare source, such as the sun in the pilot's field of view would produce similar differences in the legibilities of information presented on electronic displays installed at different locations in the cockpit, if the legibilities were not to be automatically controlled or, alternatively, manually compensated by the pilot, on a nearly continuous basis.

8.6. Strategy to Implement a Common Automatic Legibility Trim Control That Permits Aircrew Members to Adjust the Legibilities of Multiple Displays Concurrently

Because of the time changing nature of the differences in ambient illumination and veiling luminance exposure conditions experienced by aircrew members when reading information from displays installed at different locations in a cockpit, it can be concluded, based on the discussion of this subject in Sections 7.2 and 7.3, that maintaining constant legibility is not feasible if a common manual control is used to adjust the legibilities of multiple electronic displays concurrently. If other than equal legibility is acceptable, then a common manual control can be used by the pilot to make the display that is least legible, at any point in time, more legible and in so doing simultaneously increase the legibilities of the other displays as well. The primary limitation of this common manual control strategy is that the cockpit display locations, which experience the most severe legibility degradation, change over time, because of changes in the cockpit illumination and glare source exposure conditions. As a result, the latter strategy for using a common manual control makes further adjustments by the pilot a necessity to achieve and maintain the requisite display information legibility levels.

As previously described in Section 5.4, and as mentioned previously above, the historic control strategy adopted by military pilots to deal with the problem of controlling the legibility of electronic displays was to operate all electronic displays at their maximum image difference luminance levels and, therefore, at their maximum legibility, when flying under daylight ambient illumination conditions. This almost universal practice increases the need to perform maintenance on electronic displays and also reduces their useful life, but, from the perspective of freeing a pilot's time to perform primary tasks, and satisfying their visual requirements while performing a mission, it is quite satisfactory. Because of the inherent automatic legibility control capability of the human visual system, described in Section 5.3, manually setting the image difference luminance levels of electronic displays to their maximum levels, causes the grey shade or color rendition of the displayed information to be held at a nearly perceptually constant optimum level, which, in turn, allows a maximum enhancement of the interpretability of the information being portrayed to be achieved and maintained, in all but the worst-case ambient illumination and veiling luminance conditions. As previously noted, the principal advantage of using an automatic legibility control, over the manual maximum luminance setting control strategy, is that it can maintain the grey shade or color renditions of the information displayed on monochrome or color electronic displays, respectively, at constant optimal values in changing ambient illumination and veiling luminance conditions, while only operating the displays at their maximum image difference luminance output values when that is absolutely necessary.

Unlike the previously described constraints on achieving and maintaining equal legibilities on multiple cockpit displays, imposed when their image difference luminance controllers are directly connected to a single common manual control, equal legibility among multiple cockpit displays can be set, and, afterwards, automatically maintained, if a common legibility trim control signal is applied to each of the legibility trim control inputs of the dedicated automatic legibility controls used to operate the image difference luminance controllers of the individual displays. Furthermore, because each display is operated by its own individualized automatic legibility control, equal legibility is assured irrespective of the optical and physical properties of the types display being controlled. The interface of an input from a common legibility trim control with each of the individual display automatic legibility controls would be most readily accomplished by summing this control input with the aircrew legibility trim control inputs for individual displays, which were previously described in Section 5.5. Adding this common control input to each of the individual trim control settings inputs would not eliminate the need for individual display trim controls, but, once the legibility settings of the individual displays are adjusted to suit a particular aircrew member's preferences or needs, the common control input would allow the complement of display legibilities, initially set by the aircrew member, to thereafter be automatically maintained or, if necessary, trim adjusted in unison by the aircrew member to higher or lower values, using the single common control.

8.7. Overall Conclusions Regarding the Application of Automatic Legibility Control to All of the Displays in an Aircraft Cockpit

The automatic legibility control techniques described in this report are suitable for being applied not only to control the legibilities of electronic displays, but can also be used to permit simultaneous automatic control of the legibilities of displays of any type in an aircraft cockpit. Under dusk through night viewing conditions, this would, for example, include reflective operating mode flight control and engine instruments, and the light transflective operating mode integrally illuminated control panels and rotary switches used in conventionally equipped cockpits. It also includes all instances of light transmissive mode illuminated pushbutton switches, signal indicator light panels, and master caution and warning signal indicators, under both day and night viewing conditions.

The automatic control of the image difference luminance levels of conventional displays both reduce their maintenance requirements and, at night, also allow signal indicators and illuminated push button switches to be made more compatible with the aircrew's external dark adaptation requirements or with the use of night vision imaging systems in the cockpit.[171] As described in greater detail in Section 2.6.1, the greatest night vision performance benefits to be derived by aircrew members, from the application of automatic legibility

controls, would be derived from controlling the image difference luminance levels of illuminated pushbutton switches, signal indicator light panels, and master caution and warning indicators, at fixed luminance multipliers above the image difference luminance levels of the balance of the information displayed in the cockpit, which is not required to attract the attention of the aircrew.

The use of automatic legibility controls, to adjust the image difference luminance levels of the information depicted by conventional cockpit displays, allows the presentations on these displays, and, in particular, on the signal indicators and push button switches, to be continuously maintained at the minimum image difference luminance levels, set by the aircrew to achieve effective cockpit display information legibility and signal alerting capabilities. Operating these cockpit displays, as just described using automatic legibility controls, would also result in minimizing the veiling luminance induced by the image difference luminance level settings of cockpit displays, when a pilot or another aircrew member is viewing external night scenes, and, in particular, would reduce the veiling luminance induced by the light emissions from illuminated pushbutton switches and signal indicators. Moreover, operating cockpit displays in this way, using automatic legibility controls, would also reduce the interference to the operation of night vision imaging systems, caused by light emissions from the cockpit displays, and in particular those from signal indicators, as is described in greater detail in Chapter 2. The preceding advantages of applying automatic legibility control to all of the displays in a cockpit, rather than just to electronic displays, stems from the ability to maintain the overall night lighting levels in aircraft cockpits, continuously at the minimum levels required to provide satisfactory display legibility, for any particular time-variant combination of sensed night ambient illumination and veiling luminance viewing conditions.

LIST OF REFERENCES

1. Burnette, Keith T., An Evaluation of Aircraft CRT and Dot-Matrix Display Legibility Requirements, WL-TR-91-7020, Flight Dynamics Directorate, Wright Laboratory, Air Force Materiel Command, Wright-Patterson AFB, OH, June 1994, Appendix A, p. 49.

2. Burnette, Keith T., et al, Aviators Night Vision Imaging System (ANVIS) Compatible Interior Aircraft Lighting Specification, MIL-L-85762, Naval Air Engineering Center, Lakehurst, NJ, 03733, 24 January 1986 (Prepared requirements and tests for the legibility and readability of signals, monochrome and multicolor electronic displays).

3. Burnette, Keith T., et al, Night Vision Imaging System (NVIS) Compatible Interior Aircraft Lighting Specification, MIL-L-85762A, Naval Air Engineering Center, Lakehurst, NJ, 03733, 26 August 1988 (Contributions to Revision A concerning electronic and electrooptical displays).

4. Burnette, Keith T. and Donald C. Price, Modern Display Technologies and Applications, AGARD Advisory Report No. 169, NATO Advisory Group for Aerospace Research and Development (AGARD), 7 Rue Ancelle 92200 Neuilly Sur Seine, France, October 1982, pp. 112-134.

5. Burnette, Keith T. and Donald C. Price, "Light Emitting Diode Displays", Chapter 6 of Part II, Technologies, in Display Engineering , Conditioning, Technologies, Applications, Edited by D. Bosman, Elsevier Science Publishers B.V. (North-Holland), Amsterdam, The Netherlands, 1989, pp. 251-276.

6. Burnette, Keith T., A. J. Moffat and P. G. Wareberg, "Multi-Mode Matrix (MMM) Modular Flight Display Development", Proceedings of the Society for Information Display, Vol. 21, No. 2, 1980, pp. 143-156.

7. Burnette, Keith T., James A. Uphaus, and Timothy P. Barry, "Flight Simulator Evaluation of a High Speed Graphics Dot-Matrix Display While Portraying Primary Flight Control Information", Proceedings of the IEEE 1983 National Aerospace and Electronics Conference, Vol. 1, Dayton, OH, May 1983, pp. 375-388.

8. Griffith, Paul W., Percy J. Gros, Jr. and James A. Uphaus, Jr., "Evaluation of Pilot Performance and Workload as a Function of Input Data Rate and Update Frame Rate on a Dot-Matrix Graphics Display," Proceedings of the IEEE 1984 National Aerospace and Electronics Conference, Vol. 2, Dayton, OH, May 1984, pp. 988-995.

9. Burnette, Keith T., Color Aircraft Display Compatibility with the Night Vision Imaging System, WL-TR-95-3028, Flight Dynamics Directorate, Wright Laboratory, Air Force Materiel Command, Wright-Patterson AFB, OH, November 1994, pp. 112-129.

10. Sternberg, Saul, "Memory Scanning: Mental Processes Revealed By Reaction-Time Experiments," American Scientist. Vol. 57, No. 14, 1969, pp. 421-457.

11. Semple, C. A., R. J. Heapy, E. J. Conway and K. T. Burnette, Analysis of Human Factors Data for Electronic Flight Display Systems, AFFDL-TR-70-174, DDC-AD# 884 770, Air Force Flight Dynamics Laboratory, Wright-Patterson AFB, OH, April 1971, 570 pages, 397 references.

12. Burnette, Keith T., "The Status of Human Perceptual Characteristic Data for Electronic Flight Display Design", North Atlantic Treaty Organization Advisory Group for Aerospace Research and Development Conference Proceedings No. 96 on Guidance and Control Displays, AGARD-CP-96, Paris, France, 19-21 October 1971, pp. 1-1 to 1-10.

13. Burnette, Keith T., Seminar on Human Factors in Information Display Data, Sponsored by the Polytechnic Institute of Brooklyn in conjunction with the May 1973 Society for Information Display International Symposium, New York, NY, May 1973.

14. Burnette, Keith T., "The Impact of Human Factors Data on Control Display Design", 1973 SID International Symposium Digest of Technical Papers, Volume IV, Lewis Winner, New York, NY, May 1973, pp. 168-169.

15. Burnette, Keith T., Technology Assessment Display Evaluation Criteria Variables, AFFDL-TM-76-88-FGR, Air Force Flight Dynamics Laboratory, Wright-Patterson AFB, OH, January 1974, 17 pages.

16. Jainski, P., Einflub der Blendung auf das Erkennen elektronischer Anzeigen in Kanzeln moderner Hochleistungsfluqzeuge, Die Untersuchungen wurden im Rahmen eines Forschungsvertrages des Bundesministers der Verteidigung T II 3, Az.: 71-07-00-(02) mit dem Kennzeichen T-808-I-203 durchgefuhrt, Bonn-Duisdorf, 1969.

17. King, Robert C., Robert W. Wollentin, Clarence A. Semple, Jr., and Gary Gottelmann, Electroluminescent Display Legibility Research and Development, AFFDL-TR-70-89, Air Force Flight Dynamics Laboratory, Wright-Patterson AFB, OH, August 1970, 119 pages.

18. Bitterman, M.E., and J. Krauskopf, Some Determinants of Threshold for Visual Form, WADC-TR-53-311, Aero Medical Laboratory, Wright-Patterson AFB, OH, September 1953.

19. Blackwell, H. Richard, "Contrast Thresholds of the Human Eye", Journal of the Optical Society of America, Vol. 36, No. 11, November 1946, pp. 624-643.

20. Aulhorn, E. and H. Harms, "Untersuchengen Uber Des Grenzkontrastes Bericht", d. Deutschen Ophthalmologischen Gesellschaft, 1956, pp. 60-67.

21. Shurtleff, D.A., M. Marsetta, and D. Showman, Studies of Display Symbol Legibility, IX: The Effects or Resolution, Size and Viewing Angle of Legibility, ESD-TR-65-137, DDC-AD# 633 833, Electronic Systems Division, Hanscom Field, MA, May 1966.

22. Howell, W. C., and D. L. Kraft, Size, Blur and Contrast as Variables Affecting the Legibility of Alphanumeric Symbols on Radar-Type Displays, TR-59-536, DDC-AD# 232 889, Air Force Aerospace Medical Laboratory, Wright Patterson AFB, OH, September 1959.

23. Bowen, H. M., J. Andreassi, S. Traux, and J. Orlansky, Optimum Symbols for Radar Displays, Office of Naval Research Contract Number 2682(00), DDC-AD# 227 014, Office of Naval Research, Washington, D.C., September 1959.

24. Steedman, W. C., and C. A. Baker, Target Size and Visual Recognition, WADC-TR-60-93, DDC-AD# 235 129, Air Force Aerospace Medical Laboratory, Wright-Patterson AFB, Ohio, February 1960.

25. Burnette, Keith T., "Multi-Mode Matrix (MMM) Display Design and Measurement Criteria", Proceedings of the Society for Information Display, Vol. 21, No. 2, 1980, pp. 127-142.

26. Aulhorn, E. and H. Harms, "Untersuchengen Uber Des Grenzkontrastes Bericht", d. Deutschen Ophthalmologischen Gesellschaft, 1956, pp. 60-67.

27. Moon, P., and D. E. Spencer, "Visual Data Applied To Lighting Design," Journal of the Optical Society of America, Vol. 34, No. 10, 1944, pp. 605-617.

28. Burnette, Keith T., "The Status of Human Perceptual Characteristics Data for Electronic Flight Display Design", North Atlantic Treaty Organization Advisory Group for Aerospace Research and Development Conference Proceedings No. 96 on Guidance and Control Displays, AGARD-CP-96, Paris, France, 19-21 October 1971, pp. 1-1 to 1-10.

29. Chapanis, A., How We See; A Summary of the Basic Principles, NAVTRADEVCEN 166-I-85, DDC-AD# 204 769, U.S. Naval Training Device Center, Port Washington, NY, 1949.

30. Carel, W. L., Pictorial Displays for Flight, Office of Naval Research Contract Number NONR 4468(00), DDC-AD# 673 669, Office of Naval Research, Washington, D.C., December 1965.

31. Kelley, C. R., J. M. Ketchel, and P. H. Strudwick, Experimental Evaluation of Head-Up Display High Brightness Requirements, HFR 9765-1, DDC-AD# 626 657, Kaiser Aerospace and Electronics Plant, Palo Alto, CA, November 1965.

32. Chapanis, A., op. cit.

33. Carel, W. L., Pictorial Displays for Flight, Office of Naval Research Contract Number NONR 4468(00), DDC-AD# 673 669, Office of Naval Research, Washington D.C., December 1965, p. 109.

34. Semple, C. A., R. J. Heapy, E. J. Conway and K. T. Burnette, Analysis of Human Factors Data for Electronic Flight Display Systems, AFFDL-TR-70-174, DDC-AD# 884 770, Air Force Flight Dynamics Laboratory, Wright-Patterson AFB, OH, April 1971, p. 261.

35. Burnette, Keith T., "The Effects of Glare on Display Image Luminance Requirements", Interim Summary Report of Display Working Group Joint DARCOM/NMC/AFLC/AFSC Panel on the Field of Night Vision Technology, AMRL-TR-79-101, Air Force Aerospace Medical Research Laboratory, Wright-Patterson AFB, OH, October 1979, pp. 191-218.

36. Jainski, P., Prof. Dr.-Ing, The Effect of Dazzle on Electronic Display Visibility in Modern High-Performance Aircraft Cockpits. A Summary, Translator: Dr. Norris, Translation Editor: Dr. Huddleston, DDC-AD# 888 701, Royal Aircraft Establishment Library Translation No. 1545, Ministry of Aviation Supply, Farnborough, Hants, England, March 1971.

37. Aulhorn, E. and H. Harms, "Untersuchengen Uber Des Grenzkontrastes Bericht", d. Deutschen Ophthalmologischen Gesellschaft, 1956, pp. 60-67.

38. Blackwell, H. R., "Contrast Thresholds of the Human Eye", Journal of the Optical Society of America, Vol. 36, No. 11, 1946, pp. 624-643.

39. Ibid, pp. 627-629.

40. Carel, W. L., op. cit., p. 107.

41. Ibid, p. 111.

42. DeBruine, C. J., and J. R. Milligan, In-Flight Test Results on Mission-Oriented Cockpit Lighting Requirements, AFFDL-TR-71-142, Air Force Flight Dynamics Laboratory, Wright-Patterson AFB, OH, September 1971, 137 pages.

43. Burnette, Keith T., An Evaluation of Aircraft CRT and Dot-Matrix Display Legibility Requirements, WL-TR-91-7020, Flight Dynamics Directorate, Wright Laboratory, Air Materiel Command, Wright-Patterson AFB, OH, 45433-7562, June 1994, 73 pages.

44. Jainski, P., Einflub der Blendung auf das Erkennen elektronischer Anzeigen in Kanzeln moderner Hochleistungsflugzeuge, Die Untersuchungen wurden im Rahmen eines Forschungsvertrages des Bundesministers der Verteidigung T II 3, Az.: 71-07-00-(02) mit dem Kennzeichen T-808-I-203 durchgefuhrt, Bonn-Duisdorf, 1969.

45. Holladay, L. L., "The Fundamentals of Glare and Visibility," Journal of the Optical Society of America, Vol. 12, No. 4, April 1926, pp. 271-319.

46. Sweet, A. J., "An Analysis of Illumination Requirements in Street Lighting," Journal of the Franklin Institute, Vol. 169, 1910, pp. 359-384.

47. Holladay, L. L., "The Fundamentals of Glare and Visibility," Journal of the Optical Society of America, Vol. 12, No. 4, April 1926, pp. 271-319.

48. Nowakowski, B. A., "The Measurement of Glare", American Journal of Hygiene, Vol. 6, No. 1, January 1926, pp. 1-31.

49. Stiles, W. S., "The Effect of Glare on the Brightness Difference Threshold", Proceedings of the Royal Society of London, Vol. 104B, Issue 731, 4 March 1929, pp. 322-351.

50. Crawford, B. H., "Integration of the Glare Effects from a Number of Glare Sources," Proceedings of the Physical Society, Vol. 48, 1936, pp. 35-37.

51. Fry, Glenn A. and Mathew Alpern, "The Effect of a Peripheral Glare Source Upon the Apparent Brightness of an Object", Journal of the Optical Society of America, Vol. 43, No. 3, March 1953, pp. 189-195.

52. Moon, P. and D. E. Spencer, "Visual Data Applied to Lighting Design", Journal of the Optical Society of America, Vol. 34, No. 10, 1944, pp. 605-617.

53. Ireland, F. H., W. Kinslow, E. Levin, and D. Page, Experimental Study of the Effects of Surround Brightness and Size on Visual Performance, AMRL-TR-67-102, DDC-AD# 666 045, Air Force Aerospace Medical Research Laboratories, Wright-Patterson AFB, Ohio, September 1967.

54. Hartmann, Erwin, "Die Schwelle der Physiologischen Blendng," (Threshold for Physiological Glare), Lichttechnik, Vol. 15, No. 10, 1963, pp. 503-505.

55. Jainski, P., Einflub der Blendung auf das Erkennen elektonischer Anzeigen in Kanzeln moderner Hochleistungsflugzeuge, Die Untersuchungen wurden im Rahmen eines Forschungsvertranges des Bundesministers der Verteidigung T II 3, Az.: 71-07-00-(02) mit dem Kennzeichen T-808-II-203 durchgefuhrt, Bonn-Duisdorf, 1969.

56. Ibid., Equation 6a, p. 140.

57. Holladay, L. L., "Action of a Light Source in the Field of View in Lowering Visibility," Journal of the Optical Society of America, Vol. 14, No. 1, January 1927, pp. 1-15.

58. Stiles, W. S., op. cit., pp. 322-351.

59. Fry, Glenn A., "A Re-Evaluation of the Scattering Theory of Glare," Illuminating Engineering, February 1954, pp. 98-102.

60. Fry, Glenn A. and Mathew Alpern, "The Effect of a Peripheral Glare Source Upon the Apparent Brightness of an Object," Journal of the Optical Society of America, Vol. 43, No. 3, March 1953, pp. 189-195.

61. Nowakowski, Brunon A., "The Measurement of Glare," American Journal of Hygiene, Vol. 6, No. 1, January 1926, pp. 1-31.

62. Ibid., p. 20.

63. Holladay, L. L., "The Fundamentals of Glare and Visibility," Journal of the Optical Society of America, Vol. 12, No. 4, April 1926, pp. 271-319.

64. Stiles, W. S., "The Effect of Glare on the Brightness Difference Threshold," Proceedings of the Royal Society of London, Vol. 104B, Issue 731, 4 March 1929, pp. 322-351.

65. Fry, Glenn A. and Mathew Alpern, op. cit., pp. 189-195.

66. Ireland, Fred H., Effect of Surround Illumination on Visual Performance, AMRL-TR-67-103, DDC# AD 822 012, Air Force Aerospace Medical Research Laboratory, Wright-Patterson AFB, OH, July 1967.

67. Crawford, B. H., "The Change of Visual Sensitivity with Time," Proceedings of the Royal Society of London, Vol. 123B, Issue 830, 15 June 1937, pp. 69-89.

68. Fry, Glenn A. and Mathew Alpern, op. cit., pp. 189-195.

69. Stiles, W. S., op. cit., pp. 322-351.

70. Sweet, Arthur J., "An Analysis of Illumination Requirements in Street Lighting," Journal of the Franklin Institute, Vol. 169, 1910, pp. 359-384.

71. Nowakowski, Brunon A., op. cit., pp. 1-31.

72. Stiles, W. S., op. cit., pp. 322-351.

73. Nowakowski, Brunon A., op. cit., pp. 1-31.

74. Holladay, L. L., op. cit., pp. 295-298.

75. Jainski, P., Einflub der Blendung auf das Erkennen elektonischer Anzeigen in Kanzeln moderner Hochleistungsflugzeuge, Die Untersuchungen wurden im Rahmen eines Forschungsvertranges des Bundesministers der Verteidigung T II 3, Az.: 71-07-00-(02) mit dem Kennzeichen T-808-II-203 durchgefuhrt, Bonn-Duisdorf, 1969.

76. Holladay, L. L., "Action of a Light Source in the Field of View in Lowering Visibility," Journal of the Optical Society of America, Vol. 14, No. 1, January 1927, pp. 1-15.

77. Luckiesch, B. A., and L. L. Holladay, "Glare and Visibility," Transactions of the Illuminating Engineering Society, Vol. 20, March 1925, pp. 221-258.

78. Riggs, Lorrin A., "Visual Acuity," Chapter 11 in Vision and Visual Perception, Edited by Clarence H. Graham, John Wiley & Sons, Inc., New York, NY, 1965, p. 331.

79. Wyszecki, Gunter and W. S. Stiles, Color Science, John Wiley & Sons, Inc., New York, NY, 1967, p. 213.

80. Crawford, B. H., "The Dependence of Pupil Size upon External Stimuli under Static and Variable Conditions," Proceedings of the Royal Society of London, V121B, 1936, pp. 376-395.

81. Wyszecki, Gunter and W. S. Stiles, op. cit., p. 213.

82. Holladay, L. L., "The Fundamentals of Glare and Visibility," Journal of the Optical Society of America, Vol. 12, No. 4, April 1926, pp. 295-298.

83. Ireland, Fred H., Effect of Surround Illumination on Visual Performance, AMRL-TR-67-103, DDC-AD# 822 012, Air Force Aerospace Medical Research Laboratory, Wright-Patterson AFB, OH, July 1967.

84. Holladay, L. L., op. cit., p. 293.

85. Ibid., p. 296.

86. Fry, Glenn A. and Mathew Alpern, "The Effect of a Peripheral Glare Source Upon the Apparent Brightness of an Object," Journal of the Optical Society of America, Vol. 43, No. 3, March 1953, p. 189.

87. Ibid., p. 189.

88. Holladay, L. L., op. cit., p. 298.

89. Stiles, W. S. and B. H. Crawford, "The Luminous Efficiency of Rays Entering the Eye Pupil at Different Points," Proceedings of the Royal Society of London, Vol. 112B, 1933, pp. 428-450.

90. Riggs, Lorrin A., "Light as a Stimulus of Vision," Chapter 1 in Vision and Visual Perception, Edited by Clarence H. Graham, John Wiley & Sons, Inc., New York, NY, 1965, p. 12.

91. Luckiesch, B. A., and L. L. Holladay, "Glare and Visibility," Transactions of the Illuminating Engineering Society, Vol. 20, March 1925, pp. 221-258.

92. Holladay, L. L., "The Fundamentals of Glare and Visibility," Journal of the Optical Society of America, Vol. 12, No. 4, April 1926, pp. 295-298.

93. Holladay, L. L., "Action of a Light Source in the Field of View in Lowering Visibility," Journal of the Optical Society of America, Vol. 14, No. 1, January 1927, pp. 1-15.

94. Stiles, W. S., "The Effect of Glare on the Brightness Difference Threshold," Proceedings of the Royal Society of London, Vol. 104B, Issue 731, 4 March 1929, pp. 322-351.

95. Crawford, B. H., "The Integration of the Glare Effects from a Number of Glare Sources," Proceedings of the Physical Society, Vol. 48, 1936, pp. 35-37.

96. Fry, Glenn A. and Mathew Alpern, "The Effect of a Peripheral Glare Source Upon the Apparent Brightness of an Object," Journal of the Optical Society of America, Vol. 43, No. 3, March 1953, pp. 189-195.

97. Blackwell, H. Richard, "Contrast Thresholds of the Human Eye", Journal of the Optical Society of America, Vol. 36, No. 11, November 1946, p.641.

98. Judd, Deane B., "Basic Correlates of the Visual Stimulus," Chapter 22 in Handbook of Experimental Psychology, Edited by S. S. Stevens, John Wiley and Sons, Inc., New York, NY, 1951 (Seventh printing, February 1965), p. 811.

99. Bartlett, N. R., "Thresholds as Dependent on Some Energy Relations and Characteristics of the Subject," Chapter 7 in Vision and Visual Perception, Edited by Clarence H. Graham, John Wiley and Sons, Inc., New York, NY, 1965 (Second printing, October 1966), pp. 158-159.

100. Judd, Deane B., op. cit., pp. 811-820.

101. Wyszecki, Gunter and W. S. Stiles, Color Science, John Wiley & Sons, Inc., New York, NY, 1967, Table 3.3, p. 239-252.

102. Judd, Deane B., op. cit., pp. 818-820.

103. Wyszecki, Gunter and W. S. Stiles, op. cit., p. 279.

104. Ibid., Table 2.1, p. 383.

105. Bartlett, N. R., op. cit., p. 161.

106. Graham, C. H., "Discriminations that Depend on Wavelength," Chapter 12 in Vision and Visual Perception, Edited by Clarence H. Graham, John Wiley and Sons, Inc., New York, NY, 1965 (Second printing, October 1966), p. 356.

107. Graham, C. H., op. cit., p. 356.

108. Graham, C. H., op. cit., p. 355.

109. Bartlett, N. R., "Dark Adaptation and Light Adaptation," Chapter 8 in Vision and Visual Perception, Edited by Clarence H. Graham, John Wiley and Sons, Inc., New York, NY, 1965 (Second printing, October 1966), p. 195.

110. Brown, John Lott, "The Structure of the Visual System," Chapter 2 in Vision and Visual Perception, Edited by Clarence H. Graham, John Wiley & Sons, Inc., New York, 1965 (Second printing, October 1966), p. 49.

111. Wyszecki, Gunter and W. S. Stiles, Color Science, John Wiley & Sons, Inc., New York, NY, 1967, Table 2.1, p. 205.

112. Ibid., Table 2.1, p. 205.

113. Brown, John Lott, op. cit., p. 47.

114. Brown, John Lott, op. cit., p. 51.

115. Brown, John Lott, op. cit., p. 51.

116. Judd, Deane B., "Basic Correlates of the Visual Stimulus," Chapter 22 of Handbook of Experimental Psychology, Edited by S. S. Stevens, John Wiley and Sons, Inc., New York, NY, 1951 (Seventh printing, February 1965), p. 812.

117. Schade, Otto H., "Optical and Photoelectric Analog of the Eye," Journal of the Optical Society of America, Vol. 46, No. 9, September 1956, pp. 721-739.

118. Ibid, p. 724.

119. De Palma, J. J. and E. M. Lowery, "Sine-Wave Response of the Visual System, II, Sine-Wave and Square-Wave Contrast Sensitivity," Journal of the Optical Society of America, Vol. 52, No. 3, March 1962, pp. 328-335.

120. Campbell, F. W. and D. G. Green, "Optical and Retinal Factors Affecting Visual Resolution," Journal of Physiology, Vol. 181, 1965, pp. 576-593.

121. Campbell, F. W. and R. W. Gubisch, "Optical Quality of the Human Eye," Journal of Physiology, Vol. 186, 1966, pp. 558-578.

122. Shannon, C. E., "Communications in the Presence of Noise," Proceedings of the IRE, Vol. 37, January, 1949, p. 11.

123. Bumette, Keith T., "Multi-Mode Matrix (MMM) Display Design and Measurement Criteria," Proceedings of the Society for Information Display, Vol. 21, No. 2, 1980, pp. 140-141.

124. Ginsburg, Arthur, P., "Specifying Relevant Spatial Information for Image Evaluation and Display Design: An Explanation of How We See Certain Objects," Proceedings of the Society for Information Display, Vol. 21, No. 3, 1980, pp. 219-227.

125. Ginsburg, Arthur, P., Proposed New Vision Standards for the 1980's and Beyond: Contrast Sensitivity, AFAMRL-TR-80-121, Air Force Aeromedical Research Laboratory, Wright-Patterson AFB, OH, September 1981, 25 pages.

126. Bartley, Howard S., "The Psychophysiology of Vision," Chapter 24 in Handbook of Experimental Psychology, Edited by S. S. Stevens, John Wiley & Sons, Inc. New York, NY, 1951 (Seventh Printing, 1965), p. 947.

127. Bartlett, N. R., "Dark Adaptation and Light Adaptation," Chapter 8 in Vision and Visual Perception, Edited by Clarence H. Graham, John Wiley & Sons, Inc., New York, 1965, pp. 193-195.

128. Bartlett, N. R., "Thresholds as Dependent on Some Energy Relations and Characteristics of the Subject," Chapter 7 in Vision and Visual Perception, Edited by Clarence H. Graham, John Wiley & Sons, Inc., New York, 1965, p. 161.

129. Crawford, B. H., "The Dependence of Pupil Size upon External Stimuli under Static and Variable Conditions," Proceedings of the Royal Society of London, Vol. 121B, 1936, p. 377.

130. Riggs, Lorrin A., "Light as a Stimulus of Vision," Chapter 1 in Vision and Visual Perception, Edited by Clarence H. Graham, John Wiley & Sons, Inc., New York, 1965, p. 13.

131. Luckiesch, M. and L. L. Holladay, "Glare and Visibility," Transactions of the Illuminating Engineering Society, Vol. 20, March 1925, pp. 221-258.

132. Nowakowski, B. A., "The Measurement of Glare," American Journal of Hygiene, Vol. 6, No. 1, January 1946, pp. 1-31.

133. Holladay, L. L., "The Fundamentals of Glare and Visibility," Journal of the Optical Society of America, Vol. 12, No. 4, April 1926, pp. 271-319.

134. Crawford, B. H., "The Integration of the Glare Effects from a Number of Glare Sources," Proceedings of the Physical Society, Vol. 48, 1936, pp. 35-37.

135. Hartmann, E., "Die Schwelle der Physiologischen Blendng," ("Threshold for Physiological Glare"), Lichttechnik, Vol. 15, No. 10, 1963, pp. 503-505.

136. Luckiesch, M. and L. L. Holladay, "Glare and Visibility," Transactions of the Illuminating Engineering Society, Vol. 20, March, 1925, pp. 221-258.

137. Holladay, L. L., "The Fundamentals of Glare and Visibility," Journal of the Optical Society of America, Vol. 12, No. 4, April 1926, p. 291.

138. Davadov, A. S., Quantum Mechanics, Pergamon Press, Addison-Wesley Publishing Company, Inc., Reading, MA, 1965, Appendix A, pp. 654-657.

139. Schwartz, Ralph J. and Bernard Friedland, Linear Systems, McGraw-Hill Book Company, New York, NY, 1965, Chapter 3.

140. Burnette, Keith T., An Evaluation of Aircraft CRT and Dot-Matrix Display Legibility Requirements, WL-TR-91-7020, Flight Dynamics Directorate, Wright Laboratory, Air Force Materiel Command, Wright-Patterson AFB, OH, June 1994, 73 pages (Originally documented in a Bunker Ramo Corporation Report, Document# 4506-020-2506-11, Contract F33615-78-C-3614, 12 June 1980).

141. Burnette, Keith T., "Electronic Display Luminance and Grey Scale Control," Proceedings of the IEEE 1985 National Aerospace and Electronics Conference, Dayton, OH, 20-24 May 1985, pp. 1500-1510.

142. Burington, Richard S., Handbook of Mathematical Tables and Formulas, Handbook Publishers, Inc. Sandusky, Ohio, 1948, Table XXVb Probability Functions, pp. 272-276.

143. DeBruine, C. J., and J. R. Milligan, In-Flight Test Results on Mission-Oriented Cockpit Lighting Requirements, AFFDL-TR-71-142, Air Force Flight Dynamics Laboratory, Wright-Patterson AFB, OH., September 1971, 137 pages.

144. Merrifield, Robin and Louis D. Silverstein, "The ABC's of Automatic Brightness Control," Society for Information Display International Symposium Digest of Technical Papers, 1988, pp. 178-181.

145. Burnette, Keith T., "The Status of Human Perceptual Characteristic Data for Electronic Flight Display Design", North Atlantic Treaty Organization Advisory Group for Aerospace Research and Development Conference Proceedings No. 96 on Guidance and Control Displays, AGARD-CP-96, Paris, France, 19-21 October 1971, pp. 1-1 to 1-10.

146. Merrifield, Robin and Louis D. Silverstein, "The ABC's of Automatic Brightness Control," Society for Information Display International Symposium Digest of Technical Papers, 1988, p. 181.

147. Burnette, Keith T., "The Effects of Glare on Display Image Luminance Requirements", Interim Summary Report of Display Working Group Joint DARCOM /NMC/AFLC/AFSC Panel on the Field of Night Vision Technology, AMRL-TR-79-101, Air Force Aerospace Medical Research Laboratory, Wright-Patterson AFB, OH, October 1979, pp. 191-218.

148. Carel, W. L., Pictorial Displays for Flight, Office of Naval Research Contract Number NONR 4468(00), DDC-AD # 637 669, Office of Naval Research, Washington, D.C., December 1965.

149. Semple, Jr., C.A., R.J. Heapy, E.J. Conway, Jr., and K.T. Burnette, Analysis of Human Factors Data for Electronic Flight Display Systems, AFFDL-TR-70-174, DDC-AD # 884 770, Air Force Flight Dynamics Laboratory, Wright-Patterson AFB, OH, April 1971, Figure 199, p. 478.

150. Bartlett, George W., Editor, National Association of Broadcasters Engineering Handbook, National Association of Broadcasters, Washington, D.C., 1975, p. 639.

151. Munsell, A. H., A Color Notation, Munsell Color, Macbeth, A Division of Kollmorgen Corporation, Baltimore, MD, 1979.

152. Munsell, A. E. O., L. L. Sloan and I. H. Godlove, "Neutral Value Scales I, Munsell Neutral Value Scale," Journal of the Optical Society of America, Vol. 23, November 1933, pp. 394-411.

153. Newhall, S. M., D. Nickerson and D. B. Judd, "Final Report of the Optical Society of America Subcommittee on Spacing of the Munsell Colors," Journal of the Optical Society of America, Vol. 33, No. 7, July 1943, p. 385-418.

154. Burnette, Keith T., Dot-Matrix Video Display Design Criteria and Test Results, Volume I, Luminance Control and Grey Scale Requirements, Air Force Flight Dynamics Laboratory, Wright-Patterson AFB, OH, 16 November 1984, 112 pages.

155. Burnette, Keith T., "Electronic Display Luminance and Grey Scale Control," Proceedings of the IEEE 1985 National Aerospace and Electronics Conference, Dayton, OH, May 1985, pp. 1500-1510.

156. Burnette, Keith T., "Multi-Color Display Design Criteria", Proceedings of the IEEE 1984 National Aerospace and Electronics Conference, Dayton, OH, May 1984, pp. 1348-1363.

157. Silverstein, Louis D., Robin M. Silverstein, and Fredrick C. Hoerner, "A Systematic Program for the Development and Evaluation of Airborne Color Display Systems," Sixth Advanced Aircrew Display Symposium, Naval Air Test Center, Patuxent River, Maryland, 15-16 May 1984, p. 22.

158. Loughlin, Bernard D. "Nonlinear Amplitude Relations and Gamma Correction," in Color Television, Edited by Ted Rzeszewsi, IEEE Press Selected Reprint Series, John Wiley & Sons, Inc. New York, NY, 1983, pp. 63-91. Originally published in Chapter 11 of Principles of Color Television, Edited by K.McIlwain and C. Dean, Wiley, New York, NY, 1956, pp. 200-256.

159. Rogers, J. C. and W. L. Carel, Development of Design Criteria for Sensor Displays, Joint Army-Navy Aircraft Instrumentation Research (JANAIR) Annual Report, Contract No. N00014-72-C-0415, NR 213-107, Office of Naval Research, Arlington, VA, December 1972, 115 pages.

160. Burnette, Keith T., Dot-Matrix Video Display Design Criteria and Test Results, Volume I, Luminance Control and Grey Scale Requirements, Air Force Flight Dynamics Laboratory, Wright-Patterson AFB, OH, 16 November 1984, 112 pages.

161. Burnette, Keith T., "Electronic Display Luminance and Grey Scale Control," Proceedings of the IEEE 1985 National Aerospace and Electronics Conference, Dayton, OH, 20-24 May 1985, pp. 1505-1507.

162. DeBruine, C. J., and J. R. Milligan, In-Flight Test Results on Mission-Oriented Cockpit Lighting Requirements, AFFDL-TR-71-142, Air Force Flight Dynamics Laboratory, Wright-Patterson AFB, OH, September, 1971, 137 pages.

163. Semple, C. A., R. J. Heapy, E. J. Conway and K. T. Burnette, Analysis of Human Factors Data for Electronic Flight Display Systems, AFFDL-TR-70-174, DDC-AD# 884 770, Air Force Flight Dynamics Laboratory, Wright-Patterson AFB, OH, April 1971, pp. 268-270.

164. Ibid., pp. 267-268.

165. Bartlett, N. R., "Dark Adaptation and Light Adaptation," Chapter 8 of Vision and Visual Perception, Edited by Clarence H. Graham, John Wiley and Sons, Inc., New York, NY, 1965 (Second Printing, October, 1966), pp. 185-207.

166. Bartley, Howard S., "The Psychophysiology of Vision," Chapter 24 of Handbook of Experimental Psychology, Edited by S. S. Stevens, John Wiley and Sons, Inc., New York, NY, 1951 (Seventh Printing, February, 1965), Figure 23, p. 950.

167. Bartlett, N. R., op. cit., p. 189.

168. Ibid, p. 190.

169. Brown, J. L. and C. G. Mueller, "Brightness Discrimination and Brightness Contrast," Chapter 9 of Vision and Visual Perception, Edited by Clarence H. Graham, John Wiley and Sons, Inc., New York, NY, 1965 (Second Printing, October, 1966), pp. 209 - 211.

170. Bartlett, N. R., "Thresholds as Dependent on Some Energy Relations and Characteristics of the Subject," Chapter 7 in Vision and Visual Perception, Edited by Clarence H. Graham, John Wiley and Sons, Inc., New York, NY, 1965 (Second Printing, October, 1966), pp. 170-172.

171. Burnette, Keith T., Color Aircraft Display Compatibility With the Night Vision Imaging System, WL-TR-95-3028, Flight Dynamics Directorate, Wright Laboratory, Air Force Materiel Command, Wright-Patterson AFB, Ohio, November 1994, pp. 112-115.

APPENDIX A

Quantitative Data for Image Difference Luminance Versus Background Luminance Comparisons

The purpose of this appendix is to present and compare the quantitative data of Aulhorn and Harms, Chapanis and Blackwell. A discussion of the similarities and differences between these experimenters' data is contained in the body of the report. The test data of these experimenters' was selected for presentation and comparison because their test results were restricted to the use of a 50% probability of correct identification or detection criteria, for assessing the perceptibility of the test image. Applying this restriction allows the results of different experimenters using the same, or equivalent, sets of test variables, under nearly the same test conditions, to be directly compared. In the first section, the image identification data of Chapanis, and that of Aulhorn and Harms, are introduced and compared to show the agreement that exists between their test results, and to infer from this quantitative comparison that both sets of data can be considered valid. In the second section, the image detection data of Blackwell, which are already accepted as a standard of comparison in the literature, are compared with the Chapanis and Aulhorn and Harms image identification data. The twofold purpose of the latter comparisons is to show that the slopes of the image difference luminance characteristics are in reasonably good quantitative agreement, in the photopic background luminance range, and to provide a quantitative basis for a possible theoretical relationship between the image difference luminance requirements for image detection and identification tasks.

A.1. Comparisons of Different Experimenters Image Identification Test Data

Image identification data collected by Chapanis, as graphed by Carel, is shown in Figure A.1. Comparable data of Aulhorn and Harms, as presented by Semple, et al, were shown previously in Figure 3.7. The data extracted from these graphs and the procedures used to extract that data are described in the two subsections that follow. A final subsection presents data for use in the comparison of the Chapanis and Aulhorn and Harms image difference luminance versus background luminance characteristics.

A.1.1. Chapanis Data

The procedure used to extract the image difference luminance values from the Carel graph of the Chapanis data, shown in Figure A.1, involved extracting background luminance values corresponding to the intersections of constant critical detail dimension horizontal lines with the constant contrast characteristics. Image difference luminance values, corresponding to each of the background luminance values were then calculated by applying the appropriate percent contrast to the background luminance value.

The image difference luminance values for the Chapanis data shown in Table A.1, for critical detail dimensions of 2, 3.6 and 9 minutes of arc, were obtained using the above procedure. Because the Carel graph in Figure A.1 contains seven contrast characteristics, this procedure for extracting data results in at most seven background and image difference luminance levels for each critical detail dimension parameter value in Table A.1.

A.1.2. Aulhorn and Harms Data

The procedure used to extract the image difference luminance values from the Aulhorn and Harms graph, shown in Figure 3.7A, used a procedure similar to the one previously described for the Chapanis data. Differences between the data extraction procedures were relatively minor. In particular, the horizontal lines, of constant image critical detail dimension in this graph, intercept constant background luminance rather than

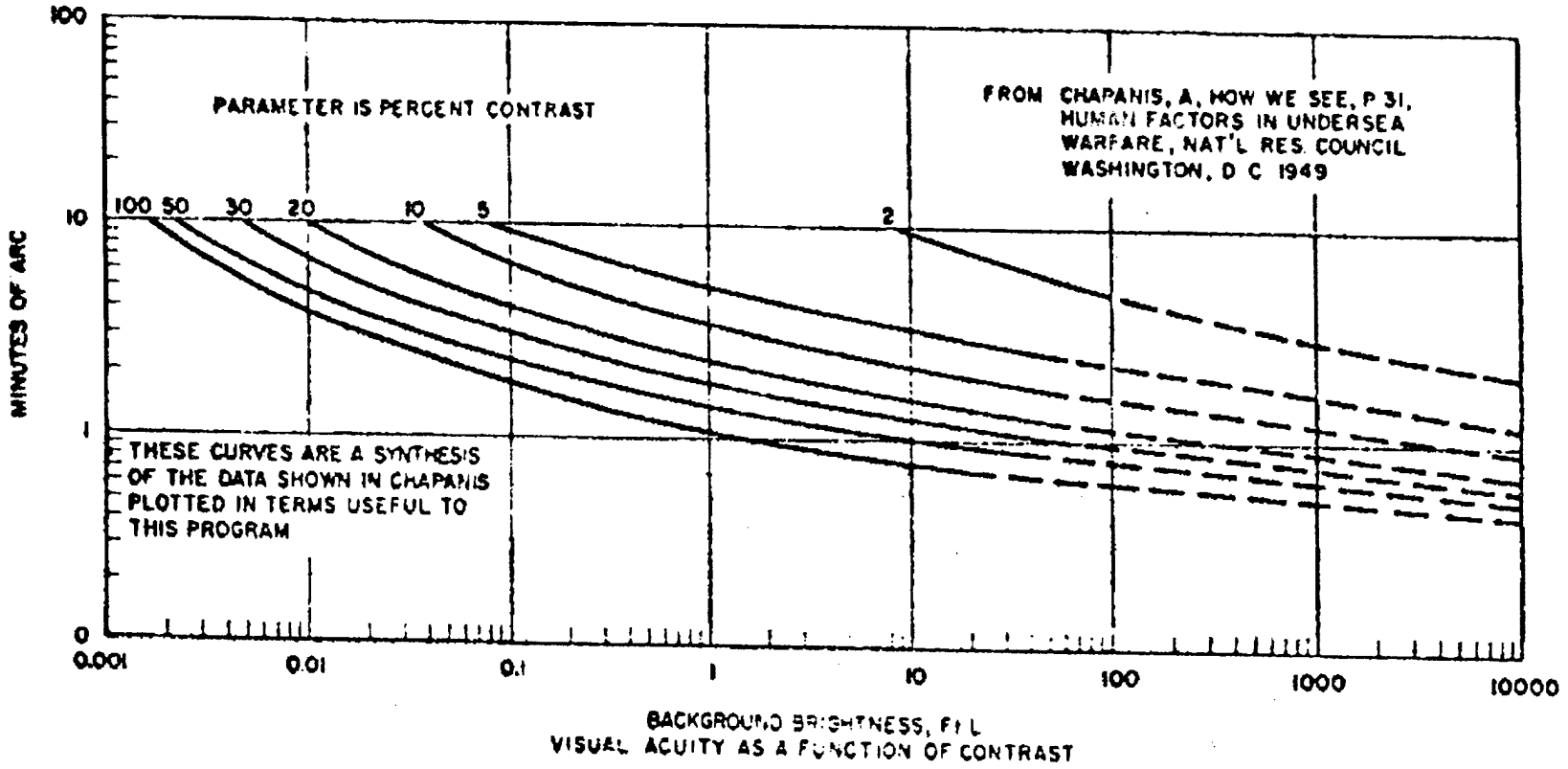


Figure A.1. Chapanis Image Critical Detail Dimension Versus Background Luminance with the Percent Contrast of the Image as a Parameter.

Table A.1. Image Difference Luminance Data of Chapanis for Different Background Luminance Levels with Critical Detail Dimension as a Parameter.

$\alpha_c = 2'$			$\alpha_c = 3.6'$			$\alpha_c = 9'$		
L_D	C	ΔL	L_D	C	ΔL	L_D	C	ΔL
fL	%	fL	fL	%	fL	fL	%	fL
0.0656	100	0.0653	0.0109	100	0.0109	0.00191	100	0.00191
0.170	50	0.0852	0.0206	50	0.0103	0.00262	50	0.00131
0.541	30	0.162	0.0558	30	0.0167	0.00572	30	0.00170
2.023	20	0.405	0.156	20	0.0313	0.0121	20	0.00242
17.18	10	17.18	0.773	10	0.0773	0.0470	10	0.00470
—	5	—	6.076	5	0.3038	0.1109	5	0.00554
—	2	—	—	2	—	11.09	2	0.2218

constant contrast characteristics. The effect of this is that the values of the image difference luminance values, for each background luminance intercept, are read directly from the logarithmic scale on the horizontal axis.

Table A.2 shows image difference luminance values extracted from a magnified version of Figure 3.7A, using the above procedure, for critical detail dimensions of 2, 3.6 and 9 minutes of arc. This procedure had been applied previously in 1972 to draw the graphs of image difference luminance versus background luminance for the constant 1, 2 and 9 minute of arc critical detail dimension characteristics of Aulhorn and Harms shown in Figure 3.8. Revised versions of these graphed characteristics, based on the data from Table A.2, were used to obtain the data compared with the data of Chapanis later in this section. This was done both

Table A.2. Aulhorn and Harms Image Difference Luminances for Different Background Luminance Levels with Critical Detail Dimension as a Parameter.

		$\alpha_c = 2.0'$		$\alpha_c = 3.6'$		$\alpha_c = 9'$	
L_D	L_D	ΔL	ΔL	ΔL	ΔL	ΔL	ΔL
mL	fL	mL	fL	mL	fL	mL	fL
0	0	0.0243	0.0226	0.00755	0.00701	0.00198	0.00184
0.01	0.00929	0.0243	0.0226	0.00873	0.00811	0.00231	0.00214
0.1	0.0929	0.0570	0.0530	0.0205	0.0190	0.00560	0.00520
1	0.929	0.287	0.267	0.104	0.0964	0.0411	0.0382
10	9.29	1.171	1.088	0.662	0.615	0.374	0.347
100	92.9	10.926	10.150	5.826	5.413	3.517	3.267

as a check on the accuracy of the original characteristics and because plotting the 3.6 minute of arc data from Table A.2 was necessary to have a characteristic for comparison later with the 3.6 minute of arc image difference luminance requirements data of the Blackwell image detection task. An attempt to draw a smooth characteristic through the plotted nine minute of arc image difference luminance data points of Aulhorn and Harms in Table A.2, showed that an approximately straight line can be drawn through the last three points in the table. The resultant slope of the line in the photopic vision range is just greater than that of the 9.68 minute of arc characteristic of Blackwell and less than that of the deviant portion of the Aulhorn and Harms nine minute of arc critical detail dimension characteristic shown in Figure 3.8.

A.1.3. Comparisons of Chapanis and Aulhorn and Harms Data

Image difference luminance values of Chapanis are compared in Table A.3, Table A.4 and Table A.5 of this subsection with the image difference luminance values extracted from the graphed Aulhorn and Harms characteristics, for corresponding background luminance values. Due to the limited background luminance ranges of the Chapanis data, described previously in Section 3.3.1, the background luminance data points from Table A.1 were used directly to make image difference luminance comparisons to the Aulhorn and Harms data. To improve accuracy of this comparison, large area graphed renditions of the Aulhorn and Harms data were used to extract image difference luminance values at the background luminance values listed Tables A.1 for the Chapanis data. The Aulhorn and Harms data were selected for graphing, rather than the Chapanis data, because of their larger range of background luminance values and the finding that smoother characteristics could be drawn through their image difference luminance data points. The assumption that this data can be graphed, using smooth continuous characteristics, was based on the shapes of the Blackwell and Jainski characteristics for the mesopic and photopic background luminance ranges. Both investigations involved a large enough number of experimentally determined data points to act as a statistically significant pool of test data.

The image difference luminance values of Chapanis in Table A.1 for 2, 3.5 and 9 minute of arc critical detail dimension images are compared in Table A.3, the left-hand side of Table A.4 and Table A.5, respectively,

Table A.3. Comparison of Chapanis and Aulhorn and Harms 2 Minute of Arc Critical Detail Dimension Image Difference Luminance Characteristics.

	Chapanis	Aulhorn &Harms	Aulhorn &Harms and Chapanis
L_D	ΔL_C	$\Delta L_{A\&H}$	$\Delta L_{High} / \Delta L_{Low}$
fL	fL	fL	
0.0656	0.0656	0.0483	1.358
0.170	0.0852	0.079	1.078
0.541	0.162	0.177	1.093
2.023	0.405	0.510	1.259
17.18	1.718	2.601	1.514
Mean Value of $\Delta L_{High} / \Delta L_{Low}$			1.260

Table A.4. Comparisons of Chapanis and Aulhorn and Harms 3.6 Minute of Arc Critical Detail Dimension Image Difference Luminance Characteristics.

	Chapanis	Aulhorn & Harms	Aulhorn & Harms and Chapanis		Aulhorn & Harms	Chapanis	Aulhorn & Harms and Chapanis
L_D	ΔL_C	$\Delta L_{A\&H}$	$\Delta L_{High} / \Delta L_{Low}$	L_D	$\Delta L_{A\&H}$	ΔL_C	$\Delta L_{High} / \Delta L_{Low}$
fL	fL	fL		fL	fL	fL	
—	—			0	0.00701	—	—
0.0109	0.0109	0.0084	1.298	0.00929	0.00811	0.0106	1.307
0.0206	0.0103	0.0101	1.020	0.034	0.0120	0.0128	1.067
0.0558	0.0167	0.0147	1.136	0.0929	0.0190	0.0220	1.158
0.156	0.0313	0.0260	1.204	0.34	0.0445	0.0475	1.067
0.773	0.0773	0.0825	1.067	0.929	0.0964	0.0885	1.089
—	—			3.4	0.258	0.214	1.206
6.076	0.304	0.415	1.365	6.076	0.415	0.304	1.365
—	—			9.29	0.615	—	—
Mean Value of $\Delta L_{High} / \Delta L_{Low}$			1.182	Mean Value of $\Delta L_{High} / \Delta L_{Low}$			1.179

Table A.5. Comparison of Chapanis and Aulhorn and Harms 9 Minute of Arc Critical Detail Dimension Image Difference Luminance Characteristics.

	Chapanis	Aulhorn & Harms	Chapanis and Aulhorn &Harms
L_D	ΔL_C	$\Delta L_{A\&H}$	$\Delta L_{High} / \Delta L_{Low}$
fL	fL	fL	
0.00191	0.00191	0.00184	1.038
0.00262	0.00131	0.00184	1.405
0.00572	0.00170	0.00202	1.188
0.0121	0.00242	0.00233	1.039
0.0470	0.00470	0.00363	1.295
0.111	0.00554	0.00599	1.081
Mean Value of $\Delta L_{High} / \Delta L_{Low}$, Mesopic Range			1.174
11.09	0.222	0.415	1.869
Overall Mean Value of $\Delta L_{High} / \Delta L_{Low}$			1.273

with the corresponding image difference luminance data extracted from the graphed Aulhorn and Harms characteristics, at each background luminance value in Table A.1. For the comparisons made on the right side of Table A.4, the preceding comparison process is reversed. Namely, the 3.5 minute of arc data points of Aulhorn and Harms, from the right-hand side of Table A.2, are compared with data extracted from a graph of the Chapanis characteristic. In this instance the error associated with extracting intermediate data from the graphed characteristic is expected to make this comparison less accurate.

The method chosen to make the individual image difference luminance value comparisons in each table involved taking the ratio of the larger to the smaller of the Chapanis and Aulhorn and Harms image difference luminance values, at each background luminance level to be compared. This approach is compatible with the logarithmic dependence in evidence in the image difference luminance characteristics and enables comparison results in any of the tables to be directly compared with each other.

A.2. Comparisons of Image Detection and Image Identification Test Data

Comparisons of the image detection data of Blackwell with the image identification data of Chapanis and Aulhorn and Harms, described in the preceding section, are contained in Tables A.6, A.7, A.8 and A.9. The detection task test data in the tables was taken from Table II of the previously cited Blackwell article or, where the background luminance values do not agree, from a large scale plot of the Blackwell data.

Table A.6. Comparison of Chapanis, Aulhorn and Harms and Blackwell Image Difference Luminance Characteristics.

	Aulhorn & Harms	Chapanis	Aulhorn &Harms and Chapanis	Blackwell	Aulhorn &Harms and Blackwell
	$\alpha_c = 9'$	$\alpha_c = 10'$	$\alpha_c = 9'$ & $10'$	$\alpha = 9.68'$	$\alpha_c = 9'$, $\alpha = 9.68'$
L_D	$\Delta L_{A\&H}$	ΔL_C	$\Delta L_{High} / \Delta L_{Low}$	ΔL_B	$\Delta L_{High} / \Delta L_{Low}$
fL	fL	fL		fL	
0.00167	0.00184	0.00167	1.102	0.00160	1.150
0.00231	0.00184	0.00116	1.568	0.00180	1.022
0.00478	0.00197	0.00143	1.378	0.00234	1.188
0.0101	0.00223	0.00202	1.104	0.00312	1.399
0.0382	0.00333	0.00382	1.147	0.00554	1.664
0.0790	0.00477	0.00395	1.208	0.00790	1.656
0.90	0.0372	—	—	0.0345	1.078
Mean Value of $\Delta L_{High} / \Delta L_{Low}$, Mesopic Range			1.254	—	1.308
9.37	0.352	0.187	1.882	0.209	1.684
92.9	3.267	—	—	1.770	1.846
Overall Mean Value of $\Delta L_{High} / \Delta L_{Low}$			1.344	—	1.410

Table A.7. Interpolation of Chapanis 9 and 10 Minute of Arc and Comparison with Blackwell 9.68 Minute of Arc Image Difference Luminance Characteristics.

Chapanis for $\alpha_c = 9'$		Chapanis for $\alpha_c = 10'$		Interpolation of L_D & ΔL Values between $\alpha_c = 9'$ & $10'$ Chapanis Characteristics for $\alpha_c = 9.68'$		Graphical Data of Blackwell for $\alpha = 9.68'$	Blackwell and Interpolated Chapanis Data for $\alpha = 9.68'$
Data from Table A.1, Columns 7 & 9		Data from Table A.6, Columns 1 & 3					
L_D	ΔL_C	L_D	ΔL_C	L_D	ΔL_C	ΔL_B	$\Delta L_{High} / \Delta L_{Low}$
fL	fL	fL	fL	fL	fL	fL	
0.00191	0.00191	0.00167	0.00167	0.00175	0.00175	0.00160	1.094
0.00262	0.00131	0.00231	0.00116	0.00241	0.00120	0.00184	1.533
0.00572	0.00170	0.00478	0.00143	0.00508	0.00152	0.00239	1.572
0.0121	0.00242	0.0101	0.00202	0.0107	0.00215	0.00320	1.488
0.0470	0.00470	0.0382	0.00382	0.0410	0.00410	0.00570	1.390
0.111	0.00554	0.0790	0.00395	0.0892	0.00446	0.00790	1.771
11.09	0.2218	9.366	0.1873	9.918	0.1956	0.219	1.106
Overall Mean Value of $\Delta L_{High} / \Delta L_{Low}$							1.422

Table A.8. Comparison of 3.6 Minute of Arc Image Difference Luminance Characteristics Chapanis and Blackwell.

	Chapanis	Blackwell	Chapanis and Blackwell
L_D	ΔL_C	ΔL_B	$\Delta L_{High} / \Delta L_{Low}$
fL	fL	fL	
0.0109	0.0109	0.0147	1.349
0.0206	0.0103	0.0194	1.883
0.0558	0.0167	0.0304	1.820
0.156	0.0313	0.050	1.597
0.773	0.0773	0.124	1.604
Mean Value of $\Delta L_{High} / \Delta L_{Low}$, Mesopic Range			1.651
6.076	0.3038	0.541	1.781
Overall Mean Value of $\Delta L_{High} / \Delta L_{Low}$			1.672

Table A.9. Comparisons of 3.6 Minute of Arc Image Difference Luminance Data of Blackwell with that of Chapanis and Aulhorn & Harms.

	Blackwell	Chapanis	Blackwell and Chapanis	Aulhorn & Harms	Blackwell and Aulhorn & Harms
L_D	ΔL_B	ΔL_C	$\Delta L_{High} / \Delta L_{Low}$	$\Delta L_{A\&H}$	$\Delta L_{High} / \Delta L_{Low}$
fL	fL	fL		fL	
0	—	—	—	0.00701	—
0.0034	0.00980	—	—	0.00720	1.361
0.00929	0.0135	0.0106	1.274	0.00811	1.665
0.034	0.0240	0.0128	1.875	0.0120	2.000
0.0929	0.0390	0.0220	1.773	0.0190	2.053
0.34	0.0760	0.0475	1.600	0.0445	1.708
0.929	0.140	0.0885	1.582	0.0964	1.452
Mean Value of $\Delta L_{High} / \Delta L_{Low}$, Mesopic Range			1.621	—	1.707
3.4	0.350	0.214	1.636	0.258	1.357
6.076	0.541	0.304	1.780	0.415	1.304
9.29	0.740	—	—	0.615	1.203
11.09	0.850	—	—	0.735	1.156
92.9	—	—	—	5.413	—
Mean Value of $\Delta L_{High} / \Delta L_{Low}$ Photopic Range			1.708	—	1.255
Overall Mean Value of $\Delta L_{High} / \Delta L_{Low}$			1.646	—	1.526

Table A.6 compares the image difference luminance data of Aulhorn and Harms, for a nine minute of arc critical detail dimension image, with the data for the Chapanis ten minute of arc critical detail dimension image, and also with the data of Blackwell for an image that subtends a total angle of 9.68 minutes of arc. Due to the close spacing of the nine and ten minute of arc lines used to extract the background luminance data of Chapanis, corresponding to each of the different percent contrast characteristics in Figure A.1, the background luminance data for the nine and ten minute of arc characteristics, in Tables A.1 and A.6, respectively, were placed in Table A.7, along with the image difference luminance values, and the former were interpolated to obtain the Chapanis background values corresponding to a 9.68 minute of arc image. The image difference luminance values, calculated after interpolating the background luminance values, are compared with the corresponding values extracted from the Blackwell 9.68 Minute of Arc image difference luminance characteristics, at each of the interpolated background luminance values.

Tables A.8 and A.9 compare the image difference luminance data of Chapanis and Aulhorn and Harms, for 3.6 minute of arc critical detail dimension images, with those of Blackwell for an image that subtends a total

angle of 3.5 minutes of arc. In Table A.8, the background luminance data points of Chapanis, from Table A.1, are used as a baseline for comparison of the image difference luminance values of Chapanis and of Blackwell. The 3.6 minute of arc characteristic of Blackwell was graphed to permit extracting the image difference luminance levels shown in the table at each of the background luminance values of the Chapanis shown in the table. This data extraction procedure was used to improve the accuracy of the comparison, since the Blackwell characteristic has more data points available for use in drawing its characteristic. To make the data comparison results in Table A.8 directly comparable with the earlier comparison between the image difference luminance values of Chapanis and Aulhorn and Harms for 3.6 minute of arc critical detail dimension images presented in the left-hand side of Table A.4, the same background luminance values were used in both tables.

The data comparison in Table A.9 employs many of the same background luminance values formerly used in the comparison between image difference luminance values of Chapanis and Aulhorn and Harms, for 3.6 minute of arc critical detail dimension images, presented in the right-hand side of Table A.4. As was true in Table A.4, only image difference luminance values at the background luminances listed in Table A.2, that is, at decade intervals from 0.00929 to 92.9 fL, correspond to data directly extracted from the Aulhorn and Harms 3.6 minute of arc characteristic in Figure 3.7A. All of the other image difference luminance values in Table A.9 had to be extracted from graphs of the characteristics drawn using the available experimental data points of the three experimenters. This includes all of the image difference luminance values of Chapanis in Table A.9, and those of Aulhorn and Harms that are intermediate between the background luminance levels in Figure 3.7A.

Because of the correspondence between the background luminance values used in Table A.4 and in Table A.9, the results of the earlier comparison of the image identification task results of Chapanis and Aulhorn and Harms can be readily compared with the results of the latter comparison between the Chapanis and the Aulhorn and Harms image identification tasks and the Blackwell image detection task. Although the equal spacing of the background luminance data points in Table A.9 would usually be expected to produce a more reliable analysis result, the need to interpret the Chapanis data between the background luminance data points, shown in Table A.8, makes the latter comparison less accurate for the Chapanis data.

Figure A.2 shows a comparison of the image detection data of Blackwell, for test images that subtend total angles of 3.6 and 9.68 minutes of arc, with the image identification characteristics of Aulhorn and Harms and the corresponding individual data points of Chapanis, for test images that subtend critical detail dimensions of 3.6 and 9 minutes of arc. The comparisons are shown for only two image critical detail dimensions because Blackwell's data only included images subtending angles of 3.6, 9.68, 18.2, 55.2 and 121 minutes of arc, and, consequently, only two detection target sizes are within, or near, the critical detail dimension ranges of the Aulhorn and Harms and Chapanis test images. As a further comparison, all five of the Blackwell characteristics are shown graphed in Figure 3.31, with the scotopic background luminance range included. Figure A.2 shows seven individual data points for nine minute of arc critical detail dimension Chapanis test image and six for 3.6 minutes of arc image. Not all of the data points are easily seen, due to their close proximity to the depictions of the continuous Blackwell and Aulhorn and Harms characteristics.

It should be noted that the nine minute of arc characteristic in Figure 3.8 was originally drawn with a small constant slope between the lowest background luminance values of 0.00929 fL and 0 fL (i.e., nominally 10^{-6} fL). In contrast to this choice for drawing the characteristic in Figure 3.8, and based on an analogy to the Jainski characteristics, shown in subsequent figures, the nine minute of arc characteristic in Figure A.2 was drawn so that it melded into the zero slope characteristic, drawn at the image difference luminance corresponding to the zero background luminance data point of Aulhorn and Harms in Table A.2. The latter interpretation of the Aulhorn and Harms nine minute of arc characteristic is suggested by the shape of the 3.6 minute of arc characteristic, which is supported by the experimental results of Aulhorn and Harms shown in Figure 3.7A, and Table A.2.

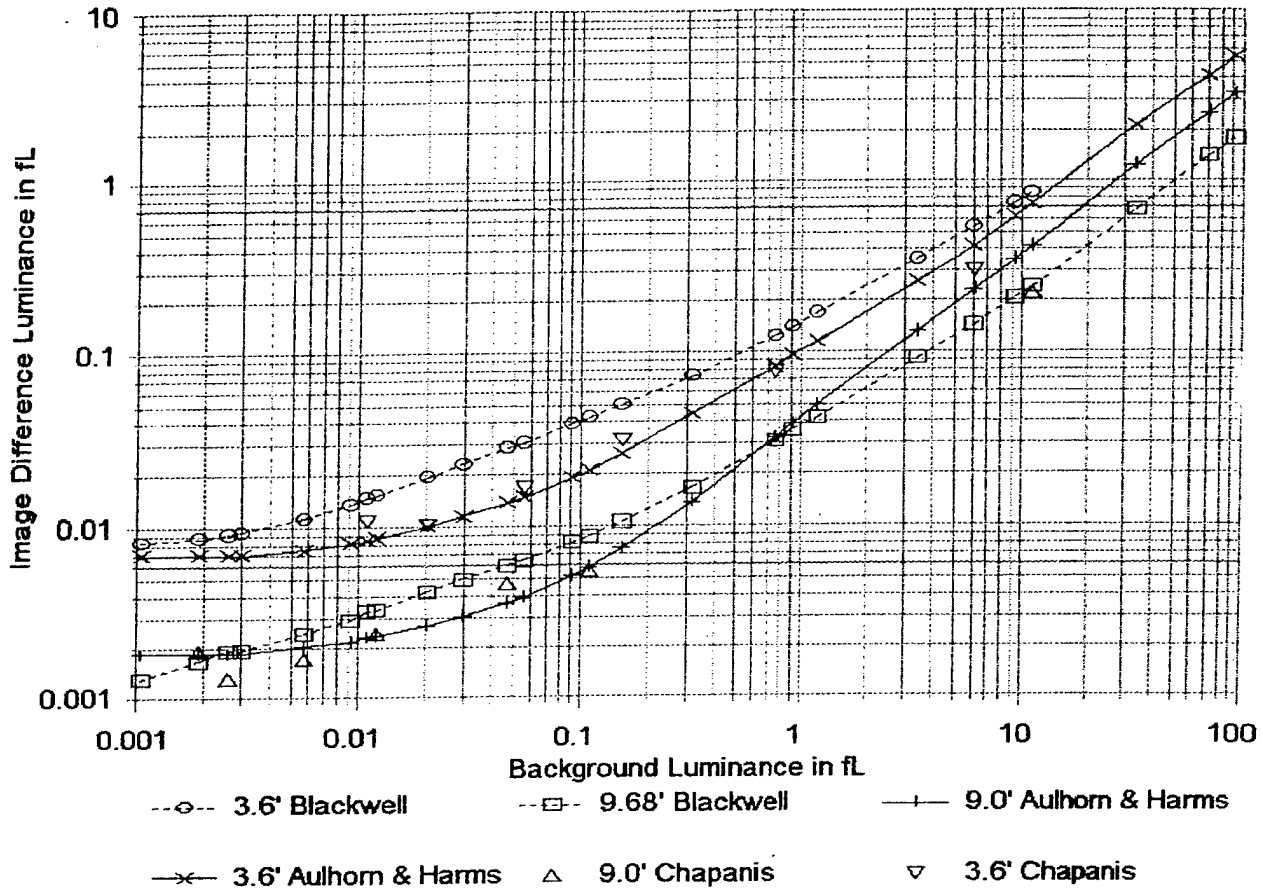


Figure A.2. Comparison of the Image Detection Data of Blackwell with the Image Identification Data of Aulhorn & Harms and Chapanis.

As described in Section 3.3.1, in the body of the report, the comparison of the image detection and identification task results are not expected to produce agreement in the scotopic or in much of the mesopic background luminance vision ranges. Unfortunately, in the photopic range of background luminance values, which is variously reported as starting between one and three foot-Lamberts, the range of background luminances over which image difference luminance data can be compared is quite limited. The maximum values of the Chapanis background luminance data points only went to values ranging from about 6.7 to 17 fL. Similarly, the Blackwell background luminance data was limited to about 11 fL, for the 3.6 minute of arc data, and to nominally 100 fL, for the 9.86 minute of arc data. Only the Aulhorn and Harms data went as high as 92.9 fL for each of its characteristics. This, of necessity, limits the accuracy of the quantitative comparisons that are possible, in that only one or two data points can be compared in the photopic vision range.

A.3. Luminance Ratio Baseline for Assessing Quantitative Comparisons Results

To provide a baseline for assessing the physical significance of the ratios between different experimenters' image difference luminance characteristics shown in Tables A.3 through Table A.9, the image difference luminance ratios between the different constant image critical detail dimension characteristics were calculated, using the Aulhorn and Harms data from Table A.2. For this comparison, image difference

luminance levels extracted from Figure 3.7A, for the one minute of arc critical detail dimension characteristic shown in Figure 3.8, have also been included in the table. The image difference luminance data from Table A.2, which were used in this comparison and the results obtained are shown in Table A.10, using the letter, R, to designate the values of the image difference luminance ratios. To clarify which data are being used to form the ratios between the image different luminance levels in the table, subscripts have been added to the letter, R, to identify the image critical detail dimensions of the image difference luminance characteristics being compared.

Table A.10. Spacing Between the Aulhorn and Harms Critical Detail Dimension Characteristics.

L_D fL	ΔL $\alpha_c = 1.0'$ fL	$R_{1'-2'}$	ΔL $\alpha_c = 2.0'$ fL	$R_{2'-3.6'}$	ΔL $\alpha_c = 3.6'$ fL	$R_{3.6'-9'}$	ΔL $\alpha_c = 9.0'$ fL	$R_{2'-9'}$	$R_{1'-9'}$
0.00929	0.143	6.32	0.0226	2.79	0.00811	3.79	0.00214	10.56	66.82
0.0929	0.281	5.30	0.0530	2.78	0.0190	3.65	0.00520	10.19	54.04
0.929	1.324	4.96	0.267	2.77	0.0964	3.05	0.0316	8.45	41.90
9.29	4.172	3.84	1.088	1.77	0.615	1.77	0.347	3.14	12.02
92.9	39.18	3.86	10.15	1.88	5.413	1.66	3.267	3.11	11.99

Besides providing a baseline for assessing the physical significance of the ratios between different experimenters' image difference luminance characteristics, the image difference luminance ratios in Table A.10 illustrate that the Aulhorn and Harms characteristics are in good quantitative agreement with the assertion that such characteristics can be represented by parallel straight lines on a full logarithmic graph in the photopic background luminance range. For the constant image critical detail dimension characteristic lines to be parallel, a necessary, but not sufficient, condition is that the ratios of their image difference luminance values have to be equal to one another at different photopic background luminance values. To assert that the characteristics are parallel requires that they not only be equidistant but they also can be represented by straight lines when plotted using full logarithmic axis presentations of the image difference luminance and background luminance variables. With only two data points per characteristic in the photopic background luminance range, the Aulhorn and Harms experimental data is insufficient to support a claim that their characteristics are parallel in the photopic background luminance range. The experimental results of Blackwell and of Jainski are the basis for asserting that the image difference luminance versus background luminance characteristics are parallel in the photopic background luminance range.

A comparison of the image difference luminance ratios at the two photopic background luminance levels in the Table A.10, that is, at 9.29 and 92.9 fL, shows that the values of the ratios are approximately equal. The largest deviation from equality is about 6.4% and occurs for the 1.77 and 1.66 ratios between the image difference luminance values for the 3.6 and 9 minute of arc critical detail dimension characteristics. Since the $R_{2'-9'}$, $R_{1'-2'}$, and $R_{1'-9'}$ ratios differ by only 0.96%, 0.52%, and 0.25%, respectively, by a process of elimination this points to an error in either or both the 0.615 and 5.413 fL image difference luminance values in Table A.10 for the 3.6 minute of arc characteristic being a potential source for the deviation from equality. For example, if the value of 0.615 is high by 3.2%, and the 5.413 fL value is low by 3.2%, the corrected image difference luminance values of 0.596 and 5,586 fL, respectively, would produce $R_{2'-3.6'}$ and $R_{3.6'-9'}$ ratios for the 9.29 and 92.9 fL background luminance levels that agree with each other to within less than 1%, without changing the corresponding $R_{2'-9'}$ ratios. It is reasonable to expect data extraction errors of this magnitude, from even a magnified copy of Figure 3.7A. In fact, it is the extent of the agreement between the photopic

image difference luminance ratios in Table A.10 that was unexpected.

A comparison of the image difference luminance values in Table A.10 at the two photopic background luminance levels, 9.29 and 92.9 fL, shows that the image difference luminance values increase by less than a multiple of ten when the background luminance increases by a factor of ten, and that this is true for data at each critical detail dimension shown in the table. This result shows that the slope of the photopic portions of each characteristic have a slope of less than unity. The mean slope for the four critical detail dimension characteristics in Table A.10 was 0.965 with about a 3% variation between the values. This slope is higher by 4.2% than the 0.926 mean slope developed from the data of Blackwell and Jainski used elsewhere in this report.

Another noteworthy feature of the image difference luminance ratios in Table A.10 is the increase in the magnitudes of the ratios for mesopic background luminance levels. As can be observed in Figures 3.8 and Figure A.2, the mesopic background luminance levels in Table A.10 correspond to the transition between the image difference luminance spacings of the characteristics, for the daylight background luminance range, and the larger spacings among the zero slope characteristics that apply at night. An unexpected aspect of these comparisons was the nearly equidistant spacing of the image difference luminance ratios for the 2 and 3.6 and the 3.6 and 9 minute of arc characteristics at the 0.00929 and 0.0929 fL levels of background luminance. These particular image difference luminance ratio comparisons of Aulhorn and Harms data suggest that most of the change in the spacing of the characteristics, in going from the photopic (day) to the scotopic (night) background luminance levels, occur before 0.1 fL in the upper part of the mesopic background luminance vision range, even though the image difference luminance levels continue to decrease for another decade and a half. Since this feature of these characteristics does not hold for the comparisons of the image difference luminance ratios, for the one and two minute of arc data, of Aulhorn and Harms in Table A.10, and the data of Jainski, for the same range of critical detail dimension images, is both quite limited and somewhat ambiguous on this point of comparison, the available data is considered is insufficient to draw any firm conclusions.

A.4. Comments on the Validity and Accuracy of the Quantitative Comparison Results

The small number of data points used to make the comparisons in this appendix are considered insufficient to test the statistical significance of the comparison results. Consequently, the observed similarities between the results are interpreted as data trends that indicate, but do not in isolation prove, the correspondence that appears to exist between the data being compared. The accuracies of the data comparisons presented in this appendix were limited by the need to interpret and draw smooth characteristics through the data points extracted from one experimenter's original characteristics, to permit comparisons to be made at the same background luminance values, at which image difference luminance values were extracted from the other experimenters' original characteristics. Despite the preceding limitations, the correspondence between the comparison results is quite striking, in view of the extensive potential ranges of the image difference luminance, background luminance and image critical detail dimension variables being tested.

APPENDIX B

Glare Source Illuminance Versus Luminance

B.1. Illuminance Relationship to Luminance

One form of the defining equation for the luminance of a glare source, L_B, is as the quotient formed by dividing the differential illuminance (i.e., the differential luminous flux density incident on a differential surface area), received from the glare source, dE_B, by the projected differential solid angle subtended by the glare source, $d\Omega_P$, at its vertex, where the differential illuminance is determined, therefore,

$$L_B = dE_B / d\Omega_P . \tag{B.1}$$

This equation is valid provided the variables used in it adhere to a self-consistent system of units. The three different systems of units, used in the references cited in this report, are briefly described in relation to Equation B.1. As Equation B.1 is written, if the illuminance is expressed in the standard international (SI) unit of lux, which was formerly called the meter-candle (i.e., lumen per meter squared - lm/m^2), the luminance unit is the nit (i.e., abbreviated as nt and equivalent to candela per square meter - cd/m^2 or lumen per steradian and square meter - $lm/sr \cdot m^2$). If instead the illuminance is expressed in the centimeter-gram-second (CGS) system unit of phot (i.e., lumen per centimeter squared - lm/cm^2), the luminance unit is the stilb (i.e., abbreviated as sb and equivalent to candela per square centimeter - cd/cm^2 or lumen per steradian and square centimeter - $lm/sr \cdot cm^2$). Finally, if the illuminance is expressed in the English system unit of foot-candle (i.e., abbreviated as fc and equivalent to lumen per foot squared - lm/ft^2), the luminance unit is the candela per square foot (i.e., abbreviated as cd/ft^2 or lumen per steradian and square foot - $lm/sr \cdot ft^2$). In each coordinate system described above the differential solid angle is expressed in steradians.

Equation B.1 can be solved for the glare source illuminance, E_B, by integrating the glare source luminance distribution, $L_B(\theta,\phi)$, over the solid angle encompassing the glare source, Ω_B. Carrying out this integration, the glare source illuminance may be expressed using the following integral equation:

$$E_B = \oint_{\Omega_B} L_B(\theta,\phi)\, d\Omega_P . \tag{B.2}$$

The projected glare source differential solid angle, $d\Omega_P$, appearing in Equation B.2, represents the projection of the glare source differential solid angle, $d\Omega$, onto the normal to a differential surface area, dA_{SA}, on which the incident luminance from the glare source is measured. Expressing this relationship mathematically, the projected differential solid angle, $d\Omega_P$, can be written in equation form, as follows:

$$d\Omega_P = \cos\theta\, d\Omega . \tag{B.3}$$

Because the illuminance of the glare source, E_B, is defined as the illuminance incident on a differential surface area, which is perpendicular to the direction of light, from the center of the glare source to the eyes, the $\cos\theta$ term in Equation B.3 compensates for incident luminances, $L_B(\theta,\phi)$, from glare source differential solid angles, $d\Omega$, located anywhere on the glare source surface, onto the planar differential surface area, dA_{SA}, at angles, θ, other than zero degrees, with respect to the normal to that surface. The glare source differential solid angle term, $d\Omega$, in Equation B.3, is, by the definition of a solid angle in spherical coordinates, given by the quotient of any differential area, dA_{GS}, on the glare source surface, divided by the square of the distance, ρ, between the glare source and the vertex of the differential solid angle. When expressed in equation form, the differential solid angle can therefore be represented as follows:

$$d\Omega = \frac{dA_{GS}}{\rho^2} = \frac{(\rho\, d\theta)(\rho \sin\theta\, d\phi)}{\rho^2} = \sin\theta\, d\theta\, d\phi . \tag{B.4}$$

Substituting this relationship into Equation B.3, the projected glare source differential solid angle, $d\Omega_P$, can

therefore be written as follows:

$$d\Omega_P = \cos\theta\, d\Omega = \cos\theta \sin\theta\, d\theta\, d\phi \qquad \text{(B.5)}$$

With the vertex of all of the differential glare solid angles, positioned at the eyes, Equation B.2 gives the total glare source illuminance, E_B, incident on the eyes from the glare source, by calculating the integral summation, at the eyes, of the differential illuminance contributions, attributable to the normal components of the incident luminance, from each of the glare source differential solid angles, contained within the total glare source solid angle, Ω_B.

Making the substitution, for the projected differential glare source solid angle from Equation B.5, into Equation B.2 for the total glare source illuminance, and then including the integration limits on θ, from zero radians, at the center of the glare source, to half its total subtended angle (i.e., a circular glare source luminous surface area is assumed), $\theta_s/2$, and from 0 to 2π radians for ϕ, yields the following equation:

$$E_B = \int_0^{2\pi} \int_0^{\theta_s/2} L_B(\theta,\phi) \cos\theta \sin\theta\, d\theta\, d\phi\,. \qquad \text{(B.6)}$$

Depending on whether the spatial luminance distribution, $L_B(\theta,\phi)$, is expressed using the unit nit, candela per square foot or stilb, the illuminance calculated using this equation will be in the units of lux, foot-candles, or phot, respectively.

Since very few of the references cited in this report employed the combinations of luminance and illuminance units, just mentioned, different formulations of the illuminance equation will be considered with alternative combinations of luminance and illuminance units. For the purposes of this discussion, the angular dimensions of glare sources will be expressed in units of radians. By applying appropriate units conversion multipliers to Equation B.6, the variables E_B and $L_B(\theta,\phi)$ do not need to have inherently self-consistent sets of units.

Alternative forms of Equation B.6, which were in common use in the literature until recently, most typically use units of lux (lx) or foot-candles (fc) for illuminance, but substitute a luminance expressed in apostilbs (asb) in place of nits (nt), foot-Lamberts (fL) in place of candela per square foot (cd/ft^2) and millilamberts (mL) in place of stilbs (sb), where a millilambert is one thousandth of a Lambert (L). The corresponding equations for carrying out these unit conversions are as follows:

$$\begin{aligned} L(\text{asb}) &= \pi L(\text{nt}) \\ L(\text{fL}) &= \pi L(\text{cd/ft}^2) \\ L(\text{mL}) &= 10^3 L(L) = \frac{\pi}{10} L(\text{nt}), \end{aligned} \qquad \text{(B.7)}$$

where the quantity, L, is the numerical value of luminance, when luminance is expressed using the unit designated inside the bracket. As an example of using these equations, 1 L = 1,000 mL, and 1 nt = 0.3142 mL.

To compensate for the insertion of a luminance variable that uses the preceding units, into Equation B.5, the right side of the equation must be multiplied by the inverse of the conversion factor applied to the luminance variable. The equation for the illuminance of the glare source, when the luminance variable substituted is either in units of nt or fL, and the illuminance is in units of lx or fc, respectively, can be expressed as follows:

$$E_B = \frac{1}{\pi} \oint_{\Omega_B} L_B(\theta,\phi)\, d\Omega_P = \frac{1}{\pi} \int_0^{2\pi} \int_0^{\theta_s/2} L_B(\theta,\phi) \cos\theta \sin\theta\, d\theta\, d\phi\,. \qquad \text{(B.8)}$$

The equation for the illuminance of the glare source, when the luminance variable substituted is in units of mL

and the illuminance is in units of lx, can be expressed as follows:

$$E_B = \frac{10}{\pi} \oint_{\Omega_B} L_B(\theta,\phi)\, d\Omega_p = \frac{10}{\pi} \int_0^{2\pi} \int_0^{\theta_s/2} L_B(\theta,\phi) \cos\theta \sin\theta\, d\theta\, d\phi\,. \tag{B.9}$$

B.2. Coordination of the Values of Luminance and Illuminance and the Illuminance of a Uniform Luminance Sky

It should be noted that the application of the π luminance multiplier term to define a new photometric unit of luminance was not an arbitrary choice in any of the conversions shown in Equation B.6. Instead, the intention of incorporating the π luminance multiplier was to coordinate the numerical magnitudes of luminance and illuminance variables.

To illustrate this point, Equation B.8 is used below to calculate the illuminance incident on a plane surface from a uniform (i.e., constant) luminance, $L_B(\theta,\phi)$, hemisphere, such as the sky vault or half of an integrating sphere located above the surface. For a hemisphere, the subtended angle, θ_s, is π radians (i.e., 180°) and the illuminance incident on the surface can be calculated as follows:

$$E_B = \frac{1}{\pi} \int_0^{2\pi} \int_0^{\pi/2} L_B(\theta,\phi) \cos\theta \sin\theta\, d\theta\, d\phi \tag{B.10}$$

Removing the constant luminance, L_B, from inside the integral, and substituting the trigonometric identity,

$$\cos\theta \sin\theta = 1/2 \sin 2\theta\,, \tag{B.11}$$

Equation B.10 can then be evaluated, as follows:

$$E_B = \frac{L_B}{2\pi} \int_0^{2\pi} \int_0^{\pi/2} \sin 2\theta\, d\theta\, d\phi = -\frac{L_B}{4\pi} \int_0^{2\pi} \Big[\cos 2\theta\Big]_0^{\pi/2} d\phi$$

$$E_B = -\frac{L_B}{4\pi} [\cos\pi - \cos 0] \int_0^{2\pi} d\phi = -\frac{L_B}{4\pi} [-1 - 1] \Big[\phi\Big]_0^{2\pi} \tag{B.12}$$

$$E_B = -\frac{L_B}{4\pi} [-2] [2\pi] = L_B$$

This result shows that while the units of illuminance and luminance in this equation differ, the numerical value of the incident illuminance calculated is equal to the numerical value of the incident luminance.

Two important practical consequences of the above relationship follow. In a diffuse surround luminance environment of any luminance, say for example a cloud at 10,000 fL (i.e., 107,600 asb) the illuminance incident on a flat surface will be of equal magnitude, in this case 10,000 fc (i.e., 107,600 lx). Possibly the most important application of this property occurs for illumination engineering. When light from any direction illuminates a diffusely reflective surface (i.e., as approximated by a surface coated with "flat" paint), the numerical value of the luminance reflected by the surface, in any direction, is equal to the product of the diffuse reflectance of the surface and the magnitude of the incident illuminance.

B.3. Assorted information for Natural Sources of Luminance and Illuminance

To demonstrate the effectiveness of Equation B.8 for calculating the illuminance due to a glare source, this equation is used below to calculate the illuminance incident on the Earth, above its atmosphere, due to the sun. By substituting the trigonometric identity used previously from Equation B.11, Equation B.8 may be solved as follows:

$$E_B = \frac{L_B}{2\pi}\int_0^{2\pi}\int_0^{\theta_s/2} \sin 2\theta\, d\theta\, d\phi = -\frac{L_B}{4\pi}\int_0^{2\pi}\Big[\cos 2\theta\Big]_0^{\theta_s/2} d\phi$$

$$E_B = -\frac{L_B}{4\pi}\Big[\phi\Big]_0^{2\pi}[\cos\theta_s - \cos 0] = -\frac{L_B}{4\pi}[2\pi][\cos\theta_s - 1] \qquad \text{(B.13)}$$

$$E_B = \frac{L_B}{2}[1 - \cos\theta_s].$$

To solve for the illuminance of a glare source using this equation, the average luminance, L_B, and angle, θ_s, subtended by the glare source, with respect to the point where the illuminance is to be determined, must be known. Table B.1 contains the luminance values for several discrete and distributed glare sources, which can be substituted directly into Equation B.13. Values of the sun's luminance, as attenuated by transmission through the atmosphere are shown in this table, characterized in terms of the air mass parameter, m. An air mass of unity, that is, one air mass, corresponds to the sun at its zenith. According to Walsh, the clear day transmittance of the atmosphere from the surface of the Earth, straight up to above the atmosphere is $\tau_Z = 0.796$, and can be approximated as 0.8. The transmittance through multiple air masses is then given by the equation, $\tau_m = \tau_Z^m$, where the angle with respect to the zenith, θ_Z, corresponding to the sun's transmittance through m air masses is given by the equation, $\theta_Z = \sec^{-1} m$ or, equivalently, $\theta_Z = \cos^{-1} 1/m$.*

It should be noted that the sky luminance level ranges given in Table B.1 for different atmospheric conditions do not represent either the lowest or highest ranges of sky luminances encountered in practice and in fact are inconsistent with the clear average sky luminance values given near the bottom of the table. Sky luminances vary spatially, with the time of year and with the time of day, as is described in greater detail by Walsh.

Table B.2 contains additional physical dimensional data required to calculate the glare source angle, θ_s, subtended by two important discrete glare sources, the sun and the moon. If the diameter of a glare source is represented by d and the distance to it is ρ, then by trigonometry the angle subtended by the glare source is given by the equation,

$$\tan(\theta_s/2) = \frac{d}{2\rho}. \qquad \text{(B.14)}$$

Solving this equation for the angle subtended by the glare source, the result is as follows:

$$\theta_s = 2\tan^{-1}\frac{d}{2\rho}. \qquad \text{(B.15)}$$

The sun and moon subtended angles, listed in Table B.3, were obtained by substituting the values of the corresponding diameters, and distances, to the earth, from the first data column in Table B.2 into Equation B.15. Using the values for the subtended angles from Table B.3, with luminance values for the sun and moon from Table B.2, Equation B.13 was used to calculate the sun and moon illuminance values shown in Table B.3.

---

* Walsh, John W.T., The Science of Daylight, Pittman Publishing Corporation, New York, NY, 1961, pp. 39-64.

Table B.1. Luminance Information for Natural Sources.

Object Measured and Conditions Present During the Measurement	Luminance L_B in fL	Chromaticity Coordinates		Correlated Color Temperature in °K
		x	y	
Sun Air Mass, m, & (Angle from Zenith)*				
m = 0 (above atmosphere)	5.84×10^8	0.318	0.330	6200
m = 1 (0°)	4.38×10^8	0.331	0.344	5600
m = 2 (60.0°)	3.65×10^8	0.343	0.357	5100
m = 3 (70.5°)	2.92×10^8	0.356	0.369	4700
m = 4 (75.5°)	2.34×10^8	0.368	0.379	4400
m = 5 (78.5°)	1.90×10^8	0.380	0.388	4100
Sky (Minimum range of luminances) *				
Clear Blue	175	0.262	0.270	15,000
Clear Blue	1170	0.247	0.251	30,000
Partly Cloudy	292	0.294	0.309	8,000
Partly Cloudy	1170	0.279	0.291	10,000
Overcast	584	0.313	0.329	6,500
Overcast	1460	0.313	0.329	6,500

Observations from Earth's Surface	Luminance in fL **	Luminance in fL ***
Sun at Meridian	4.67×10^8	4.82×10^8
Sun near Horizon	1.75×10^6	1.75×10^6
Moon, Mean Luminance	721	
Moon, Bright Spot	729.8	743.2
Clear Average Sky	2,340	2,323
Lightning Flash	2.34×10^{10}	
Atomic Fission Bomb (0.1 ms after firing - 90 foot diameter ball)	5.84×10^{11}	

* Bolz, Ray E. and George L. Tuve, CRC Handbook of Tables for Applied Engineering Science, The Chemical Rubber Company, Cleveland, OH, pp. 172, 173.

** IES Lighting Handbook, 4 th. ed., Illuminating Engineering Society, 1966

*** Weast, Robert C. and Sameul M. Selby, Handbook of Chemistry and Physics, The Chemical Rubber Company, Cleveland, OH, 1966, p. E-125.

Table B.2. Physical Data for Sun and Moon.

Glare Source & Physical Parameter	Dimensional Data *	Dimensional Data **
Sun		
Diameter	864,000 mi (1,390,476 km)	864,100 mi (1,390,600 km)
Mean distance from Earth	92,956,000 mi (149,598,000 km)	92,900,000 mi (149,500,000 km)
Perihelion distance	91,600,000 mi (147,416,000 km)	
Aphelion distance	94,750,000 mi (152,856,000 km)	
Moon		
Mean Diameter	2,160 mi (3,476 km)	2,159.9 mi (3,476 km)
Mean distance from Earth	238,857 mi (384,404 km)	238,854 mi (384,393 km)

Note: 1 km = 0.62137 mi

Table B.3. Subtended Angles and Illuminances for the Sun and Moon.

Glare Source & Physical Parameter	Glare Source Subtended Angle	Glare Source Illuminance
Sun Luminance above the Atmosphere = 5.84 X 10^8 fL		
Sun at Mean distance from Earth	0.5325° (0.009294 radians)	12,611 fc (117,160 lx)
Sun at Perihelion distance	0.5404° (0.009432 radians)	12,988 fc (120,660 lx)
Sun at Aphelion distance	0.5225° (0.009119 radians)	12,142 fc (112,800 lx)
Moon Luminance at the Earths Surface = 721 fL		
Moon at Mean distance from Earth	0.5181° (0.009043 radians)	0.0147 fc (0.1366 lx)

Based on the calculated values shown in Table B.3, the illuminance due to the sun above the earth's atmosphere varies in a range between 12,142 and 12,988 fc, depending on the position of the earth in its elliptical orbit about the sun. These values of illuminance are in good enough agreement with the 12,300 to

---

* Bolz, Ray E. and George L. Tuve, CRC Handbook of Tables for Applied Engineering Science, The Chemical Rubber Company, Cleveland, OH, Table 5-70. The Sun, Table 5-71. The Moon, Page 482.

** Weast, Robert C. and Sameul M. Selby, Handbook of Chemistry and Physics, The Chemical Rubber Company, Cleveland, OH, 1966, pp. F-116 & F-117.

13,600 fc range of illuminance values reported by Walsh,* as having been measured from aircraft at high altitudes by Tousey and Hulbert, ** to validate the glare source calculation technique presented in this appendix.

In practice, the spatial luminance distribution of the sun is not only not a constant, as has been assumed here for the purposes of discussion, but its luminance distribution is time variant. Sun spot activity, slow changes in the ellipticity the Earth's orbit around the sun, and other factors, not yet that well documented, also cause the sun's spatially averaged mean luminance to change as a function of time. One effect of the changes in the sun's area-averaged luminance over time, is that measurements of the illuminance levels incident on the Earth from the sun, above the atmosphere, have shown these values can reach 14,000 fc and higher.

---

* Walsh, John W.T., The Science of Daylight, Pittman Publishing Corporation, New York, NY, 1961, p. 42.

** Tousey, R. and E. O. Hulbert, Journal of the Optical Society of America, Vol. 37, 1947, p. 78.